Analysis of Physiologically Relevant Signalling Events via GLP-1R in Insulinoma cells

Kavita Pabreja

BPharm, MPharm (Pharmacology)

A thesis submitted for the degree of (*Doctor of Philosophy*) at

Monash University in 2015

Monash Institute of Pharmaceutical Sciences

Copyright Notices

Notice 1

Under the Copyright Act 1968, this thesis must be used only under the normal conditions of scholarly fair dealing. In particular, no results or conclusions should be extracted from it, nor should be copied or closely paraphrased in whole part or in part without written consent of the author. Proper written acknowledgement should be made for any assistance obtained from this thesis.

Notice 2

I certify that I have made all reasonable efforts to secure copyright permissions for third-party content included in this thesis and have not knowingly added copyright content to my work without the owner's permission.

Table of Contents

Analysis of Physiologically Relevant Signalling Events via GLP-1R in Insulinoma cells. i

Table of Contents ..... **iii**

ABSTRACT ..... **viii**

Peer-reviewed Review article ..... **xiii**

Published abstracts ..... **xiii**

Invited Seminar ..... **xiv**

ABBREVIATIONS ..... **xv**

LIST OF TABLES ..... **xix**

LIST OF FIGURES ..... **xxii**

CHAPTER 1: INTRODUCTION **1**

1.1. G protein-coupled receptors **2**

1.1.1 Introduction 2

1.1.2 Classification of GPCRs 2

1.1.2.4 Class F GPCRs 7

1.2 GPCR activation: Signalling and Regulation **8**

1.2.1 G proteins and signalling 8

1.2.2 Regulation of GPCRs and G protein mediated signals 9

1.2.3 G protein-independent signalling 12

1.2.4 GPCRs and Biased-Signalling 14

1.3 Allosteric modulation of GPCRs **17**

1.3.1 Introduction to GPCR allostery 17

1.3.2 Therapeutic advantages of allosteric modulation 17

1.3.3 Differential effects of allosteric ligands on orthosteric affinity vs efficacy 18

1.3.4 Probe dependence and allosteric modulation 20

1.3.5 The interplay of allosteric modulation, probe dependence and biased signalling 21

1.3.6 The challenges of identifying allosteric ligands in vitro and their application therapeutically 21

1.4 Pharmacological models and quantification of biased signalling and allosterism **23**

1.4.1 Measuring biased signalling 23

1.4.2 Measuring Allostery 25
1.5. Glucose homeostasis and the incretin system 28
1.5.1 General Introduction 28
1.5.2 The enteroinsular axis and the incretin effect 29
1.5.3 The incretin hormones 29
1.6 The glucagon-like peptide-1 receptor (GLP-1R) system 31
1.6.1 Biology of GLP-1 synthesis, secretion and metabolism 31
1.6.2 Biological actions of endogenous GLP-1 33
1.6.3 The glucagon like peptide-1 receptor (GLP-1R) 39
1.7 GLP-1R ligands 48
1.7.1 Endogenous GLP-1R peptide ligands 48
1.7.2 Exogenous long acting GLP-1R peptide ligands 49
1.7.3 Non-peptide and allosteric ligands of GLP-1R 53
1.8 GLP-1R biased signalling and allosteric modulation 55
1.8.1 Biased signalling by orthosteric and allosteric agonists 55
1.8.2 Allosteric modulation at the GLP-1R 55
1.9 Type 2 diabetes and the GLP-1R 56
1.9.1 Diabetes Mellitus 56
1.9.2 The GLP-1R as a therapeutic target for type 2 diabetes 57
1.9.3 Currently approved incretin threapies for T2DM 58
1.10 Future directions for GLP-1 based therapeutics and challenges facing discovery 60
1.11 Summary 61
CHAPTER 2: MATERIALS AND METHODS 64
2.1 Cell culture 65
2.1.1 Maintenance of Cells 65
2.1.2 Freezing and thawing cells 65
2.1.3 Counting cells 66
2.1.4 Laminin coating of cell culture plates 66
2.2 cAMP Accumulation 66
2.2.1 Preparation of 10X Earle's balanced salt solution (EBSS) 67
2.2.2 cAMP accumulation assay 67
2.2.3 cAMP detection assay 67
2.3 ERK1/2 Phosphorylation 68
2.3.1 pERK1/2 phosphorylation 68

2.3.2 ERK detection assay 69
2.4 Insulin secretion 69
2.4.1 Insulin secretion assay 69
2.4.2 Insulin detection 70
2.5 Apoptosis 70
2.5.1 Apoptosis assay 71
2.5.2 Detection of apoptotic cell death 71
2.6 Proliferation 72
2.6.1 Proliferation assay 72
2.6.2 BrdU incorporation and detection 73
2.7 Intracellular Ca^{2+} $[Ca^{2+}]_i$ mobilization 73
2.7.1 $[Ca^{2+}]_i$ mobilization assay 74
2.8 mRNA extraction 74
2.8.1 Treatment of cells 74
2.8.2 RNA extraction 75
2.9 mRNA Library generation 75
2.9.1 mRNA Library preparation 76
2.9.2 Sample preparation for RNA Sequencing 81
2.10 Reagents 82
2.10.1 Peptides 82
2.10.2 Small Molecules 82
2.10.3 General Reagents 82
2.11 Data analysis 83
2.11.1 Equations 83
CHAPTER 3: SELECTION AND OPTIMISATION OF MODEL β-CELL LINES 85
3.1 INTRODUCTION 86
3.2 RESULTS 88
3.2.1 Screening for a model β-cell line 88
3.2.2 Identification of suitable coating agent for INS-1 832/3 cells: 93
3.2.3 Further optimization of cAMP accumulation assays 102
3.2.4 Optimizing conditions for glucose-dependent insulin secretion 103
3.2.4 Optimizing conditions for phosphorylation of ERK1/2 107
3.2.6 Optimizing conditions for evaluating apoptosis in INS-1 832/3 cells 117
3.2.7 Optimizing conditions for proliferation of INS-1 832/3 cells 126

3.2.8 Optimizing conditions for assessing intracellular calcium ([Ca2+]i) mobilization in INS-1 832/3 cells 127
3.3 DISCUSSION 134
3.4 CONCLUSION 139
CHAPTER 4: BIASED SIGNALLING AND ALLOSTERIC MODULATION OF GLP-1R IN INS-1 832/3 CELLS 140
4.1 INTRODUCTION 141
4.2 RESULTS 144
4.2.1 GLP-1R activation of signalling pathways by different GLP-1R agonists 144
4.2.2 Stimulus bias and GLP-1R in INS-1 832/3 cells 158
4.2.3 GLP-1R biased allostery and probe-dependence 177
4.3. DISCUSSION 193
CHAPTER 5: GLOBAL ANALYSIS OF SIGNALLING BIAS AT GLP-1R 204
5.1 INTRODUCTION 205
5.2 METHODS 207
5.2.1 Incubation of INS-1 832/3 cells with GLP-1R peptides and insulin detection 207
5.2.2. RNA extraction 208
5.2.3 Sample preparation for RNA-sequencing and outsourcing to BGI for transcriptomics 209
5.2.4 RNA-Sequencing (Transcriptomics): BGI-Hong Kong Co. Ltd. 210
5.2.5 Ingenuity pathway analysis software 216
between the dataset genes and the genes that are regulated in a pathway or by upstream regulators. It is calculated using Fisher's Exact Test, and significance is generally attributed to p-values < 0.01. 222
5.2.6 Validation of RNA-seq data using RT-qPCR array 222
5.3 RESULTS 222
5.3.1 Sample treatments and GSIS 222
5.3.2 RNA quantity and quality assessment 224
5.3.3 Sequencing assessment: Sequence quality 224
5.3.4 Global and differential genes expression (DGE) analysis performed by BGI 227
5.3.5 Functional bioinformatics analysis of regulated genes 233
5.4. DISCUSSION 256
5.4.1 Transcriptomic regulation in response to GLP-1 257
5.4.2. Differential regulation of transcriptome in presence of GLP-1 and exendin-4 261
5.4.3. Differential regulation of transcriptome in presence of GLP-1 and oxytnomodulin 265

5.5 CONCLUSION **266**

CHAPTER 6: **267**

FUTURE DIRECTIONS AND PERSPECTIVES **267**

Summary and Future directions **268**

REFERENCES **281**

ABSTRACT

Glucagon-like peptide-1 (GLP-1) is an incretin hormone secreted in response to nutrient ingestion following it's binding to the GLP-1 receptor (GLP-1R). Long-acting GLP-1R peptidomimetics have become an important class of therapeutics for treating type 2 diabetes (T2D) because of their gluco-regulatory actions. However, they have been associated with adverse side-effects. Pharmaceutical companies are actively pursuing development of small molecule ligands as alternatives, but with little success to date.

GLP-1R ligands can stabilize distinct subsets of receptor conformations that can "traffic" stimulus to diverse functional outputs with varying prominence, a concept referred to as biased agonism. Allosteric modulators can also alter the signalling profiles of orthosteric ligands in a ligand-dependent manner, termed probe-dependence. While GLP-1R biased agonism and allosteric probe dependence are established, to date most studies are from recombinant systems overexpressing the GLP-1R. This thesis utilizes a reductionist (cAMP accumulation, glucose-stimulated insulin secretion (GSIS), ERK1/2 phosphorylation, proliferation and apoptosis) and non-reductionist approach (transcriptomics) to understand GLP-1R biased agonism and allosteric modulation in natively expressing cells that display glucose dependence, addressing some of the issues of translation from recombinant to more physiologically relevant systems mimicking β-cell physiology.

Extensive and systemic analysis performed using GLP-1R peptides in INS-1 832/3 insulinoma cells, revealed that cAMP accumulation, proliferation and anti-apoptosis were glucose-independent, whereas, insulin secretion, $[Ca^{2+}]_i$ mobilization and aspects of the ERK1/2 phosphorylation kinetics were glucose-dependent. Furthermore, attenuation of glucose-mediated activation of ERK1/2 at 5 min by GLP-1R peptides was a novel, unexpected observation. Assessment of ligand signalling profiles revealed that biased agonism occurred with distinct ligands; however the bias profile was different in two physiologically relevant glucose concentrations. One significant observation was a large degree of bias at the therapeutically relevant endpoints of proliferation and apoptosis, where for equivalent amounts of cAMP generated, GLP-1 was more efficacious compared to exendin-4 and oxyntomodulin. For small molecule ligands there was bias relative to GLP-1 between the amount of cAMP production and insulin secretion that was not observed with peptide ligands. In addition, both BETP and Compound 2 allosterically altered the signalling profiles of peptide ligands, in a peptide-dependent

manner that differed depending on the glucose concentration assessed, observations that have clinical relevance for the development of allosteric drugs.

In the final chapter, analysis of transcriptomics data identified a number of genes associated with functions of cell to cell signalling, signal transduction, proliferation, cell death and survival, along with number genes for GPCRs and GPCR ligands that were up or down-regulated following GLP-1R activation. In addition, a number of genes associated with T2D, but not previously with GLP-1R signalling also emerged. Exendin-4 and oxyntomodulin displayed bias relative to GLP-1 at the level of gene transcription with a number of differentially regulated genes identified.

Thus, this thesis expands the existing knowledge around GLP-1R pharmacology and signalling. This will facilitate ligand profiling and better understanding of biased agonism in natively expressing systems that may be useful for future therapeutic development.

DECLARATION

This thesis contains no material which has been accepted for the award of any other degree or diploma at any university or equivalent institution and that, to the best of my knowledge and belief, this thesis contains no material previously published or written by another person, except where due reference is made in the text of the thesis.

This thesis includes one original manuscript (review) as a primary author, published in a peer-reviewed journal, reflecting the core theme of the thesis "Analysis of physiologically relevant events via glucagon-like peptide-1 receptor in insulinoma cells". The ideas, development and writing of this paper, arising from this thesis was the principal responsibility of myself, the candidate, working within the Drug Discovery Biology Theme under the supervision of Prof. Patrick Sexton, Dr. Denise Wootten and Dr. Sebastian Furness.

The inclusion as co-author on other two original manuscripts reflects the fact that the work came from active collaboration between researchers and acknowledges input into team-based research.

(Kavita Pabreja)

ACKNOWLEDGEMENT

Firstly, I wish to express my sense of gratitude and indebtedness to my primary and associate supervisors, Professor Patrick Sexton, Dr. Denise Wootten and Dr. Sebastian Furness. I deeply acknowledge their constructive guidance and unwavering support throughout my tenure of doctoral studies, along with their devotion in providing me with many personal hours to guide and mentor me in reviewing my numerous drafts of thesis.

I would like to convey my special thanks to Dr. Denise Wootten, for her enormous contribution, continuous support, guidance and immense patience right from my candidature confirmation through to the thesis writing phase including exit seminar that was incredible. I am forever grateful for her inspiration that motivated me to finalise my Doctoral thesis where she will always be my role model.

I also express my thanks to Dr Trevor Biden, Garvan Institute of Medical Research, Sydney, along with Dr Nicole Wong, Melbourne University, Melbourne, Professor Ken Walder, Deakin University, Geelong and Professor Christopher B. Newgard, Duke University, North Carolina USA for generously providing MIN6, INS-1, INS-1E and INS1-1 832/3 Beta cell lines expressing GLP-1R respectively that were applied in this research project.

My sincere thanks also go to my PhD. Review Panel members, Professor Matthew Watt, Dr Erica Sloan and Dr Bronwyn Evans for their valuable feedback and constant support at various stages of my doctoral studies.

A big thank you to past and present members of the Drug Discovery Biology (DDB) Laboratory, particularly “the Family B” group, for the constant support, encouragement and sharing the abundance of knowledge with me, along with inspiring involvements in making my journey gratifying.

I would like to extend my thanks to the Monash Research Graduates School for providing me this wonderful opportunity to study and carry out my Higher Degree Research (HDR) by awarding me with the Monash Graduate Scholarship (MGS) and Monash International Postgraduate Research Scholarship (MIPRS) including the Monash Institute of Pharmaceutical Sciences (MIPS) for providing me with the MIPS Faculty Scholarship. Furthermore, I would like to acknowledge and sincerely thank Dr. Karen

McConalogue and Karen Drakatos for their efforts, support and guidance provided during my PhD tenure from time to time.

On a personal level, this achievement would not have been ever possible without the immense support, constant encouragement and sacrifice from my loving five year old daughter Tannishtha, ever loving parents, spouse Dr Kamal, in-laws and extended family Mrs. Upward and Stuart. I owe sincere thanks to my dear friends Nabila, Sajjad and Prabuddha, whose contributions during my journey would be cherished for a life-time. I am eternally grateful to you all for standing by my side in good or trying scenarios by continuously infusing me with motivation and strength. I would also like to thank all other people who have directly or indirectly contributed to my thesis but have not been individually listed.

Moreover, the axioms provided by dear family acted as restorative therapy “Each passing day is a step closer to home”; “Nearly there” and “Keep going” , which will be endured over my lifetime. Lastly but not least, I acknowledge all those who knowingly and unknowingly contributed in my doctoral studies and making me to reach this step of my research journey.

PUBLICATIONS AND COMMUNICATIONS

Peer-reviewed articles

Koole C, **Pabreja Kavita**, Savage EE, Wootten D, Furness SG, Miller LJ, Christopoulos A, Sexton PM. *Recent advances in understanding GLP-1R (glucagon-like peptide-1 receptor) function*, Biochemical Society Transactions, 2013, 41(1):172-179.

Amy N.Y. Chen, Daniel T. Malone, **Kavita Pabreja,** Patrick M. Sexton, Arthur Christopoulos, and Meritxell Canals. *Detection and quantification of allosteric modulation of endogenous M4 muscarinic acetylcholine receptor using impedance-based label-free technology in a neuronal cell line***.** Journal of Biomolecular Screening, 2015 Jun; 20(5):646-54.

Peer-reviewed Review article

Kavita Pabreja, M A Mohd, C Koole, D Wootten and S G B Furness. *Molecular mechanisms underlying physiological and receptor pleiotropic effects mediated by GLP-1R activation*. British Journal of Pharmacology, Mar 2014, Volume 171, Issue 5: 1114–1128.

Published abstracts

Kavita Pabreja, Shannen Lau, Emilia E Savage, Sebastian G.B. Furness, Patrick M. Sexton, Denise Wootten. *Characterizing Novel Aspects of GLP-1 Receptor Signalling* at ASCEPT- MPGPCR 2014 Joint Scientific Meeting, 7-11 Dec 2014, Melbourne, Australia.

Kavita Pabreja, Denise Wootten, Sebastian GB Furness, Patrick M Sexton. *Characterization of INS-1 832/3 cell line as a model system for studying GLP-1R regulation in diabetes* at 47th Annual Scientific Meeting, December 2013, Melbourne, Australia.

Kavita Pabreja, Denise Wootten, Patrick M Sexton and Sebastian G.B. Furness. *Preliminary investigation to identify and characterize model cell system for studying GLP-1R regulation* at Molecular pharmacology of G Protein-Coupled Receptors (MP-GPCR) meeting (2012), Melbourne, Australia.

Mohd M.A., **Pabreja Kavita**, Sexton P.M., Koole C., Wootten D., Furness SGB. *Pharmacological comparison of human, rat and mouse glucagon-like peptide-1 (GLP-1) receptors* at MPGPCR meeting 2012 Melbourne, Australia.

Invited Seminar

Kavita Pabreja, Shannen Lau, Emilia E Savage, Sebastian G.B. Furness, Patrick M. Sexton, Denise Wootten. *Characterizing Novel Aspects of GLP-1 Receptor Signalling* at Joint IUBMB- RCB Advanced School -2014, 24-29 Nov 2014, India

ABBREVIATIONS

5-HT – 5-hydroxytryptamine AA – arachidonic acid

AC – adenylyl cyclase

ACh - acetylcholine

AM – acetoxymethyl

AP-2 – activating protein 2

β-**Arrestin** – beta arrestin

ANOVA – analysis of variance

ARF6 – ADP-ribosylation factor 6

ARNO – ARF nucleotide exchange factor

ATCM – allosteric ternary complex model

ATP – adenosine triphosphate

ATSM – allosteric two-state model

BCA – bicinchoninic acid

BETP – 4-(3-(benzyloxy)phenyl)-2-(ethylsulfinyl)-6-(trifluoromethyl)pyrimidine

Boc5 - 1,3-bis [[4-(tert-butoxy-carbonylamino)benzoyl]amino]-2,4-bis[3-methoxy-4-(thiophene-2-carbonyloxy)-phenyl]cyclobutane-1,3-dicarboxylic acid

Bpa – p-benzoylphenylalanine

BRET - bioluminescence resonance energy transfer

BSA – bovine serum albumin

Ca^{2+} – calcium

cAMP – cyclic adenosine monophosphate

CaS – Ca^{2+} sensing

CHO – Chinese hamster ovary

CCP – clathrin coated pits

Compound 1 – 2-(2'-methyl)thiadiazolylsulfanyl-3-trifluoromethyl-6,7-dichloroquinoxaline

Compound 2 – 6,7-dichloro2-methylsulfonyl-3-tert-butylaminoquinoxaline

CREB – cAMP response element-binding

CRF – corticotropin-releasing factor

c-Src – proto-oncogene tyrosine kinase Src

DAG – diacylglycerol

DM – diabetes mellitus

DMEM – Dulbecco's modified eagle medium

DOI – (6)-1-(2,5-dimethoxy-4-iodophenyl)-2-aminopropane

DPPIV – dipeptidyl peptidase IV

ECL – extracellular loop

EGF – epidermal growth factor

Epac – exchange protein activated by cAMP

ERK1/2 – extracellular signal regulated kinases 1 and 2

FBS – fetal bovine serum

GDP – guanosine diphosphate

GHRH – growth hormone-releasing hormone

GIP – glucose-dependent insulinotropic polypeptide, gastric inhibitory polypeptide

GLP – glucagon-like peptide

GLP-1R – glucagon-like peptide 1 receptor

GPCR – G protein-coupled receptor

G protein – guanine nucleotide-binding protein

GPS – GPCR proteolytic site

GRK – G protein receptor kinase

GRPP – glicentin-related polypeptide

GSK – glucogen synthase kinase

GTP – guanosine triphosphate

HIV – human immunodeficiency virus

HTS – high throughput screen

$[Ca^{2+}]_i$ - intracellular Ca^{2+}

IBMX – 3-isobutyl-1-methylxanthine ICL – intracellular loop

InP – intervening peptide

IP – inositol phosphate

IRS – insulin receptor substrate

IUPHAR – International Union of Basic and Clinical Pharmacology

JNK – c-Jun N-terminal kinases

K^+ – potassium

mACh – muscarinic acetylcholine

MAPK – mitogen-activated protein kinase

McN-A-343 – 4-(m-chlorophenylcarbamoyloxy)-2-butynyltrimethylammonium chloride

MEK – mitogen-activated protein kinase kinase

MPGF – major proglucagon fragment

Na+ – sodium

NAM – negative allosteric modulator

NEP – neutral endopeptidase 24.11

NFxviB – nuclear factor kappa B

NMR – nuclear magnetic resonance

NMS – N-methylscopolamine

NSF – N-ethylmaleimide-sensitive fusion

OPD – o-phenylenediamine dihydrochloride

ORG – Organon research

PAC – PACAP receptor

PACAP – pituitary adenylate cyclase-activating peptide

PAM – positive allosteric modulator

PBS – phosphate buffered saline

PC – prohormone convertase

PDB – Protein Data Bank

PEG – polyethylene glycol

pERK1/2 – phosphorylated ERK1/2

PI3K – phosphatidylinositol-3 kinase

PIP2 – phosphatidylinositol 4,5-bisphosphate

PFA – paraformaldehyde

PLC – phospholipase C

PLD – phospholipase D

PKA – protein kinase A

PKB – protein kinase B

PKC – protein kinase C

PTH – parathyroid hormone

QNB – quinuclidinyl benzilate

Quercetin – 3,3’,4,5,7-pentahydroxyflavone

Raf – mitogen-activated protein kinase kinase kinase

RAMP – receptor activity modifying protein

RhoA – Ras homolog gene family member A

Forskolin - (3R,4aR,5S,6S,6aS,10S,10aR,10bS)-6,10, 10b-trihydroxy- 3,4a,7,7,10apentamethyl-1-oxo-3- vinyldodecahydro-1H-benzo[f]chromen-5-yl acetate

SAR – structure activity relationship

SCR – short consensus repeat

SOCS – suppressor of cytokine signaling proteins

SU – sulfonylurea

TM – transmembrane

TZD – thiazolidinedione

VDCC – voltage-dependent Ca2+ channel

VIP – vasoactive intestinal peptide

VPAC – VIP and PACAP receptors

LIST OF TABLES

S. No.	*Title of table*	*Page. No.*
3.1	Effect of GLP-1 on cAMP accumulation in different insulinoma cell lines.	87
3.2	Effect of GLP-1 and 11 mM glucose on cAMP accumulation in INS-1 832/3 cells stimulated for 5 min and 30 min, after 48 h of seeding on plates treated with different coating agents at varying cell densities.	92
3.3	Summarized key findings from the optimization process involved to identify a suitable coating agent so as to investigate various functional outputs in INS-1 832/3 cells. The best conditions are highlighted in yellow.	95
3.4	Effect of GLP-1 on cAMP accumulation in INS-1 832/3 cells stimulated in DMEM and EBSS, 72 h post-seeding on laminin coated plates respectively, for 30 min in presence of 2.8 mM and 11 mM glucose.	103
3.5	Effect of GLP-1 on cAMP accumulation in different passages of INS-1 832/3 cells stimulated in DMEM for 30 min in presence of varying glucose concentrations after 72 h of seeding on plates coated with laminin.	104
3.6	Effect of starvation periods (2 h and overnight starvation) on GLP-1 mediated GSIS, prior to insulin secretion assay.	105
3.7	Summarized key findings from the MTT assay used as a part of the optimization process followed to identify ideal set of conditions to investigate apoptosis in INS-1 832/3 cells.	115
3.8	Summarized key findings from the Annexin V 488 conjugate and PI staining of INS-1 832/3 cells analysed using InCell analyser, as a part of the optimization process followed to identify ideal set of conditions to investigate apoptosis.	117
3.9	Summarized key findings from the Annexin V 647 conjugate and PI staining of INS-1 832/3 cells analyzed using FACS , as part of the	118

	optimization process followed to identify ideal set of conditions to investigate apoptosis.	
3.10	Effect of 24 h incubation of INS-1 832/3 cells in presence of GLP-1 on BrdU incorporation as a measure of cell proliferation.	129
4.1	Effect of GLP-1R peptide and allosteric agonists on cAMP accumulation in the endogenously expressing GLP-1R cell line INS-1 832/3.	142
4.2	Effect of GLP-1R peptide and allosteric agonists on glucose-dependent insulin secretion in the endogenously expressing GLP-1R cell line INS-1 832/3 in 11 mM glucose.	144
4.3	Effect of GLP-1R agonists on ERK1/2 phosphorylation at varying time points in endogenously expressing GLP-1R cell line INS-1 832/3.	148
4.4	Anti-apoptotic effects of GLP-1R peptide agonists in endogenously expressing GLP-1R cell line INS-1 832/3.	153
4.5	Proliferative effects of GLP-1R peptide agonists in endogenously expressing GLP-1R cell line INS-1 832/3.	156
4.6	Ligand-directed stimulus bias exhibited by GLP-1R peptide ligands when comparing individual pathways in varying glucose conditions relative to the reference agonist GLP-1 in INS-1 832/3 cells.	164
4.7	Stimulus bias of all pathways (except pERK1/2) exhibited by GLP-1R peptide ligands relative to the reference agonist GLP-1 in INS-1 832/3 cells.	165
4.8	Stimulus bias exhibited GLP-1R peptide ligands at all pathways relative to pERK1/2 and the reference agonist GLP-1 in INS-1 832/3 cells.	167
4.9	Functional cooperativity estimates for the interaction between Compound 2 or BETP and GLP-1R peptide ligands.	177
5.1	Biofunctions and diseases affected by differential regulation of genes in response to time-dependent treatment of GLP-1 (30 min, 2 h, 6 h and 24 h) relative to vehicle control at 30 min in INS-1 832/3 cells.	207
5.2	Canonical Pathways affected by differential regulation of genes in response to time-dependent treatment of GLP-1 (30 min, 2 h, 6 h and 24 h) relative to vehicle control at 30 min in INS-1 832/3 cells.	208

5.3	Canonical pathways affected by differential regulation of genes in response to acute and chronic treatment with glucose alone, GLP-1 and exendin-4 relative to the appropriate vehicle control in INS-1 832/3 cells.	211
5.4	Criteria for designing RT-qPCR array. Assorted sub-list of differentially regulated genes at 30 min and 24 h in response to GLP-1 and exendin-4 compared to glucose control (vehicle) at the same time points genes representing criteria (cell to cell signalling, signal transduction, cell death and survival and genes linked to type 2 diabetes) considered for designing of RT-qPCR array.	217
5.5.	Biofunctions and diseases affected by differential regulation of genes in response to time-dependent treatment of GLP-1 (30 min, 2 h, 6 h and 24 h) relative to vehicle control at 30 min in INS-1 832/3 cells.	237
5.6 A	Top canonical pathways predicted to be activated based on the genes regulated response to GLP-1.	245
5.6 B	Canonical pathways that were predicted to be activated or inhibited based on the gene expression profiles of GLP-1 treatments at 30 min, 2 h, 6 h or 24 h.	247
5.7	Canonical pathways affected by differential regulation of genes in response to acute and chronic treatment with glucose alone, GLP-1 and exendin-4 relative to the appropriate vehicle control in INS-1 832/3 cells.	250
5.8	Examples of genes linked to functions of interest when considering GLP-1R activation for therapeutic development.	252
Supplementary Section		
S5.1	RNA quality analysis	36
S5.8	Selection criteria and Primer Sequences	59

LIST OF FIGURES

S. No.	*Title of Figure*	*Page. No.*
1.1	Classification of G protein-coupled receptors	4
1.2	Diversity of G-protein-coupled receptors (GPCRs) signalling	11
1.3	Identification of signalling bias in pharmacological assays	16
1.4	Schematic representation of allosteric actions	19
1.5	Models of allosteric interactions	26
1.6	Physiological actions of glucagon-like peptide-1 (GLP-1)	33
1.7	Signalling pathways mediated by GLP-1R activation in pancreatic β-cell.	42
1.8	Amino acid sequence of various GLP-1 mimetics	48
1.9	Small molecule synthetic ligands of the GLP-1R	50
3.1	Effect of GLP-1 on cAMP accumulation in different insulinoma cell lines in 11 mM (high) glucose conditions	86
3.2	Effect of GLP-1 on Insulin secretion in different insulinoma cell lines.	88
3.3	Effect of GLP-1 in 11 mM glucose on cAMP accumulation in INS-1 832/3 cells 48 h post-seeding at a density of 25,000 cells/well on laminin (A-C) and fibronectin (D-F) coated 96 well cell culture plates.	91
3.4	Effect of GLP-1 on cAMP accumulation in presence of varying glucose concentration (2.8 mM and 11 mM) after 48 h (A, B, E and F) and 72 h(C, D, G and H) of seeding 25,000 cells/well on laminin (A-D) and fibronectin (E-H) coated 96 well cell culture plates.	99
3.5	Effect of GLP-1 on INS-1 832/3 cells assessed using cAMP accumulation performed in (A) DMEM and (B) EBSS as stimulation buffers supplemented with 2.8 mM and 11 mM glucose at a seeding density of 25,000 cells/well on laminin coated 96 well cell culture plates	100
3.6	Effect of GLP-1 on cAMP accumulation in presence of varying glucose concentrations on two different passages of INS-1 832/3 cells.	101
3.7	Sensitivity oftwo different insulin detection methods	108

3.8	Effect of starvation periods (overnight Vs 2 h starvation) prior to assay on GLP-1 mediated glucose-dependent insulin secretion (GSIS).	109
3.9	Time-dependent phosphorylation of ERK1/2 in response to 100 nM GLP-1 in INS-1 832/3 cells seeded at a density of 25,000 cells/well on laminin coated plate and stimulated in different buffers, RPMI 1640 (A-D) and EBSS (E-H) and different glucose concentrations, 2.8 mM (A, B, E, F) and 11 mM (C, D, G, H).	110
3.10	AnnexinV- 488 and propidium iodide staining of INS-1 832/3 cells after 6 h (A, B, E, F) and 24 h (C, D, G, H) incubation in presence and absence of 100 nM (A-D) and 300 nM (E-H) staurosporineco-added with and/or without GLP-1in RPMI 1640 supplemented with 11 mM glucose and 10% serum.	112
3.11	Dose-dependent effect of GLP-1 on annexinV- 647 and propidium iodide staining of INS-1 832/3 cells after 24 h of co-addition and incubation in presence of 100 nM staurosporine and GLP-1 with RPMI 1640 supplemented with 10% serum and 2.8 mM or 11 mM glucose. Percent apoptotic was assessed as percent of staurosporine treatment in 2.8 mM glucose (A) 5 x 10^5 cells/well; (B) 7 x 10^5 cells/well. Percent live cells was determined after 24 h of incubation of (A) 5 x 10^5 cells/well; (B) 7 x 10^5 cells/well, as percent of 2.8 mM glucose media.	120
3.12	Dose-dependent effect of GLP-1 on annexinV- 647 and propidium iodide staining of INS-1 832/3 cells after 24 h of co-addition and incubation in presence of 100 nM staurosporine and GLP-1with RPMI 1640supplemented with 10% serum and 2.8 mM or 11 mM glucose.	121
3.13	BrdU incorportaion after 24h incubation in presence of GLP-1 (10 nM and 100 nM) at a cell density of (A) 5000 cell/well ; (B) 10,000 cells/well ; (C) 15,000 cells/well ; (D) 20,000 cells/well ; (E) 30,000 cells/well and (F) 40,000 cells/well.	125
3.14	Dose-dependent uptake of BrdU after 24h incubation in presence GLP-1 at a cell density of (A) 20,000 cell/well; (B) 12,000 cells/well.	126
3.15	Effect of GLP-1(7-36) NH_2 on intracellular calcium mobilization in both low and high glucose conditions at a cell density of 25,000 cells/well.	127

3.16	Summary of various glucose-dependent and -independent functional screens optimised in INS-1 832/3 cells using GLP-1R ligand GLP-1.	128
4.1	cAMP accumulation by GLP-1R agonists in INS-1 832/3 cells. Characterization of cAMP accumulation in presence of (A) GLP-1, (B) Exendin-4, (C) Oxyntomodulin, (D) BETP and (E) Compound 2 in INS-1 832/3 cells. Green represents low (2.8 mM) glucose and red represents high (11 mM) glucose.	141
4.2	Insulin secretion by GLP-1R agonists in INS-1 832/3 cells. Characterization of glucose-dependent insulin secretion in presence of (A) GLP-1, (B) Exendin-4, (C) Oxyntomodulin, (D) BETP and (E) Compound 2 in INS-1 832/3 cells. Green represents low (2.8 mM) glucose and red represents high (11 mM) glucose.	143
4.3	Time-dependent activation of pERK1/2 by different GLP-1R agonists in INS-1 832/3 cells. Characterization of time-dependent activation of ERK1/2 in presence of (A) vehicle, (B) GLP-1 (100 nM), (C) Exendin-4 (100 nM), (D) Oxyntomodulin (1µM), (E) BETP (3 µM), (F) Compound 2(3 µM) and (G) DMSO in INS-1 832/3 cells.	146
4.4	Concentration response curves for pERK1/2 of different GLP-1R agonists in INS-1 832/3 cells.	147
4.5	Concentration response curves for pERK1/2 of different GLP-1R small molecule agonists in INS-1 832/3 cells.	151
4.6	Concentration response curves for anti-apoptotic effects mediated by different GLP-1R peptides agonists in INS-1 832/3 cells.	152
4.7	Concentration response curves for proliferative effects mediated by different GLP-1R peptides agonists in INS-1 832/3 cells.	155
4.8	Signalling profiles of GLP-1R ligands in low and high glucose.	157
4.9	Bias factors of peptide ligands between high and low glucose. Quantification of stimulus bias [$\Delta(\tau/K_A)$] displayed by various GLP-1R peptide ligands relative to the reference ligand GLP-1 for individual pathways where a response could be detected in both 2.8 mM glucose and 11 mM glucose in INS-1 832/3 cells.	159
4.10	Bias of peptide ligands when comparing different signalling pathways in	160

	low glucose.	
4.11	Bias of peptide ligands when comparing different signalling pathways in high glucose.	161
4.12	Bias of small molecule ligands relative to GLP-1.Quantification of stimulus bias [$\Delta(\tau/K_A)$] displayed by various GLP-1R small molecule ligands relative to the reference ligand GLP-1 in the presence of low and high glucose using INS-1 832/3 cells.	163
4.13	Web of bias with GLP-1R ligands relative to the reference ligand GLP-1 and reference pathway cAMP in respective glucose conditions.	172
4.14	Allosteric modulation of GLP-1R peptide-mediated responses in cAMP by compound 2.	174
4.15	Allosteric modulation of GLP-1R peptide-mediated cAMP responses by BETP.	175
4.16	Allosteric modulation of GLP-1R peptide responses in insulin secretion by compound 2 and BETP.	176
4.17	Allosteric modulation of GLP-1R peptide responses in pERK1/2 assay performed at the transient ERK1/2 peak for both peptide and small molecule Compound 2.	182
4.18	Allosteric modulation of GLP-1R peptide responses in pERK1/2 assay performed at the transient ERK1/2 peak for both peptide and small molecule BETP.	183
4.19	Allosteric modulation of GLP-1R peptide responses in pERK1/2 assay performed at the transient ERK1/2 peak for both peptide and small molecule Compound 2.	184
4.20	Allosteric modulation of GLP-1R peptide responses in pERK1/2 assay performed at the transient ERK1/2 peak for both peptide and small molecule BETP.	185
4.21	Potency changes in 5 min pERK1/2 inverse agonism by peptide ligands in the presence of increasing concentration of small molecules.	186
4.22	Allosteric modulation of GLP-1R peptide responses in pERK1/2 assay performed at the transient ERK1/2 peak for peptide and sustained ERK1/2 response for small molecule Compound 2.	187

4.23	Allosteric modulation of GLP-1R peptide responses in pERK1/2 assay performed at the transient ERK1/2 peak for peptide and sustained ERK1/2 response for BETP.	188
5.1	Insulin Secretion. Glucose-dependent insulin secretion in presence of 100 nM GLP-1, 100 nM exendin-4, and 1μM oxyntomodulinin supernatants collected from INS-1 832/3 cells at 2 h, prior to RNA extraction and sequencing.	219
5.2	Global and differential gene expression analysis (performed by BGI-Hong Kong Co. Ltd): Number of significantly regulated genes in response to GLP-1R peptide agonists at varying time points.	225
5.3	Description of functional hierarchical clustering as illustrated using an example.	231
5.4	Hierarchical functional clustering analysis in response to 100 nM GLP-1.	233
5.5	Hierarchical functional clustering in response to glucose.	235
5.6	Global Analysis. Venn diagrams showing overlap of differentially ($p < 0.05$) expressed genes at different time points (30 min and 24 h) in presence of 100 nM GLP-1 (G_30 and G_24) and 100 nM exendin-4 (Ex_30 and Ex_24) compared to 11 mM glucose at the same time points (U_30 and U_24) that are unique and shared	249
6.1	Probe dependence, signal bias and physiological relevance in presence of compound 2 and GLP-1R peptides.	272
6.2	Probe dependence, signal bias and physiological relevance in presence of BETP and GLP-1R peptides.	273
Supplementary Section		
S3.1	Microscopic images of INS-1 832/3 cells representing their phenotype and distribution after 24 h (panels A-F; 20X) and 48 h (panels G-L; 20 X and panels M-R; 4X) of seeding on uncoated 96 well cell culture plates at different cell densities.	5
S3.2	Effect of 30 min GLP-1 stimulation in 11 mM glucose on cAMP accumulation in absence of IBMX after 48 h of cell seeding at varying cell densities on uncoated 96-well cell culture plates.	6

S3.3	Microscopic images of INS-1 832/3 cells representing their phenotype and distribution after 24 h (panels A-E; 20X) and 48 h (panels G-J; 20 X) of seeding on poly-D-Lysine coated 96 well cell culture plates at different cell densities.	7
S3.4	Microscopic images of INS-1 832/3 cells representing their phenotype and distribution after 24 h (panels A-F; 20X) and 48 h (panels G-L; 20 X; panels M-R; 4X) of seeding on poly-D-Lysine coated 96 well cell culture plates at different cell densities.	8
S3.5	Effect of 30 min GLP-1 stimulation in 11 mM glucose on cAMP accumulation in presence of IBMX after 48 h of cell seeding at varying cell densities on poly-D-lysine coated 96-well cell culture plates.	9
S3.6	Microscopic images of INS-1 832/3 cells representing their phenotype and distribution after 24 h (panels A-F; 20X) and 48 h (panels G-L; 20 X and panels M-R; 4X) of seeding on collagen coated 96-well cell culture plates at different cell densities.	10
S3.7	Effect of 30 min GLP-1 stimulation in 11 mM glucose on cAMP accumulation in presence of IBMX after 48 h of cell seeding at varying cell densities on collagen coated 96-well cell culture plates.	11
S3.8	Microscopic images of INS-1 832/3 cells representing their phenotype and distribution after 24 h (panels A-F; 20X) and 48 h (panels G-L; 20 X and panels M-R; 4X) of seeding on foetal bovine serum (FBS) coated 96-well cell culture plates at different cell densities.	12
S3.9	Effect of 30 min GLP-1 stimulation in 11 mM glucose on cAMP accumulation in presence of IBMX after 48 h of cell seeding at varying cell densities on FBS coated 96-well cell culture plates.	13
S3.10	Microscopic images of INS-1 832/3 cells representing their phenotype and distribution after 24 h (panels A-F; 20X) and 48 h (panels G-L; 20 X and panels M-R; 4X) of seeding on gelatin coated 96-well cell culture plates at different cell densities.	14
S3.11	Effect of 30 min GLP-1 stimulation in 11 mM glucose on cAMP accumulation in presence of IBMX after 48 h of cell seeding at varying cell densities on gelatin coated 96-well cell culture plates.	15

S3.12	Microscopic images of INS-1 832/3 cells representing their phenotype and distribution after 24 h (panels A-F; 20X) and 48 h (panels G-L; 20 X and panels M-R; 4X) of seeding on laminin coated 96-well cell culture plates at different cell densities.	16
S3.13	Effect of 30 min GLP-1 stimulation in 11 mM glucose on cAMP accumulation in presence of IBMX after 48 h of cell seeding at varying cell densities on laminin coated 96-well cell culture plates.	17
S3.14	Effect of GLP-1 on cAMP accumulation in INS-1 832/3 cells after 48 h of seeding 40,000 cells/well on laminin (A-D) and fibronectin (E-H) coated 96 well cell culture plates.	18
S3.15	Effect of GLP-1 on cAMP accumulation in presence of varying glucose concentration after 48 h (A, B, E and F) and 72 h (C, D, G and H) of seeding 40,000 cells/well on laminin (A-D) and fibronectin (E-H) coated 96 well cell culture plates.	19
S3.16	Staurosporine induced apoptosis assessed using MTT (3-[4,5-dimethylthiazol-2-yl]-2,5 diphenyl tetrazolium bromide) assay at different time points, 2 h (A-C), 6 h (D-F) and 24 h (G-I) in INS-1 832/3 cells seeded at varying cell densities, 20,000 cells/well (A, D, G), 30,000 cells/well (B, E, H) and 40,000 cells/well (C, F, I).	20
S3.17	Staurosporine induced apoptosis assessed using annexinV- 647 and propidium iodide staining of INS-1 832/3 cells after 6 h (A, B, E, F) and 24 h (C, D, G, H) incubation in presence and absence of 100 nM staurosporine with and without GLP-1 in RPMI 1640 supplemented with 11 mM glucose.	21
S4.1	Comparison of pathway bias mediated by GLP-1R peptide ligands in low and high glucose.	23
S4.2	Bias plots of GLP-1R peptide ligands in low glucose.	24
S4.3	Bias plots of GLP-1R peptide ligands in high glucose	25
S4.4	Allosteric modulation of GLP-1R peptide responses in pERK1/2 assay performed at the sustained ERK1/2 peak for both peptide and small molecule compound 2.	26
S4.5	Allosteric modulation of GLP-1R peptide responses in pERK1/2 assay	27

	performed at the sustained ERK1/2 peak for both peptide and small molecule BETP.	
S5.1	Gel Images and RNA integrity number (RIN) of RNA samples (n=3) prepared for RNA sequencing assessing RNA quality performed using R6K ScreenTape® and 2200 tapeStation Software (A.01.01).	29
S5.2	Measure of pre-alignment quality	30
S5.3	Measure of pre-alignment quality	31
S5.4	Measure of post-alignment quality	32
S5.5	Measure of post-alignment quality	33
S5.6	Distribution of gene coverage	34

CHAPTER 1: INTRODUCTION

1.1. G protein-coupled receptors

1.1.1 Introduction

G protein-coupled receptors (GPCRs), also known as 7-transmembrane receptors, heptahelical receptors, serpentine receptors, or G protein-linked receptors, are the largest family of membrane proteins involved in transmitting extracellular environmental signals into the cells. These receptors are activated by diverse set of extracellular messengers, including light, odorant molecules, peptide and non-peptide neurotransmitters, hormones, growth factors, lipids, etc. (Flower, 1999; Marinissen *et al.*, 2001). GPCRs have emerged as the most important targets for human therapeutics due to their large numbers and critical roles in the physiology of vital systems, such as cardiovascular, nervous, immune, metabolic, and endocrine systems. This makes them a central focus of basic pharmacology studies and drug discovery efforts. GPCRs are preferentially targeted for the development of new therapeutics and account for about 40% of the currently exploited drug targets (Allen *et al.*, 2011; Rask-Andersen *et al.*, 2011).

Altering the activity of GPCRs via therapeutic intervention has been successfully employed in the treatment of numerous ailments including cardiac malfunction, asthma, metabolic disorders and migraines (Moore *et al.*, 2012; Arvanitakis *et al.*, 1998). Given the tremendous diversity of GPCRs, there remains enormous potential for the development of additional drugs to ameliorate neurological disorders, inflammatory diseases, cancer and metabolic imbalances. All GPCRs present a canonical fold of seven hydrophobic α-helical transmembrane (TM) segments, with an extracellular amino terminus and an intracellular carboxyl terminus. Once activated by a ligand, they can couple to four different families of heterotrimeric proteins (G_s, G_i/G_o, G_q/G_{11} and G_{12}/G_{13}) and other signalling molecules such as arrestins, which in turn regulate the activity of one or several effectors such as second-messenger-producing enzymes or ion channels.

1.1.2 Classification of GPCRs

GPCRs were classified by Kolakowski into six families that include GPCRs present in both vertebrates and invertebrates: the rhodopsin family (A) the secretin-receptor family, (B) the metabotropic glutamate receptor family, (C) fungal pheromone P- and α-factor receptors, (D) and cAMP receptors from Dictyostelium, (Kolakowski, 1994). Later, Fredriksson and colleagues, on the basis of phylogenetic relationship between the GPCRs in the human genome, classified this superfamily into

what is known as the GRAFS classification system: glutamate, rhodopsin, adhesion, frizzled/taste2 and secretin (Fredriksson *et al.,* 2003) (Figure 1.1).

1.1.2.1 Class A GPCRs

Class A GPCRs (the Rhodopsin receptor family) is the largest family of GPCRs (Gloriam *et al.,* 2007) and contains the majority of receptors that are targeted by clinically used drugs (Tyndall *et al.,* 2005). Class A GPCRs are highly diverse with respect to their primary structure and ligand preference. They bind a vast variety of ligands, such as peptides, fatty acids, prostaglandins, amines and purines (Tyndall *et al.,* 2005). Class A GPCRs are further divided into four groups- alpha, beta, gamma and delta (Fredriksson *et al.,* 2003). The α-group consists of histamine receptors 1 and 2; the dopamine receptors 1 and 2; the serotonin receptors 1A, 1D and 2A; the adrenoceptors 1A, 2A, B1 and B2; the muscarinic receptor 3; the prostanoid receptors TP, EP1, EP3, IP1 and FP; and the cannabinoid receptor 1 (CNR1) (Jacoby *et al.,* 2006; Tyndall *et al.,* 2005). Drugs that target these receptors include antihistamines, antacids, cardiovascular drugs and antipsychotics. The β-group of the rhodopsin family includes mainly peptide-binding receptors such as endothelin, gonadotropin-releasing hormone and vasopressin/oxytocin receptor ligands (Tyndall *et al.,* 2005). The γ-group includes receptors for peptides and lipid-like compounds comprising three opioid receptors, somatostatin receptor 2 and 5 (SSTR2 and SSTR5) and the angiotensin receptor 1 (AGTR1) (Fredriksson *et al.,* 2003; Tyndall *et al.,* 2005). The δ-group includes purinergic receptors (P2YRs), glycoprotein binding receptors (FSHR, TSHR, LHCGR), protease activated receptors (PARs) and olfactory receptors (Fredriksson *et al.,* 2003).

Most of the family A group receptors contain highly conserved motifs within their TM bundle, including the D/ERY motif at the cytoplasmic border of helix III, a CWXP motif in TMVI and an NSXXNPXXY motif in helix VII, which are important for protein stabilization and receptor activation (Ballesteros *et al.,* 2001; Kristiansen, 2004)

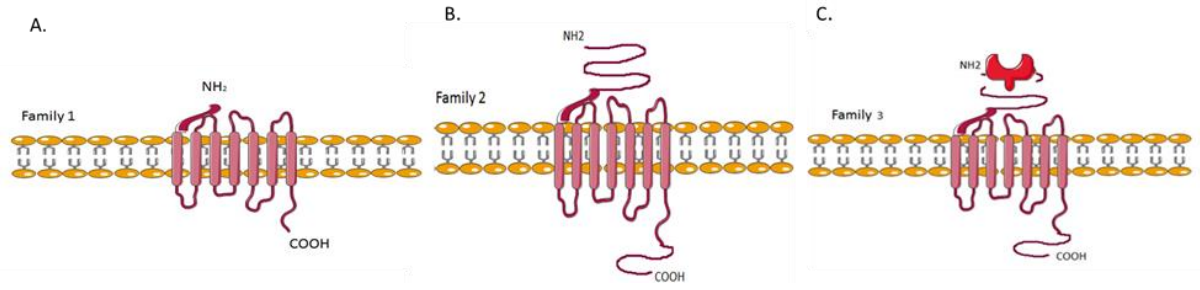

Figure 1.1: Classification of G protein-coupled receptors. Schematic representations of G protein-coupled receptor (GPCR) monomers showing some key structural aspects of the three main families. a) Class A or the rhodopsin-like family, characterized by several highly conserved amino acids and a disulphide bridge that connects the first and second extracellular loops; (b) Class B, characterized by a relatively long amino terminus that contains several cysteines, which form a network of disulphide bridges and c) Class C, characterized by a long amino terminus and carboxyl tail with the ligand binding domain located in the amino terminus, which is often described as being like a 'Venus fly trap' (adapted from George *et al.*, 2002).

1.1.2.2 Class B GPCRS

Class B GPCRs can be subdivided into two families, the secretin family and the adhesion/ Frizzled family.

The Adhesion receptor family/class B GPCRs

According to the GRAFS GPCR classification, the Adhesion family is the second largest GPCR family in humans, with 33 members (Fredriksson *et al.,* 2003). This family is also referred to as the LNB7TM family (Foord *et al.,* 2005), whereby LN stands for long N termini and B for the sequence similarity between the TM regions of Adhesion GPCRs and the secretin receptors (Harmar, 2001; Stacey *et al.,* 2000). The Adhesion family has been categorized as a distinct GPCR family and not as a part of the secretin family of receptors due to their highly variable architecture of the N- terminal domain and the presence of a GPCR proteolytic (GPS) domain that is absent in the secretin receptor family (Fredriksson *et al.,* 2003).

The Adhesion receptors also have conserved cysteine residues in extracellular loops 1 and 2, like the other GPCR families (Harmar, 2001). They are rich in functional domains and most receptors have a long and diverse N- terminus (Bjarnadottir *et al.,* 2004), which is anticipated to be highly glycosylated and form a rigid structure that protrudes from cell surface (Baud *et al.,* 1995). These extracellular regions contain a GPS domain that acts as an intracellular autocatalytic processing site that yields two non-covalently attached sub-units (Krasnoperov *et al.,* 1997). Members of the adhesion family of receptors have N termini that contain adhesion like motifs, such as epidermal growth factor (EGF) and mucin-like repeats, which might mediate cell–cell adhesion (Kristiansen, 2004; Stacey *et al.,* 2000).

The secretin family/class B GPCRs

The secretin family is a small family of GPCRs that all have a large extracellular hormone-binding domain and bind peptide hormones. The 15 members of this family include the calcitonin and calcitonin receptor-like receptors (CALCR, CALCRL); the corticotropin-releasing hormone receptors (CRHR1, CRHR2); the glucagon receptor (GCGR); the gastric inhibitory polypeptide receptor (GIPR); the glucagon-like peptide receptors (GLP-1R, GLP-2R); the growth-hormone-releasing hormone receptor (GHRHR); the adenylate cyclase activating polypeptide receptor (PAC1/ADCYAP1R1); the parathyroid hormone receptors (PTHR1, PTHR2); the secretin receptor (SCTR); and the vasoactive intestinal peptide receptors (VIPR1, VIPR2) (Harmar, 2001; Lagerstrom *et al.,* 2008).

The secretin family receptors contain a globular N-terminal extracellular domain (ECD) defined by three conserved disulfide bonds (Hoare, 2005; Hofmann *et al.,* 2001; Pal *et al.,* 2012) and the common GPCR seven TM domain. The extracellular N terminal domain forms a conserved three layer α-β-β/α fold, also termed as the 'secretin-family recognition fold', that serves as the principle binding site of class B GPCR peptide ligands (Kumar *et al.,* 2011; Runge *et al.,* 2008; Underwood *et al.,* 2010). Binding of the peptide ligand to family B GPCRs is currently described by a two domain model in which the C-terminus of the peptide binds to the N-terminal domain of the receptor with high affinity in an α-helical conformation (Hoare, 2005; Parthier *et al.,* 2009). This acts as an affinity trap, promoting the interaction of N-terminus of the ligand with the lower affinity sites within the TM domain and/or extracellular loops of the receptor, which leads to receptor activation (Dong *et al.,* 2004a; Dong *et al.,* 2004b; Grace *et al.,* 2004; Unson *et al.,* 2002).

The members of this family have been targeted for the treatment of major diseases. This includes glucagon, GLP-1 and GIP receptors for diabetes (Bhavsar *et al.,* 2013; Drucker, 2006; Inzucchi *et al.,* 2008), GLP-2 receptors for short bowel syndromes (Jeppesen, 2006), PTH and calcitonin receptors for osteoporosis (Epstein, 2007; Mulder *et al.,* 2006), pituitary adenylate cyclase-activating peptide (PACAP) receptors for neurodegenerative diseases (Brenneman, 2007; Sherwood *et al.,* 2000), GRF receptors for dwarfism (Campbell *et al.,* 1995), VIP receptors for inflammatory diseases (Brenneman, 2007; Gomariz *et al.,* 2001), CRF receptors for chronic stress, depression and anxiety (Gilligan *et al.,* 2004) and CGRP receptors for migraine (Ho *et al.,* 2010). The structures of the extracellular domains of several members of this family have been solved by X-ray crystallography (Pioszak *et al.,* 2008a; Pioszak *et al.,* 2008b) or by NMR spectroscopy (Grace *et al.,* 2004), and more recently two crystal structures of 7TM domain have been solved (Hollenstein *et al.,* 2013; Siu *et al.,* 2013).

For the remainder of this thesis, Class B GPCRs will refer to the secretin family of Class B GPCRs.

1.1.2.3 Class C GPCRs

Class C GPCRs, also termed the glutamate family of GPCRs (Fredriksson *et al.,* 2003; Kolakowski, 1994), consists of 22 human proteins: eight metabotropic glutamate receptors (GRMs), two γ-amino butyric acid B ($GABA_B$) receptors (also referred to as one receptor with two subunits), the calcium-sensing receptor (CASR), the sweet and umami taste receptors (TAS1R1-3), GPRC6A and seven

orphan receptors (Bjarnadottir *et al.,* 2004). These receptors also perform important physiological functions due to their central and peripheral localization and expression. Class C GPCRs share similar topology to other GPCRs in their TM domain, but they possess a large globular N terminal domain and they exist as obligate homodimers. Most Class C receptors possess nine highly conserved cysteine residues, in what is termed the cysteine rich region (CRR) between the extracellular amino terminaldomain (ATD) and 7TM, however, the CRR is absent in $GABA_B$ receptors (Pin *et al.,* 2004). Class C GPCRS bind their respective endogenous ligand within the unusually large N-terminal region that is comprised of 500-600 residues (Brauner-Osborne *et al.,* 1999; Malitschek *et al.,* 1999; Ohara *et al.,* 1993; Okamoto *et al.,* 1998). Glutamate family receptors have a characteristic 'Venus flytrap' N terminus that is composed of two lobes (one from each protomer) that close around the ligand thereby activating the receptor (Kunishima *et al.,* 2000). To date, two drugs, baclofen and cinacalcet, targeting family C GPCRs are on the market and used clinically (Campbell *et al.,* 1995; Tfelt-Hansen *et al.,* 2005).

1.1.2.4 Class F GPCRs

Class F GPCRs are also known as the frizzled and smoothened receptor**s.** Frizzled receptors represent the cell membrane receptors for a family of secreted glycoprotein ligands termed "Wnts" that play essential roles in development, including cell fate, adhesion, polarity, migration, and proliferation (Malbon, 2004). This group consists of ten frizzled receptors (FZD1–10) and the smoothened receptor (SMO) (Fredriksson *et al.,* 2003). The FZDs bind the family of Wnt glycoproteins (Bhanot *et al.,* 1996), whereas the SMO protein is not directly activated by its endogenous ligand Hedgehog (Murone *et al.,* 1999). The extracellular part of the FZDs range from 200 to 320 amino acids in length with most variations present in the linker region between the TM part and the extracellular ligand binding domain (Wang *et al.,* 1996). The Wnt ligands bind to a cysteine-rich region in the extracellular part of the receptor protein where the positions of nine cysteines are conserved (Dann *et al.,* 2001; Murone *et al.,* 1999).

Taste-2 receptors are also Class F GPCRs and have a short N terminus but share several consensus sequences with other members of the family (Fredriksson *et al.,* 2003). The human genome contains 25 functional *T2R* genes, which are mostly localized in clusters on chromosome 7q31 and 12p13 (Adler *et al.,* 2000; Bufe *et al.,* 2002; Conte *et al.,* 2002; Go *et al.,* 2005; Matsunami *et al.,* 2000; Shi *et al.,* 2003). The T2Rs can be divided into five different subgroups based on phylogenetic analyses, in which

the degree of sequence conservation between the T2R subgroups differs remarkably (20–90%) (Conte *et al.,* 2002). The T2Rs are relatively short GPCR receptor proteins, spanning from 290 to 340 amino acids, intronless and display short N termini and C termini (Adler *et al.,* 2000; Matsunami *et al.,* 2000). They seem to lack the otherwise well-conserved cysteine bridge between two of the extracellular loops.

1.2 GPCR activation: Signalling and Regulation

GPCRs are highly flexible within the membrane and can exist in number of conformational states, ranging from inactive ground state (R) to one or more fully activated states (R*). Ligands and drugs binding to the extracellular surface of the receptor alter the equilibrium between the different conformational states (Kenakin, 2004; Kristiansen, 2004) resulting in the interaction of the receptor with heterotrimetric G proteins.

1.2.1 G proteins and signalling

Heterotrimeric G proteins have a crucial role as molecular switches in signal transduction pathways mediated by GPCRs and can define the specificity and temporal characteristics of the cellular response. They are composed of three subunits, α, β and γ, and their function depends on the ability of the G protein α-subunit (Gα) to cycle between an inactive GDP-bound conformation that is primed for interaction with an activated receptor, and an active GTP-bound conformation that can modulate the activity of downstream effector proteins (Oldham *et al.,* 2008).

In humans, there are 21 Gα subunits encoded by 16 genes, 6 Gβ subunits encoded by 5 genes, and 12 Gγ subunits (Downes *et al.,* 1999). Heterotrimers are typically divided into four main classes based on the primary sequence similarity of the Gα subunit: Gαs, Gαi, Gαq and Gα12 (Simon *et al.,* 1991; Wettschureck *et al.,* 2005). The structures of Gα subunits reveal a conserved protein fold that is composed of a GTPase domain and a helical domain. The GTPase domain is conserved in all the members of the G protein superfamily. This domain hydrolyses GTP and provides binding surfaces for the Gβγ dimer, GPCRs and effector proteins (Lambright *et al.,* 1994; Noel *et al.,* 1993). The helical domain is unique to Gα proteins and is composed of a six α-helix bundle that forms a lid over the nucleotide binding pocket. Post-translational modifications of Gα subunits regulate membrane localization and protein-protein interactions (Chen *et al.,* 2001; Smotrys *et al.,* 2004).

The interaction of agonists with GPCRs induces conformational modifications in the receptor that results in their interaction with the heterotrimetric G proteins. This interaction results in the exchange of GDP for GTP bound to the Gα-subunit that leads to the dissociation of Gα from the dimeric Gβγ subunits (Bourne *et al.,* 1991). Consequently, the Gα- and Gβγ-subunits stimulate downstream effector molecules, which include adenylyl and guanylyl cyclases, phosphodiesterases, phospholipase A_2 (PLA_2), phospholipase C (PLC) and phosphoinositide-3-kinases (PI3Ks). This results in activation or inhibition of the production of a variety of second messengers such as cAMP, cGMP, diacylglycerol, inositol (1,4,5)-trisphosphate [Ins(1,4,5)P_3], phosphatidyl inositol (3,4,5)-trisphosphate [PtdIns(3,4,5)P_3], arachidonic acid and phosphatidic acid, in addition to promoting increases in the intracellular concentration of Ca^{2+} and the opening or closing of a variety of ion channels (Marinissen *et al.,* 2001). The particular pathwyas activated/inhibited depend on the subtype of G protein that couples to the particular GPCR being avtivated (Figure 1.2). G protein activation is terminated by the hydrolysis of GTP to GDP by the intrinsic GTPase activity of the α-subunit. Once GTP is cleaved to GDP, α and βγ subunits re-associate and become inactive, thereby terminating G protein dependent signalling.

1.2.2 Regulation of GPCRs and G protein mediated signals

In addition to interacting with G proteins, agonist bound GPCRs associate with GPCR kinases (GRKs), leading to receptor phosphorylation and β-arrestin recruitment, resulting in the inactivation, internalization, trafficking and signalling of transmembrane receptors (Alvarej *et al.,* 2008). GRKs are a family of seven related kinases (GRK1–GRK7) that have differential patterns of distribution across tissues and distinct preferences for binding to certain receptors (Reiter and Lefkowitz, 2006; Premont and Gainetdinov, 2007). GRKs are comprised of three functional domains, an amino-terminal regulator of G protein signalling (RGS) homology (RH) domain, a central catalytic domain and carboxyl-terminal membrane targeting domain. GRKs are targeted to the plasma membrane through multiple mechanisms to phosphorylate serine and threonine residues within the third intracellular loop and carboxyl-terminal tail domains of agonist-activated receptors (Koch *et al.,* 1993; Touhara *et al.,* 1994; Pitcher *et al.,* 1995). GRKs regulate GPCR desensitization by both phosphorylation-dependent and -independent mechanisms (Dhami and Ferguson, 2006; Ferguson, 2007).

A common outcome of GPCR phosphorylation by GRKs is a decrease in GPCR interactions with G proteins and an increase in GPCR interactions with arrestins (members of a family of four closely

related scaffold proteins). The interaction of GPCRs with arrestins further inhibits GPCR signalling through G proteins and simultaneously turns on other signalling pathways that are initiated by the arrestin-mediated recruitment of signalling proteins to activated GPCRs. Thus, G protein-mediated signalling by agonist-activated GPCRs can be terminated through GPCR phosphorylation by GPCR kinases (GRKs) (Lefkowitz, 1998) and concomitant GPCR association with arrestins. Arrestins can interact with clathrin and the clathrin adaptor AP2 to drive GPCR internalization into endosomes (Goodman *et al.,* 1996; Reiter and Lefkowitz, 2006; Moore *et al.,* 2007). GPCR internalization regulates the functional process of receptor desensitization. Following internalization after association with arrestins, GPCRs can be trafficked to lysosomes, where they are ultimately degraded, or to recycling endosomes for recycling back to the cell surface in the functional process of resensitization, whereby the cell is resensitized for another round of signalling.

Both β-arrestin1 and β-arrestin2 specifically bind to the clathrin heavy chain and the β2-adaptin subunit of the heterotetrameric adaptor complex to facilitate endocytosis (Goodman *et al.,* 1996; Laporte *et al.,* 1998). In addition, Src-mediated phosphorylation of β2-adaptin regulates the dissociation of the β2-adaptin/β-arrestin complex (Zimmerman *et al.,* 2009). The β-arrestin domain involved in clathrin binding is localized to amino acid residues 373–377 in the carboxyl-terminus of β-arrestin2 (Krupnick *et al.,* 1997). β-arrestins can also interact with a variety of other protein complexes that have been implicated in the regulation of clathrin-mediated endocytosis including E3 ubiqitin ligases such as mdm2 (Shenoy *et al.,* 2001). Thus, β-arrestins play an essential role in recruiting proteins that are not only essential for the internalization of GPCRs but also for the regulation of the endocytic machinery.

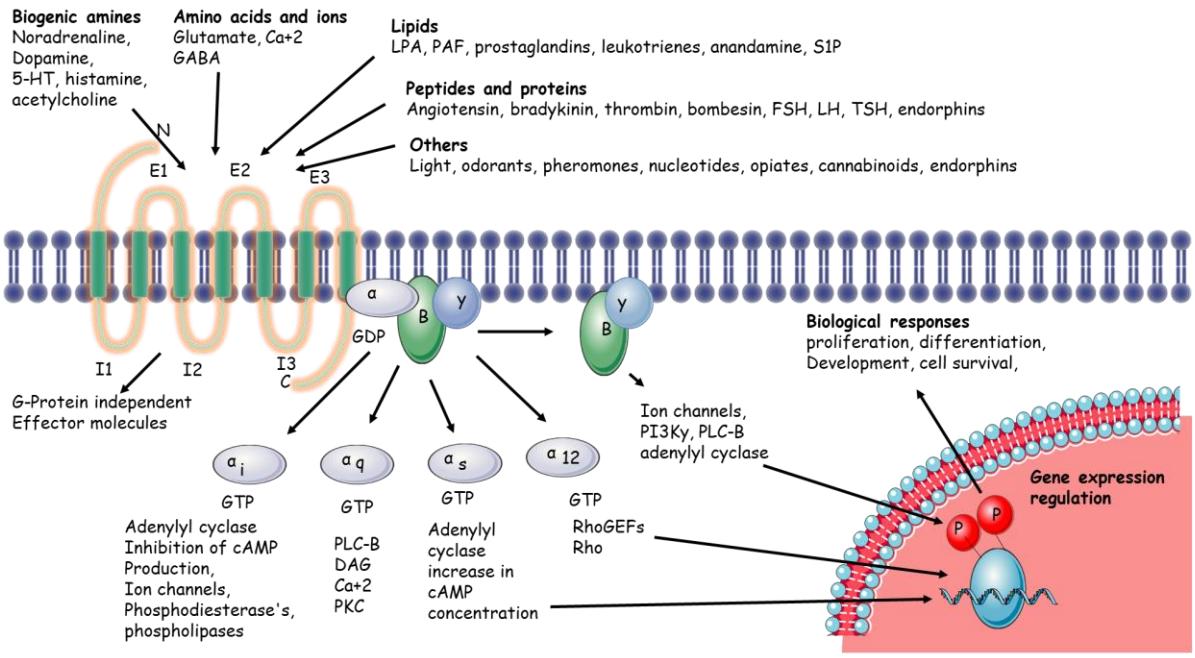

Figure 1.2: Diversity of G protein-coupled receptors (GPCRs) signalling. Various ligands/stimuli including biogenic amines, amino acids, ions, lipids, peptides and proteins, bind to GPCRs and stimulate cytoplasmic and nuclear targets through heterotrimeric G protein-dependent and -independent pathways. Activation of distinct Gα protein subunits results in activation of specific downstream signalling cascade. Consequently, activated downstream signalling pathways regulate key biological functions such as cell proliferation, cell survival and angiogenesis (adapted from Marinissen and Gutkind 2001).

Abbreviations: DAG, diacylglycerol; FSH, follicle-stimulating hormone; GEF, guanine nucleotide exchange factor; LH, leuteinizing hormone; LPA, lysophosphatidic acid; PAF, plateletactivating factor; PI3K, phosphoinositide 3-kinase; PKC, protein kinase C; PLC, phospholipase C; S1P, sphingosine-1-phosphate; TSH, thyroid-stimulating hormone.

1.2.3 G protein-independent signalling

Recent evidence shows that activation of GPCRs can lead to biochemical responses that are not mediated by heterotrimeric G proteins, thereby overcoming the dogma of canonical G protein-mediated signalling. It is now being recognized that GPCRs can transmit signals to effectors in a G protein-independent manner (Abdulla *et al.,* 1997; Heuss *et al.,* 1999; Quoyer *et al.,* 2010; Sonoda *et al.,* 2008) by interacting with a myriad of proteins (Becamel *et al.,* 2001; Hall *et al.,* 1998; Hu *et al.,* 2000; Tu *et al.,* 1999) such as cytoplasmic scaffolding proteins, and direct interactions with effectors, thereby promoting protein-to-protein interactions (Liu *et al.,* 2000; Stacey *et al.,* 2000). Thus the variety of cellular responses mediated by GPCRs is not the result from a single biochemical route but an integration of the functional activity of multiple intricate networks of intracellular signalling pathways. Some GPCRs are able to mediate intra-cellular signalling through other transducers apart from heterotrimeric G proteins, including PDZ-containing proteins and non-PDZ scaffolding proteins like β-arrestin, A-kinases of anchor proteins (AKAPs), Homer proteins, proteins containing Src homology 2 (SH2) and Src homology 3 (SH3) (Fisyunov, 2012; Hall *et al.,* 2002).

Scaffold proteins are capable of binding with two or more partners, resulting in an increase in the efficacy and/or specificity of intracellular signalling pathways. The three most widely accepted modes of interaction of GPCRs with scaffold proteins include (a) binding of a PDZ scaffold protein with a distal part of the C terminus; (b) interaction of non-PDZ scaffolding proteins to proximal regions of the C terminus and (c) association of β-arrestin and other scaffold proteins with C-terminus and/or the third intracellular loop of GPCRs (Fisyunov, 2012). Mechanistically, the scaffolding proteins convey information from the receptor to the effector molecule either by physically binding to the receptor or through an indirect mechanism via which they are involved in the transduction of the signal. Furthermore, they can play a role in regulating receptor localization and transportation and act as allosteric modulators, resulting in varied pharmacological characteristics and/or functions of the receptors (Fisyunov, 2012).

Many GPCRs such as serotonergic receptors (5HT2) (Ullmer *et al.,* 1998), metabotropic glutamate receptors (Boudin *et al.,* 2001; Tu *et al.,* 1999), β2 adrenoceptors (Weinman *et al.,* 2000), α-adrenergic receptors (Raman *et al.,* 1996) contain a PDZ binding motif at their C-terminus enabling PDZ proteins to associate and scaffold multi-protein complexes, which can modulate different receptor properties such as trafficking, signalling, receptor stability and cell distribution. Two different A-kinases of

anchor proteins (AKAPs), AKAP250 (gravin) and AKAP79 have been known to interact with β-adrenoreceptors thereby promoting their interactions with protein kinase A (PKA), PKC, phosphatases (PPs) (Colledge *et al.,* 1999; Shih *et al.,* 1999). Apart from this, other non-PDZ scaffolding proteins like homer proteins can promote the interaction between metabotropic receptors (mGluR1 and mGluR5) and other intracellular effector proteins, such as syntaxin 13 (Minakami *et al.,* 2000), Shank proteins (Tu *et al.,* 1999), and inositol trisphosphate (IP3) receptors (Tu *et al.,* 1998). Furthermore, tyrosine Janus kinase (Jak) has been reported to serve as a scaffold protein by directly interacting with angiotensin receptor 1 (AT1) (Ali *et al.,* 2000; Ali *et al.,* 1997), resulting in phosphorylation of the transcriptional factor STAT1, leading to the formation of a complex consisting of receptor AT1, Jak2, and factor STAT1 (Ali *et al.,* 2000; Sayeski *et al.,* 2001).

GPCR stimulation and subsequent phosphorylation of C-terminal serine/threonine residues by G protein-coupled receptor kinases (GRKs) relay the primary steps in the induction of G protein–independent signalling by inducing the recruitment of β-arrestins. GRKs and β-arrestins, classically regarded as terminators of G protein signalling, (Lefkowitz, 1998; Leftowitz *et al.,* 2005), have emerged as G protein-independent transducers, that are able to promote signalling independent of G protein activation. β-arrestins act as multifunctional scaffolding protein that play critical roles in GPCR signalling (Luttrell, 2008; Rajagopal *et al.,* 2010; Reiter *et al.,* 2006) by interacting with many protein partners such as small GTPases, guanine nucleotide exchange factors, E3 ubiquitin ligases, phosphodiesterases and transcription factors (Xiao *et al.,* 2007) and a wide variety of protein kinases, thereby leading to phosphorylation of numerous intracellular targets (Xiao *et al.,* 2010). Initial studies demonstrated that these adaptor proteins interacted with Src family kinases via a polyproline motif and couple the receptor to MAPK pathways (Luttrell *et al.,* 1999; Luttrell *et al.,* 2001; Miller *et al.,* 2000). β-arrestin mediated signalling mechanisms also include RhoA-dependent stress fiber formation (Barnes *et al.,* 2005), inhibition of nuclear factor κB (NFκB)-targeted gene expression through IκB stabilization (Witherow *et al.,* 2004), protein phosphatase mediated dephosphorylation of Akt, resulting in activation of glycogen synthase kinase 3 and dopaminergic behavior (Beaulieu *et al.,* 2005), extracellular-signal regulated kinase (ERK)-dependent induction of protein translation (Dewire *et al.,* 2008) and anti-apoptotic effects (Ahn *et al.,* 2009; Quoyer *et al.,* 2010). β-arrestin recruitment mediates activation of MAPK and ERK1/2 signalling at many GPCRs such as vasopressin V_2 receptor (V_2R) (Charest *et al.,* 2007; Ren *et al.,* 2005), GLP-1R (Sonoda *et al.,* 2008), angiotensin type 1a receptor (Kim *et al.,* 2005b), β2 adrenergic receptor (Shenoy *et al.,* 2006) and FSH-R (Kara *et al.,* 2006).

1.2.4 GPCRs and Biased-Signalling

Historically, efficacy at GPCRs was considered to be linear, such that the downstream events of a given proximal receptor activation event was considered to be linked sequentially, thereby predicting that any differences in the agonist efficacy was due to the differential strength of coupling and the location along the signalling pathway where agonist activity is sampled. More recently, the signalling from GPCRs has been described as pluridimensional with the efficacy of the ligand being collateral instead of linear (Kenakin, 2007). GPCRs are pleiotropically coupled receptors that, on activation, possess the ability to signal via multiple different effectors that can be G protein-dependent and independent. Distinct ligands acting at the same GPCRs have the ability to differentially activate these signalling effectors. The ability of different ligands to engender discrete signalling activities at a given GPCR has been termed biased signalling, stimulus trafficking, stimulus bias, collateral efficacy, biased agonism or functional selectivity (Kenakin and Miller, 2010; Leach 2007). This is accomplished by engendering unique ensembles of receptor conformations that can give rise to discrete signalling profiles (Kenakin 2011). This behavior can be observed through differences in the activation of second messengers and also through the changes as to how receptors are desensitized and downregulated. A common indicator of stimulus bias is the reversal of potency order or maximal effects for different agonists at a given receptor, when they are examined across alternative signalling pathways (Figure 1.3). Stimulus bias can also be predicted, if potency or efficacy preferences of a test agonist do not match with the endogenous agonist across different pathways (Gregory 2010; Koole 2010).

The first clear demonstration of signalling bias was shown for the PAC1R, where the agonist PACAP(1-38) stimulated cAMP with greater potency than the agonist PACAP(1-27), conversely PACAP(1-38) was more potent for inositol phosphate (IP) stimulation than PACAP(1-27) *(Spengler et al.,* 1993). Other examples include, the neurokinin 1 receptor (NK-1R), where the agonists [Pro9]substance-P and septide display similar potencies for IP hydrolysis, but [Pro9]substance-P potently stimulates cAMP, whereas septide induces only weak coupling to cAMP (Sagan *et al.,* 1996); the serotonin 5HT receptor, where the agonist (6)-1-(2,5-dimethoxy-4- iodophenyl)-2-aminopropane (DOI) favors PLC-mediated IP accumulation with low efficacy for phospholipase A2-mediated arachidonic acid (AA) release, whereas quipazine has low efficacy in IP accumulation and high efficacy in AA release (Berg *et al.,* 1998); the PTH1R, where PTH(1-34) activates both PKA downstream of cAMP and PKC downstream of IP, whereas PTH(1-31) solely activates PKA, and PTH(3-38) solely activates PKC (Luttrell and Kenakin, 2011). Furthermore, biased signalling has also

been identified at the μ-opioid receptor (Keith *et al.,* 1996), DAR (Urban *et al.,* 2007), V2 vasopressin receptor (V2R) (Barak *et al.,* 2001), cannabinoid receptors (Georgieva *et al.,* 2008) and GLP-1R (Koole *et al.,* 2010), among others. In particular, there is now extensive evidence indicating that GPCR activation by ligands can selectively promote G protein versus β-arrestin mediated signalling pathways by facilitating the formation of distinct receptor conformational states required for receptor association with either heterotrimeric G proteins or β-arrestins (Gesty-Palmer *et al.,* 2008; Rajagopal *et al.,* 2010). Examples of reeptors where ligands have been identified that induce β-arrestin biased signalling include the β2AR (Azzi *et al.,* 2003; Drake *et al.,* 2008), AT1aR (Wei *et al.,* 2003), V2R (Azzi *et al.,* 2003) and PTH1R (Gesty-Palmer *et al.,* 2009; Rominger *et al.,* 2014).

Observations of biased signalling at GPCRs have led to speculation that the optimal mix of efficacies for different signalling pathways will determine the ultimate clinical efficacy of therapeutics. This is demonstrated by examples in literature of ligands with positive therapeutic effects that predominantly activate β-arrestin-mediated signalling pathways and where unwanted side effect profiles are associated with activation of G protein mediated signalling at the same GPCR (or vice versa). For example, the β-blocker carvedilol acts as β-arrestin-biased ligand at both β1-adrenergic receptor (β1AR) and β2AR subtypes and provides cardioprotective effects. In contrast, β-AR-mediated activation of G protein-dependent signalling (Gαs coupling) has been reported to be cardiotoxic (Zhang *et al.,* 2013). In addition, for many years it was not understood why some β-blockers were more effective therapeutics than others as all had the ability to block receptor mediated activation of G proteins. For example, carvedilol, possess superior efficacy in the treatment of heart failure, compared to other β-blockers. This ligand, like all β-blockers, was observed to be an inverse agonist for cAMP production, but unlike the other β-blockers displayed positive agonism for β-arrestin mediated ERK1/2 phosphorylation (Weiser *et al.,* 2007). This suggests that ultimate clinical efficacy of a molecule can be determined by developing a correct blend of collateral efficacies, therefore suggesting that in drug discovery and optimization, ligands should be screened in multiple functional endpoints, rather than just a single assay. In addition, biased ligands that can selectively influence beneficial signalling pathways at the expense of pathways that lead to significant side effects may have a high therapeutic potential as drug candidates. The challenge, however, for most receptor systems is an understanding of signalling pathways that lead to beneficial and undesirable therapeutic effects and the ideal mix of efficacies for the best therapeutic outcome.

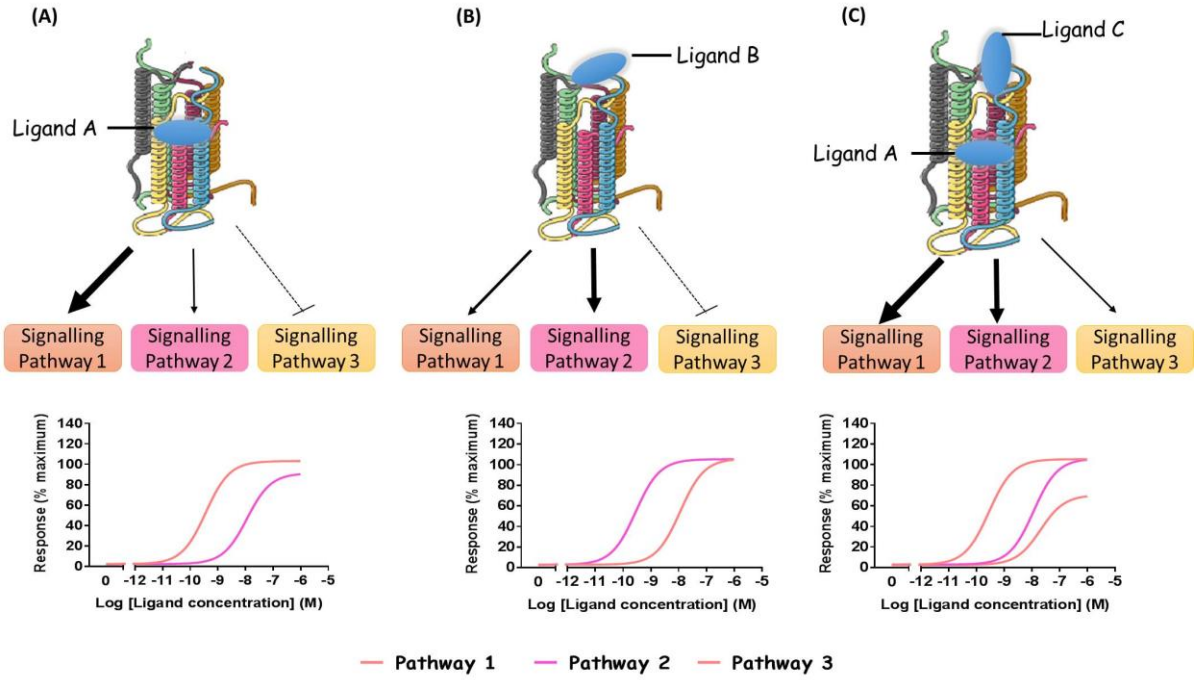

Figure 1.3: Identification of signalling bias in pharmacological assays. Signalling bias describes the ability of different ligands binding at the same receptor to activate unique combinations of various signalling pathways. A common indicator of signalling bias is a reversal in the rank order of potency or efficacy (that is, the maximal agonist effect) of distinct agonists when they are examined across different signalling pathways. (A) Ligand A has high potency and full agonist activity at signalling pathway 1, a lower potency and weaker agonist effects at signalling pathway 2, and no signalling at signalling pathway 3; (B) Ligand B binds to a topographically distinct site to ligand A and has a reverse profile whereby it has a higher potency for signalling pathway 1 than for signalling pathway 2. The reversal of potency between these two ligands in pathways 1 and 2 is a clear indicator of biased aginism. (C) Although an orthosteric ligand bound to a receptor on its own may preferentially signal to a particular subset of pathways, the co-binding of an allosteric modulator can differentially alter the signalling bias of the receptor. When ligand C is co-bound with ligand A, it potentiates a stimulus through signalling pathway 2 and signalling pathway 3, but negatively affects signalling pathway 1, as evidenced by a switch in the potency and maximal response between signalling pathway 2 and signalling pathway 3 compared with signalling pathway 1 (adapted from Wootten *et al.*, 2013).

Therefore, there is an interplay between allosteric modulation and biased signalling, where an allosteric ligand can alter the signalling profile of the orthosteric ligand in a pathway-dependent manner.

1.3 Allosteric modulation of GPCRs

1.3.1 Introduction to GPCR allostery

Targeting allosteric sites on GPCRs has emerged as an attractive approach for drug discovery. Moreover, the use of functional assays for screening has accelerated the discovery of allosteric compounds that have the potential of being developed either as a therapeutics or drug discovery research tools. According to the IUPHAR nomenclature recommendations, the orthosteric ligand binding site is the site occupied by the endogenous agonist, whereas, the allosteric site is defined as any domain on the GPCR that is topographically distinct from the orthosteric site, such that GPCRs can concomitantly bind both orthosteric and allosteric ligands (Neubig *et al.,* 2003).

As ligands can simultaneously bind to two (or more) topographically distinct sites on the same receptor complex, the binding to one site can change the nature and extent of binding (or signalling) at the other site; this is referred to as an allosteric interaction (Neubig *et al.,* 2003; Monod *et al.,* 1963, Christopolous 2002). These allosteric interactions are reciprocal in nature i.e. binding of one ligand to its site affects the binding of the second ligand at the other site and vice-versa. Allosteric agonists bind to allosteric sites to activate downstream signalling cascades, whereas allosteric modulators are ligands that bind to GPCRs at an allosteric site and promote a conformational change that modulates orthosteric ligand affinity and/or efficacy (Kenakin amd Miller 2010; Conn, 2009) (Figure 1.4). They are classified as positive modulators (PAM) and negative modulators (NAM), based on their mechanism of action to either enhance or inhibit the binding/efficacy of orthosteric ligands respectively. In addition, some allosteric ligands may possess both agonist and modulatory properties.

1.3.2 Therapeutic advantages of allosteric modulation

Allosteric modulators that do not display agonism on their own, have the ability to fine tune the effect of orthosteric ligands, thus maintaining spatial and temporal characteristics of endogenous signalling. In addition, these compounds have the potential to achieve subtype selectivity due to lack of sequence conservation amongst the allosteric binding sites when compared to orthosteric sites of related GPCRs that are often highly conserved. Moreover, these modulators exhibit saturability in their effect, that is, there is a limit to the allosteric effect where no further modulation of orthosteric ligand would be

observed in presence of increasing concentrations of the allosteric ligand. Saturability of allosteric effects applies to both positive and negative allosteric modulators and therefore is useful for the drug candidates that are aimed at either enhancing or antagonizing receptor-mediated effects. The modulators can be administered in relatively high doses without fear of overstimulating or overinhibiting the system. Thus, there is ceiling to the effects of an allosteric modulators that is retained even with the excessive doses, therefore providing mechanistic safety in cases of overdose if allosteric compounds are used as therapeutics (Christopolous 2002), at least with respect to on-target activity.

Furthermore, exploitation of allosteric sites on GPCRs provides means by which important issues associated with difficulty in discovering small molecule ligands of certain GPCRs can be overcome. In particular, for GPCRs in which the orthosteric site is highly conserved between subtypes (Kenakin and Miller 2010; Conn 2009). Additionally, these compounds are attractive tools to target GPCRs that possess diffuse and/or poorly druggable orthosteric sites, such as in the Class B and Class C GPCRs (Kenakin and Miller, 2010; Wootten *et al.,* 2013).

Recently, another class of ligand called bitopic or dualsteric has emerged that are hybrid molecules, possessing both an orthosteric and allosteric pharmacophore in one ligand. These ligands offer the potential of achieving selectivity by virtue of targeting less conserved allosteric regions on GPCRs, while ensuring activation via concomitant interaction with the orthosteric site (Mohr, 2010; Valant, 2009; Dasingrini 2006).

1.3.3 Differential effects of allosteric ligands on orthosteric affinity vs efficacy

The ability of an allosteric ligand to modulate the affinity of an orthosteric ligand does not necessarily correlate with effects of the modulator on orthosteric ligand efficacy and vice versa. Thus a modulator can have opposite effects on orthosteric ligand binding relative to function. This can be exemplified with the allosteric modulator at CB1 receptor, Org27569, which when tested against orthosteric ligand binding and function, was observed to be a positive modulator of agonist affinity but was a negative modulator of agonist signalling efficacy in both recombinant and native tissue bioassays (Price *et al.,* 2005).

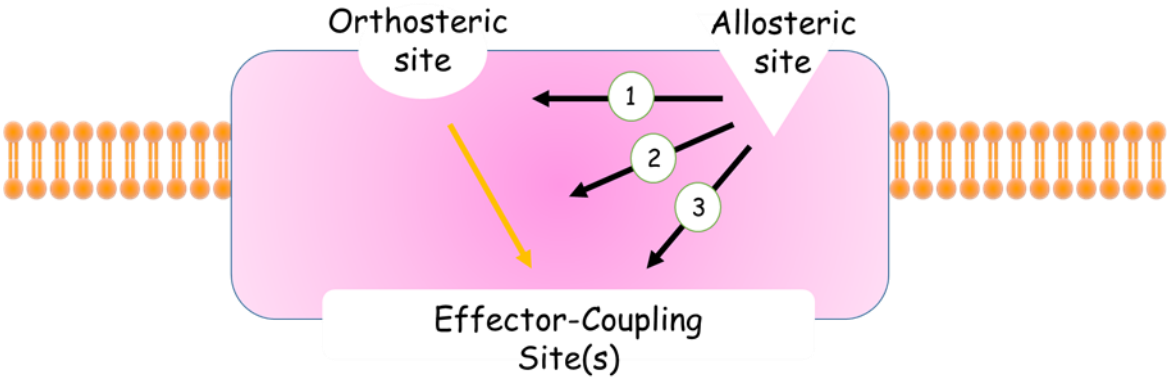

Figure 1.4: Schematic representation of allosteric actions. Allosteric ligands, binding at a site distinct to that of the orthosteric site, can affect receptor function in three general ways (1) Allosteric modulation of orthosteric-ligand binding affinity (2) Allosteric modulation of orthosteric ligand efficacy (3) Direct allosteric agonism (adapted from Langmead and Christopolous, 2006).

1.3.4 Probe dependence and allosteric modulation

Probe-dependence highlights the fact that the extent and direction of an allosteric interaction can vary with the nature of the orthosteric ligand used as a probe of receptor function (Kenakin, 2005). The phenomemon of probe-dependence highlights the requirement for careful consideration in the choice of orthosteric ligands to assess the effects of an allosteric modulator (Kenakin, 2008; Leach *et al.,* 2007). Ideally, the choice of orthosteric probe would be dictated by the endogenous agonist for a given receptor. However, some GPCRs have more than one endogenous agonist and selective focus on one of these endogenous ligands, at the exclusion of others can lead to substantial compound misclassification, if probe dependence is evident in these systems.

Probe dependence is clearly illustrated at the human M4 muscarinic acetylcholine (mACh) receptor, whereby the allosteric ligand, 3-amino-5-chloro-6-methoxy-4-methyl-thieno(2,3-b)pyridine-2-carboxylic acid cyclopropylamide (LY2033298), positively modulates the binding affinity of the endogenous orthosteric agonist ACh, but not the binding affinity of the orthosteric antagonists, [^{3}H]-N-methylscopolamine (NMS) and [^{3}H]-quinuclidinyl benzilate (QNB) (Leach *et al.,* 2010). In another example, LY2033298 demonstrated a robust potentiation of ACh and oxotremorine, but not xanomeline in ERK1/2 signalling (Suratman *et al.,* 2011) at the mouse M4 mACh receptor. In the same study, LY2033298 potentiated oxotremorine but not ACh in glycogen synthase kinase (GSK)-3β activity (Suratman *et al.,* 2011). In addition, LY2033298 also displays probe dependence at the M2 mACh receptor, examples of which include differential modulation in pERK1/2, whereby LY2033298 positively modulates oxotremorine, negatively modulates pilocarpine and xanomeline, but does not clearly modulate ACh signalling (Valant *et al.,* 2011).

Probe-dependence could affect both the therapeutic application and the mode of discovery of allosteric modulators. The ability of allosteric ligands to have differential probe-dependence across multiple receptor subtypes (even if these receptor subtypes bind to the same allosteric and orthosteric ligand pairs) is an additional consideration that can have major implications on the screening process so as to achieve a robust target validation. Careful consideration when pharmacologically characterizing allosteric ligands also applies to receptors possessing multiple endogenous ligands. When all endogenous ligands for a given GPCR exert similar physiological profiles, probe-dependence provides several opportunities for the identification of novel therapeutics. Moreover, screening against alternative endogenous ligands such as metabolites of ligands (Wootten et al, 2012), even if they have

lower affinity or efficacy, may yield novel chemical leads that might not be identified if screening for co-operative effects is only performed using the primary endogenous ligand.

1.3.5 The interplay of allosteric modulation, probe dependence and biased signalling

Allosteric modulation of GPCRs and biased signalling are described as separate phenomena, but both arise from ligand-specific conformational changes in the GPCR. Just as the binding of an orthosteric agonist can give rise to distinct conformational changes that can lead to biased signalling, allosteric ligands can also give rise to a distinct signalling profile compared to an orthosteric ligand. In addition, the co-binding of an orthosteric and allosteric ligand simultaneously can stabilize distinct conformational states of the GPCR compared to the binding of one ligand alone. A consequence is that some pathways may be selectively modulated (either positively or negatively) at the expense of others (Figure 1.3). The most extreme situation of this is where the allosteric effect is in opposite directions for two different pathways (ie. positive in one and negative in the other). For example, gadolinium is an allosteric modulator of $mGluR_{1\alpha}$ where it potentiates glutamate-mediated calcium mobilization ($G_{q/11}$-protein linked pathway) and inhibits glutamate-mediated cAMP pathway (G_s-protein linked pathway) (Abe *et al.,* 2003, Tateyama and Kubo 2006.). However, on its own, gadolinium can selectively trigger calcium mobilization via $G_{q/11}$-protein linked pathway, while having no effect on the G_s-protein linked pathway, thus demonstrating true stimulus bias (Tateyama and Kubo, 2006).

The interplay of the probe-dependent nature of allosteric ligands and stimulus bias adds a further level of complexity as this can lead to a situation where the stimulus imparted by one orthosteric ligand in the presence of an allosteric ligand, may be different to the stimulus of a second orthosteric ligand in the presence of the same allosteric ligand (even if the signalling profile of the two orthosteric ligands on their own are similar) (Knudsen *et al.,* 2007; Sloop *et al.,* 2010; Koole *et al.,* 2010; Wootten *et al.,* 2011). This is particularly relevant when there are multiple endogenous ligands for one receptor, or where the othosteric ligand used in screening is not the endogenous ligand.

1.3.6 The challenges of identifying allosteric ligands in vitro and their application therapeutically

The potential therapeutic advantages of allosteric ligands as drugs are well accepted, but have yet to be widely realized in practice because the clinical translation of such compounds is still in its early days. The ever-expanding portfolio of complex behaviours ascribed to allosteric ligands including probe dependence and biased signalling also presents both challenges opportunities to preclinical lead

discovery, validation and optimization. To date, only two allosteric ligands have been approved as therapeutics: cinacalcet (Sensipar; Amgen), which is a positive allosteric modulator of the calcium-sensing receptor (Block *et al.,* 2004; Brown, 2007); and maraviroc (Selzentry/ Celsentri; Pfizer), which is a negative allosteric modulator of CCR5 (Fatkenheuer *et al.,* 2005; Wood and Armour, 2005). Thus, there are substantial challenges in the design and identification of allosteric ligands that fulfil their desired effect in vitro that can subsequently be translatable to in vivo settings.

The principal approach that is currently used to identify allosteric modulators is high-throughput functional screening (HTS), which generally involves one signalling output and assesses effects in the presence of one orthosteric ligand (usually the most physiologically relevant endogenous ligand). However, this approach has proven to be successful in the past (for example, for identifying ligands of the calcium-sensing receptor and of CCR5), it suffers from various limitations inclusive of inability to take into consideration pleiotropically coupled GPCRs, the potential for biased signalling the possibility of probe-dependent effects (which is particularly important for receptor systems that have multiple endogenous ligands) or ligands that are rapidly metabolized. Ideally, all of these concepts should be taken into account when screening for novel compounds (reviewed in Wootten *et al.,* 2013).

Practically, screening programs would take into accovunt only one pathway for the primary screens but it is important to make sure that there is a clear link between the chosen signalling pathway and at least one of the main therapeutic goals. Likewise, it is important that a parallel assessment of alternative signalling pathways is undertaken at a relatively early stage of candidate selection. Furthermore, investigating and targeting alternative endogenous ligand (such as oxyntomodulin that possess low affinity for GLP-1R compared to GLP-1) or the metabolic products that were initially considered inert (Wootten *et al.,* 2012), would help explore the maximum potential for the chemical space and identifying alternative candidates and/or chemotypes that could underpin a drug discovery and development programme.

Moreover, it is even important to test the allosteric modulator screening hits in primary tissues or other physiologically relevant systems natively expressing receptor of interest. This is because of the effect mediated by cellular milieu, the level of endogenous receptor expression and the disease state on the therapeutic goal. The level of information attained by this approach would be physio(patho)logically more relevant compared to artificial recombinant system, however, the challenges of working with

physiological levels of receptor expression would include development and identification of functional assays sensitive enough to provide an acceptable signal window (as these would not ususally be as large or reproducible compared with those obtained in cell lines over-expressing GPCRs in recombinant systems) and optimization of counter-screening methods for confirming receptor specificity under such HTS conditions (Burford *et al.,* 2011).

Drug discovery at these tractable targets is considerably challenging because for many GPCR targets, the required spectrum of signalling needed to attain optimal therapeutic benefit is currently unknown, which limits the rational selection of both allosteric and orthosteric drug candidates. As the field acquires greater knowledge on these concepts, it will be increasingly important to perform an extensive pharmacological profile of ligands to enable the exploration of biased signalling and probe dependence. These types of studies will facilitate the effective translation of in vitro findings into preclinical models and eventually into clinical trials. The increasing number of GPCR crystal structures will also yield information that may aid in the rational design of allosteric ligands. The pursuit of crystal structures in the presence of different agonists (both orthosteric and allosteric) and different effector proteins, if successful, may allow the rational design not only of ligands that target allosteric sites but also of potentially probe-dependent biased allosteric modulators (Wootten *et al.,* 2013; Burford *et al.,* 2011).

1.4 Pharmacological models and quantification of biased signalling and allosterism

1.4.1 Measuring biased signalling

The concept of "stimulus bias" is revolutionizing receptor biology and drug discovery by providing a means of selectively targeting receptor signalling pathways that have therapeutic impact and help in identification and development of novel biased ligands as therapeutics. Many complementary computational approaches are present for the quantification of ligand bias that have been compared by Rajagopal *et al.,* 2011. The first approach referred to as "equimolar comparison" is a qualitative method where data for a single ligand is collected in two different assays. The responses of these two different assays at the same concentration are then plotted against each other thus generating a curve (bias plot), which is a direct comparison of the signalling through the two different pathways. Thus, to identify biased ligands using this method, the shape of the equimolar curve for the test ligand must be qualitatively compared with that of the reference ligand (Gregory *et al.,* 2010; Rajagopal *et al.,* 2011). The weakness associated with this method is that it is unable to identify weakly biased ligands, when

assays with markedly different levels of amplification are compared, and, it is unable to quantify bias. The second approach cited as "equiactive comparison" between two different assays for a ligand is a quantitative process. In this approach, the comparison can be performed by working out the intrinsic relative activities using maximal effects and potencies for each of the two pathways; extrapolated from individual fits of each concentration-response curve (CRC) (Figueroa *et al.,* 2009). A "bias factor" is calculated as the logarithmic of the ratio of intrinsic relative activities for a ligand at two different assays compared with a reference agonist. This bias factor can be an estimate for molecular efficacy of pathway 1 versus pathway 2 on logarithmic scale (a bias factor of 1 between two pathways means that ligand is 10 times better at generating the active receptor conformation for one pathway over the other pathway compared with reference agonist (Figueroa *et al.,* 2009; Rajagopal *et al.,* 2011). Though this method allows quantification of bias, the resulting bias factors are prone to error with partial agonists or strongly biased compounds because of the poor fits of concentration response data with weak signal to noise levels. The third approach includes the use of the operational model of Black and Leff (1983), which allows the calculation of coupling efficiency (τ) to each of the downstream signalling pathway (Evans *et al.,* 2011; Kenakin and Miller, 2010). Calculation of coupling efficiency requires separate binding experiments so as to identify the dissociation constant of the ligand for the receptor (McPherson *et al.,* 2010). Comparison of these coupling efficiencies to that of the reference compounds results in calculation of effective signalling (σ) by a ligand in each assay. Further, bias factors can be calculated by comparing the effective signalling between different pathways, thereby allowing the identification of biased ligands (Rajagopal *et al.,* 2011). Additional information required from a separate ligand binding experiment, constrains the fits and yields a better assessment of bias along with the estimation of efficacy, thus making operational model the best approach, nonetheless, this method requires equivalent functional K_As, which is not always the case (Christopoulos and Kenakin, 2002). A better and improved method, derives, transduction ratios (τ/K_A) (K_A = dissociation constant), derived directly from fitting the operational model to concentration-response data that can be used to calculate ligand bias (Figueroa *et al.,* 2009; Kenakin and Miller 2010; Koole *et al.,* 2010). By including the natural/reference ligand in the analysis, this method simultaneously nullifies the impact of cell background and natural bias (bias associated with binding of natural ligand to the receptor thus yielding active conformation). Furthermore, this method can be used where the functional K_A may be different between two assays. This facilitates the determination of true bias factors that describe the ability of test ligands to promote distinct receptor conformational states (Kenakin *et al.,* 2012; Gregory *et al.,*

2012). Thus, the ability to quantify signalling bias can facilitate the mechanistic understanding of both desirable and undesirable properties of therapeutics.

1.4.2 Measuring Allostery

1.4.2.1 The allosteric ternary complex model (ATCM)

The simplest manifestation of an allosteric interaction occurs when the binding of the allosteric modulator either enhances or inhibits the affinity of the orthosteric ligand for the receptor (Christopolous and Kenakin, 2002; Stockton, 1983; Ehlert 19888; Lazareno 1995); the modulator is assumed not to mediate any effect in its own right in the absence of orthosteric ligand. This simple mechanism is referred to as the allosteric ternary complex model (ATCM). In this model, binding of orthosteric and allosteric ligand to the receptor is governed by the concentration of each ligand, their equilibrium dissociation constants and an additional, cooperativity parameter termed, α, which describes the magnitude of allosteric change in ligand affinity that occurs between the two sites when they are concomitantly bound (Christopoulos and Kenkin 2002; Christopoulos, 2000).

The ATCM describes the simplest allosteric effect, namely reciprocal modulation of ligand affinity in terms of the respective dissociation constants (K_A, K_B), that an orthosteric ligand A and allosteric ligand B have for their binding sites on the unoccupied receptor, and the extent to which the dissociation constant of each ligand is modified in presence of the other, quantified by α (Figure 1.5 A). Values of α greater than 1 denotes an allosteric enhancement of affinity for the receptor (positive cooperativity); value of α between 0 and 1 represents allosteric reduction in affinity (negative cooperativity) while α=1 indicates no net effect on binding affinity at equilibrium (neutral cooperativity) (Keov 2011). The limitations associated with the use of the ATCM includes (a) it does not explicitly consider the isomerization of GPCR between active and inactive states (b) it cannot account for allosteric modulators that change orthosteric ligand signalling efficacy in addition to or instead of any observed effects on orthosteric binding affinity (Keov *et al.,* 2011)

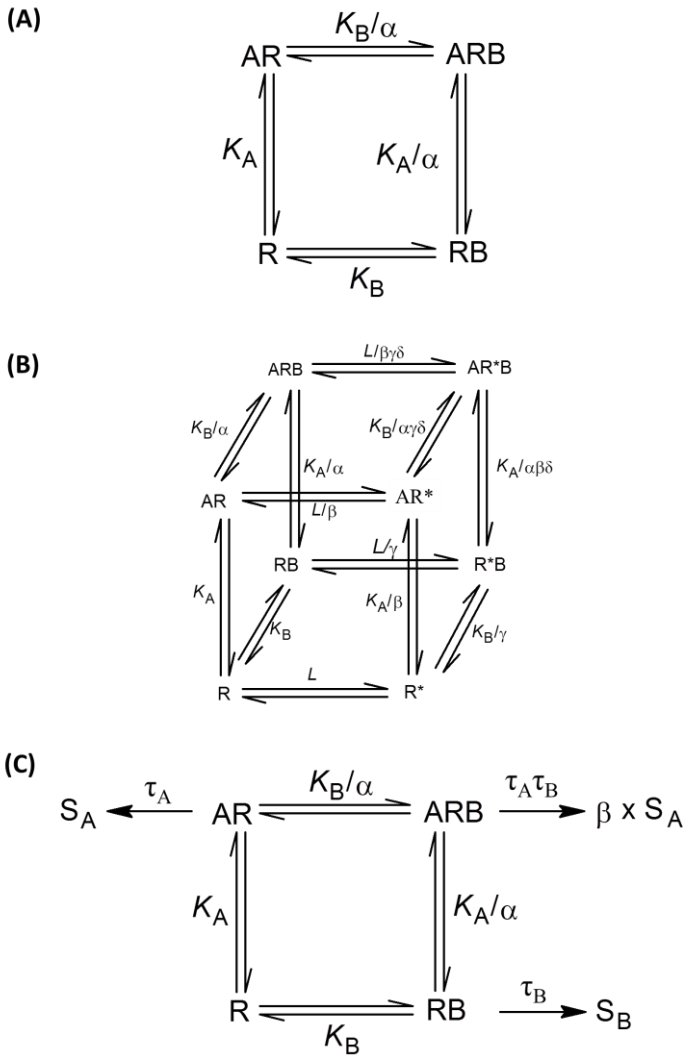

Figure 1.5: Models of allosteric interactions. (A) the allosteric ternary complex model (ATCM), (B) the allosteric two state model (ATSM) and (C) the basic operational model of allosterism. In all models, R denotes inactive receptor conformations, R* denotes active receptor conformations, and L is the isomerization constant describing the transition between R and R* states. A and B represents orthosteric and allosteric ligands, respectively, for which their binding affinities are denoted by K_A and K_B. α describes the cooperativity in binding between orthosteric and allosteric ligands, respectively. β and γ describe the cooperativity in efficacy of the orthosteric and allosteric ligand to achieve receptor isomerization/activation, respectively. δ denotes the activation cooperativity between both ligands to form the active state of the ternary complex (Hall, 2000; Keov *et al.*, 2011). Stimulus in any given system is governed by S_A and S_B for the orthosteric and allosteric ligand, respectively, while τ_A and τ_B are the transducer constants describing system variables (cell surface expression, coupling efficacy) (Leach *et al.*, 2007).

1.4.2.2 The allosteric two state model (ATSM)

This model explicitly incorporates the isomerization of receptor between active (R*) and inactive (R) states and introduces additional coupling constants to describe the selective stabilization of these states by orthosteric and allosteric ligands (Hall 2000). This model accommodates the effect of allosteric ligand affinity, efficacy and the ability to modulate the orthosteric ligand across both receptors' active and inactive states. The transition between R and R* states has been denoted as L, the additional efficacy parameters β and γ denotes cooperativity in efficacy of orthosteric and allosteric ligand to achieve receptor isomerization/activation respectively and δ denotes the activation cooperativity between both ligands to form the active state of ternary complex (Hall 2000) (Figure 1.5 B). The model also accounts for allosteric agonism at a receptor unoccupied by an orthosteric ligand (R*B). Despite the fact that this model accommodates both an allosteric effect on efficacy and affinity, it is impractical to use this model experimentally due to the exhaustive number of parameters. An alternative approach to tackle the quantification challenge is to adopt an operational approach where both mechanistic and empirical parameters are combined in a model to yield system-independent molecular descriptors of the interactions and absolute experimental models that are completely dependent on biological system in which the allosteric behavior is studied.

1.4.2.3 The operational model of allosterism

An operational model of allosteric modulation and agonism (Ehlert 2005; Kenakin 2005, Leach *et al.*, 2007; Price *et al.*, 2005) has been derived by combining the classic operational model of agonism (Black and Leff 1983) and the ATCM (Figure 1.5 C). Similar to the ATCM, it includes α that denotes cooperativity in binding between orthosteric ligand (A) and allosteric ligand (B). This model takes into consideration the stimulus of the system (S) that initiates the pharmacological response derived from three species AR, BR and the ternary complex ARB. In addition to allosteric effects on the binding affinity (governed by α), allosteric effects on efficacy are incorporated by introducing an additional parameter β. In the resultant operational model of allosterism, the parameters τ_A and τ_B denote the capacity of orthosteric and allosteric ligands, respectively, to exhibit agonism and incorporate the intrinsic efficacy of each ligand, the total density of receptors and the efficiency of stimulus-response coupling. The terms E_m and n denote the maximal possible system response and the slope factor of the transducer function that links occupancy to response, respectively (Leach *et al.*, 2007). In this model, allosteric modulation is governed by α and β, which can vary for each and every pair of interacting

ligands but should not change for a given set of ligands and GPCRs across different assay systems measuring same signalling output.

$$E = \frac{E_m\left(\tau_A[A]\left(K_B + \alpha\beta[B]\right) + \tau_B[B]K_A\right)^n}{\left([A]K_B + K_AK_B + [B]K_A + \alpha[A][B]\right)^n + \left(\tau_A[A]\left(K_B + \alpha\beta[B]\right) + \tau_B[B]K_A\right)^n}$$

In a system with low stimulus-response coupling efficiency or very low receptor expression levels (low τ values), the efficacy of the allosteric ligand might not be evident and the manifestations of the allosteric effect will be observed primarily as changes in the location and/or the maximum response to the orthosteric agonist. Under the conditions of high coupling efficiency and/or high receptor expression levels (high τ values), allosteric ligand efficacy is detected as changes in the basal responsiveness of the system of the system, in addition to changes in the location parameter of the orthosteric agonist, but it might not be possible to detect allosteric modulation of maximum orthosteric agonist response because of the latter approaching the ceiling imposed by cellular system.

1.5. Glucose homeostasis and the incretin system

1.5.1 General Introduction

Glucose metabolism is critical to normal physiological functioning. It acts both as a source of energy and as a source of starting material for nearly all types of biosynthetic reactions. Despite periods of feeding and fasting, plasma glucose remains in a narrow range between 4 and 7 mM in normal individuals. This tight control is governed by the balance between glucose absorption from the intestine, production by the liver and uptake and metabolism by peripheral tissues. The pancreas plays a crucial role in regulating this tight control (Aronoff *et al.*, 2004).

The pancreas is comprised of small groups of cells distributed throughout the organ known as the islets of Langerhans. The islets contain five principle endocrine cell types defined by the hormone they secrete. These include insulin-producing β-cells, glucagon-producing α-cells, somatostatin-producing δ-cells, ghrelin-producing ε-cells and pancreatic polypeptide-producing PP-cells that consist of four cell types (α, β, δ, and F) (Cabrera *et al.*, 2006). The secretion of islet hormones is highly regulated and collectively maintains glucose homeostasis through actions on many peripheral tissues such as liver, muscle and adipose tissue. Insulin stimulates glucose uptake by peripheral tissues, whereas glucagon

mobilizes glucose from the liver into the circulation. Somatostatin inhibits both α- and β-cell secretions (Kanno *et al.,* 2002). Pancreatic polypeptide (PP) may exert an inhibitory role in pancreatic exocrine secretion (Kojima *et al.,* 2007), and ghrelin inhibits insulin secretion (Dezaki *et al.,* 2007). All islet endocrine cells therefore play a central role in maintaining appropriate levels of blood glucose.

Insulin is a peptide hormone secreted by pancreatic β-cells in response to meal ingestion. It is synthesized in the rough endoplasmic reticulum as part of an 11.5 kDa precursor protein called pre-proinsulin and mediates its actions binding to the insulin receptor (Rosen, 1987). Insulin increases glucose uptake in muscle and fat, and inhibits hepatic glucose production, thus serving as the primary regulator of blood glucose concentration. Insulin also stimulates cell growth and differentiation, and promotes the storage of substrates in fat, liver and muscle by stimulating lipogenesis, glycogen and protein synthesis, and inhibiting lipolysis, glycogenolysis and protein breakdown (Guo, 2014; Saltiel and Khan, 2001). Insulin resistance or deficiency results in profound dysregulation of these processes, and produces elevations in fasting and postprandial glucose and lipid levels (Saltiel and Khan, 2001).

1.5.2 The enteroinsular axis and the incretin effect

The incretin concept dates back to early observations that ingested glucose leads to a considerably larger and more sustained insulin response than intravenously administered glucose. This implied that glucose sensing within the gastrointestinal tract resulted in potentiated insulin secretion (Elrick *et al.,* 1964; Nauck *et al.,* 1986). Subsequently it was shown that gut-derived hormones, known as incretins, are secreted in response to meal ingestion and stimulate insulin secretion, thereby making a significant contribution to overall postprandial insulin release (Creutzfeldt *et al.,* 1992; Holst *et al.,* 2001). This phenomenon of postprandial enhancement of insulin secretion by factors from the gut was termed “the incretin effect” (Creutzfeldt, 1979). Two incretin hormones were identified; glucose-dependent insulinotropic polypeptide (GIP), secreted by enteroendocrine K-cells in the proximal gut and glucagon-like peptide-1 (GLP-1) secreted by L-cells in the distal gut. Both GIP and GLP-1 have no effect on insulin secretion in the absence of elevated plasma glucose, obviating the risk of hypoglycaemia (Nauck *et al.,* 1993a).

1.5.3 The incretin hormones

GIP is a 42 amino acid peptide that binds to its GPCR, the GIP receptor (GIPR) to elicit its biological effects. GIPRs have been reported to be present on pancreatic islets, gut, adipose tissue, heart, pituitary,

adrenal cortex and several regions of brain (Fehmann *et al.,* 1995). GIP exerts glucose-dependent stimulatory effects on insulin secretion and also inhibits gastric acid secretion (Andersen *et al.,* 1978; Dupre *et al.,* 1973). It has also been investigated for its effects on fat metabolism in adipocytes (Yip and Wolfe, 2000), β-cell proliferation and cell survival (Trumper *et al.,* 2001).

The physiological actions of GLP-1 appear to be entirely mediated by the GLP-1 receptor (GLP-1R). Like GIP, GLP-1 potentiates glucose-dependent insulin secretion (Kreymann *et al.,* 1987). It also suppresses glucagon release (Creutzfeldt *et al.,* 1996; Schirra *et al.,* 2006), slows of the rate of gastric emptying (Delgado-Aros *et al.,* 2002), decreases hepatic glucose production (Prigeon *et al.,* 2003; Dardevet *et al.,* 2004), enhances insulin biosynthesis, improves insulin sensitivity in target tissues and induces satiety (Drucker, 2006). The activation of GLP-1 receptors on pancreatic β-islets is also associated with trophic and protective effects, including regulation of beta cell mass, proliferation, anti-apoptotic effects and stimulation of islet neogenesis. These functions make GLP-1 clinically relevant for the treatment of diabetes (Buteau *et al.,* 1999; Wang *et al.,* 2001).

The action of both GIP and GLP-1 is terminated by the action of the enzyme dipeptidyl-peptidase 4 (DPPIV), which is ubiquitously expressed in the central nervous system, kidney, lung, adrenal gland, liver, intestine, spleen, testis, pancreas, and on surface of macrophages and lymphocytes. DPPIV cleaves the biologically active form of GIP and GLP-1 at position 2 alanine (N-terminal). The plasma half-life of exogenously administered incretins GIP and GLP-1 is up to 5-7 min and 2-5 min respectively (Hansen *et al.,* 1999; Mentlein, 1999). A few studies have examined the involvement of other enzymes in GLP-1 degradation *in vivo,* one of them being neprilysin. GLP-1 has been found to be a substrate for this metalloendopeptidase enzyme also known as neutral endopeptidase 24.11, prominently found in kidney and proposed to play a role in the renal clearance of peptide hormones (Roques *et al.,* 1993; Hupe-Sodmann *et al.,* 1995). The significance of this observation in terms of GLP-1 degradation *in vivo* is not well-established.

The insulinotropic effects of GIP are lost in type 2 diabetics (T2DM) (Nauck *et al.,* 1993b), while the physiological effects from GLP-1 are maintained, leaving GLP-1 as the primary candidate incretin for clinical use. Thus, the GLP-1 system forms the basis of two classes of glucose lowering agents, incretin mimetics (i.e. GLP-1 receptor agonists) and inhibitors of dipeptidyl peptidase 4 (DPPIV or CD26) (incretin enhancers) (Deacon *et al.,* 2006; Drucker *et al.,* 2006; Nauck *et al.,* 2005). Even though GIP

and GLP-1 are the only two classified incretins, many other proglucagon derived peptides such as glicentin, glucagon, oxyntomodulin, and GLP-2 represent physiologically important regulators of nutrient intake and digestion and are currently being used clinically or under active investigation for clinical use.

1.6 The glucagon-like peptide-1 receptor (GLP-1R) system

1.6.1 Biology of GLP-1 synthesis, secretion and metabolism

Tissue specific posttranslational processing of proglucagon (18-kDa protein) yields specific peptide profiles containing different sets of peptides with opposing biological activities in the pancreas and intestine (Mojsov *et al.*, 1986). Although several prohormone convertase (PC) enzymes have been identified, only PC1/3 and PC2 appear to be important for proglucagon processing (Rouille *et al.*, 1995). Evidence suggests the tissue-specific processing is due to differential expression of PC1 (Tucker *et al.*, 1996) and PC2 (Rouille *et al.*, 1994).

The prohormone convertase 2 (PC2) enzyme cleaves proglucagon in pancreatic α-cells (Rouille *et al.*, 1994) predominantly to glucagon, glicentin-related pancreatic peptide (GRPP), intervening peptide-1 (IP-1), and the major proglucagon fragment (MPGF; proglucagon-(72-158)) (Patzelt *et al.*, 1979; Patzelt and Schiltz, 1984). In pancreatic α cell, proglucagon is initially cleaved to produce glicentin and the major proglucagon fragment (MPGF; proglucagon-(72-158)). Glicentin is later processed to yield GRPP, glucagon and intervening peptide-1 (IP-1). MPGF had been identified to encompass the GLP-1, intervening peptide-2 (IP-2), and GLP-2 sequences (Holst *et al.*, 1994). Thus, the pancreatic processing of proglucagon occurs with an initial inter-domain cleavage, followed by efficient processing of the N-terminal domain (glicentin) and very little processing of the C-terminal domain (MPGF) (Rouille *et al.*, 1995). Glucagon, the major counter-regulatory hormone to insulin, regulates hepatic glucose production via activation of glycogenolysis and gluconeogenesis and inhibition of glycolysis, and is essential for maintaining glucose homeostasis in the fasting state.

In contrast, in the intestinal L cells, cleavage of proglucagon is by prohormone convertase 1 (PC1) results in the efficient formation of GLP-1, intervening peptide-2 (IP-2), and GLP-2 (Orskov *et al.*, 1986). Glucagon levels are very low in the intestine (Kervran *et al.*, 1987). The N-terminal domain remains relatively unprocessed in the form of glicentin (Thim and Moody, 1982) and is only partially

cleaved into GRPP and oxyntomodulin (proglucagon-(33-69)) (Bataille *et al.,* 1982). An additional cleavage occurs within the GLP-1 sequence (Arg77), yielding shortened active forms of GLP-1, GLP-1-(7-37) (proglucagon-(78-108)) and GLP-1-(7-36)NH_2 (proglucagon-(78-107)), collectively known as truncated GLP-1 (tGLP-1) (Orskov *et al.,* 1989). The processing of proglucagon in intestinal L cells thus may involve an initial inter-domain cleavage, probably at the same site as observed in the pancreas, and is followed by extensive processing of only the C-terminal domain.

Glicentin is a 69 amino acid proglucagon-derived peptide that contains the 29 amino acid sequence of glucagon flanked by peptide extensions at both the amino and the carboxyl terminus. Although secreted together with GLP-1 and GLP-2 from enteroendocrine L cells, glicentin has not been shown to regulate glucose homeostasis (Drucker, 2006). The physiological actions of glicentin are not well defined but have been investigated to exert trophic effects in the rodent small intestine (Myojo *et al.,* 1997).

To date, no physiologic actions have been identified for intervening peptide-2.

Oxyntomodulin also contains the 29 amino acid sequence of glucagon with an additional 8–amino acid carboxy-terminal extension. Oxyntomodulin stimulates intestinal glucose uptake (Collie *et al.,* 1997) and insulin secretion (Jarrousse *et al.,* 1984) and inhibits gastric emptying, food intake, and meal-stimulated gastric acid secretion (Pocai, 2012, 2014). Oxyntomodulin also induces satiety, inhibits food intake, and increases energy expenditure in humans (Wynne *et al.,* 2005, 2006). Although oxyntomodulin is a weak agonist of both GLP-1R and the glucagon receptor, the anorectic actions of oxyntomodulin are blocked by the GLP1R antagonist $exendin_{9\text{-}39}$ (Dakin *et al.,* 2001) and are eliminated in the absence of a functional GLP-1R (Baggio *et al.,* 2004).

GLP-2 is a 33 amino acid peptide secreted with GLP1 from enteroendocrine cells in a nutrient-dependent manner. GLP-2 rapidly induces hexose transport in jejunal basolateral membrane vesicles (Cheeseman and Tsang, 1996). The main biological consequence of exogenous GLP-2 administration is expansion of the mucosal epithelium in the small bowel. The intestinotrophic actions of GLP-2 have been demonstrated in rodents with intestinal injury (Boushey *et al.,* 1999, 2001) and in humans with short bowel syndrome (Jeppesen *et al.,* 2001, 2005; Jeppesen *et al.,* 2003; Hornby and Moore, 2011). Although acute GLP-2 administration increased levels of plasma glucagon, triglycerides, and FFAs in the postprandial state (Meier *et al.,* 2006), there is no evidence that acute or chronic GLP-2

administration directly regulates insulin secretion or glucose homeostasis in humans (Jeppesen *et al.*, 2001). GLP-2 stimulates cell proliferation and inhibits apoptosis in the intestinal crypt compartment (Boushey *et al.*, 2001; Estall and Drucker, 2006). GLP-2 also upregulates intestinal glucose transport, improves intestinal barrier function, and inhibits food intake, gastric emptying, and acid secretion (reviewed in Drucker, 2002; Burrin *et al.*, 2001). GLP-2 also reduces bone resorption and promotes neuronal proliferation and survival (reviewed in Marathe *et al.*, 2013).

There are multiple forms of GLP-1. GLP-1(1-37) is processed in intestinal L-cells into two equipotent circulating molecular forms GLP-1(7-37) and GLP-1(7-36)NH_2 (Holst *et al.*, 1987; Kreymann *et al.*, 1987; Mojsov *et al.*, 1987). GLP-1(7-36)NH_2 represents the majority of circulating active GLP-1 secreted in response to nutrient ingestion (Orskov *et al.*, 1994). GLP-1 is secreted in a biphasic pattern with an early phase beginning within 5-15 min and a prolonged second phase observed from 30-60 min after meal ingestion (Herrmann *et al.*, 1995). All forms of GLP-1 are rapidly degraded by DPPIV into the low affinity fragments, GLP-1(9-37) and GLP-1(9-36)NH_2 (Deacon *et al.*, 1995; Hansen *et al.*, 1999). These metabolites are antagonists to adenylyl cyclase activity in baby hamster kidney cells (Knudsen *et al.*, 1996), but have cardioprotective and glucoregulatory actions when pharmacologically dosed (Elahi *et al.*, 2008; Nikolaidis *et al.*, 2005b), and have also been reported to exert GLP-1R independent effects (Ban *et al.*, 2010; Ban *et al.*, 2008).

1.6.2 Biological actions of endogenous GLP-1

The GLP-1R is ubiquitously expressed throughout the body, and although it has been best characterized for its involvement in glucose regulation, it also has other functions in other tissues (Figure 1.6).

1.6.2.1 GLP-1 effects on the pancreas

As discussed above, activation of GLP-1R on pancreatic islets has been shown to stimulate glucose-dependent insulin secretion, enhance growth and survival of β-cells, exert proliferative and protection (heart), decreasing gastric empyting (stomach), increasing glomerular filtration and renoprotection (kidneys), modulating airway and pulmonary vascular tone (lungs) and increasing bone mineral density and strength (bone) (adapted from Baggio and Drucker, 2007; Holst *et al.*, 2008). Apart from regulation of the entero-insular axis, GLP-1 also induces effects on peripheral tissues including decreasing appetite and enhancing neuroprotection (brain), increasing cardiac function and

cytoprotective actions through engagement of signal transduction pathways linked to mitogenesis and cell survival. These functions make GLP-1 clinically relevant for the treatment of diabetes (Buteau *et al.,* 1999; Wang *et al.,* 2001).

1.6.2.2 GLP-1 effects on the gastrointestinal tract

In the gastrointestinal tract, GLP-1 inhibits antral contractions, increases pyloric tone and substantially delays the passage of both liquid and solid meals to the small intestine (Schirra *et al.,* 2000). Thus GLP-1 inhibits gastrointestinal motility, reduces gastrointestinal secretions and attenuates gastric emptying.

1.6.2.3 GLP-1 effects on the central nervous system (CNS)

GLP-1 is synthesized in caudal part of nucleus of solitary tract (Jin *et al.,* 1988) and its receptors are widespread throughout brain, particularly in hypothalamic, hippocampal, and cortical nuclei (Larsen *et al.,* 1997; Van Dijk *et al.,* 1996; Turton *et al.,* 1996). GLP-1Rs in the brain regulate appetite and energy homeostasis (Orskov *et al.,* 1996). Intra-cerebroventricular administration of GLP-1 in rodents (Turton *et al.,* 1996; Tang-Christensen *et al.,* 1996) and intravenous infusions of GLP-1 in humans (Flint *et al.,* 1998; Gutzwiller *et al.,* 1999 a, b) inhibit food intake thus promoting satiety. Chronic administration of GLP-1 has also been documented to result in weight loss (Meeran *et al.,* 1999; Zander *et al.,* 2002).

Cabou *et al.,* showed that brain GLP-1R signalling simultaneously controls heart rate, femoral arterial blood flow and glucose utilization and also regulates reactive nitric oxide and reactive oxygen species (Cabou *et al.,* 2008). In addition, some studies have reported a neurotrophic and neuroprotective role of GLP-1 in various cell lines and animal models, which may hold promise for the development of GLP-1 agonists in the treatment of various neurodegenerative disorders (Perry *et al.,* 2002; Perry and Greig, 2005; Perry *et al.,* 2007).

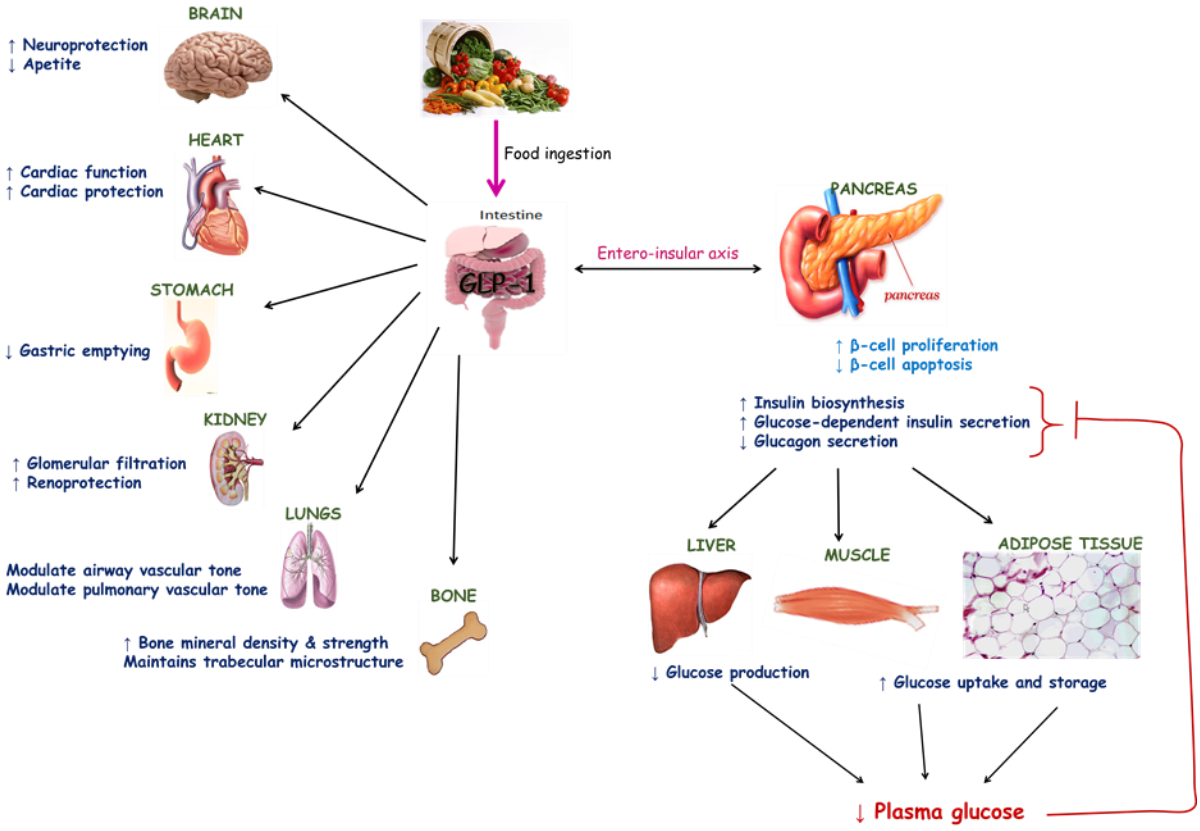

Figure 1.6: Physiological actions of glucagon-like peptide-1 (GLP-1). Ingestion of a glucose-rich meal augments secretion of GLP-1 from the gastrointestinal tract. Subsequently GLP-1 promotes glucoregulatory effects via the pancreas, liver, adipose tissue and muscle. The resultant decrease in plasma glucose acts in a negative feedback manner to inhibit insulin release from the pancreas (adapted from Baggio and Drucker, 2007; Holst *et al.*, 2008).

1.6.2.4 GLP-1 effects on the cardiovascular system (CVS)

The GLP-1R is expressed in cardiomyocytes, coronary and vascular endothelial cells as well as smooth muscles in mice (Ban *et al.,* 2008). Administration of GLP-1 elicits ionotropic and chronotropic activity that may be either mediated through the autonomic nervous system (Barragan *et al.,* 1994; Yamamoto *et al.,* 2002) or may be a consequence of direct activation of GLP-1Rs (Barragan *et al.,* 1999; Yamamoto *et al.,* 2002). These effects were attenuated in GLP-1R$^{-/-}$ mice (Gros *et al.,* 2003). Pressor and chronotropic responses of GLP-1 were not observed in normal, conscious and chronically instrumented dogs over a dose range of 1-20 pmol/kg/min (Nikolaidis *et al.,* 2004a), but these responses were improved in canine models of cardiac injury and heart failure (Nikolaidis *et al.,* 2004a). In addition to this, GLP-1 administration reduced systemic vascular resistance and improved myocardial insulin sensitivity and glucose uptake (Nikolaidis *et al.,* 2004a).

In humans, GLP-1 improves left ventricular ejection fraction and functional status in patients with congestive heart failure (Sokos *et al.,* 2006), and those who suffered myocardial infarction and angioplasty (Nikolaidis *et al.,* 2004b; Sokos *et al.,* 2007). Some studies have also revealed a role of GLP-1 in improving endothelial dysfunction (Nystrom *et al.,* 2004) and providing protection against myocardial infarction (Bose *et al.,* 2005). Thus, the GLP-1 is cardioprotective (Nikolaidis *et al.,* 2004 a,b; Nikolaidis *et al.,* 2005a; Bose *et al.,* 2005), with improved cardiac functions including cardiac output, blood pressure and contractility (Barragan *et al.,* 1999; Golpon *et al.,* 2001; Yamamoto *et al.,* 2002; Sokos *et al.,* 2006). In addition, GLP-1(9-36)NH_2, the principal metabolite of GLP-1 has been observed to improve myocardial glucose uptake and ventricular contractility in animal models of cardiomyopathies (Nikolaidis *et al.,* 2005b).

1.6.2.5 GLP-1 effects on the liver

In the liver, GLP-1 promotes glycogen accumulation, reduces hepatic glucose production and lipogenesis, and attenuates macrophage infiltration, thus preventing inflammatory response in hepatocytes isolated from diabetic, obese and transgenic rats and mice (Valverde *et al.,* 1994; Alcantara *et al.,* 1997; Lopez-delgado *et al.,* 1998, Moreno *et al.,* 2012; Panjwani *et al.,* 2013). Some studies also suggest a role of GLP-1(9-36) in suppressing hepatic glucose production (Elahi *et al.,* 2008).

1.6.2.6 GLP-1 effects on adipose tissue

The expression of GLP-1Rs in adipose tissue has been controversial but convincing studies show the presence of these receptor in epididymal fat tissue of mice and a differentiated 3T3L1 adipocyte cell line (Valverde etal., 1993; Merida *et al.,* 1993; Egan *et al.,* 1994) and humans (Sancho *et al.,* 2007; Vendrell *et al.,* 2011). GLP-1 enhanced insulin-mediated lipid synthesis and glucose uptake, improving insulin responsiveness in 3T3L1 adipocytes and rodent epididymal adipose tissues (Oben *et al.,* 1991; Egan *et al.,* 1994). Both GLP-1(7-36)NH_2 and GLP-1(1-36)NH_2 exhibit dose-dependent lipolytic effect, measured as glycerol release, in isolated rat adipocytes from epididymal pads (Ruiz-Grande *et al.,* 1992). Anti-inflammatory effects of GLP-1on adipose tissue have also been proposed and investigated in the ob/ob mouse model of diabetes (Lee *et al.,* 2012), and in isolated 3T3L1 adipocytes (Chung *et al.,* 2009; Lee *et al.,* 2012). Both GLP-1 and a synthetic long acting analogue of GLP-1 (liraglutide) regulate adipogenesis in a GLP-1R dependent manner, both *in vitro* and *in vivo,* by stimulating the differentiation of primary pre-adipocytes (Challa *et al.,* 2012).

1.6.2.7 GLP-1 effects on the lungs

The GLP-1R is expressed at high density in rat lung membrane (Kanse *et al.,* 1988; Richter *et al.,* 1990; Campos *et al.,* 1994) and on vascular smooth muscle (Richter *et al.,* 1993,) although its physiological role in the lungs remains unclear. Treatment of rat trachea and pulmonary artery with GLP-1 resulted in increased mucous secretion and relaxation of smooth muscle, respectively, thus modulating airway and pulmonary vascular tone (Richter *et al.,* 1993). Stimulation of the GLP-1R in type II pneumocytes (Bullock *et al.,* 1996), results in secretion of surfactant from these cells (Wright and Clements, 1987; Benito *et al.,* 1998; Vara *et al.,* 2001).

1.6.2.8 GLP-1 effects on the kidney

GLP-1 prevents renal damage in streptozotocin-induced diabetic rats (Ojima *et al.,* 2013), and the GLP-1 mimetic, exendin-4, exhibits natriuretic and diuretic effects in mice, which was found to be absent in GLP-$1^{-/-}$ mice (Reig *et al.,* 2012). Hirata *et al.,* 2009 and Liu *et al.,* 2010 demonstrated that GLP-1 analogues can attenuate hypertension in a salt-sensitive mouse model (Hirata *et al.,* 2009), and Dahl salt-sensitive rats (Liu *et al.,* 2010). Regulation of sodium reabsorption by GLP-1 and its analogues (Carraro-Lacroix *et al.,* 2009) may be one of the mechanisms contributing to the antihypertensive action of GLP-1. In addition to this, chronic treatment with GLP-1 analogues

ameliorates diabetic nephropathy by modulating metabolic abnormalities, such as reducing body weight, lipid accumulation and improving renal function (Park *et al.,* 2007).

1.6.2.9 Effect of GLP-1 on bones

GLP-1 and exendin-4 have been reported to control bone reabsorption and promote bone anabolic and osteogenic effects by increasing bone mineral density, strength of the bone, preventing deterioration of trabecular microstructure, reducing bone fat mass and improving/normalizing biochemical factors representing increased bone turnover in streptozotocin-induced and fructose-induced insulin resistant rats (Nuche-Berenguer *et al.,* 2009; Nuche-Berenguer *et al.,* 2010a), as well as aged ovariectomized rats (Ma *et al.,* 2013). Genetic deletion of GLP-1 has been demonstrated to result in cortical osteopenia and bone fragility, probably due to increased bone resorption by osteoclasts in association with reduced thyroid calcitonin expression (Yamada *et al.,* 2008). Furthermore, GLP-1 prevents adipogenic differentiation and promotes proliferation, cytoprotection and osteogenic differentiation in bone marrow mesenchymal stem cells of humans (Sanz *et al.,* 2010) and rats (Ma *et al.,* 2013). All these effects were mediated independent of insulin and glucose concentration (Nuche-Berenguer *et al.,* 2009, 2010a; Kim *et al.,* 2013).

1.6.2.10 Miscellaneous effects of GLP-1

Apart from the above mentioned tissues, GLP-1R expression has also been detected in the inner layer of the retina of Sprague-Dawley rats (Zhang *et al.,* 2009). The expression of GLP-1R is being speculated in dorsal root ganglia and sciatic nerve of mice and rats (Jolivalt *et al.,* 2011), where the activation of the receptor has been determined to provide protection from diabetes-associated complications (Zhang *et al.,* 2009; Fu *et al.,* 2012; Jolivalt *et al.,* 2011). Furthermore, there is a report of GLP-1R in hair follicles of the skin in mice and cultures of skin-derived cells, suggesting a role in skin development and folliculogenesis (List *et al.,* 2006). In addition, the psoriasis condition of two geriatric type 2 diabetic adults has been shown to improve when treated with the long acting GLP-1 analogues exenatide and liraglutide (Faurschou *et al.,* 2011; Buysschaert *et al.,* 2012), which may be due to the increased expression of GLP-1R in psoriasis plaques or due to the increased infiltration of the immune cells (Faurschou *et al.,* 2013).

Anti-inflammatory properties of GLP-1 and its analogues have been explored in LPS activated mouse peritoneal macrophages (Arakawa *et al.,* 2010), THP-1 macrophage cells (Kodera *et al.,* 2011), LPS

activated Raw 264.7 macrophage cells (Chang *et al.,* 2013) and insulin resistant macrophages isolated from insulin receptor knock-out mice and obese mice (Liang *et al.,* 2012). Anti-inflammatory effects were mediated either by inhibition of the expression of inflammatory mediators such as TNF-α and monocyte chemoattractant protein-1 (Arakawa *et al.,* 2010), iNOS (Chang *et al.,* 2013) or by reducing the release of cytokines (TNF-α and IL-1β). A recent study of human macrophages identified the ability of GLP-1 to induce macrophage differentiation into the M2 phenotype (Shiraishi *et al.,* 2012), which is responsible for the production of anti-inflammatory factors, angiogenesis, tissue remodeling and repair (Porcheray *et al.,* 2005). Thus this provides new opportunities for the treatment of chronic inflammatory diseases.

GLP-1 is therefore a candidate for treatment of various metabolic disorders, although currently it is primarily being pursued by the pharmaceutical industry as a target for type II diabetes and obesity. Its role as a treatment for various neurodegenerative, cardiovascular and renal disorders still needs to be better-elucidated.

1.6.3 The glucagon like peptide-1 receptor (GLP-1R)

The GLP-1R contains 463 amino acids and belongs to the secretin-like Class B (II) GPCR family. It comprises a characteristic extracellular N-terminal domain containing six conserved cysteine residues (the N-domain) and a core domain comprising the 7TMs (seven transmembrane helices) separated by three intracellular loops (ICL1–ICL3) and three extracellular loops (Palczewski *et al.,* 2000). According to the two domain model for peptide binding (Runge *et al.,* 2008; Underwood *et al.,* 2010; Al-Sabah and Donnelly, 2003), the N-domain is primarily responsible for providing most of the peptide binding energy, whereas the core domain is responsible for binding the N-terminal region of the peptide agonists and transmitting the signal to the intracellular G proteins. In these structures, the C-terminus of the peptide interacts with the receptor N-terminal domain, while the N-terminus of the peptide is thought to associate with the core of the receptor, predominantly the ECLs to influence transmission of signal and signalling specificity to intracellular effectors (Al-Sabah and Donnelly, 2003; Coopman *et al.,* 2011). This broadly recognized two-domain model of ligand binding is also supported experimentally by chimeric receptors (Runge *et al.,* 2003), photolabile peptide cross-linking (Chen *et al.,* 2009; Chen *et al.,* 2010; Miller *et al.,* 2011), and by mutagenesis analysis (López de Maturana and Donnelly, 2002; Koole *et al.,* 2012).

Although there are no TM bundle structures of the GLP-1R, the recent structures of the CRF1R and GCGR TM domains allows for homology modeling of the TM bundle of the closely related GLP-1R that may provide a better mechanistic understanding of receptor function (Siu *et al.,* 2013; Hollenstein *et al.,* 2013).

1.6.3.1 The glucagon like peptide-1 receptor (GLP-1R) signalling

The ability of GLP-1 to enhance glucose-dependent insulin secretion and promote trophic and survival effects by regulating apoptosis and proliferation in pancreatic beta cells makes it a promising candidate from a clinical perspective. The actions of GLP-1 are predominantly mediated through cAMP-dependent pathways (cAMP/PKA, cAMP/Epac and PI3K/Akt pathways) (Drucker *et al.,* 1987; Taylor *et al.,* 1990; Dyachok *et al.,* 2006; Gromada *et al.,* 1998; Kawasaki *et al* ., 1998), and recruitment of β-arrestin-1 (Sonoda *et al.,* 2008; Quoyer *et al.,* 2010). Activation of the GLP-1R results in coupling to Gαs and activation of adenylyl cyclase to generate cAMP, which sequentially activates protein kinase A and cAMP regulated guanine nucleotide exchange factors of the Epac family (Gromada *et al.,* 1998; Holz *et al.,* 1995; Kang *et al.,* 2001) to promote downstream effects. In addition to coupling to Gαs, the GLP-1R has also been reported to couple to other G proteins, including Gαi, Gαq and Gα12/13 (Bavec *et al.,* 2003; Hallbrink *et al.,* 2001). GLP-1 and its analogues have also been reported to stimulate the p44/42 mitogen activated protein kinase (ERK1/2) cascade by diverse pathways such as influx of calcium, Gαs/cAMP/PKA or β-arrestin-1 recruitment (Arnette *et al.,* 2003; Gomez *et al.,* 2002; Briaud *et al.,* 2003; Costes *et al.,* 2006). Early activation of ERK1/2 has been reported to be dependent on PKA leading to nuclear translocation of ERK, whereas long lasting ERK1/2 activation is mediated through the β-arrestin-1 pathway (Quoyer *et al.,* 2010).

The GLP-1R is primarily expressed in pancreatic islets, predominantly in β-cells, where it is responsible for regulating glucose-dependent insulin biosynthesis and release, inducing β-cell proliferation, decreasing β-cell apoptosis and inhibiting glucagon secretion (Orskov and Poulsen, 1991; Tornehave *et al.,* 2008), as well as in other tissues such as the kidney (Schlatter *et al.,* 2007), lung (Kanse *et al.,* 1988; Lankat-Buttgereit *et al.,* 1994), heart and brain (Hoosein and Gand, 1984; Shimizu *et al.,* 1987; Korner *et al.,* 2007). A thorough elucidation of the signalling pathways originating from GLP-1Rs is required and how this links to downstream physiological effects, both to understand the basic cell biology of GLP-1, and to understand the signalling requirements that would be desirable for identification and development of small molecule ligands that may mimic the actions of GLP-1. GLP-

1 signalling in the pancreas, in terms of pathways leading to insulin synthesis and secretion have been explored in detail, however to date, less is known on the roles of individual signalling components leading to β-cell survival, and for functions of GLP-1 outside of the pancreas.

1.6.3.2. Signalling mechanisms of GLP-1R in the pancreas: GLP-1R activated signalling pathways/mediators that promote glucoregulatory effects

GLP-1R activation promotes pancreatic insulin biosynthesis and release (Husokawa *et al.,* 1996) and induces insulin gene transcription (Drucker *et al.,* 1987) by inducing the transcription of Pdx1, leading to enhanced insulin gene expression (Wang *et al.,* 1999, 2000). GLP-1R signalling inhibits ATP-sensitive and voltage-dependent K^+ channels (MacDonald*et al.,* 2003), thus reducing cell depolarization, and increasing cytosolic calcium (Flamez *et al.,* 1999), which potentiates calcium-dependent exocytosis of insulin probably by accelerating the mobilization of insulin secretory granules from the reserve pool to readily releasable pool, which is responsible for the sustained insulin secretion (Gromada *et al.,* 1998). PKA phosphorylation has been implicated in the regulation of K_{ATP} channels (Holz *et al.,* 1993), voltage dependent calcium channels (VDCCs) (Gromada *et al.,* 1998), voltage dependent K^+ channels (K_v) (Dukes and Philipson, 1996), mobilization of intracellular Ca^{2+} stores (Bootman and Berridge, 1995; Holz *et al.,*1999), docking and fusion of insulin secretory vesicles (Renstrom *et al.,* 1997) and intracellular energy homeostasis through hormone-sensitive lipase (HSL) (Yaney *et al.,* 2001) (Figure 1.7) .

Glucokinase is considered as the glucose sensor and forms the rate-limiting step in the process of glycolysis. Increase in its activity by GLP-1 was demonstrated to enhance GSIS by activating the cAMP/Epac2 pathway, which further linked interacting proteins Rim2 (interacting molecules of small G protein) and Ras-associated protein, Rab3A, thus forming a complex that improved sensitization of β-cells to glucose (Park *et al.,* 2012). In addition, GLP-1 mediated modulation of glucokinase activity was observed to be absent at low glucose concentrations indicating a role for these proteins in mediating the glucose-dependent effects of GLP-1 (Park *et al.,* 2012).

VAMP8 has been predicted to play a dual and non-redundant role in insulin exocytosis and β-cell proliferation (Zhu *et al.,* 2012). GLP-1 potentiates glucose-stimulated insulin secretion by accelerating VAMP8-mediated recruitment of newcomer insulin secretory granules to the plasma membrane (Zhu *et al.,* 2012). Paradoxically, VAMP8 has also been identified as a negative regulator of β-cell

proliferation. VAMP8$^{-/-}$ mice exhibited high basal cyclin D1 levels and polo-like kinase-1 (Plk1) enzyme activity compared to wild type mice, which was further amplified with exendin-4 treatment resulting in increased β-cell mass. Moreover no effects were observed on apoptotic processes in VAMP-/- mice when compared to wild type (Zhu *et al.,* 2012).

β-arrestin1 has been reported to regulate insulin synthesis in insulinoma cell lines by coupling to agonist-activated GLP-1R and activating downstream effector molecules including phosphorylation of CREB, ERK1/2 and stimulation of IRS2 via both PKA-dependent and independent mechanisms (Sonoda *et al.,* 2008). In a separate study, β-arrestin1 regulated the levels of IRS-1 by competitively binding to E3 ubiquitin ligase Mdm2 (Usui *et al.,* 2004), modulating gene expression through CREB phosphorylation, p300 (Kang *et al.,* 2005) and IRS2 (Jhala *et al.,* 2003, Park *et al.,* 2006). Furthermore, rap1-regulated phospholipase C-epsilon (PLC-ε) was identified to link Epac2 activation to potentiation of calcium-dependent exocytosis of insulin secretion by studying islets from Epac$^{(-/-)}$ and PLC$^{(-/-)}$ knockout mice (Dzhura *et al.,* 2011). In a study by Sindhu and colleagues, small ubiquitin-related modifier proteins (SUMO) was reported to downregulate GLP-1R during hyperglycemia by developing a covalent association that attenuated cell surface trafficking of GLP-1R, thus contributing to significant reductions in insulin secretion and incretin responsiveness (Sindhu *et al.,* 2012).

Other effects that have been identified to play a role in GSIS include, transcellular interaction of neuroligin 2 (Suckow *et al.,* 2008, 2012), downregulated expression of neurexin-1α (Mosedale *et al.,* 2012), scaffolding role of Double C2 domain (Doc2b), regulation of receptor tyrosine kinase c-Kit (Feng *et al.,* 2012), role of PDZ domain proteins bridge 1 and PDZD2 as transducers (Thomas *et al.,* 2009), PKA-mediated phosphorylation of Snapin (Song *et al.,* 2011), attenuation of AGEs (Puddu *et al.,* 2010), enhanced expression of acetyl-CoA carboxylase-1 (Ronnebaum *et al.,* 2008), synt1A (Ohara-Imaizumi *et al.,* 2007), NKx6.1 homeodomain transcription factor (Schisler *et al.,* 2005), neuronal calcium sensor-1 (NCS-1) (Gromada *et al.,* 2005), activation of Raf-1 kinase (Alejandro *et al.,* 2010) and gene HadhSc encoding short-chain-3-hydroxyacyl-coenzymeA dehydrogenase (Hardy *et al.,* 2007).

1.6.3.3 Signalling mechanisms of GLP-1R in the pancreas: GLP-1R activated signalling pathways/mediators that promote proliferation and anti-apoptosis

β-arrestin-1 recruitment is established as a G protein-independent mechanism that contributes to GPCR signalling, in addition to its known role in receptor regulation and termination of G protein-mediated signalling. β-arrestin-1-mediated phosphorylation of ERK1/2 has been implicated in the anti-apoptotic action of GLP-1 via activation of p90RSK and inactivation of the pro-apoptotic protein Bad (Quoyer *et al.*, 2010). This scaffolding protein has also been recently reported to facilitate the proliferative effects of GLP-1 by recruiting c-Src to the agonist occupied receptor (Talbot *et al.*, 2012).

Transcriptional control of gene expression mediated by GLP-1, such as via PKA-dependent phosphorylation of transcription factor CREB, which further stimulates IRS2 expression (Jhala *et al.*, 2003), and PI3K/Akt dependent nuclear exclusion of transcription factors (Buteau *et al.*, 2006) have also been reported to increase the expression of Pdx1 (Perfetti *et al.*, 2000). And contribute to cell survival mechanisms of GLP-1. ERK1/2 has also been revealed to control the phosphorylation of CREB and plays a key role in glucose-mediated pancreatic β-cell survival (Costes *et al.*, 2006).

In addition, GLP-1R signalling induces proteolytic maturation of betacellulin by membrane bound metalloproteinases to transactivate the epidermal growth factor receptor (EGFR), thereby stimulating β-cell proliferation (Buteau *et al.*, 2003). Activation of EGFR consecutively activates phosphatidyl inositol-3-kinase (PI3K) and protein kinase B (PKB; Akt) (Buteau *et al.*, 2001, 1999), resulting in the inhibition of forkhead transcription factor FoxO1, thus relieving molecular breaks on Pdx1 and Foxa2 expression (Buteau *et al.*, 2006) and activating Wnt signalling (Liu and Habener, 2008) to mediate β-cell proliferation and survival. Another mechanism explored in context to GLP-1-mediated inhibition of FoxO1, is stunting the activity of NAD^+-dependent protein deacetylase, SirT1, resulting in nuclear exclusion of FoxO1 and increasing the expression of Pdx1 and Foxa2, triggering β-cell mass expansion (Bastein-Dionne *et al.*, 2011). Furthermore, GLP-1 also enhanced the activity of the IGF2/IGF-1R autocrine loop by upregulating the expression of insulin-like growth factor-1 receptor in a cAMP-dependent manner (Cornu *et al.*, 2009).

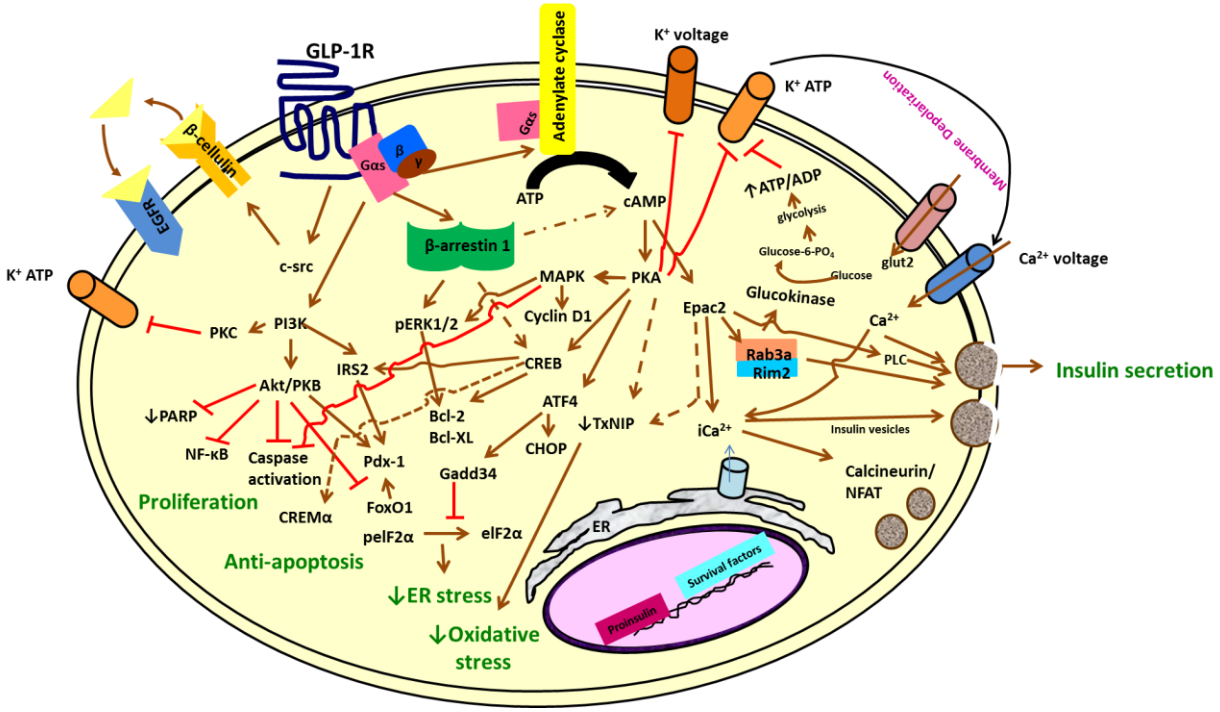

Figure 1.7: Signalling pathways mediated by GLP-1R activation in pancreatic β-cell. The activation of the GLP-1R on the pancreas regulates a plethora of downstream signalling events resulting in number of clinically and physiological relevant outcomes that can be used in management of metabolic disorders. GLP-1R activation leads to β-cell proliferation and neogenesis, inhibition of β-cell apoptosis, ER stress reduction, attenuation of oxidative stress, and insulin secretion/biosynthesis.

GLP-1R signalling also leads to decreased cleavage of pro-apoptotic molecules, including caspase-3 and poly-ADP-ribose polymerase (PARP), and increased expression of cytoprotective molecules such as Bcl-2, Bcl-xL, and the inhibitor of apoptosis protein-2 (IAP- 2) (Urosova *et al.,* 2004). A study by Brun and colleagues has established an association between paired homeodomain nuclear factor Pax4 and susceptibility of INS-1 cells to apoptosis, suggesting a role of this transcription factor in proliferation by upregulation of bcl-xL (Brun *et al.,* 2007).

The GLP-1R agonist, exendin-4 reduced thioredoxin interactin protein (TxNIP) levels (which is involved in oxidative stress, a negative regulator of cell growth and proliferation that has an established role in the pathogenesis of type 2 diabetes and other metabolic and systemic disorders) in a rat pancreatic β-cell line. In addition, Shao and colleagues demonstrated that downregulation of TxNIP was partially due to the activation of cAMP signalling, involving both PKA and Epac-dependent mechanisms, leading to enhanced ubiquitination and proteasomal degradation of TxNIP (Shao *et al.,* 2010). Moreover, carbohydrate response element binding protein (ChREBP) and nuclear coactivator p300 have also been implicated in regulation of TxNIP levels in response to glucose in separate studies (Minn *et al.,* 2005; Cha-Molstad *et al.,* 2009). cJun-N-terminal kinase (JNK), activation has been reported to deteriorate pancreatic β-cell function (Kaneto *et al.,* 2005), and was attenuated in response to exendin-4 treatment, probably in a cAMP/PKA-dependent manner accompanied by a reduction in the activation of glycogen-synthase kinase-3β (GSK3β) (Kim *et al.,* 2010). In addition to this, exendin-4 was revealed to promote β-cell protection through activation of the Akt pathway and by improving mitochondrial function (Fan *et al.,* 2010).

GLP-1 also provides protection against cell death, both apoptosis and necrosis, induced by advanced glycation end products (AGE), by attenuating AGE-induced expression of RAGE (receptors for advanced glycation end products), restoring the redox balance, improving responsiveness to glucose (Puddu *et al.,* 2010) and by reversing the detrimental effects of AGEs on transcription factors such as nuclear factor erythroid-derived-2 (Nrf2), Pdx1 and MafA (Puddu *et al.,* 2013). Moreover, GLP-1R activation has been shown to provide a mechanism for β-cell adaptation to metabolic and cellular stress by regulating pancreatic endoplasmic reticulum kinase (PERK), an unfolded protein response (UPR) to endoplasmic reticulum (ER) stress, potentiated induction of ATF-4, attenuating biochemical markers of ER stress and attenuating translational downregulation of insulin leading to improved cell survival (Yusta *et al.,* 2006) (Figure 1.7).

Apart from these mediators activated in response to GLP-1 and its analogues, other key factors that regulate proliferation and β-cell survival in response to various mitogenic signals such as glucose and growth factors, can also be predicted to play a role in GLP-1R signalling mediated events. Some of these identified players include cell cycle regulators such as cyclinD2 (Salpeter *et al.,* 2010), cyclinA2 and cyclinE1 (Metukuri *et al.,* 2012), zinc transporter ZnT8 (Egefjord *et al.,* 2009), and carbohydrate response element-binding protein (ChREBP; MIxipl) (Metukuri *et al.,* 2012).

While these studies outline many signalling effectors that may contribute to GLP-1R signalling leading to these physiologically important effects in the pancreas, it is unclear, how all these functions are relevant in relation to one another and if there is interplay and crosstalk between the various signalling proteins to exert the effects mediated by GLP-1.

1.6.3.4 Signalling mechanisms of GLP-1R in extra-pancreatic tissues

The expression of GLP-1R in extra-pancreatic tissues is still under discussion due to lack of specific antibodies targeted to GLP-1R (Panjwani *et al.,* 2013). Furthermore, two different thoughts exist regarding the downstream coupling of functional GLP-1R in these tissues. Some studies support the coupling of GLP-1R to the cAMP-PKA pathway (Ding *et al.,* 2006; Gupta *et al.,* 2010; Ayala *et al.,* 2010; Svegliati-Baroni *et al.,* 2011), while a few other studies have identified generation of inositol phosphoglycans as secondary intermediates (Trapote *et al.,* 1996; Marquez *et al.,* 1996, 1998).

GLP-1R dependent reduction in hepatic gluconeogenesis, enhanced insulin-dependent and independent uptake of glucose, and augmented fat oxidation in hepatocytes has been attributed to PI3K/PKB, and PKC mediated increases in mRNA expression and activity of glycogen synthase α, (Morales *et al.,* 1997; Redondo *et al.,* 2003), increased activation of p70s6K and MEK/MAPK (Redondo *et al.,* 2003), cAMP-dependent activation of Akt, AMPK, reduced expression of SREBP-1 (Ayala *et al.,* 2010), and attenuated hepatic expression of PEPCK, glucose-6-phosphatase and fatty acid synthase (Lee *et al.,* 2007). Furthermore, activation of GLP-1Rs has been shown to upregulate the expression of PPARα with subsequent activation of its downstream targets acetyl Co-A oxidase-1 palmitoyl (ACOX-1) and carnitine palmitoyl transferase 1A (CPT-1A) (Svegliati-Baroni *et al.,* 2011), and attenuate expression of acetyl Co-A carboxylase (ACC), SREBP-1c, Stearoyl Co-A desaturase-1(SCD-1) (Ding *et al.,* 2006), which promote β-oxidation of fatty acids and reduce hepatic lipogenesis. Activation of 3-

phosphoinositide-dependent kinase-1 (PDK-1) and phosphorylation of PKCζ elicited enhanced GLUT2 synthesis promoting glucose uptake and increased AKT phosphorylation, resulting in inhibition of glycogen synthase kinase-β (GSK-β), thus attenuating glycogen and fatty acid synthesis (Gupta *et al.*, 2010; Moreno *et al.*, 2012).

In adipose tissues, activation of PI3K, p44/p42 MAPK (ERK1/2), PKCβII and p70s6 kinase, and altered expression of GLUT4 have been identified to regulate lipogenesis, glucose and lipid metabolism (Sancho *et al.*, 2005, 2007), adipocyte formation and differentiation (Challa *et al.*, 2012 and improve glucose uptake and metabolism in adipocytes (Moreno *et al.*, 2012). GLP-1R dependent attenuation of transcription factor NFκB, secretion and expression of adiponectin, reduction in inflammatory adipokines, monocyte chemoattractant protein-1 (MCP-1), inflammatory cytokines IL-6, TNFα (Arkan *et al.*, 2005; Le *et al.*, 2009; 2012) were suggested to underlie the anti-inflammatory processes and attenuated macrophage infiltration in adipocytes.

The natriuretic and diuretic effects of GLP-1 and its analogues have been attributed to the increased phosphorylation of Na^+/H^+ exchanger NHE3, at PKA consensus sites 552 and 605, which modulates sodium homeostasis and alters both hemodynamics and tubular function such as increases in bicarbonate excretion, glomerular filteration rate, urine outflow in diabetic and transgenic mice (Schlatter *et al.*, 2007; Carraro-Lacroix *et al.*, 2009; Mima *et al.*, 2012; Crajoinas *et al.*, 2010; Reig *et al.*, 2012). PKA-independent signalling via activation of cAMP-dependent guanine nucleotide exchange protein (Epac) has also been identified as contributing to attenuated sodium reabsorption (Carraro-Lacroix *et al.*, 2009). The renoprotective effects of GLP-1 and its analogues have been observed to be mediated by attenuation of oxidative stress and inflammatory response, probably by reducing the expression of transforming growth factor-β1 (TGF-β1), caspase 3, enhancing the expression of PPAR-α, which plays a role in preventing lipid accumulation and attenuated accumulation of type IV collagen, which probably would result in suppression of macrophage infiltration (Park *et al.*, 2007), suppressing expression of receptors for advanced glycation end products (RAGE) and reducing expression of MCP-1 and ICAM-1 (Ishibashi *et al.*, 2011; Ojima *et al.*, 2011).
Even though the signalling mechanisms underlying osteogenic, anti-resorptive and anti-osteoporotic effects of GLP-1 are not well-elucidated, it is hypothesized to be cAMP/PKA dependent. Late markers of bone formation such as osteocalcin (OC) and collagen type 1 (Col1) and early markers of osteogenesis such as alkaline phosphatase (ALP) and Runt-related transcription factor 2 (Runx-2) were

shown to be upregulated in response to continuous infusion of GLP-1 and exendin-4 in diabetic rats (Nuche-Berenguer *et al.,* 2010a; Ma *et al.,* 2013). Increased mRNA expression of LRP5 (co-receptor for Wnt proteins and necessary for activation of Wnt signalling) (Nuche-Berenguer *et al.,* 2010a), increased ratio of osteoprogeterin (OPG) and receptor activator of NFκB ligand (RANKL) gene expression (that represents inhibition of osteoclastogenesis; Nuche-Berenguer *et al.,* 2010a; Ma *et al.,* 2013), downregulation of sclerostin (SOST- inhibitor of LRP5 activity) (Kim *et al.,* 2013), and modulated gene expression levels of DKK1, another inhibitor of LRP5 activity (Nuche-Berenguer *et al.,* 2010a) have been reported to promote osteoblast formation and reduce osteoclast generation in response to chronic treatment with GLP-1/exendin-4.

A few studies have investigated the role of exendin-4 in diabetic retinopathy so as to explore the underlying mechanisms. Neuroprotective effects of exendin-4 were attributed to the increased expression of Bcl2, reduced expressions of Bax, and attenuated levels of excitatory amino acid, glutamate (Zhang *et al.,* 2011). In the lung, activation of PKA, PKC and calcium-calmodulin-dependent kinase have been identified as three different signalling pathways that promote phosphatidylcholine, thus promoting surfactant secretion (Benito *et al.,* 1998; Vara *et al.,* 2001).

1.7 GLP-1R ligands

1.7.1 Endogenous GLP-1R peptide ligands

There are multiple endogenous ligands that target and activate the GLP-1R. GLP-1 is secreted in the gastrointestinal tract and pancreas (Orskov *et al.,* 1994), and exists in four different forms; full length peptide GLP-1(1-37) and a processed form GLP-1(7-37), each of which has an amidated form GLP-1(1-36)NH_2 and GLP-1(7-36)NH_2 (Drucker *et al.,* 1987). Physiological plasma level of GLP-1(7-36)NH_2 range from 5-10 pmol/L during fasting state to 15-30 pmol/L after meal ingestion (Vilsboll *et al.,* 2001). Processed peptides are more potent insulinotropic agents compared to full-length peptides (Drucker *et al.,* 1987) (Figure 1.8).

Oxyntomodulin (OXM), a member of the glucagon family of peptides, is a 37 amino acid peptide co-secreted with GLP-1 from intestinal L-cells in response to food intake (Mayo *et al.,* 2003)) and, like GLP-1, is also degraded by DPPIV. Oxyntomodulin is a full agonist of the GLP-1R (Jorgensen *et al.,* 2007; Schepp *et al.,* 1996) and the glucagon receptor (GCGR) (Depigny *et al.,* 1984) for cAMP

accumulation, but has higher affinity for the GLP-1R compared to GCGR. OXM is also a partial agonist for G protein coupled receptor kinase (GRK) 2, β-arrestin1, and β-arrestin 2 recruitment at the GLP-1R, but is a full agonist at recruiting these scaffolding proteins to the GCGR (Jorgensen *et al.*, 2007). In rodents, OXM has been shown to reduce food intake and body weight, increase energy expenditure, and improve glucose metabolism (Baggio *et al.*, 2004; Dakin *et al.*, 2001; Parlevliet *et al.*, 2008). In addition to this, glucagon and GIP also bind to GLP-1R with very low affinity (Thorens 1992; Kim and Egan, 2008).

1.7.2 Exogenous long acting GLP-1R peptide ligands

Currently there are a number of GLP-1 analogues that have been approved or are in clinical trials for treatment of T2DM. GLP-1 itself is not practical for type 2 diabetes therapy because it is rapidly inactivated in circulation resulting in a short biological half-live, therefore requiring repeated administration. There has therefore been substantial effort to extend the half-life of these mimetics for clinical use. By leveraging incretin physiology, a natural regulatory system that coordinates oral nutrient intake with mechanisms of metabolic control, GLP-1R agonists address multiple core defects in the pathophysiology of T2DM. Various long acting and DPPIV resistant analogues are being synthesized including exenatide (exendin-4), lixisenatide, liraglutide, dulaglutide, taspogltide, albiglutide (Figure 1.8), however only three including exenatide, liraglutide and dulaglutide have been approved by FDA for the management of metabolic disorder.

Exendin-4, the naturally occurring form of exenatide, was originally isolated from the salivary secretions of the lizard Heloderma suspectum (Eng *et al.*, 1992; Chen *et al.*, 2006). Exendin-4 gained interest as a potential development candidate for diabetes therapy after a number of nonclinical discoveries (1) First, exendin-4 has a 53% amino acid sequence overlap with mammalian GLP-1 (Eng *et al.*, 1992); (2) Second, seminal discovery was that exendin-4 is resistant to degradation by DPPIV due to an amino acid difference in position 2, where Ala2 is substituted by Gly2 (Deacon *et al.*, 1995; Kieffer *et al.*, 1995); (3) Third, exendin-4 and GLP-1 share many glucoregulatory actions mediated by the GLP-1R (Goke *et al.*, 1993). The GLP-1R has been demonstrated to bind exendin-4 and GLP-1 with equal affinity *in vitro*, and both peptides stimulate the receptor equipotently (Goke *et al.*, 1993; Thorens *et al.*, 1993).

Furthermore, exendin-4 is also stable to ectopeptidases, as it lacks many of the neutral endopeptidase substrate sites found in GLP-1 (Hupe-Sodmann *et al.,* 1995). These properties give exendin-4 a half-life of around 2.4 h *in vivo* and a clinical effect lasting up to 8 h (Kim *et al.,* 2007). It possesses an *in vitro* half-life in plasma of around 9.6 h, as a result of proteolytic digestion with principal proteolytic sites between Thr5 and Phe6 (T5-F6), Phe6 and Thr7 (F6-T7) and Thr7 and Ser8 (T7-S8) (Chen *et al.,* 2007; Liao *et al.,* 2015) and degradation (metabolism/elimination) of the peptide in liver and kidney (Arnes *et al.,* 2009). The ability of exendin-4, like all GLP-1 mimetics, to stimulate insulin secretion in a glucose-dependent manner minimises the risk of producing hypoglycaemia, compared to other non GLP-1R agents that stimulate insulin release, such as sulphonylureas.

The pharmacology of exenatide has been investigated extensively in nonclinical studies performed by Amylin Pharmaceuticals, Inc., and other independent research laboratories. Physiological actions shared by exendin-4 and GLP-1 in mammalian systems include reduction of hyperglycemia (Nielsen *et al.,* 2004; Young *et al.,* 1999), glucose-dependent enhancement of insulin secretion (Göke *et al.,* 1993; Thorens *et al.,* 1993; Gromada *et al.,* 1997) and insulin biosynthesis (Alarcon *et al.,* 2006), glucose-dependent suppression of inappropriately high glucagon secretion (Silvestre *et al.,* 2003; Nielsen *et al.,* 2004), slowing of gastric emptying (Nielsen *et al.,* 2004; Linnebjerg *et al.,* 2008) promotion of satiety, reducing food intake, reducing fat deposition and reducing body weight (Szayna *et al.,* 2000; Mack *et al.,* 2006; Washington *et al.,* 2010; Primeaux *et al.,* 2010). Exendin-4 also promotes β-cell proliferation and islet neogenesis from precursor cells in both in vitro and in vivo models (Young *et al.,* 1999; Xu *et al.,* 1999; Song *et al.,* 2008; Xue *et al.,* 2010). Thus, in addition to improving metabolic control, with the potential to reduce long-term diabetic complications, exenatide also has the potential to prevent the progressive loss of β-cell function and β-cell mass (Maida *et al.,* 2009; Pérez-Arana *et al.,* 2010; Wang *et al.,* 2010) associated with type 2 diabetes (reviewed in Gallwitz, 2006; Furman, 2012; Parkes *et al.,* 2013).

Exenatide (synthetic exendin-4) has been developed as a first-in-class therapy for T2DM in both immediate- and extended-release formulations. Real-world clinical experience has supported the value of exenatide in the treatment of T2DM, and this drug is now included as a recommended therapy in the American Diabetes Association (ADA) and the European Association for the Study of Diabetes (EASD) treatment algorithm.

Liraglutide is based on the mammalian GLP-1 sequence with a glutamate and 16 carbon fatty acid conjugated to the ε-amino group of Lys26 and a substitution of Lys34 with Arg. This modification increases albumin binding to 99%, thus protecting liraglutide from DPPIV degradation and giving it an 11-13 h half-life.Taspoglutide is also based on mammalian GLP-1 with substitution of Ala8 and Ala35 with methylated derivatives, thus protecting the peptide from DPPIV and giving a half-life of 10 h. Albiglutide uses 2 molecules of Gly8 substituted GLP-1 sequences covalently coupled to human albumin and have a half-life of 6-8 days. Dulaglutide uses 2 molecules of a position 8 Val substituted GLP-1 sequence fused via a linker to the human IgG4-Fc domain and has a half-life of 4 days. Lastly, exenatide-LAR is a microsphere formulated extended release formulation of exendin-4 that is suitable for once a week injection. Clinically, all GLP-1 mimetics are better at lowering fasting and post prandial plasma glucose, glycosylated haemaglobin levels and weight compared with DPPIV inhibitors (Arnolds *et al.,* 2010; Pratley *et al.,* 2010; Berg *et al.,* 2011; Pratley *et al.,* 2011) (Figure 1.8).

Figure 1.8: Amino acid sequence of various GLP-1 mimetics. The four endogenous forms of GLP-1, two of which are glycine extended at the C-terminus (GLP-1(1-37) and GLP-1(7-37)), and two of which are C-terminally amidated (NH_2) (GLP-1(1-36)NH_2 and GLP-1(7-36)NH_2). DPPIV degradation of GLP-1 yields N-terminally truncated metabolites GLP-1(9-37) and GLP-1(9-36)NH_2. The endogenous agonist exogenous agonists share high homology in the N-terminal region of the peptide, highlighted in red. Liraglutide is based on the mammalian GLP-1 sequence with a glutamate and 16 carbon fatty acid conjugated to the ε-amino group of lysine26 palmitoyl) a glutamate linker (E in circle) and a substitution of lysine34 with arginine. Dulaglutide is a genetic fusion of GLP-1 via a linker (pink) to the Fc domain of human IgG4 (blue). Albiglutide is a genetic fusion of a GLP-1 concatamer to human albumin. Taspoglutide is also based on mammalian GLP-1 with substitution of Ala8 and Ala35 with methylated derivatives α-aminoisobutyric acid (Aib), α-dimethyl-substituted non-natural amino acid with D-amino acid structural characteristics and therefore protects the surrounding peptide bonds against proteolysis.

1.7.3 Non-peptide and allosteric ligands of GLP-1R

All the therapeutic ligands of the GLP-1R are peptides. Thus, there have been continuous efforts on the development of small molecules that have better stability compared to peptides allowing an oral route of administration. Many small molecule ligands have been identified through high throughput screening of compound libraries. These include T0632 (Tibaduiza *et al.,* 2001), 6,7-dichloro-2-methylsulfonyl-3-N-tert-butylaminoquinoxaline (DMB) (Irwin *et al.,* 2010), Boc5, S4P (Chen *et al.,* 2007; Su *et al.,* 2008), WB4-24 (Liu *et al.,* 2011), Eli Lilly compound B/BETP (Sloop *et al.,* 2010), Novo Nordisk Compound 2 (Knudsen *et al.,* 2007) and Transtech Pharma TTP054 (Figure 1.9).

T0632 has been shown to have significant affinity for GLP-1R and appears to allosterically block receptor function by inhibiting GLP-1 induced cAMP production (Tibaduiza *et al.,* 2001). DMB, a non-peptide quinoxaline compound, is an agonist and an allosteric modulator of GLP-1R signalling. It has been demonstrated to induce GLP-1R mediated cAMP production and potentiate GSIS (Irwin *et al.,* 2010). Boc5, WB4-24 and S4P are cyclobutane derivatives. Boc5 dose-dependently amplifies GSIS, inhibits food intake, improves glucose tolerance, reduces body weight and induces satiety at higher doses (Chen *et al.,* 2007; Su *et al.,* 2008). WB4-24 was observed to possess more potent activities compared to Boc5 (Liu *et al.,* 2011). BETP (Compound B; 4,3(benzyloxyphenyl)-2-ethylsulfinyl-6-trifluoro-methyl) pyrimidine) is a pyrimidine based compound that possess the ability to activate GLP-1R signalling alone and can allosterically modulate GLP-1 peptide signalling. It has been investigated in normal and diabetic human islets and shown to promote receptor mediated cAMP signalling and dose-dependent GSIS (Sloop *et al.,* 2010). Furthermore, the quinoxaline compound, Compound 2 (N-tert-butyl-6,7-dichloro-3-methylsulfonyl-quinoxalin-2-amine) also elicits glucose-dependent insulin secretion in vivo (Knudsen *et al.,* 2007). Quercetin, a natural flavonoid, was shown to positively modulate the affinity and efficacy of GLP-1R (Koole *et al.,* 2010, Wootten *et al.,* 2011; Schann *et al.,* 2009).

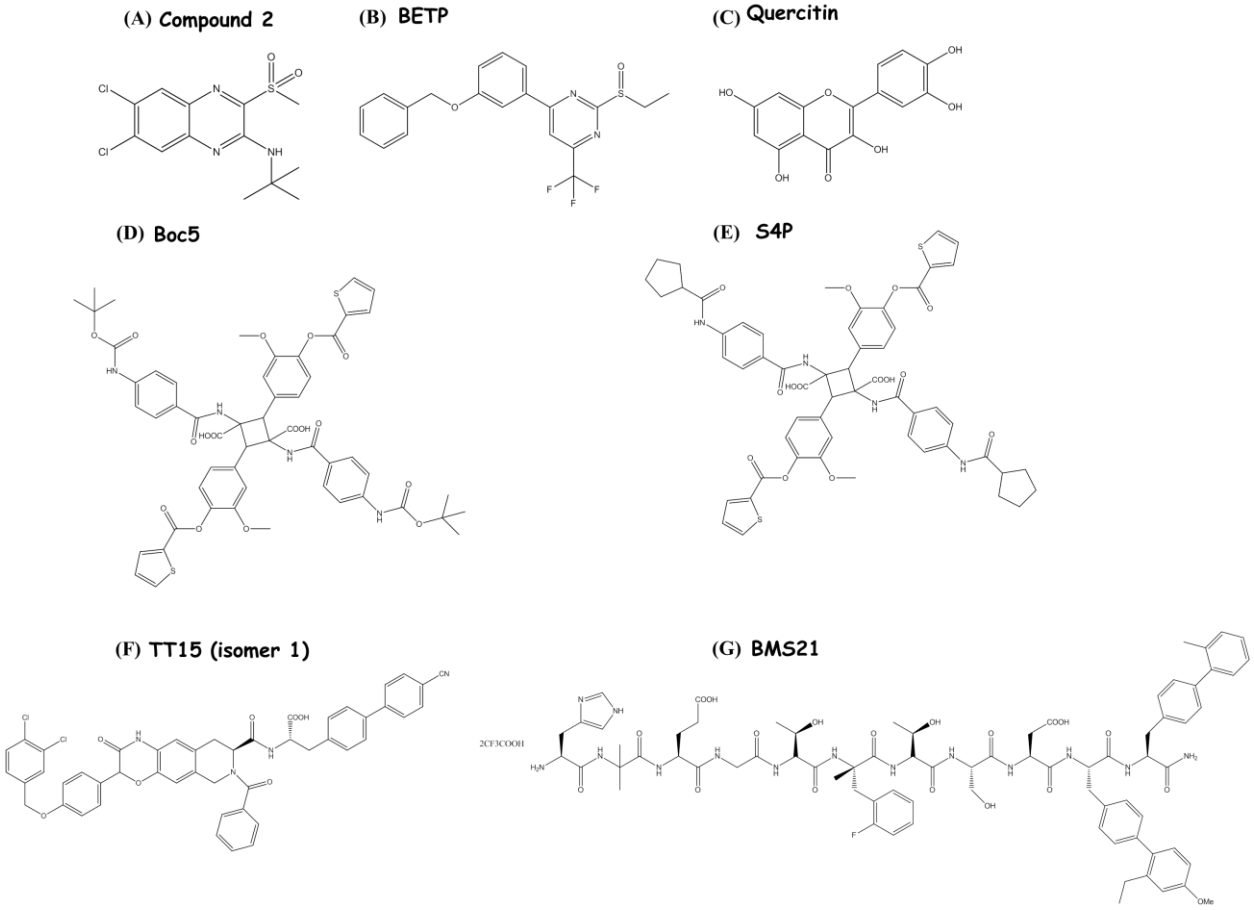

Figure 1.9: Small molecule synthetic ligands of the GLP-1R. Structures of small molecule ligands that are documented to bind to GLP-1R. (A) compound 2, (B) BETP, (C) Quercitin, (D) Boc5, (E) S4P) (F) TT15 and (G) BMS21 (adapted from Koole *et al.*, 2010 and Wootten *et al.*, 2013).

1.8 GLP-1R biased signalling and allosteric modulation

1.8.1 Biased signalling by orthosteric and allosteric agonists

Despite having a high degree of sequence conservation, the different ligands display markedly different clinical effects (Pabreja *et al.,* 2014), which may, in part, be attributed to the combination of ligand-directed signalling bias and the ability of GLP-1R to pleiotropically couple to multiple G proteins and regulatory molecules. Additionally, these different ligands have the potential to engender unique receptor conformations, giving rise to distinct signalling profiles. All GLP-1R peptide ligands preferentially activate cAMP over ERK1/2 phosphorylation and Ca^{2+} mobilization, however the relative degree of bias varies (Koole *et al.,* 2010). For example processed GLP-1 peptides and exendin-4 are strongly biased towards cAMP over ERK1/2 phosphorylation, whereas in comparison oxyntomodulin and the full length GLP-1 peptides are more weakly biased towards cAMP when compared to pERK1/2. Therefore, this provides the possibility that distinct agonists can direct cellular signalling with unique precision and specificity.

There has been significant interest from pharmaceutical companies for the development of small molecule ligands of GLP-1R for the treatment of type II diabetes. Because the endogenous ligands for the GLP-1R are peptides, it is unlikely that small molecule agonists will bind in a similar way to the GLP-1R. Small molecule agonists of the GLP-1R have been identified to be biased ligands of GLP-1R function in comparison to GLP-1 (Wootten *et al.,* 2013). Small molecules such as Compound 2 and BETP (that interact with the intracellular face of the GLP-1R) are heavily biased towards recruitment of β-arrestin over G protein-mediated signalling relative to equivalent levels of cAMP, when compared to GLP-1 peptides. In addition, small agonists such as Boc5 and BMS21 displayed bias towards ERK1/2 phosphorylation and Ca^{2+} mobilisation compared to GLP-1 peptide ligands (Wootten *et al.,* 2013). Thus, this phenomenon provides the potential to develop ligands that can fine tune physiological responses at the GLP-1R.

1.8.2 Allosteric modulation at the GLP-1R

Stimulus bias is further complicated when allosteric modulators are considered because conformational preferences of the receptor when allosteric and orthosteric binding sites are co-occupied may be different from when either site is individually occupied. Indeed, data from our lab has shown that the allosteric ligand, compound 2, which is both an agonist of the GLP-1R and a modulator of orthosteric agonist function, exhibits selective modulation of specific peptide agonists and engenders stimulus bias at GLP-1R with greatest effect on cAMP accumulation mediated by oxyntomodulin and weaker effect on processed GLP-1 peptides, and on other pathways (Koole *et*

al., 2010). However, this potentiation of oxyntomodulin efficacy occurs in a pathway-dependent manner, with augmentation of cAMP signalling and β arrestin recruitment and no effect on ERK1/2 phosphorylation or Ca^{2+} signalling (Koole *et al.,* 2010). In addition, BETP strongly potentiates oxyntomodulin-mediated cAMP signalling at the GLP-1R, whereas has only a limited ability to potentiate of GLP-1 or exendin-4. As with compound 2, this potentiation from BETP occurs in a pathway-dependent manner altering cAMP, β arrestin recruitment and calcium, but not pERK1/2. Interestingly, both allosteric compounds selectively enhance β arrestin recruitment by GLP-1 and exendin-4, despite no change in cAMP, pERK1/2 and Ca^{2+} signalling (Wootten *et al.,* 2013). In addition, BETP and compound 2 can potentiate the metabolite of GLP-1, GLP-1(9-36)NH_2 mediated cAMP accumulation and in the case of BETP, there is also evidence for enhanced glucose dependent insulin secretion (Wootten *et al.,* 2012). Hydroxyflavonols, such as quercetin, can also potentiate the effects of high affinity GLP-1R peptides, however, they do so in a pathway-dependent manner where only Ca^{2+} mobilisation is enhanced, with no effect on formation of cAMP or ERK1/2 phosphorylation (Koole *et al.,* 2010, Wootten *et al.,* 2011).

Therefore, due to the potential of peptide and small molecule agonists to display signal bias, when cobound, there is the potential for some pathways to be selectively modulated (either positively or negatively) at the expense of others. Thus, in order to understand any potential stimulus bias at GLP-1R, it is preferred to investigate the effect of allosteric modulations at several different signalling and/or regulatory pathways.

1.9 Type 2 diabetes and the GLP-1R

1.9.1 Diabetes Mellitus

Type 2 diabetes is emerging as a global epidemic, with its prevalence increasing exponentially (Davidson, 2009). The number of people globally with diabetes mellitus is projected to rise to 439 million by 2030, which represents 7.7% of the total adult population of the world aged 20–79 years (Shaw *et al.,* 2010; Chen *et al.,* 2012). The American Association of Clinical Endocrinologists (AACE) describes type II diabetes mellitus as “a progressive, complex metabolic disorder characterized by coexisting defects of multiple organ sites including insulin resistance in muscle and adipose tissue, a progressive decline in pancreatic insulin secretion, unrestrained hepatic glucose production and other hormonal deficiencies” (AACE Diabetes Mellitus Clinical Practice Guidelines Task Force, 2007). Other defects include accelerated gastric emptying (Weytjens *et al.,* 1998; Bertin *et al.,* 2001), accelerated lipolysis, hyperglucagonemia and incretin deficiency/resistance (DeFronzo, 2009).

A decrease in β-cell mass plays a significant role in the pathogenesis of type II diabetes (Butler *et al.,* 2003; Kahn, 2003), as it does in rodent models of the disease (Kaiser *et al.,* 2003; Rhodes, 2005). Since it is not possible to measure β-cell mass in *vivo* in humans noninvasively, it still remains unclear whether the type II diabetic patients had a lower β-cell mass early in life, failed to increase their β-cell mass due to insulin resistance or had a progressive β-cell loss. Moreover, the contributing factors responsible for reduced β-cell mass also need to be uncovered. In addition, it is essential to explore the underlying mechanisms as to how the administration of exogenous GLP-1 and its analogues recover the lost β-cell mass in type II diabetics. Despite the fact that there are important differences between rates and capacity for islet cell turnover and growth between rodents and humans (Butler *et al.,* 2007), rodent models are widely used to elucidate these unknown mechanisms. Various studies have demonstrated the augmentation of β-cell proliferation and attenuation of β-cell apoptosis in pancreatic islets after the administration of GLP-1 and its analogues in diabetic rodents (Farilla *et al.,* 2002; Wang *et al.,* 2002; Li *et al.,* 2003; Buteau *et al.,* 2006).

1.9.2 The GLP-1R as a therapeutic target for type 2 diabetes

The current treatments that aim to improve glycaemic control comprise orally active anti-diabetic drugs such as pioglitazones, rosiglitazones, metformin, sulfonylurea and non-sulfonylurea drugs. However, side-effects such as weight gain and hypoglycaemia diminish the benefits of available oral anti-diabetic drugs. Thus, the development of therapeutic agents that could amplify insulin secretion without hypoglycaemia and weight gain is highly desired.

Until recently diabetes was conceptualized in terms of the predominant defects in insulin secretion and insulin action. Evolving understanding of the pathogenesis of type II diabetes has highlighted another important abnormality at the forefront of diabetes research, which is the decreased incretin effect due to impairments in secretion and action of the incretin hormones glucagon-like peptide-1 (GLP-1) and glucose-dependent insulinotropic peptide (GIP) (Nauck *et al.,* 1986; Pratley and Gilbert 2008).

The receptors for the incretin hormones are very promising targets for type 2 diabetes due to their insulinotropic properties. In type 2 diabetic patients, the insulinotropic action of GIP is reduced. The functions of the GLP-1R are preserved, but the secretion of GLP-1 is diminished. GLP-1 administration significantly lowers blood glucose levels during fasting and after eating, and is associated with weight loss and a decreased rat of gastric emptying, thereby promoting satiety. In

addition, diabetic rats displayed consistent increases in β-cell mass following GLP-1 treatment. Therefore, methods of enhancing either circulating concentrations of GLP-1 and/or GLP-1R function offer attractive avenues for therapeutics for type 2 diabetes. This research paved the way for the development of promising new generation anti-diabetic drugs that include GLP-1 receptor agonists such as exenatide, liraglutide, albiglutide amongst which exenatide and liraglutide have been approved by the FDA in 2005 and 2009, respectively.

1.9.3 Currently approved incretin threapies for T2DM.

The therapeutic usefulness of GLP-1 (peptide) is limited by its metabolic instability. Thus, therapeutic strategies for increasing active GLP-1 concentrations include DPPIV resistant GLP-1 mimetics such as exenatide and liraglutide, or DPPIV inhibitors such as vildagliptin and sitagliptin are approved as monotherapies and/or adjuvant drugs with oral antidiabetics depending on the country of approval. Approved DPPIV inhibitors (known as gliptins) show very good selectivity for DPPIV over the structurally related enzymes DPP8 and DPP9 (Brandt *et al.,* 2005; Feng *et al.,* 2007; Kim *et al.,* 2005a; Wang *et al.,* 2012). DPPIV inhibitors produce modest changes in circulating levels of active GLP-1 (GLP-1(7-36)NH_2) ranging from 2-4 fold depending on the study (Ahren *et al.,* 2004, Dai *et al.,* 2008, Henry *et al.,* 2011, Herman, *et al.,* 2005). Although the available data indicate that DPPIV inhibition is a promising treatment for type 2 diabetes, there are concerns that prolonged inhibition of DPPIV activity could lead to adverse side effects. To date only a few endogenous substrates have been identified for DPPIV based on (1) *in vitro* cleavage that occurs at penultimate L-proline or L-alanine residues (Kenny *et al.,* 1976) and (2) cleavage products observed *in vivo* that are absent in the presence of selective inhibitors or $DPPIV^{-/-}$ mice (reviewed in Weber, 2004), however it is unclear how well DPPIV degradation of putative substrates has been examined. Some known and putative *in vivo* substrates of DPPIV include substance P (Heymann and Mentlein, 1978; Kato *et al.,* 1978), neuropeptide Y (Mentlein *et al.,* 1993a), peptide YY (Mentlein *et al.,* 1993a; Michel *et al.,* 1998; Keire *et al.,* 2002), endmorphins (Bird *et al.,* 2001; Sakurada *et al.,* 2003), pituitary adenylate cyclase activating polypeptide 38 (PACAP 38) (Lambier *et al.,* 2001; Zhu *et al.,* 2003; Ahren and Hughes, 2005); GLP-1 and GIP (Mentlein *et al.,* 1993b; Kieffer *et al.,* 1995; Marguet *et al.,* 2000), GLP-2 (Drucker *et al.,* 1997; Hartmann *et al.,* 2000a,b; Tavares *et al.,* 2000) and various chemokines such as CCL5 (Regulated on Activation, Normal T-cell Expressed and Secreted, RANTES) (Oravecz *et al.,* 1997; Proost *et al.,* 1998a; Khin *et al.,* 2003), CCL11 (eotaxin) (Struyf *et al.,* 1999; Oravecz *et al.,* 1997), CCL22 (Macrophage derived Chemokine, MDC) (Proost *et al.,* 19999), CCL3L1 (LD78β) (Proost *et al.,* 2000) and CXCL12 (Stromal-Cell-Derived Factor 1, SDF-1) (Ohtsuki *et al.,* 1998; Proost *et al.,* 1998b; Busso *et al.,* 2005). Thus, inhibition of DPPIV could potentially extend the circulating half-

lives of these biologically active peptides, which might conceivably affect/modulate vasoreactivity, nociception, energy homeostasis (food intake, lipid metabolism, thermogenesis, and glucose control), proliferation, angiogenesis, immune response, behavioural stress response, gastrointestinal motility and growth.

Approved GLP-1 analogues that include long acting and DPPIV resistant analogues of GLP-1 such as exenatide, liraglutide and dulaglutide, are very selective for GLP-1R activation and do not suffer from the potential off target effects of DPPIV inhibitors. Clinically, GLP-1 mimetics are better at lowering fasting & post prandial plasma glucose, glycosylated haemaglobin levels and weight (Arnolds *et al.,* 2010, Buse *et al.,* 2009, DeFronzo *et al.,* 2008, and Pratley *et al.,* 2011). A larger number of patients report gastrointestinal effects such as nausea and vomiting with GLP-1 mimetics compared to DPPIV inhibitors, although this disappears over about 3 weeks and can be lessened by ascending dosing strategies. In addition, the GLP-1 mimetic liraglatide appears to display better efficacy and reduced side effect profile compared with exenatide (Buse *et al.,* 2010).

Exenatide (Byetta ®), a synthetic version of exendin-4 has been approved by the FDA for the treatment of T2DM. Exenatide administrated parenterally reduces HbA1c, increases insulin secretion and preserves β-cell function. Similar to GLP-1 it suppresses inappropriate glucagon secretion, slows postprandial gastric emptying and suppresses appetite with longer term effects on weight reduction (DeFronzo *et al.,* 2005; Uccellatore *et al.,* 2015).

Liraglutide (Victoza®) is a human GLP-1 analog in which lysine 34 is substituted with arginine, and lysine 26 has a C16 acyl chain attached (Vilsboll, 2007). These modifications improve the absorption and extend the half-life compared to native GLP-1, allowing once-daily administration. After subcutaneous administration, maximum concentrations are achieved in 9–14 h, and the half-life is 13 h (Agerso *et al.,* 2002]. Reductions in HbA1c ranged from 0.6% to 1.6% in clinical trials of liraglutide administered once-daily at 0.6 to 1.8 mg, alone or in combination with other agents (Garber *et al.,* 2009; Marre *et al.,* 2009; Uccellatore *et al.,* 2015).

Exenatide and liraglutide have provided better glycemic control and gastrointestinal tolerance than other anti-hyperglycemic drugs in comparative studies. Exenatide LAR was more effective than maximum-labeled doses of exenatide twice-daily (Drucker *et al.,* 2008), sitagliptin and pioglitazone (Bergenstall *et al.,* 2010], and insulin glargine (Diamant *et al.,* 2010) in patients treated with oral anti-hyperglycemic drugs (Uccellatore *et al.,* 2015).

Dulaglutide (Trulicity, Eli Lily) is the fifth GLP-1R agonist approved for T2D in the United States on September 18, 2014. It is an attractive option because it is dosed once-weekly (subcutaneously), provides A1C lowering similar to liraglutide, weight loss similar to twice-daily exenatide, and GI adverse effects similar to both liraglutide and exenatide. Dulaglutide consists of 2 GLP-1 analogues that have been linked to a human immunoglobulin class 4 constant fragment (Barrington *et al.*, 2011a). This reduces the renal clearance of the drug because of the increased size of the protein (59.7 kDa) (Barrington *et al.*, 2011a). The amino acid sequence has been modified in both GLP-1 analogues at positions 8, 22, and 26 to protect the molecule from DPPIV hydrolysis (Barrington *et al.*, 2011a). Dulaglutide increases insulin secretion and decreases glucagon secretion in a glucose-dependent manner by acting as an incretin mimetic, slows gastric motility and promotes satiety (Barrington *et al.*, 2011b). Both pre-prandial and post-prandial blood glucose levels are decreased with the use of dulaglutide. Dulaglutide offers the advantage of being a once-weekly medication, but it has not been compared in head-to-head studies with the other 2 once-weekly GLP-1R agonists (Thompson and Trujillo, 2015).

The GLP-1 mimetics liraglutide and exenatide have been associated with nausea and acute pancreatitis in several patients. Liraglutide has also been associated with thyroid C-cell hyperplasia in rats (a precursor for thyroid cancer; Drucker *et al.*, 2010). In addition, GLP-1R analogues are peptides that are required to be administered by subcutaneous injection, which has low patient compliance compared to oral therapies. Exploration of alternative treatments, in particular small molecule allosteric ligands that target the GLP-1R are currently being pursued by the pharmaceutical industry as the ideal therapeutic approach to treatment of T2DM.

1.10 Future directions for GLP-1 based therapeutics and challenges facing discovery

In general, GLP-1 peptide mimetics have a mode of action that both promotes beneficial effects, but may also contribute to their side effect profile and tolerability. For example, on one side, they promote insulin secretion, which is physiologically regulated by the prevailing plasma glucose concentration (Nauck *et al.*, 2002), while on the other an important effect is their delay of gastric emptying, which can contribute to nausea (Meier *et al.*, 2003). The challenge to consider when using GLP-1 mimetics is how to combine efficacy and tolerability. Therefore, the balance will be between the effect of the GLP-1 mimetic on glycemic control and the long-term tolerability by patients.

Due to the subcutaneous route of administration and subsequent limited patient compliance, small molecule orally available allosteric modulators for the GLP-1R provide potential advantages. Furthermore allosteric modulators have the potential to maintain spatial and temporal characteristics of endogenous signalling. Allosteric ligands modulate orthosteric ligand binding and/or efficacy through mediating changes in receptor conformation. Furthermore, these molecules would reach saturability of effect thereby preventing the risks of overdose. Their ability to display probe-dependent effects can be both and advantage and a challenge in discovering novel therapeutics. As there are multiple endogenous ligand of the GLP-1R, screening programs need to focus on assessing effects of allosteric ligands at each endogenous ligand to assess the full effects of such ligands, that may occur in vivo. However, this could also be an advantage, as compounds that bind to the receptor but are unable to modulate one endogenous ligand, may have the potential to affect a different endogenous ligand, therefore providing more scope for identifying novel ligands.

The phenomenon of biased signalling also holds great promise. The design of ligands (allosteric or orthosteric) that alter signal bias offers the potential of augmenting physiologically beneficial signalling pathways to the exclusion of detrimental ones and providing a novel mechanism to enhance the positive effects of activating the GLP-1R, but further reducing unwanted side effect profiles (such as those seen with current GLP-1 mimetics). The key challenge however for most GPCRs is a limited understanding around which signalling pathways or combination of pathways are most predictive of the desired therapeutic outcome. So to rationally design biased ligands, a greater understanding of the molecular determinants and conformational dynamics will be required that would contribute to biased signalling upon GPCR activation. Additionally, a detailed understanding of the interplay of allosteric modulation, probe dependence and biased signalling at the GLP-1R could also open avenues for developing drugs to target this receptor that display improved therapeutic profiles, however this also presents a large number of challenges.

1.11 Summary

Previous studies have revealed that the glucagon-like peptides exert an increasing number of physiological actions on regulation of nutrient absorption and assimilation via actions on the gut, pancreas and central nervous system. Moreover, studies linking GLP-1R signalling to preservation of β-cell mass by regulating survival and proliferation mechanisms, have fostered considerable interest in evaluating the efficacy of GLP-1 in the clinic for the management of metabolic disorders including type 2 diabetes and obesity. But the cross-talks in between various proteins and signalling pathways accountable for the physiologically and therapeutically relevant effects downstream of

GLP-1R activation in pancreatic β-islets is still largely not well understood and requires more research to elucidate this.

Allosteric modulation and biased signalling provides opportunity to specifically target receptors and specific signalling pathways mediated by activation of GPCRs. These concepts provide many benefits, such as preserving temporal and spatial endogenous tone while fine-tuning the desired biological signalling outcome and a ceiling effect that can minimize side-effects. However, the allosteric modulators that have intrinsic activity in their own rights also provide an opportunity to activate or diminish GPCR-mediated signalling in the absence of ligands that act at the orthosteric site of action.

Currently for the GLP-1R, there is only limited understanding of which signalling pathway or combination of pathways are important physiologically and less known about the interplay of these pathways, how they are altered in disease and which profile of signalling will be most predictive of the desired therapeutic outcome. This poses key challenges in the design of better and safer therapeutics. The design and identification of ligands that display biased agonism or allosteric modulators that show biased modulatory profiles will help in translating biased profiles of ligands to their in vivo physiological effects. Understanding signalling bias profiles that lead to positive outcomes and further reduce the side-effect profiles of the therapeutics will have many advantages in the drug discovery and development processes.

Although there is evidence for biased signalling and biased modulation leading to therapeutically beneficial outcomes from the GLP-1R, these studies are limited and most of the current information is largely limited to studies in recombinant systems. A detailed understanding of allosteric modulation and biased signalling at a more physiological level is required in order to develop more effective therapeutics to target this system. In addition, as GLP-1 is secreted in presence of elevated glucose levels and that the gluco-regulatory and insulinotropic effects mediated by the activation of GLP-1R are glucose-dependent, performing key experiments exploring these is vital. In addition, GLP-1R peptide agonists are clinically prescribed for the treatment of type 2 diabetes that demands chronic therapy. Consequently, a through and deep investigation is required to understand the effect of chronic exposure on the receptor function and regulation. Investigating these long term regulatory processes of the receptor and its implications related to decreased clinical efficacy over time due to desensitization and up/down regulation of the target receptor would further help in development of new and improved therapeutics.

This thesis is a step in this direction and the results are a stepping stone towards understanding these concepts at a more physiological level for the GLP-1R. A better understanding of these concepts would form a promising platform for the development of more effective GLP-1R therapeutics (agonists or allosteric modulators), which could be developed into safe, well-tolerated formulations with prolonged *in vivo* bioactivity for the implementation of successful GLP-1 therapeutics programs.

CHAPTER 2:

MATERIALS AND METHODS

2.1 Cell culture

2.1.1 Maintenance of Cells

Cell culture was done in PS2 laminar flow hoods (Email Air Handling, NSW, Australia), under sterile conditions with sterilized equipments. Cells were maintained in tissue culture flasks at 37°C in water jacket incubator (Forma Scientific, Oh, USA) at 5% CO_2 and 85% humidity. Cells were allowed to grow in monolayer in the appropriate media. MIN6 cells were grown and maintained in Dulbecco's Modified Eagle's Medium (DMEM) #11995-065 supplemented with 25 mM D-glucose (4.5 g/L), 15% v/v foetal bovine serum (FBS) and 50 µM 2-mercaptoethanol. Rat insulinoma cell lines (INS-1E and INS-1 832/3) were grown and maintained in RPMI 1640 #11879 supplemented with 10% v/v FBS, 1 mM sodium pyruvate, 50 µM 2-mercaptoethanol, 10 mM HEPES, penicillin/streptomycin (50 µg/mL) and 11 mM glucose. The growth conditions and media for INS-1 were the same as other rat insulinoma cell lines except for the glucose concentration which was reduced to 5.5 mM.

Cells were passaged every 2-3 days approximately 20 times before new cells were brought up from the frozen stores. Upon reaching 70-80% confluence, cells were washed twice with sterile phosphate buffered saline (PBS) (sodium chloride 8 g/L, potassium chloride 0.2 g/L, di-sodium hydrogen phosphate 1.15 g/L, potassium dihydrogen phosphate 0.2 g or di-potassium hydrogen phosphate 0.24 g/L) and harvested from tissue culture flasks using versene (PBS with EDTA at 0.196 g/L). Cells were then centrifuged at 350 x g for 3 min, resuspended in media and reseeded into 75 or 175 cm^2 flasks at a dilution of 1:5 and 1:2, as required.

2.1.2 Freezing and thawing cells

The cells were expanded into 5 x T175 cm^2 flasks and upon reaching 70-80% confluence were washed twice with sterile PBS and harvested with versene followed by centrifugation at 350 x g for 3 min. Cells were resuspended in 10 ml freezing solution and 1 mL aliquots were dispensed into 10 cryo-vials (approximately 1 x 10^7 cells/mL). The freezing mix consisted of 90% v/v (total) FBS and 10% dimethylsulphoxide (DMSO). Each cryo-vial was labelled with cell type, date frozen and passage number. Cryo-vials containing cells were placed in isopropanol bath at -80°C for at least 24 h prior to transfer to vapour phase nitrogen storage system.

Cells were brought up from storage by rapid defrosting at 37°C and gently added to 10 mL pre-warmed media in a sterile 50 mL falcon tube, followed by centrifugation at 350 x g for 3 min. The pellet was resuspended in 1 mL pre-warmed media and transferred to a 75 or 175 cm^2 flask. Cells

were allowed to adhere and grow for at least two or three passages prior to use in any assays.

2.1.3 Counting cells

Cells were harvested into 50 mL sterile falcon tube using pre-warmed versene and centrifuged for 3 min at 350 × g. The supernatant was removed and cells were resuspended in 10 mL of appropriate pre-warmed media. The glass haemocytometer and cover slip were thoroughly cleaned using 80% v/v ethanol, and the cover slip was placed over the haemocytometer channels. The cell suspension was diluted appropriately in a 1.5 mL eppendorf tube, using the media such that the trypan blue solution (0.4% solution; 93595-50 mL, Sigma Aldrich) was in a ratio of 1:2 (diluted cell suspension: trypan blue). The stained cell suspension was placed drop-wise on either side of the haemocytometer, allowing the liquid to distribute evenly into the haemocytometer via capillary action. The cells were counted in five squares under the microscope using 20X objective lens and the average cell number per square was determined, which was then multiplied by the dilution factor and 1×10^4 to give cells/mL. The required number of cells was then dispensed into the new flask containing media or seeded in cell culture plates as required and finally placed in the incubator.

2.1.4 Laminin coating of cell culture plates

Laminin L4544 (Sigma Aldrich, St. Louis MO 63103 USA) stock (1 mg/mL) was diluted 200X using PBS (50 µL diluted to 10 ml with PBS). 50 µL diluted laminin (5µg/mL) was added to all the wells of 96 well plates in the laminar flow hood. Plates were placed at room temperature for 4h. The coating solution was flicked off and plates were set aside without lids to dry for couple of hours in the laminar flow hood, followed by UV sterilization.

2.2 cAMP Accumulation

All cAMP studies were performed using an ALPHA (Amplified Luminescent Proximity Homogeneous Assay) Screen cAMP Assay Kit (PerkinElmer, Vic, Australia). The cAMP assay kit contains streptavidin-coated Donor beads, anti-cAMP antibody-coated Acceptor beads, and biotinylated cAMP.

The ALPHA Screen cAMP assay measures the levels of cAMP produced upon modulation of adenylate cyclase activity by GPCRs. It is a competitive assay, where endogenous cAMP produced in the cells upon stimulation with receptor ligands competes with exogenously added biotinylated cAMP for binding to an anti-cAMP antibody conjugated to the acceptor beads. The bio-molecular

interaction between a streptavidin-coated donor bead associated with biotinylated cAMP and anti-cAMP antibody conjugated to acceptor bead, results in the close proximity (no more than 200 nm) of acceptor and donor beads. A highly amplified luminescence signal is generated as a consequence of excitation of donor bead (680 nm) which thereby provokes the release of singlet oxygen molecules that triggers a cascade of energy transfer in acceptor beads resulting in the emission of light at 520-620 nm. But, when the biotinylated cAMP is displaced by endogenous cAMP, this interaction and proximity between the beads is disrupted, singlet oxygen decays and no signals are produced resulting in reduction of signal.

2.2.1 Preparation of 10X Earle's balanced salt solution (EBSS)

10X EBSS contains potassium chloride 4 g/L (53 mM), magnesium sulphate heptahydrate 0.977 g/L (8 mM), sodium chloride 68 g/L (1170 mM), sodium bicarbonate 22 g/L (260 mM) and sodium phosphate monobasic 1.4 g/L (10 mM). Prior to assay, 10X EBSS is diluted to 1X and supplemented with calcium chloride 0.20 g/L (1.8 mM) and required glucose concentration of either 0.05 g/L (2.8 mM) or 0.198 g/L (11 mM).

2.2.2 cAMP accumulation assay

INS-1 832/3 cells were seeded at a density of 3 x 10^4 cells/well/200 µL into laminin coated 96-well cell culture plates and were grown at to a confluence of 85-95% prior to the assay. On the third day of seeding the cells were washed with 1X EBSS supplemented with 1.8 mM $CaCl_2$ and 2.8 mM glucose, pH 7.4 and starved for 90 min in RPMI containing 2.8mM glucose. Subsequently, the cells were washed twice with 1X EBSS and further incubated in 135 µL of stimulation buffer [1X EBSS containing 1.8 mM $CaCl_2$, 2.8 mM glucose, 0.1% (w/v) BSA and 1 mM 3-isobutyl-1-methylxanthine (IBMX), pH 7.4] at 37°C in 5% CO_2 for another 30 min. 10X stock of drugs was prepared in low glucose (2.8 mM glucose) and high glucose (10 X; 82 mM glucose; final 1X high glucose concentration = 11 mM) stimulation buffer. Cells were stimulated for 30 min at 37°C in 5% CO_2 with increasing concentrations of peptide ligand alone, allosteric ligand alone, or simultaneously with increasing concentrations of allosteric ligand and peptide. The reaction was terminated by rapid removal of the ligand containing buffer and addition of 100 µL of ice-cold 100% ethanol.

2.2.3 cAMP detection assay

After ethanol evaporation, 75 µ*L* of lysis buffer [0.1% (w/v) BSA, 0.3% (v/v) Tween 20, and 5 mM HEPES, pH 7.4] was added, and 10 µL of lysate was transferred to a 384-well optiplate (PerkinElmer Life and Analytical Sciences). Five microliters of acceptor bead mix (1.0%

AlphaScreen cAMP acceptor beads diluted in lysis buffer) and 15 µL of donor bead mix [0.3% AlphaScreen cAMP donor beads, 0.025% AlphaScreen cAMP biotinylated cAMP (133 units/µL) diluted in lysis buffer, and pre-incubated for a minimum of 30 min] were added in reduced light conditions. Plates were incubated at room temperature overnight before measurement of the fluorescence using Envision with standard AlphaScreen settings (emission/band width 570/100 nm; total measurement time 550 sec). All values were converted to concentration of cAMP using a cAMP standard curve performed in parallel.

2.3 ERK1/2 Phosphorylation

All ERK1/2 phosphorylation studies were performed using the AlphaScreen *Surefire* ERK1/2 phosphorylation kit TGR bioscinces (Thebarton, South AUstralia). The AlphaScreen® SureFire® ERK1/2 phosphorylation assay is based on an immuno-sandwich assay principle. A phosphorylated cellular protein (analyte) is sandwiched between a streptavidin-coated donor bead associated with an analyte antibody and a Protein A-conjugated acceptor bead associated with an anti-phospho specific antibody. The formation of these sandwich antibody complexes brings the donor and acceptor beads in close proximity (≤200 nm). A highly amplified luminescence signal is generated as a consequence of excitation of donor bead (680 nm) which thereby provokes the release of singlet oxygen molecules (short lifetime, 4 µs in aqueous solutions) that triggers a cascade of energy transfer in acceptor beads resulting in the emission of light at 520-620 nm.

2.3.1 pERK1/2 phosphorylation

INS-1 832/3 cells were seeded at a density of 3 x 10^4 cells/well/200 µL into laminin coated 96-well cell culture plates and allowed to grow to a confluence of 85-95%, prior to the assay. Initial ERK1/2 phosphorylation time course experiments were performed over 90 min to determine the time at which ERK1/2 phosphorylation was maximal/sustained after stimulation by agonists. Assays investigating concentration-response curves were generated by the addition of ligand for the indicated time periods at 37°C. The time of stimulation for concentration-response curves represents the time of peak/sustained response as determined in time course assays.

On the third day of seeding, the cells were washed with 1X EBSS supplemented with 1.8 mM $CaCl_2$ and 2.8 mM glucose, pH 7.4 and starved for 5 h in RPMI 1640 containing 2.8 mM glucose. After 5 h of starvation, the cells were washed and further starved for another 1 h in 135 µL 1X EBSS supplemented with 1.8 mM $CaCl_2$, 0.1% w/v BSA and 2.8 mM glucose, pH 7.4. Cells were stimulated with 15 µL of increasing concentrations of 10X peptide ligand and/or simultaneously with allosteric ligand in low (2.8 mM glucose) and high glucose (10X glucose concentration = 82

mM; final 1X glucose concentration = 11 mM) for the time required to generate an ERK1/2 phosphorylation response. Agonist stimulation of cells was terminated by the removal of buffer (flicking) and the addition of 50 µL of SureFire lysis buffer to each well and stored at -20°C.

2.3.2 ERK detection assay

To perform the ERK1/2 detection, the plates were thawed and agitated for 2 to 5 min on a shaker. 5 µL of lysates were added to each well of a 384-well white proxyplate assay plate. AlphaScreen® SureFire® p-ERK1/2 activation and reaction buffer were brought to room temperature. Activation buffer was diluted 7-fold in reaction buffer; acceptor and donor beads were diluted 70-fold in activation/reaction buffer mix. 8.5 µL of activation/reaction bead mix was added to the lysates in the 384-well proxyplate and covered with TOPSeal-A 384, a clear adhesive sealing film (PerkinElmer, Vic, Australia). Following 90 min incubation at 37°C, 5% CO_2, plates were allowed to rest at room temperature for 30 min. Plates were read on Fusion™ universal microplate analyzer (Packard Bioscience) with standard AlphaScreen settings.

2.4 Insulin secretion

Insulin detection was performed using Homogeneous Time Resolved Fluorescence (HTRF®) from Cisbio ASSAYS (Codolet, France). This assay is intended to be used for the quantitative detection of rat, mouse, pig or human insulin in cell-culture supernatants. This assay involves two different anti-insulin antibodies, one labelled with europium cryptate, and the other one with XL665. When a sandwich is formed with insulin molecules, the two antibodies come into close proximity, allowing FRET to occur between the europium cryptate and the cross-linked allophycocyanin. This FRET phenomenon increases proportionally with the insulin concentration.

2.4.1 Insulin secretion assay

INS-1 832/3 cells were seeded at $3x10^4$ cells/well/200 µL into laminin coated 96-well cell culture plates using RPMI 1640 complete media. Cells were allowed to grow to a confluence of 85-90%. On the third day of seeding, the cells were glucose and serum deprived for at least 12 h prior to assay in RPMI 1640. The deprivation was done in a serial manner such that the cells were left with RPMI 1640 containing 2.8 mM glucose and 2.5% v/v FBS. Prior to assay, the cells were washed twice with 1X EBSS supplemented with 2.8 mM glucose, 1.8 mM $CaCl_2$ and 0.1% w/v BSA, pH 7.4. The drugs (peptide/allosteric ligands) were prepared at 1X concentration in 1X EBSS supplemented with both 2.8 mM and 11 mM glucose separately, 1.8 mM $CaCl_2$ and 0.1% w/v BSA, pH 7.4 and laid out in 96 well, V-bottomed plates (200 µL/well) to be directly transferred on to the

cells immediately after washing. The cells were stimulated for 2 h in presence of ligands, after which the supernatants were collected into a fresh 96 well plate.

For the interaction studies, both peptides and allosteric modulators were made up in 1X EBSS at a concentration of 2X both in high and low glucose (2.8 mM/11 mM) and transferred into a 96 well plate in preparation for addition on to the cells using manual pipette. Subsequently, 100 µL of allosteric ligand followed by 100 µL of peptide were added to each well (for well without peptide, EBSS glucose buffer was added) and incubated for 2 h at 37°C, 5% CO_2. Following incubation, supernatants from each well were transferred into a fresh 96 well plate and stored at 4°C (short term) or -20°C (long term) until required for detection using Cisbio HRTF® insulin kit.

2.4.2 Insulin detection

All the samples to be assayed were diluted in a way that sample dilutions fall in 0-10 ng/mL range (linear part) of the standard curve, using 1X EBSS supplemented with 1.8 mM $CaCl_2$, 2.8 mM glucose and 0.1% w/v BSA, pH 7.4. The formerly reconstituted aliquots of anti-insulin antibodies were further diluted 1:20 using the reconstitution buffer.

To assess the insulin concentrations, 10 µL of supernatant (thawed if stored at -20°C) was transferred to 384-well, low volume optiplate. The plate was briefly centrifuged. Subsequently, the reagents were dispensed in a fixed set of order, 5 µL anti-insulin Ab-cryptate followed by 5 µL anti-insulin Ab-XL665. The plate was covered with a plate sealer, briefly spun and incubated for 2 h at room temperature in dark. The plates were read on Envision® Alpha-reader with excitation filter 320/75 and emission filter for APC665 as 665/7.5 (wavelength in nm/bandwidth in nm) and emission filter for europium as 615/8.5 (wavelength in nm/bandwidth in nm).

In case of negative control, the sample was replaced with the buffer used to dilute the collected supernatants. The standard curve was prepared using the same buffer (1X EBSS) in a concentration range of 0-15 ng/mL.

2.5 Apoptosis

Apoptosis is a regulated process of cell death that occurs as a normal part of development. In normal viable cells, phosphatidylserine (PS) is located on the cytoplasmic face of the plasma membrane. However, in apoptotic cells, PS is translocated from the inner to the outer leaflet of the plasma membrane, thus exposing PS to the external cellular environment. Annexin V, is a Ca^{2+}-

dependent phospholipid-binding protein that has a high affinity for PS. Annexin V labeled with a fluorophore or biotin can identify apoptotic cells by binding to PS exposed on the outer leaflet.

Not only are Annexin V conjugates able to bind PS on apoptotic cell surfaces in the presence of Ca^{2+}, but can also pass through the compromised membranes of dead cells and bind to PS in the interior of the cell. Therefore, it is important to use a cell-impermeant dead cell stain in combination with annexin V conjugate staining to distinguish dead cells from apoptotic cells. Propidium iodide (PI), red fluorescent, nucleic acid binding dye, is used in conjunction with annexin V conjugate so as to differentiate in between the live/apoptotic and dead cells. PI is impermeant to live and apoptotic cells but stains dead cells with red fluorescence, binding tightly to nucleic acids in the cells.

2.5.1 Apoptosis assay

INS-1 832/3 cells plated were plated on to 6-well plates at a density of 5×10^5 cells/well/3 mL, using pre-warmed RPMI 1640 complete media. The cells were allowed to grow to 85-90% confluence, prior to assay. On the third day of seeding, the cells were deprived of glucose and FBS for at least 12 h, by serially diluting the media with RPMI 1640 (no additives) so as to have a remnant glucose of 2.8 mM and 2.5% v/v FBS in 3 mL supernatant in the wells.

Following deprivation, the cells were washed twice with 1X EBSS supplemented with 2.8 mM glucose and 1.8 mM $CaCl_2$, pH 7.4. Subsequently, 1X drugs with and without 100 nM staurosporine were prepared in RPMI 1640 complete media supplemented separately with 2.8 mM and 11 mM glucose, separately. 2 mL of the prepared drug combination was added on to the cells immediately after washings. Cells were incubated for a further 24 h.

Following incubation supernatant was collected and remaining cells were washed with 1.5 mL PBS and then harvested from the plate using 1.5 mL pre-warmed versene. Cells were added to the previously collected supernatant and were then centrifuged for 3 min at 350 × g. 10X HBSS (14065-056, Life technologies; pH 4.4 - 4.7) was diluted to 1X HBSS and supplemented with 0.35 g/L sodium bicarbonate (4.7 mL/L of 7.5% w/v solution of sodium bicarbonate) with pH adjusted to 7.2. The supernatant was discarded and pellet was gently resuspended in 90 µl 1X HBSS, pH 7.2.

2.5.2 Detection of apoptotic cell death

A 10X master mix of AlexaFluor® 647 annexin V conjugate (1:10) (A13201, Molecular Probes ®) and PI (1 mg/mL in water; 1:100) (P4864, Sigma Aldrich) was prepared in 1X HBSS. 10 µL of this

master mix was added to each sample and incubated for 15 min at room temperature, after which they were transferred on ice. 400 µL of 1X HBSS was gently mixed with the samples. Stained cells were promptly analyzed on flow cytometer (BD FACS Canto^{TM} II) using 640 nm laser with a 670 LP filter.

2.6 Proliferation

The BrdU Cell Proliferation ELISA (chemiluminescence) is used to measure DNA synthesis during cell activation and proliferation by quantifying 5-bromo-2'-deoxyuridine (BrdU) incorporated into the newly synthesized DNA of replicating cells. When cells are incubated in presence of labelling medium that contains BrdU, this pyrimidine analogue is incorporated in place of thymidine into the newly synthesized DNA of proliferating cells. After removing the labelling medium, cells are fixed with partially denatured BrdU-labelled DNA. The denaturing of DNA is necessary to improve the accessibility of the incorporated BrdU to the detection antibody. Subsequently, anti-BrdU antibody labelled with peroxidase is added to detect the bound BrdU. Finally, addition of chemiluminescence substrate (luminol) allows the measurement of cell proliferation. All proliferation assays were performed using Cell Proliferation ELISA, BrdU (chemiluminescent) Roche #11669915001 (Basel, Switzerland).

2.6.1 Proliferation assay

INS-1 832/3 cells were seeded at 1.2×10^4 cells/well/200 µL in laminin coated, 96-well, clear bottomed, black view plates using pre-warmed RPMI 1640 complete media. The cells were allowed to grow to a confluence of 40-45%. After 24 h, the cells were deprived of glucose and FBS for at least 12 h, by serially diluting the media with RPMI 1640 having no supplements. After 12 h of starvation, the media was again serially diluted in a way so that the cells are left with 100 µL of RPMI 1640 with almost 0% w/v glucose and 0% v/v FBS. The peptides/allosteric modulators are prepared at a concentration of 2X in RPMI 1640 supplemented with twice the amounts of additives and laid out in fresh 96-well plate, prior to addition. The RPMI 1640 (2X media) required for proliferation assay studies contains 1% v/v FBS, 0.2% w/v BSA, 2 mM sodium pyruvate, 100 µM β-mercaptoethanol, and 20 mM HEPES with low glucose represented as 5.6 mM glucose and high glucose represented as 22.2 mM. 100 µL of drugs were added to the wells containing 100 µL media (with all the additives diluted to negligible amounts). 10% FBS v/v was used at a positive control, whereas media itself was used as a negative control.

2.6.2 BrdU incorporation and detection

Following incubation, 100 μL of the supernatant was removed from all the wells and discarded. Cells were labelled with 10 μl/well BrdU working solution (1:10 dilution of the BrdU stock solution with the culture media; low light conditions) and incubated for 2 h. Labelling media was gently removed using a manual pipette, and replaced with 100 μL/well of FixDenat solution and further incubated for 30 min at room temperature. Subsequently, FixDenat was gently removed and replaced with 100 μL/well anti-BrdU-POD and further incubated for 90 min at room temperature. 10 min prior to completion of incubation period with the antibody, wash buffer and substrate solution was prepared. Wash buffer was prepared by diluting one part of the wash concentrate with four parts of milli-Q water. Substrate was prepared in a 15 mL tube covered in foil and mixing the two substrates A and B at a ratio of 100:1, prior to its placing on a spinning wheel for 15 min at room temperature. Anti-BrdU POD was removed and cells were washed 3 times with 200 μL/well wash buffer (1X) over a 15 min period. A black cover sticker was placed over the bottom of the plate and 100 μL of pre-mixed substrate was added. The plate was covered in foil, and placed on a shaker for 3 min (room temperature). Directly after shaking, the plate was then read on luminescence only protocol (emission filter settings 410-480 nm, measurement interval time 0.50 sec) using the LumiSTAR Omega instrument (BMG LABTECH GmbH, Ortenberg, Germany).

2.7 Intracellular Ca^{2+} $[Ca^{2+}]_i$ mobilization

The Flexstation calcium assay is a fluorimetric assay that quantitates the elevation of intracellular calcium concentration in response to receptor agonists and calcium ionophores.

Intracellular calcium, $[Ca^{2+}]_i$, mobilization assay is a non-ratiometric, fluorescence based assay. The mobilization of calcium from the intracellular stores in mammalian cells can be measured using the Fluo-4, acetoxymethyl (Fluo-4-AM) ester. Fluo-4-AM is a cell permeable and non-fluorescent molecule. Once inside the cell, the fluo-4-AM ester is hydrolysed by intra-cellular esterases to cell membrane impermeable negatively charged form of the dye which is capable of binding to calcium ions that are released from the intra-cellular stores upon activation of GPCR. A dye efflux inhibitor, probenecid, is added during the process so as to prevent the active export of anionic dye from the cell by the organic anion transporters expressed in the cells, which otherwise would lead to reduced fluorescence signals.

2.7.1 $[Ca^{2+}]_i$ mobilization assay

INS-1 832/3 cells were seeded at a density of 3×10^4 cells/well into laminin coated 96-well cell culture plates in RPMI 1640 complete media. On the third day of seeding (85-95% confluent), the cells were washed with 1X EBSS containing 1.8 mM $CaCl_2$ and 2.8 mM of glucose, pH 7.4. Subsequently, the cells were glucose and serum deprived for 2 h in 200 µL RPMI 1640 supplemented with 2.8 mM glucose. After 2 h, the supernatant was removed and cells were washed once with 200 µl pre-warmed 1X EBSS supplemented with 2.8 mM glucose, 1.8 mM $CaCl_2$, 0.1% w/v BSA and 4 mM probenecid, pH 7.4. Successively, 135 uL of 1X EBSS was added to each well supplemented with 1µM Fluo-4-AM (#F-14217; Invitrogen, Carlsbad, CA; in low light conditions). The plate was wrapped in aluminium foil and incubated for 45 min at 37°C. Increasing concentrations of peptide agonist (10X) was added in the FlexStation (Molecular Devices, Palo Alto, CA). Fluorescence was determined immediately with an excitation wavelength set to 485 nm and an emission wavelength set to 538 nm, and readings were taken every 1.36 sec for 120 sec. Peak magnitude was calculated using five-point smoothing, followed by correction against basal fluorescence. The peak value was used to create concentration-response curves. Data were normalized to the maximal response elicited by 10 µM ionomycin.

2.8 mRNA extraction

2.8.1 Treatment of cells

INS-1 832/3 cells plated were plated on to 6- well plates at a density of 7×10^5 cells/well/3 mL, using pre-warmed RPMI 1640 complete media. The cells were allowed to grow to 85-95% confluence, prior to the treatment. On the third day of seeding, the cells washed with 1X EBSS supplemented with 1.8 mM $CaCl_2$ and 2.8 mM glucose, pH 7.4. Subsequently, the cells were starved for 2 h in RPMI 1640 supplemented with only 2.8 mM glucose at 37°C, 5% CO_2. During the starvation period, 1X drugs were prepared in 1X EBSS with low (2.8 mM glucose) and high (11 mM glucose) glucose containing 1.8 mM $CaCl_2$, 0.1% w/v BSA, pH 7.4. Moreover for longer incubation groups (6 h and 24 h) the drugs were prepared in similar way but using RPMI 1640 supplemented with 0.1% w/v BSA and glucose (2.8 mM and 11 mM) as the vehicle.

After 2 h of starvation, the cells were washed twice with 1X EBSS, pH 7.4 (1.5 mL/well) with immediate addition of 2 mL drugs to each well. Similarly, the drugs prepared in RPMI 1640 was added in new 6-well plates (without cells) and kept at 37°C, 5% CO_2 so as to mimic *in-situ* conditions when added on to the cells. The cells were incubated for 30 min, 2 h, 6 h and 24 h. For

the treatment groups requiring 6 h and 24 h incubations, the supernatants were collected after 2 h of stimulation and stored at -20ºC. Pre-warmed drugs prepared in RPMI 1640 were immediately added on to the cells.

After the treatment duration was over, the supernatants of each treatment group were collected, labelled and stored at -20°C for insulin detection. The cells were collected using PBS and pelleted by centrifuging for 3 min at 300 x g. The supernatants were discarded and cell pellets were stored at -80°C until ready for RNA extraction.

2.8.2 RNA extraction

RNeasy® plus Mini kit from Qiagen was used to extract the RNA from the pelleted cells as per the manufacturer's instructions. Briefly, the pelleted cells were thawed at room temperature. 350 µL of buffer RLT plus was added to the cells and vortexed for 30 sec so as to lyse the cells. The homogenized lysate was transferred to gDNA eliminator spin column placed in 2 mL collection tube. It was centrifuged for 30 sec at ≥8000 x g. Column was discarded and flow through was saved for the next step. One volume (350 µL) of freshly prepared 70% v/v ethanol was added to the flow through and mixed well with pipetting. Subsequently, 700 µL of sample including any formed precipitates was transferred to RNeasy spin column placed in 2 mL collection tube. The lid was closed and column was centrifuged for 15 sec at ≥8000 x g. Flow through was discarded. 700 µL of buffer RW1 was then added to the RNeasy spin column; lid closed and centrifuged for 15 sec at ≥ 8000 x g. The flow through was again discarded. Following this, 500 µL of buffer RPE was added to the column, lid closed and centrifuged for 15 sec at ≥ 8000 x g. The flow through was discarded. The addition of buffer RPE was repeated and was centrifuged for 2 min at ≥ 8000 x g. The column was placed in a new collection tube and centrifuged at full speed for 1 min to further dry the membrane. Finally, the RNeasy spin column was placed in 1.5 mL LoBind eppendorf tube and RNA was eluted by adding 15 µL RNase free water directly to the column membrane followed by centrifugation for 1 min at ≥ 8000 x g. The concentration of RNA was determined using NanoDrop spectrophotometer (ND-1000) and further the quality was determined using RNA nanochip on Bioanalyzer (Agilent 2100). The RNA was aliquoted and stored at -80°C so as to avoid repeated freeze-thaw cycles.

2.9 mRNA Library generation

SureSelect Strand Specific RNA Library Prep Kit for Illumina Multiplexed Sequencing (SureSelect strand specific RNA reagent kit, Illumina platforms (ILM), 96 samples, p/n G9691B; Agilent Technologies) was used to generate mRNA library for RNA sequencing which thereby help in

providing a deeper understanding of gene regulation and transcriptome in a cell, in response to a particular ligand/treatment. The protocol used the oligo-dT methods to purify polyA RNA from total RNA, resulting in generation of libraries comprised of mRNA.

2.9.1 mRNA Library preparation

To start with the library generation protocol a clean work area was maintained during the process. The bench space was thoroughly cleaned with 80% v/v ethanol, bleach (0.5% sodium hypochlorite) followed by RNaseZap® (AM 9780, Ambion®, Life Technologies) and DNaseZap™ (AM9890, Ambion®, Life Technologies) solutions so as to get rid of any contaminants such as DNA or nucleases. Similarly all the things required during the process such as pipettes, tubes and eppendorfs were thoroughly cleaned (as the bench space) and UV sterilized for at least 20 min. Furthermore, sterile, nuclease free, DNA & RNA free aerosol barrier tips was only used during the process.

2.9.1.1 Purification of poly(A) RNA from total RNA

Poly(A) RNA was purified from total RNA using two serial rounds of binding to oligo(dT) magnetic particles. The total amount of RNA used to prepare the library was optimized to be 1 µg and possessed a RNA integrity number (RIN) of not less than 8, 260/280 ratio ≥2 and 260/230 ratio ≥1.8 based on analysis using Agilent's 2100 Bionalyzer and Bioanalyzer picoRNA chip. 1 µg total RNA was diluted to a final volume of 25 µL using nuclease-free water and the samples were placed in separate wells of 96-well PCR plate (AB0700, 0.2 mL, Thermofast 96 PCR plate, low profile, non-skirted, Thermo Scientific). The oligo(dT) beads were vortexed, until a homogenous and consistent suspension was obtained and 25 µL of these beads were added to each sample. The plates were sealed using a sealer (product# 729757001, LightCycler® 480 sealing foil, Roche), gently vortexed for 5 sec and spun in a centrifuge so as to collect the liquid without pelleting the beads. The plate was incubated in a T100™ thermal cycler (Bio-Rad Laboratories) with heated lid ON and denaturing the RNA by increasing the temperature to 65°C for 5 min with immediately dropping it and holding it at 4°C.

The plate was removed and incubated at room temperature for 5 min so as to allow the poly(A) RNA binding to the oligo(dT) beads. The plate was then moved to magnetic separation device (A001322, 96S Super Magnet Plate, ALPAQUA Liquid Handling Products, US) and further incubated for 5 min at room temperature. While keeping the plate in the magnetic stand, the cleared solution was carefully removed and discarded without disturbing the beads. The plate was removed from the stand, and 200 µL of RNA Seq Bead Washing buffer was added to each well. Plate was

sealed, vortexed, briefly centrifuged and again placed on the magnetic stand for 2 min. While keeping the plate on the magnetic stand, the cleared solution was removed and discarded.

After removing the plate from the magnetic stand, 25 µL of RNA Seq Bead Elution buffer was added to each sample. Plate was sealed, vortexed, briefly centrifuged and incubated on thermal cycler (heated lid ON) at 80°C for 2 min followed by immediate hold at 4°C. Subsequently, 25 µL of RNA Seq Bead Binding buffer was added to each well. Plate was sealed, vortexed, briefly centrifuged and incubated at room temperature for 5 min (allow re-binding of poly(A) RNA to beads). The plate was placed on magnetic stand, and clear solution was removed and discarded after 2 min of incubation. Plate was removed from the magnetic stand and 200 µL of RNA Seq Bead Washing buffer was added to each well. Plate was sealed, vortexed, briefly centrifuged and placed on the magnetic stand for at least 2 min so as to carefully remove and discard the clear solution.

2.9.1.2 Fragmentation of poly(A) RNA

The purified poly(A) RNA was chemically-fragmented to a size appropriate for RNA sequencing library preparation.The plate was removed from the magnetic stand and 19 µL of RNA Seq Fragmentation Mix was added to each sample well. The plate was sealed, gently vortexed, briefly centrifuged and incubated in the thermal cycler (heated lid ON) at 94°C for 8 min followed by a hold at 4°C.

During the incubation period, previously aliquoted stock (stored at -20°C, protected from light and prepared less than a month ago prior to use) of Actinomycin D (A1410, Sigma-Aldrich) solution (4 µg/µL), prepared in DMSO (D8418-50mL for molecular biology, Sigma-Aldrich) was diluted to 120 ng/µL using nuclease-free water. Additionally, appropriate amount of RNA Seq First Strand Master Mix with actinomycin D (120 ng/µL) was prepared and kept on ice. The RNA Seq first strand master mix from SureSelect strand specific RNA library kit, Box 1 was thawed and thoroughly vortexed before using.

2.9.1.3 Synthesizing first strand cDNA

The plate containing fragmented RNA and beads was transferred to the magnetic stand and incubated for 5 min. While the plate still on the magnetic stand, 17 µL of the fragmented RNA-containing supernatant was transferred to fresh plate well and placed on ice. Subsequently, 8.5 µL of the previously prepared first stand master mix/actinomycin D mixture was added to each RNA sample well. Plates were sealed, gently vortexed and centrifuged at 1500 x g for 1 min. The plate

was then incubated in thermal cycler (heated lid ON) at 25°C for 10 min, 37°C for 40 min and finally held at 4°C.

2.9.1.4 Purification of first strand cDNA using AMPure XP beads

The Agencourt AMPure XP beads (Beckman Coulter Genomics, p/n A63880) was brought to room temperature at least 30 min prior to use. The bead suspension was mixed well so as to have a homogeneous and consistent suspension. The plate was removed from the thermal cycler and 46 µL of homogenous bead suspension was added to each sample (25.5 µL volume) in the PCR plate. The plate was sealed, vortexed and incubated for 5 min at room temperature, followed by 5 min incubation on magnetic stand. While keeping the plate in the magnetic stand, the clear solution was carefully removed and discarded without disturbing the beads. The plate still being on the magnetic stand, 200 µL of freshly prepared 70% v/v ethanol was dispensed in each sample well carefully. After waiting for 1 min so as to allow settling of any disturbed beads, the ethanol was removed. The ethanol wash was repeated once again after which the plate was briefly spun in the centrifuged and placed back on the magnetic stand. Any residual amount of ethanol was removed using pipette and the samples were air dried at room temperature for about 2-5 min. 27 µL of nuclease-free water was added to each sample well and covered with a sealer, vortexed, briefly centrifuged and incubated for 2 min at room temperature. The plate was placed back on the magnetic stand, incubated for 2 min and 25 µL of cleared supernatant was removed to a fresh plate and the beads were discarded.

2.9.1.5 Synthesizing second-strand cDNA and repairing the ends

RNA Seq second strand + end repair master mix (SureSelect strand specific RNA library kit, Box 1) was thawed, thoroughly vortexed and kept on ice. The samples and enzyme mixtures were kept on ice during all the steps followed on from now in the protocol.

25 µL of RNA Seq second strand + end repair master mix was mixed to 25 µL purified first strand cDNA sample. The plates were sealed, vortexed, centrifuged at 1500 x g for 1 min and incubated in thermal cycler (heated lid OFF) at 16°C for 30 min followed by 4°C hold.

2.9.1.6 Purification of cDNA using AMPure XP beads

The Agencourt AMPure XP beads was brought to room temperature at least 30 min prior to use and mixed well so as to have a homogeneous and consistent suspension. The plate was removed from the thermal cycler and 90 µL of homogenous bead suspension was added to each sample (50 µL volume) in the PCR plate. The plate was sealed, vortexed, briefly centrifuged and incubated for 5 min at room temperature, followed by 5 min incubation on magnetic stand. While keeping the plate

in the magnetic stand, the clear solution was carefully removed and discarded without disturbing the beads. The plate still being on the magnetic stand, 200 µL of freshly prepared 70% v/v ethanol was dispensed in each sample well carefully. After waiting for 1 min so as to allow settling of any disturbed beads, the ethanol was removed. The ethanol wash was repeated once again. Any residual amount of ethanol was removed using pipette and the samples were air dried at room temperature for about 2-5 min. 22 µL of nuclease-free water was added to each sample well and covered with a sealer, vortexed, briefly centrifuged and incubated for 2 min at room temperature. The plate was placed back on the magnetic stand, incubated for 2 min and 20 µL of cleared supernatant was removed to a fresh plate and the beads were discarded. The plate was sealed and stored at -20°C and the remaining protocol was followed the next day.

2.9.1.7 Adenylation of cDNA 3' ends

RNA Seq dA tailing Master Mix (SureSelect strand specific RNA library kit, Box 1) was thawed, thoroughly vortexed prior to use and kept on ice. 20 µL of RNA Seq dA tailing master mix was added to 20 µL purified, end-repaired cDNA samples. The plates were sealed, vortexed, centrifuged at 1500 x g for 1 min and incubated in thermal cycler (heated lid OFF) at 37°C for 15 min followed by a hold at 4°C. The plate was kept on ice after removing from the thermal cycler.

2.9.1.8 Ligation of adaptors

SureSelect Ligation Master Mix and the SureSelect Oligo Adaptor Mix (SureSselect strand specific RNA library kit, box 1) was thawed, thoroughly mixed using vortex and kept on ice.

5 µL of SureSelect ligation master mix was added to each A-tailed cDNA sample well and mixed well with pipetting. Subsequently, 5 µL of SureSelect oligo adaptor mix was added to each sample. The plate was sealed, vortexed, briefly centrifuged and incubated in thermal cycler (heated lid OFF) at 20°C for 15 min and then held at 4°C.

2.9.1.9 Purifying adaptor-ligated DNA using AMPureXP beads

The Agencourt AMPure XP beads was brought to room temperature at least 30 min prior to use and mixed well so as to have a homogeneous and consistent suspension. The plate was removed from the thermal cycler and 60 µL of homogenous bead suspension was added to each sample (50 µL volume) in the PCR plate. The plate was sealed, vortexed, briefly centrifuged and incubated for 5 min at room temperature, followed by 5 min incubation on magnetic stand. While keeping the plate in the magnetic stand, the clear solution was carefully removed and discarded without disturbing the beads. The plate still being on the magnetic stand, 200 µL of freshly prepared 70% v/v ethanol was dispensed in each sample well carefully. After waiting for 1 min so as to allow settling of any

disturbed beads, the ethanol was removed. The ethanol wash was repeated once again. Any residual amount of ethanol was removed using pipette and the samples were air dried at room temperature for about 2-5 min.

20 µL of nuclease-free water was added to each sample well and covered with a sealer, vortexed, briefly centrifuged and incubated for 2 min at room temperature. The plate was placed back on the magnetic stand, incubated for 3 min and 17 µL of cleared supernatant was removed to a fresh plate and the beads were discarded.

2.9.1.10 Amplifying and indexing the adaptor-ligated cDNA library

RNA Seq ILM Reverse PCR Primer, RNA Seq PCR master Mix, Uracil DNA Glycosylase (UDG) and SureSelect primer (forward primer) were thawed, thoroughly vortexed and kept on ice.

Sufficient amount of 1:20 dilution of RNA Seq ILM reverse PCR primer was prepared in nuclease-free water. Appropriate volume of PCR reaction mix was prepared (for 1 sample: 25 µL RNA Seq PCR master mix, 1 µL UDG, 1 µL SureSelect forward primer and 1 µL of 1:20 diluted RNA Seq ILM reverse PCR primer) and vortexed thoroughly. 28 µL of this PCR reaction mix was added to each sample containing 17 µL of purified, adaptor-ligated cDNA and mixed thoroughly by pipetting. Subsequently, 5 µL of appropriate indexing primer (RNA Seq Index 1-18, 8 bp) was added individually to each PCR reaction mixture well. The plate was sealed and incubated in thermal cycler (heated lid ON) at 37°C, 15 min, 1 cycle; 95°C, 2 min, 1 cycle; 95°C for 30 sec, 65°C for 30 sec and 72°C for 1 min, 12 cycles; 72°C, 5 min, 1 cycle and finally held at 4°C.

2.9.1.11 Purification of the amplified library with AMPure XP beads

The Agencourt AMPure XP beads was brought to room temperature at least 30 min prior to use and mixed well so as to have a homogeneous and consistent suspension. The plate was removed from the thermal cycler and 60 µL of homogenous bead suspension was added to each sample (50 µL volume) in the PCR plate. The plate was sealed, vortexed, briefly centrifuged and incubated for 5 min at room temperature, followed by 5 min incubation on magnetic stand. While keeping the plate in the magnetic stand, the clear solution was carefully removed and discarded without disturbing the beads. The plate still being on the magnetic stand, 200 µL of freshly prepared 70% v/v ethanol was dispensed in each sample well carefully. After waiting for 1 min so as to allow settling of any disturbed beads, the ethanol was removed. The ethanol wash was repeated once again. Any residual amount of ethanol was removed using pipette and the samples were air dried at room temperature for about 2-5 min. 27 µL of nuclease-free water was added to each sample well and covered with a

sealer, vortexed, briefly centrifuged and incubated for 2 min at room temperature. The plate was placed back on the magnetic stand, incubated for 3 min and 25 µL of cleared supernatant was removed to a fresh plate and the beads were discarded.

2.9.1.12 Removing adaptor-dimers with AMPure XP beads

The Agencourt AMPure XP beads was brought to room temperature at least 30 min prior to use and mixed well so as to have a homogeneous and consistent suspension. The plate was removed from the thermal cycler and 60 µL of homogenous bead suspension was added to each sample (50 µL volume) in the PCR plate. The plate was sealed, vortexed, briefly centrifuged and incubated for 5 min at room temperature, followed by 5 min incubation on magnetic stand. While keeping the plate in the magnetic stand, the clear solution was carefully removed and discarded without disturbing the beads. The plate still being on the magnetic stand, 200 µL of freshly prepared 70% v/v ethanol was dispensed in each sample well carefully. After waiting for 1 min so as to allow settling of any disturbed beads, the ethanol was removed. The ethanol wash was repeated once again. Any residual amount of ethanol was removed using pipette and the samples were air dried at room temperature for about 2-5 min. 27 µL of nuclease-free water was added to each sample well and covered with a sealer, vortexed, briefly centrifuged and incubated for 2 min at room temperature. The plate was placed back on the magnetic stand, incubated for 2 min and 25 µL of cleared supernatant was removed to a fresh plate and the beads were discarded.

2.9.1.13 Assessing quality with 2100 Bioanlyzer DNA1000 assay

The library was aliquoted and 3.5 µL of library (1 µL for Bioanalyzer and 2 µL for Cubit analysis) was sent away for the quality assessment using 2100 Bioanalyzer and Cubit.

2.9.2 Sample preparation for RNA Sequencing

The number of indexed libraries that may be multiplexed in a single sequencing lane is determined by output specifications of the platform used and the amount of sequencing data required. The libraries are combined in a way that each index-tagged sample is present in equimolar amounts in the pool. Below formula is used so as to determine the volume of index sample required in the library.

$$Volume\ of\ Index = \frac{V(f) x\ C(f)}{\#\ x\ C(i)}$$

Where,

V(f) = final desired volume of the pool

C(f) = desired final concentration of all DNA in the pool

= the number of indexes

C(i) = initial concentration of each indexed sample

The final volume of pooled library was adjusted to desired final concentration using 1X low TE buffer (10 mM Tris-HCl, pH 8.0, 0.1M EDTA; p/n 12090-015, Life Technologies).
0.1 % v/v Tween 20 was added to the pooled library so as to store it for a short term at -20°C prior to sequencing (paired- end sequencing).

2.10 Reagents

2.10.1 Peptides

GLP-1(7-36)NH_2, exendin-4 and oxyntomodulin were purchased from American peptides (Sunnyvale, CA, USA).

2.10.2 Small Molecules

The small molecule GLP-1R ligands 4-(3-benzyloxyphenyl)-2-ethylsulfinyl-6-(trifluoromethyl)pyrimidine (BETP) (Sloop *et al*., 2010) was provided by Eli Lilly, 6.7-dichloro-2-methylsulfonyl-3- tert-butylaminoquinoxaline (Compound 2) (Knudsen *et al*., 2007) was generated in-house by Dr. Celine Valant, according to a method published previously (Teng *et al*., 2007) to a purity of ~95%, and compound integrity was confirmed by NMR.

2.10.3 General Reagents

Dulbecco's Modified Eagle's Medium (DMEM), RPMI 1640 # 11879 and Fluo-4 acetoxymethyl ester (Fluo-4 AM) were purchased from Invitrogen (Carlsbad, CA, USA). Foetal bovine serum (FBS) was purchased from Thermo Electron Corporation (Melbourne, VIC, Australia).

AlphaScreen reagents, 384-well proxiplates and 384-well optiplates were purchased from PerkinElmer Life and Analytical Sciences (Waltham, MA, USA). SureFire^{TM} ERK1/2 reagents were obtained from TGR Biosciences (Thebarton, SA, Australia). All other reagents were purchased from Sigma- Aldrich (St. Louis, MO, USA) or BDH Merck (Melbourne, Victoria, Australia) and were of an analytical grade.

2.11 Data analysis

2.11.1 Equations

All data obtained were analyzed in Prism 6.0 (GraphPad Software Inc., San Diego, CA). Concentration response signaling data were analyzed using a three-parameter logistic equation as described previously (May, 2007).

Equation (1)

$$Y = Bottom + \frac{(Top - Bottom)}{1 + 10^{(LogEC_{50} - \log[A])}}$$

cAMP interaction data were also analyzed with an operational model of allosterism:
Equation (4)

$$Y = Basal \frac{(E_{\max}) - Basal \times (([A] \times (K_B + \alpha\beta \times [B]) + \tau[B] \times [B] \times EC_{50})^n)}{(([A] \times (K_B + \alpha\beta \times [B]) + \tau[B] \times [B] \times EC_{50})^n) \times (EC_{50}{}^n) \times (K_B + [B])^n)}$$

where E_{max} is the maximal possible response of the system (not the agonist), basal is the basal level of response in the absence of agonist, K_B denotes the functional equilibrium dissociation constant of the agonist (B), τis an index of the coupling efficiency (or efficacy) of the agonist and is defined as the total concentration of receptors divided by the concentration of agonist-receptor complex that yields half the maximum system response (E_{max}), and n is the slope of the transducer function that links occupancy to response. αβ is the combined affinity-efficacy parameter that measures the magnitude and direction of the functional interaction between the modulator and peptide agonist.

To quantify signaling bias, which may be manifested either as functional affinity (K_A) and/or efficacy (τ) of an agonist for a given pathway, agonist concentration-response curves data were analyzed with an operational model (Gregory, 2007), but modified to directly estimate the ratio of τ/K_A, in a manner similar to that described by (Figueroa, 2009), for each pathway:

Equation (5)

$$\frac{E_{\max} \times (\tau/K_A)^n \times [B]^n}{[B]^n \times (\tau/K_A)^n + (1 + [B]/K_B)^n}$$

Where, all other parameters are as defined for eq. 4. All estimated parameters are expressed as logarithms (mean ± S.E.M.); where relevant, statistical analysis was performed by one-way analysis of variance and Dunnett's post test using GraphPad Prism 6.0, and statistical significance was accepted at $p < 0.05$.

CHAPTER 3: SELECTION AND OPTIMISATION OF MODEL β-CELL LINES

3.1 INTRODUCTION

The GLP-1R is ubiquitously expressed throughout the body primarily in the β-cells of pancreatic islets, where it is best characterized for its involvement in glucose regulation, despite having other functions throughout the body. There are multiple endogenous ligands that target and activate the GLP-1R namely, four different forms of GLP-1, full length peptide GLP-1(1-37) and a processed form GLP-1(7-37), each of which has an amidated form GLP-1(1-36)NH_2 and GLP-1(7-36)NH_2 (Drucker *et al.,* 1987; Orskov *et al.,* 1994) and oxyntomodulin. There are also a number of long-acting GLP-1 analogues that have been approved and/or are in clinical trials for treatment of type 2 diabetes mellitus (T2DM) such as exenatide, liraglutide, dulaglutide and lixisenatide (Gallwitz, 2015). Activation of the GLP-1R regulates many key physiological functions but the most well characterized are in glucose-homeostasis. This includes glucose-dependent insulin biosynthesis and release (Kreymann *et al.,* 1987), inducing β-cell proliferation, decreasing β-cell apoptosis (Buteau *et al.,* 1999; Wang *et al.,* 2001; Quoyer *et al.,* 2010) and inhibiting glucagon secretion (Orskov and Poulsen, 1991; Garcia-Flores *et al.,* 2001; Korner *et al.,* 2007; Tornehave *et al.,* 2008). The ability of GLP-1 to enhance glucose-stimulated insulin secretion (GSIS) and promote trophic and survival effects by regulating apoptosis and proliferation in pancreatic beta cells makes it a promising candidate from clinical perspectives.

The known actions of GLP-1 are predominantly mediated through cAMP-dependent pathways (cAMP/PKA, cAMP/Epac and PI3K/Akt pathways) (Drucker *et al.,* 1987; Taylor *et al.,* 1990; Dyachok *et al.,* 2006; Gromada *et al.,* 1998; Kawasaki *et al* ., 1998), and recruitment of β-arrestin-1 (Sonoda et al., 2008; Quoyer *et al.,* 2010). Activation of the GLP-1R results in coupling to $G\alpha_s$ and activation of adenylyl cyclase to accumulate cAMP which sequentially activates protein kinase A and cAMP regulated guanine nucleotide exchange factors of the Epac family (Gromada *et al.,* 1998; Holz *et al.,* 1995; Kang *et al.,* 2001) to promote downstream effects. GLP-1 and its analogs have also been reported to stimulate p44/42 mitogen activated protein kinase (ERK1/2) cascade by diverse pathways such as influx of calcium, $G\alpha_s$/cAMP/PKA or β-arrestin-1 recruitment (Arnette *et al.,* 2003; Gomez *et al.,* 2002; Briaud *et al.,* 2003; Costes *et al.,* 2006; Sonoda *et al.,* 2008). Two phases of ERK1/2 have been reported. Early activation of ERK1/2 that is dependent on PKA and long lasting ERK1/2 activation, mediated through the β-arrestin-1 pathway (Sonoda *et al.,* 2008; Quoyer *et al.,* 2010).

Functional and molecular studies of β-cells have been performed *in vitro* using islet cell culture and/or cell lines. Although it is preferable to use primary cells (pancreatic islets) in order to gain a detailed understanding of islet function at molecular and biochemical level, the use of primary islets

is limited, in that large numbers of islets are required which is both work and cost intensive. There are also other disadvantages that include the presence of mixed population of cells (β-, α-, and δ-cells) in the culture and poor proliferative capacity of the cells isolated from islets. Thus, several pancreatic rodent β-cell lines that retain many key functional attributes of normal islets have been established and characterized and have become useful tools in the study of β-cell function. Some of these rodent β-cell lines include MIN6, INS-1, INS-1E, INS-1 832/3.

The MIN6 insulinoma cell line was derived from tumors of transgenic mice harboring the insulin promoter followed by SV40 T-antigen gene. Characterization of MIN6 cells revealed that this cell line retained its differentiated phenotype in culture and secreted high levels of insulin (six to seven fold increase) in response to an elevation of extracellular glucose concentration (Miyazaki *et al.,* 1990; Ishihara *et al.,* 1993). INS-1 cells were isolated by dispersion of a transplantable radiation-induced INS tumor from NEDH rats into a tissue culture medium containing mercaptoethanol (Asfari *et al.,* 1992). The non-clonal nature of these cells is proposed to contribute to the limited stability of this cell line andmay be responsible for the inconsistencies in reported data sets from these cells (Asfari *et al.,* 1992). To overcome the problems associated with INS-1 cells, two different lab groups established clonal cell lines using parental INS-1 cells namely, INS-1E and INS-1 832/3 that were selected on the basis of robust GSIS. INS-1E cells are one of the well differentiated clones available without any genetic manipulation in the parental INS-1 cell culture (Merglen *et al.,* 2004). INS-1 832/3 cells were derived from parental INS-1 cells after stable transfection with a plasmid containing the human insulin gene under the control of the cytomegalovirus promoter and a neomycin resistance gene (plasmid pCMV8/INS/IRES/Neo containing the human insulin cDNA). These cells overexpress the human insulin gene and therefore produce human insulin, in addition to endogenous rat insulin, rendering it impossible to judge the differentiated state based on insulin content alone (Hohmeier *et al.,* 2000). These particular cells were selected based on their ability to secrete glucose and GLP-1-mediated insulin secretion (Hohmeier *et al*., 2000; Dyachok *et al.*, 2006; Maida *et al.*, 2008; Ronnebaum *et al*., 2008).

To date, all work assessing GLP-1R, signalling bias and allostery within Monash Institute of Pharmaceutical Sciences (MIPS) has been performed on recombinant cell lines. In order to understand this phenomenon and their physiological importance and relevance, a reliable β-cell model is of paramount importance. The present study was aimed to identify an appropriate model for investigating the signalling pathways underlying GLP-1R mediated potentiation of GSIS as well as trophic and survival effects in pancreatic β-cells. In addition, once a cell line was selected, conditions were established and optimized to assess various functional outputs, enabling assessment

elements of GLP-1R signalling and to gain insight into the underlying molecular mechanisms in an endogenously expressing GLP-1R cell line that contains physiologically relevant end points of GLP-1R signalling.

3.2 RESULTS

3.2.1 Screening for a model β-cell line

The GLP-1R preferentially couples to the $G_{\alpha s}$ pathway, activating adenylate cyclase and augmenting intracellular levels of cAMP, which in turn plays an important role in secretion of insulin (Drucker *et al.*, 1987). Additionally, the GLP-1R agonist peptides are reported to enhance GSIS (Creutzfeldt and Nauck, 1992; Holst and Orskov, 2001). Therefore, in order to select a model cell line, that depicts GLP-1R function in a beta cell, GLP-1(7-36)NH_2 peptide-mediated cAMP accumulation and potentiation of GSIS were chosen as functional screens.

Four cell lines were sourced from various laboratories around the world. INS-1 rat insulinoma and MIN6 mouse insulinoma cell lines were generously provided Dr. Trevor Biden affiliated to the Garvan Institute of Medical Research, St. Vincent's Hospital, Sydney. INS-1E rat insulinoma cell line was kindly received from Dr. Nicole Wong of the Melbourne University as well as from Prof. Ken Walder associated with the Metabolic Research Unit of Deakin University, Geelong. INS-1 832/3 cells were a generous gift from Prof. Christopher B. Newgard affiliated with Duke University, North Carolina.

From here on GLP-1(7-36)NH_2 will be referred as GLP-1 throughout the thesis.

3.2.1.1 cAMP Production

To quantify cAMP accumulation in all the available cell lines, the broad specificity phosphodiesterase (PDE) inhibitor, IBMX was included to enhance cellular cAMP levels to potentially provide a larger window with a greater ability to detect small changes in cAMP concentration. Stimulation of MIN6 (Figure 3.1A) and INS-1E (Figure 3.1C) cells in the presence of increasing concentration of GLP-1 in 11mM glucose, exhibited a very weak cAMP response (Table 3.1).

In contrast, robust dose-dependent accumulation of intracellular cAMP accumulation was observed in INS-1 cells ($pEC_{50} = 9.17 \pm 0.14$) (Figure 3.1B; Table 3.1). In addition, exposure of INS-1 832/3 cells to 11 mM glucose and increasing concentrations of GLP-1 also resulted in a robust dose-

dependent accumulation of cAMP (pEC_{50} = 9.02 ± 0.14) (Figure 3.1 D, Table 3.1), with a larger range (maximum - minimum) than that of INS-1 cells (Table 3.1).

3.2.1.2 Insulin secretion

In order to identify an ideal cell line for insulin secretion, the cell line needed to display glucose-mediated insulin secretion, in addition to augmentation of this response in high glucose by GLP-1, and with no GLP-1 response in low glucose. In measurements of insulin secretion, MIN6 cells showed a very high basal constitutive insulin secretion in low glucose (2.8mM glucose) with no further augmentation of insulin secretion observed upon stimulation with 11mM glucose and 100 nM GLP-1 (Figure 3.2 A). While INS-1 cells had low basal insulin secretion in low glucose, these cells did not respond to high glucose or GLP-1 (Figure 3.2 B). The glucose responsiveness of INS-1E cells was robust, but GLP-1-mediated potentiation was poor (Figure 3.2 C). However, in INS-1 832/3 cells, robust glucose responsiveness was detected, which was significantly potentiated by 100 nM GLP-1 (Figure 3.2 D). No GLP-1-mediated insulin secretion was observed in low glucose conditions with either INS-1E or INS-1 832/3 cells (Figure 3.2 C and D).

Thereby, based on these functional screens of cAMP and glucose-dependent insulin secretion, INS-1 832/3 cells were selected as a model cell line for our studies due to their ability to respond robustly and reproducibly to GLP-1 stimulation compared to the other cell lines, despite all cell lines reportedly expressing the GLP-1R (Kieffer *et al.*, 1996; Maida *et al.*, 2011; Yamato *et al.*, 1997).

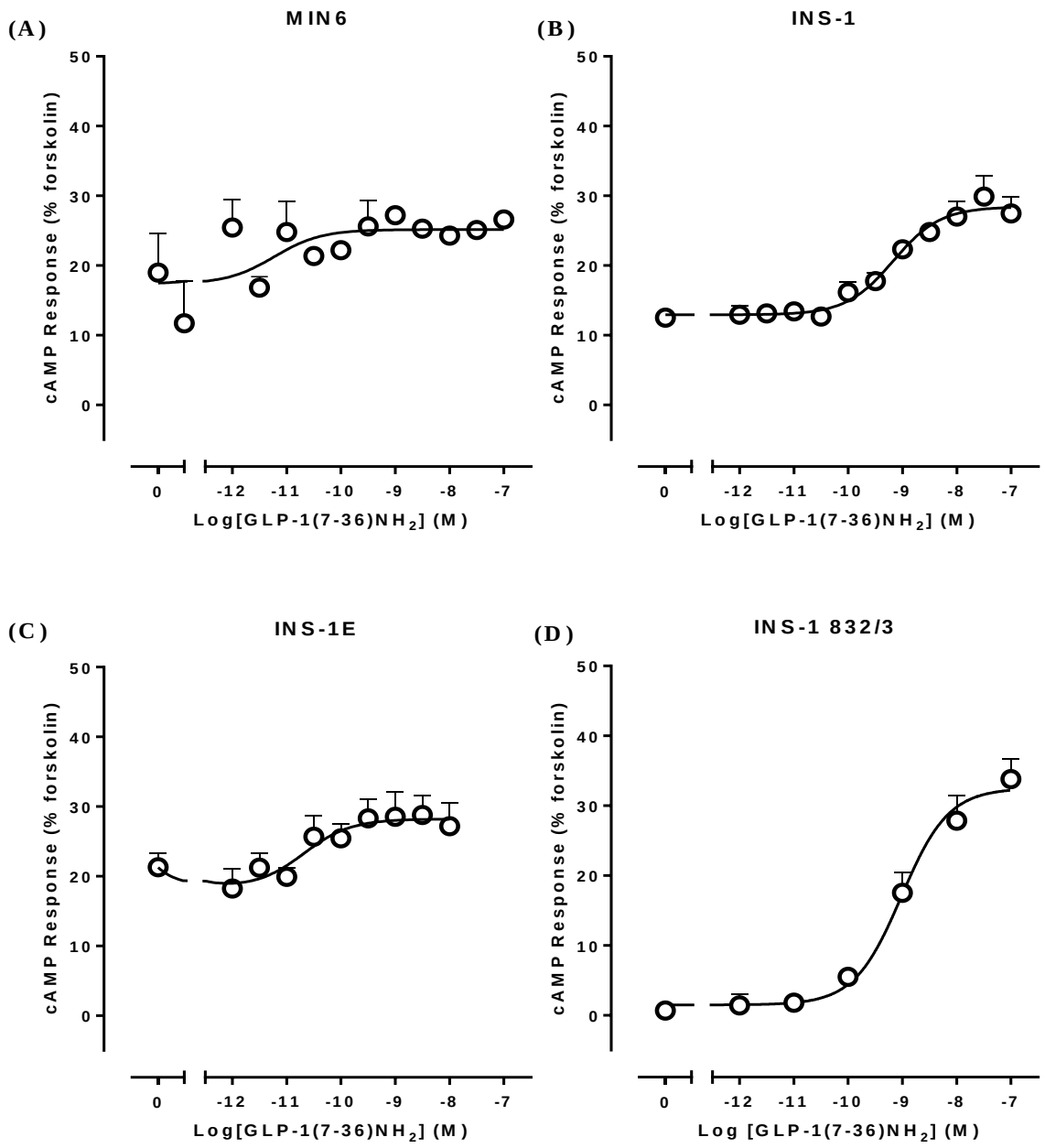

Figure 3.1: cAMP accumulation in different insulinoma cells. Effect of GLP-1 on cAMP accumulation in different insulinoma cell lines in 11 mM (high) glucose conditions. (A) mouse insulinoma cell line, MIN6, plated at cell density 50,000 cells/well; (B) rat insulinoma cell line, INS-1, plated at cell density 60,000 cells/well; (C) rat clonal insulinoma cell line, INS-1E, plated at cell density 30,000 cells/well; (D) rat clonal insulinoma cell line, INS-1 832/3, plated at cell density 30,000 cells/well. cAMP accumulation was normalised to maximum forskolin (10µM)response.

Cell densities were selected based on those reported previously in the literature for the relevant cell lines. Each were assayed 72 h following cell plating. Data is analysed with three-parameter logistic equation. All values are mean + SEM of three to six independent experiments conducted in triplicate. The average forskolin response observed in various cells lines are (A) MIN6 =2.08 nM, (B) INS-1 = 7.87 nM, (C) INS-1E= 7.87 nM and (D) INS-1 832/3 cells= 79.84 nM.

Table 3.1: Effect of GLP-1 on cAMP accumulation in different insulinoma cell lines.

Data was analyzed using a three parameter logistic equation. pEC_{50} values represent the negative log of the concentration of agonist GLP-1, that produces half the maximal response. E_{max} values are GLP-1 response normalized to the response elicited by 10 µM forskolin, basal response is presented as the baseline cAMP response as a percent of forskolin stimulated response. The range is the assay window (i.e. E_{max} - basal). All values are mean ± SEM of three to six independent experiments, conducted in triplicate.

	MIN6	**INS-1**	**INS-1E**	**INS-1 832/3**
Basal response (% forskolin)	17.3 ± 2.4	12.9 ± 0.6	21.5 ± 1.7	1.5 ± 1.2
E_{max} (% forskolin)	25.1 ± 1.3	28.4 ± 0.9	30.3 ± 1.7	32.5 ± 1.8
Range (E_{max} – Basal)	7.8 ± 2.6	15.5 ± 1.0	8.8 ± 2.3	31.0 ± 2.1
pEC_{50}	11.23 ± 0.66	9.17 ± 0.14	10.52 ± 0.58	9.02 ± 0.14

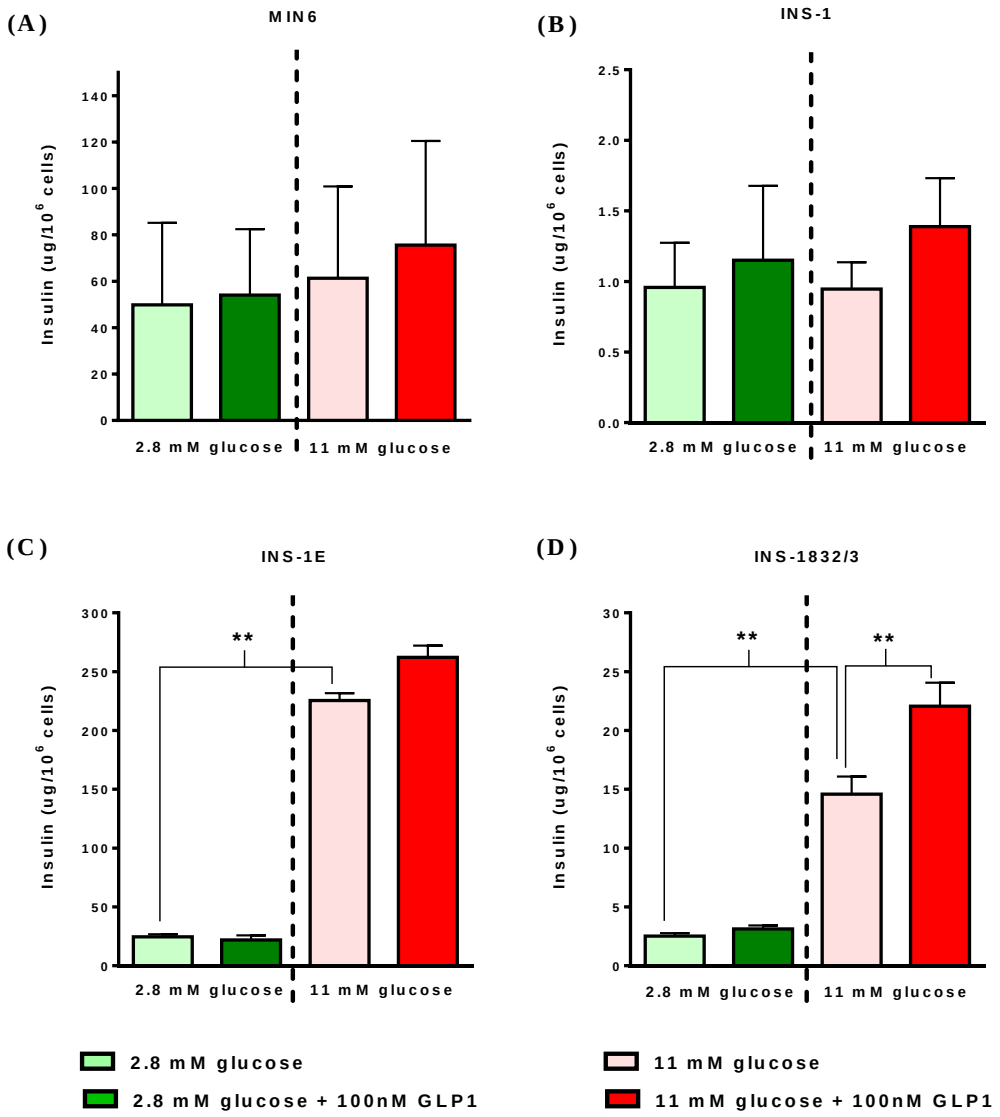

Figure 3.2: Insulin secretion from various insulinoma cell lines. Effect of GLP-1 on insulin secretion in different insulinoma cell lines. (A) MIN6 plated at cell density of 50,000 cell/well; (B) rat insulinoma cell line INS-1, plated at a cell density of 60,000 cells/well; (C) rat clonal insulinoma cell line, INS-1E, plated at a cell density of 30,000 cells/well; (D) rat clonal insulinoma cell line, INS-1 832/3, plated at a cell density of 30,000 cells/well. Insulin secretion is presented as µg insulin per one million cells. Cell numbers chosen were based on previously published work with these individual cell lines. Data were analysed with paired t-test. Statistically significant at $*P < 0.05$ and $**P < 0.01$. All values are mean + SEM of three independent experiments conducted in triplicate.

3.2.2 Identification of suitable coating agent for INS-1 832/3 cells:

In order to assess signalling of the GLP-1R, multiple functional assays will be studied in our chosen cell line. Many of these assays require multiple wash steps and INS-1 832/3 cells detach from the wells of plates under these conditions. Therefore, before any further optimisation of this cell line in multiple assays could be performed, different coating materials were tested so as to achieve firm adherence and uniform spread of INS-1 832/3 cells, prior to and during the functional assays.

We tested multiple coatings for their suitability. The wells of the cell culture plates were coated with poly-D-lysine(PDL; 5 µg/mL in 1X PBS), gelatin (0.1% w/v in Milli-Q water), collagen (rat tail, type 1) (0.1% w/v stock prepared in 0.1M acetic acid; diluted to a working solution of 0.01% with MQ water), FBS, laminin (5 µg/mL in 1X PBS) and fibronectin (5 µg/mL in 1X PBS) according to the manufacturer's instructions.

INS-1 832/3 cells were plated on these coated plates at different cell densities varying from 20,000 to 45,000 cells/well and their morphology, growth and distribution were visually compared to those seeded on uncoated plates using a Nikon Eclipse TS100 inverted microscope (4X and 20X objectives).Images were captured over regular intervals following plating prior to performing a cAMP accumulation assay. This was used as a functional screen to aid identification of the most appropriate coating, with the visual examination used to identify the ideal cell number that could attain sufficient confluency (> 90%) prior to assay and the condition, that allowed cells to remain adherent following multiple wash steps during the cAMP assay. As many assays require multiple washing steps, we also performed extra test washings on the cells, two to four times continuously, to assess their adherence.

For all conditions 5 min and 30 min cAMP assays were performed in the absence (5 min) and presence (30 min) of IBMX. But for fibronectin (which was introduced later in the assay design), only 25,000 (Figure 3.3 D-F) and 40,000 cells/well (Appendix 1, Figure S3.15 E-H) were assessed with cAMP assay performed only at 30 min (Figure 3.3 F and S3.15 H). In all cases 5 min cAMP resulted in inconsistent and variable levels of cAMP accumulation, irrespective of the coatings and cell numbers (Table 3.2). Therefore, only cAMP at 30 min will be discussed further. The key findings from these experiments are summarised in the Table 3.3 and all the raw data is contained in Appendix 1.

Briefly, at cell densities above 30,000 cells/well, cells were confluent, rounded and aggregated in all conditions, 24 and 48 h after plating (Table 3.3). Not surprisingly, this resulted in considerable cell

loss during the washing procedures in all conditions (although some coatings were more prone to higher cell loss than others) (Figure S3.1, S3.3, S3.4, S3.6, S3.8, S3.10). Additionally, in the majority of these conditions, cAMP could not be detected, and where it could, results were often variable (Table 3.3, Figure S3.2, S3.5, S3.7, S3.9, S3.11, S3.13). For cell numbers of 30,000 and less, some coatings did not alter INS-1 832/3 behaviour whereas others were unfavourable (Tables 3.2 and 3.3). 24 h post-plating, cells seeded on FBS coatings were not uniformly dispersed (Figure S3.11) and this was worse at 48 h. Cells seeded on gelatin appeared to form disc-like structures that were non-adherent even after 48 h post-plating (Figure S3.10). Cells plated on both FBS and gelatin coated plates were easily washed off and not surprisingly, they did not produce robust, reproducible cAMP responses (Figure S3.9 and S3.11; Table 3.2).

For PDL and collagen coating, cells were evenly dispersed at 24 h post-seeding, however, some cells had a rounded and more randomly distributed at 48 h (Figure S3.4 and S3.6). Washing the cells seeded on collagen coated plates resulted in considerable cell loss and cAMP responses with large error bars (Figure S3.7; Table 3.2), whereas, cells plated on PDL remained adherent with washing and produced robust cAMP responses (Figure S3.5 and S3.7).

Cells plated onto fibronectin (Figure 3.3 D-F andS3.15 E-H) and laminin (Figure 3.3 A-C, S3.14 A-D) plates were uniformly dispersed with the expected morphology (compared to uncoated plates) at 24 h, and unlike PDL-coated plates retained expected morphology at 48 h post-seeding. After washing, these cells maintained adherence whereas on uncoated plates (Appendix 1, Figure S3.1), cells were lost with larger numbers of washes. Cells plated on both fibronectin and laminin coatings produced robust and reproducible cAMP responses for these cells (Figure 3.3; Table 3.2 and 3.3).

Based on the visual microscopic evaluation, combined with evaluation of multiple washing procedures and the cAMP accumulation data, fibronectin and laminin were chosen as suitable coating agents (Figure 3.3) and laminin was used in all subsequent assays.

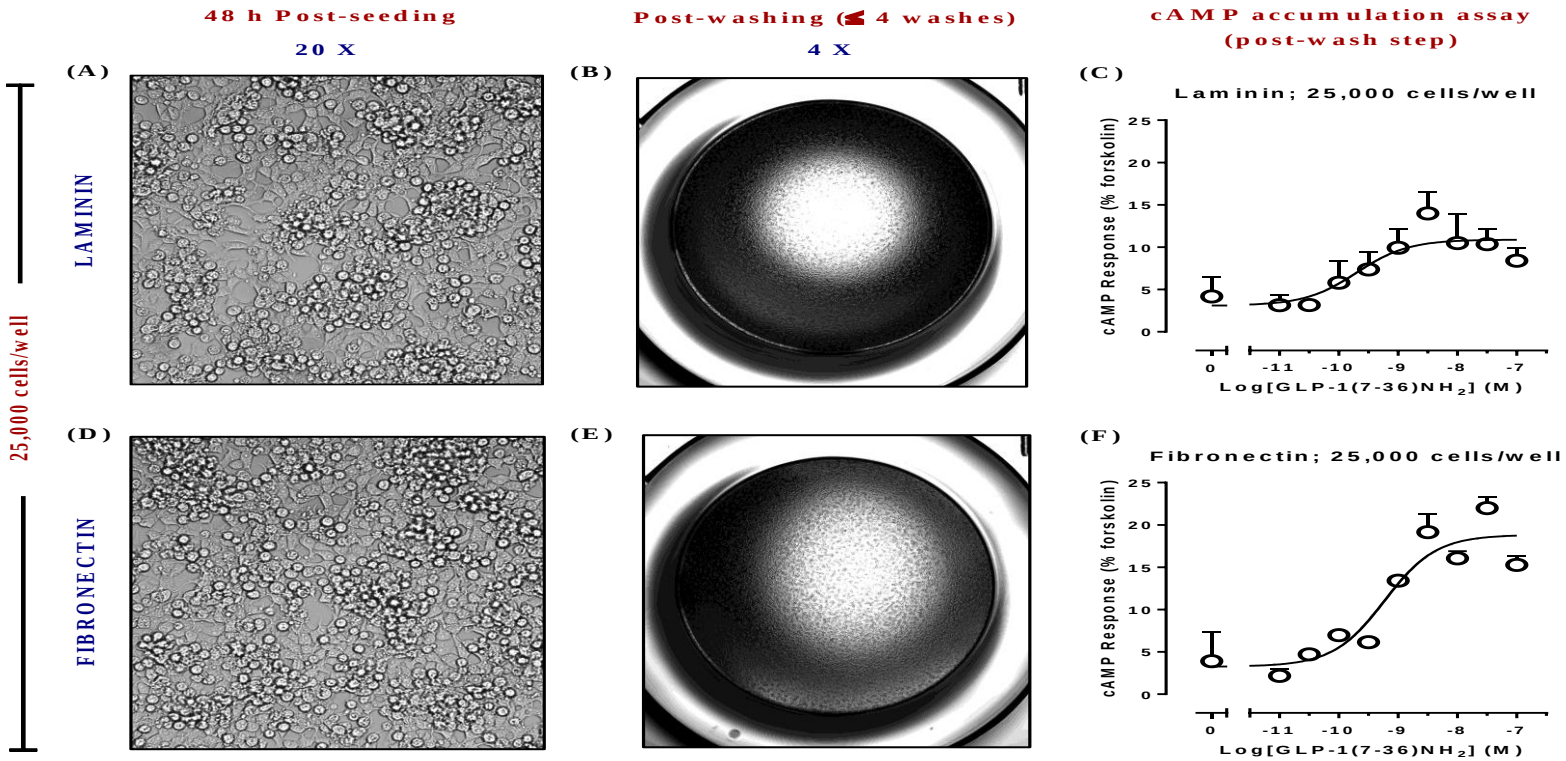

Figure 3.3: Effect of seeding duration and washing of cells on cAMP accumulation. Effect of GLP-1 in 11 mM glucose on cAMP accumulation in INS-1 832/3 cells 48 h post-seeding at a density of 25,000 cells/well on laminin (A-C) and fibronectin (D-F) coated 96 well cell culture plates. (A) cell confluence on the day of assay on laminin coated plate prior to wash step; (B) washing of cells prior to assay on laminin coated plates; (C) concentration dependent cAMP response with cells seeded on laminin coated plate following washing; (D) cell confluence on the day of assay on fibronectin coated plate prior to wash step; (E) washing of cells prior to assay on fibronectin coated plates; (F) concentration dependent cAMP response with cells seeded on fibronectin coated plate following washing. cAMP accumulation was normalised to maximum forskolin response at 10 µM. Data was analysed with a three parameter logistic equation. All values are mean + SEM of three to six independent experiments conducted in triplicate.

Table 3.2: Effect of GLP-1 and 11 mM glucose on cAMP accumulation in INS-1 832/3 cells stimulated for 5 min and 30 min, after 48 h of seeding on plates treated with different coating agents at varying cell densities.

Data was analyzed using a three parameter logistic equation. pEC_{50} values represent the negative log of the concentration of agonist GLP-1, that produces half the maximal response. E_{max} values are GLP-1 response normalized to the response elicited by 10 µM forskolin, basal response is presented as the baseline cAMP response as a percent of forskolin stimulated response. The range is the assay window (i.e. E_{max} - basal). All values are mean ± SEM of three to six independent experiments, conducted in triplicate. The cells were starved for 2 h prior to assay with basal glucose concentration being 2.8 mM and serum reduced to 0%. Conditions highlighted in yellow routinely produce cAMP within the expected potency range based on the reported values in the literature.

Coating	Cell density (cells/ well)	5 min stimulation (In absence of IBMX)				30 min stimulation (in presence of IBMX)			
		Basal response (% forskolin)	E_{max} (% forskolin)	Range (E_{max} - Basal)	pEC_{50}	Basal response (% forskolin)	E_{max} (% forskolin)	Range (E_{max} - Basal)	pEC_{50}
Uncoated	20,000	17.8 ± 6.2	10.1 ± 6.1	-7.7 ± 8.2	10.26 ± 2.27	2.7 ± 1.3	24.3 ± 4.5	21.5 ± 4.5	7.80 ± 0.34
	25,000	0.7 ± 10.6	61.4 ± 5.3	60.6 ± 11.4	10.82 ± 0.35	0.7 ± 2.2	11.2 ± 4.1	10.4 ± 4.4	8.61 ± 0.91
	30,000	25.7 ± 6.6	85.8 ± 68.5	60.0 ± 67.1	7.33 ± 1.37	3.2 ± 2.2	14.8 ± 2.8	11.7 ± 3.4	9.21 ± 0.64
	35,000	ND	ND	ND	ND	0.3 ± 0.3	4.1 ± 1.3	3.8 ± 1.3	7.67 ± 0.52
	40,000	4.4 ± 5.7	16.8 ± 13	12.4 ± 13.5	8.34 ± 2.44	3.5 ± 2.8	15.8 ± 4.6	12.3 ± 5.2	8.81 ± 0.88
	45,000	6.62 ± 5.7	19.1 ± 6.9	12.5 ± 8.5	9.54 ± 1.63	0.5 ± 0.9	13.6 ± 1.9	13.2 ± 2.0	8.49 ± 0.36
Poly-D-Lysine	20,000	64.0 ± 1113	14.3 ± 7.1	-49.7 ± 1110	ND	5.6 ± 3.7	23.5 ± 5.8	17.9 ± 6.6	8.94 ± 0.78
	25,000	19.2 ± 18.9	46.0 ± 25.6	26.7 ± 30.2	9.28 ± 3.01	0.7 ± 0.9	19.2 ± 0.9	18.5 ± 1.2	9.79 ± 0.15

(PDL)	30,000	13.2 ± 4.9	71.8 ± 24.3	58.5 ± 23.8	7.58 ± 0.60	3.5 ± 2.9	11.7 ± 2.9	8.1 ± 3.9	9.95 ± 1.09
	35,000	12.3 ± 11.9	31.8 ± 12.7	19.5 ± 16.7	9.63 ± 2.06	1.1 ± 0.6	5.5 ± 1.8	4.6 ± 1.8	7.98 ± 0.70
	40,000	24.42 ± 7.0	9.2 ± 5.0	-15.2 ± 8.23	10.76 ± 1.48	2.9 ± 1.5	9.7 ± 1.3	6.8 ± 1.8	9.41 ± 0.55
	45,000	35.0 ± 21.7	10.0 ± 8.1	-25.0 ± 22.34	11.88 ± 1.60	0.2 ± 0.7	2.2 ± 0.7	2.0 ± 0.9	10.01 ± 1.08
Collagen	20,000	53.0 ± 18.8	3.3 ± 9.2	-48.6 ± 19.8	11.58 ± 0.82	1.3 ± 1.7	4.9 ± 3.5	3.6 ± 3.7	8.50 ± 2.16
	25,000	13.5 ± 4.3	0.9 ± 7.0	-12.6 ± 7.9	8.86 ± 1.32	ND	ND	ND	ND
	30,000	20.0 ± 4.7	6.5 ± 6.5	-13.4 ± 7.6	9.26 ± 1.29	1.3 ± 1.3	6.1 ± 1.0	4.8 ± 1.5	10.67 ± 0.75
	35,000	8.9 ± 6.7	35.3 ± 17.7	26.5 ± 18.2	8.14 ± 1.24	4.2 ± 1.0	15.6 ± 1.5	11.4 ± 1.7	9.06 ± 0.32
	40,000	26.5 ± 3.7	6.4 ± 3.3	-20.1 ± 4.7	10.67 ± 0.52	7.0 ± 1.0	-6.2 ± 28.3	-13.2 ± 28.0	6.94 ± 1.60
	45,000	ND	ND	ND	ND	2.2 ± 1.7	20.8 ± 4.8	18.6 ± 4.9	8.01 ± 0.46
FBS	20,000	8.0 ± 3.4	52.5 ± 11.9	44.4 ± 11.9	8.01 ± 0.46	4.9 ± 1.7	16.5 ± 3.6	11.6 ± 3.8	8.44 ± 0.68
	25,000	51.9 ± 12.1	10.4 ± 8.3	-41.5 ± 14.1	11.06 ± 0.66	ND	ND	ND	ND
	30,000	14.0 ± 4.4	190.2 ± 1166	176.2 ± 1164	6.50 ± 3.78	0.9 ± 1.1	3.5 ± 0.9	2.5 ± 1.4	10.46 ± 1.28
	35,000	21.4 ± 12.2	43.6 ± 54.5	22.2 ± 35.3	8.04 ± 2.74	3.2 ± 1.7	4.6 ± 1.5	1.3 ± 2.1	10.38 ± 3.79
	40,000	37.2 ± 17.5	9.3 ± 4.8	-28.0 ± 17.5	12.22 ± 0.99	1.1 ± 2.1	16.4 ± 2.0	15.3 ± 2.8	10.15 ± 0.42
	45,000	18.8 ± 20.5	44.7 ± 15.5	26.0 ± 25.3	10.01 ± 2.11	2.8 ± 1.6	22.7 ± 22.0	20.0 ± 21.6	7.23 ± 1.11
Gelatin	20,000	ND	ND	ND	ND	ND	ND	ND	ND

	25,000	ND	ND	ND	ND	9.0 ± 2.3	-3.3 ± 16.1	-12.4 ± 15.7	7.43 ± 1.72
	30,000	ND	ND	ND	ND	10.1 ± 4.2	4.11 ± 5.9	-6.0 ± 6.9	9.26 ± 2.62
	35,000	22.4 ± 6.4	4.1 ± 5.9	-18.3 ± 8.7	10.45 ± 1.41	ND	ND	ND	ND
	40,000	53.0 ± 16.3	0.9 ± 24.6	-52.1 ± 28.3	10.20 ± 1.01	1.8 ± 5.5	48.0 ± 7.2	46.2 ± 8.6	9.35 ± 0.51
	45,000	ND	ND	ND	ND	10.2 ± 3.5	3.5 ± 7.3	-6.6 ± 7.7	8.50 ± 2.44
Laminin	20,000	34.3 ± 9.3	8.3 ± 4.1	-25.9 ± 9.6	11.62 ± 0.75	ND	ND	ND	ND
	25,000	47.3 ± 9.2	7.9 ± 3.6	-39.4 ± 9.5	11.82 ± 0.44	3.1 ± 1.5	10.9 ± 1.1	7.8 ± 1.7	9.70 ± 0.44
	30,000	45.2 ± 15.7	11.1 ± 9.2	-34.2 ± 17.4	11.21 ± 1.08	0.4 ± 2.0	7.4 ± 2.5	7.0 ± 3.0	9.51 ± 1.04
	35,000	77.7 ± 101.6	10.6 ± 9.6	-67.1 ± 99.2	12.70 ± 1.77	1.8 ± 2.2	10.6 ± 6.0	8.8 ± 6.1	8.10 ± 1.21
	40,000	37.6 ± 36.5	5.5 ± 11.1	-32.0 ± 36.9	12.14 ± 1.86	6.1 ± 1.7	14.5 ± 1.6	8.4 ± 2.1	9.33 ± 0.53
	45,000	ND	ND	ND	ND	5.9 ± 4.8	24.6 ± 5.0	18.6 ± 6.7	9.88 ± 0.81
Fibronectin	25,000	-	-	-	-	3.3 ± 1.1	18.8 ± 1.1	15.6 ± 1.4	9.23 ± 0.20
	40,000	-	-	-	-	5.3 ± 1.3	16.1 ± 0.8	10.8 ± 1.4	9.87 ± 0.26

Table 3.3: Summarized key findings from the optimization process involved to identify a suitable coating agent so as to investigate various functional outputs in INS-1 832/3 cells. The best conditions are highlighted in yellow.

Coating	VISUAL				WASHING (≤ 4 washes)		cAMP accumulation assay (30 min stimulation)		cAMP accumulation assay (5 min stimulation)	
	≤ 30,000 cells/well		> 30,000 cells/well		≤ 30,000 cells/well	> 30,000 cells/well	≤ 30,000 cells/well	> 30,000 cells/well	≤ 30,000 cells/well	> 30,000 cells/well
	> 24 h	> 48 h	> 24 h	> 48 h	> 48 h		> 48 h		> 48 h	
Uncoated (Appendix 1, Figure S3.1-S3.2; Table 3.2)	• Uniformly dispersed cells • 60-80% confluent	• Cells adherent and uniformly dispersed • >90% confluent	• Over-confluent, aggregated and rounded cells • > 80% confluent	• aggregated and rounded cells	With subsequent washes cells start to detach	Considerable cell loss	cAMP in potency range (pEC50 ~ 1 nM)	cAMP in potency range but with variability and large errors	Inconsistent and variable cAMP responses	
Poly-D-Lysine (PDL) (Appendix 1, Figure	• Uniformly dispersed cells • 40-60% confluent	• aggregated and rounded cells distributed randomly • 80-90% confluent	• Over-confluent, aggregated and rounded cells • > 80% confluent	• aggregated and rounded cells distributed randomly	Cells remain adherent and uniformly dispersed	Considerable cell loss	cAMP in potency range (pEC50 ~ 1 nM)	cAMP in potency range but with high errors	Inconsistent and variable cAMP responses	

S3.3 - S3.5; Table 3.2)									
Collagen (Appendix 1, Figure S3.6-S3.7; Table 3.2)	• Cells distributed randomly • 30-40% confluent	• aggregated and rounded cells distributed randomly • 40-60% confluent	• Over-confluent, aggregated and rounded cells • > 70% confluent	• aggregated and rounded cells distributed randomly	Considerable cell loss	Considerable cell loss	cAMP in potency range but with high errors (pEC50 ~ 1 nM)	cAMP in potency range but with high errors	Inconsistent and variable cAMP responses
FBS (Appendix 1, Figure S3.8 - S3.9; Table 3.2)	• Cells not evenly dispersed	• Over-confluent, aggregated and rounded cells dispersed unevenly	• aggregated and rounded cells dispersed unevenly	• aggregated and rounded cells dispersed unevenly	Considerable cell loss	Considerable cell loss	Weak cAMP response Inconsistent EC50	Weak cAMP response Inconsistent EC50	Inconsistent and variable cAMP responses
Gelatin (Appendix 1, Figure S3.10-S3.11; Table 3.2)	• Uniformly dispersed cells	• Non-adherent, disc structures	• Over-confluent, aggregated and rounded cells	• Non-adherent, disc structures	Considerable cell loss	Considerable cell loss	Weak cAMP response Inconsistent EC50	Weak cAMP response Inconsistent EC50	No cAMP response detected
Laminin (Figure 3.3 A – C,	• Uniformly dispersed cells in monolayers	• Uniformly dispersed cells • ~90% Confluent	• Over-confluent, aggregated and rounded	• Over-confluent, aggregated and rounded	Cells remain adherent	Considerable cell loss	cAMP detected within the	cAMP detected within the	Inconsistent and variable cAMP responses

Appendix 1, Figure S3.12-S3.14; Table 3.2)			cells	cells			potency range (pEC50 ~ 1 nM)	potency range	
Fibronectin (Figure 3.3 D - F, Appendix 1, Figure S3.15; Table 3.2)	• Uniformly dispersed cells in monolayers	• Uniformly dispersed cells • ~90% Confluent	• Over-confluent, aggregated and rounded cells	• Over-confluent, aggregated and rounded cells	Cells remain adherent	Considerable cell loss	cAMP detected within the potency range (pEC50 ~ 1 nM)	cAMP detected within the potency range	---------

3.2.3 Further optimization of cAMP accumulation assays

Conditions for the cAMP accumulation assay were optimised using laminin and fibronectin coated plates. Based on protocols in the literature, cAMP assays have been performed up to 72 h post-seeding of INS-1 832/3 cells. Cells were seeded at a density of 25,000 cells/well and cAMP assays were performed at 48 h (as per all preliminary experiments) and 72 h post-seeding. Glucose and GLP-1 mediated cAMP accumulation was observed on each coating (laminin and fibronectin), when the assay was performed 72 h post-seeding (Figure 3.4). cAMP was also assessed in both low (2.8 mM) and high (11 mM) glucose conditions. A right shift in the potency of peptide was observed with increase in glucose concentration from 2.8 mM to 11 mM glucose (Figure 3.4 D and H).The cAMP assay performed after 48 h of seeding showed a dose-dependent accumulation of cAMP but the response was more variable than 72 h (Figure 3.4 B and F). From these studies, we selected laminin coating with cells seeded at 25,000 cells/well and incubation for 72 h post-seeding prior to performing the cAMP assay, as these conditions provided the most robust and reproducible cAMP responses from stimulation of the GLP-1R in conditions assessed. All cAMP assays described above were performed in DMEM as vehicle. Many different buffers have been used for assaying these cells in the literature; these include DMEM, HBSS and EBSS. To further optimise our assay, these three buffers were assessed for performance of the cAMP assay with 30 min stimulation in presence of 2.8 and 11 mM glucose concentrations (Figure 3.5). cAMP responses in HBSS were variable with large errors (Figure 3.5B; Table 3.4). Both EBSS and DMEM resulted in robust, potent dose-dependent accumulation of cAMP (Figure 3.5 A and C). Though the potency of GLP-1, was comparable in both DMEM and EBSS (Figure 3.5 A and C; Table 3.4), the response window observed was larger in EBSS and the results were very reproducible. In addition, in both buffers the response was slightly (although not statistically significant) more potent in 2.8 mM glucose compared to 11 mM glucose (Figure 3.5 A and C). Thus, based on the observations, 25,000 cells/well stimulated after 72 h of seeding on laminin coated plates, for 30 min in EBSS containing IBMX resulted in highly robust reproducible cAMP responses.

Finally, we also assessed the impact of passage number on the potency and maximal GLP-1 response observed as the literature suggests that these cells may show a loss of GLP-1R responsiveness at high passage numbers (Hohmeier *et al.,* 2000; Merglen *et al.,* 2004). Assessment of cAMP at passage 31-33 revealed higher potencies than those of passage 46-48 (Figure 3.6 A and B; Table 3.5). Therefore, INS-1 832/3 cells of passage 30-45 (p30 is the lowest passage in the laboratory) were used for all subsequent experiments in this thesis.

Despite a slightly higher maximal response in the higher passage cells, we opted to use only low passage cells as pEC_{50} of 8.86 ± 0.62 has been reported previously for cAMP production in INS-1 832 cells (Ehses *et al.,* 2003), consistent with that of our lower passage cells. Moreover, pEC_{50} values reported for cAMP accumulation in low expressing recombinant cell systems was also similar to that observed in our study with low passage INS-1 832/3 cells, with pEC_{50} values similar to the affinity of GLP-1 (Koole *et al.,* 2010, 2012, 2015; Wootten *et al.,* 2013). The reduced GLP-1 and glucose responsiveness of INS-1 832/3 with increase in passage numbers is also consistent with data reported in the literature (Hohmeier *et al.,* 2000; Merglen *et al.,* 2004).

3.2.4 Optimizing conditions for glucose-dependent insulin secretion

To assess glucose-dependent insulin secretion, we compared a number of different detection methods. This included ELISA based kits and a HTRF based kit. The ELISA based kit only detects rodent insulin, however, the HTRF kit detects both human and rat insulin. As INS-1832/3 cell line is a modified cell line that contains the gene for human insulin, it secretes both human and rat insulin.

For cell treatment, we followed a published protocol supplied by our collaborators at Eli lily (Indianapolis, Indiana, United States). This consisted of a two hour glucose starvation in EBSS containing 2.8mM glucose, followed by 2 h ligand treatment in the presence of 11 mM glucose and collection of the supernatant. Treatments were performed on cells plated at the optimised cell density of 25,000 cells/well in 96 well plates, 72 h post-seeding on laminin coated plates. Each kit was then used following the manufacturer's instructions. With the ELISA kit we were unable to detect any GLP-1-mediated insulin release, however, with the HTRF kit, GLP-1-mediated insulin response could be detected only in the presence of high glucose (Figure 3.7B) (Brisson *et al.,* 1972). This is consistent with expectations based on published results. Following identical conditions a concentration response curve was produced and this revealed that while a concentration-dependent insulin secretion could be detected in high glucose, there was considerable error associated with the data, making accurate determination of EC_{50} values through curve fitting problematic.

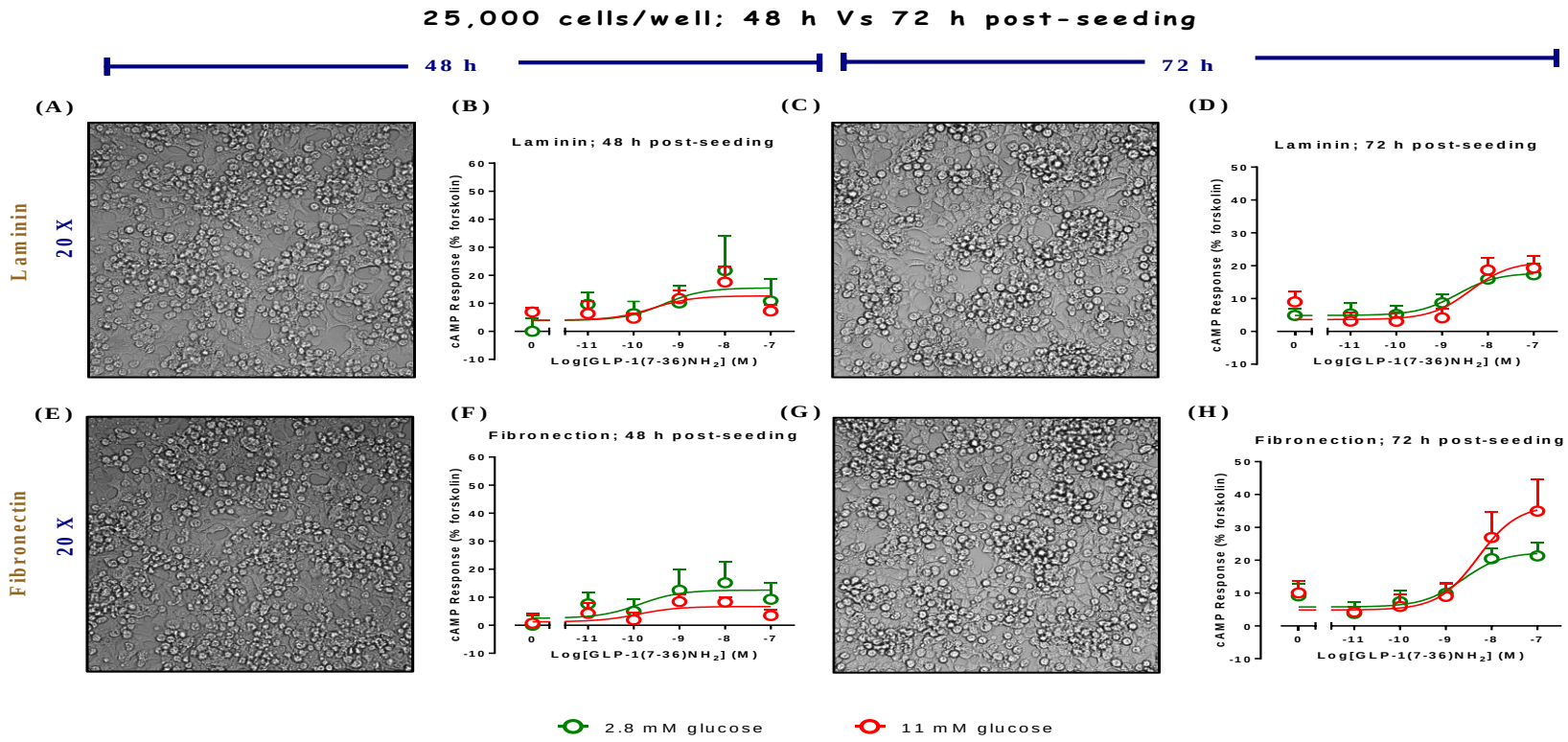

Figure 3.4: Effect of GLP-1 on cAMP accumulation in presence of varying glucose concentration (2.8 mM and 11 mM) after 48 h (A, B, E and F) and 72 h (C, D, G and H) of seeding 25,000 cells/well on laminin (A-D) and fibronectin (E-H) coated 96 well cell culture plates. (A) 25,000 cells/well on laminin coated plate after 48 h; (B) cAMP assay after 48 h of post-seeding on laminin coated plate; (C) 25,000 cells/well on laminin coated plate after 72 h; (D) cAMP assay after 72 h of post-seeding on laminin coated plate; (E) 25,000 cells/well on fibronectin coated plate after 48 h; (F) cAMP assay after 48 h of post-seeding on fibronectin coated plate; (G) 25,000 cells/well on fibronectin coated plate after 72 h; (H) cAMP assay after 72 h of post-seeding on fibronectin coated plate. cAMP accumulation was normalised to maximum forskolin (10^{-5}M) response. Data was analysed with a three parameter logistic equation. All values are mean + SEM of three to six independent experiments conducted in triplicate.

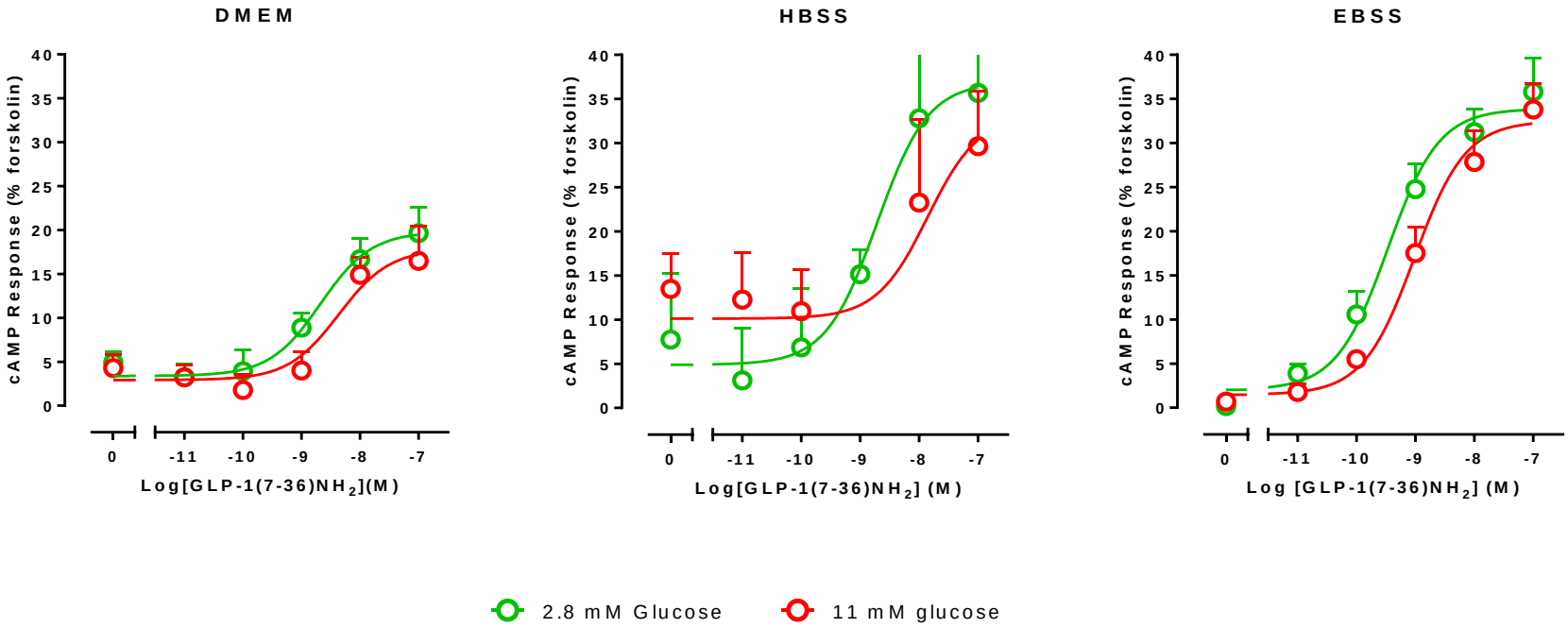

Figure 3.5: Effect of different buffers on cAMP accumulation. Effect of GLP-1 on INS-1 832/3 cells assessed using cAMP accumulation performed in (A) DMEM and (B) EBSS as stimulation buffers supplemented with 2.8 mM and 11 mM glucose at a seeding density of 25,000 cells/well on laminin coated 96 well cell culture plates. cAMP accumulation was normalised to maximum forskolin, 10 µM (10^{-5}M) response. Data was analysed with a three parameter logistic equation. All values are mean + SEM of three to six independent experiments conducted in triplicate.

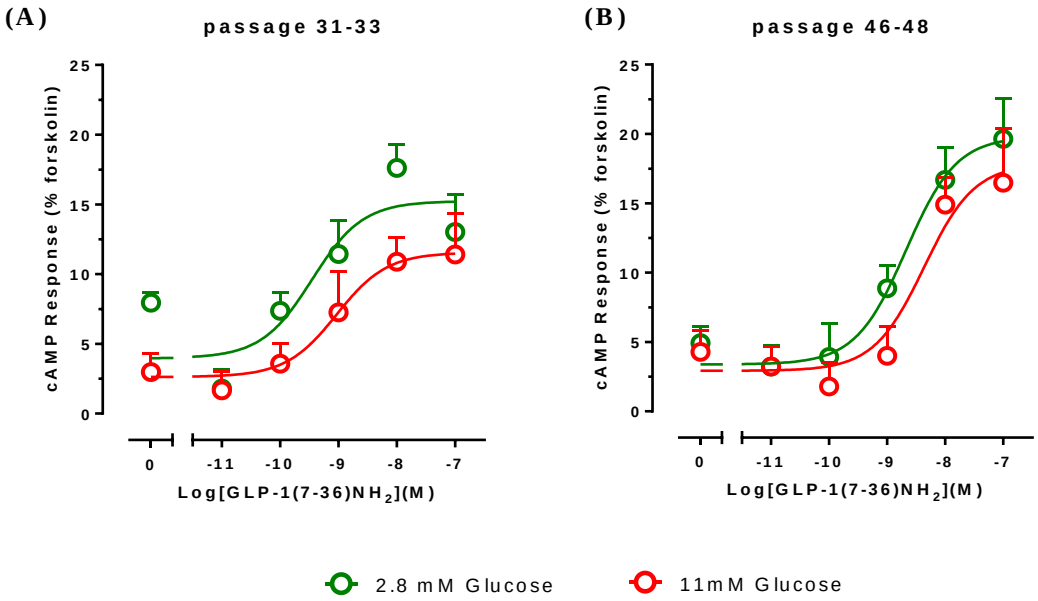

Figure 3.6: Effect of different passages of INS-1 832/3 cells on cAMP accumulation. Effect of GLP-1 in presence of varying glucose concentrations on two different passages of INS-1 832/3 cells, (A) passage 31-33 and (B) passage 46-48, seeded on laminin coated plates. cAMP accumulation was normalised to maximum forskolin(10^{-5}M) response. Data was analysed with a three parameter logistic equation. All values are mean + SEM of three to six independent experiments conducted in triplicate.

In an attempt to improve the assay conditions and reproducibility of results, optimisation of the glucose starvation conditions was performed, in addition to a serum starvation. Overnight glucose and serum starvation (2.8 mM glucose and 2.5 % v/v FBS) was compared to 2 h starvation (2.8 mM glucose and no FBS) before stimulating the cells with GLP-1 in both low (2.8mM) and high (11mM) glucose. GLP-1 mediated insulin secretion was observed in high glucose, but not in low glucose (consistent with the literature) following both overnight and 2 h starvation conditions (Figure 3.8), but the response observed following overnight starvation was more reproducible and the potency was consistent with what would be expected from those reported in primary islets (pEC_{50} = 9.41 ± 0.34) (Table 3.6, Figure 3.8) (Goke *et al.,* 1993; Baggio and Drucker, 2007). Therefore, these conditions were selected as optimal.

3.2.4 Optimizing conditions for phosphorylation of ERK1/2

ERK1/2 is often used as a general marker of convergent activation of multiple pathways including G protein-independent signalling (Lee *et al.,* 2008). The GLP-1R is known to signal to this pathway and it has been identified to be of physiological importance. Therefore, we wanted to optimize conditions to detect pERK1/2 in INS-1 832/3 cells. To initiate the optimization process and identify an ideal set of conditions to study GLP-1R dependent ERK1/2 phosphorylation, we followed the protocol used for CHO FlpIn cells (Koole *et al.,* 2010; Woottern *et al.,* 2012). This consisted of serum starving the cells for a minimum of 5 h prior to ligand treatment and pERK1/2 detection using an alphascreen assay.

After 72 h of seeding, the cells were serum starved for 6 h prior to assay. Treatments were performed on cells plated at a cell density 25,000 cells/well on laminin coated 96 well plates (optimised using cAMP accumulation and insulin assay).These studies were performed in EBSS to be consistent with those of cAMP accumulation and insulin. In addition this assay was also performed in normal growth media (RPMI 1640). An ERK1/2 phosphorylation time course for GLP-1 was performed at a saturating concentration of 100nM and in presence of both low (2.8 mM) and high (11 mM) glucose. In both buffers, a GLP-1-mediated response could be observed in 2.8 mM glucose that peaked at 2 min and returned to baseline although this was larger in RPMI than EBSS (compared to the 10% v/v FBS response) (Figure 3.9 B and F). Peak ERK1/2 phosphorylation was detected at 5 min and 2 min in response to 11 mM glucose and GLP-1, respectively, in EBSS (Figure 3.9G)and RPMI (Figure 3.9C).

Table 3.4: Effect of GLP-1 on cAMP accumulation in INS-1 832/3 cells stimulated in DMEM and EBSS, 72 h post-seeding on laminin coated plates respectively, for 30 min in presence of 2.8 mM and 11 mM glucose.

Data was analyzed using a three parameter logistic equation. pEC_{50} values represent the negative log of the concentration of agonist GLP-1, that produces half the maximal response. E_{max} values are GLP-1 response normalized to the response elicited by 10 µM forskolin, basal response is presented as the baseline cAMP response as a percent of forskolin stimulated response. The range is the assay window (i.e. E_{max} - basal). All values are mean ± SEM of three to six independent experiments, conducted in triplicate. The cells were starved for 2 h prior to assay with basal glucose concentration being 2.8 mM and serum reduced to 0%.

	DMEM (72 h post- seeding)		**HBSS (72 h post-seeding)**		**EBSS (72 h post-seeding)**	
	2.8 mM glucose	**11 mM glucose**	**2.8 mM glucose**	**11 mM glucose**	**2.8 mM glucose**	**11 mM glucose**
Basal response (% forskolin)	3.4 ± 1.0	3.0 ± 1.1	4.9 ± 4.0	10.1 ± 3.0	2.0 ± 1.4	1.5 ± 1.2
E_{max} (% forskolin)	19.8 ± 1.9	17.8 ± 2.5	36.9 ± 7.3	33.2 ± 10.1	33.8 ± 1.8	32.5 ± 1.8
Range (E_{max} – Basal)	16.4 ± 2.0	14.9 ± 2.6	32.0 ± 8.0	23.1 ± 10.2	31.9 ± 2.1	31.0 ± 2.1
pEC_{50}	8.68± 0.27	8.36 ± 0.35	8.72 ± 0.71	7.85 ± 0.71	9.47 ± 0.16	9.02 ± 0.14

Table 3.5: Effect of GLP-1 on cAMP accumulation in different passages of INS-1 832/3 cells stimulated in DMEM for 30 min in presence of varying glucose concentrations after 72 h of seeding on plates coated with laminin.

Data was analyzed using a three parameter logistic equation. pEC_{50} values represent the negative log of the concentration of agonist GLP-1, that produces half the maximal response. E_{max} values are GLP-1 response normalized to the response elicited by 10 µM forskolin, basal response is presented as the baseline cAMP response as a percent of forskolin stimulated response. The range is the assay window (i.e. E_{max} - basal). All values are mean ± SEM of three to six independent experiments, conducted in triplicate. The cells were starved for 2 h prior to assay with basal glucose concentration being 2.8 mM and serum reduced to 0%.

	Passage 31-33		**Passage 46-48**	
	2.8 mM glucose	**11 mM glucose**	**2.8 mM glucose**	**11 mM glucose**
Basal response (% forskolin)	4.0 ± 1.1	2.6 ± 1.1	3.4 ± 1.0	2.9 ± 1.1
E_{max} (% forskolin)	15.2 ± 1.4	11.5 ± 1.7	19.8 ± 1.9	17.8 ± 2.5
Range (E_{max} – Basal)	11.3 ± 1.7	8.9 ± 2.0	16.4 ± 2.1	14.9 ± 2.6
pEC_{50}	9.45 ± 0.35	9.03 ± 0.47	8.67 ± 0.27	8.36 ± 0.35

Table 3.6: Effect of starvation periods (2 h and overnight starvation) on GLP-1-mediated GSIS, prior to insulin secretion assay.

Data was analyzed using a three parameter logistic equation. pEC_{50} values represent the negative log of the concentration of agonist GLP-1, that produces half the maximal response. Data are normalized to the response elicited by 11 mM glucose (baseline) and 100 nM GLP-1 in 11 mM glucose (E_{max}). The range is the assay window (i.e. E_{max} - basal) of individual conditions. All values are mean ± SEM of four independent experiments, conducted in triplicate. NDR = No detectable response; ND = Curve could not be defined despite response

	2 h starvation prior to assay		**Overnight starvation prior to assay**	
	2.8 mM glucose	**11 mM glucose**	**2.8 mM glucose**	**11 mM glucose**
Basal response (% GLP-1 max in high glucose)	-73.5 ± 2.0	13.0 ± 18.3	-195.6 ± 41.7	9.7 ± 7.8
E_{max} (% GLP-1 max in high glucose)	-52.2 ± 93.1	98.04 ± 7.8	-200.5 ± 36.9	94.5 ± 9.1
Range (Max – Basal)	21.35 ± 92.4	85.02 ± 19.5	-4.8 ± 53.6	84.7 ± 11.5
pEC_{50}	NDR	ND	NDR	9.41 ± 0.34

A peak ERK1/2 phosphorylation of a higher magnitude to GLP-1 was observed in high glucose when compared to low glucose at 2 min (Figure 3.9).

In RPMI, a robust ERK1/2 activation was observed in response to 11 mM glucose at 2 min, which was sustained until 5 min (Figure 3.9 C). A peak ERK1/2 phosphorylation in response to GLP-1 in 11 mM glucose was observed at 2 min(Figure 3.9 C) which unlike in EBSS, where peak ERK1/2 activation persisted for about 7 min before attenuating (Figure 3.9 G), was back to basal within 10 min of stimulation in RPMI 1640 (Figure 3.9 C and G). Moreover, a weak sustained glucose-mediated and GLP-1-mediated response in 11 mM glucose with GLP-1 was detected after 15 min stimulation of the cells in EBSS, which was not evident in RPMI 1640 (Figure 3.9 D and H). To distinguish GLP-1 effects from 11 mM or 2.8 mM glucose effects, we subtracted the relevant glucose only response from the GLP-1-mediated response in 2.8 mM and 11 mM glucose (Figure 3.10 B, F, D and H). This produced a similar profile for GLP-1-mediated response in both RPMI and EBSS, although the magnitude of the response for the transient peak at 2 min is larger in RPMI 1640 in both high and low glucose conditions. However, the literature reports that isolated primary islets cells produce a sustained late ERK1/2 response (Larsen *et al.*, 1998; Quoyer *et al.*, 2010). When activated by GLP-1 in high glucose conditions, this phase was evident in EBSS buffer but not RPMI 1640. Moreover, at 5 min post-ligand addition, in both buffers, GLP-1 suppresses the ERK1/2 response mediated by 11 mM glucose which was unexpected (Figure 3.9 D and H).

We selected the ideal set of conditions to assess the effect of GLP-1R peptides on ERK1/2 phosphorylation in time-dependent manner. The optimised conditions include seeding cells at a density of 25,000 cells/well and serum starving for 6 h prior to assay, 72 h post-seeding. Subsequently, cells are treated with the peptide in EBSS supplemented with calcium chloride and the appropriate glucose concentration and assessed for their pERK1/2 response.

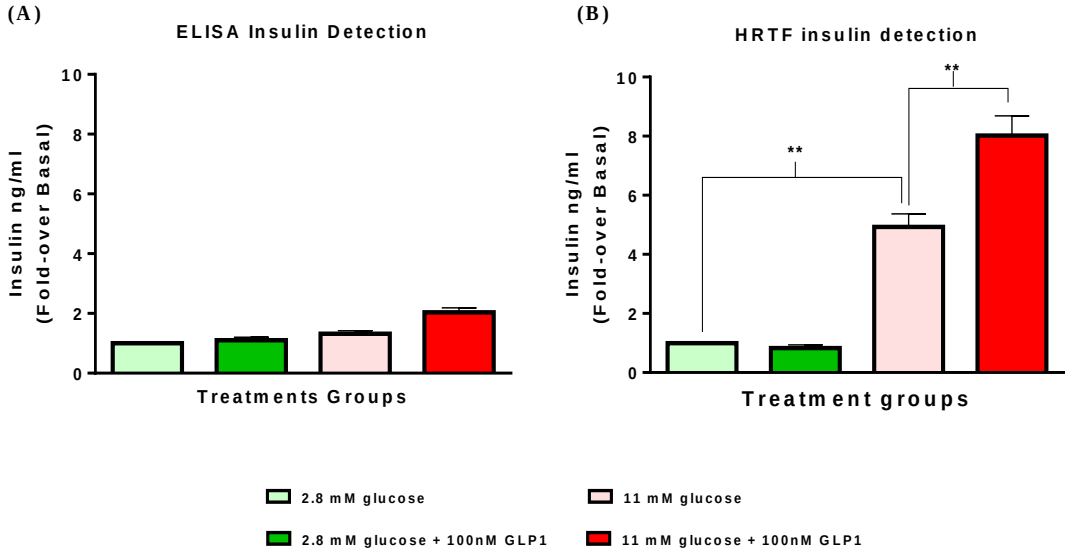

Figure 3.7: Sensitivity of two different insulin detection methods, (A) ELISA and (B) HRTF in INS-1 832/3 cells seeded at 25,000 cells/well on laminin coated plates. Insulin secretion was plotted as fold over basal to 2.8 mM glucose. Data were analysed with paired t-test. Statistically significant at **P < 0.01. All values are mean + SEM of three to six independent experiments conducted in triplicate.

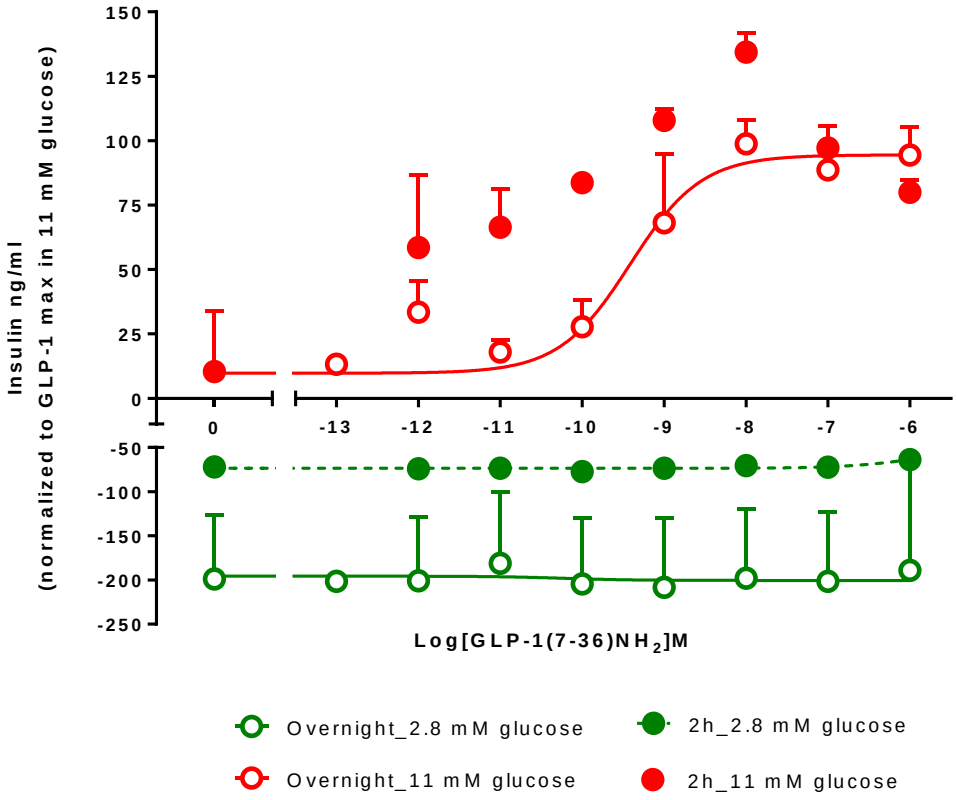

Figure 3.8: Comparison of Insulin secretion detection methods. Effect of starvation periods (overnight *vs* 2 h starvation) prior to assay on GLP-1- mediated glucose-dependent insulin secretion (GSIS). Insulin secretion was normalised to maximum peptide, 100 nM (10^{-7}M) response. All values are mean + SEM of four independent experiments, conducted in triplicate. Data is analysed with a three parameter logistic equation.

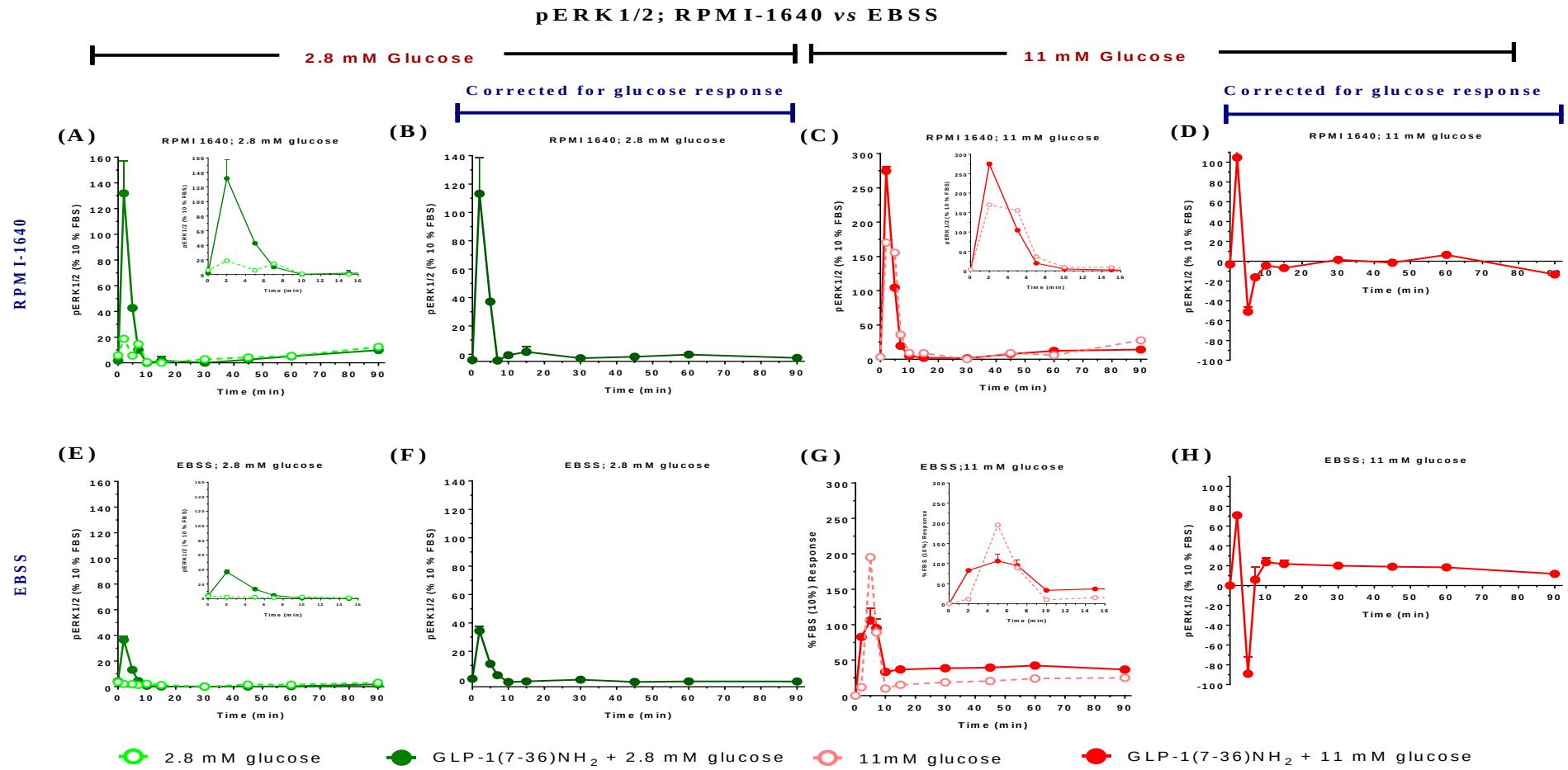

Figure 3.9: Kinetics of ERK1/2 phosphorylation. Time-dependent phosphorylation of ERK1/2 in response to 100 nM GLP-1 in INS-1 832/3 cells seeded at a density of 25,000 cells/well on laminin coated plate and stimulated in different buffers, RPMI 1640 (A-D) and EBSS (E-H) and different glucose concentrations, 2.8 mM (A, B, E, F) and 11 mM (C, D, G, H). In all figures open circles represent the response to relevant glucose concentration in the absence of GLP-1; with closed circles, the GLP-1 response in the presence of the relevant glucose concentration; ERK1/2 response with insets, a close up of

the peak of time-course (A,E); ERK1/2 response for GLP-1 corrected for 2.8 mM glucose response (B, F); ERK1/2 activation in 11 mM glucose and GLP-1 with inset, a close up of the peak region of the time course (C, G) and ERK1/2 activation mediated by GLP-1 in high glucose corrected for the glucose-mediated response. Data is normalised to maximum 10% v/v FBS response at 2 min. All values are mean ± SEM of four independent experiments, conducted in triplicate. All values are mean + SEM of four independent experiments, conducted in triplicate.

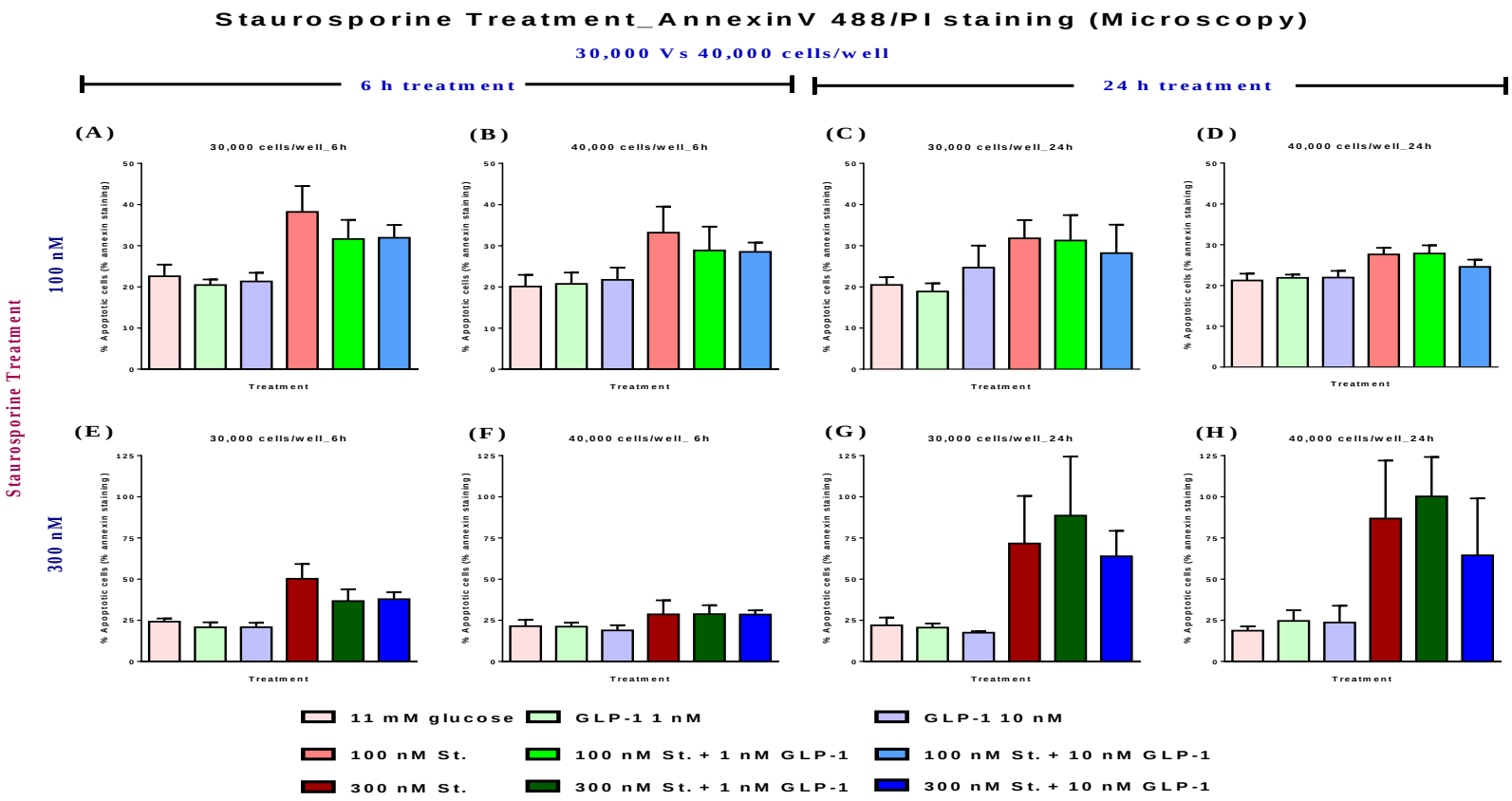

Figure 3.10: Anti-apoptotic study using microscopy. AnnexinV- 488 and propidium iodide staining of INS-1 832/3 cells determined by microscopy after 6 h (A, B, E, F) and 24 h (C, D, G, H) incubation in presence and absence of 100 nM (A-D) and 300 nM (E-H) staurosporine co-added with and/or without GLP-1 in RPMI 1640 supplemented with 11 mM glucose and 10% serum. (A) 30,000 cells/well, 6 h incubation; (B) 40,000 cells/well, 6 h incubation; (C) 30,000 cells/well, 24 hours incubation; (D) 40,000 cells/well, 24 h incubation in presence of 100 nM staurosporine. (E) 30,000 cells/well, 6 h incubation; (F) 40,000 cells/well, 6 h incubation; (G) 30,000 cells/well, 24 h incubation; (H) 40,000 cells/well, 24 h incubation in presence of 300 nM staurosporine. Percent apoptosis was assessed by normalizing to annexinV 488 staining. All values are mean + SEM of four independent experiments, conducted in triplicate.

3.2.6 Optimizing conditions for evaluating apoptosis in INS-1 832/3 cells

GLP-1 is reported to be protective against apoptosis of β-islets (Brubaker and Drucker, 2004). We therefore embarked on establishing conditions to study protection from apoptosis via GLP-1R activation in our INS-1 832/3 cells. To assess the protective effects of GLP-1, apoptosis was induced in INS-1 832/3 cells. Apoptotic versus live healthy cells was assessed usingtwo different approaches, namely 3-[4,5-dimethylthiazol-2-yl]-2,5-diphenyl tetrazolium bromide (MTT; thiazolyl blue) assay, and analysis of AnnexinV-PI stained cells using two techniques, Microscopy (AnnexinV488 and PI staining)analysed with the InCell analyser on 96 well clear bottom black plates and flow cytometry (AnnexinV-647 and PI staining).

A range of different conditions were assessed and optimised, including different apoptotic-inducing agents at varying concentrations (TNF-α and staurosporine), seeding densities of cells (not all assays were in 96-well format) and treatment durations for GLP-1 (2 h, 6 h, 12 h and 24 h). These conditions were selected to identify effective conditions to induce a cell death (early - late apoptosis) of 65-70% using the inducing agents, that could be inhibited to some extent by GLP-1. The key findings from these experiments are summarised in the Table 3.7, 3.8 and 3.9 and all the raw data is contained in Appendix 1 (Figure S3.16). Briefly, although the MTT assay is associated with limitations, in that it cannot differentiate between cells undergoing apoptosis or necrosis, it isless sensitive than PI and annexin V staining and it also measures a combination of cell events around cell survival (proliferation, metabolic activity, cell viability and cell death), the assay is easy to perform and the preliminary results obtained aided in narrowing down the initial optimisation conditions. Acute toxicity was observed with TNF-α and staurosporine was toxic at a high concentration (1000 nM) (Table 3.7). The results from MTT optimization are summarised in Table 3.7, however due to the limitations in differentiating between apoptosis and other cell viability measures (as mentioned above), this assay was not pursued further.

Apoptosis detected using AnnexinV/PI staining protocols was quantified as cells stained with AnnexinV conjugate alone (early apoptosis) and AnnexinV conjugate and PI both (late apoptosis). PI positive cells were excluded as these cells followed a necrotic fate of the cell death without entering an apoptotic pathway. Cells that did not stain with either AnnexinV or PI were considered viable. During optimisation, the concentration of AnnexinV 647 conjugate was also optimised to 1:100 in contrast to 1:20 as stated according to manufacturer's protocol. Analysis of staurosporine-induced apoptosis by microscopy revealed that 300 nM staurosporine was associated with toxic effects resulting in high cell death at 24 h. In addition GLP-1 mediated protection was also observed (Figure 3.10; Table 3.8). However, although, this method could identify cells that had entered into

apoptosis, it was difficult to assess every cell (especially cells in late apoptotic phase) due to the cells detaching from the plate. The InCell analyser has limitations of focussing only to specific area in the wells and cells that were less healthy due to the induced apoptosis had a tendency to lift off from the bottom of the well, therefore were not measured in the analysis. Consequently, flow cytometry was next assessed to measure stained cells using AnnexinV 647 conjugate and propidium iodide.

To improve the window and reproducibility of the data using the FACS protocol, the cells were glucose and serum deprived overnight prior to the assay. Due to a larger number of cells required for FACS, cell density was optimised in 6 well plates. Cell densities of 30,000 cells/well and 40,000 cells/well used in the MTT and microscopy protocols were scaled up to 1.2 x 10^6 cells/well. Staurosporine at 100 nM was used in this assay (based on the results from the MTT and microscopy study), as the inducing agent that was shown to produce approximately 60-70% death in all conditions. In addition, the effect of low glucose (2.8 mM glucose) was added for consideration in further studies (Figure 3.1; Table 3.9). The results from this study are summarised in Table 3.9.

Conditions chosen to assess the effect of GLP-1R peptides on rescue and survival of cells from staurosporine-induced apoptosis, included cells seeded at a density of 5 x 10^5 cell/well and subsequently, starved overnight (approximately 60 h post seeding) in RPMI 1640 (2.5% v/v FBS and 2.8mM glucose) (Figure 3.11). Cells were then treated with 100 nM stauroporine to achieve 65-70% cell death and ligands (co-added) to assess survival. The final protocol is present in materials and methods (chapter 2).

Using these conditions we observed 11 mM glucose itself was protective against apoptosis (25-30%). This could be further enhanced in the presence of GLP-1. In addition, GLP-1 was also protective against staurosporine-induced apoptosis in low glucose (~30%). To assess if a dose-dependent GLP-1R response could be observed, a concentration response curve was performed in both low and high glucose conditions. A GLP-1 concentration response curve was observed in both glucose conditions with a more potent response observed in high glucose (pEC50 = 10.14 ± 0.36) compared to low glucose (pEC_{50} = 9.24 ± 0.37) (Figure 3.12).

Table 3.7: Summarized key findings from the MTT assay used as a part of the optimization process followed to identify ideal set of conditions to investigate apoptosis in INS-1 832/3 cells.

		MTT assay								
		% viable cells (Percent of apoptotic-inducing agent max in 2.8 mM glucose)								
Apoptosis inducing agents	**Glucose**	**2h**			**6h**			**24 h**		
		20,000 cells/well	30,000 cells/well	40,000 cells/well	20,000 cells/well	30,000 cells/well	40,000 cells/well	20,000 cells/well	30,000 cells/well	40,000 cells/well
TNF-α (1 ng/mL; 10 ng/mL; 50 ng/mL)	2.8 mM glucose	Variable and inconsistent	High susceptibility to cell death	High susceptibility to cell death	Variable and inconsistent	Variable and inconsistent	Variable and inconsistent	Bell shaped distribution of cell viability with increased viability observed at 10 ng/ml	Bell shaped distribution of cell viability with max viability observed at 10 ng/ml	Variable and inconsistent
	11 mM glucose	Variable and inconsistent	High concentrations observed in-effective in producing apoptosis	Variable and inconsistent	Increased cell viability observed in dose-dependent manner	Increased cell viability observed in dose-dependent manner	Variable and inconsistent	Bell shaped distribution of cell viability with max viability observed at 10 ng/ml	cell viability observed in dose-dependent manner	Variable and inconsistent
Staurosporine	2.8 mM glucose	High susceptibility to cell death	Variable and inconsistent apoptosis of	Variable and inconsistent apoptosis of	Dose-dependent reduction in	Dose-dependent reduction in	Dose-dependent reduction in	Dose-dependent reduction in	Dose-dependent reduction in	Dose-dependent reduction

(50 nM; 250 nM; 1000 nM)			the cells	the cells	viability	viability	viability	viability	viability	in viability
	11 mM glucose	Variable; reduction in cell viability observed at lower concentrations	Variable; reduction in cell viability observed at lower concentrations	Reduction in cell viability observed at lower concentrations	Dose-dependent reduction in viability	Dose-dependent reduction in viability	Dose-dependent reduction in viability	Dose-dependent reduction in viability	Dose-dependent reduction in viability	Dose-dependent reduction in viability
Inference	Variable effects observed with TNF-α therefore excluded from further studies 1000 nM staurosporine observed to be toxic at 6 h and 24 h with minimal effect of 50 nM stauroprine.									
Limitation	Cannot differentiate between apoptotic and necrotic cell death									
Considered for further optimization	Apoptotic inducing agent: Staurosporine (100 nM and 300 nM) Seeding density: 30,000 and 40,000 cells/well Treatment duration: 6h and 24 h									

Table 3.8: Summarized key findings from the Annexin V 488 conjugate and PI staining of INS-1 832/3 cells analysed using InCell analyser, as a part of the optimization process followed to identify suitable set of conditions to investigate apoptosis.

Microscopy: Annexin V 488 conjugate and PI staining					
		Percent apoptotic cells (%annexinV staining)			
Staurosporine	Glucose	6h		24 h	
		30,000 cells/well	40,000 cell/well	30,000 cells/well	40,000 cell/well
100 nM	11 mM	• ~ 40 % apoptosis observed • ~10% GLP-1 - dependent rescue from apoptosis	• ~30-35 % apoptosis observed • No GLP-1 - dependent rescue from apoptosis	• ~ 30-35 % apoptosis observed • No GLP-1 -dependent rescue from apoptosis	• ~30% apoptosis observed • No GLP-1 - dependent rescue from apoptosis
300 nM	11 mM	• ~50-55 % apoptosis observed • 20% GLP-1 - dependent rescue from apoptosis	• ~ 30-40 % apoptosis observed • No GLP-1 - dependent rescue from apoptosis	• High percentage of apoptosis observed (70-90%) • No GLP-1 -dependent rescue from apoptosis	• High percentage of apoptosis observed (~90%) • No GLP-1 - dependent rescue from apoptosis
Inference	300 nM staurosporine is toxic at 24 h				
Limitation	difficult to assess every cell as some cells did not stay completely adhered to the wells restricted focus area				
Considered for further optimization	Similar conditions considered for optimization of FACS protocol				

Table 3.9: Summarized key findings from the Annexin V 647 conjugate and PI staining of INS-1 832/3 cells analyzed using FACS, as part of the optimization process followed to identify suitable set of conditions to investigate apoptosis. Highlighted in yellow are the best conditions identified.

FACS: Annexin V 647 conjugate and PI staining									
Treatment	**Glucose concentration**	**Percent Apoptosis (as a Percent of Staurosporine treatment)**							
		1.2 x 10^6 cells/well		9 x 10^5 cells/well		7 x 10^5 cells/well		5 x 10^5 cells/well	
		6 h	24 h	6 h	24 h	6 h	24 h	6 h	24 h
100 nM Staurosporine	11 mM glucose	Effect of glucose cannot be predicted because of absence of low glucose treatment groups during preliminary studies. Variable effects in presence of GLP-1	Effect of glucose cannot be predicted because of absence of low glucose treatment groups during preliminary studies. ~25-30% rescue in presence of GLP-1	~25-30% rescue in presence of GLP-1	~20% protection in presence of glucose alone Further ~20% rescue in presence of GLP-1	Not performed	~20% protection in presence of glucose alone ~40% rescue in presence of GLP-1; dose-dependent	Not performed	~20% protection in presence of glucose alone ~25-30 % rescue in presence of GLP-1 GLP-1 observed to be dose-dependent and more potent

	2.8 mM glucose	Not performed	Not performed	Not performed	Not performed	Not performed	~ 25 % rescue in presence of GLP-1; dose-dependent	Not performed	~ 25 % rescue in presence of GLP-1 GLP-1 observed to be dose-dependent and more potent

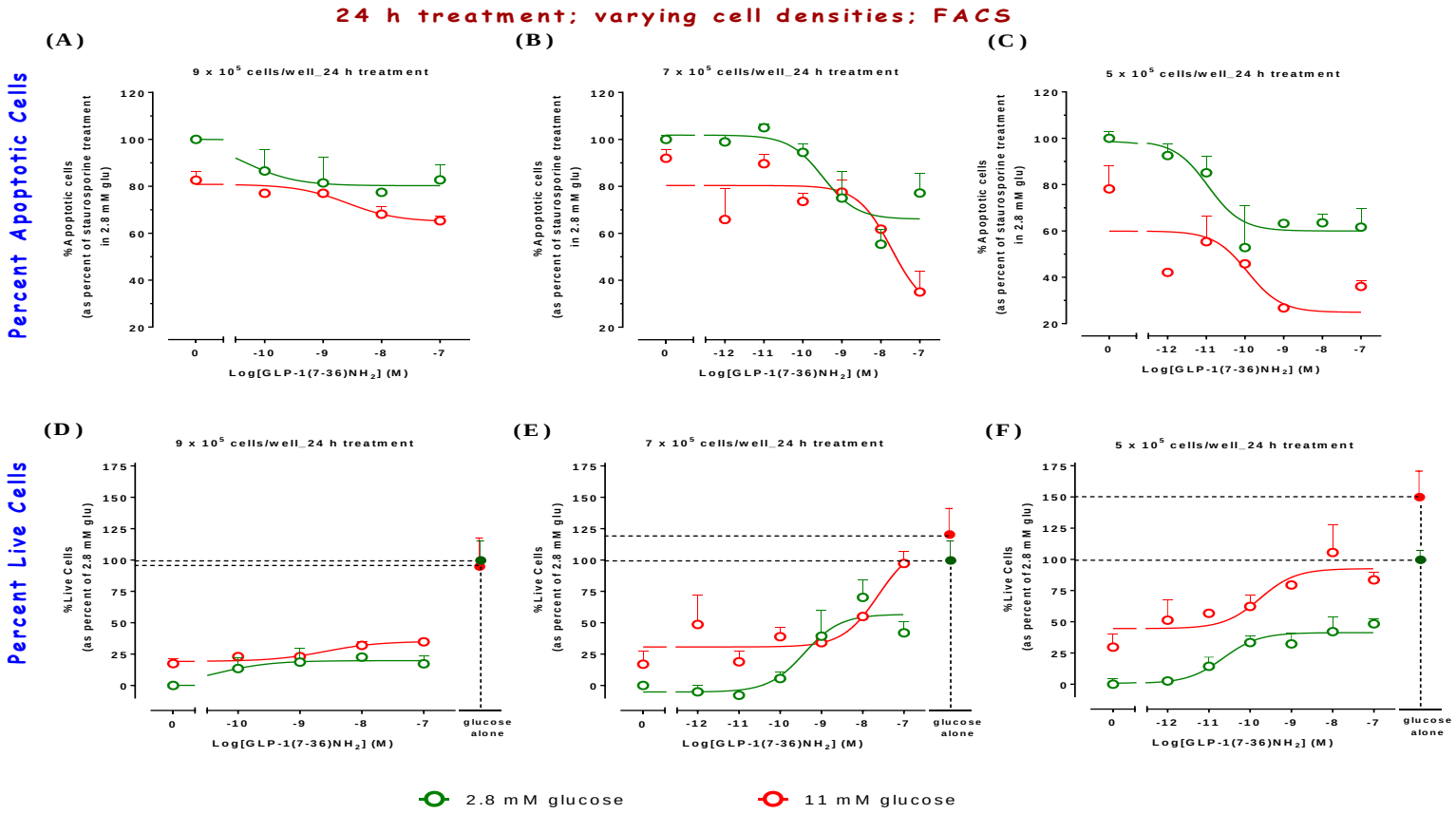

Figure 3.11: Optimisation of cell density for apoptosis assay. Dose-dependent effect of GLP-1 on annexinV- 647 and propidium iodide staining of INS-1 832/3 cells after 24 h of co-addition and incubation in presence of 100 nM staurosporine and GLP-1 with RPMI 1640 supplemented with 10% serum and 2.8 mM or 11 mM glucose. Percent apoptotic was assessed as percent of staurosporine treatment in 2.8 mM glucose (A) 5 x 10^5 cells/well; (B) 7 x 10^5 cells/well.Percent live cells was determined after 24 h of incubation of (A) 5 x 10^5 cells/well; (B) 7 x 10^5 cells/well, as percent of 2.8 mM glucose media. Data was analysed using a three parameter logistic equation. All values are mean + SEM of four independent experiments, conducted in triplicate.

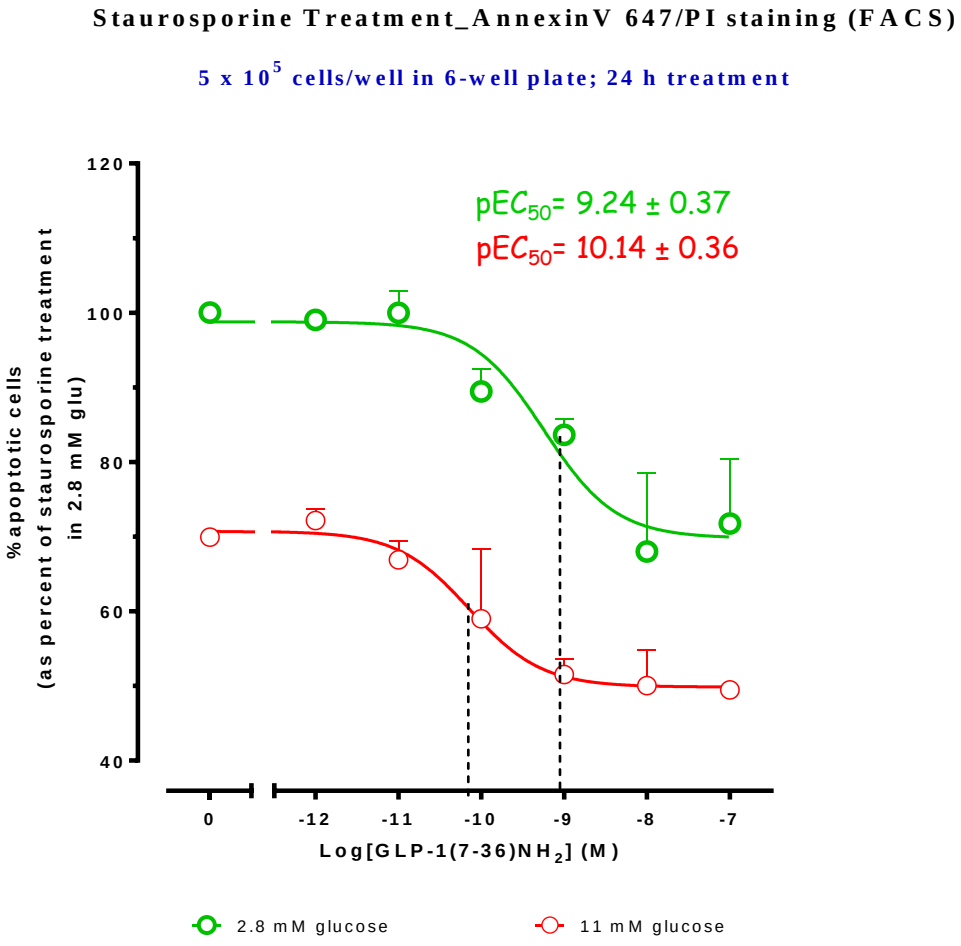

Figure 3.12: Anti-apoptotic study in INS-1 832/3 cells. Dose-dependent effect of GLP-1 on annexinV- 647 and propidium iodide staining of INS-1 832/3 cells after 24 h of co-addition and incubation in presence of 100 nMstaurosporine and GLP-1 with RPMI 1640supplemented with 10% serum and 2.8 mM or 11 mM glucose. Percent apoptotic cells was assessed as percent of staurosporine treatment in 2.8 mM glucose. Data was analysed using three parameter logistic equation. All values are mean + SEM of four independent experiments, conducted in triplicate.

3.2.7 Optimizing conditions for proliferation of INS-1 832/3 cells

To test whether the activation of GLP-1R induces proliferation of INS-1 832/3 cells, two different protocols were compared, namely, 3-[4,5-dimethylthiazol-2-yl]-2,5-diphenyl tetrazolium bromide (MTT; thiazolyl blue) assay and 5-bromo-2′-deoxyuridine (BrdU) incorporation. The first requirement for standardizing the assay was the optimal seeding density and the required incubation periods in presence of low glucose, high glucose and GLP-1 in low and high glucose (24 h, 48 h and 72 h). Additionally, other optimizing conditions taken into consideration included varying concentrations of FBS (10% v/v, 2% v/v, 0.5% v/v and 0% v/v) in order to identify the minimum concentration of FBS essential for survival of cells, which would allow optimization of the window for peptide mediated responses.

In the MTT assay, varying the incubation period of treated cells with sodium dodecyl sulphate (SDS), used to promote cell lysis and solubilisation of formazan crystals between 5 h and overnight (18 – 24 h), was also assessed so as to obtain consistent, measurable and comparable colour production. While limited differences in signals were observed, overnight lysis was chosen as overnight incubation with SDS after 24 h treatment with GLP, showed comparable proliferation at different cell densities. Although GLP-1R mediated proliferation was observed in 2.8 mM glucose after 24 h exposure to GLP-1, higher cell numbers and longer incubation periods (48 h and 72 h) produced more variable results. Marked proliferation of cells in FBS and 11 mM glucose further reduced the window of response for the peptide, making it difficult to identify a reasonable and reproducible response window to assess GLP-1R agonists effects.

While optimizing conditions for MTT assay, 0.5% v/v FBS was identified to be the minimum concentration required for maintenance of INS-1 832/3 cells and to minimize any proliferative effects contributed by the growth factors present in FBS. With 0.5% v/v FBS concentration, the cell numbers and peptide exposure periods were optimized using a chemiluminescence approach to measure BrdU incorporation to detect DNA synthesis in replicating cells.

These assays were optimised in a 96-well plate format, using a wide range of seeding densities varying from 5,000 cells/well to 40,000 cells/well using 10 nM and 100 nM GLP-1 in low (2.8mM) and high (11 mM) glucose following incubation for 24 h (Figure 3.13), 48 h and 72 h post-seeding. The proliferative effect of FBS (positive control) and glucose was evident at all cell densities and exposure conditions. However, GLP-1-mediated proliferative responses were very weak. The largest GLP-1-mediated response occurred at 12,000 and 20,000 cells/well with a proliferation response of almost 20% observed after 24 h exposure using 20,000 cells/well and 100 nM GLP-1

regardless of the glucose concentration (Figure 3.13D). Although the response in high glucose are more variable, large variability was observed in the extent of proliferation measured at longer incubation periods of 48 h and 72 h for GLP-1. In addition, cells seeded at high cell densities did not proliferate much even at 24 h (particularly in high glucose)and this was probably a result of confluency attained by the cells seeded in these conditions, as when cells reach 100% confluency they may undergo contact inhibition slowing their proliferation rate or they begin to die. Additionally, wells with very low seeding density did not proliferate in presence of GLP-1 and this may be due to too few cells and lack of contacts at the seeded densities causing them to proliferate much slower, and, therefore little proliferation was observed (Figure 3.13). Despite this, however, at 20,000 cells/well seeding density dose-dependent GLP-1 responses were obtained beyond that of glucose alone (pEC_{50} = 9.06 ± 1.24) in low glucose, however the response window was small (~5%) (Figure 3.14; Table 3.10). More robust responses were seen with 12,000 cells. Treatment for 24 h in 2.8 mM glucose (Figure 3.14) gave a lower potency (pEC_{50} = 9.35 ± 0.42) than high glucose (pEC_{50} = 11.35 ± 0.78) (Table 3.10; Figure 3.14 B). However, in high glucose GLP-1 -mediated proliferation could be observed, the windows were small and perhaps due to the high proliferative effects of glucose alone in these cells, the ability to detect enhanced proliferation from GLP-1 may be limited (Figure 3.14).

Thus, the ideal set of conditions identified to assess the effect of GLP-1R peptides on proliferation by measuring BrdU incorporation includes a seeding density of 12,000 cells/well incubated in presence of peptide and 0.5% v/v FBS for 24 h.

3.2.8 Optimizing conditions for assessing intracellular calcium ([Ca2+]i) mobilization in INS-1 832/3 cells

Calcium signalling downstream of GLP-1R activation is known to have physiologically significance. To optimise assays to measure calcium signalling, we adopted a method that has been used successfully in the laboratory to measure GLP-1R mediated calcium signalling in recombinant cell lines. This involves assessing intracellular calcium using the dye Fluo4, following the protocol described in the materials and methods section (Chapter 2, section 2.7). To optimise the assay for the Ins1823/3 cell line, a range of cell numbers and seeding durations were selected. These were limited to 20,000, 25,000 and 30,000 cells per well in 96 well clear bottomed plates coated with laminin, and assays were performed 72 hours post seeding (conditions were selected based on the optimisation for cAMP accumulation assays). On the day of assay, cells were stimulated with 2.8mM glucose, or 11mM glucose in the absence or presence of increasing concentrations of GLP-1 and intracellular calcium was measured over a 2 minute time period. All data are normalised to a

positive control, ionomycin. In all instances, cells were starved of glucose and FBS (2.5 % v/v FBS) overnight prior to assay. The only cell number that produced a detectable response was 30 000 cells/well (Figure 3.15)

Concentration response curves were generated for GLP-1 in high and low glucose. No calcium response was observed following GLP-1R stimulation in low glucose or from low glucose alone. High glucose resulted in calcium signalling, which was further enhanced by GLP-1 although the window was relatively small. The peak response was plotted for each concentration, corrected for the glucose only response (Figure 3.15). In 11mM glucose, this produced a concentration response curve in high glucose with a pEC50 of 7.4 ± 0.36 M, with no concentration response detectable in 2.8 mM glucose conditions. The conditions selected as final assay conditions were 30000 cells/well followed by assay 72 h post seeded, conditions that are in line with the cAMP, insulin and pERK1/2 assays Figure 3.15

Hence, the favourable conditions for investigating GLP-1R-mediated physiologically and clinically relevant outcomes were established in INS-1 832/3 cells and can be categorized as glucose-dependent (GSIS, pERK1/2, and calcium mobilization) and -independent (cAMP accumulation, anti-apoptosis and proliferation). All the functional endpoints are summarised in Figure 3.16.

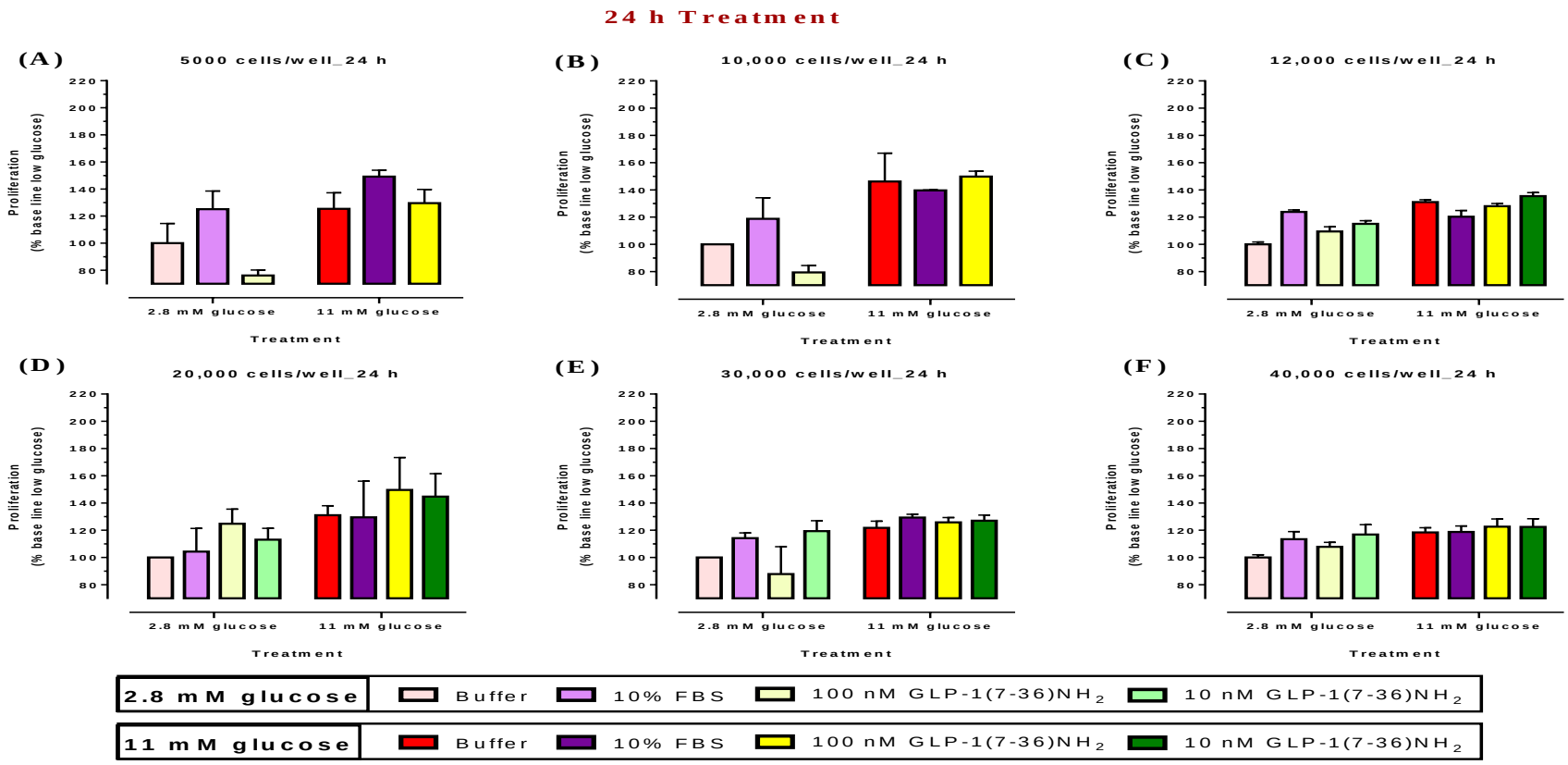

Figure 3.13: BrdU incorportaion after 24h incubation in presence of GLP-1 (10 nM and 100 nM) at a cell density of (A) 5000 cell/well; (B) 10,000 cells/well; (C) 15,000 cells/well; (D) 20,000 cells/well; (E) 30,000 cells/well and (F) 40,000 cells/well. Proliferation was quantified as a percent 2.8 mM glucose response. Data is presented as percent of response elicited in 2.8 mM glucose (where, 100% is defined as total apoptotic cells in 2.8 mM glucose only). All values are mean + SEM of three to five experiments conducted in triplicate.

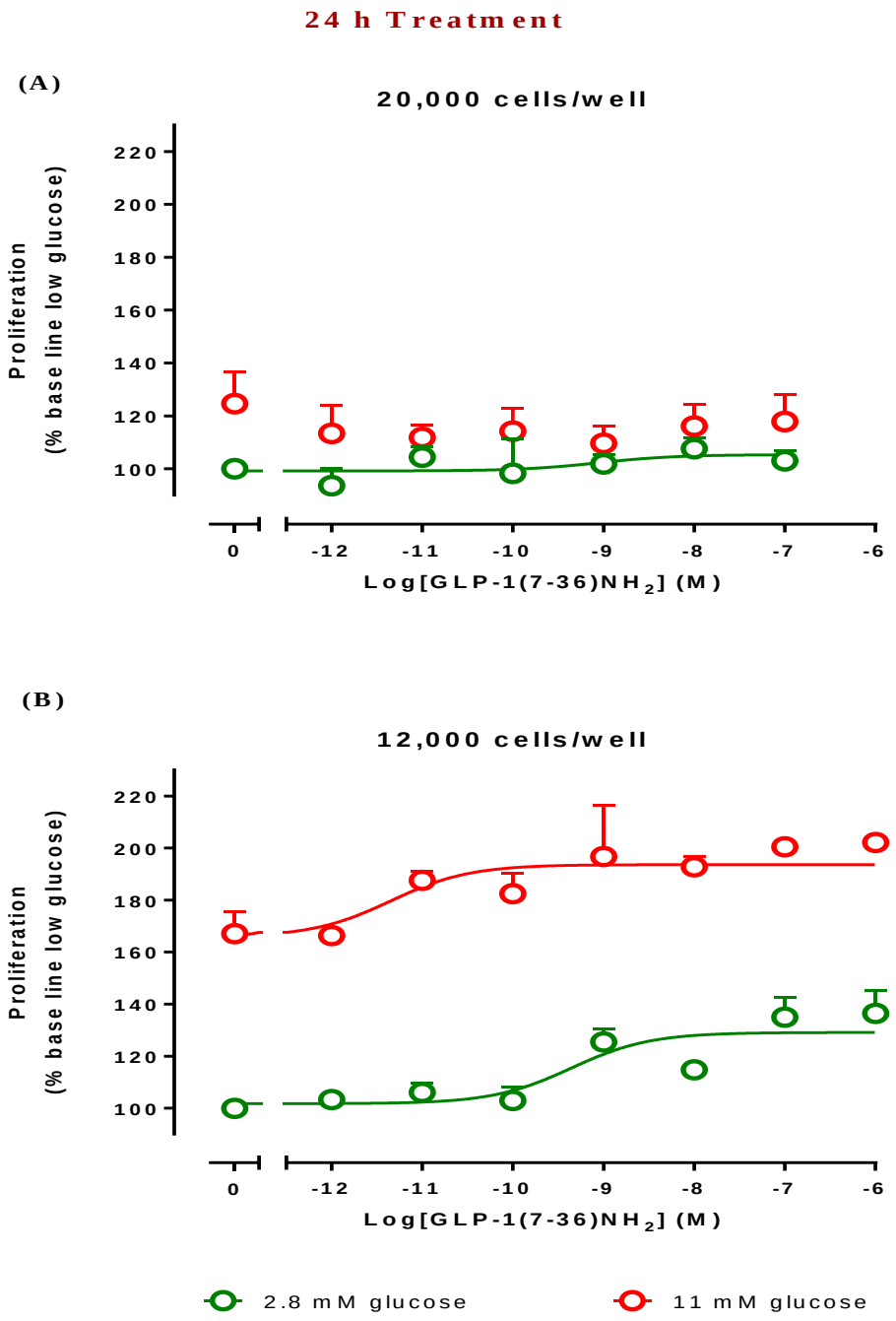

Figure 3.14: Proliferation assay using BrdU incorporation (chemiluminesence approach). Dose-dependent uptake of BrdU after 24 h incubation in presence GLP-1 at a cell density of (A) 20,000 cell/well; (B) 12,000 cells/well. Proliferation was quantified as a percent 2.8 mM glucose response. Data is normalised to the response elicited by vehicle alone (2.8 mM glucose). All data was analysed with a three-parameter logistic equation. All values are mean + SEM of three experiments conducted in triplicate.

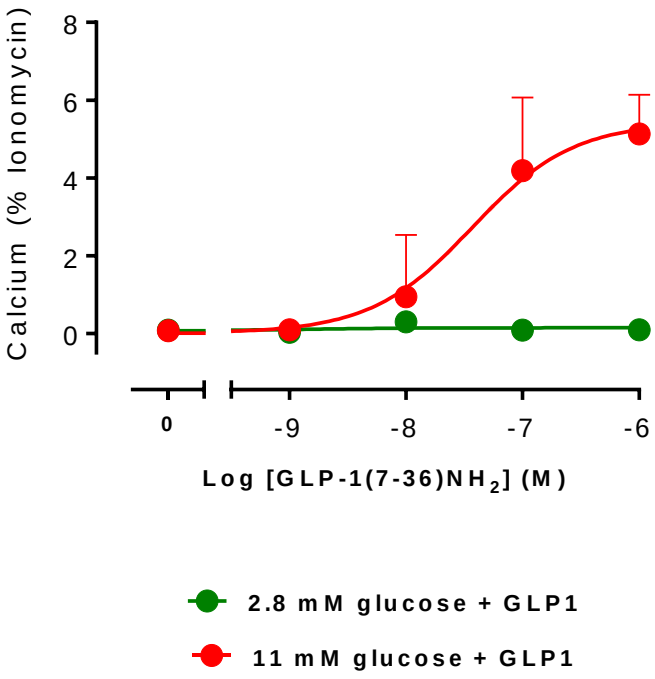

Figure 3.15: Intracellular calcium signaling. Effect of GLP-1 on intracellular calcium mobilization in both low and high glucose conditions at a cell density of 25,000 cells/well. Calcium mobilization was quantified as a percent ionomycin response. Data was analysed using three parameter logistic equation. All values are mean + SEM of four independent experiments, conducted in triplicate.

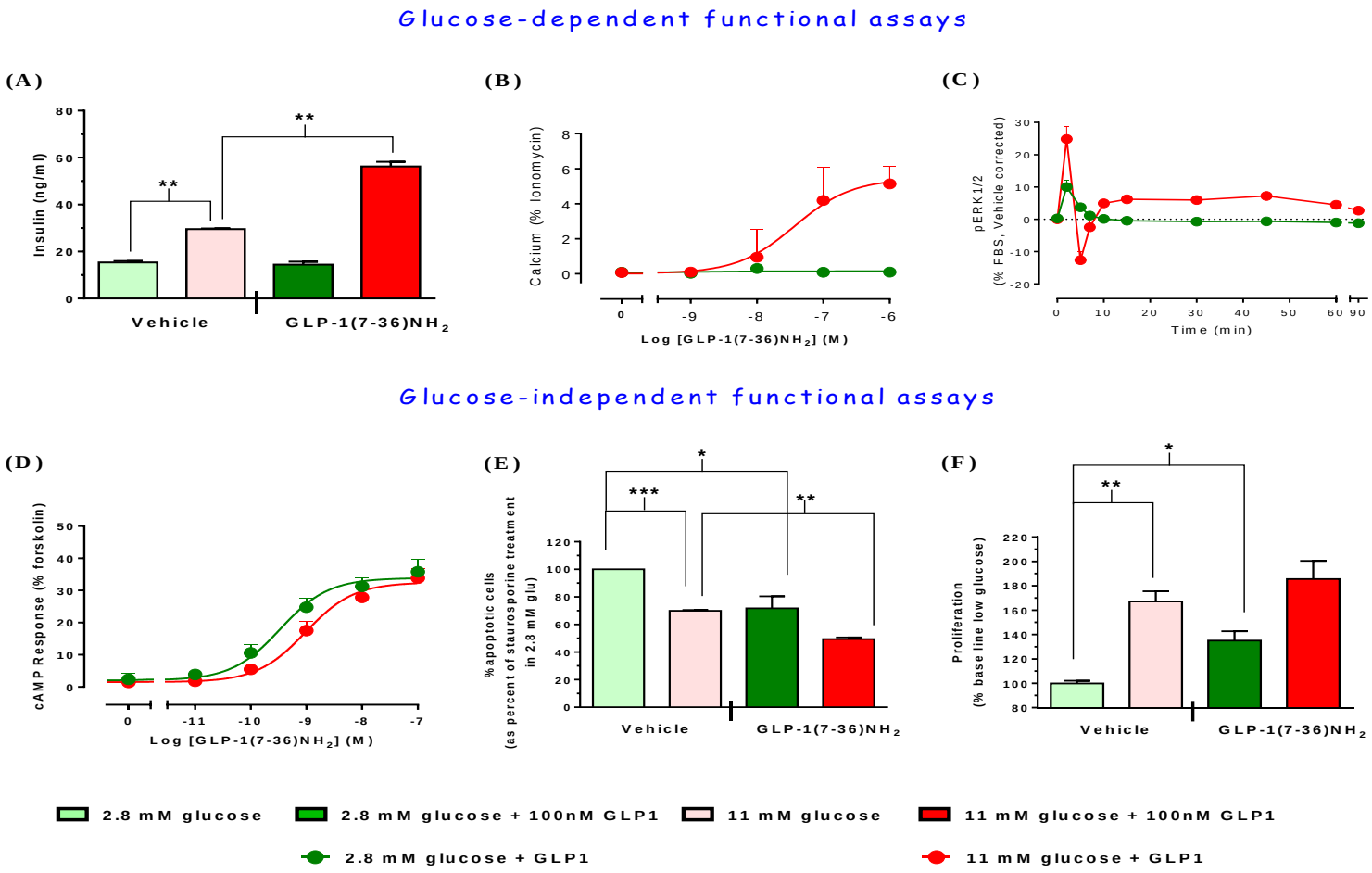

Figure 3.16: Glucose-dependent and independent signaling in INS-1 832/3 cells. Summary of various glucose-dependent and -independent functional screens optimised in INS-1 832/3 cells using GLP-1R ligand GLP-1.

Table 3.10: Effect of 24 h incubation of INS-1 832/3 cells in presence of GLP-1 on BrdU incorporation as a measure of cell proliferation.

Data was analyzed using a three parameter logistic equation. pEC_{50} values represent the negative log of the concentration of agonist GLP-1, that produces half the maximal response. Data are normalized to the response elicited by 2.8 mM glucose (baseline) and 100 nM GLP-1 in 2.8 mM glucose (E_{max}). The range is the assay window (i.e. E_{max} - basal) of individual conditions. All values are mean ± SEM of four independent experiments, conducted in triplicate. ND = Curve could not be defined despite response

	20,000 cells/well		**12,000 cells/well**	
	2.8 mM glucose	**11 mM glucose**	**2.8 mM glucose**	**11 mM glucose**
Basal response (% baseline low glucose)	99.2 ± 2.6	ND	101.7 ± 3.6	165.7 ± 10.8
E_{max} (% baseline low glucose)	105.3 ± 3.0	ND	129.1 ± 3.7	193.6 ± 5.0
Range (E_{max} – Basal)	6.1 ± 3.8	ND	27.4 ± 4.9	27.9 ± 11.5
pEC_{50}	9.06 ± 1.24	ND	9.56 ± 0.54	11.35 ± 0.78

3.3 DISCUSSION

GLP-1 is produced by post-translational processing of the proglucagon gene in enteroendocrine L-cells and is a potent gluco-regulatory peptide hormone. It is released into blood stream in response to nutrient ingestion (Drucker, 2006; Holst, 2007) and controls blood glucose through pleiotropic effects on pancreatic islets, central nervous system and gastrointestinal tract. The principal gluco-regulatory mechanisms activated by GLP-1R agonists include GSIS, inhibition of glucagon secretion, reduction of food intake and inhibition of gastric emptying (Doyale and Egan, 2007; Drucker and Nauck, 2006). Besides its insulinotropic action, GLP-1 favours the maintenance of correct β-cell glucose sensing, regulates transcriptional responses, induces β-cell proliferation and provides protection against apoptosis (Stoffers *et al.,* 2000; Buteau *et al.,* 2003; Klinger *et al.,* 2008). This taken together has attracted interest from pharmaceutical companies to develop therapeutics mimicking endogenous GLP-1 to counteract the defects underlying the pathogenesis of type 2 diabetes that involves β-cell dysfunction and death. Therefore, knowledge of the signalling pathways linked to the activated GLP-1R within β-cells and a better understanding of their functions are of major significance.

Poor and incomplete understanding of the physiology and pharmacology of GLP-1R activation has limited progress in developing improved and better GLP-1R therapeutics for the treatment of type 2 diabetes. One impediment to gaining full understanding of GLP-1R mediated functions in pancreatic β-cells has been the procurement of insulinoma cell lines that faithfully and stably mimic the performance of β-cells within normal pancreatic islets of Langerhans. Immortalized pancreatic β-cell lines represent a valuable model in order to study and understand β-cell function and biology in physiological and pathological states such as diabetes. These cell lines mimic major functions of β-cells amongst which GSIS is prominent and the most studied. Furthermore, cAMP is a well-reported secondary messenger contributing to the process of GLP-1 mediated potentiation of GSIS (Drucker *et al.,* 1987).

Thus, the goal of this chapter was to identify a model pancreatic β-cell line from those reported in the literature that would efficiently mimic the functional attributes of pancreatic β-islets and optimise conditions to measure multiple functional signalling endpoints. To confirm that a cell line behaves like a β-cell, at the minimum we know it has to produce cAMP, display GSIS, signal to Ca^{2+}, pERK1/2 and promote anti-apoptosis and proliferation. However, only insulin is known to be dependent on glucose concentration. cAMP is reported to be glucose-independent (Brisson *et al*., 1992; Lan *et al*., 2012).

Four cell lines reported in the literature to display GLP-1-mediated GSIS, were assessed for both cAMP and GSIS. Of these, only INS-1E and INS-1 832/3 reliably and reproducibly produced GSIS mediated by GLP-1. INS-1 and MIN6 cell lines failed to show both glucose-dependent as well as GLP-1-mediated potentiation of insulin secretion in our study, and that was inconsistent with the literature reports where both the cell lines have been described to stably maintain physiological characteristics of normal β-cell particularly in regards to their glucose-responsiveness (Miyazaki *et al*., 1990; Ishihara *et al.*, 1993; Asfari *et al.*, 1992). The observed discrepancy can be attributed to the non-clonal and heterogenous nature of these cells (Chick *et al*., 1977; Madsen *et al*., 1986) whereby regular and continuous subculturing can result in the expansion of the non-beta cell pool overtime. Furthermore, insulinoma cell lines to become glucose unresponsive and lose their ability to secrete insulin with high passages probably due to the associated metabolic transformations as well as changes in their gene and protein expression levels (Dowling *et al*., 2006; Hohmeier and Newgard, 2004; O'Driscoll *et al*., 2004, 2006).

Following extensive optimisation of cAMP and insulin secretion, we have identified suitable conditions to measure both cAMP and insulin secretion in INS-1 832/3 cells reproducibly and robustly. Consistent with the literature, the insulin response mediated by GLP-1 was only observed in high glucose conditions but not in low glucose conditions, which is also consistent with what would be expected from primary β-islets cells (Holz *et al*., 1993; Fridolf *et al*., 1991; Ishihara *et al.*, 1993). Interestingly, the cAMP response mediated by GLP-1 was glucose-independent. This has been reported previously (Widmann *et al*., 1994). Subsequently, the study targeted the identification and optimization of conditions to set up robust and reproducible functional assays using INS-1 832/3 cells in our lab, specifically, cAMP accumulation, glucose-dependent insulin secretion, ERK1/2 phosphorylation, $[Ca^{2+}]_i$ mobilization, anti-apoptosis and proliferation, all of which have been reported to contribute to the physiological effects associated with GLP-1R activation (eg GSIS and β-cell survival).

In addition to cAMP, there are other signalling messengers that aid in facilitation of physiological outcomes of GLP-1R activation, one of them being calcium (Ca^{2+}). Ca^{2+} is not only a pre-requisite for insulin secretion but it also exerts direct stimulatory effects on insulin secretion (Devis *et al*., 1975; Hellman, 1976). Insulin secretion from β-cell is Ca^{2+}-dependent. Glucose metabolism in β-cells elevates cytosolic ADP/ATP ratio and closes ATP-sensitive K^+ channels (K_{ATP}) resulting in membrane depolarization, Ca^{2+} influx through voltage-dependent Ca^{2+} channels (VDCCs), and Ca^{2+} dependent exocytosis of insulin. Additionally, when blood glucose levels are elevated, GLP-1 has also been reported to mediate the opening of intracellular Ca^{2+} release channels (inositol

triphosphate receptors, IP3R; ryanodine receptors, RYR; nicotinic acid adenine dinucleotide phosphate receptors, NAADPR) to mobilize Ca^{2+} from intracellular stores (Dyachok and Gylfe, 2004; Kang and Holz, 2003), such as endoplasmic reticulum, endosomes, lysosomes and secretory granules,thus facilitating Ca^{2+}-induced Ca^{2+} release (CICR) (Gromada *et al*., 1995; Dyachok and Gylfe, 2004; Islam, 2010).

Since, depolarization-induced Ca^{2+} influx is already well established to be a direct stimulus for insulin secretion (Eliasson *et al.,* 2008) and GLP-1 has been illustrated to potentiate this effect by various signal transduction mechanismsincluding facilitating Ca^{2+} influx and CICR, this presents functional significance of intracellular Ca^{2+} in promoting insulin secretagogic effect of GLP-1, and emphasises the importance of considering Ca^{2+} mobilization when accounting for GLP-1R mediated effects.Through our optimization studies, we identified favourable conditions to measure GLP-1-mediated changes in intracellular calium. From these studies we observed GLP-1-mediated increases in intracellular Ca^{2+} only in high glucose conditions, which is when a β-cell is electrically active (Roe *et al.,* 1993; Gromada *et al.,* 1995). Moreover, we also observed a dose-dependent increase in intracellular calcium in response to GLP-1 which is consistent with earlier studies (Suga *et al.,* 1997; Gromada *et al*., 1995).

Cells can initiate apoptotic pathways in response to multiple diverse triggers including cytokines, free fatty acids, reactive oxygen and nitrogen species, hyperglycaemia, serum or growth factor withdrawal and chemicals such as streptozotocin and staurosporine. Because diabetes results in part from an impaired balance between β-cell proliferation and apoptosis, it becomes highly relevant to study molecular mechanisms whereby insulinotropic hormones promote β-cell growth. This is particularly relevant for ligands that activate the GLP-1R as it is a therapeutic target for diabetes treatment (Holst *et al.,* 2000). GLP-1 exhibits trophic effects on β-cells (Farilla *et al.,* 2003) in addition to stimulating proliferation, inhibiting/preventing apoptosis and enhancing differentiation of β-cells (Drucker, 2003). The signalling mechanisms that underlie these effects include PI3K (Park *et al.,* 2006), PKA, transcription factors such as CREB (Hui *et al.,* 2003; Shin *et al.,* 2014) and Pdx1 (Li *et al.,* 2005; Perfetti *et al.,* 2000; Habener and Stoffers, 1998), kinases such as Akt (Wang *et al.,* 2004, Li *et al.,* 2005), ERK1/2 (Gomez *et al.,* 2002, Quoyer *et al.,* 2010), PKB (Wang *et al.,* 2004; Fan *et al.,* 2010), phosphorylation and nuclear exclusion of FoxO1 (Buteau *et al.,* 2006), transactivation of epidermal growth factor receptor (EGFR) (Buteau *et al.,* 2003), regulation of IGF-1R expression and stimulation of associated IGF-2/IGF-1 receptor autocrine loop in β-cell (Cornu *et al.,* 2009), and induction and expression of cellular anti-apoptotic proteins like Bcl-2, Bcl-xL (Hui *et al.,* 2003). Although studies are ongoing to investigate and understand the signal

transduction mechanisms coupled to regulation of β-cell mass mediated by GLP-1R activation, to date there are still many unanswered questions.

Thus, keeping in mind the associated importance of promoting β-cell survival and function in treatment of type 2 diabetes and to understand the involvement of GLP-1R activation, conditions to measure anti-apoptotic and proliferation effects in INS-1 832/3 cells were investigated and optimised using Annexin-V 647-PI staining and BrdU incorporation in the cellular DNA respectively. High glucose (11 mM glucose) provided a protection against staurosporine-induced apoptosis, 24 h post-treatment, which is consistent with reports in literature (Andersson, 1978; Efanova *et al.,* 1998). β-cell survival has been reported to be both positively and negatively regulated in response to glucose conditions. Although there is no direct correlation between the β-cell apoptosis and glucose concentration, glucose concentrations between 6 and 11 mmol/L are reported to promote survival of β-cells due to synthesis of proteins that inhibit the cells endogenous suicide program (Hoorens *et al.,* 1996; Casteele *et al.,* 2003). In contrast chronic exposure of rat islets or β-cells to glucose concentrations beyond this range (15-30 mmol/L glucose) results in β-cell dysfunction and death (Robertson 2004; Efanova *et al.,* 1998; Maedler *et al.,* 2001, McKenzie *et al.,* 2010).The discrepancies and inconsistencies seen in this range of glucose concentrations being protective or apoptotic can be attributed to the effects of conditions such as serum and different culture media (Andersson, 1978; Davalli *et al.,* 1993). This protective effect was further improved by approximately 15% in presence of GLP-1. Our results align with the literature reports where GLP-1R activation has been revealed to prevent against apoptosis, which has been attributed to either activation of various signalling molecules/pathways such as PKB (Li *et al.,* 2005), CREB (Shin *et al.,* 2014), IRS2 (Assmann *et al.,* 2009; Park *et al.,* 2006), cAMP/PKA/PI2K pathway (Hui *et al.,* 2003) or regulation of endogenous cellular defence mechanisms like bad, Bcl2, caspases (Farilla *et al.,* 2002, 2003; Quoyer *et al.,* 2010) or by modifying the susceptibility of β-cells to apoptotic injury and maintaining the three-dimensional islet morphology (Farilla *et al.,* 2003) thereby preserving the viability and function of pancreatic islets.

Dose-dependent proliferation of INS-1 832/3 cells could be observed in presence of GLP-1, but a reasonable proliferation window (20%) was detected only in low glucose conditions (2.8 mM glucose). In comparison, although effects mediated by GLP-1 could also be observed in high glucose concentration (11 mM), the response window was small. However, there may be a limited ability to recognize peptide mediated proliferation in high glucose conditions due to the mitogenic potential of glucose (King *et al.,* 1978; Swenne *et al.,* 1980; Kaung, 1983). Thus, to achieve an improved window in high glucose may require additional optimization that may involve using

different cell densities for high versus low glucose conditions to assess the different concentrations so as to detect GLP-1 mediated proliferation in state of high glucose. Nevertheless, the proliferative effects mediated by GLP-1R activation were observed during the study and complied with the literature reports (Buteau *et al.,* 1999; Tornehave *et al.,* 2008; Bastein-Dionne *et al.,* 2011). In combination, the anti-apoptotic and proliferative effects of glucose that is potentiated by GLP-1 promotes INS-1 832/3 survival, by increasing viable cells, and this is consistent with what would be expected from a β-islet.

In β-cells, GLP-1R activation has been reported to activate the ERK1/2 cascade via diverse pathways dependent on influx of calcium, $G\alpha_s$/cAMP/PKA or β-arrestin-1 (Gomez *et al.,* 2002; Trumper *et al.,* 2005; Sonoda *et al.,* 2008; Quoyer *et al.,* 2010). Phosphorylation of ERK1/2 has been well documented for its role in many cellular functions such as proliferation, differentiation and survival effects depending on its spatial and temporal activation patterns (Aplin *et al.,* 2001; Klinger *et al.,* 2008; Quoyer *et al.,* 2010). In this chapter, we identified suitable conditions to assess ERK1/2 phosphorylation in INS-1 832/3 cells. While investigating the kinetic profile of ERK1/2 phosphorylation in these cells in response to GLP-1, we observed that in low glucose conditions, only a transient first phase of ERK1/2 activation was detected, which has also been observed previously in β-cells but mediated by activation of other family B GPCR such as the PACAP receptor (Broca *et al.,* 2009). In contrast, we observed a three phase kinetic pattern of ERK1/2 activation with GLP-1 in high glucose conditions, after the response was corrected for the ERK1/2 response mediated by 11 mM glucose alone. A rapid and transient first phase of increased ERK1/2 phopsphorylation was followed by a later phase of pERK1/2 activation that occurred for the duration of the experiment (90 min), which complied with the study performed by Quoyer *et al.,* 2010. Although, the pattern of ERK1/2 activation observed was the same, Quoyer and colleagues detected the peak activation of ERK at 5 min in MIN6 cells in contrast to 2 min observed in our study using INS-1 832/3 cells, which may be contributed to the different cell backgrounds.

ERK1/2 has the ability to shuttle between the cytoplasm and the nucleus, leading to its subcellular compartmentalization and formation of two different pools of cellular ERK1/2.The early phase of ERK1/2 activation has been reported to be mediated by the $G\alpha_s$/cAMP/PKA pathway that favours the nuclear translocation of ERK1/2. This nuclear pool of active ERK1/2 may provide a transcriptional response and/or mitogenic stimulus by directly activating transcription factors such as beta2/NeuroD1, MafA or Elk-1 (Klinger *et al.,* 2008; Raman *et al.,* 2007; Lawrence *et al.,* 2007). In contrast, the sustained activation of ERK1/2 has been described to be exclusively β-arrestin-1 dependent and restricted to the cytoplasm (Quoyer *et al.,* 2010). This pool of ERK1/2 has been

proposed to phosphorylate non-nuclear ERK1/2 substrates involved in translation, cell survival and proliferation and cytoskeletal rearrangements with no direct involvement in the regulation of various transcriptional events. Furthermore, cytoplasmic retention of ERK1/2 may affect the duration of ERK1/2 signalling while the nucleus can act as a site for both ERK1/2 action as well as ERK1/2 signal termination by dephosphorylation via nuclear phosphatases (Volmat *et al.*, 2001).

Unexpectedly, a trough was observed at 5 min of ERK1/2 time course in response to GLP-1 treatment in high glucose, which was attributed to the abilty of the peptide to attenuate the ERK1/2 activation mediated by glucose alone. However, this phase of ERK1/2 activation has not been reported previously in the literature, and may have some physiological relevance, which has not yet been accounted for.

3.4 CONCLUSION

In conclusion, the INS-1 832/3 cell line was identified as a suitable model to study and understand GLP-1R mediated effects that are translatable to what may occur in pancreatic β-islets. Furthermore, the optimization process revealed that cAMP accumulation, proliferation and anti-apoptosis processes facilitated by GLP-1 occurred independent of glucose concentration, whereas, potentiation of GSIS, $[Ca^{2+}]_i$ mobilization and aspects of the ERK1/2 phosphorylation kinetics were observed to be glucose-dependent.

After optimisation of conditions to study downstream signalling pathways and physiologically and therapeutically relevant end points, we have now identified a suitable cell line that mimics primary β-islets in order to address key questions associated with GLP-1R activation and physiology that will be addressed in the subsequent chapters.

CHAPTER 4: BIASED SIGNALLING AND ALLOSTERIC MODULATION OF GLP-1R IN INS-1 832/3 CELLS

4.1 INTRODUCTION

Due to the ability of GLP-1 to promote glucose-dependent insulin release from pancreatic β-cells (Holst *et al.,* 1987; Holz *et al.,* 1993), its receptor, the GLP-1R is an established target for the treatment of type 2 diabetes. In addition to insulin secretion, activation of the GLP-1R contributes to glucose homeostasis by increasing insulin biosynthesis, suppressing glucagon secretion, stimulating β-cell mass, slowing gastric emptying and suppressing appetite. However, due to a very short plasma half-life via degradation by DPPIV (Mentlein *et al.,* 1993) and rapid renal clearance (Deacon *et al.,* 1995), GLP-1 is unsuitable for therapeutic use. There are a range of DPPIV resistant analogues of GLP-1 with improved pharmacokinetic profiles that have been developed and approved for the treatment of type 2 diabetes, including dulaglutide, liraglutide and exenatide (Gallwitz, 2015). Despite the undoubted advantages that these mimetics provide in immediate weight loss and in managing previously uncontrolled type 2 diabetes, a number of concerns remain regarding their long term use, including an increased risk of pancreatitis and cancer (Butler *et al.,* 2013). In addition, due to the need for these drugs to be administered via subcutaneous injection, there has been a drive for the development of small molecule, orally active compounds that activate the GLP-1R. However, despite huge investment from the pharmaceutical industry, novel small molecule drug candidates targeting this receptor have not emerged.

GPCRs are targets of many clinically used drugs, however some drugs yield better therapeutics than others. Two phenomena that may account for this and the high attrition rate in development of novel drugs are the concepts of ligand-directed stimulus bias and allosteric modulation. These avenues of investigation have gained traction in GPCR research over the last decade and are being pursued as a means to develop novel therapeutics. Ligand-directed stimulus bias describes the ability of different ligands acting at the same GPCR to give rise to distinctive signalling profiles due to their ability to engender unique receptor conformations. Stimulus bias is further complicated when allosteric ligands (that bind at distinct sites from orthosteric ligands) are considered because conformational preferences of the receptor, when allosteric and orthosteric binding sites are co-occupied, may be different from when either site is individually occupied. As a consequence, some signalling pathways may be selectively modulated (either positively or negatively) at the expense of others. This therefore provides the potential to promote signalling to pathways that provide therapeutic benefit, while limiting signalling to those that lead to unwanted side effect profiles. Furthermore, the extent and direction of an allosteric interaction can vary with the nature of the orthosteric ligand used as a probe of receptor function, a phenomenon termed as "probe dependence" (Kenakin, 2005; Knudsen *et al.,* 2007; Sloop *et al.,* 2010; Koole *et al.,* 2010; Wootten *et al.,* 2011). Probe-dependence could affect both the therapeutic application and the mode of

discovery of allosteric modulators. Both stimulus bias and allostery are particular relevant to systems such as the GLP-1R that have multiple endogenous ligands and can couple to multiple signalling pathways (May *et al.,* 2007; Koole *et al.,* 2010; Wootten *et al.,* 2013).

In addition to the endogenous GLP-1R peptides (GLP-1, oxyntomodulin) and clinically used ligands (exenatide, liraglutide, dulaglutide), a number of structurally diverse small molecule ligands of the GLP-1Rhave been identified, all of which have been shown to promote insulin secretion in vivo. These include a series of quinoxalines (e.g. compound 2), pyrimidines (BETP), substituted cyclobutanes (Boc5), flavonoids (quercetin) and azoanthracenes (reported in patents by transtech Pharma) (Willard *et al.,* 2012). While most of these small molecules developed to date are not drug-like compounds, they represent pharmacophores that can be further optimized for clinical evaluation and provide a range of useful tools to understand receptor function and biology.

From studies performed in recombinant Chinese Hamster Ovary (CHO) cells that overexpress the GLP-1R, ligand directed stimulus bias from a number of these distinct ligands has been identified (Koole *et al.,* 2010; Wootten *et al.,* 2013). Assessment of cAMP, pERK1/2 and calcium signalling revealed oxyntomodulin to be a biased ligand compared to GLP-1 and exendin-4, with significant bias towards the pERK1/2 pathway over cAMP and calcium mobilization (Koole *et al.,* 2010). In addition, small molecule ligands have also been assessed in these pathways, where significant bias profiles were also observed for both Compound 2 and BETP with a strong bias in the calcium responses observed compared to cAMP and pERK1/2. When compared to GLP-1, BETP produced significantly more calcium compared to equivalent amounts of cAMP, while Compound 2 had the opposite effect (Koole *et al.,* 2010).

BETP and Compound 2 are also allosteric modulators of the GLP-1R with the ability to alter the signalling properties of othosteric ligands in both a pathway and ligand-dependent manner. Both small molecules potentiate the affinity of oxyntomodulin with little effect on the four endogenous variants of GLP-1 and exendin-4. Moreover, these allosteric ligands engendered biased signalling in the responses induced by oxyntomodulin. They potentiated cAMP production, but did not potentiate intracellular calcium mobilization or ERK1/2 phosphorylation (Koole *et al.,* 2010; Willard *et al.,* 2012). Compound 2, but not BETP was also able to significantly enhance β-arrestin recruitment. Additionally, modulation of oxyntomodulin-mediated responses by BETP both in vivo and ex vivo enhanced insulin secretion without having any synergistic effect on GLP-1 responses (Willard *et al.,* 2012; Sloop *et al.,* 2010). Importantly these effects are distinct from those imposed by the allosteric liagnds on GLP-1 and exendin-4 signalling. In addition to the above studies, BETP has

been demonstrated to modulate the signalling mediated by the inactive GLP-1 metabolite, GLP-1(9-36)NH_2, in a pathway-selective manner (Wootten *et al.*, 2012).

For the GLP-1R, targeting allosteric sites by development of small molecule compounds allows for maintenance of spatial-temporal signalling and selectivity, while stimulus bias offers the opportunity for attaining pathway selective therapies. However, successful translation of these phenomena requires multi-pathway profiling of ligands to identify stimulus bias and allosterically imposed effects on this signalling, in addition to an understanding of the ideal repertoire of signalling pathways required to be activated for clinical translation of these phenomena to therapeutic success. This chapter addresses the first of these questions and provides information on the signalling by different ligands that may allow the later question to be addressed in the future, at least in terms of linking ligand fingerprints to physiological outcomes.

Nearly all the accounted studies investigating signalling bias and allosterically induced bias at the GLP-1R have been performed in recombinant cell systems. From these studies it is evident that biased signalling exists and that this is further complicated with the addition of an allosteric modulator. However, the physiological conditions in which GLP-1 is secreted and/or is functionally active and the etiology of type 2 diabetes are both associated with altered glucose conditions, a setting that cannot be mimicked in a recombinant system. Therefore, the physiological importance of phenomena such as biased signalling and allosteric modulation still remains largely unexplored. Now ligand-directed stimulus bias has been identified for the GLP-1R, understanding what this bias means physiologically and how the ligand fingerprint of the studies explored in recombinant cells relates to a physiological system is required. Exploiting pharmacological characteristics (probe-dependence, signalling bias and allosteric modulation) and understanding their cross-talk in a physiologically relevant system presents both a challenging yet potentially advantageous avenue for the design and development of better drug molecules.

Therefore, the present study aims to investigate the signalling profile of GLP-1R in the presence of endogenous and exogenous peptide ligands (GLP-1, exendin-4 and oxyntomodulin) and small molecule allosteric ligands(Compound 2 and BETP) using the endogenously GLP-1R expressing model beta cell system and assays that were optimized in chapter 3.This includes both acute signalling pathways that have been assessed in recombinant cell systems (cAMP, pERK1/2 and calcium) for direct comparison to the CHO cells, in addition to physiologically relevant endpoints downstream of GLP-1R activation, including insulin secretion and cell survival assays (proliferation and anti-apoptosis). Subsequently, qualitative and quantitative analytical approaches

were applied to the data to assess and quantify stimulus bias for the ligands (peptides and small molecules) used in the study performed in both high (11mM) and low (2.8mM) glucose conditions.

4.2 RESULTS

4.2.1 GLP-1R activation of signalling pathways by different GLP-1R agonists

4.2.1.1cAMP Accumulation in INS-1 832/3 cells

Activation of the GLP-1R by the orthosteric peptide agonists, GLP-1, exendin-4 and oxyntomodulin increased cAMP levels in INS-1 832/3 cells in concentration-dependent manner in both high (11 mM) and low (2.8 mM) glucose (Figure 4.1A-C). Although all the peptide agonists were able to produce a similar E_{max}, GLP-1 (pEC_{50} 9.47 ± 0.16 in 2.8 mM glucose and pEC_{50} 9.02 ± 0.14 in 11 mM glucose) and exendin-4 (pEC_{50} 9.89 ± 0.17 in 2.8 mM glucose and pEC_{50} 9.56 ± 0.19 in 11 mM glucose) were more potent than oxyntomodulin (pEC_{50} 7.92 ± 0.08 in 2.8 mM glucose and pEC_{50} 7.78 ± 0.09 in 11 mM glucose), irrespective of glucose concentration (Figure 4.1 A-C; Table 4.1). Additionally, the allosteric agonists, compound 2 and BETP, both stimulated cAMP accumulation with partial agonism and lower potencies in both low and high glucose (Figure 4.1 D and E; Table 4.1).

4.2.1.2 Insulin Secretion in INS-1 832/3 cells

GLP-1R peptide agonists promoted insulin secretion in a concentration-dependent manner in 11 mM glucose (Figure 4.2 A-C). GLP-1 and exendin-4 were equipotent with pEC_{50} values of 9.23 ± 0.06 and 9.32 ± 0.07 respectively (Table 4.2). Oxyntomodulin was the least potent amongst the three peptides with pEC_{50} of 8.18 ± 0.12 (Figure 4.2 C; Table 4.2). A glucose-dependent insulinotropic effect was also observed in the presence of compound 2 (40% of the maximum GLP-1 response) (Figure 4.2 E), while incubation with BETP demonstrated a weaker effect on insulin secretion (Figure 4.2 D; Table 4.2). No insulin secretion was observed in 2.8 mM glucose with any of the peptides or small molecule agonists (Figure 4.2).

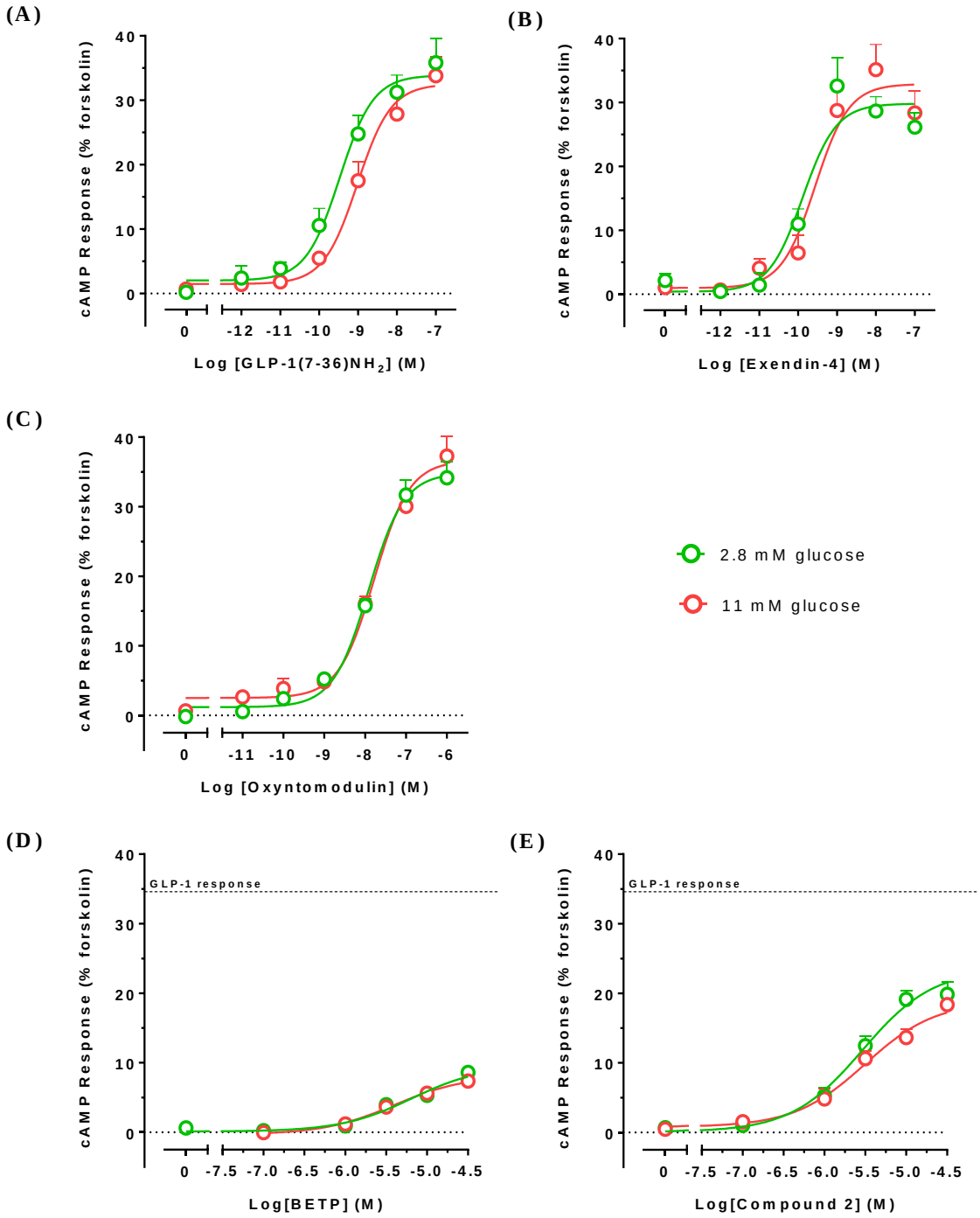

Figure 4.1: cAMP accumulation by GLP-1R agonists in INS-1 832/3 cells. Characterization of cAMP accumulation in presence of (A) GLP-1, (B) Exendin-4, (C) Oxyntomodulin, (D) BETP and (E) Compound 2 in INS-1 832/3 cells. Green represents low (2.8 mM) glucose and red represents high (11 mM) glucose.Data is normalised to the response elicited by 100 µM forskolin and analysed with a three-parameter logistic equation. All values are mean + SEM of five to ten experiments conducted in triplicate.

Table 4.1: Effect of GLP-1R peptide and allosteric agonists on cAMP accumulation in the endogenously expressing GLP-1R cell line INS-1 832/3.

Concentration response data (Figure 4.1) was analyzed using a three parameter logistic equation to derive pEC_{50} values that represent the negative log of the concentration of agonist that produces half the maximal response. E_{max} values are peptide response normalized to the response elicited by 100 µM forskolin, basal response is a percent of the baseline cAMP response in 11 mM glucose expressed as a percent of forskolin stimulated response. The range is the assay window (i.e. E_{max} - basal). All values are mean ± SEM of five to ten independent experiments, conducted in triplicate.

cAMP Accumulation (% forskolin)	**GLP-1**		**Exendin-4**		**Oxyntomodulin**		**Compound 2**		**BETP**	
	2.8 mM Glucose	**11 mM Glucose**	**2.8 mM Glucose**	**11 mM Glucose**	**2.8 mM Glucose**	**11 mM Glucose**	**2.8 mM Glucose**	**11 mM Glucose**	**2.8 mM Glucose**	**11 mM Glucose**
Basal response (% forskolin)	2.0 ± 1.4	1.5 ± 1.2	0.38 ± 1.6	0.9 ± 1.7	1.2 ± 0.7	2.5 ± 0.8	0.1 ± 1	0.7 ± 1.0	-0.2 ± 0.8	-0.4 ± 0.7
E_{max} (% forskolin)	33.9 ± 1.8	32.5 ± 1.8	29.8 ± 1.7	32.9 ± 2.0	34.8 ± 1.1	36.6 ± 1.8	23.5 ± 1.8	18.9 ± 1.9	6.3 ± 1.9	7.5 ± 1.9
Range (max - min)	31.9 ± 2.1	31.0 ± 2.1	29.4 ± 2.2	31.9 ± 2.5	33.6 ± 1.3	23.5 ± 1.8	23.5 ± 1.8	18.1 ± 1.9	6.5 ± 1.8	7.8 ± 1.7
pEC_{50}	9.47 ± 0.16	9.02 ± 0.14	9.89 ± 0.17	9.56 ± 0.19	7.92 ± 0.08	7.78 ± 0.09	5.43 ± 0.17	5.61 ± 0.24	5.48 ± 0.39	5.48 ± 0.32

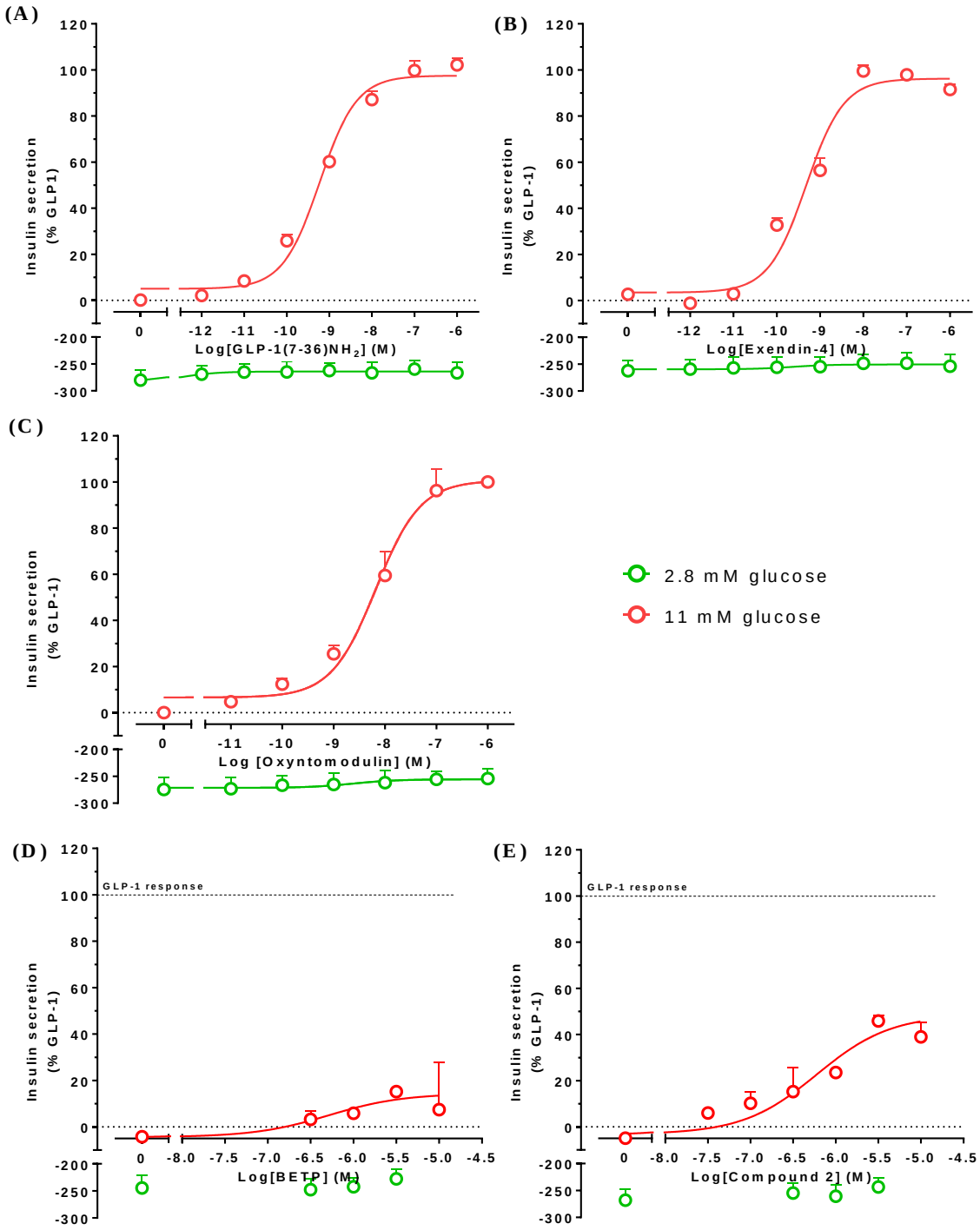

Figure 4.2: Insulin secretion by GLP-1R agonists in INS-1 832/3 cells. Characterization of glucose-dependent insulin secretion in presence of (A) GLP-1, (B) Exendin-4, (C) Oxyntomodulin, (D) BETP and (E) Compound 2 in INS-1 832/3 cells. Green represents low (2.8 mM) glucose and red represents high (11 mM) glucose. Data is normalised to GLP-1basal and maximal responses in 11 mM glucose and analysed with a three-parameter logistic equation. All values are mean + SEM of five to ten experiments conducted in triplicate.

Table 4.2: Effect of GLP-1R peptide and allosteric agonists on glucose-dependent insulin secretion in the endogenously expressing GLP-1R cell line INS-1 832/3 in 11 mM glucose.

Concentration response data (Figure 4.2) was analyzed using a three parameter logistic equation to derive pEC_{50} values that represent the negative log of the concentration of agonist GLP-1 that produces half the maximal response. Data were normalized to the response elicited by 11 mM glucose (baseline) and 100 nM GLP-1 in 11 mM glucose (E_{max}). The range represents the assay window (i.e. E_{max} - basal) of individual conditions. All values are mean ± SEM of five to ten independent experiments, conducted in triplicate.

Insulin Secretion (% peptide max)	**GLP-1**	**Exendin-4**	**Oxyntomodulin**	**Compound 2**	**BETP**
Basal response (%GLP-1 max)	5.0 ± 1.7	3.5 ± 1.9	6.6 ± 3.3	0.5 ± 0.3	1.0 ± 1.8
E_{max} (% peptide max)	97.5 ± 1.9	96.2 ± 2.1	100.7 ± 4.5	47.5 ± 2.2	26.4 ± 6.7
Range (max – min)	92.5 ± 2.5	92.8 ± 2.7	94.1 ± 5.3	47.0 ± 2.3	25.3 ± 6.2
pEC_{50}	9.23 ± 0.06	9.32 ± 0.07	8.18 ± 0.12	5.57 ± 0.13	5.87 ± 0.32

4.2.1.3 ERK1/2 phosphorylation in INS-1 832/3 cells

As described earlier in chapter 3, a robust pERK1/2 response was observed that peaked a maximum response at 5 min upon change of glucose concentration from 2.8 mM to 11 mM glucose (Figure 4.3 A). After correction for the response elicited by glucose alone, a peptide-mediated peak pERK1/2 response was observed at 2 min in both low and high glucose when the GLP-1R was activated by GLP-1, exendin-4 and oxyntomodulin, at saturating concentrations of ligands (Figure 4.3 B-D). However, the magnitude of this response was 1.5 to 2-fold greater in high glucose compared to low glucose conditions in all three cases. Additionally, weak and sustained pERK1/2 activation was detected after 10 min, which was sustained for the duration of the experiment (90 min) in the presence of all three peptides in 11 mM glucose, however, this sustained response was not observed in 2.8 mM glucose. Interestingly, after correction for the 11mM glucose response, there was a reduction in baseline response (i.e. the pERK1/2 induced by 11 mM glucose) at 5 min by all the three peptides, to a similar degree (approximately 10%) in high glucose. Thus, after the subtraction of vehicle (11 mM or 2.8mM glucose alone) induced response, there was a characteristic peptide-mediated pERK1/2 response in 11mM glucose that peaked at 2 min followed by a trough at 5 min and a subsequent sustained activation after 10 min of stimulation for all three peptide ligands, whereas in 2.8mM, there was only a peak response at 2 mins observed for all peptides (Figure 4.3 B-D). The allosteric ligands, BETP (Figure 4.3 E) and compound 2 (Figure 4.3 F) at a concentration of 3 µM demonstrated a peak activation of pERK1/2 at 5 min in high glucose conditions after which there was a sustained response throughout the 90 min time course. Furthermore, no ERK1/2 was detected in low glucose conditions for either of the small molecules ligands (Figure 4.3 F and E). The vehicle, DMSO, that was used to solubilize the allosteric ligands, had no effect on pERK1/2 in either low or high glucose concentration (Figure 4.3 G).

Based on the observed time-dependent profiles of peptide-induced ERK1/2 activation, multiple dose-response curves were performed by stimulating the INS-1 832/3 cells at varying time points along the kinetic profile. 2 min, 5 min and 45 min were assessed for activation of GLP-1R induced pERK1/2 by individual peptides, GLP-1, exendin-4 and oxyntomodulin, in both 2.8 mM and 11 mM glucose. A robust concentration-dependent phosphorylation of ERK1/2 was mediated at 2 min by GLP-1 (Figure 4.4 A and B), exendin-4 (Figure 4.4 C and D) and oxyntomodulin (Figure 4.4 E and F) irrespective of glucose concentration. Nevertheless, consistent with the kinetic data, the maximum response of pERK1/2 at 2 min was greater in 11 mM glucose (Figure 4.4 B, D, F) when compared to 2.8 mM glucose. In addition the responses were more potent in 11 mM glucose compared to 2.8 mM glucose (Figure 4.4; Table 4.3).

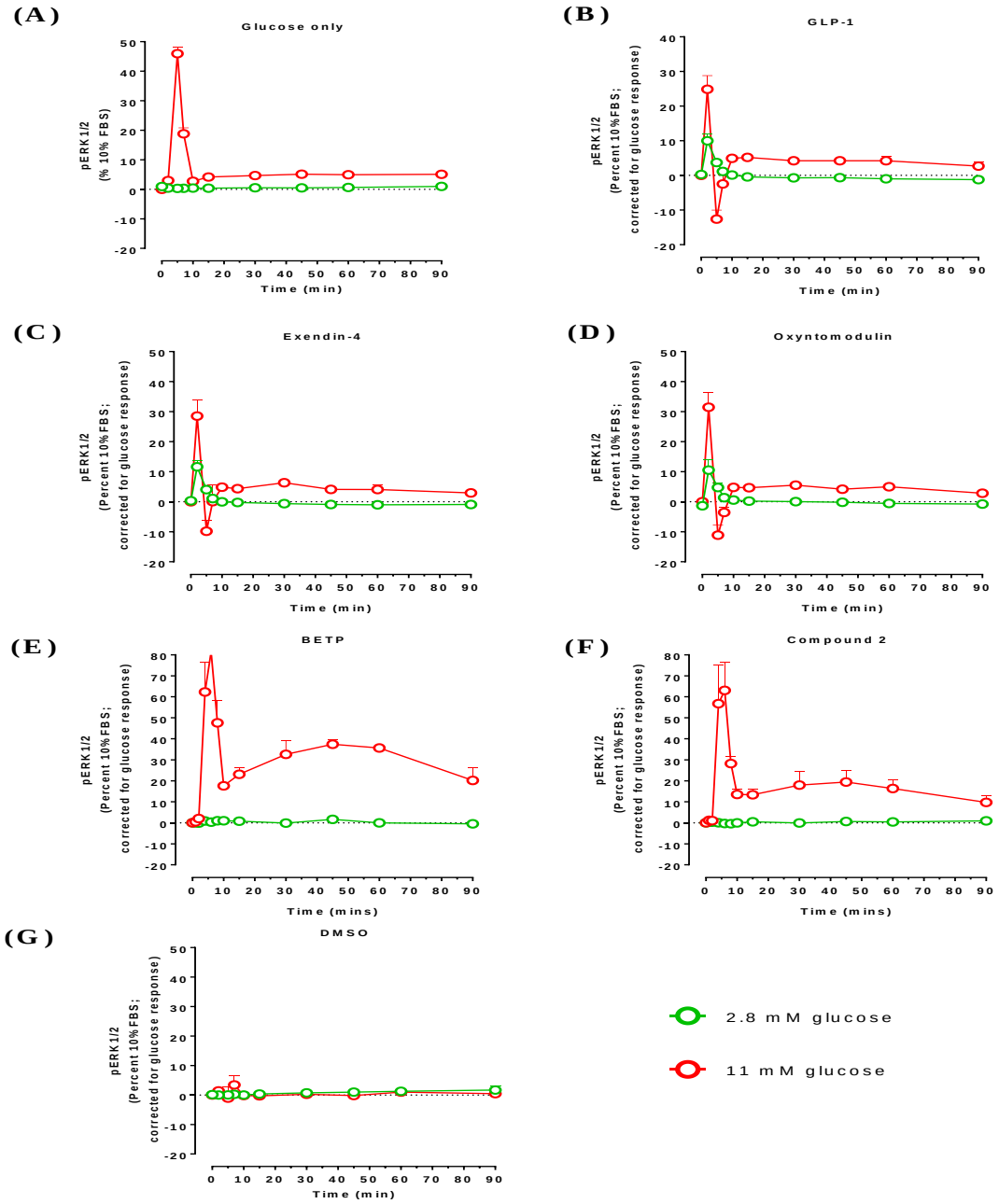

Figure 4.3: Time-dependent activation of pERK1/2 by different GLP-1R agonists in INS-1 832/3 cells. Characterization of time-dependent activation of ERK1/2 in presence of (A) vehicle, (B) GLP-1 (100 nM), (C) Exendin-4 (100 nM), (D) Oxyntomodulin (1µM), (E) BETP (3 µM), (F) Compound 2 (3 µM) and (G) DMSO in INS-1 832/3 cells. In all cases low and high glucose were used such that in A, either low (2.8 mM) or high (11 mM) glucose alone was added and in B-F, agonist ligands were co-added with low or high glucose. Green represents low (2.8 mM) glucose and red represents high (11 mM) glucose. Data is normalised to the maximal response elicited by 10% v/v FBS at 2 min. In B-F the response was then corrected for the relevant glucose response to depict the GLP-1R agonist dependent effects on the glucose-mediated pERK1/2. All values are mean + SEM of three to five experiments conducted in triplicate.

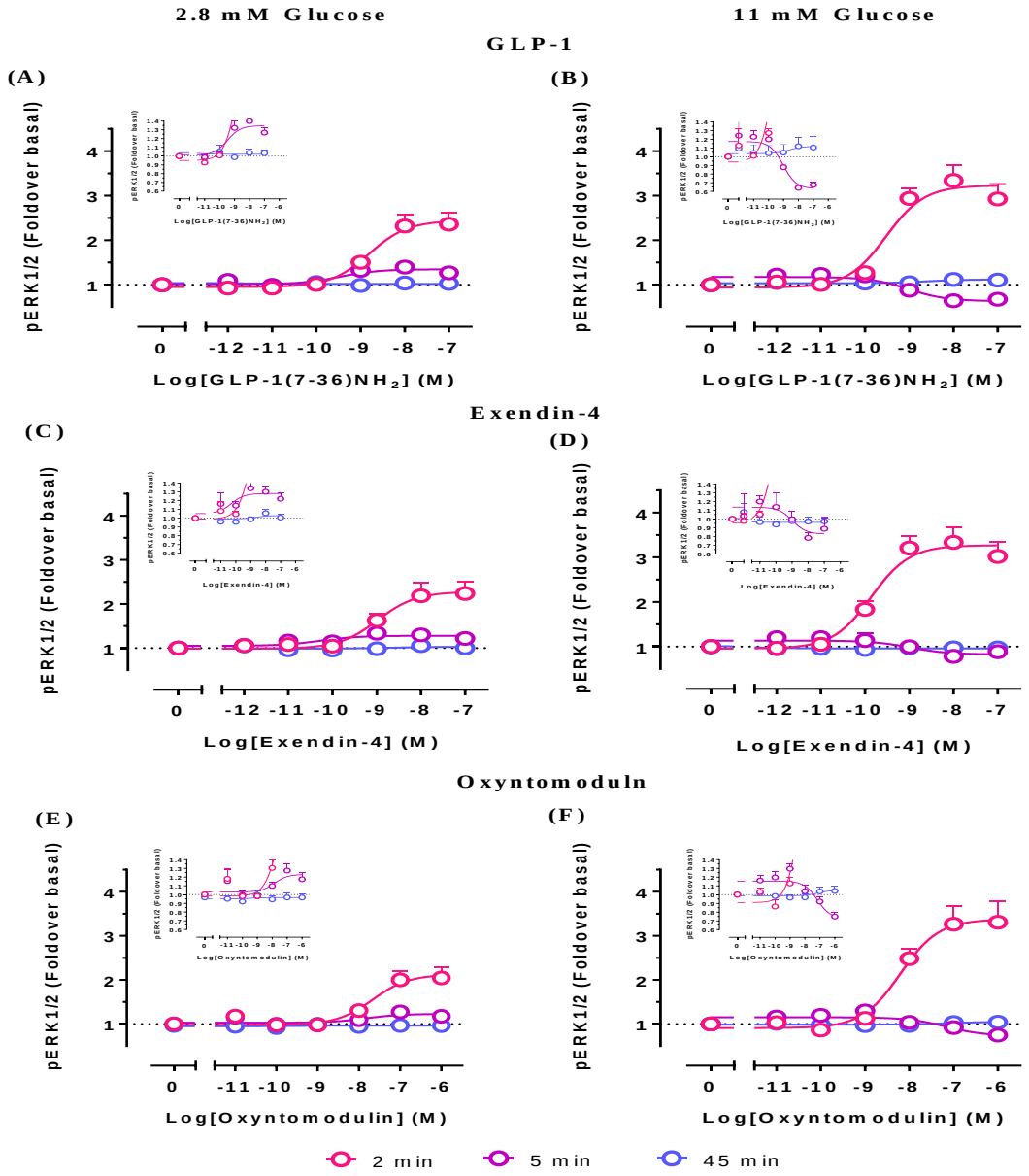

Figure 4.4: Concentration response curves for pERK1/2 of different GLP-1R agonists in INS-1 832/3 cells. Characterization of ERK1/2 phosphorylation in INS-1 832/3 cells at varying time points (2 min in pink, 5 min in purple, and 45 min in blue) in the presence of GLP-1R peptides under conditions of both low (A, C, E) and high (B, D, F) glucose conditions. (A) GLP-1, 2.8 mM glucose; (B) GLP-1, 11 mM glucose; (C) Exendin-4, 2.8 mM glucose; (D) Exendin-4, 11 mM glucose; (E) oxyntomodulin, 2.8 mM glucose and (F) oxyntomodulin, 11 mM glucose. The insets show a limited view of the y-axis such that visualization of the weaker 5 min and 45 min response can be observed.

Data is represented as fold-over basal for the respective glucose condition and analysed with a three parameter logistic equation. All values are mean + SEM of five to ten experiments conducted in triplicate.

Table 4.3: Effect of GLP-1R agonists on ERK1/2 phosphorylation at varying time points in endogenously expressing GLP-1R cell line INS-1 832/3.

Concentration response data (Figure 4.4 and 4.5) was analyzed using a three parameter logistic equation to derive pEC_{50} values that represent the negative log of the concentration of agonist that produces half the maximal response. E_{max} values are peptide response normalized to the response elicited by vehicle in high or low glucose as appropriate (2.8 mM and/or 11 mM) concentration (fold over basal), basal response is presented as the baseline ERK1/2 response elicited by vehicle in the corresponding glucose. The range represent the assay window (i.e. E_{max} - basal). All values are mean ± SEM of four independent experiments, conducted in triplicate. NDR = No detectable response; ND = Curve could not be defined despite response.

Time	ERK1/2 Phosphorylation	2.8 mM Glucose					11 mM Glucose				
		GLP-1	Exendin-4	Oxyntomodulin	BETP	Compound 2	GLP-1	Exendin-4	Oxyntomodulin	BETP	Compound 2
2 min	Basal response (foldover basal)	0.94 ± 0.11	1.00 ± 0.12	0.99 ±0.08	NR	NR	0.93 ± 0.17	0.96 ± 0.20	0.91 ± 0.19	NR	NR
	E_{max} (foldover basal)	2.44 ± 0.14	2.28 ± 0.15	2.12 ± 0.13	NR	NR	3.23 ± 0.16	3.27 ± 0.16	3.38 ± 0.22	NR	NR
	Range (max – min)	1.50 ± 0.17	1.28 ± 0.18	1.14 ± 0.14	NR	NR	2.29 ± 0.22	2.31 ± 0.24	2.46 ± 0.27	NR	NR
	pEC_{50}	8.82 ± 0.23	8.97 ± 0.29	7.66 ± 0.27	NR	NR	9.53 ± 0.17	9.86 ± 0.21	8.20 ± 0.23	NR	NR
	Basal response (foldover basal)	1.02 ± 0.03	1.06 ± 0.04	1.03 ± 0.04	ND	ND	1.17 ± 0.03	1.14 ± 0.05	1.14 ± 0.03	1.04 ± 0.09	ND

5 min	**E_{max} (foldover basal)**	1.40 ± 0.05	1.28 ± 0.04	1.23 ± 0.06	ND	ND	0.63 ± 0.05	0.83 ± 0.83	0.72 ± 0.08	3.20 ± 0.58	ND
	Range (max – min)	0.40 ± 0.06	0.22 ± 0.06	0.20 ± 0.07	ND	ND	-0.54 ± 0.05	-0.31 ± 0.09	-0.42 ± 0.08	2.16 ± 0.55	ND
	pEC_{50}	9.38 ± 0.37	10.22 ± 0.62	7.83 ± 0.73	ND	ND	9.03 ± 0.21	8.97 ± 0.65	7.11 ± 0.35	5.79 ± 0.28	ND
45 min	**Basal response (foldover basal)**	1.04 ± 0.05	1.05 ± 0.03	0.95 ± 0.03	ND	ND	1.03 ± 0.04	1.01 ± 0.04	1.01 ± 0.03	0.99 ± 0.11	1.04 ± 0.13
	E_{max} (foldover basal)	1.02 ± 0.03	0.99 ± 0.02	0.96 ± 0.02	ND	ND	1.12 ± 0.08	0.96 ± 0.02	1.00 ± 0.02	ND	1.88 ± 0.20
	Range (max – min)	-0.02 ± 0.05	-0.05 ± 0.03	0.01 ± 0.02	ND	ND	0.08 ± 0.09	-0.05 ± 0.05	0.011 ± 0.04	ND	0.83 ± 0.20
	pEC_{50}	ND	ND	ND	ND	ND	ND	ND	ND	ND	6.27 ± 0.39

A concentration dependent peptide-mediated inverse agonism of the 11 mM glucose alone response was observed at 5 min stimulation in 11 mM glucose (Figure 4.4 B, D and F) which was in contrast to the weak agonism exhibited by the peptides at the same time point in low glucose (Figure 4.4 A, C, E). Furthermore, a very weak pERK1/2 activity was observed in high glucose at a stimulation time point of 45 min, which was not observed in low glucose conditions (Figure 4.4 B, D, and F, see inset for more clear indication).

Based on the time-profile observed for small molecules, 5 min and 45 min time points were assessed in concentration response curves. Concentration-dependent activation of pERK1/2 was observed at both 5 min and 45 min in presence of 2.8 mM and 11 mM glucose when the cells were treated with either BETP or Compound 2 (Figure 4.5). However, both the molecules showed a higher response in 11 mM glucose. Both ligands displayed similar E_{max} values to peptide ligands for the 45 min response in low and high glucose. Similarly, both ligands have a comparable maximal response to peptide ligands in low glucose conditions at 5 mins. Interestingly, whereas peptide ligands displayed inverse agonism in high glucose at 5 mins, both small molecules displayed agonism (Figure 4.5).

4.2.1.4 Evaluation of Anti-apoptosis in INS-1 832/3 cells

The anti-apoptotic effects mediated by activation of the GLP-1R was assessed by flow cytometric analysis of dual stained (annexinV 647 conjugate and PI) INS-1 832/3 cells, treated with 100 nM staurosporine co-added with varying concentrations of individual peptides in both 2.8 mM and 11 mM glucose, using conditions identified in chapter 3.Interestingly, a cyto-protective effect of approximately 25-30% was observed when cells were incubated in 11 mM glucose alone suggesting that glucose itself is protective against staurosporine-induced apoptosis in INS-1 832/3 cells (Figure 4.6 A-C; Table 4.4). This anti-apoptotic effect was further augmented in the presence of GLP-1R orthosteric peptides in a concentration-dependent manner (Figure 4.6 A-C). The maximal effect of the peptides was comparable between the three orthosteric peptide ligands, with equipotent effects mediated by GLP-1 and exendin-4 (Table 4.4). In line with its reduced affinity as defined by radioligand binding in recombinant cells stably expressing GLP-1R (Koole *et al.*, 2010, 2012, 2015), oxyntomodulin was approximately 75-fold less potent at protecting against staurosporine induced apoptosis compared to GLP-1 and exendin-4 (Table 4.4). In addition to high glucose conditions, all peptides were protective against apoptosis in 2.8 mM glucose conditions with a similar window of protection (approx 25% of the staurosporine-induced apoptosis). However, while exendin-4 and oxyntomodulin were equally potent in both low and high glucose, GLP-1 was 10-fold less potent in 2.8 mM glucose compared to 11 mM glucose (Figure 4.6; Table 4.4).

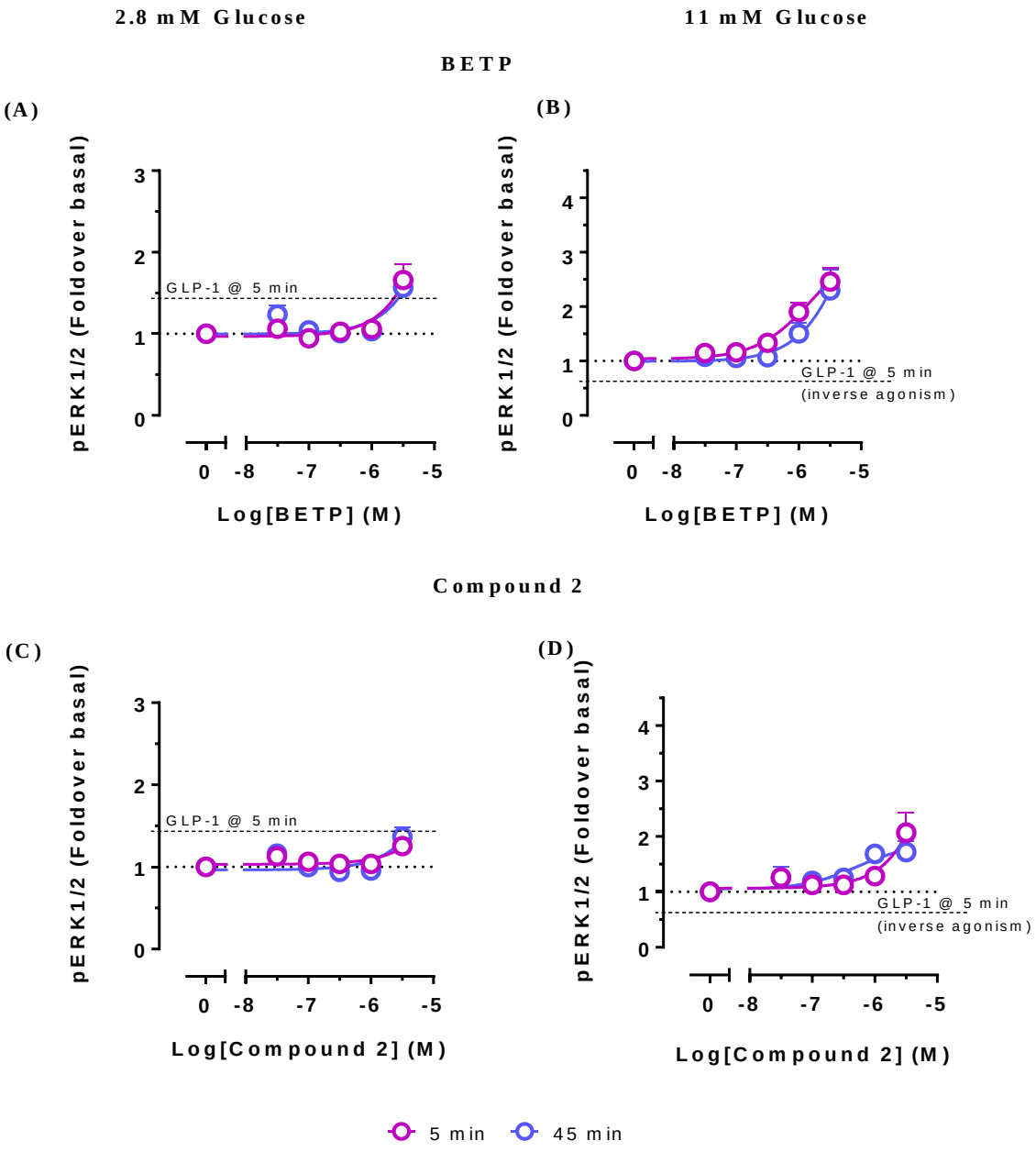

Figure 4.5: Concentration response curves for pERK1/2 of different GLP-1R small molecule agonists in INS-1 832/3 cells. Characterization of ERK1/2 phosphorylation in INS-1 832/3 cells at varying time points (5 and 45 min) in presence of small molecule allosteric agonists of the GLP-1R under conditions of both low and high glucose. (A) BETP, 2.8 mM glucose; (B) BETP, 11 mM glucose; (C) Compound 2, 2.8 mM glucose; (D) Compound 2, 11 mM glucose. Data is represented as fold over basal for the respective glucose condition and analysed with a three-parameter logistic equation. All values are mean + SEM of five to ten experiments conducted in triplicate.

Dotted lines in the graphs represent the maximal ERK1/2 activation at 5 min in response to 100 nM GLP-1 at corresponding glucose concentrations of 2.8 mM and 11 mM.

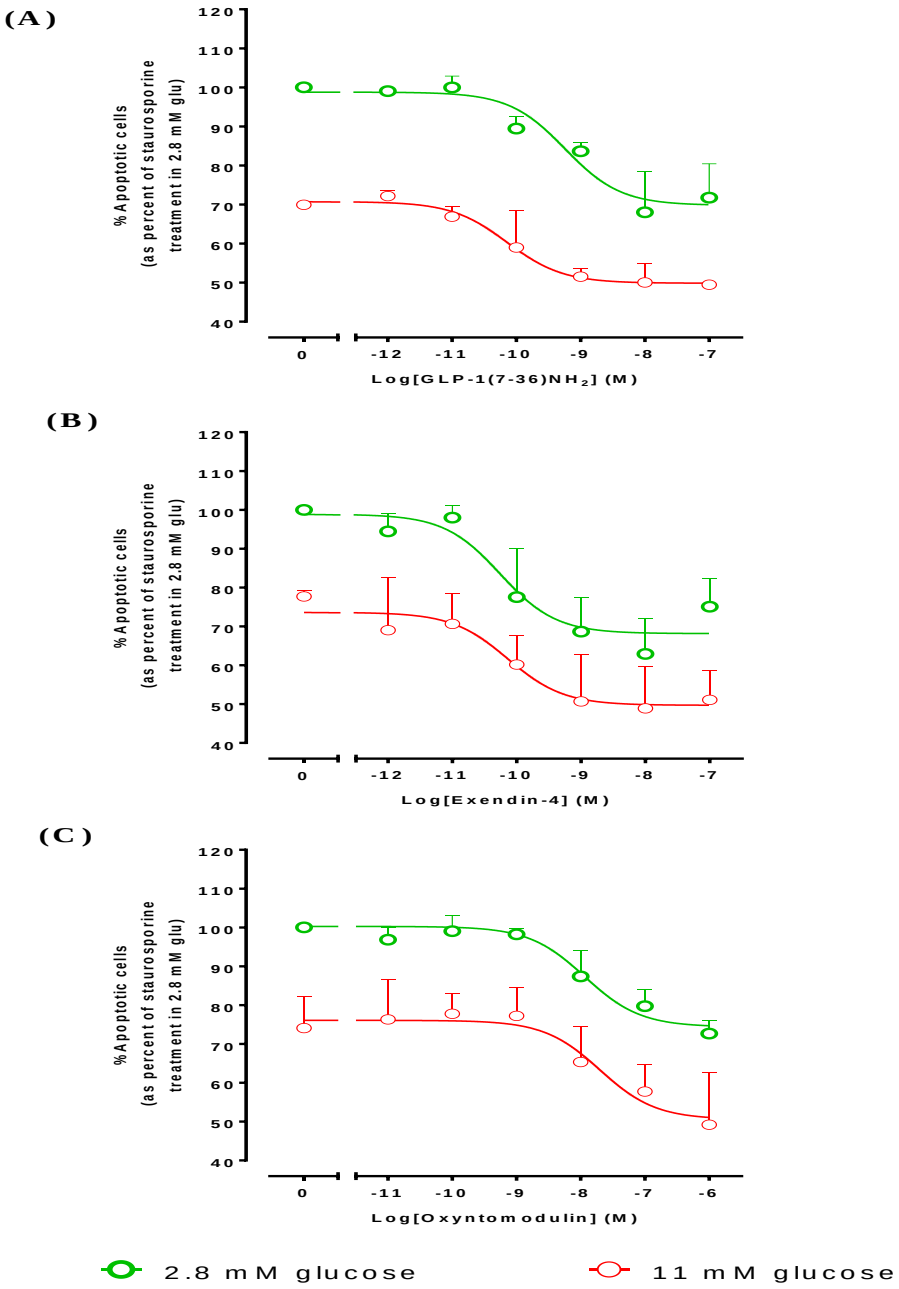

Figure 4.6: Concentration response curves for anti-apoptotic effects mediated by different GLP-1R peptides agonists in INS-1 832/3 cells. Characterization of anti-apoptotic effects of GLP-1R peptides in presence of both low and high glucose using INS-1 832/3 cells. (A) GLP-1, (B) Exendin-4, and (C) Oxyntomodulin. Data is normalised to the response elicited by 100 nM staurosporine in 2.8 mM glucose (where, 0% is defined as total apoptotic cells in 2.8 mM glucoseonly and 100% is defined as total apoptotic cells in presence of staurosporine in 2.8 mM glucose). Concentration response data is analysed with a three parameter logistic equation. All values are mean + SEM of three to five experiments conducted in triplicate.

Table 4.4: Anti-apoptotic effects of GLP-1R peptide agonists in endogenously expressing GLP-1R cell line INS-1 832/3.

Concentration response data (Figure 4.6) was analyzed using a three parameter logistic equation to yield pEC_{50} values that represent the negative log of the concentration of agonist that produces half the maximal level of protection against staurosporine-induced apoptosis. Basal response is presented as the number of apoptotic cells detected in vehicle, 2.8 mM glucose (0%). E_{max} values are maximum peptide mediated reduction in apoptotic cells normalized to the response elicited by vehicle in 2.8 mM (baseline) glucose concentration and 100 nM staurosporine treatment in 2.8 mM glucose (100%). The range represents the assay window (i.e. E_{max} - basal). Dose response curve of glucose was not performed hence pEC_{50} was not derived. All values are mean ± SEM of four independent experiments, conducted in triplicate. All values are mean ± SEM of three to five independent experiments, conducted in triplicate. A dose response curve was not performed for glucose alone, therefore pEC_{50} was not reported. Percent apoptotic cells observed in presence of glucose alone was determined to be 99.3 ± 0.5% in 2.8 mM glucose 73.5 ± 1.6% in 11 mM glucose.

Apoptotic Cells	**GLP-1**		**Exendin-4**		**Oxyntomodulin**	
	2.8 mM Glucose	**11 mM Glucose**	**2.8 mM Glucose**	**11 mM Glucose**	**2.8 mM Glucose**	**11 mM Glucose**
Basal response (% apoptotic cells)	98.8 ± 2.9	70.7 ± 2.5	98.9 ± 4.9	73.6 ± 5.6	100.3 ± 1.6	76.1 ± 3.2
E_{max} (% apoptotic cells)	69.8 ± 4.0	49.9 ± 2.4	68.1 ± 4.4	49.7 ± 5.3	74.4 ± 3.0	50.6 ± 6.3
Range (max – min)	-28.9 ± 4.7	-20.9 ± 3.3	-30.7 ± 6.3	-23.9 ± 7.4	-25.9 ± 3.2	-25.5 ± 6.8
pEC_{50}	9.24 ± 0.37	10.14 ± 0.36	10.26 ± 0.47	10.14 ± 0.70	7.94 ± 0.27	7.70 ± 0.57

4.2.1.5 Evaluation of Proliferation in INS-1 832/3 cells

GLP-1R mediated proliferative responses were evaluated by a chemiluminescence approach to calculate BrdU incorporation into the DNA of cells undergoing mitosis as described in chapter 3. Similar to that observed for anti-apoptosis, glucose itself promoted proliferation of the INS1832/3 cells (Figure 4.7). Peptide-induced proliferation of cells was observed in a concentration-dependent manner for GLP-1 and exendin-4 in both high and low glucose conditions (Figure 4.7A-D). Exendin-4 exhibited equivalent potencies in high and low glucose (pEC_{50} 10.02 ± 0.48 in 2.8 mM glucose and 10.15 ± 0.98 in 11 mM glucose), whereas GLP-1 was 100-fold more potent in high glucose (pEC_{50} 11.35 ± 0.78) compared to low glucose (pEC_{50} 9.35 ± 0.42) (Figure 4.7A-D; Table 4.5). In addition, the actual magnitude of the proliferative effects mediated solely by GLP-1R activation was similar between the two peptides and between the peptides in both low and high glucose (Figure 4.7 B and D). Oxyntomodulin also exhibited proliferative effects on INS-1 832/3 cells in low glucose conditions at the maximum concentration assessed (1 µM), however a concentration response curve could not be derived within the concentration range tested. In high glucose conditions oxyntomodulin failed to produce proliferative effects beyond that of glucose alone, even at the highest concentration assessed (Figure 4.7). While concentration curves were not defined for this ligand, this data suggests that, in contrast to GLP-1, proliferative effects of oxyntomodulin are greater in conditions of low glucose compared to high glucose conditions (Figure 4.7 E-F).

4.2.2 Stimulus bias and GLP-1R in INS-1 832/3 cells

In the previous sections, the GLP-1R agonists, GLP-1, exendin-4, oxyntomodulin, BETP and Compound 2 were investigated for their ability to activate cAMP accumulation, insulin secretion, pERK1/2 (at multiple time points), apoptosis and proliferation, under different glucose conditions in INS-1 832/3 cells. By normalising each of the responses of these ligands in each of the signalling pathways to that of the primary endogenous agonist GLP-1 and plotting each of the signalling pathways for an individual ligand on the same graph (one graph for each ligand) (Figure 4.8), it is evident that there is stimulus bias in both high and low glucose conditions; one of the easiest ways to observe ligand-directed stimulus bias is to look for a switching of potency or maximal response between two ligands when comparing one pathway to another (Kenakin and Christopoulos, 2013). However, a change in the relative potency of one pathway to another, when comparing two different ligands is also indicative of ligand-directed signalling bias, even if there is not an obvious switch in the potency.

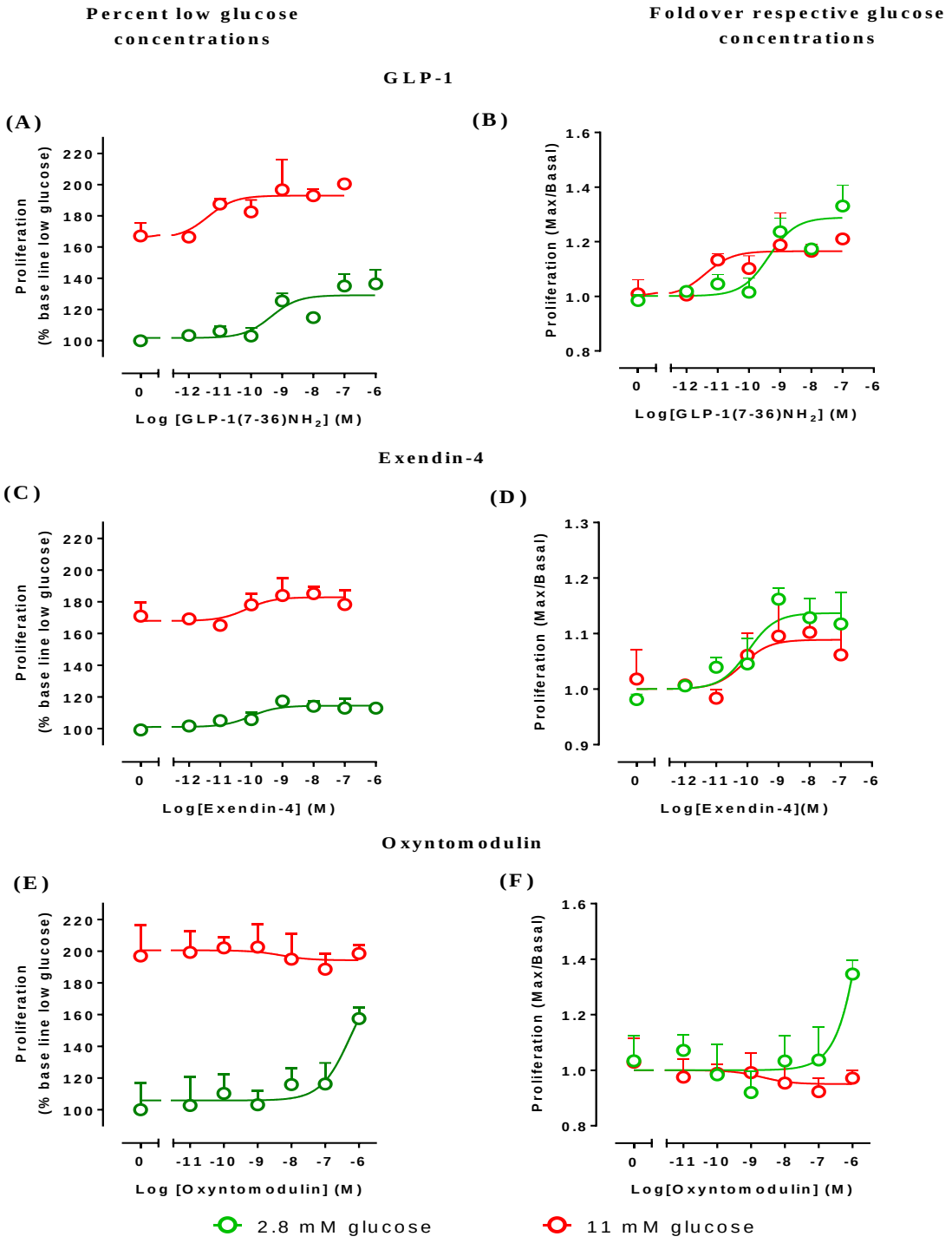

Figure 4.7: Concentration response curves for proliferative effects mediated by different GLP-1R peptides agonists in INS-1 832/3 cells. Characterization of proliferative effects of GLP-1R peptides in presence of both low (green) and high (red) glucose using INS-1 832/3 cells. (A) GLP-1, (B) Exendin-4, and (C) Oxyntomodulin. Data is normalised to the response elicited by vehicle alone (2.8 mM glucose) (A, C, E), and as fold-over basal (Max/Basal) (B, D, F). All data was analysed with a three-parameter logistic equation. All values are mean + SEM of three experiments conducted in triplicate.

Table 4.5: Proliferative effects of GLP-1R peptide agonists in endogenously expressing GLP-1R cell line INS-1 832/3.

Concentration response data (Figure 4.7) was analyzed using a three parameter logistic equation to derive pEC_{50} values that represent the negative log of the concentration of agonist that produces half the maximal response. Data were normalized to the response elicited by vehicle in 2.8 mM (baseline) glucose concentration. E_{max} values are represented as the percent of base line proliferation mediated by the peptide in corresponding glucose (2.8 mM and 11 mM) concentrations, basal response is presented as the baseline proliferative response elicited by vehicle with 2.8 mM glucose (100%). The range represents the assay window (i.e. E_{max} - basal). All values are mean ± SEM of three independent experiments, conducted in triplicate. Data were analyzed with one way ANOVA and Dunnett's multiple comparison post-test to calculate statistical significance from corresponding buffer (2.8 mM or 11mM glucose), statistically significant at $*P < 0.05$, $**P < 0.01$. A dose response curve was not performed for glucose alone, therefore pEC_{50} was not reported. ND = not defined; NR = no response detected.

Proliferation of cells in response to glucose alone was determined to be 102.9 ± 1.5% in 2.8 mM glucose and 168.9 ± 2.2% in 11 mM glucose.

Proliferation (% baseline low glucose)	**2.8 mM Glucose**			**11 mM Glucose**		
	GLP-1	**Exendin-4**	**Oxyntomodulin**	**GLP-1**	**Exendin-4**	**Oxyntomodulin**
Basal response	101.7 ± 3.6	101.1 ± 2.5	105.9 ± 5.3	165.7 ± 10.7	167.9 ± 5.6	200.5 ± 6.5
E_{max}	129.1 ± 3.7**	114.5 ± 1.8	ND	193.6 ± 5.03*	182.9 ± 4.5	194.30 ± 8.9
Range (max –min)	27.38 ± 4.9	13.4 ± 3.0	ND	27.89 ± 11.55	14.92 ± 6.9	ND
pEC_{50}	9.35 ± 0.42	ND	ND	11.35 ± 0.78	ND	ND

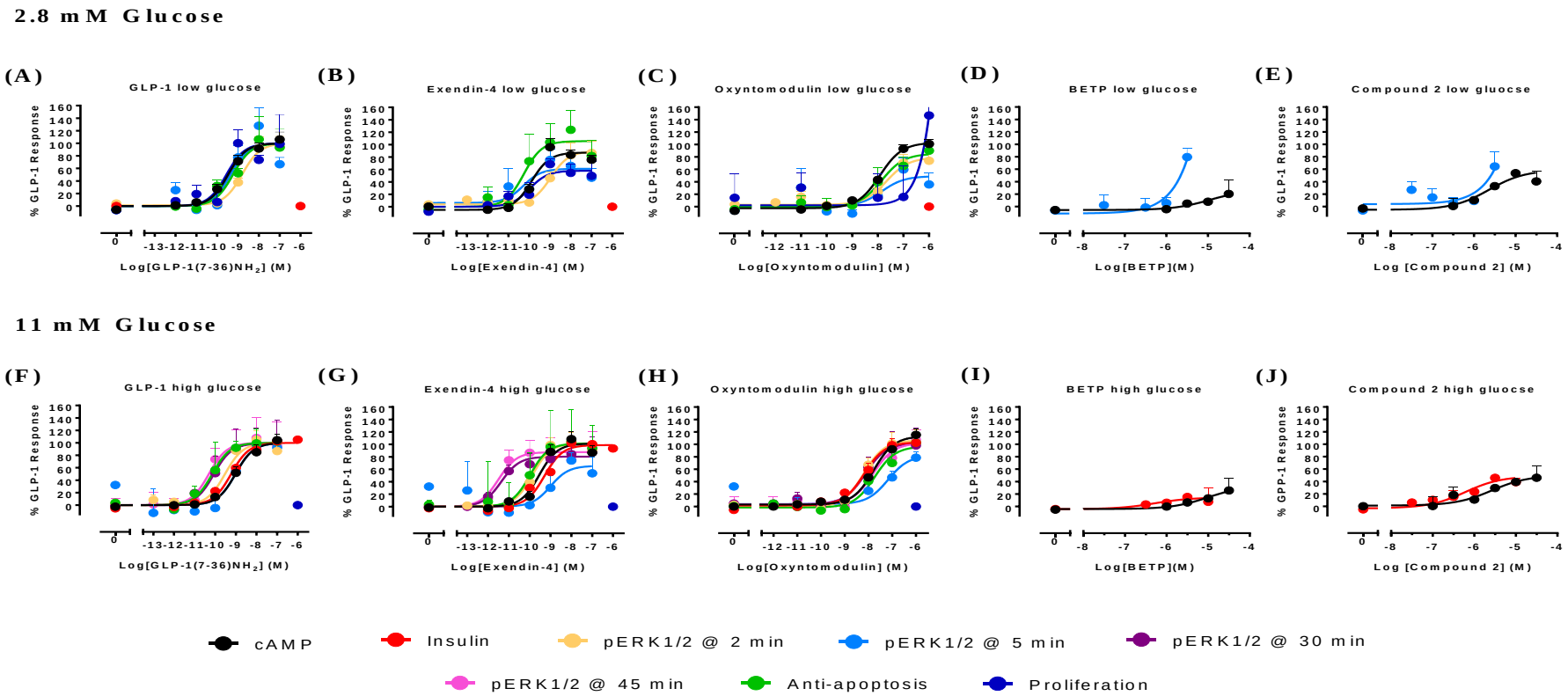

Figure 4.8: Signalling profiles of GLP-1R ligands in low and high glucose. Concentration response curves for cAMP accumulation; insulin; pERK1/2 at 2 min, 5 min, 30 min and 45 min; anti-apoptosis; and proliferation for (A) GLP-1, 2.8 mM glucose; (B) Exendin-4, 2.8 mM glucose; (C) Oxyntomodulin, 2.8 mM glucose; (D) BETP, 2.8 mM glucose; (E) Compound 2, 2.8 mM glucose; (F) GLP-1, 11 mM glucose; (G) Exendin-4, 11 mM glucose; (H) Oxyntomodulin, 11 mM glucose; (I) BETP, 11 mM glucose; (J) Compound 2, 11 mM glucose. Responses are all normalised to GLP-1 maximal response in respective glucose and respective pathways. Data is analysed with three parameter logistic equation. All values are mean + SEM of five to ten experiments conducted in triplicate.

The bias associated with each ligand can be more readily observed in bias plots (Appendix 2, Figure S4.1-S4.3), which display the response observed to equimolar concentrations of ligand for one pathway relative to another. These highlight more clearly that, for selective pathways, there is apparent bias of exendin-4 and/or oxyntomodulin compared to GLP-1. For example, in comparison to GLP-1, exendin-4 appears to be biased towards pERK1/2 (at 5 and 45 min), anti-apoptosis and proliferation relative to cAMP (Appendix 2, Figure S4.2 B, C, D and E) and towards anti apoptosis and pERK1/2 (at 5 and 45 min) relative to proliferation (Appendix 2, Figure S4.2 I and J) in low glucose conditions. In contrast, oxyntomodulin is biased towards pERK1/2 (at 2 and 5 min, but not 45 min) relative to cAMP and anti-apoptosis (Appendix 2, Figure S4.2 A, B, C, F, G and H) in 2.8 mM glucose conditions. While these types of analysis allow easy visualisation of ligand-directed signalling bias, to quantify and assess signalling bias in a measure that can be statistically tested provides advantages over these qualitative measures. Therefore, relative bias has been quantified using the operational model of agonism defined by Black and Leff (Black and Leff 1983, and Chapter 1 section 1.5.2.3; Chapter 2 section 2.11) to derive a transduction ratio (τ/K_A) that is a measure of intrinsic efficacy for a given pathway. Relative bias of two pathways/conditions can be compared to a reference ligand, such as the primary endogenous ligand GLP-1, to calculate bias factors ($\Delta\tau/K_A$) (Figure 4.9-4.12, Tables 4.6-4.8) from which statistical analysis of bias can be performed.

4.2.2.1 Distinct signalling profiles from the GLP-1R in different glucose conditions

When comparing individual signalling pathways in high and low glucose conditions relative to reference ligand GLP-1, there is evidence that peptide ligands display a differential behaviour in their signalling depending on the physiological glucose concentration. There was no insulin secretion in low glucose for any ligand, whereas robust responses were observed in high glucose. In addition, the time profile of pERK1/2 phosphorylation was distinct between high and low glucose conditions. Only a transient pERK1/2 response was observed in low glucose, whereas in addition to this transient 2 min response, there was a later reduction in pERK1/2 at 5 min and a late sustained response in conditions of high glucose. Peptide-induced cAMP accumulation was observed to be independent of the glucose concentration with similar amounts of cAMP produced in 2.8 mM and 11 mM glucose for all the peptides when compared to GLP-1 (Figure 4.9A, S4.1A; Table 4.6).

In contrast, both the small molecules (BETP and compound 2) trended towards greater levels of cAMP in high glucose conditions than low glucose relative to GLP-1, however, due to large error (through propagation of error in calculating these bias factors), this was not statistically significant (Figure 4.12 A).

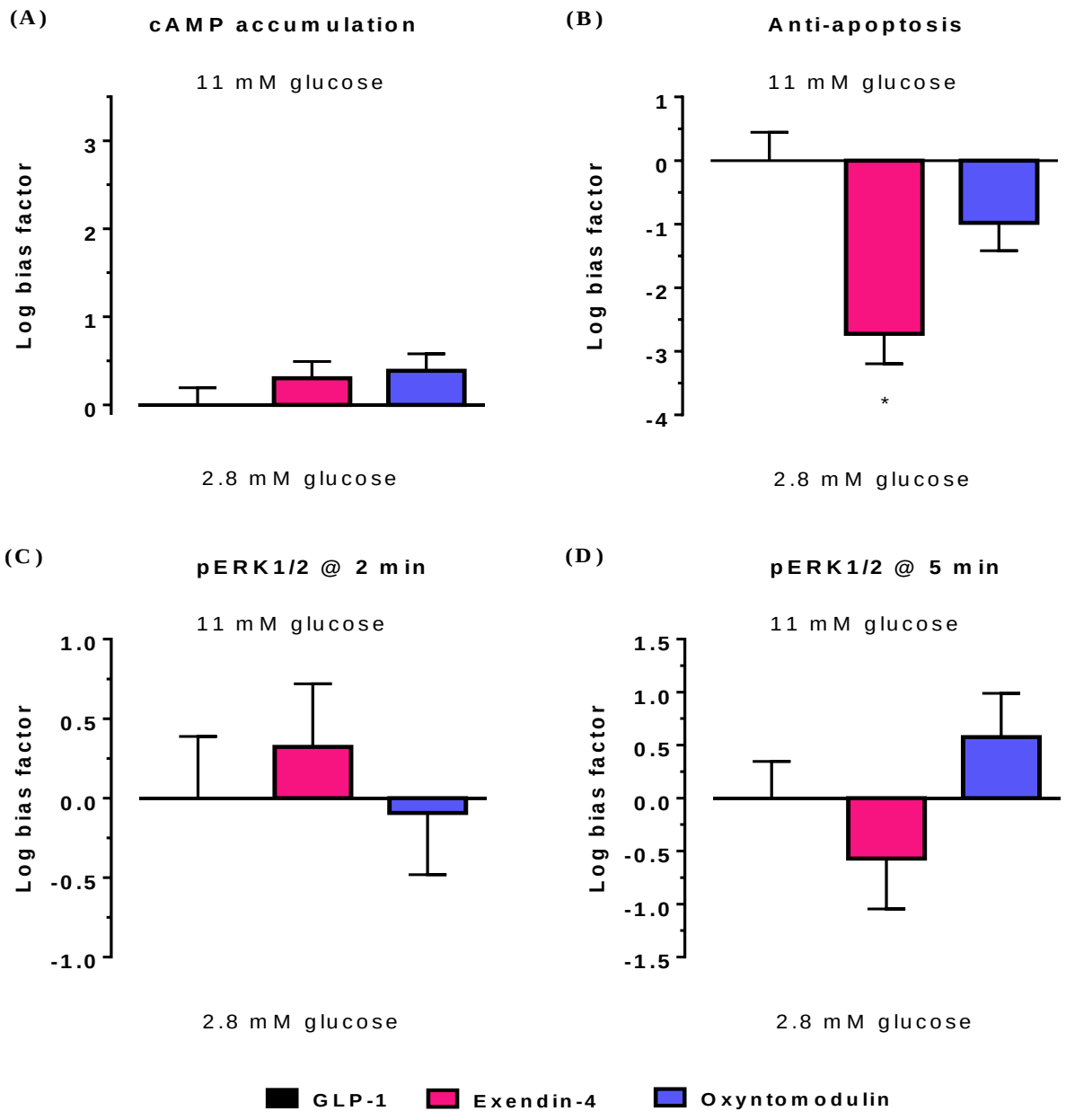

Figure 4.9: Bias factors of peptide ligands between high and low glucose. Quantification of stimulus bias [$\Delta(\tau/K_A)$] displayed by various GLP-1R peptide ligands relative to the reference ligand GLP-1for individual pathways where a response could be detected in both 2.8 mM glucose and 11 mM glucose in INS-1 832/3 cells. (A) cAMP accumulation, (B) anti-apoptosis, (C) pERK1/2 at 2 min and (D) pERK1/2 at 5 min.Statistical significance of changes in bias with respect to the reference ligand GLP-1 were determined by one way analysis of variance and Dunnett's post-test and are indicated with an asterisk (*, $p< 0.05$). All the values are $\Delta(\tau/K_A)$ + SEM of 5-10 independent experiments conducted in triplicate.

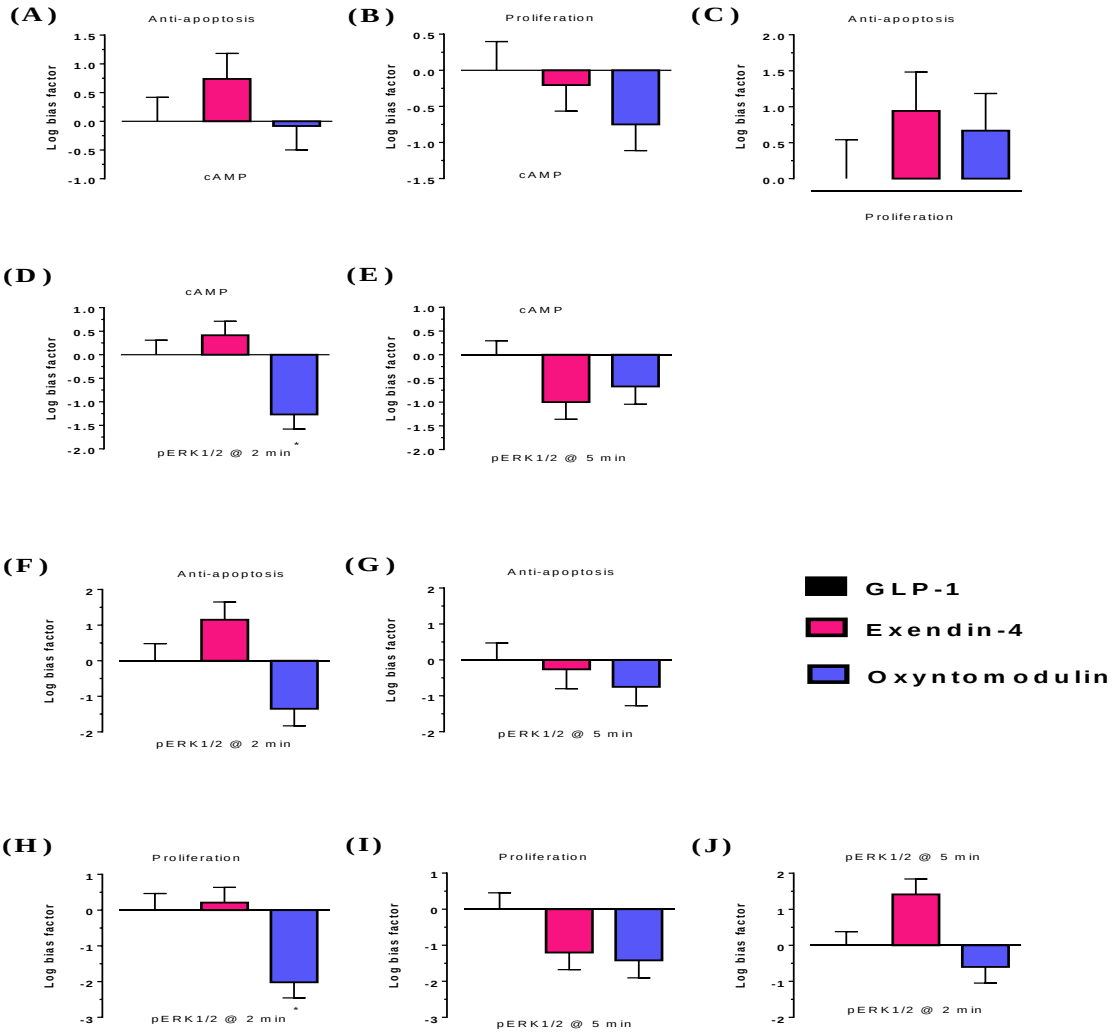

Figure 4.10: **Bias of peptide ligands when comparing different signalling pathways in low glucose.** Quantification of stimulus bias [$\Delta(\tau/K_A)$] displayed by various GLP-1R peptide ligands relative to the reference ligand GLP-1in presence of 2.8 mM glucose using INS-1 832/3 cells. (A) anti-apoptosis *vs* cAMP accumulation, (B) proliferation *vs* cAMP accumulation, (C) anti-apoptosis *vs* proliferation (D) cAMP accumulation *vs* pERK1/2 at 2 min, (E) cAMP accumulation *vs* pERK1/2 at 5 min, (F) anti-apoptosis *vs* pERK1/2 at 2 min, (G) anti-apoptosis *vs* pERK1/2 at 5 min, (H) proliferation *vs* pERK1/2 at 2 min, (I) proliferation *vs* pERK1/2 at 5 min and (J) pERK1/2 at 5 min *vs* pERK1/2 at 2 min.

Statistical significance of changes in bias with respect to GLP-1 were determined by one way analysis of variance and Dunnett's post-test and are indicated with an asterisk (*, $p < 0.05$). All the values are $\Delta(\tau/KA)$ + SEM of 5-10 independent experiments conducted in triplicate. The stimulus bias for pathways not presented here is due to the inability of either detecting the response for one of the compared pathway (insulin and sustained pERK1/2) in each panel or the failure to fit operational model to the data obtained.

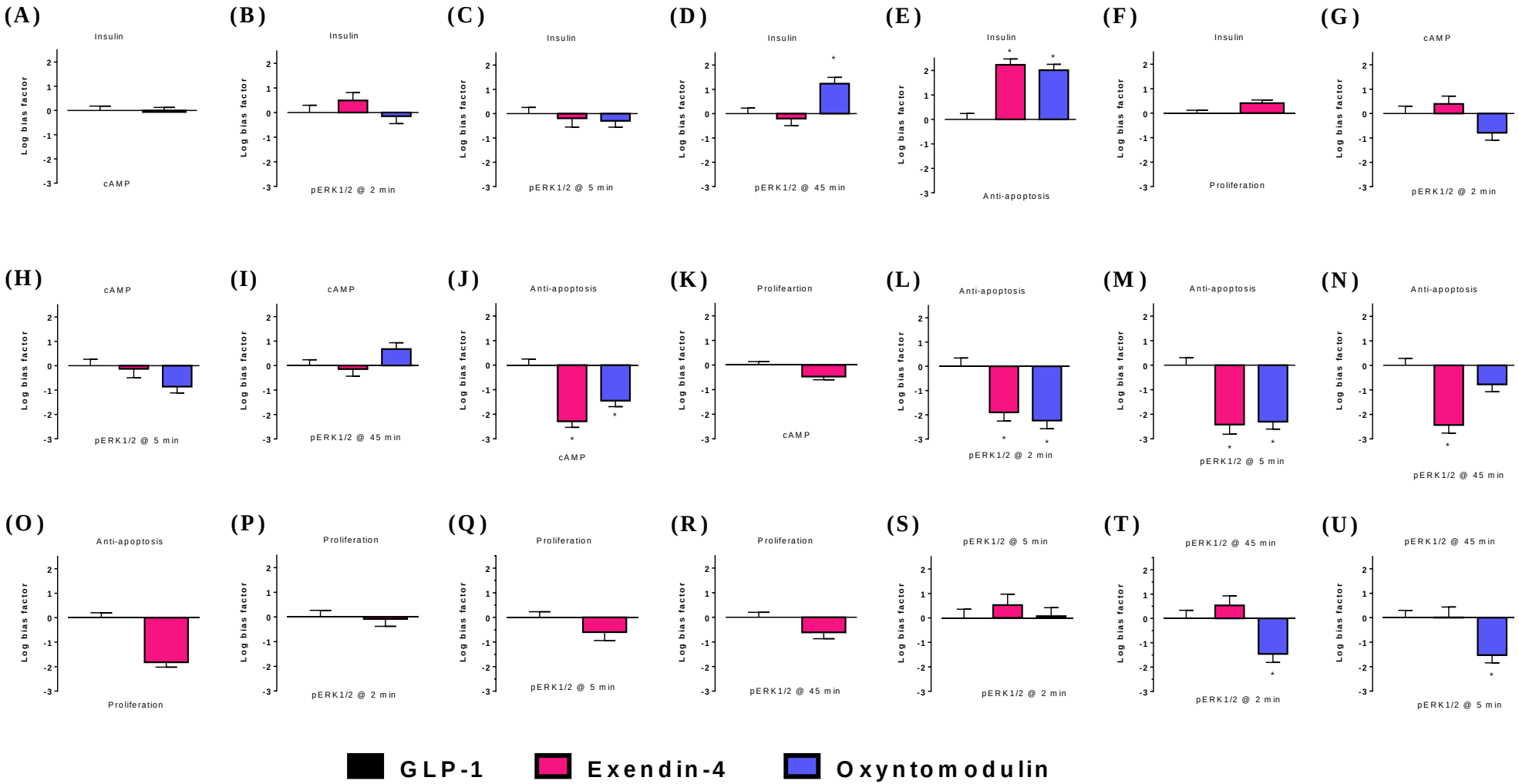
(A)
Insulin
cAMP
(B)
Insulin
pERK1/2 @ 2 min
(C)
Insulin
pERK1/2 @ 5 min
(D)
Insulin
pERK1/2 @ 45 min
(E)
Insulin
Anti-apoptosis
(F)
Insulin
Proliferation
(G)
cAMP
pERK1/2 @ 2 min
(H)
cAMP
pERK1/2 @ 5 min
(I)
cAMP
pERK1/2 @ 45 min
(J)
Anti-apoptosis
cAMP
(K)
Prolifeartion
cAMP
(L)
Anti-apoptosis
pERK1/2 @ 2 min
(M)
Anti-apoptosis
pERK1/2 @ 5 min
(N)
Anti-apoptosis
pERK1/2 @ 45 min
(O)
Anti-apoptosis
Proliferation
(P)
Proliferation
pERK1/2 @ 2 min
(Q)
Proliferation
pERK1/2 @ 5 min
(R)
Proliferation
pERK1/2 @ 45 min
(S)
pERK1/2 @ 5 min
pERK1/2 @ 2 min
(T)
pERK1/2 @ 45 min
pERK1/2 @ 2 min
(U)
pERK1/2 @ 45 min
pERK1/2 @ 5 min
Log bias factor
GLP-1
Exendin-4
Oxyntomodulin

Figure 4.11: **Bias of peptide ligands when comparing different signalling pathways in high glucose.** Quantification of stimulus bias [$\Delta(\tau/K_A)$] displayed by various GLP-1R peptide ligands relative to the reference ligand GLP-1 in presence of 11 mM glucose using INS-1 832/3 cells. (A) insulin *vs* cAMP accumulation, (B) insulin*vs*pERK1/2 at 2 min, (C) insulin *vs* pERK1/2 at 5 min, (D) insulin *vs* pERK1/2 at 45 min, (E) insulin *vs* anti-apoptosis, (F) insulin *vs* proliferation,(G) cAMP accumulation *vs* pERK1/2 at 2 min, (H) cAMP accumulation *vs* pERK1/2 at 5 min, (I) cAMP accumulation *vs* pERK1/2 at 45 min, (J) anti-apoptosis *vs* cAMP, (K) proliferation *vs* cAMP,(L) anti-apoptosis*vs* pERK1/2 at 2 min, (M) anti-apoptosis *vs* pERK1/2 at 5 min (N) anti-apoptosis *vs* pERK1/2 at 45 min, (O) anti-apoptosis *vs* proliferation, (P) proliferation *vs* pERK1/2 at 2 min, (Q) proliferation *vs* pERK1/2 at 5 min, (R) proliferation *vs* pERK1/2 at 45 min, (S)pERK1/2 at 5 min *vs* pERK1/2 at 2 min, (T) pERK1/2 at 45 min *vs* pERK1/2 at 2 min and (U) pERK1/2 at 45 min *vs* pERK1/2 at 5 min. Statistical significance of changes in bias with respect to GLP-1 were determined by one way analysis of variance and Dunnett's post-test and are indicated with an asterisk (*, $p< 0.05$). All the values are $\Delta(\tau/KA)$ + SEM of 5-10 independent experiments conducted in triplicate.The stimulus bias for pathways not presented here is due to the inability of either detecting the response for one of the compared pathway (proliferation) in each panel or the failure to fit operational model to the data obtained.

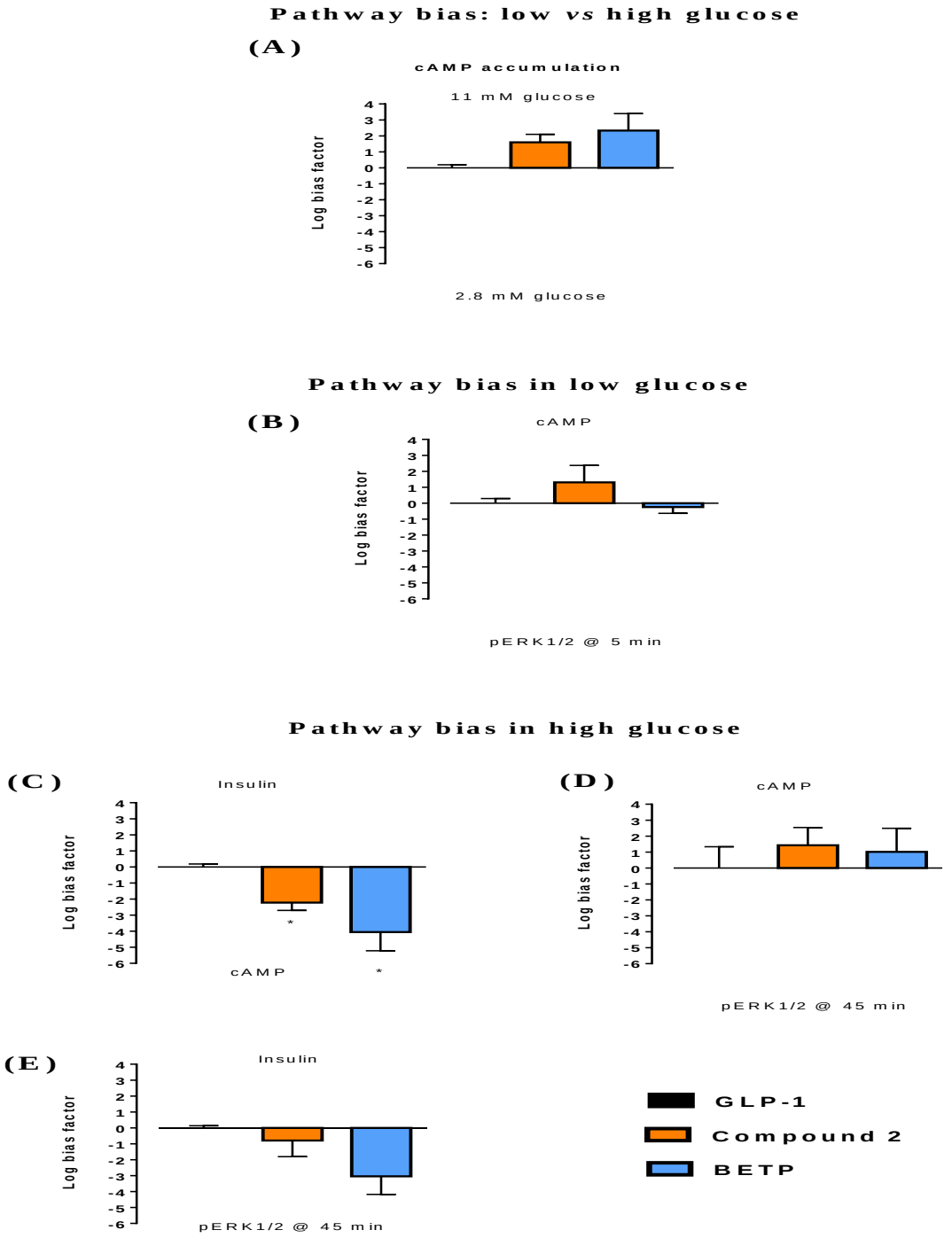

Figure 4.12: **Bias of small molecule ligands relative to GLP-1.**Quantification of stimulus bias [$\Delta(\tau/K_A)$] displayed by various GLP-1R small molecule ligands relative to the reference ligand GLP-1 in the presence of low and high glucose using INS-1 832/3 cells. (A) cAMP accumulation in low glucose *vs* high glucose, (B) cAMP accumulation *vs* pERK1/2 at 5 min, (C) insulin *vs* cAMP accumulation, in high glucose (D) cAMP accumulation *vs* pERK1/2 at 45 min in high glucose and (E) insulin *vs* pERK1/2 at 45 min in high glucose.Statistical significance of changes in bias with respect to GLP-1 were determined by one way analysis of variance and Dunnett's post-test and are indicated with an asterisk (*, $p < 0.05$). All the values are $\Delta(\tau/KA)$ + SEM of 5-10 independent experiments conducted in triplicate. The stimulus bias for pathways not presented here is due to the inability of either detecting the response for one of the compared pathway (insulin and sustained pERK1/2 in low glucose; transient pERK1/2 in high glucose) in each panel or the failure to fit operational model to the data obtained.

Table 4.6: Ligand-directed stimulus bias exhibited by GLP-1R peptide ligands when comparing individual pathways in varying glucose conditions relative to the reference agonist GLP-1 in INS-1 832/3 cells.

Concentration response data from each ligand in each signalling pathway was analysed using an operational model of agonism to estimate log τ/K_A ratios. Changes in log τ/K_A ratios were calculated to provide a measure of the differences in signalling exhibited between low and high glucose conditions at individual signalling pathways relative to that of reference agonist (GLP-1). Values are expressed as mean ± SEM of three to five independent experiments conducted in triplicate. Data were analyzed with one way ANOVA and Dunnett's multiple comparison post-test to calculate statistical significance from reference ligand GLP-1, statistically significant at $*P < 0.05$. ND = not defined as data did not fit well to operational model of agonism.

Signalling High : Low glucose			
	GLP-1 $\Delta\log \tau/K_A$ **(**τ/K_A)	**Exendin-4** $\Delta\log \tau/K_A$ **(**τ/K_A)	**Oxyntomodulin** $\Delta\log \tau/K_A$ **(**τ/K_A)
cAMP accumulation	0 ± 0.19 (1)	0.30 ± 0.19 (1.99)	0.39 ± 0.19 (2.43)
pERK1/2 @ 2min	0 ± 0.39 (1)	0.32 ± 0.40 (2.10)	-0.09 ± 0.39 (0.81)
pERK1/2 @ 5 min	0 ± 0.35 (1)	-0.57 ± 0.47 (0.27)	-0.58 ± 0.41 (3.77)
Anti-apoptosis	0 ± 0.44 (1)	-2.72 ± 0.47* (0.002)	-0.98 ± 0.44 (0.10)
Proliferation	0 ± 1.76 (1)	-1.12 ± 1.60 (0.07)	ND

Table 4.7: Stimulus bias of all pathways (except pERK1/2) exhibited by GLP-1R peptide ligands relative to the reference agonist GLP-1 in INS-1 832/3 cells.

Concentration response data from all ligands in each signalling pathway was analysed using an operational model model of agonism to estimate log τ/K_A ratios. Changes in log τ/K_A ratios were calculated to provide a measure of the degree of stimulus bias between two pathways relative to that of the reference agonist (GLP-1). Values are expressed as means ± SEM of three to five independent experiments conducted in triplicate. Data were analyzed with one way ANOVA followed by Dunnett's multiple comparison post-test to calculate statistical significance from reference ligand GLP-1, statistically significant at $*P < 0.05$. ND = not defined due to no detectable insulin response in conditions of low glucose.

	2.8 mM Glucose	**11 mM Glucose**
Insulin : cAMP accumulation $\Delta\log \tau/K_A$ **(**τ/K_A)		
GLP-1	ND	0 ± 0.18 (1)
Exendin-4	ND	0.06 ± 0.19 (0.87)
Oxyntomodulin	ND	0.56 ± 0.19 (3.65)
Compound 2	ND	-2.22 ± 0.49* (0.006)
BETP	ND	-4.05 ± 1.16* (8.81e-05)
Insulin : Anti-apoptosis $\Delta\log \tau/K_A$ **(**τ/K_A)		
GLP-1	ND	0 ± 0.24 (1)
Exendin-4	ND	2.23 ± 0.24* (169.04)
Oxyntomodulin	ND	2.01 ± 0.24* (101.86)
Insulin : Proliferation $\Delta\log \tau/K_A$ **(**τ/K_A)		
GLP-1	ND	0 ± 0.12 (1)
Exendin-4	ND	0.41 ± 0.13 (2.58)
Oxyntomodulin	ND	-0.57 ± 0.14 (0.27)
Anti-apoptosis : cAMP accumulation $\Delta\log \tau/K_A$ **(**τ/K_A)		
GLP-1	0 ± 0.42 (1)	0 ± 0.25 (1)

Exendin-4	0.74 ± 0.44 (5.46)	-2.29 ± 0.24* (0.005)
Oxyntomodulin	-0.08 ± 0.41 (0.83)	-1.45 ± 0.24* (0.036)
Proliferation : cAMP accumulation $\Delta\log \tau/K_A$ **(**τ/K_A)		
GLP-1	0 ± 0.40 (1)	0 ± 0.14 (1)
Exendin-4	-0.20 ± 0.36 (0.62)	-0.47 ± 0.13 (0.34)
Oxyntomodulin	-0.75 ± 0.36 (0.18)	-1.13 ± 0.14 (13.55)
Anti-apoptosis : Proliferation $\Delta\log \tau/K_A$ **(**τ/K_A)		
GLP-1	0 ± 0.54 (1)	0 ± 0.20 (1)
Exendin-4	0.94 ± 0.54 (8.73)	-1.82 ± 0.20* (0.015)
Oxyntomodulin	0.67 ± 0.51 (4.65)	-2.58 ± 0.20* (0.003)

Table 4.8: Stimulus bias exhibited GLP-1R peptide ligands at all pathways relative to pERK1/2 and the reference agonist GLP-1 in INS-1 832/3 cells.

Concentration response data from all ligands in each signalling pathway was analysed using an operational model model of agonism to estimate log τ/K_A ratios. Changes in log τ/K_A ratios were calculated to provide a measure of the degree of stimulus bias between two pathways relative to that of the reference agonist (GLP-1). Values are expressed as means ± SEM of three to five independent experiments conducted in triplicate. Data were analyzed with one way ANOVA followed by Dunnett's multiple comparison post-test to calculate statistical significance from reference ligand GLP-1, statistically significant at *$P < 0.05$. ND = not defined due to no detectable response.

	GLP-1 $\Delta\log \tau/K_A$ **(**τ/K_A)		**Exendin-4** $\Delta\log \tau/K_A$ **(**τ/K_A)		**Oxyntomodulin** $\Delta\log \tau/K_A$ **(**τ/K_A)	
	2.8 mM Glucose	**11 mM Glucose**	**2.8 mM Glucose**	**11 mM Glucose**	**2.8 mM Glucose**	**11 mM Glucose**
Insulin : pERK1/2 @ 2 min	ND	0 ± 0.3 (1)	ND	0.50 ± 0.32 (3.10)	ND	-0.15 ± 0.30 (0.71)
Insulin : pERK1/2 @ 5 min	ND	0 ± 0.26 (1)	ND	-0.19 ± 0.386 (0.64)	ND	0.30 ± 0.26 (0.50)
Insulin : pERK1/2 @ 45 min	ND	0 ± 0.23 (1)	ND	-0.20 ± 0.29 (0.62)	ND	1.23 ± 0.26* (17.10)

cAMP : pERK1/2 @ 2 min	0 ± 0.31 (1)	0 ± 0.30 (1)	0.41 ± 0.30 (2.60)	0.40 ± 0.32 (2.47)	-1.27 ± 0.31* (0.05)	-0.79 ± 0.30 (0.16)
cAMP : pERK1/2 @ 5 min	0 ± 0.30 (1)	0 ± 0.26 (1)	-1.00 ± 0.36 (0.1)	-0.13 ± 0.36 (0.74)	-0.67 ± 0.38 (0.21)	-0.86 ± 0.26 (0.14)
cAMP : pERK1/2 @ 45 min	ND	0 ± 0.24 (1)	ND	-0.14 ± 0.30 (0.72)	ND	0.671 ± 0.26 (4.69)

In transient ERK1/2 phosphorylation at 2 min and 5 min, despite small variations in the overall level of pERK1/2, there were no significant differences in the amount of pERK1/2 produced in the two different glucose concentrations for oxyntomodulin and exendin-4 relative to GLP-1 between the peptide ligands (Figure 4.9C and D; Table 4.6). In contrast, anti-apoptotic effects of exendin-4 and oxyntomodulin were more prominent in low glucose conditions relative to high glucose when compared to that of GLP-1 (Appendix 2, Figure S4.1E). Calculation of bias factors revealed this effect to be significant ($p < 0.05$) for exendin-4 (Figure 4.9B, Table 4.6). In addition, the bias plots for proliferation assay suggest that there may be ligand bias between low and high glucose conditions by GLP-1 when compared to exendin-4 (Appendix 2, Figure S4.1F), however due to large errors on the high glucose values and the requirement for propagation of errors, reliable bias factors could not be calculated.

4.2.2.2 Peptide-mediated signal bias in low glucose conditions

Comparison of the ability of individual peptide ligands to signal to each pathway in comparison to another in conditions of low gluocse, resulted in limited, significant ligand-directed signalling bias (Figure 4.10, S4.2; Table 4.7). In comparison to GLP-1, both exendin-4 and oxyntomodulin displayed some degree of bias although, in the majority of cases, this did not reach statistical significance (Figure 4.10). Oxyntomodulin was revealed to be statistically more biased towards transient pERK1/2 (measure at 2 min) relative to cAMP and proliferation when compared to GLP-1 (and exendin-4) (Figure 4.10 D,H; Table 4.7). However, due to the nature of propagation of errors when calculating bias factors, large differences in bias often need to be observed or very high n numbers performed to reach statistical significance. Nonetheless, those that do not reach significance may still be of physiological relevance, as for some therapies, only very small physiological changes are required for therapeutic effect (ie DDPIV inhibitors only increase circulating GLP-1 by 2-fold) (Dai *et al.*, 2008; Aulinger *et al.*, 2014). Further experiments would be required to improve the statistical power to confirm if these parameters do reach statistical significance.

4.2.2.3 Peptide-mediated stimulus bias in high glucose conditions

In high glucose conditions, both exendin-4 and oxyntomodulin displayed significant degrees of bias in their signalling relative to GLP-1 (Figure 4.11, S4.3; Table 4.7 and 4.8). In comparison to GLP-1, exendin-4 was significantly biased towards cAMP (Figure 4.11 J) and ERK1/2 activation (at all time points) relative to anti-apoptosis (Figure 4.11 L, M and N). However, similar bias was observed when compared with proliferation but it did not reach statistical significance (Figure 4.11 Q, R and S). Relative to GLP-1, oxyntomodulin also exhibited significant bias towards cAMP and

ERK1/2 at 2min and 5 min, but not sustained pERK1/2 relative to anti apoptosis (and presumable proliferation given none was detectable) (Figure 4.11 J, L, M and N). In addition, oxyntomodulin was also significantly biased towards insulin secretion relative to sustained ERK1/2 activation at 45 min in comparison to GLP-1 (Figure 4.11 D). Furthermore, there were also indications of bias between different phases of ERK1/2 responses with oxyntomodulin significantly biased towards transient pERK1/2 (2min) and inhibition of pERK1/2 (5 min) relative to sustained pERK1/2 (45 min) (Figure 4.11 T and U) compared to GLP-1. As with low glucose conditions, due to the nature of propagation of errors when calculating bias factors, large differences in bias need to be observed or high n numbers performed to reach statistical significance and therefore those that do not reach significance may still be of physiological relevance.

4.2.2.4 Small molecule ligands also induce distinct bias in GLP-1R signalling

The signalling bias of small molecule agonists relative to GLP-1 could only be calculated between a limited number of pathways where signalling was detectable. This included cAMP and sustained 45 min pERK1/2 in low glucose and insulin, cAMP and sustained pERK1/2 in high glucose (Figure 4.12, Table 4.7). BETP and compound 2, in the presence of 11 mM glucose significantly biased the receptor towards cAMP accumulation over insulin secretion relative to GLP-1 (Figure 4.12 C). There was also potential bias towards cAMP over sustained pERK1/2 responses for both compounds, however due to large errors introduced by propagation of errors, these did not reach significance (Figure 4.12 D). In addition, the receptor trended towards bias for sustained pERK1/2 at 45 min over insulin secretion, when BETP was added in conjunction with glucose (Figure 4.12 E), however this do not achieve significance.

4.2.2.5 Webs of Bias allow visualisation of the extent of ligand-directed signalling bias in different glucose concentrations.

In addition, to comparing two pathways against one another, multiple pathways/conditions can be compared and easily visualised simultaneously by producing a web of bias where the (τ/K_A) value of each ligand in each signalling pathway is normalised to that of a reference ligand (GLP-1) as well as a reference signalling pathway (cAMP) producing $\Delta\Delta(\tau/K_A)$ values (Figure 4.13). Comparison of the webs of bias of ligands in 2.8 mM *vs* 11 mM glucose reveals convincing evidence for quite distinct biased profiles of signalling for the individual ligands in the two physiologically relevant concentrations of glucose that were assessed (Figure 4.13). Relative to GLP-1 (and exendin-4), in low glucose conditions, oxyntomodulin produces significantly more transient pERK1/2 (2 min) for equivalent amounts of cAMP. However, for all other pathways assessed, there was no significant ligand-directed signalling (relative to cAMP), although there

were some observed minor differences in pERK1/2 at 5 mins and anti-apoptotic effects between these peptide ligands (Figure 4.13). However, in high glucose conditions, a distinct biased agonism profile is observed. While the bias of oxyntomodulin towards transient pERK1/2 is still evident, this does not reach statistical significance as the magnitude of effect for oxyntomodulin is smaller (10-fold) than that observed in low glucose conditions (>10-fold). However, in high glucose there are significant differences for both oxyntomodulin and exendin-4 compared to GLP-1 that were not evident in low glucose. Both these ligands are less efficient at promoting cell survival pathways with significantly less anti-apoptosis and proliferation observed for equivalent amounts of cAMP relative to GLP-1 (Figure 4.13).

Similar to analysis of peptide ligands, bias factors were derived to compare compound 2 and BETP to GLP-1 (Figure 4.12). Since, both the molecules were unable to produce insulin secretion in low glucose conditions, there were only two pathways available for comparison. As a consequence, a web for low glucose conditions was not generated. In high glucose conditions, for the same amount of cAMP response as GLP-1, compound 2 produced 10-fold less sustained pERK1/2, while no bias was observed with BETP. Furthermore for the same amount of cAMP response, both ligands produce significantly less insulin compared to GLP-1, for compound 2 this was 100-fold whereas for BETP, this reached >100-fold (Figure 4.13).

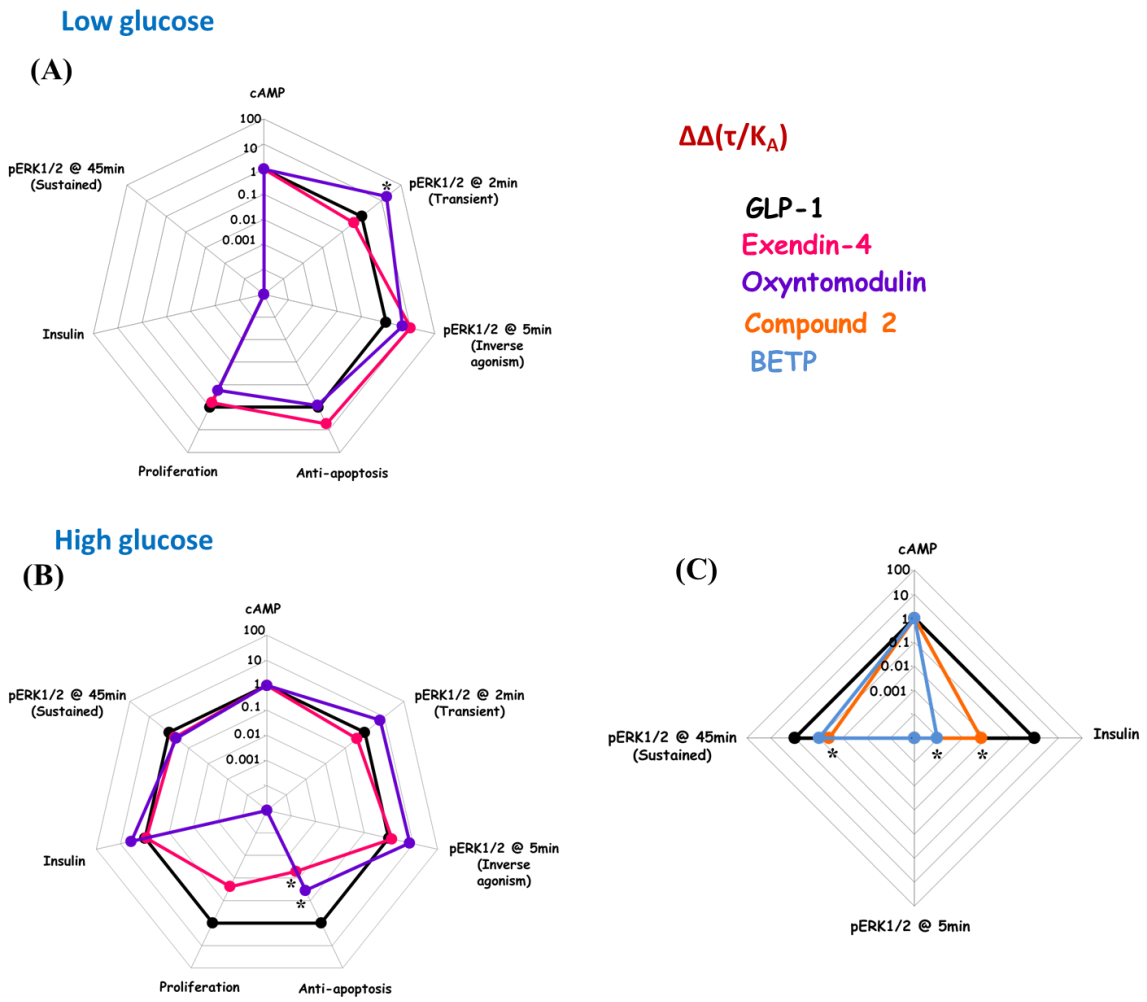

Figure 4.13: Web of bias with GLP-1R ligands relative to the reference ligand GLP-1 and reference pathway cAMP in high and low glucose conditions.(A) GLP-1R peptide ligands, 2.8 mM glucose; (B) GLP-1R peptide ligands, 11 mM glucose; (C) small molecules allosteric modulators of GLP-1R, 11 mM glucose. The transduction coefficient (τ/K_A ratio) is extracted by applying the operational model of agonism to standard dose-response curves to calculate bias factors τ/K_A, that are normalised to a reference ligand, GLP-1 and a reference pathway cAMP to obtain $\Delta\Delta$ (τ/K_A) values which are then plotted. Normalised data points are plotted on the log scale in the web of bias. Data were analyzed with one way ANOVA followed by Dunnett's multiple comparison post-test to calculate statistical significance from reference ligand GLP-1, statistically significant at $*P < 0.05$.

4.2.3 GLP-1R biased allostery and probe-dependence

4.2.3.1 Modulation of agonist-mediated cAMP accumulation in INS-1 832/3 cells

In the previous section both compound 2 and BETP displayed weak, low potency, agonism in multiple pathways. As these compounds bind to an allosteric site (Knudsen *et al.*, 2007; Sloop *et al.*, 2010), and have been identified to behave as allosteric modulators in a probe dependent manner, interaction studies between the small molecules and individual peptides were performed in order to investigate the allosteric effects that these two ligands have on peptide-mediated signalling in INS-1 832/3 cells in the two distinct physiologically relevant glucose conditions. Concentration response curves were generated for each of the three orthosteric peptides in the presence of increasing concentrations of either BETP or compound 2 for cAMP accumulation Figure 4.14 - 4.15), insulin secretion (Figure 4.16) and the various phases of the pERK1/2 response (Figure 4.17 - 4.23, S4.5 and S4.6). These data were analysed using the allosteric operational model that allowed calculation of combined affinity-efficacy cooperativity (αβ) estimates to quantify allosteric modulation (Table 4.9). The co-addition of compound 2 with GLP-1 resulted in a weak modulation of cAMP response in both low and high glucose conditions (Figure 4.14 A and D) with log αβ estimates of 0.96 ± 0.21 and 0.95 ± 0.34, respectively (approx. 9-fold positive modulation) (Figure 4.14 A and D; Table 4.9). No modulation was observed for exendin-4 (Figure 4.14 B and E). In contrast, compound 2 robustly modulated oxyntomodulin responses with combined log αβ estimates of 1.14 ± 0.33 (14-fold) and 1.31 ± 0.41 (20-fold) in 2.8 mM and 11 mM glucose, respectively (Figure 4.14 C and F; Table 4.9) thereby suggesting a strong positive modulation. Co-addition of increasing concentrations of BETP showed no modulation of either GLP-1 or exendin-4-mediated cAMP (Figure 4.15 A, D, B and E; Table 4.9). However, positive modulation (approximately 20-fold) of oxyntomodulin cAMP was observed in presence of BETP in both low and high glucose (log αβ = 1.33 ± 0.40 in 2.8 mM glucose andlog αβ = 1.41 ± 0.29 in 11 mM glucose) (Figure 4.15 C and F; Table 4.9).

4.2.3.2 Modulation of agonist-mediated insulin secretion in INS-1 832/3 cells

Compound 2 and BETP, were identified as low potency partial agonists for insulin secretion in conditions of high glucose. These allosteric ligands did not promote modulation of either GLP-1 or exendin-4-mediated GSIS, when co-added with these ligands in high glucose conditions (Figure 4.16 A, B, D and E). However, both BETP and compound 2 positively modulated oxyntomodulin-mediated insulin secretion in high glucose (compound 2, log αβ = 1.52 ± 0.15 and BETP, log αβ = 1.45 ± 0.48) (Figure 4.16 C and F; Table 4.9). No insulin response was observed when these ligands were added alone or in combination with peptides in low glucose conditions (data not shown).

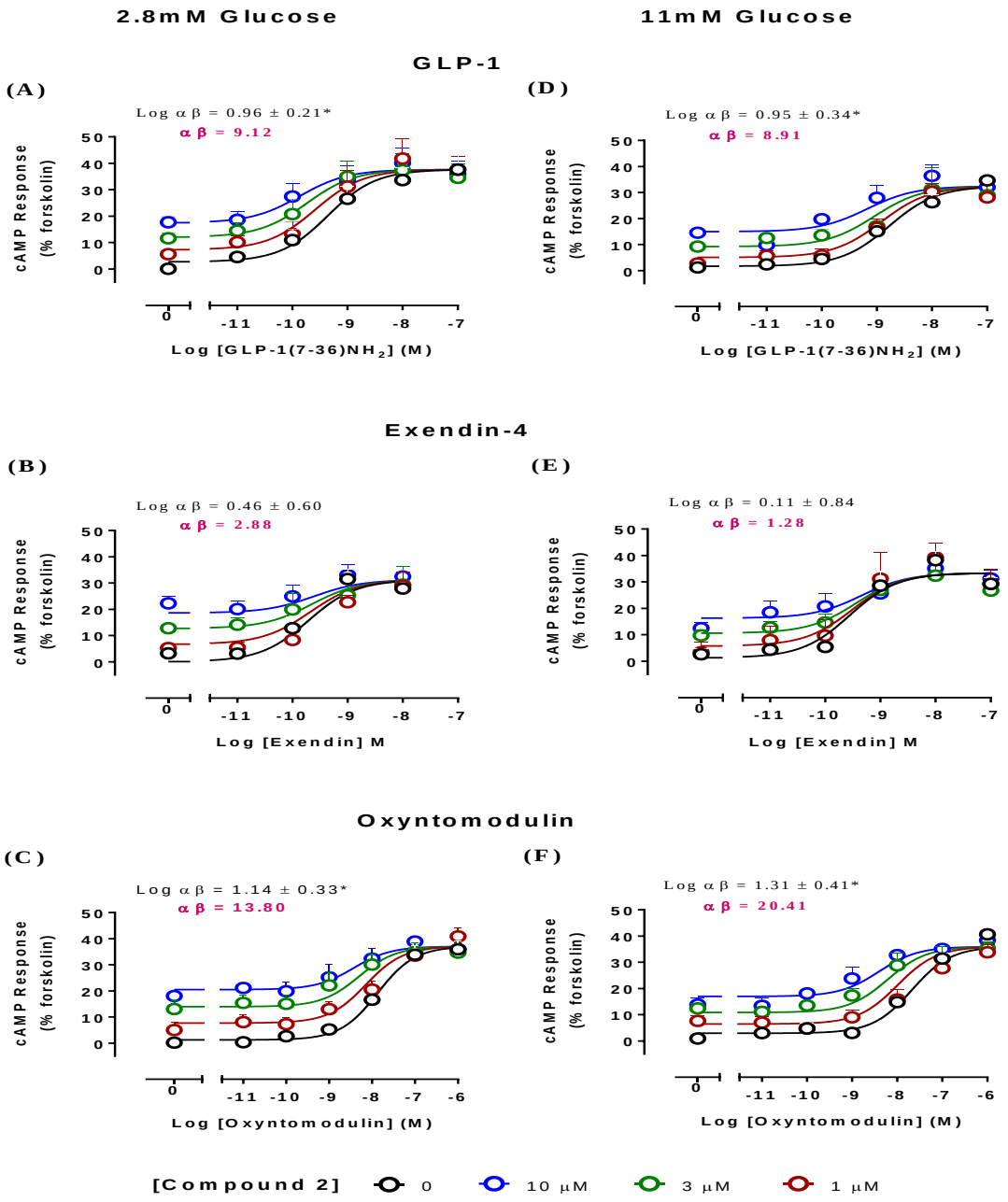

Figure 4.14: Allosteric modulation of GLP-1R peptide-mediated responses in cAMP by compound 2 Characterization of the interaction between Compound 2 and GLP-1R peptide ligands in conditions of both low and high glucosein cAMP accumulation assay using INS-1 832/3 cells. Concentration response curves were generated for peptide ligands in the absence and presence of increasing concentrations of compound 2 (A) GLP-1, 2.8 mM glucose; (B) Exendin-4, 2.8 mM glucose; (C) Oxyntomodulin, 2.8 mM glucose; (D) GLP-1, 11 mM glucose; (E) Exendin-4, 11 mM glucose; (F) Oxyntomodulin, 11 mM glucose.Data is normalised to the response elicited by 100 μM forskolin and analysed with the operational model of allosterism with the curves representing the best global fit. All values are mean + SEM of three to five experiments conducted in triplicate.Derived log αβ values were analysed with one way ANOVA and Dunnett's post test to determine significant modulation (*$P < 0.05$).

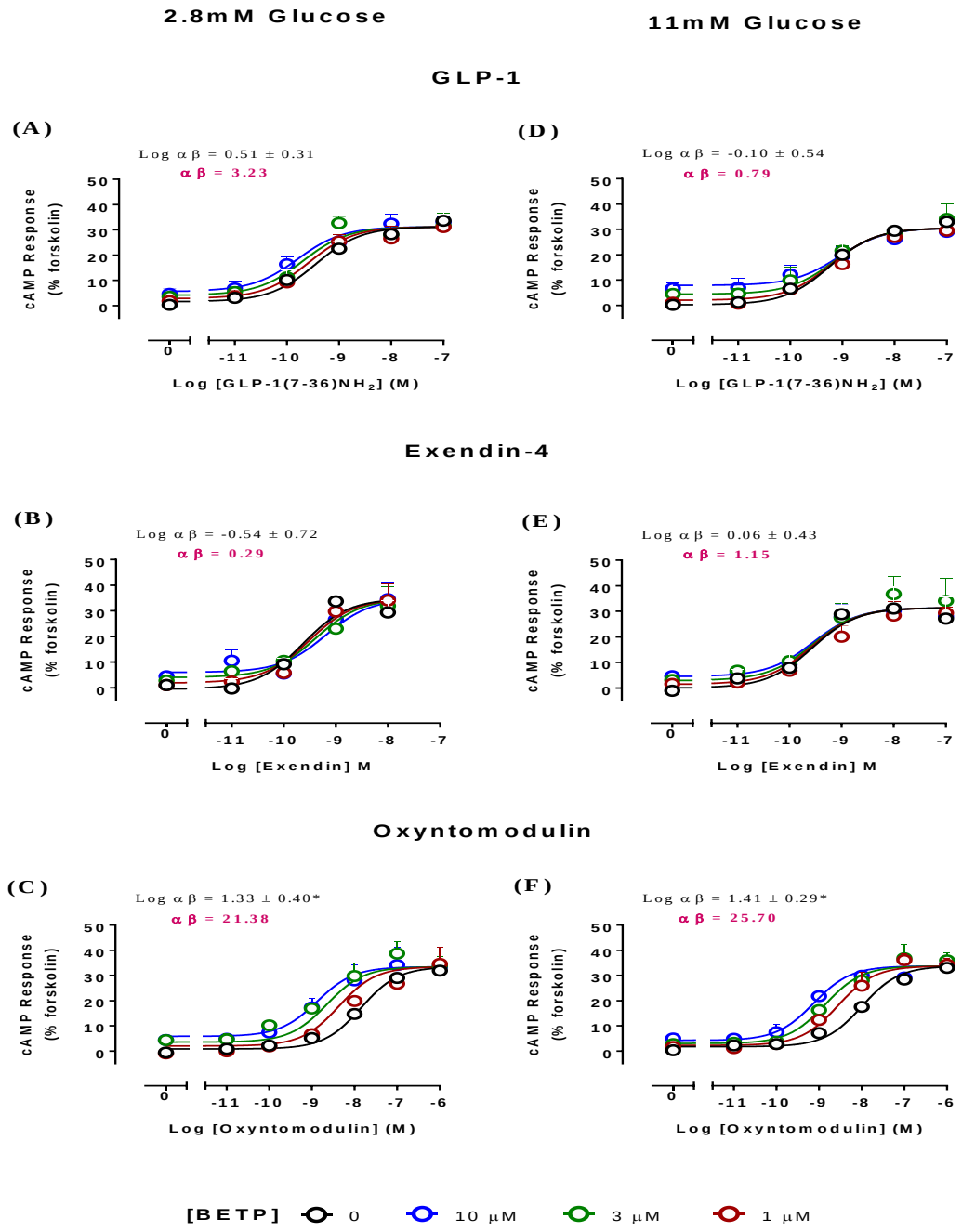

Figure 4.15: Allosteric modulation of GLP-1R peptide-mediated cAMP responses by BETP Characterization of the interaction between BETP and GLP-1R peptide ligands under conditions of both low and high glucose in cAMP accumulation assay using INS-1 832/3 cells. Concentration response curves were generated for peptide ligands in the absence and presence of increasing concentrations of BETP(A) GLP-1, 2.8 mM glucose; (B) Exendin-4, 2.8 mM glucose; (C) Oxyntomodulin, 2.8 mM glucose; (D) GLP-1, 11 mM glucose; (E) Exendin-4, 11 mM glucose; (F) Oxyntomodulin, 11 mM glucose.Data is normalised to the response elicited by 100 µM forskolin and analysed with the operational model of allosterism with the curves representing the best global fit. All values are mean + SEM of three to five experiments conducted in triplicate. Derived log αβ values were analysed with One way ANOVA and Dunnett's post test to determine significant modulation (*$P < 0.05$).

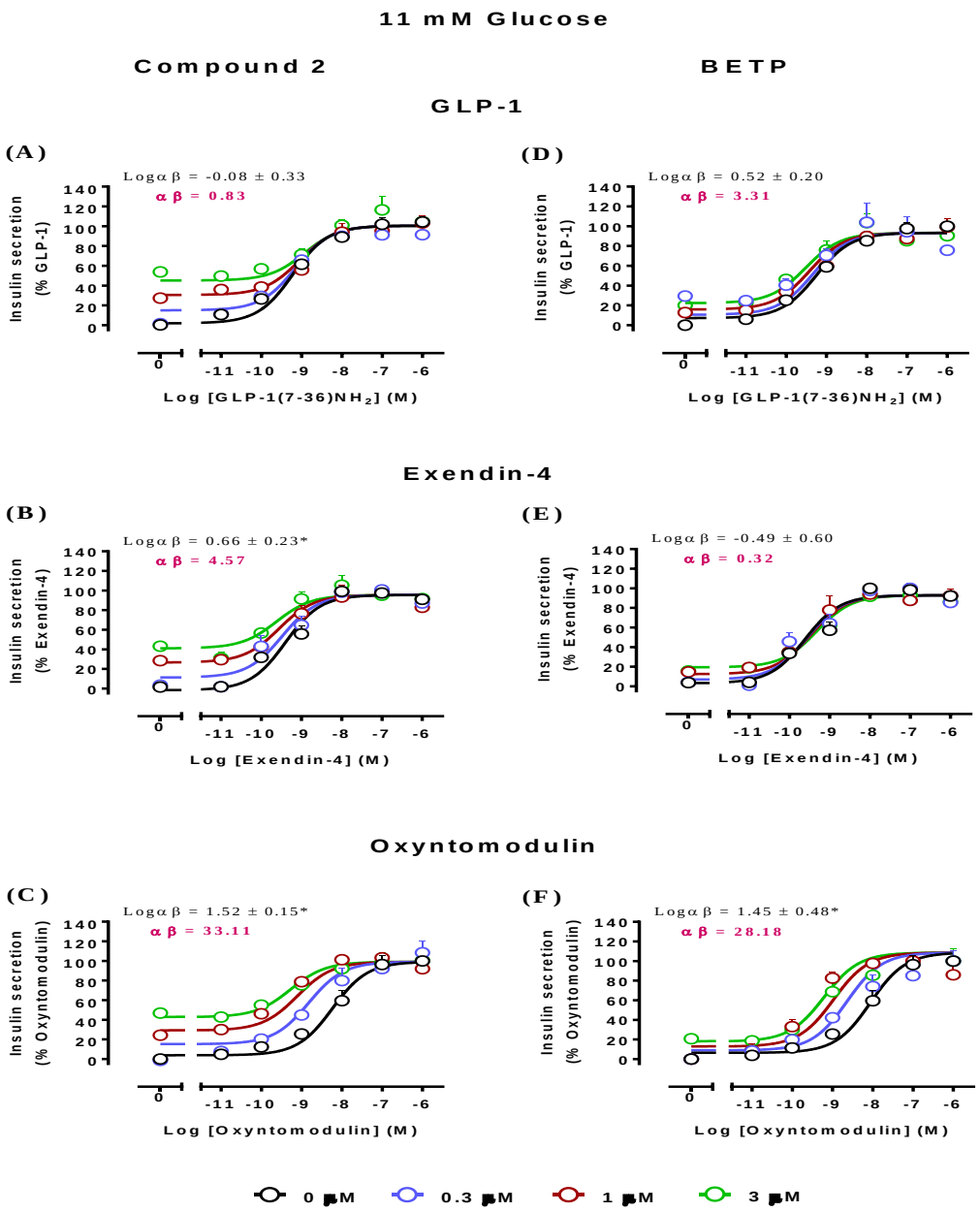

Figure 4.16: Allosteric modulation of GLP-1R peptide responses in insulin secretion Characterization of the interaction between GLP-1R peptide ligands and Compound 2 (A-C) and BETP (D-F) in the presence of 11 mM glucose using the glucose-stimulated insulin secretion assay in INS-1 832/3 cells. Concentration response curves were generated for peptide ligands in the absence and presence of increasing concentrations of small molecules(A) GLP-1with compound 2 (B) Exendin-4 with compound 2; (C) Oxyntomodulin with compound 2; (D) GLP-1 with BETP; (E) Exendin-4, with BETP; (F) Oxyntomodulin, with BETP. Data is normalised to the maximal peptide response and analysed using the operational model of allosterism with the curves representing the best global fit. All values are mean + SEM of three to five experiments conducted in triplicate. Calculated log αβ values were analysed with one way ANOVA and Dunnett's post test to determine significant modulation (*$P < 0.05$).

Table 4.9: Functional cooperativity estimates for the interaction between Compound 2 or BETP and GLP-1R peptide ligands.

Data derived from the analysis of interaction concentration response curves with an operational model of allosterism between allosteric ligands and peptide ligands in various signalling pathways and different glucose conditions. Log αβ represents the combined cooperativity between allosteric ligand and the orthosteric peptide ligand. Values represent mean + SEM of 3-5 experiments performed in duplicate. The data is presented as Log αβ with αβ values in parenthesis.

Logαβ (αβ) =0 (1) equals neutral co-operativity; Logαβ (αβ) > 0 (1) equals positive co-operativity and Logαβ (αβ) < 0 (1) equals negative co-operativity. Data were analyzed with one way ANOVA followed by Dunnett's multiple comparison post-test, statistically significant at *$P < 0.05$. ND = not defined due to no detectable response NR = no response detected.

	Log αβ (αβ)			
	Compound 2		**BETP**	
	2.8 mM Glucose	**11 mM Glucose**	**2.8 mM Glucose**	**11 mM Glucose**
cAMP Accumulation				
GLP-1	0.96 ± 0.21* (9.12)	0.95 ± 0.34* (8.19)	0.51 ± 0.31 (3.23)	-0.10 ± 0.54 (0.79)
Exendin-4	0.46 ± 0.60 (2.88)	0.11 ± 0.84 (1.29)	-0.54 ± 0.72 (0.29)	0.06 ± 0.43 (1.15)
Oxyntomodulin	1.14 ± 0.33* (13.80)	1.31 ± 0.41* (20.42)	1.33 ± 0.40* (21.38)	1.41 ± 0.29* (25.70)
Glucose-stimulated Insulin Secretion				
GLP-1	NR	-0.08 ± 0.33 (0.83)	NR	0.52 ± 0.20 (3.31)
Exendin-4	NR	0.66 ± 0.23* (4.57)	NR	-0.49 ± 0.60 (0.32)
Oxyntomodulin	NR	1.52 ± 0.15* (33.11)	NR	1.45 ± 0.48* (28.18)

ERK1/2 Phosphorylation @ 2 min (3 min Pre-incubation with allosteric modulator)				
GLP-1	0.84 ± 0.32* (6.92)	0.80 ± 0.34 (6.31)	1.28 ± 0.15* (19.05)	0.94 ± 0.20* (8.71)
Exendin-4	0.80 ± 0.37 (6.31)	1.22 ± 0.38* (16.60)	1.26 ± 0.20* (18.20)	0.88 ± 0.26* (7.60)
Oxyntomodulin	1.20 ± 0.21* (15.85)	1.02 ± 0.28* (10.47)	1.27 ± 0.50* (18.62)	0.86 ± 0.40 (7.24)
ERK1/2 Phosphorylation @ 5 min (Co-addition with allosteric modulator)				
GLP-1	1.21 ± 0.50* (16.22)	ND	0.83 ± 0.13* (6.76)	ND
Exendin-4	1.01 ± 0.49 (10.23)	ND	1.09 ± 0.20* (12.30)	ND
Oxyntomodulin	1.44 ± 0.52* (27.54)	ND	1.14 ± 0.27* (13.80)	ND
ERK1/2 Phosphorylation @ 2 min (43 min Pre-incubation with allosteric modulator)				
GLP-1	0.27 ± 0.62 (1.86)	0.21 ± 0.24 (1.62)	1.07 ± 0.22 (11.75)	1.02 ± 0.20 (10.50)
Exendin-4	0.39 ± 0.56 (2.45)	0.10 ± 0.26 (1.26)	1.15 ± 0.16 (14.12)	0.77 ± 0.20 (5.89)
Oxyntomodulin	0.75 ± 0.16 (5.62)	0.99 ± 0.41 (9.77)	0.88 ± 0.42 (7.60)	0.56 ± 0.24 (3.63)
ERK1/2 Phosphorylation @ 45 min (Co-addition with allosteric modulator)				
GLP-1	ND	1.61 ± 2.82 (40.74)	ND	ND

Exendin-4	ND	ND	ND	ND
Oxyntomodulin	ND	1.15 ± 2.02 (14.12)	ND	ND

4.2.3.3 Modulation of agonist-mediated ERK1/2 phosphorylation in INS-1 832/3 cells

The modulatory effects of allosteric compounds on GLP-1R peptide-mediated pERK1/2 was assessed at differential time points selected based upon their individual kinetic profiles. As Compound 2 and BETP pERK1/2 response peaked at 5 min, whereas, peptide-mediated responses were observed to peak at 2 min, therefore concentration response curves for peptides were assessed at 2 min post-stimulation in the presence of increasing concentration of either compound 2 or BETP that had been pre-incubated prior to peptide addition for 3 min (thus in theory measuring the response at the peak for both small molecule and peptide) (Figure 4.17 and 4.18).

Weak positive modulation of peptide-mediated pERK1/2 was observed with compound 2 in high glucose, however only exendin-4 and oxyntomodulin were significantly modulated (Figure 4.17; Table 4.9). Under the same conditions, BETP also augmented efficacy promoting left shifts in potency of the peptides, however, in this case the modulation of GLP-1 and exendin-4 reached statistical significance, but oxyntomodulin did not (Figure 4.18; Table 4.9). In low glucose, although compound 2 augmented responses for all three peptides, only oxyntomodulin (16-fold) reached statistical significance (Figure 4.17, Table 4.9). In contrast BETP positively modulates peptide responses to a higher degree in low glucose, significantly modulating all three peptides to a similar extent (approx. 20-fold) (Figure 4.18, Table 4.9).

Similarly, positive modulation of the pERK1/2 response was observed when GLP-1R peptide ligands were co-added with compound 2 and BETP and response measured at 5 min in presence of 2.8 mM glucose (Figure 4.19 and 4.20). For Compound 2, modulation of both GLP-1 and oxyntomodulin reached statistical significance (16 and 28-fold respectively), whereas for BETP all peptides reached statistical significance, but modulated responses to a lesser extent than that observed for compound 2 (7-14 fold). Furthermore, the peptides showed inverse agonism in high glucose at 5 min, whereas the allosteric ligands displayed agonism. Due to this, the operational model of allosterism could not be used to determine quantitative functional estimates of cooperativity ($\alpha\beta$). However, by plotting the changes observed in the pEC_{50} value of the peptide inverse agonism response with increasing concentrations of small molecules, the presence of allosteric modulation can be predicted (Figure 4.21). Assessment of allosteric effects in this manner reveals BETP positively modulates all peptide-mediated pERK1/2 responses at 5 min in high glucose, however compound 2, showed no modulation of potency (Figure 4.21).

Additionally, pre-incubation of allosteric ligands for 45 minutes prior to assessment of transient pERK1/2 peptide responses was assessed (Figure 4.22 and 4.23) so as to gain an insight into the

modulation engendered by pre-incubation of allosteric modulator on the peptide-mediated transient activation of pERK1/2. Following pre-incubation of compound 2 measurements of transient peptide-mediated ERK1/2 responses (2 min) revealed weak positive modulation of oxyntomodulin only (in both high and low glucose), however, this did not reach statistical significance (Figure 4.22).

In contrast, weak positive modulation of all peptides (to varying degrees) by BETP was observed in high and low glucose but this did not reach statistical significance (Figure 4.23). No modulation of peptide-mediated sustained pERK1/2 was observed in presence of increasing concentration of either compound 2 (Appendix 2, Figure S4.5) or BETP (Appendix 2, Figure S4.6) irrespective of glucose conditions when both peptide and small molecule were co-incubated.

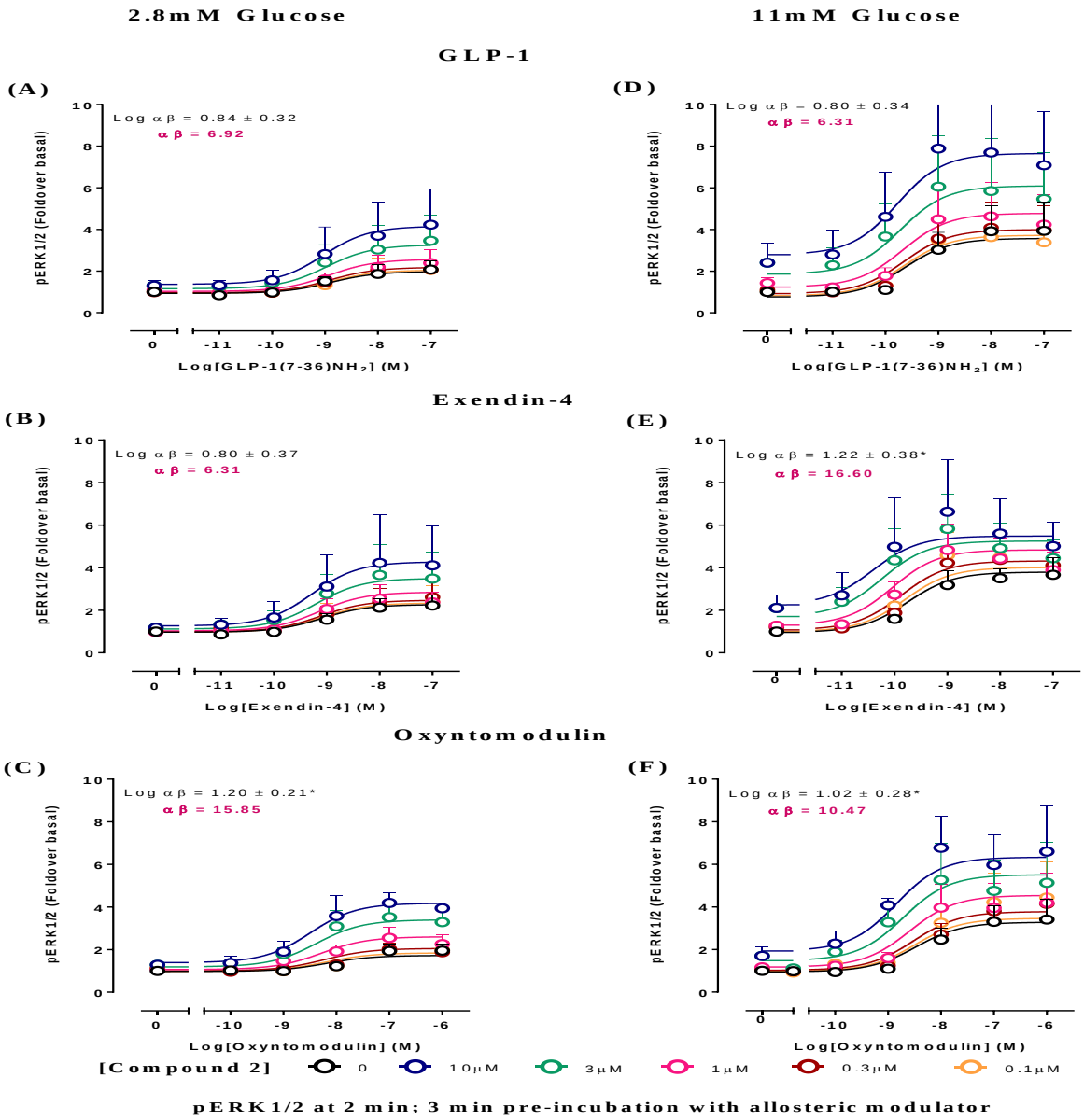

Figure 4.17: Allosteric modulation of GLP-1R peptide responses in pERK1/2 assay performed at the transient ERK1/2 peak for both peptide and small molecule Compound 2. Characterization of the interaction between Compound 2 and GLP-1R peptide ligands under conditions of both low and high glucose in ERK1/2 phosphorylation using INS-1 832/3 cells. Concentration response curves were generated for peptide ligands in the absence and presence of increasing concentrations of compound 2. (A) GLP-1, 2.8 mM glucose; (B) Exendin-4, 2.8 mM glucose; (C) Oxyntomodulin, 2.8 mM glucose; (D) GLP-1, 11 mM glucose; (E) Exendin-4, 11 mM glucose; (F) Oxyntomodulin, 11 mM glucose. Cells were pre-incubated for 3 min with compound 2 in 2.8 mM glucose and subsequently exposed to the peptide for 2 min, which was prepared in both low and high glucose. Data is represented as fold over basal corresponding to respective glucose concentration and analysed using the operational model of allosterism with the curves representing the best global fit. All values are mean ± SEM of three to five experiments conducted in triplicate. Calculated log αβ values were analysed with one way ANOVA and Dunnett's post test to determine significant modulation (*$P < 0.05$).

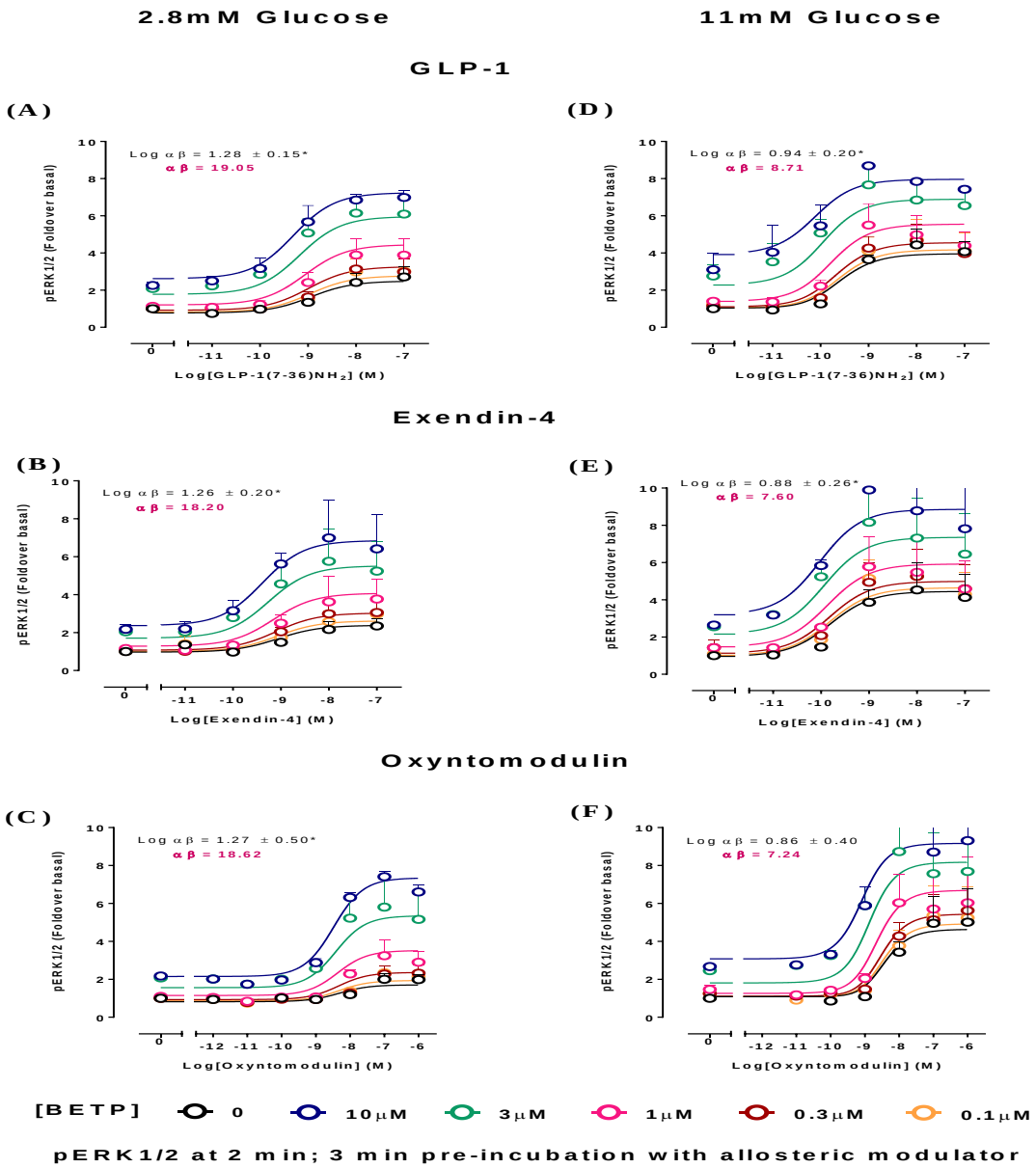

Figure 4.18: Allosteric modulation of GLP-1R peptide responses in pERK1/2 assay performed at the transient ERK1/2 peak for both peptide and small molecule BETP. Characterization of the interaction between BETP and GLP-1R peptide ligands under conditions of both low and high glucose in ERK1/2 phosphorylation in INS-1 832/3 cells. Concentration response curves were generated for peptide ligands in the absence and presence of increasing concentrations of BETP (A) GLP-1, 2.8 mM glucose; (B) Exendin-4, 2.8 mM glucose; (C) Oxyntomodulin, 2.8 mM glucose; (D) GLP-1, 11 mM glucose; (E) Exendin-4, 11 mM glucose; (F) Oxyntomodulin, 11 mM glucose. Cells were pre-incubated for 3 min with BETP in presence of 2.8 mM glucose, and subsequently exposed to the peptide for 2 min, which was prepared in both low and high glucose. Data is represented as foldover basal corresponding to respective glucose concentration and analysed using the operational model of allosterism with the curves representing the best global fit. All values are mean ± SEM of three to five experiments conducted in triplicate. Calculated log αβ values were analysed with one way ANOVA and Dunnett's post test to determine significant modulation (*$P < 0.05$).

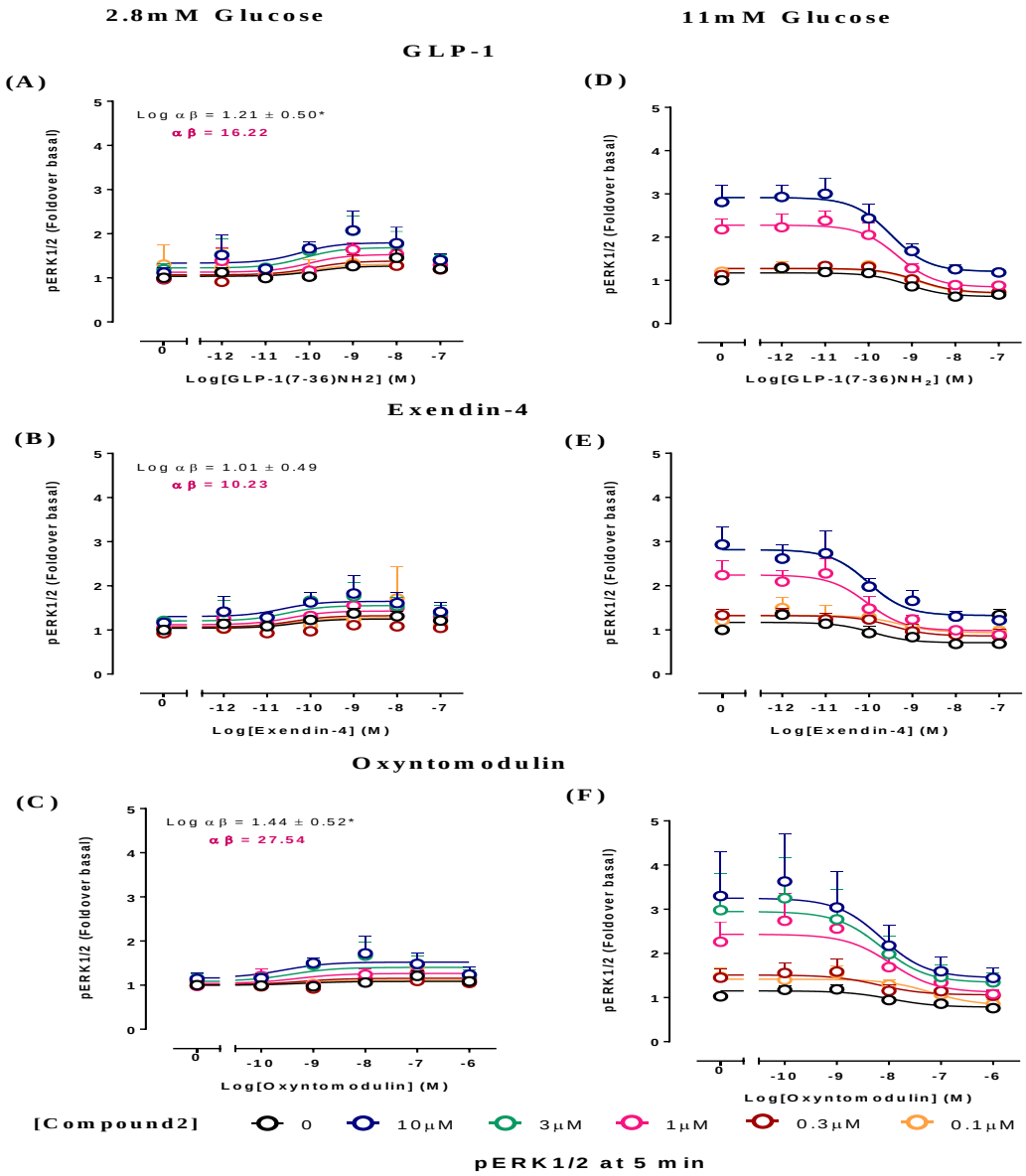

Figure 4.19: Allosteric modulation of GLP-1R peptide responses by compound 2 in pERK1/2 assay measured at 5 min. Characterization of the interaction between Compound 2 and GLP-1R peptide ligands under conditions of both low and high glucose in ERK1/2 phosphorylation assay using INS-1 832/3 cells. Concentration response curves were generated for peptide ligands in the absence and presence of increasing concentrations of compound 2 (A) GLP-1, 2.8 mM glucose; (B) Exendin-4, 2.8 mM glucose; (C) Oxyntomodulin, 2.8 mM glucose; (D) GLP-1, 11 mM glucose; (E) Exendin-4, 11 mM glucose; (F) Oxyntomodulin, 11 mM glucose. The compound 2 was co-added with each peptide for 5 min. Data is represented as fold over basal corresponding to respective glucose concentration. A-C were analysed with the operational model of allosterism with the curves representing the best global fit. Calculated log αβ values were analysed with one way ANOVA and Dunnett's post test to determine significant modulation (*$P < 0.05$). D-F were fitted to a three parameter logistic equation. All values are mean ± SEM of three to five experiments conducted in triplicate.

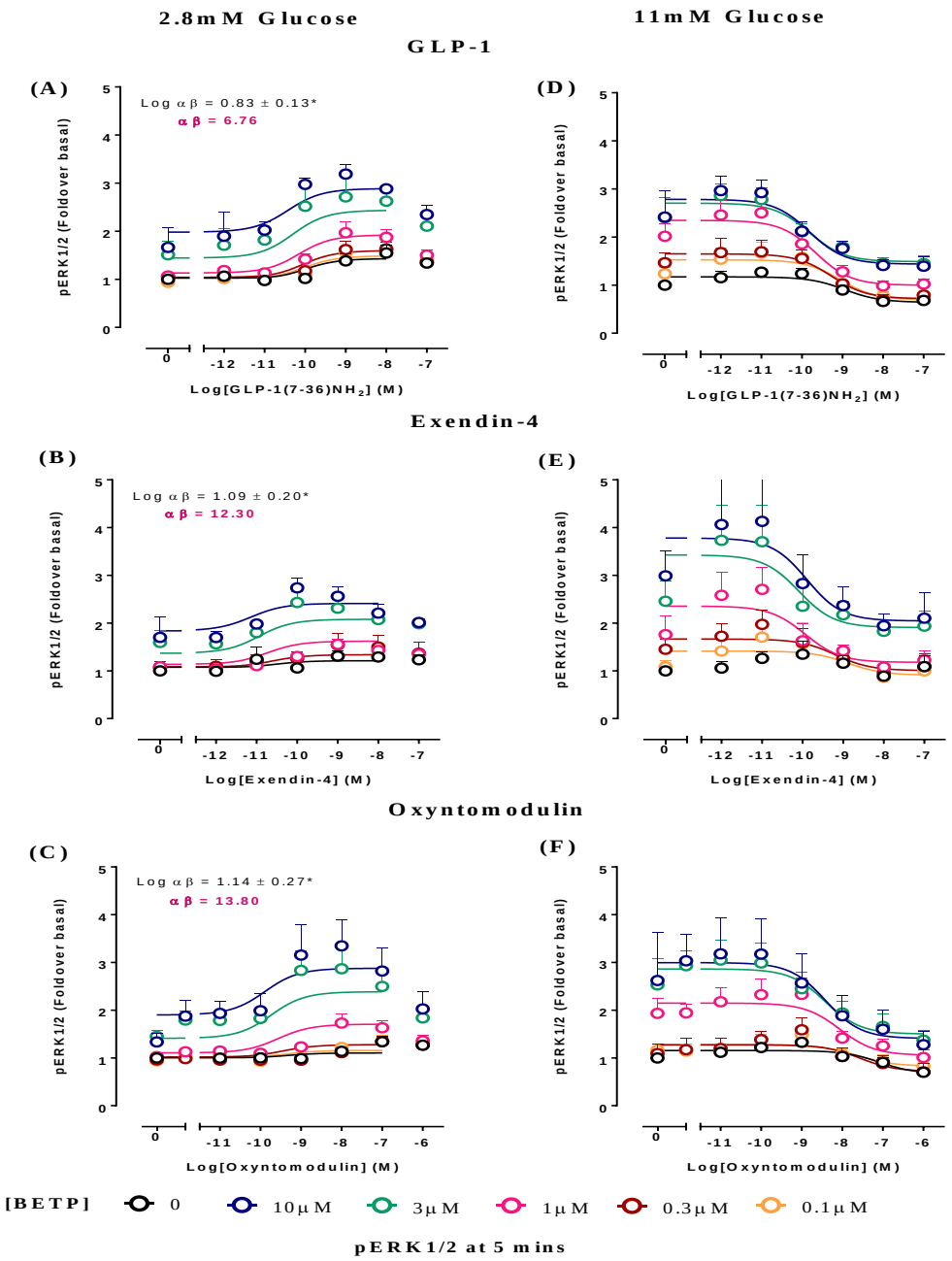

Figure 4.20: Allosteric modulation of GLP-1R peptide responses by BETP in pERK1/2 assay measured at 5 min. Characterization of the interaction between BETP and GLP-1R peptide ligands under conditions of both low and high glucose in ERK1/2 phosphorylation assay using INS-1 832/3 cells. Concentration response curves were generated for peptide ligands in the absence and presence of increasing concentrations of BETP (A) GLP-1, 2.8 mM glucose; (B) Exendin-4, 2.8 mM glucose; (C) Oxyntomodulin, 2.8 mM glucose; (D) GLP-1, 11 mM glucose; (E) Exendin-4, 11 mM glucose; (F) Oxyntomodulin, 11 mM glucose. BETP was co-added with each peptide for 5 min. Data is represented as fold-over basal corresponding to respective glucose concentration. A-C were analysed with the operational model of allosterism with the curves representing the best global fit. Calculated log αβ values were analysed with one way ANOVA and Dunnett's post test to determine significant modulation (*$P < 0.05$). D-F were fitted to a three parameter logistic equation. All values are mean ± SEM of three to five experiments conducted in triplicate.

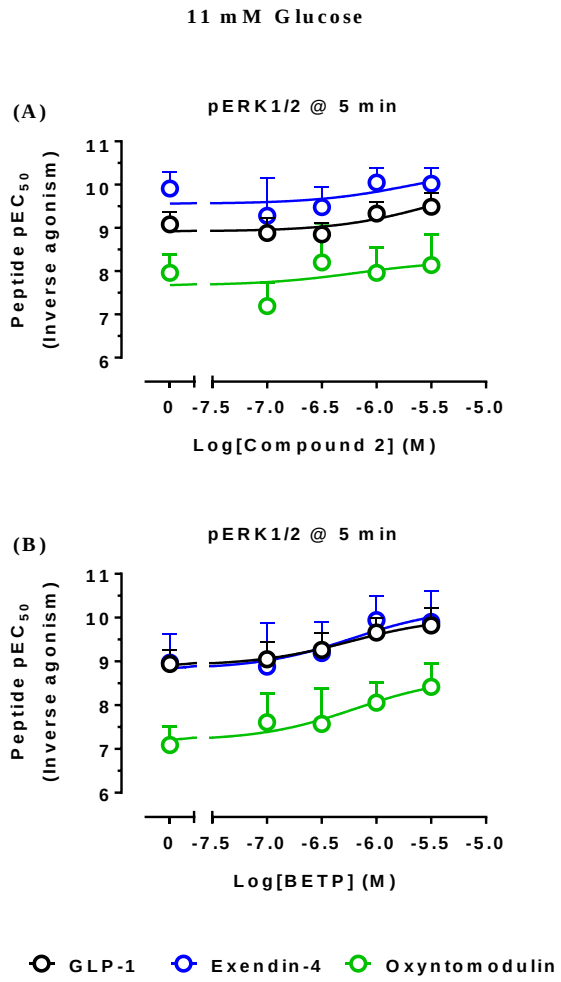

Figure 4.21: Potency changes in 5 min pERK1/2 inverse agonism by peptide ligands in the presence of increasing concentration of small molecules. pEC50 values of the inverse agonism of peptide ligands in the presence and absence of increasing concentrations of small molecule allosteric modulators (A) compound 2 and (B) BETP in 11 mM glucose. Cells were simulated for 5 min after co-addition of peptides with the small molecules.pEC_{50} values are the negative logarithms of concentration of agonists that produces half the maximal response derived from the data in figure 4.19 and 4.20. Data is analysed with a three-parameter logistic equation. All values are mean ± SEM of five to ten experiments conducted in triplicate. Peptide EC_{50} values were analysed with one way ANOVA and Dunnett's post test to determine significant modulation (*$P < 0.05$).

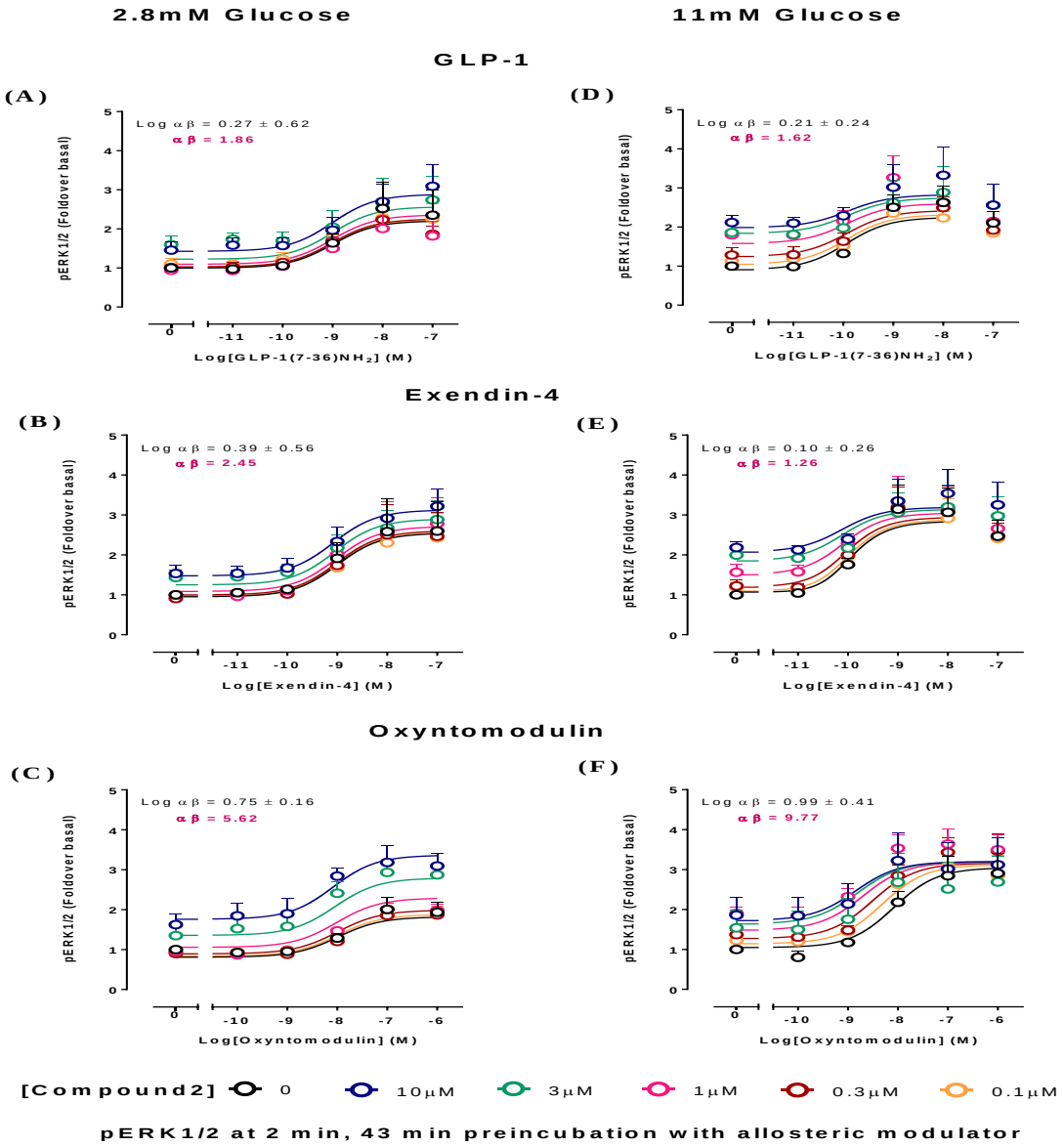

Figure 4.22: Allosteric modulation of GLP-1R peptide responses in pERK1/2 assay performed at the transient ERK1/2 peak for peptide and sustained ERK1/2 response for Compound 2. Characterization of the interaction between Compound 2 and GLP-1R peptide ligands under conditions of both low and high glucose in ERK1/2 phosphorylation assay using INS-1 832/3 cells. Concentration response curves were generated for peptide ligand in the absence and presence of increasing concentrations of compound 2(A) GLP-1, 2.8 mM glucose; (B) Exendin-4, 2.8 mM glucose; (C) Oxyntomodulin, 2.8 mM glucose; (D) GLP-1, 11 mM glucose; (E) Exendin-4, 11 mM glucose; (F) Oxyntomodulin, 11 mM glucose. Cells were pre-incubated for 43 min with compound 2 in presence of 2.8 mM glucose and subsequently exposed to the peptide for 2 min under conditions of both low and high glucose. Data is represented as foldover basal corresponding to respective glucose concentration and analysed using the operational model of allosterism with the curves representing the best global fit. All values are mean ± SEM of three to five experiments conducted in triplicate. Calculated log αβ values were analysed with One way ANOVA and Dunnett's post test to determine significant modulation (*$P < 0.05$).

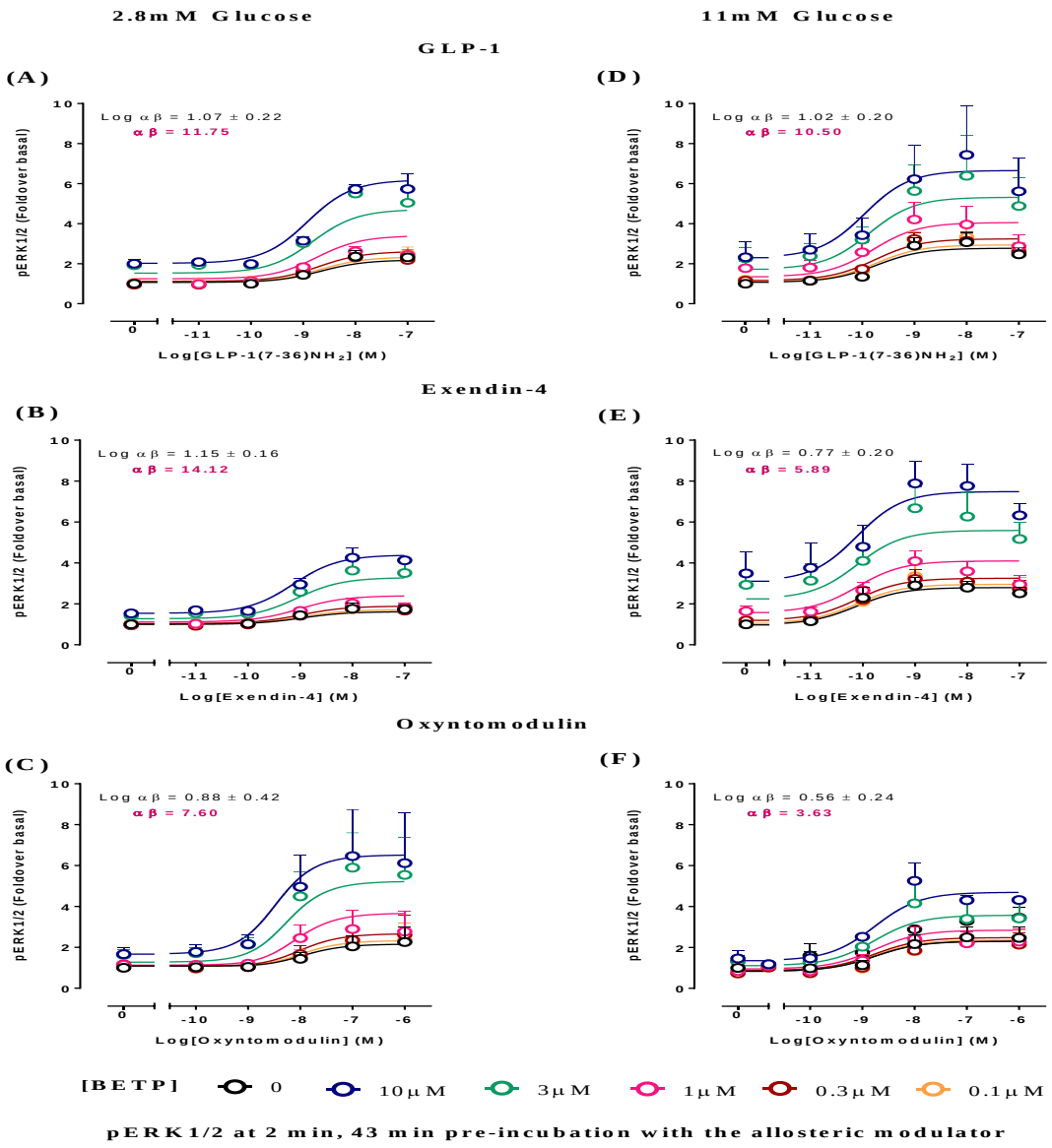

Figure 4.23: Allosteric modulation of GLP-1R peptide responses in pERK1/2 assay performed at the transient ERK1/2 peak for peptide and sustained ERK1/2 response for BETP. Characterization of the interaction between BETP and GLP-1R peptide ligands under conditions of both low and high glucose in ERK1/2 phosphorylation assay using INS-1 832/3 cells. Concentration response curves were generated for peptide ligand in the absence and presence of increasing concentrations of BETP (A) GLP-1, 2.8 mM glucose; (B) Exendin-4, 2.8 mM glucose; (C) Oxyntomodulin, 2.8 mM glucose; (D) GLP-1, 11 mM glucose; (E) Exendin-4, 11 mM glucose; (F) Oxyntomodulin, 11 mM glucose. Cells were pre-incubated for 43 min with BETP in presence of 2.8 mM glucose and subsequently exposed to the peptide for 2 min, under conditions of low and high glucose. Data is represented as fold-over basal corresponding to respective glucose concentration and analysed using the operational model of allosterism with the curves representing the best global fit. All values are mean ± SEM of three to five experiments conducted in triplicate. Calculated log αβ values were analysed with One way ANOVA and Dunnett's post test to determine significant modulation (*$P < 0.05$).

4.3. DISCUSSION

Ligand-mediated signal bias is evident at many GPCRs and this may be beneficial for treating various diseases (Kenakin, 2007; Kenakin and Christopoulos, 2013; Zhao *et al.,* 2014; Khoury *et al.,* 2014). One of the earliest known examples of biased drugs that display improved therapeutic profiles are βAR antagonists (β-blockers) used for treatment of sustained acute myocardial infarction and heart failure. While all β-blockers have the ability to block G protein-mediated effects, those that simultaneously stimulate β-arrestin–mediated signalling provide additional advantages (Wisler *et al.,* 2007). In addition, selective activation of β-arrestins at the angiotensin II type 1 receptor and the PTH receptor provide theoretical therapeutic advantages, through increasing cardiac performance by reducing blood pressure and improved treatments for osteoporosis, respectively (Violin *et al.,* 2010; Gesty-Palmer *et al.,* 2009; Schmid *et al.,* 2008). In animal models of disease, selectively decreasing β-arrestin activation for GPR109, α_2-adrenoreceptors and opioid receptors promotes decreased triglycerides with no cutaneous flushing (GPR109) (Wlaters *et al.,* 2009), hypotension with reduced sedation (α_2-adrenoreceptors) (Cullen and Bohn., 2009) and analgesia with decreased tolerance, respiratory repression and constipation (opioid receptors) (Xu *et al.,* 2007, Bohn *et al.,* 1999; Groer *et al.,* 2007). At the arginine vasopressin receptor blocking classical G protein signalling (IP_3 pathway), while promoting ERK1/2 phosphorylation, has shown potential advantages for treatment of small cell lung cancers (MacKinnon *et al.,* 2005). Whereas, decreasing MAPkinase phosphorylation and receptor internalization following D2 dopamine receptor activation provides an improved profile for the treatment of schizophrenia and Parkinson's disease (Urban *et al.,* 2007, Ryman-Rasmussen *et al.,* 2007).

From these studies, it is evident that exploitation of ligand-directed signalling bias to selectively target signalling pathways that enhance some physiological functions downstream of specific signalling pathways, while avoiding others linked to different signalling pathways, could have numerous advantages in GPCR drug development. This phenomenon may also account for the large attrition rate of drugs entering into clinical trials, as many of these properties are not understood for most GPCRs, and screening programs in drug development are normally focused entirely on targeting the primary G protein signalling pathway when searching for novel drug-like compounds.

While clinically used GLP-1R peptide ligands approved by the FDA (exenatide, liraglutide and dulaglutide) (Gallwitz, 2015) have been very successful in the treatment and management of type 2 diabetes (and obesity), they have been linked to numerous side effect profiles, including nausea, increased risk of pancreatitis, pancreatic and thyroid cancers. In addition, there are reports that these

drugs cause a desensitisation to GLP-1R mediated inhibition of gastric emptying (Baggio *et al.*, 2004; Nauck *et al.*, 2011). The pharmaceutical industry has attempted to discover novel GLP-1R small molecule, orally available, drugs, however these efforts to date have been unsuccessful (Chen *et al.*, 2007; Knudsen *et al.*, 2007). This may in part be due to a lack of mechanistic understanding of the very basic pharmacology and signalling properties of this receptor and a lack of understanding of ligand-directed signalling bias.

There is now a substantial body of evidence that reveals ligand-directed stimulus bias occurs at the GLP-1R by either direct agonist activation or via allosteric modulation of orthosteric ligand responses. To date, the majority of these studies have been performed in recombinant cell systems that overexpress the GLP-1R (Knudsen *et al.*, 2007; Koole *et al.*, 2010; Sloop *et al.*, 2010; Wootten *et al.*, 2011, 2012, 2013). While these studies identify fingerprints for distinct ligands, and identify those that have biased behaviour, it is unclear what the physiological impact of this is, and how this information may be used to exploit biased signalling therapeutically. This chapter expands the knowledge around GLP-1R ligand-directed signalling bias assessing both acute signalling pathways (cAMP, pERK1/2) and more physiologically relevant endpoints (insulin secretion, proliferation and anti-apoptosis) in an endogenously expressing system that is used to mimic primary beta islet cells. This allows us to begin to speculate on the importance of various pathways for targeting physiological functions and highlights the importance of understanding signalling bias profiles of ligands in different cell backgrounds. In addition, the assessment of signalling bias in two physiologically relevant glucose conditions highlights the need to not only understand the impact of signalling bias on physiologically relevant events, but also to understand this in different physiological and pathophysiological conditions, as the bias observed changes under these different conditions.

Here, we provided a detailed analysis of the ability of various GLP-1R peptide ligands, GLP-1, exendin-4 and oxyntomodulin, to mediate cAMP accumulation, insulin secretion, ERK1/2 phosphorylation, cell protection/survival and proliferation using the insulinoma cell line INS-1 832/3 that endogenously expresses the GLP-1R. These studies revealed that like, GLP-1 (as identified in Chapter 3), exendin-4 and oxyntomodulin mediated cAMP accumulation, anti-apoptosis and proliferation mechanisms were glucose-independent, while insulin secretion and elements of the pERK1/2 response were glucose-dependent; an outcome that cannot be produced using a transfected cell system that lacks the capacity to respond to glucose regulation. Furthermore, each of the peptide agonists produced three distinct phases of pERK1/2; a peak at 2 min, a trough at 5 min and a prolonged sustained phase, in high glucose conditions. Based on the

literature, two phases of this ERK response (the transient peak and sustained response) may be linked to different pools of ERK that are responsible for distinct physiological functions such as insulin secretion and cell survival, respectively (Sonoda *et al.,* 2008; Quoyer *et al.,* 2010). However, in conditions of low glucose that would normally represent physiological concentrations of glucose during the fasting state, only a transient ERK phosphorylation is observed. This is consistent with the pERK1/2 profile that has been reported for CHO FlpIn cells overexpressing the GLP-1R (Koole *et al.,* 2011; Wootten *et al.,* 2013). Therefore, it appears that some elements of the GLP-1R signalling profiles identified in recombinant cells may have some relevance to what occurs in natively expressing cells, but the full effects of GLP-1R function in β-islets can only be observed in a system that displays glucose-dependence.

Assessment of the signalling profile by different peptides in low glucose conditions and high glucose conditions, through the generation of webs of bias revealed that not only are there general differences in the overall profiles of the peptides between the two glucose concentrations, but that the profile of ligand-directed signalling bias is also different in these two glucose conditions. Specifically, in low glucose, oxyntomodulin is biased compared to GLP-1 and exendin-4 in that for the same amount of cAMP it produces significantly more transient ERK (>10 fold). This bias has been reported previously in recombinant cell systems and is linked to its ability to stabilise a different subset of receptor conformations compared to the other two ligands (Koole *et al.,* 2010; Wootten *et al.,* 2013, Wootten *et al.,* 2013b).

Interestingly, in low glucose conditions, there was no significant bias between the three peptide ligands in the other pathways measured. Although there is no reported data in CHO FlpIn cells regarding proliferative and anti-apoptotic effects mediated by GLP-1R ligands, from the data available, it appears that the elements of the signalling profile of the GLP-1R in low glucose conditions that have been assessed in recombinant systems are consistent to that reported in the insulinoma cell line in low glucose conditions. Therefore information from these overexpressed systems may have some translation to endogenous physiology. While, this may not be directly relevant for endogenous GLP-1R function, as GLP-1 is only released when blood glucose levels are elevated, it is important to understand this for therapeutic development as drugs may be present during periods when blood glucose levels may not be significantly elevated.

The oxyntomodulin bias, relative to GLP-1 and exendin-4, observed in low glucose for cAMP to transient pERK1/2 was also detected in high glucose conditions, but to a lesser extent (<10-fold) that was not statistically significant. However, due to the complexity of glucose dependent

responses in the model beta cell line, there is much more information that can be extrapolated from the web of bias under high glucose conditions, compared to what we could previously identify from recombinant cell systems or by assessing the low glucose conditions. When assessing these effects in high glucose, there was no peptide-mediated ligand-directed signalling bias between cAMP and insulin responses suggesting that, as expected, there is a correlation between cAMP formation and insulin secretion. However, there was a large degree of bias observed between the ligands at the therapeutically relevant endpoints of proliferation and apoptosis that control beta cell mass. While both oxyntmodulin and exendin-4 could promote cell survival against staurosporine-induced apoptosis, for an equivalent amount of cAMP produced, these ligands were less able to promote anti-apoptotic effects compared to GLP-1. Exendin-4 was also less efficient at promoting proliferative effects (for equivalent amounts of cAMP) compared to GLP-1, while oxyntomodulin could not promote any detectable proliferation, at least under the conditions of assay. This is interesting as this data suggests that in high glucose conditions, distinct mechanisms downstream of GLP-1R activation may be driving ligand-induced cell survival pathways to those in low glucose conditions where these ligands were equivalent at promoting cAMP, proliferation and anti-apoptosis.

Sustained pERK1/2 has been linked to GLP-1-mediated cell survival (Quoyer *et al.,* 2010) and this profile of pERK1/2 was only detectable in our system in conditions of high glucose. In addition, cAMP-mediated activation of Bcl-2 and Bcl-xl via CREB has been linked to inhibition of apoptosis of beta cells (Urosova *et al.,* 2004; Quoyer *et al.,* 2010). Therefore, it may be expected that the differences in signalling bias between GLP-1, exendin-4 and oxyntomodulin in cell survival pathways would be translated to changes in the relative amounts of sustained pERK1/2 and cAMP, however, no ligand-directed signalling bias was detected between these ligands for these pathways. Therefore, for equivalent amounts of cAMP, there were similar amounts of sustained pERK1/2 produced, but less promotion of cell survival mechanisms for oxyntomodulin and exendin-4 compared to GLP-1. In addition, similar total amounts of cAMP and sustained pERK1/2 were also produced (at least with GLP-1 and exendin-4) with similar pEC_{50} and E_{max} values for these pathways. This suggests that while sustained activation of pERK1/2 and production of cAMP may contribute to cell survival mechanisms that promote enhanced beta cell mass, they may not be the most significant drivers of proliferative and anti-apoptotics effects mediated downstream of GLP-1R activation in high glucose conditions.

Identification of upstream signalling pathways that lead to agonist signal bias profiles observed in proliferation and protection against apoptosis may help to distinguish individual pathways that may

be more efficacious in promotion of β-cell survival, only in conditions of elevated glucose. This would reveal potential pathways to target therapeutically for improved profiles of potential drug candidates. It would therefore be important to extend the types of studies in this chapter to explore additional downstream pathways of GLP-1R activation that may be linked to proliferative or inhibition of apoptotic pathways. Potentially, proteins such as PKC and Akt (protein kinase B) could play a role in these cell survival mechanisms mediated by the GLP-1R as activation of these proteins have been linked to proliferation and differentiation of β-cells (Buteau *et al.,* 2001, 1999; Brun *et al.,* 2007). In addition, inhibition of β-cell apoptosis can be regulated by Akt/PKB downstream of PI-3 kinase activation though inhibition of caspases, NFkB and Foxo1 (Buteau *et al.,* 2006). The GLP-1R is known to activate PI-3 kinase, potentially through Gβγ and/or transactivation of EGRF that can result in activation of numerous downstream effectors including PKC, IRS2 and phosphorylation of Akt (protein kinase B) (Jhala *et al.,* 2003), although to date, these have not been specifically linked to proliferation and apoptosis when activated downstream of the GLP-1R.

In this chapter the signal bias profiles of Compound 2 and BETP were also assessed. Both ligands were low potency agonists for cAMP accumulation and compound 2 displayed a strong partial agonism and BETP weaker partial agonism, relative to the response of peptide agonists. This is in accordance with previous studies conducted in CHO FlpIn cells stably expressing the GLP-1R (Wootten *et al.,* 2013, Koole *et al.,* 2010). Distinct responses and weak agonism exhibited by these allosteric ligands could arguably be due to the limited number of contacts they can form with the receptor (compared to peptide ligands), but could also be due to the mode in which they activate the receptor. Both compounds bind to a region in intracellular loop 3, at the intracellular face of the GLP-1R, whereas peptide ligands interact at the extracellular face to promote activation (Nolte *et al.,* 2014). In addition to cAMP, these compounds also display weak partial agonism in insulin secretion, with BETP being a weaker agonist compared to compound 2. This may be expected, and supports previous observations that insulin secretion is linked to cAMP formation with these relative effects on insulin secretion in line with the observed pharmacology in cAMP when compound 2 and BETP are compared to one another (Drucker *et al.,* 1987; Park *et al.,* 2012). However, when compared with responses of GLP-1, in high glucose conditions, both these ligands produce significantly less insulin secretion compared to equivalent amounts of cAMP. This suggests that while there is a correlation between cAMP and insulin (cAMP is essential for insulin secretion), it is not the only element linked to insulin-secretion. It has been reported in the literature that both intracellular calcium mobilisation and β-arrestin-1 are also important for GLP-1 mediated insulin secretion (Gomez *et al.,* 2002; Sonoda *et al.,* 2008; Quoyer *et al.,* 2010). Interestingly, in

CHO FlpIn cells BETP is biased towards both of these pathways, producing significantly more calcium and β-arrestin-1 recruitment for equivalent amounts of cAMP (compared to GLP-1) (Koole *et al.*, 2010). In addition, in these recombinant cells, compound 2 is also biased towards β-arrestin1 recruitment (Willard *et al.*, 2012). This suggests that perhaps these pathways are not responsible for the observed differences the bias profile of these small molecule agonists compared to GLP-1 in the INS-1 832/3 cells. However, given that the ligand-directed signalling bias profiles of the peptide ligands differ between the two physiologically relevant glucose concentrations, it would be important to measure both calcium mobilisation and β-arrestin 1 recruitment in high and low glucose conditions in the insulinoma cells, to establish if the bias profile observed in CHO FlpIn cells translates, before further conclusions around this can be drawn. Identification of relative amounts of individual signalling pathways that could account for the observed differences in the amount of cAMP vs insulin secretion produced by the small molecule ligands vs GLP-1 may aid in identification of additional signalling pathways beyond cAMP (in addition to the relative amounts of cAMP vs other pathways), that may produce an improved therapeutic profile in terms of insulin secretion in drug development.

In contrast to differences in insulin relative to cAMP, there was significant bias in the small molecule ligands and GLP-1 responses when considering sustained pERK1/2 (relative to cAMP). pERK1/2 has been linked to both insulin secretion and beta cell survival, however, in these studies there seems to be no correlation between the amount of pERK1/2 produced and the amount of insulin secretion or the ability of these two allosteric ligands to promote cell survival (as neither compound2 or BETP could promote anti-apoptosis or proliferation in these insulinoma cells regardless of the glucose concentration). Interestingly, these ligands promote very sustained pERK1/2 responses and are stronger agonists in pERK1/2 phosphorylation than in cAMP accumulation (albeit low potency) relative to GLP-1, exhibiting similar maximal responses to those of peptide ligands. However, when the generated concentration response curves were analysed in the operational model and bias factors were assessed, no bias, relative to GLP-1 was observed, potentially due to their lower potencies in sustained pERK1/2 compared to cAMP. Therefore, although no bias was calculated, the different kinetic profiles of these ligand responses may have some relevance in terms localisation of the pERK1/2 responses versus cAMP responses produced by peptide ligands and the small molecule ligands. The location of signalling within a cell may explain some of these differences in the concentration response curve profiles of these ligands and should be explored further to assess if this could have clinical relevance. Indeed, there is already evidence that distinct pools of pERK1/2 (nuclear vs cytosolic), produced following GLP-1R activation, promote quite distinct physiological effects (Sonoda *et al.*, 2008; Quoyer *et al.*, 2010).

The results for Compound 2 and BETP also highlight that sustained pERK1/2 may not always contribute to β-cell survival as has been proposed (Subramaniam and Unsicker, 2010), as these ligands did not promote proliferation and anti-apoptotic effects. Again, this may suggest that sustained pERK1/2 may not be the driver (rather a contributor) to β-cell survival.

The bias of ligands may, in part be related to the location of their binding pocket. For example compound 2 and BETP bind intracellularly (Nolte *et al.,* 2014) and have a distinct bias to peptide ligands that bind the orthosteric binding site (Hoare, 2005). Nonetheless, peptide ligands also display bias despite binding within the same site, suggesting that distinct contacts formed between receptor and ligands within these sites can also account for biased signalling profiles.

In this chapter, the ability of compound 2 and BETP to alter orthosteric ligand signalling profiles in different glucose conditions was also assessed. Co-binding of small synthetic ligands of the GLP-1R with an orthosteric ligand has the potential to alter the signalling output from the receptor either in a pathway dependent manner, (one pathway can be enhanced while another pathway is reduced) or in a probe-dependent manner (May *et al.,* 2007). Understanding of both the probe dependent nature of allosteric modulation and the effects of this on downstream signalling bias has the potential to affect the the success/failure of allosteric drugs during clinical development. However, for these concepts to be exploited, a detailed understanding of what these allosteric ligands do to orthosteric ligand signalling profiles is required, alongside a detailed understanding of what profile of signalling is required for the best therapeutic output.

There is significant evidence from recombinant cells that both BETP and compound 2 can alter the signalling profile of GLP-1R orthosteric peptide ligands in a probe dependent manner. This has also been explored to some degree in *ex vivo* and *in vivo* assays assessing glucose-stimulated insulin secretion and cAMP (Lamont *et al.,* 2012; Sloop *et al.,* 2010). Similar to that observed in recombinant cells and primary islets, in INS1 832/3 cells, compound 2 displayed weak positive modulation of GLP-1 mediated cAMP responses that was observed in both high and low glucose conditions (Koole *et al.,* 2010; Wootten *et al.,* 2011). However, the same allosteric ligand enhanced the oxyntomodulin in both high and low glucose to a greater extent, but was unable to modulate exendin-4 cAMP response in either glucose condition. These oxyntomodulin results are consistent with those reported previously in recombinant systems with both compound 2 and BETP (Koole *et al.,* 2010; Wootten *et al.,* 2013) and in primary β-islets with BETP (Willard *et al.,* 2012). In addition, as expected based on previous studies (Willard *et al.,* 2012; Wootten *et al.,* 2013), glucose-stimulated insulin secretion mediated by oxyntomodulin, was positively modulated by

compound 2, however there was no modulation observed on GLP-1 responses by this allosteric ligand. Unexpectedly, there was a small degree of positive modulation with exendin-4, albeit very weak. The literature reports that GLP-1R-mediated formation of cAMP is essential for glucose-mediated insulin secretion (Drucket *et al.,* 1987; Doyle and Egan 2007). This would be supported by the oxyntomodulin data, whereby compound 2 positively potentiates both cAMP and insulin secretion in conditions of high glucose. There is also support for this from the interaction studies performed here using the other allosteric ligand, BETP. In this case, there was no enhancement of GLP-1 or exendin-4-mediated cAMP (in low or high glucose) or glucose-stimulated insulin secretion. Nonetheless, both cAMP and insulin secretion were positively modulated when BETP was co-added to the cells with oxyntomodulin. Whereas for BETP there was a similar degree of potentiation of both oxyntomodulin mediated cAMP and insulin secretion, a greater potentiation of insulin secretion compared to cAMP (33-fold and 20-fold, respectively) was observed with compound 2. Like the small molecule biased signalling profile for these two pathways, this also suggests that while cAMP enhancement has the potential to lead to enhance glucose-stimulated insulin secretion, other pathways may also be important. This is supported by the data on interaction of compound 2 with GLP-1 and exendin-4; compound 2 can enhance both insulin and cAMP mediated by oxyntomodulin, but for exendin-4 there was weak insulin enhancement with no effect on cAMP whereas for GLP-1, there was weak cAMP enhancement with no modulation on insulin secretion response.

Currently, based on the data in this thesis, it is still not clear what the most important pathways to be modulated are. As mentioned above, calcium signalling, β-arrestin-1 and sustained pERK1/2 have been reported in the literature to have a role in insulin secretion (Sonoda *et al.,* 2008; Gromada *et al.,* 1998). Therefore these additional pathways (along with others yet to be identified) may modulate the level of insulin secretion beyond that of cAMP itself. Modulating just one of these pathways may be sufficient, or it may require a combination. Currently, there is not enough information in these studies to speculate further on this, however data from recombinant cells suggests that both Compound 2 and BETP can enhance β-arrestin 1 signalling by all peptide ligands (Wootten *et al.,* 2012). If this is translatable to the INS1 cells in high glucose, then this would suggest that modulation of β-arrestin-1 recruitment does not always promote enhanced insulin secretion, as no modulation of insulin secretion was observed for GLP-1 by compound 2. In addition, BETP can also promote enhanced calcium signalling by exendin-4, but not GLP-1 (Koole *et al.,* 2010), however no insulin secretion was seen in this study with this orthosteric-allosteric ligand combination.

It is also unclear from these studies, how much of the ERK1/2 measured using a global assay of pERK1/2 contributes to insulin secretion responses. The literature reports that transient pERK1/2 responses contribute to insulin secretion. Our studies may support this to some extent as both exendin-4 and oxyntmodulin transient pERK1/2 responses were positively enhanced (17 and 10-fold respectively), however in this pathway exendin-4 displays greater potentiation than oxyntomodulin, whereas in insulin secretion oxyntomodulin is enhanced to a greater degree than exendin-4. As oxyntomodulin responses are also enhanced in cAMP, this may indicate interplay between transient pERK1/2 and cAMP for generation of greater levels of insulin secretion. Interaction studies using BETP revealed that transient pERK1/2 responses for all peptide ligands are enhanced in high glucose conditions, however only very weakly (7-8 fold). In the case of insulin secretion, only oxyntomodulin was modulated by BETP, however to a slightly weaker extent than observed with compound 2, but with greater cAMP modulation. This could therefore also support the involvement of both cAMP and transient pERK1/2 in enhancing insulin secretion. Therefore based on this, we could speculate that allosteric drug design where ligands enhance both transient pERK1/2 and cAMP may provide a better therapeutic profile than enhancement of one of these pathways alone.

Assessment of allosteric modulation of sustained pERK1/2 responses that have been proposed in the literature to have a protective role leading to enhanced β cell mass (Wootten *et al.,* 2013) by compound 2 and BETP revealed some positive modulation of the peptide ligand responses in high glucose conditions, although none reached statistical significance. Oxyntomodulin responses were weakly enhanced by approximately 10-fold by compound 2, but not BETP, whereas the opposite profile was observed with GLP-1 (a 10-fold potentiation with BETP, but no effect with compound 2). Within this study, endpoints of β cell survival were not assessed. As sustained pERK1/2 has been linked to cell survival effects previously, it is difficult to interpret these results in terms of their physiological relevance with the current dataset. It would be interesting to explore the allosteric effects on orthosteric ligands in proliferation and anti-apoptotic studies to observe if there is a link between modulation of sustained pERK1/2 and cell survival mechanisms that may lead to enhanced β cell mass.

In addition to modulation of cAMP and pERK1/2 responses in high glucose, modulation of these pathways with the different peptides occurs in low glucose conditions, however the nature of the modulation was not necessarily consistent. cAMP profiles were almost identical in low glucose with strong positive modulation of oxyntomodulin-mediated cAMP by both BETP and compound 2. However, for transient and sustained pERK1/2, different profiles were observed in low compared

to high glucose conditions. In transient pERK1/2, only oxyntomodulin responses were enhanced by compound 2, whereas all three peptide responses were strongly enhanced by BETP. For sustained pERK1/2 responses, no significant modulation was seen with either compound 2 or BETP, although there was a trend towards weak modulation with BETP of all three peptide responses. While most studies *in vivo* and *ex vivo* in physiological systems explore the effect of drugs on physiological outputs (such as insulin secretion and β cell survival), very little work has been completed in vivo in low glucose conditions. Therefore, it is difficult to speculate on the relevance of the INS-1 832/3 cell results physiologically. However, it is important to try to understand these effects for allosteric drug development. If used alone as drugs, these effects may not be relevant, as physiological ligands such as GLP-1 and oxyntomodulin are secreted in the presence of high glucose. However, if used in combination with another drug (for example, exendin-4), then it is important to understand what these drugs do in the presence of normal physiological glucose concentrations, not just in conditions of elevated blood glucose.

In this chapter we also identified, an unexpected pERK1/2 profile from peptide ligands, where, at the 5 min time point, they inhibited the pERK1/2 response of 11 mM glucose in a concentration-dependent manner. Nonethless, while compound 2 was unable to alter this effect, BETP was able to enhance the pEC50 of the inverse agonism response of all three peptide ligands. This has not been reported before in the literature and may have some clinical relevance and should be explored further.

In conclusion, pharmacological and allosteric effects observed in response to ligands are distinct in different glucose concentrations in insulinoma cells, which may have physiological relevance. In addition, while some information on signalling bias translates from a recombinant cell system to low glucose conditions in INS1 832/3 cells, additional information can be gained from assessing effects at two relevant glucose conditions. Therefore, the use of a more physiological system that displays glucose dependence has more relevance for understanding normal physiology and for potential translation to pathophysiological conditions. In addition, we observed that the probe-dependent nature of allosteric ligands translates from our recombinant systems for the primary acute pathway, cAMP (Koole *et al.*, 2010; Wootten *et al.*, 2013), but not for pathways such as pERK1/2 that have a much more complex response profile to that observed in recombinant cells. In addition, effects on insulin can only be detected in a physiological system that displays glucose dependence. Thus, this chapter has identified additional information to what was previously known around biased ligands and allosteric modulation that have the ability to sculpt cellular signalling profiles. With the information gained some hypothesis can be drawn around the relative importance of some

of the pathways we have assessed, but there is a lot of work still to do to obtain enough information to be able to exploit these complicated concepts therapeutically for the GLP-1R, including validation of results in primary islets of mouse and human origin. In addition, while the work presented here explores biased signalling and allostery to try to understand elements of GLP-1R signalling in β-islets, for many therapeutically important effects of GLP-1R activation, including modulation of appetite, delayed gastric emptying, cardio-protective and neuroprotective effects, the underlying GLP-1R mediated signalling pathways are unknown and this requires further exploration. From the results presented in this chapter, it could be predicted that the GLP-1R may display distinct signal bias profiles depending on its location in the body, and therefore to therapeutically target the GLP-1R for numerous diseases such as for diabetes, obesity, neuroprotection and cardiovascular disease may require an understanding of the importance of signalling and signal bias for its protective effects different across tissues, such as the pancreas, brain and heart.

CHAPTER 5: GLOBAL ANALYSIS OF SIGNALLING BIAS AT GLP-1R

5.1 INTRODUCTION

GLP-1R activation caused by various orthosterically binding peptides such as GLP-1, oxyntomodulin and exendin-4 (used in the current study) stimulates insulin release in the postprandial state, inhibits glucagon release and slows the rate of gastric emptying, along with acid secretion (Doyle and Egan, 2007). In addition to these well-known functions, it has been related to the maintenance of β-cell mass by promoting islet cell neogenesis and inhibiting β-cell apoptosis (Gaddy *et al.,* 2010; Boutant *et al.,* 2012; Hui *et al.,* 2003; Farilla *et al.,* 2002). GLP-1R-dependent differentiation of pancreatic precursor cells into mature β-cells has also been proposed (Hui *et al.,* 2001; Hui *et al.,* 2010). Although oxyntomodulin and GLP-1 are co-secreted in response to nutrient load, oxyntomodulin possess the abilty to activate to both the glucagon receptor and the GLP-1R. Data in the literature suggests that treatment of human islets with exogenous GLP-1 could improve function and survival of pancreatic islets (Farilla *et al.,* 2002; Mancuso *et al.,* 2006), thus attracting interest in developing and/or finding a better GLP-1 analogue for the type 2 diabetes. Exendin-4 is one of the long acting GLP-1 analogues that was identified and is used clinically for the management/treatment of type 2 diabetes.

GLP-1R peptide agonists have been demonstrated to exhibit signalling bias (Koole *et al*., 2010, Wootten *et al.,* 2013, Chapter 4), a phenomenon whereby these agonists differentially activate cellular signalling pathways. The implication is that these peptides may elicit differential physiological responses as a consequence of this observed signal bias. Although there is considerable published data on the molecular pathways contributing to the pleiotropic effects of GLP-1R agonists on pancreatic β-cells, it is not clear which, or to what extent, each of the GLP-1R stimulated pathways contributes to the various physiological outcomes. Furthermore, there may be a number of as yet unidentified pathways leading to both physiological and adverse effects associated with GLP-1R therapeutics. This chapter describes a global analysis approach to study GLP-1R dependent effects in the model insulinoma cell line INS-1 832/3 used in chapters 3 and 4.

The last 20 years has seen significant developments in a variety of global approaches to help understand cell biology including a variety of proteomic and transcriptomic approaches. In terms of transcriptomic approaches, the longest established is that of oligonucleotide array technology. Microarrays have been very useful in providing an overall view of gene expression changes between two or more biological conditions (Croze, 2010) and have the ability to explore many diverse stimuli and to build up extensive maps of expression profiles, the identification of biomarkers or development of prognostic signatures for many diseases (Song *et al.,* 2012; Wood *et*

al., 2014; Eizirik *et al.,* 2012; Akeno *et al.,* 2011). By using this technology, expression of nearly 8,000 genes in rat and human islet cells has been determined (Eizirik *et al.,* 2008; Ortis *et al.,* 2010; Gurzov *et al.,* 2011). This technology however, has some limitations; (Wang *et al.,* 2009): (i) it depends on existing knowledge about genome sequences and hence does not identify novel mRNA transcript that are absent from databases, (ii) it has high background that occurs mainly due to cross or non-specific hybridization; (iii) its detection range is limited by background on the lower side and by saturation on the upper one; (iv) gene expression is measured indirectly in that scanned intensity of fluorescent hybridized probes occurs through a process that may require complex normalization. This can limit the ability to compare across different experiments. Altogether this makes the technique a valuable resource but with room for improvement. RNA-Seq (transcriptomics) replaces the hybridization of nucleotide probes with sequencing individual cDNAs produced from the target RNA. (Ledford, 2008; Gevaert and De Moor, 2009; Hurd and Nelson, 2009) and thus is considered a better approach.

Transcriptomics can be defined as the complete set of transcripts in a cell and their quantity in a specific developmental stage or physiological condition (Wang *et al.,* 2009). Transcriptomics aims to (i) catalogue all species of RNA, both coding and non-coding; (ii) determine the transcriptional structure of genes in terms of their start sites, 5' and 3' ends, splicing patterns and other post-transcriptional modifications and (iii) quantify the changing expression levels of each of these during development or under different conditions (Wang *et al.,* 2009). As such, it can overcome many of the limitations of microarrays. In addition, unlike microarrays, the RNA-seq method has high reproducibility, sensitivity and capability of capturing splicing variants. However, a principal concern with RNA based profiling is RNA degradation, thus a careful handling of tissue/assessment of RNA integrity via bioanalyzer-based assessment is required (Hatiz *et al.,* 2011).

In RNA-seq (total or messenger) the RNA population is converted to a library of cDNA fragments with adaptors attached to one or both the ends (Wang *et al.,* 2009; Head *et al.,* 2014). Each library, with or without amplification, is then sequenced to obtain short sequence reads from one end (single-end sequencing) or both ends (paired-end sequencing). The read sequences are typically 30-400 bp in length, depending on the sequencing platform: illumina, Roche 454 or SOLiD system. Following sequencing, the resulting reads are either aligned to a reference genome or transcripts, or assembled de novo without the genomic sequence (Wang *et al.,* 2009). Owing to the high depth of gene coverage, RNA-seq produces a more accurate measurement of the level of transcripts and their isoforms than other available tools (Zheng and Wang, 2008).

Against this background, this chapter describes RNA-Seq analysis of transcripts from INS-1 832/3 cells. A time-dependent profile (30 min, 2 h, 6 h and 24 h) of transcriptome alteration/regulation was studied in response to GLP-1 in the presence of 11 mM glucose, while early (30 min) and late (24 h) phase time-points were chosen to examine oxyntomodulin and exendin-4 relative to GLP-1. The data produced showed a good consistency amongst different samples sequenced and allowed us to (i) describe the kinetic profile of the complete INS-1 832/3 cell transcriptome in response to GLP-1, including splice variants, thus providing a novel and valuable resource for future genetic and functional studies; (ii) explore/investigate various factors/genes/signalling networks associated with glucoregulatory, proliferation and survival effects mediated by GLP-1R activation on model pancreatic islets and (iii) show that many early (30 min) and late (24 h) genes were differentially expressed/regulated in the presence of different GLP-1R peptide ligands. From these data sets, future experiments have been designed to validate some of the key findings obtained through RNA-seq by other methods such as real time RT-qPCR in independent samples of INS-1 832/3 cells. In addition, this work has enabled the identification of technical challenges associated with the experimental design (biological replication; mapping to the reference genome; read count, sequence depth) of the RNA-seq data prior to planning and executing a RNA-seq experiment.

5.2 METHODS

This section describes methods that were specific to this chapter of the thesis and were not covered in the main materials and methods section. Methods such as insulin secretion were covered previously in the main materials and methods section (Chapter 2).

5.2.1 Incubation of INS-1 832/3 cells with GLP-1R peptides and insulin detection

INS-1 832/3 cells were seeded at a density of 7 x 10^5 cells/well/3 ml in 6-well cell culture plates for approximately 72 h. Cells were washed twice with EBSS buffer (1.5 mL/well/wash), pH 7.4 and starved for 2 h in serum free RPMI-1640 supplemented with 2.8 mM glucose. Subsequently, cells were stimulated for 30 min, 2 h, 6 h or 24 h in the presence of 100 nM GLP-1 prepared in RPMI-1640 supplemented with 0.1% w/v BSA and 11 mM glucose. Furthermore, the cells were incubated for 30 min and 24 h with 11 mM glucose alone (vehicle control) or saturating concentrations of exendin-4 (100 nM) or oxyntomodulin (1 µM) prepared in RPMI 1640 supplemented with 0.1% w/v BSA and high (11 mM) glucose

Saturating concentrations of the peptide ligands was defined as the concentration of peptide required to saturate the dose response curve and this was obtained by performing cell based assays in INS-1 832/3 cells (Chapter 4). Moreover, the objective of using the maximal concentration was

to ensure that ligands provided their maximal activity enhancing the probability of observing changes in the transcriptome.

Following these incubation periods, the supernatants were collected and stored at -80 °C until ready for insulin detection (see Chapter 2: Materials and methods) to ensure that the cells responded in the expected manner. Subsequently, the cells were harvested and the cell pellet snap frozen on dry ice and transferred to -80 °C until ready for RNA extraction. For treatments of longer duration than 2 h, (6 h and 24 h), two insulin samples were collected, one after 2 h of stimulation and a second prior to harvesting the cells for RNA extraction. All supernatants from cells that exhibited glucose-stimulated insulin secretion (GSIS) (vehicle control) and augmentation of GSIS in response to GLP-1R peptides were further processed for RNA extraction.

5.2.2. RNA extraction

Total RNA was isolated using the RNeasy Mini Kit (Qiagen, Venlo, The Netherlands) according to manufacturer's instructions. The protocol favours purification of all RNA molecules longer than 200 nucleotides. This kit combines the selective binding properties of a silica-based membrane with the speed of microspin technology. A specialized high-salt buffer system allows up to 100 µg of RNA longer than 200 bases to bind to the RNeasy silica membrane. Biological samples are first lysed and homogenized in the presence of a highly denaturing guanidine-thiocyanate–containing buffer, which immediately inactivates RNases to ensure purification of intact RNA. Ethanol is added to provide appropriate binding conditions, and the sample is then applied to an RNeasy Mini spin column, where the total RNA binds to the membrane and contaminants are efficiently washed away. High-quality RNA is then eluted in water.

The cells were disrupted by brief vortexing and adding appropriate volume of Buffer RLT (350µl). The lysate was homogenized and pipetted directly into a QIAshredder spin column placed in a 2 ml collection tube, and centrifuged for 2 min at ≥8,000 x g. One volume of 70% v/v ethanol was added to the homogenized lysate, and mixed well by pipetting. Up to 700 µl of the sample was transferred, including any precipitate that formed, to an RNeasy spin column placed in a 2 ml collection tube (supplied by the manufacturer). Columns were centrifuged for 15 s at ≥8000 x g (≥10,000 rpm). The flow-through was discarded, buffer RW1 (700 µl) was added and the column centrifuged for 15 s at ≥8000 x g (≥10,000 rpm) to wash the spin column membrane. The flow-through was discarded and 500 µl of Buffer RPE was added, followed by centrifugation for 15 s at ≥8000 x g (≥10,000 rpm), and the flow-through was discarded. A 500 µl Buffer RPE was added and the column was centrifuged again for 2 min at ≥8000 x g (≥10,000 rpm) to wash the spin column membrane. The

RNeasy spin column was placed in a new 2 ml collection tube (supplied), and centrifuged at full speed (15 s at ≥8000 x g) for 1 min. The RNeasy spin column was placed in a new 1.5 ml collection tube. Finally, 15 µl RNase-free water was added directly to the spin column membrane and centrifuged for 1 min at ≥8000 x g (≥10,000 rpm). Eluted RNA was stored at -80°C until required.

The RNA quality assessment indicating the amount and quality of the samples was performed using both a NanoDrop spectrophotometer (Monash University) and a Bioanalyzer (Facility in WEHI, Melbourne).

Using the nanodrop, quantity and quality assessment using spectrometric analysis was performed at multiple wavelengths 260 nm, 280 nm and 230 nm. The quantity, quality and purity can be verified on basis of the optical density (OD) at 260 nm, the ratio of the OD at 260/280 nm and the OD at 260/230 nm respectively. An OD 260/280 ratio greater than 1.8 is usually considered an acceptable indicator of good RNA quality (Sambrook *et al.,* 1989; Manchester, 1996). By the presence of genomic DNA the OD 260 measurement can be compromised resulting in the over-estimation of the actual and real RNA concentration.

Using the bioanalyzer, electrophoretical separation of RNA is performed using an RNA ladder as an indicator of molecular weight / length. Integrity of the RNA may be assessed by visualization of the 18S and 28S ribosomal RNA bands. An elevated threshold baseline and a decreased 28S:18S ratio, both are indicative of degradation (Mueller *et al.,* 2004). Conventionally, the proportion of the ribosomal bands (28S/18S) with a ratio of > 1.8 corresponds to a high quality intact RNA. Another checkpoint of quality includes RNA Integrity Number (RIN, developed by Agilent Technologies) (Mueller *et al.,* 2004). This tool is based on a neuronal network that determines the RIN from the shape of the curve in the electropherogram. The software and the algorithm classifies total RNA on a numbering system from 1 to 10, with 1 being the most degraded profile and 10 being the most intact thus facilitating the interpretation of an electropherogram (Mueller *et al.,* 2004; Imbeaud *et al.,* 2005).

5.2.3 Sample preparation for RNA-sequencing and outsourcing to BGI for transcriptomics

Because of the constraints related to the cost of the RNA-seq, single samples were assessed for insulin secretion and quality of extracted RNA for each treatment at each timepoint. To reduce contribution of biological/experimental variation to the analysis, RNA-seq was performed on pooled samples. On the basis of results from the quality analysis and insulin response, the samples from individual treatments (n=3, performed in triplicate) were pooled to a sample concentration of

65 ng/µl; total RNA quantity of 5 µg and sample purity indicated by OD260/280 = 1.8~2.2, OD260/230 ≥2.0 and RIN ≥ 7.0. Ten total RNA samples were sent to BGI-Hong Kong Company Ltd. (provider) for transcriptome sequencing using Illumina HiSeq2000 next generation sequencing (NGS) technology. The provider agreed to deliver 4 Gb clean data per sample, along with bioinformatics analysis performed on the sequencing data.

5.2.4 RNA-Sequencing (Transcriptomics): BGI-Hong Kong Co. Ltd.

5.2.4.1 Sample background information and description

The information related to the sample treatments is contained in Table 5.1. The samples were named based on the treatment performed and was abbreviated as in Table 5.2. At this point onwards, the abbreviated names contained in this table will be used in reference to the corresponding treatment.

5.2.4.2 Library generation

RNA-seq is a method of transcriptome analysis that consists of sequencing a cDNA library by high throughput next generation sequencing (NGS). The number of reads aligning to a specific gene sequence is proportional to the abundance of that gene in the sample from which the cDNA library was prepared. The library was generated by BGI that would be compatible with illuminaHiSeq 2000 sequencing platform. A target insert size of 200 bp was selected to perform paired-end sequencing, to generate read lengths of 2 x 91 bp.

5.2.4.3 Data processing/analysis and bioinformatics (BGI-Hong Kong Co. Ltd.)

Data processing included data filtering and standard bioinformatic analysis (sequencing assessment). The rat reference genome sequence (ftp://ftp.ensembl.org/pub/release-69/fasta/rattus_norvegicus/dna/Rattus_norvegicus.RGSC3.4.69.dna.toplevel.fa.gz) was used to perform the bioinformatics analysis. Data filtering included removing adaptors and low-quality reads from the raw reads. The bioinformatics analysis service provided assessment of sequencing (alignment statistics, randomness assessment of sequencing, and distribution of reads on the reference genome), gene expression and annotation (gene coverage and coverage depth).

Table 5.1. Treatment groups assessed in the transcriptomic analysis. Outlined in the table the treatment groups chosen for transcriptomic analysis are represented in the following table using the symbol +. Those treatments excluded (due to cost limitations) are highlighted using the symbol -. All treatments performed were in 11mM glucose.

Treatment duration	**GLP-1R peptide treatment (all treatments in 11mM glucose)**			
	Vehicle (Untreated)	**GLP-1**	**Exendin-4**	**Oxyntomodulin**
30 min	+	+	+	+
2 h	-	+	-	-
6 h	-	+	-	-
24 h	+	+	+	+

Table 5.2. Abbreviated names of all treatment groups. Highlighted are the treatment groups and duration and the abbreviated name given to the various sample groups, that will be used throughout the remainder of this chapter.

No.	Sample Name	Sample Name (Abbreviation)
1	Untreated 30 min (11mM glucose alone)	U_30
2	GLP-1 30 min (in 11mM glucose)	G_30
3	Exendin-4 30 min (in 11mM glucose)	Ex_30
4	Oxyntomodulin 30 min (in 11mM glucose)	Ox_30
5	GLP-1 2 h (in 11mM glucose)	G_2
6	GLP-1 6 h (in 11mM glucose)	G_6
7	Untreated 24 h (11mM glucose alone)	U_24
8	GLP-1 24 h (in 11mM glucose)	G_24
9	Exendin-4 24 h (in 11mM glucose)	Ex_24
10	Oxyntomodulin 24 h (in 11mM glucose)	Ox_24

5.2.4.3.1 Raw sequence data and quality control

Raw sequence data generated from the transcriptomics experiments was transferred into sequence data via base calling, which is defined as raw data or raw reads and saved as FASTQ file. The quality control process was performed by using several software packages. Base composition and quality along with filtering of raw reads were used as criteria to detect which data was included. In addition, filtering of raw data was needed to decrease data noise. “Dirty” raw reads, defined as reads that contained the sequence of adapter and/or high content of unknown bases were filtered out. After filtering, the remaining reads ("clean reads") was used for downstream bioinformatics analysis.

5.2.4.3.2 Alignment/mapping of reads to reference genes

Clean reads were mapped to a reference sequence using SOAPaligner/SOAP2 (soap.genomics.org.cn). No more than 5 mismatches were allowed in the alignment. Mapping was performed to the reference rat genome (ftp://ftp.ensembl.org/pub/release69/fasta/rattus_norvegicus/dna/Rattus_norvegicus. RGSC 3.4.69.dna.toplevel.fa.gz). Proportion of clean reads mapped back to the genome provides an overall assessment of the sequencing. Distribution of reads located on the genes was used to evaluate the randomness. Since, the reference genes have different lengths, the read location on each gene was standardized to a relative position (calculated as the ratio between read location on the gene and the gene length), and then the number of reads in each relative position was counted. If the randomness was good, this indicated an even distribution of reads. Furthermore, gene coverage was calculated as the percentage of a gene covered by reads. This value is equal to the ratio of the base number in a gene covered by unique mapping reads to the total base number of coding region in that gene.

5.2.4.3.3 Gene expression

The gene expression level is calculated by using the RPKM method (Reads per kilobase transcriptome per million mapped reads) (Mortazavi et al., 2008), and the formula is shown as follows:

$$RPKM = \frac{10^6\, C}{NL/10^3}$$

Given to be the expression of gene A,

C = number of reads that are uniquely aligned to gene A,

N = total number of reads that are uniquely aligned to all genes, and

L = number of bases on gene A.

The RPKM method is able to eliminate the influence of different gene length and sequencing discrepancy on the calculation of gene expression. Therefore, the calculated gene expression can be directly used for comparing the difference of gene expression among samples.

5.2.4.4 Screening of differentially expressed genes (DEGs)

The screening of differentially expressed genes was based on a pairwise comparison. The samples considered for the pairwise comparison and their relationship (control or treatment) has been specified in Table 5.3. A strict algorithm was developed based on the significance of digital gene expression profiles (Audic and Claverie, 1997) and used to identify differentially expressed genes between two samples. The method used is described as follow: Denote the number of unambiguous clean tags (which means reads in RNA_Seq) from gene A as x, given every gene's expression occupies only a small part of the library, x yields to the Poisson distribution:

$$p(x) = \frac{e^{-\lambda}\lambda^{x}}{x!} \quad (\lambda \text{ is the real transcript of the gene})$$

While identifying differential regulation in between two different genes the following formula was applied. Considering, the total clean tag number of sample 1 is N_1, and total clean tag number of sample 2 is N_2; gene A holds x tags in sample 1 and y tags in sample 2. The probability of gene A being expressed equally between two samples can be calculated with

$$2\sum_{i=0}^{i=y} p\left(\frac{i}{x}\right)$$

Or,

$$2 * (1 - \sum_{i=0}^{i=y} p\left(\frac{i}{x}\right) \ (if \sum_{i=0}^{i=y} p\left(\frac{i}{x}\right) > 0.5$$

$$p\left(\frac{y}{x}\right) = \left(\frac{N_2}{N_1}\right)^{y} \frac{(x+y)!}{x!\,y!\left(1+\frac{N_2}{N_1}\right)^{(x+y+l)}}$$

Table 5.3. List of treatment groups compared in a pairwise comparison. 18 different pairwise comparisons were performed. Listed in the table is each of these along with the treatment groups compared.

Comparison	Treatment groups compared		Comparison	Treatment groups compared	
1	U_30	G_30	**10**	U_24	G_24
2	U_30	Ex_30	**11**	U_24	Ex_24
3	U_30	Ox_30	**12**	U_24	Ox_24
4	U_30	U_24	**13**	G_24	Ex_24
5	U_30	G_2	**14**	G_24	Ox_24
6	U_30	G_6	**15**	Ex_24	Ox_24
7	G_30	Ex_30	**16**	U_30	G_24
8	G_30	Ox_30	**17**	U_30	Ex_24
9	Ex_30	Ox_30	**18**	U_30	Ox_24

The p-value corresponds to the differential gene expression test. Since DEG analysis generates large multiplicity problems in which thousands of hypotheses (is gene x differentially expressed between the two groups) are tested simultaneously, correction for false positive (type I errors) and false negative (type II) errors are performed using the Benjamini and Yekutieli, 2001 false discovery rate (FDR) method. Assume that we have picked out R differentially expressed genes in which S genes really show differential expression and the other V genes are false positive. If we decide that the error ratio "Q = V / R" must stay below a cutoff (e.g. 5%), we should preset the FDR to a number no larger than 0.05 (see Benjamini and Yekutieli, 2001 for details). We have used FDR ≤ 0.001 (Benjamini and Yekutieli, 2001) and the absolute value of Log_2 ratio ≥ 1 as the threshold to judge the significance of gene expression difference. More stringent criteria with smaller FDR and bigger fold-change value can be used to identify DEGs.

This analysis identifies genes with different expression levels among samples.

5.2.4.5 Advanced analysis

Based on the expression profile of genes, further advanced analysis was performed on these comparisons. The latest version of related databases including KEGG, NR and Gene Ontology were used for the analysis. However, for the present study only the gene expression and annotation and gene differential analysis was considered and assessed further. Limiting to these analyses allows the objectives of investigating various signalling mechanisms mediated by the activation of GLP-1R and identification of differentially regulated genes/networks associated with activation of the GLP-1R by different orthosteric binding peptides to be accomplished.

5.2.4.6 Data delivery

Data delivery was done through BGI's FTP site (amount of data >80G).

5.2.5 Ingenuity pathway analysis software

IPA is a web-based software application that was applied for the analysis, integration, and interpretation of data derived from RNA sequencing. Powerful analysis and search tools associated with this software helped in uncovering the significance of data and identifying/speculating new targets within the context of biological systems. The Core analysis in IPA was performed on significantly and differentially regulated genes in each of our comparisons to identify relationships, mechanisms, functions, and pathways relevant to the uploaded dataset. A cut-off of minimum two-fold change in expression (Log_2 fold change ≥ 1, $P < 0.05$) was set up to identify differentially expressed genes.

5.2.5.1 Downstream effects analysis: Functional hierarchy

Downstream effects analysis performed using IPA enables quick visualization of biological trends in the experimental data set and predicts the effect of gene expression changes in the data set on biological processes and disease or on toxicological functions. A color-coded heatmap illustrates and explores the function hierarchy in the Ingenuity® Knowledge Base (e.g. Figure 5.3 in results section of this chapter). Downstream effects analysis is based on the expected causal effects between genes and functions. The expected causal effects are derived from the literature compiled in the Ingenuity® Knowledge Base. The analysis examines genes in uploaded (experimental) datasets that are known to affect functions, compares the genes' direction of change to expectations derived from the literature, and then issues a prediction for each function based on the direction of change. The direction of change is the gene expression in the experimental samples relative to a control. If the direction of change is (i) consistent with the literature for activation of that function across most genes, IPA predicts that the function will increase in the experimental sample (orange); (ii) mostly inconsistent with the literature for activation of that function, IPA predicts that the function will decrease in the experimental sample (blue); (iii) if there is no clear pattern related to the literature, IPA does not make a prediction (grey). IPA uses the z-score algorithm to make predictions. The z-score algorithm is designed to reduce the chance that random data will generate significant predictions. The p-value of overlap is calculated by the Fisher's Exact Test and p-values < 0.05 (-log = 1.3) indicate a statistically significant, non-random association.

5.2.5.2 Canonical signalling

The Canonical Pathways application of IPA displays the most significantly affected canonical pathways across the entire dataset, and across multiple datasets while reviewing a comparison analysis on the uploaded experimental data sets. The significance value for the canonical pathways is calculated by Fisher's exact test, right-tailed. The significance indicates the probability of association of molecules from the experimental dataset with the canonical pathway by random chance alone. By default, IPA applies a -log (p-value) cutoff of 1.3 ($p < 0.05$).

5.2.5.3 Calculation of z-score

The primary purpose of the activation z-score is to infer the activation states of predicted biological functions, canonical pathways and transcriptional regulators. The basis for inference are relationships in the molecular network that represent experimentally observed gene expression or transcription events, and are associated with a literature-derived regulation direction, which can be either activating or inhibiting. For each of those regulated genes we can make a prediction about the activation state.

The z-score is a statistical approach where, by defining a quantity, we can determine whether a biological function, a pathway or an upstream transcription regulator, has significantly more "increased/activated" predictions than "decreased/inhibited" predictions (z>0) or vice versa (z<0). Here, significance means that we reject the hypothesis that predictions are random with equal probability. The distribution underlying this null hypothesis is defined by a random variable:

$$x_i \epsilon \{-1,1\}$$

Where, +1 corresponds to an "increased/activated" state predictions and -1 to a "decreased/inhibited' state and both values are chosen with probability 1/2. Index iruns from 1 to N with N being the number of genes affecting the function or regulated by the regulator. Let

$$x = \sum_i x_i = N_+ - N_-$$

Where $N_{+/-}$ are the numbers of "increased/activated" or decreased/inhibited predictions and $N_+ + N_- = N$. The variance of x_i is $\sigma^2 = 1$, so the variance of x is given by:

$$\sigma^2_x = N\sigma^2 = N$$

And the z-score statistic (with mean equal to zero and variance equal to 1) is defined by:

$$z = \frac{x}{\sigma_x} = \frac{\sum_i x_i}{\sqrt{N}} = \frac{N_+ - N_-}{\sqrt{N}}$$

Since z is approximately normally distributed with zero mean and standard deviation of one under the null hypothesis, it can be used to assess statistical significance of the observed number of "increased/activated" and "decreased/inhibited" predictions. If the absolute value of the z-score calculated from those numbers is large (i.e. falls into the "tail" of the Gaussian distribution) it would be unlikely to occur by chance. Moreover, the sign of the calculated z-score will reflect the overall predicted activation state of the regulator (<0: inhibited/decreased, >0: activated/increased). In practice, z-scores greater than 2 or smaller than -2 are considered significant.

So far it has been assumed that a direction of regulation (either activating or inhibiting) can be unambiguously assigned to an edge/relation. This is not always the case because generally a single

edge/relation is associated with a number of findings that represent experimental observations reported in the literature. Since these observations have not necessarily been obtained under the same experimental conditions but could represent different contexts (e.g. organism, tissue, cell line, or more complex situations) it is not surprising that the direction of regulation can be different for different findings underlying the same edge. Ideally only findings that are applicable to the experimental context at hand (i.e. the biological context in which the data was observed) should be considered, however since this context is unknown, the approach taken puts less weight on edges/relation with fewer findings or ambiguous direction of regulation (a larger weight would in principle make it more likely that the given direction of regulation is applicable to the context at hand). Let $M_{activating}$ be the number of activating findings underlying a relationship, and $M_{inhibiting}$ be the number of inhibiting findings. Then we define the weight of the edge leading to the ith gene (index i runs from 1 to N being the number of genes regulated by the regulator as:

$$w_i = \frac{|M_{activating} - M_{inhibiting}|}{M_{activating} + M_{inhibiting} + 1}$$

$$x = \sum_i w_i x_i$$

$$\sigma^2_x = \sum_i w_i^2$$

and the z-score statistic used by IPA to compute activation is given by

$$z = \frac{x}{\sigma_x} = \frac{\sum_i w_i x_i}{\sqrt{\sum_i w_i^2}}$$

5.2.5.4 Calculation of p-value or overlap p-value used to identify significantly altered function of pathway regulation.

The p-value associated with a biological process or pathway annotation is a measure of its statistical significance with respect to the functions/pathways/lists of eligible molecules for the experimental dataset and a reference set of molecules (which define the molecules that could possibly have been functions/pathways/lists eligible). p-value calculation is based on hypergeometric distribution that calculates probabilities without replacement, thus reflecting the constraint that a particular molecule can appear in a given set only once. The p-value is calculated with the right-tailed Fisher's Exact Test. The p-value for a given function is calculated by considering the (i) number of functions/pathways/lists eligible molecules that participate in that annotation as defined by the molecules in the selected reference set; (ii) total number of molecules in the selected reference set

known to be associated with that function; (iii) total number of functions/pathways/lists eligible molecules in the selected reference set; (iv) total number of molecules in the reference set; and (v) the reference set selected. In the right-tailed Fisher's Exact Test, only over-represented functions or pathways that have more functions/pathways/lists of eligible molecules than expected by chance are significant. Under-represented functions or pathways ('left-tailed' p-values), which have significantly fewer molecules than expected by chance are not shown. While the number of functions/pathways/lists eligible molecules associated with a given function/pathway is an important measure when calculating the p-value for functional analyses, the p-value does not only depend on this number. The smaller the p-value, the less likely the association is random and the more significant the association. In general, p-values less than 0.05 indicate a statistically significant, non-random association.

For calculating the p-value for global functional analysis and canonical pathways, a 2X2 contingency table can be considered (Table 5.4).

The probability of observing an individual combination according to Fisher is:

$$P = \frac{(row_1!\, row_2!\, col_1!\, col_2!)}{(N!\, n_{11}!\, N_{12}!\, N_{21}!\, N_{22}!)}$$

Using this formula, we can calculate a table containing all the possible combinations of N_{11}, N_{12}, N_{21}, and N_{22} with the same row and column sums. Because the row and column sums remain fixed, it turns out that the only number that can be freely chosen is N_{11}. The p-value corresponding to a particular occurrence of N_{11} is the sum of all probabilities associated with overlaps (subnetwork and annotation genes) greater than or equal to N_{11}.

A corrected p-value calculation can be performed to identify the most significant results in IPA's functional, canonical pathway, my pathway and list analyses. This calculation returns corrected p-values based on the Benjamini Hochberg method of accounting for multiple testing, and enables to control of the error rate in analysis results and allows focus in on the most significant biological functions associated with genes of interest. This corrected p-value can be interpreted as an upper bound for the expected fraction of false positives. Furthermore, the purpose of the overlap p-value is to identify transcriptional regulators/canonical pathways that are able to explain observed gene expression changes. The overlap p-value measures whether there is a statistically significant overlap

Table 5.4. Contigency table formulation. The 2X2 contingency table used for calculating p-values for global functional analysis, where the frequency of molecules are represented as N_{11}, N_{12}, N_{21}, and N_{22} and the marginal totals represented by Row_1, Row_2, Col_1, Col_2 and N.

	Focus molecules	**Non-focus molecules**	**Row totals**
Molecules associated with a function	N_{11}	N_{12}	Row_1
Molecule not associated with a function	N_{21}	N_{22}	Row_2
Column totals	Col_1	Col_2	N

between the dataset genes and the genes that are regulated in a pathway or by upstream regulators. It is calculated using Fisher's Exact Test, and significance is generally attributed to p-values < 0.01.

5.2.6 Validation of RNA-seq data using RT-qPCR array

To follow up and validate the alteration of gene expression by GLP-1R peptide agonists observed by RNA-Seq analysis a real time qPCR array was designed. 384-well RT-qPCR array was custom designed where 192 genes were selected based on the analysis of RNA-Seq data and arranged on the array plates in duplicate. Gene array plates were produced by (Bioharbor, USA).

5.3 RESULTS

5.3.1 Sample treatments and GSIS

Insulin detection was performed on the supernatants of INS-1 832/3 cells treated for 2 h with the GLP-1R peptides, GLP-1, exendin-4 and oxyntomodulin to confirm that this physiologically relevant pathway was activated prior to extracting RNA for sequencing. Glucose-dependent insulin secretion was observed with INS-1 832/3 cells that was further potentiated in the presence of the three GLP-1R peptides. No effect of peptides was observed on insulin secretion in low glucose conditions (2.8 mM glucose) (Figure 5.1). Insulin was also detected from supernatants in the 30 min treatment groups, and at 2 h for the treatment groups that were stimulated for 6 h and 24 h.

These revealed that all treatments displayed GSIS

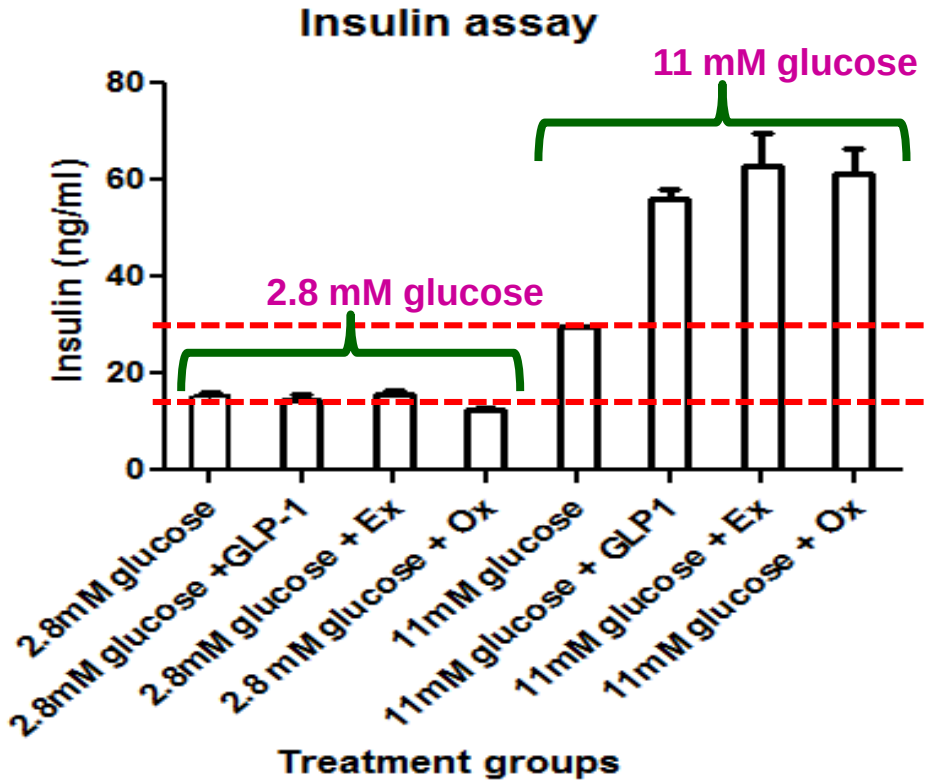

Figure 5.1: Insulin secretion assay from supernatents of cells treated for RNA extraction. Glucose-dependent insulin secretion was detected from supernatents of cells treated for 2 hours with either 2.8 mM glucose or 11 mM glucose in the absence and presence of either 100 nMGLP-1, 100 nM exendin-4 or 1µM oxyntomodulin, prior to RNA extraction for sequencing. All values are mean + SEM of three experiments conducted in triplicate.

5.3.2 RNA quantity and quality assessment

The quantity and quality of all RNA samples extracted following cell treatments was assessed using both the NanoDrop as well as Tape Station 2200 (Bioanalyser) .All the samples had a RIN of > 9 and both OD ratio's (260/280 and 260/230) were >2.0, which are indicators of good RNA quality and integrity (Appendix 3, Figure S5.1; Appendix 4, Table S5.1). However, the ribosomal ratio (28S/18S) of some samples was variable with a range from 1.4 to 2.1 (Appendix 4, Table S5.1). A conventionally accepted value of >1.8 is normally used. The lower numbers can be attributed to the 28S/18S evaluation process whereby the values are compromised by the fact that their calculation is based on area measurements and therefore heavily dependent on definition of start and end points of peaks. Moreover, due to the lack of reliability, it cannot be used as a gold standard for assessing RNA integrity (Watson, 2014). Since, RIN is considered as a reliable and widely acceptable tool for RNA quality control and all samples had a high RIN, the transcriptome study was pursued using these samples.

5.3.3 Sequencing assessment: Sequence quality

5.3.3.1 Pre-alignment quality assessment

The pre-alignment quality control was used to determine the mapping potential of the raw reads. This was done by assessing base composition (nucleotide distribution) (Appendix 3, Figure S5.2) and distribution along the reads (Appendix 3, Figure S5.3).

5.3.3.1.1 Distribution of base sequence content/composition

A balanced base composition percentage is considered when the A (adenosine nucleotide) curve overlaps with the T (thymidine nucleotide) curve and the G (guanidine nucleotide) curve overlaps with the C (cytosine nucleotide) curve as opposed to an unbalanced base composition percentage, where the curves are not in accordance with their complementary bases when they unqualified for mapping. This can also be used to check the nucleotide composition bias. All samples showed overlapping of complementary curves, thus representing balanced composition (Appendix 3, Figure S5.2).

5.3.3.1.2 Quality distribution of bases

For the assessment of base quality, a good quality sequence is represented by a base quality score > 20. The bases in each sample used for the study showed a good quality score on the heatmaps. Each dot in the heat map represents the quality value of the corresponding position along reads (Appendix 3, Figure S5.3). All the samples sent for RNA sequencing to BGI-Hong Kong Co. Ltd.

demonstrated good quality of raw reads and were pursued further for mapping to the reference genome/gene

5.3.3.2 Post-alignment quality assessment

After performing pre-alignment quality checks, the raw data was filtered for dirty reads that included removing reads with adaptors, reads with >5% unknown bases and low quality reads (base sequence quality < 10). Clean reads were mapped to the reference sequence using SOAPaligner/SOAP2 (soap.genomics.org.cn). The standards were set with an allowable limit of no more than 5bp mismatches in the alignment. The post-alignment quality control was assessed in terms of read alignment (sequenced, mapped and unmapped reads) (Tables S5.2 and S5.3), reads distribution on the reference gene (Appendix 3, Figure S5.4), reads distribution on the reference genome (Appendix 3, Figure S5.5) and gene coverage (Appendix 3, Figure S5.6).

5.3.3.2.1 Alignment statistics to genes within the reference genome

The clean reads were mapped to mapped genes within the reference genome and the alignment statistics are presented in Appendix 4, Table S5.2 - S5.5, where total reads refers to the total number of sequencing reads; total base pairs represents the total number of base pairs; total mapped reads depicts the reads that aligned to the reference sequence and its percentage and total unmapped reads indicates reads that could not be aligned to the reference sequence. The total mapped reads were further sub-divided into 4 ranks that included perfect match (Rank 1), referring to no mismatches observed in total mapped reads, ≤ 5bp mismatch (Rank 2) indicating that the mismatch number was less than 5bp in the total mapped reads, unique match (Rank 3) represents reads aligned to only one position in the total mapped reads and lastly multi-position match (Rank 4) showing reads that aligned to two or more positions in the total mapped reads.

The basic read metrics revealed that more than 70% of the total reads for all the samples in the study aligned to genes in the reference genome, leaving <30% of reads that did not map to genes. Moreover, in all samples, approximately 50% of the total reads were ranked as perfect match, > 65% as unique matches and only 20% of the reads representing mismatch of ≤ 5bp (Appendix 4, Table S5.2 and S5.3)

5.3.3.2.2 Distributions of reads on genes within the reference genome

The distribution of the reads located on mapped genes within the reference genome was used to evaluate randomness. Since reference genes have different lengths, the read location on each gene was standardized to a relative position (which was calculated as the ratio between read location on

the gene and the gene length), and then the number of reads in each relative position was counted. All samples showed that the reads were evenly distributed on the reference genes depicting a good randomness (Appendix 3, Figure S5.4) and therefore, all samples were pursued further for downstream analysis.

5.3.3.2.3 Alignment statistics to reference genome

Alignment tools report a few standard values, including the number of matches, mismatches, insertions and deletions in a mapping. These statistics together provide a direct measure of how well a read is aligned to a position in the reference genome. Alignment stats revealed that about 80% of the total reads for all the samples in the study aligned to the reference genome with ~20% of reads unmapped. Furthermore, >50% of the total reads were ranked as perfect match and ~75% as unique matches. However, some of the reads represented a mismatch of ≤ 5bp (< 25%) (Appendix 4, Table S5.4 and S5.5).

The percent of reads aligned vary in different datasets as well as from reported study to study because the alignment sensitivity is determined by sequencing quality and the parameter setting of each alignment tool (Li *et al.,* 2009). Even the best mapping algorithms cannot align all reads to the reference genome, probably due to sequencing errors, structural rearrangements or insertions in the query genome, or deletions in the reference. Moreover, analyses of unmapped reads can be used for the identification of structural variants and non-reference insertions (Hatem *et al.,* 2013; Mijuskovic *et al.,* 2012). However, the percentages of aligned read depth can vary from 60% to 90% and can also fluctuate depending on the sample source (humans or cell lines) (Mortazavi *et al.,* 2008; Djebali *et al.,* 2012; Lunter and Goodson, 2011). Consequently, it is important to assess the uniformity of coverage, which in our study is consistent across samples as shown by the alignment stats.

5.3.3.2.4 Distributions of reads on reference genome

This analysis gives the distribution of reads on Chromosome 1 and location of reads including exon, intron and intergenic region. The reads of each sample used in the study mapped to the chromosome 1 and displayed uniform coverage and sequence depth. The alignment was computed across the genome and those alignment scores were log transformed (base 2) to better visualize the full range of data (Appendix 3, Figure S5.5).

5.3.3.2.5 Gene coverage

Gene coverage is calculated as the percentage of a gene covered by reads. This value is equal to the ratio of the base number in a gene covered by unique mapping reads to the total base number of coding region in that gene. Different colours in the pie chart (Appendix 3, Figure S5.6) represent proportions of genes with different levels of coverage. In each sample used for the RNA-seq study, ~60% genes had coverage between 90-100%, followed by ~10% genes that had coverage between 80-90% and <5% genes had coverage in other ranges specifically below 60%. Thus, different quality checks performed for each sample used in the transcriptome study assured uniformity and consistency in terms of handling, processing and sequencing of the samples both at pre- and post-alignment phases. This provides confidence in the analysis that would be performed from hereon (appendix 3, Figure S5.6).

5.3.4 Global and differential genes expression (DGE) analysis performed by BGI

Gene expression levels were expressed as RPKM. The threshold to judge the significance of gene expression differences when comparing two samples was set to a FDR ≤ 0.001 and absolute value of Log_2 ratio ≥1 (greater than a 2-fold change between samples).

5.3.4.1 Genes differentially regulated by glucose alone

Chronic treatment (24 h) of the cells in the presence of high glucose (11 mM) alone resulted in a significant differential expression of 948 genes, relative to acute exposure to 11mM glucose (30 min). Amongst these 948 genes, 534 genes were upregulated and 414 genes were down regulated (Figure 5.2 A, D).

5.3.4.2 Global analysis of kinetics of gene regulation in response to GLP-1 compared to acute glucose treatment alone (30 min)

A high number of statistically significant differentially expressed genes (DEGs) were detected after 24 h (713 genes; 317 genes upregulated and 396 genes downregulated) treatment of INS-1 832/3 cells with 100 nM GLP-1 in high glucose conditions. While this number is lower than that for glucose treatment alone there were 107 non-overlapping DEGs when treatment with glucose alone compared with treatment with glucose and 100 nM GLP-1 (green colour in stacked bar graph 5.2(A) and bar graph 5.2(C)). At earlier times in the GLP-1 time course smaller numbers of DEG's were identified compared to the 30 min glucose alone treatment, with 174 genes regulated at 30 min (126 genes upregulated and 48 genes downregulated), 579 genes at 2 h (330 upregulated and 249 down regulated) and 218 genes at 6 h (138 genes upregulated and 80 genes downregulated) (Figure 5.2 A).

As the GLP-1 time course gene regulation profiles all compared to 30 min glucose alone treatment, figure 5.2 A actually displays a composite profile due to the GLP-1 effects of GLP-1R activation and combined effects by glucose stimulation. The exception to this is the the 30 min time point where all are effects from GLP-1 alone as glucose effects have been omitted from these due to the comparison to the 30 min glucose alone treatment. Genes only regulated by GLP-1 alone can also be assessed at 24 h as a glucose alone control was also generated for this timepoint. These non-overlapping genes (and therefore regulated by GLP-1, not glucose) can be inferred from the stacked bar graph in Figure 5.2 (A and B) and in Figure 5.2 D (24 h GLP-1R peptide treatments relative to 24 h glucose control).

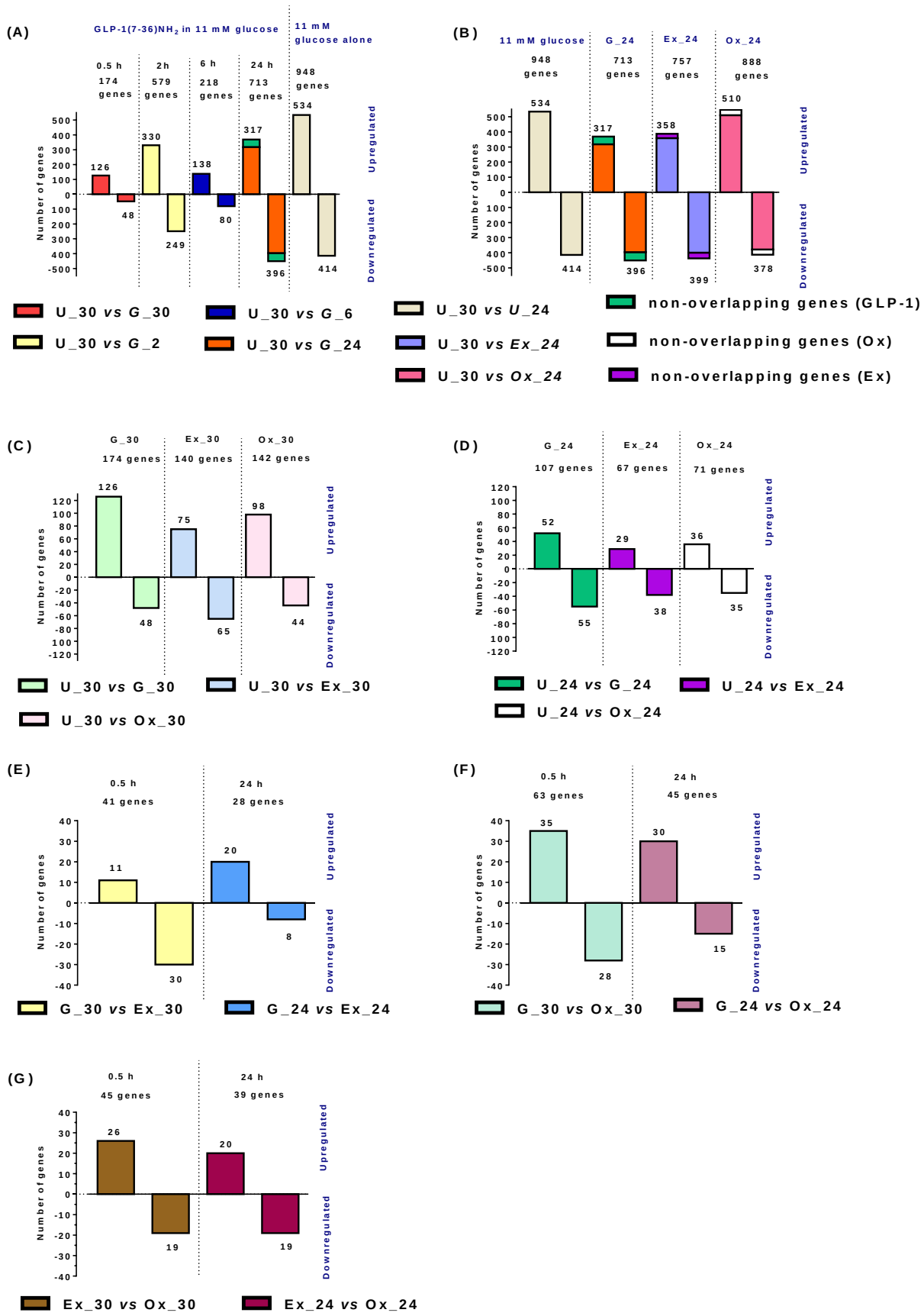

Figure 5.2: Significantly regulated genes in response to GLP-1R peptide agonists at varying time points. (A) time-dependent regulation of transcriptome in response to 100 nM GLP-1 in the

presence of 11 mM glucose compared to 11 mM glucose alone at 30 min (U_30) or glucose alone over the 24h period (last 2 bars). Non-overlapping DEGs (between 11 mM glucose and GLP-1 in 11mM glucose) are shown for the 24 h time point in green of the stacked bars; (B) differential gene expression in response to 24 h exposure to either 11mM glucose or different GLP-1R peptides in 11mM glucose compared to control (11 mM glucose, U_30). Non-overlapping DEGs in the top colour of the stacked bars; (C) differential gene expression at 30 min exposure of GLP-1R peptides (100 nM GLP-1, 100 nM exendin-4 or 1 µM oxyntomodulin) in 11mM glucose compared to vehicle control (11 mM glucose alone (U_30)); (D) differential gene expression following 24 h exposure to GLP-1R peptides compared to 11 mM glucose alone at 24 h; (E)) differential gene expression by exendin-4 (Ex_30 and Ex_24 respectively), relative to 100 nM GLP-1 (G_30 and G_24) following 30 min and 24 h treatment in 11mM glucose; (F) differential gene expression in response 1 µM oxyntomodulin (Ox_30 and Ox_24 respectively), relative to 100 nM GLP-1 (G_30 and G_24) for 30 min or 24 h in 11mM glucose (G) differential gene expression by 1 µM oxyntomodulin (Ox_30 and Ox_24), compared to 100 nM exendin-4 (Ex_30 and Ex_24) treated for 30 min and 24 h in high glucose. The gene regulation observed was statistically significant (FDR ≤ 0.001 and absolute value of Log_2 ratio ≥ 1.

As glucose alone treatments were omitted for the 2 h and 6 h time point due to cost constraints, the number of genes regulated specifically by GLP-1 at these timepoints cannot be assessed. Thus, to maintain uniformity in data analysis all the treatment groups were compared to a common vehicle control (30 min glucose treatment). Ideally, a vehicle control corresponding to each time-point should have been assessed. This would aid in presentation of actual number of genes regulated by the peptide itself at that particular time. Thus, a real estimate of differentially regulated genes in response to GLP-1 can be provided only for 30 min and 24 h. This revealed that GLP-1 in high glucose statistically up/downregulated 174 genes when measured at 30 min (126 up, 48 down) and 107 genes when measured at 24 h (52 up, 55 down) when compared to their relevant glucose only control (Figures 5.2C-D).

To clarify ligand dependent DEGs at the 2 h time point, where a large number of total genes were upregulated by coaddition of glucose and GLP-1, a pilot RNA-sequencing study was planned that consisted of vehicle, 100 nM GLP-1 and 100 nM exendin-4 treatment, all performed in both low (2.8 mM) and high (11 mM) glucose. Due to time constraints this experiment was not completed, but is actively being pursued by other members of the laboratory.

5.3.4.3 Global analysis of differentially regulated genes in response to acute treatment with GLP-1R peptides (30 min)

174 genes were up/downregulated when exposed to 100 nM GLP-1 treatment for 30 min compared to glucose alone at the same time point. 100 nM exendin-4 resulted in up/downregulation of 140 genes, whereas 1 µM oxyntomodulin changed the expression profiles of 142 genes compared to vehicle control at 30 min. Of these, 75 and 98 genes were upregulated in response to exendin-4 and oxyntomodulin respectively, and 65 and 44 genes were down regulated in response to exendin-4 and oxyntomodulin respectively (Figure 5.2 C).

Differential expression analysis between different peptide treatment groups were also performed at 30 min. This comparison provides further evidence for ligand-directed signalling bias, providing a gene fingerprint for differential effects of these ligands and may, in part, explain some mechanisms that underlie the signalling bias and pleiotropic effects mediated by GLP-1R that have been observed in both recombinant studies and in particular chapter 4 of this thesis.

Comparisons between GLP-1 and exendin-4 revealed differential expression profiles for 41 genes at the 30 min timepoint (11 upregulated and 30 downregulated in exendin-4 treatment vs GLP-1) (Figure 5.2 E). When comparing GLP-1 treatment with equimolar concentrations of

oxyntomodulin, 63 genes were differentially regulated at 30 min by the two peptides (35 upregulated and 28 downregulated in oxyntomodulin treated samples compared to those treated with GLP-1) (Figure 5.2 F). In addition, comparison of oxyntomodulin with equimolar concentrations of exendin-4 revealed differential expression of 45 genes at the 30 min treatment time between the two ligands. From this 26 genes were upregulated and 19 genes downregulated in oxyntomodulin treatment compared to equipotent concentrations of exendin-4 (Figure 5.2 G).

5.3.4.4 Global analysis of differentially regulated genes in response to chronic GLP-1R peptide treatment compared to 24 h treatment with glucose alone

Long term exposure of insulinoma cells to 100 nM GLP-1 in high glucose resulted in altered expression levels of 107 genes (52 genes up-regulated and 55 genes down regulated) when compared to glucose alone treatment at the same time point. In addition, 24 h treatment with either 100 nM exendin-4 or 1 µM oxyntomodulin in high glucose altered the expression levels of 67 (29 up-regulated and 38 down regulated) genes and 71 (36 up-regulated and 35 genes down regulated) genes, relative to the 11 mM glucose alone control at 24 h post treatment (Figure 5.2 C).

Exposure of cells for 24 h to different GLP-1R peptides revealed ligand induced signalling bias at the gene level. When comparing GLP-1 and exendin-4, there were 28 genes that displayed differential gene expression (20 upregulated and 8 downwregulated in exendin-4 compared to GLP-1) (Figure 5.2 C). Oxyntomodulin differentially regulated 45 genes (30 up-regulated and 15 downregulated) compared to equimolar concentrations of GLP-1 treatment (Figure 5. 2F), whereas 39 genes (24 up-regulated and 19 down regulated) genes were differentially regulated by oxyntomodulin compared to 100 nM exendin-4 (Figure 5.2 G).

5.3.4.5 Equal expression of glucagon receptors and GLP-1Rs in INS-1 832/3 cells and oxyntomdoulin responses.

This transcriptomic study revealed that INS-1 832/3 cells express similar levels of mRNA encoding glucagon and GLP-1 receptors. Since oxyntomodulin is an agonist for both the glucagon receptor and the GLP-1R, it is speculated that some of the gene expression changes observed with oxyntomodulin may be a result of activation of both receptors. Nonetheless, the affinity of oxyntomodulin, K_B (pK_B), at the glucagon receptor is reported to be lower, 8.27 (5.30 nM) (Baldissera *et al.,* 1988; Gros *et al.,* 1993; Baggio *et al.,* 2004) than the GLP-1R, affinity reported to be 7.53 (29.51 nM) in FlpIn CHO cells stably expressing GLP-1R (Koole *et al.,* 2010).

To define oxyntomodulin dependent GLP-1R mediated gene expression changes, these studies would need to be performed in a glucagon receptor knock down model or specific antagonism would be required. This is limitation in the design of the experimental dataset and as such this requires additional work to really understand which receptor is responsible for the observed gene expression changes. While this information is of interest, further analysis at this point was only pursued for GLP-1 and exendin-4 treatment groups.

5.3.5 Functional bioinformatics analysis of regulated genes

5.3.5.1 Investigation of time-dependent GLP-1 induced transcriptome alteration in INS-1 832/3 cells through IPA analysis

Downstream effects were analysed for functional hierarchical clustering of genes. Figure 5.3 represents the complete description of the heat map displaying the gene expression changes observed in response to GLP-1 exposure in high glucose for 2 h (compared to U30). The squares in the heatmap are divided into three hierarchical levels (i) Level 1: High-level functional category (for example, cell death and survival) (Figure 5.3 A); (ii) Level 2: Mid-level functional category (for example, survival) (Figure 5.3 B) and (iii) Level 3: Specific functions that are significantly represented in the data (for example, cell survival) (Figure 5.3C). At Level 3, the evidence for effects tool enables visualization of the genes in the uploaded experimental dataset, their direction of change and the literature evidence of their effect on a disease or function. Furthermore, the colour and size of the squares in the heatmap reflects the z-score, the negative log p-value, or the number of genes, depending upon the option chosen while performing data analysis. Heat maps considered and presented in this chapter display the colour of squares by their z-score and their size by the negative log p-value. The colour reflects the direction of change for the function, based on the regulation z-score. Orange indicates a positive z-score indicating that the biological process or disease is trending towards an increase. Z-scores ≥ 2 indicate that the function is statistically significantly increased. Blue reflects a negative z-score thus predicting that the biological process or disease is trending towards a decrease. Z-scores ≤ -2 indicate that the function is statistically significantly decreased. The intensity of the colours indicates the prediction strength. The square size reflects the magnitude of the associated negative log of the calculated p-value (larger square for larger magnitude). P-values < 0.05 (negative log = 1.3) have been taken as statistically significant, non-random association. The categories with the largest p-values are displayed on the left side of the heatmap (Figure 5.3).

Functional cluster analysis of regulated genes in response to 100 nM GLP-1 treatment in high glucose conditions at 30 min (G_30), 2 h (G_2), 6 h (G_6) and 24 h (G_24) compared to 11 mM glucose treatment at 30 min (U_30) is presented as heat maps (Figure 5.4). In addition, the functional clustering of genes regulated by 11 mM glucose alone between the 30 min and 24 h are also presented in this format. These illustrate a diversified pattern of gene regulation at different time points following simultaneous treatment of GLP-1 with 11mM glucose or glucose alone that relate mutually to the global analysis (Figure 5.2 A). However, visualization of these heat maps only enables qualitative analysis of the data due to difficulties comparing two functional clusters simultaneously. This is attributed to the way the heat maps are laid out by the software where the categories with the most significant p-values are displayed on the left side of the heat map and this tends to alter with the treatment. Consequently, high-level functional categories change positions.

In order to make further analysis and statistically relevant comparisons, the hierarchical analysis was adapted to a table (Table 5.5). However, a vast number of functional clusters appeared post-analysis, as such the focus was directed to clusters of genes that could account for GLP-1R mediated effects on pancreatic β-islets function and survival, along with the categories that could potentially suggest therapeutic potential as well as side-effects potentially mediated by GLP-1R peptides in the clinic (especially for type 2 diabetes and obesity).

The hierarchical analysis displayed a significant modulation of 75, 460, 164 and 563 genes, after 30 min, 2 h, 6 h and 24 h treatment with GLP-1 and high glucose respectively, which were widely spread across various functional clusters comprising of bio-functions and diseases. Two of the most relevant and significantly enriched bio-functions (metabolism of carbohydrates and lipids (p-value ranging from 1.86×10^{-14} to 1.15×10^{-02} over time) and cellular growth and proliferation (p-value ranging from 1.88×10^{-07} - 1.25×10^{-02} over time) are presented as examples (Table 5.5) amongst the multitude of gene assemblages represented in the heat maps (Figure 5.4).

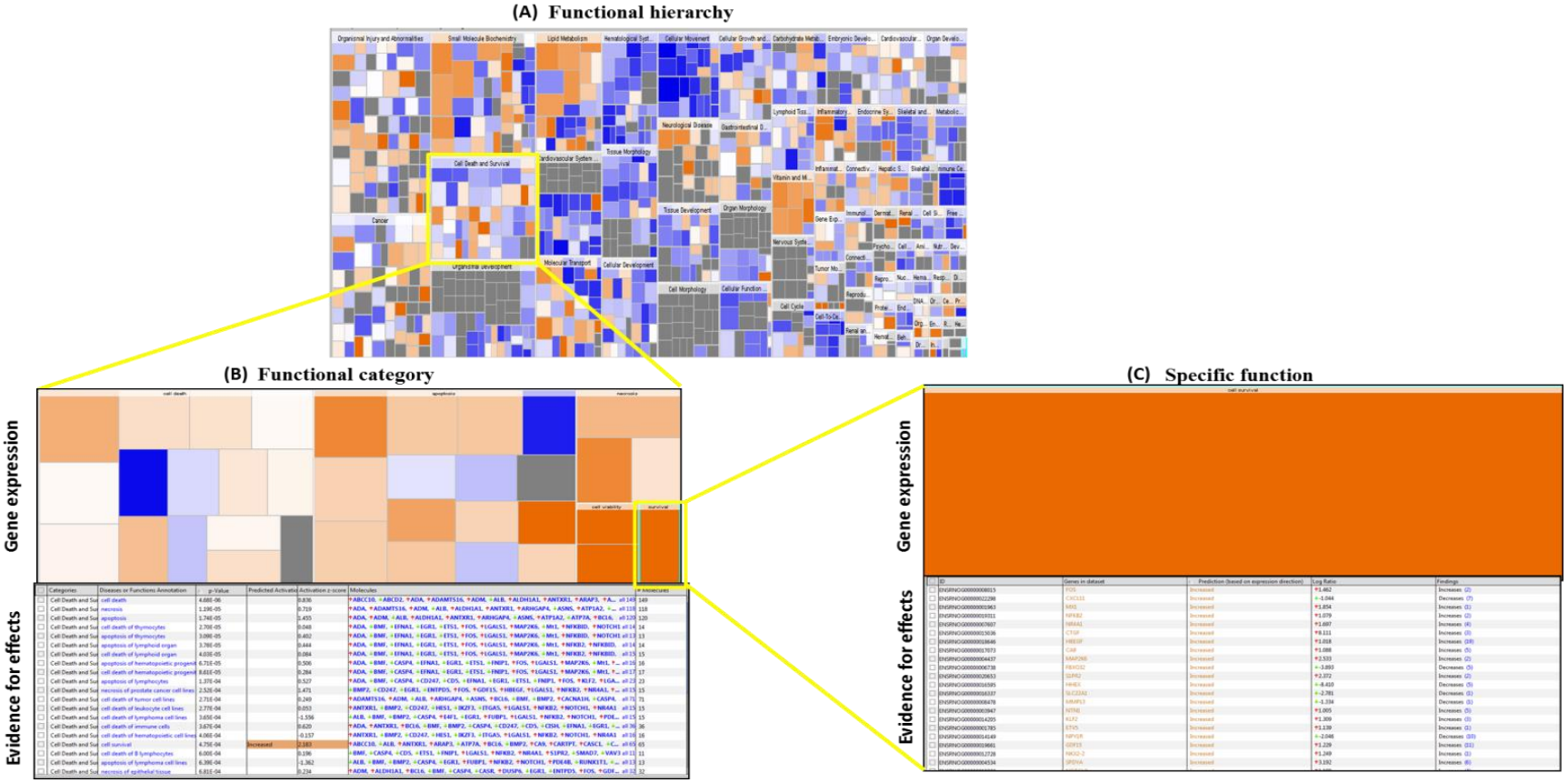

Figure 5.3: Description of functional hierarchical clustering as illustrated using an example. The heat map shows the expression of significantly regulated and differentially expressed genes after treatment with 100 nM GLP-1 for 2 h relative to acute treatment with vehicle control (glucose only treatment for 30 min, U_30). The squares in the heat map are divided into three hierarchical levels. (A) Level 1 refers to high-level functional category, example cell death and survival as highlighted in yellow Square; (B) Level 2 refers to mid-level functional category, example survival as highlighted in yellow square; (C) Level 3 represents specific functions (example cell survival) that that are significantly represented in the data. Evidence for effect window displays the related genes and their predicted effects on the function. The colour code of the heat map is based on z-score and reflects the direction of change; orange predicts that biological process/disease is trending towards increase, blue indicates trend towards a decrease, while grey represents to the

cluster where software was unable to predict the direction of change and white represents the clusters predicted by IPA but not present in the uploaded dataset. Intensity of colour indicates the prediction strength. Z-scores ≥ 2 indicate that the function is statistically significantly increased. Z-scores ≤ -2 indicate that the function is statistically significantly decreased. Size of the rectangle represents p-value. Larger squares indicate more significant overlap between the genes perturbed in the dataset and the function or disease. p-values< 0.05 ($-\log = 1.3$) indicate a statistically significant, non-random association.

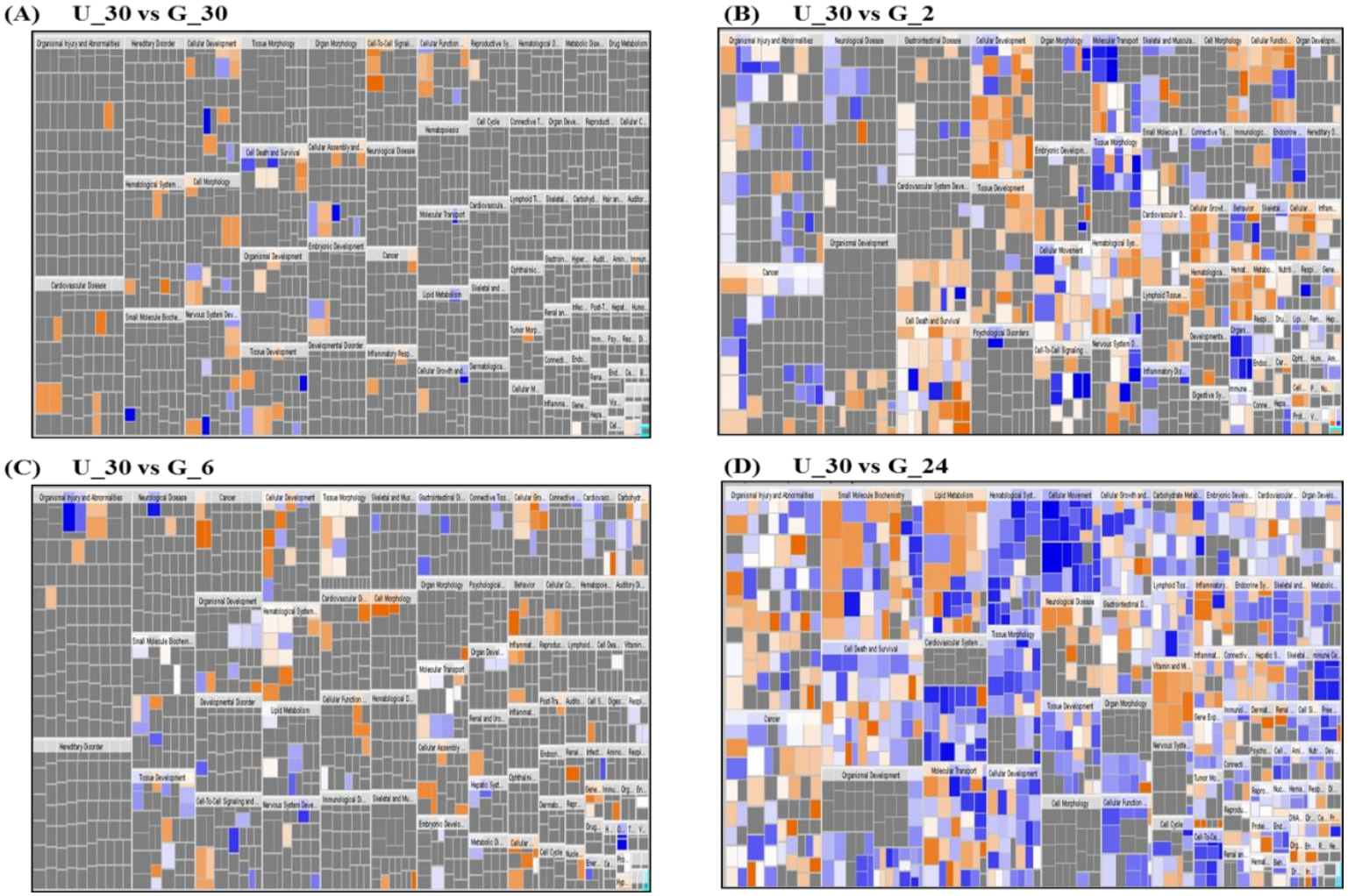

Figure 5.4: Hierarchical functional clustering analysis for gene expression changes in response to 100 nM GLP-1. The heat map shows the kinetic profile of significantly and differentially expressed genes after time-dependent treatment with GLP-1 relative to acute treatment with vehicle control (glucose only treatment for 30 min, U_30). (A) 30 min post-treatment with GLP-1 in 11mM glucose; G_30; (B) 2 h post-treatment with GLP-1; G_2; (C) 6 h post-

treatment with GLP-1; G_6; (D) 24 h post-treatment with GLP-1; G_24. All results were reported relative to 30 min vehicle control supplemented with 11 mM glucose, U_30. The orange predicts that biological process /disease is trending towards increase, blue indicates trend towards a decrease, while grey represents clusters where software was unable to predict the direction of change. White represents clusters predicted by IPA but not present in the uploaded dataset. Intensity of colour indicates the prediction strength. Size of the rectangle represents p-value. Z-scores ≥ 2 (orange), z-scores ≤ -2 (blue) and p-values < 0.05 indicate a statistically significant functionality.

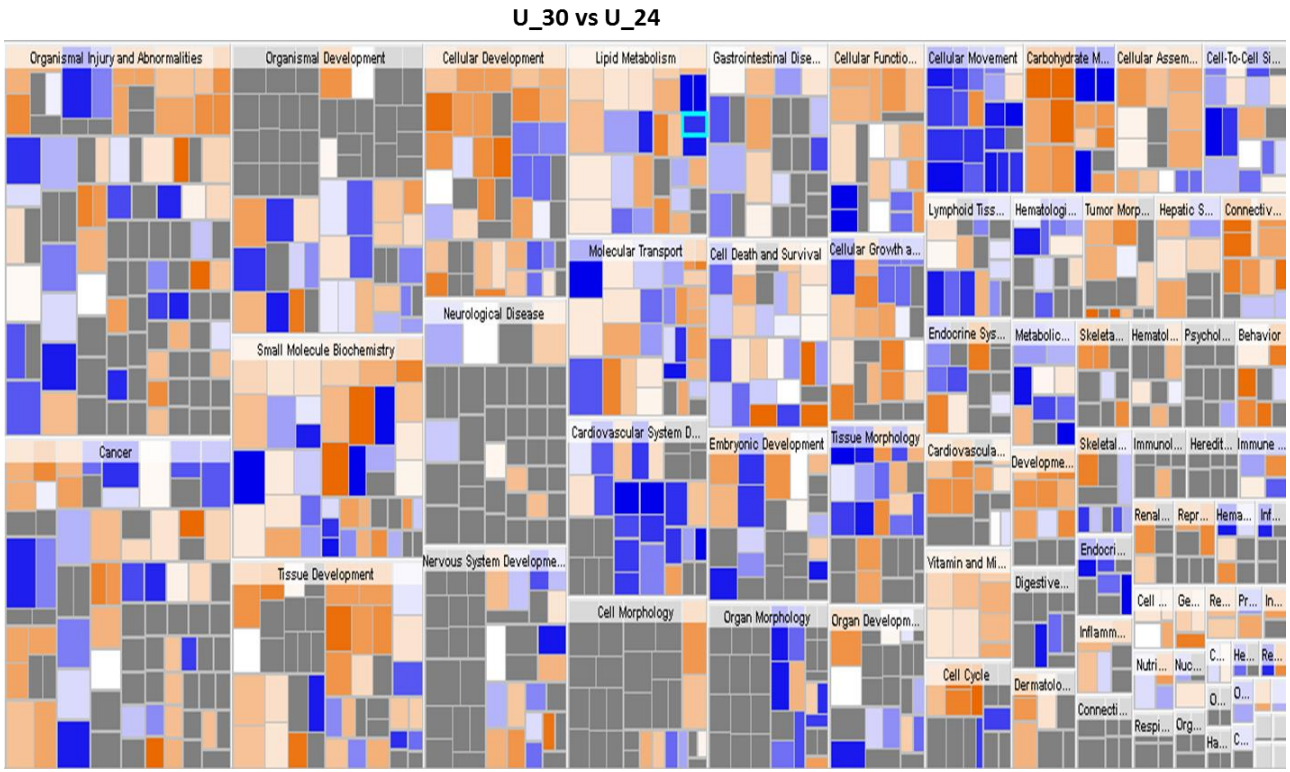

Figure 5.5: Hierarchical functional clustering in response to 11mM glucose over a 24 h period. The heat map shows the significantly and differentially expressed genes after 24 h treatment with 11 mM glucose (U_24) relative to 30 min glucose treatment (U_30). The orange colour predicts that biological process /disease is trending towards increase, blue indicates a trend towards a decrease, while grey represents clusters where the software was unable to predict the direction of change, and white represents the clusters predicted by IPA but not present in the uploaded dataset. Intensity of colour indicates the prediction strength. Size of the rectangle represents p-value. Z-scores ≥ 2 (orange), z-scores ≤ -2 (blue) and p-values < 0.05 indicate a statistically significant functionality.

Similarly, to understand the regulatory elements contributing to the management of diabetes in patients (therapeutic outcomes associated with GLP-1R activation), as well as the side-effects reported for various GLP-1 therapeutics (such as pancreatitis and pancreatic cancer), two of the most significantly enriched diseases from the analysis, metabolic diseases (7.41×10^{-09}– 1.66×10^{-02}) and cancer (2.55×10^{-12} – 1.73×10^{-02}) were chosen for description (Table 5.5). Though cancer emerged as one of the diseases during analysis, there is a high degree of overlap amongst genes that were regulated in this processes and those involved with cell death and survival, cellular growth and proliferation, cellular compromise, cell cycle, cell function and maintenance, cell viability and differentiation all of which may be interpreted independent of cancer. Moreover the β-cell model employed for the study was derived from a rat tumor, which may also be one of the reasons for cancer emerging as a linked disease during the analysis.

A number of significantly enriched canonical pathways were also seen across all time points in response to 100 nM GLP-1 in 11 mM glucose compared to the transient treatment in presence of 11 mM glucose alone (U_30) (Table 5.6). Different mechanisms of endocytosis signalling emerged post-GLP-1 treatment, where caveolar-mediated endocytosis was prominent at 30 min (p-value 6.61×10^{-04}), 2 h (p-value 2.42×10^{-02}) and 6 h (p-value 3.3×10^{-03}) while clathrin-coated endocytosis (p-value 1.77×10^{-02}) was noticeable after 24 h. Clathrin-mediated endocytosis has been reported to regulate the cell surface levels of GLP-1R (Marchese *et al.,* 2003; Syme *et al.,* 2006). In addition there is evidence that GLP-1R can continue to signal from endocytic vesicles and that this might be important in GSIS (Kuna *et al.,* 2013; Roed *et al.,* 2014). Another pathway that has been implicated as one of the downstream events contributing to GLP-1R-mediated potentiation of GSIS, proliferation and survival effects is protein kinase A (PKA) signalling which is modulated over the time-course duration of GLP-1 except at 30 min (p-value range 6.29×10^{-03} - 1.8×10^{-02}) (Table 5.6 A).

In addition to these pathways being enriched across multiple time points, there were a large number of pathways that were predicted to be activated or inhibited at various time points (30 min, 2 h, 6 h or 24 h) based on the gene expression profiles on the GLP-1 treated samples (Table 5.6 B). While some would be expected based on what is known about GLP-1R signalling (i.e. PKA signalling, cAMP signalling, PI3-kinase signalling), many others appeared that have not been previously reported (Table 5.6 B).

Table 5.5: Biofunctions and diseases affected by differential regulation of genes in response to time-dependent treatment of GLP-1 (30 min, 2 h, 6 h and 24 h) relative to vehicle control at 30 min in INS-1 832/3 cells. The analysis was performed using Ingenuity Pathway analysis software. Genes highlighted in red represents up-regulated genes, while genes highlighted in green indicate down-regulated genes.

			GLP-1 for 30 min (G_30)	**GLP-1 for 2 h (G_2)**	**GLP-1 for 6 h (G_6)**	**GLP-1 for 24 h (G_24)**
Bio-functions and Diseases	**Number of significantly regulated molecules**		**75**	**460**	**164**	**563**
	BIO-FUNCTIONS					
	Metabolism (carbohydrate and lipid)	**p-value range**	$3.95 \times 10^{-03} – 1.66 \times 10^{-02}$	6.14×10^{-04} - 2.30×10^{-03}	$2.20 \times 10^{-04} – 1.15 \times 10^{-02}$	$1.86 \times 10^{-14} – 4.62 \times 10^{-04}$
		Subset of Genes (Upregulated/ downregulated)	Abcb1b, ALB, ANGPTL6, APOE, CD59, CPE, EGR1, EHHADH, EXTL1, FOS, KITLG, NR4A1, Gsta4, EGR1	ACP6, ADA, ADM, ALB, ALDH1A1, BCAT2, BRS3, CARTPT, CEL, CTGF, FES, GATM, GDF15, GLIS3, HAS3, Irs3, KLF2, LIFR, Mt1, NPY1R, NR0B2, NR4A1, NUAK2, PRLR, SGMS2, SLC22A1, SLC23A1, SLC9B2, TP53INP1, BMP2, CASR, CCL24, CTGF, DUSP6, GALE, GALM, GALR1, GCNT3, GLCE, GMPPB, GNE, HAS3, HBEGF,	ALB, CYP1A1, GSTP1, HPX, RDH16, SCD, SGMS2, LCAT, SCD, FES, NR4A1, RGS16, EHHADH, FES, GATM, MFSD2A, NUAK2, PDE10A, PFKFB1, PNOC, PPP1R3C, SLC6A4, SRGAP3, TH, CYP1A1, CSF1R, G0S2, PFKFB3, APLNR, CCL24, HBEGF, PFKFB3, PPP1R3C, PPP1R3E, RENBP, S1PR2,	ABCB1, Abcb1b, ADCY10, ANGPT1, BRS3, CASR, CCL24, CHKA, COQ3, CPT1A, CX3CL1, DGAT2, DUSP6, EDN1, ENPP2, EPM2AIP1, ERBB2, FBP2, GALM, GRK5, HAS3, HBEGF, HLA-A, IGF1, IGFBP5, IL1R2, INS, IRS2, MAS1, MYC, NEU2, NGFR, NPY1R, NR1D1, NRG1, NTRK3, OAS1, ONECUT1,

				HYAL2, HYAL3, LRP5, NPY1R, NR4A1, PDGFB, PFKFB3, PGM3, PIGV, PLA2G4B, PLCD1, S1PR2, SOCS3, ST6GAL1, TGFB2, ZFPM2, ABCD2, ABCG8, CYP1A1, CYP26B1, EGR1, EHHADH, ENTPD5, FOS, MFSD2A, NTN1, NUAK2, PLVAP, PNOC, PRLR, PTGS1, PYCARD, SCNN1B, SGMS2, SLC16A2, SLC22A1, SLC6A4, SRGAP3, TH, VAV3, BCL6, CHRM4, GRIN2A, HCAR1, IL16, LGALS1, P2RX2, PTGS1, TRPM4	SCD, ST6GAL1, APLNR, CSF1R, NR4A1, PPP1R3C, PPP1R3E, APLNR, CCL24, CSF1R, LIFR, NRIP1, SH2B2, TRIB3, MAP2K6, CAMK2A, Sik1	PDGFB, PIGV, PPARGC1A, PPP1R3B, PTGER4, USP2, VEGFC, XYLT1, ZFPM2, ABAT, ABCD2, ABCG8, ACACB, Acot5, AKR1C1/AKR1C2, ALB, ANO4, BCL2, CAV1, CPT1B, CYP1A1, DEGS2, EGR1, EHHADH, F2RL1, FA2H, GIPR, IL15, IL16, INSIG1, LDLR, MSMO1, NRG1, PITPNC1, SLC1A3, SLC27A3, TLR2, TRIB3
	Cellular growth and proliferation	**p-value range**	5.56×10^{-03} - 5.56×10^{-03}	1.88×10^{-07} – 4.14×10^{-03}	1.76×10^{-05} – 1.25×10^{-02}	1.07×10^{-06} – 6.42×10^{-04}
		Subset of Genes (Upregulated/ downregulated)	Abcb1b, ADCY1, AFAP1, ALB, ANGPTL6, ANTXR1, APOE, ATP6V1G2, C10orf90, CD59, CDH3, EFNA4, EGR4, EMP3, ERBB3, EXTL1, FAM107A,	ADA, ADAMTS8, ADM, AFAP1L1, ALB, ALDH1A1, ANTXR1, ARHGAP24, ARX, ASNS, ATP7A, BCL6, BMF, BMP2, BRSK1, CA9, CAMK2A, CASR, CCL24, CCNO, CD247,	ADAMTS8, ADCY1, ALB, ANTXR1, APLNR, ASCL2, BCL6, CAMK2A, CCL24, CCNG2, CD6, CITED2, CSF1R, CYP1A1, CYTIP, EBF1, EFNA4, EGR4,	AR, ATF3, BACH2, BCL2, BCL6, CABLES1, CAV1, CCL24, EDN1, EGR1, EPHA2, ERBB2, HCK, IFIH1, IGF1, IGFBP2, MLLT11, MYC, NFIL3,

	Cellular growth and proliferation	**Subset of Genes (Upregulated/ downregulated)**	FBXL2, FOS, HNRNPA0, IFNLR1, ITGA2, ITGA2B, KCNQ1, KITLG, KNDC1, Kng1/Kng1l1, LIN9, MID1, MT-ND6, NFKBID, NPTX1, NR4A1, PDIA5, PIWIL1, SCARF1, SIX3, STK38L, TRIM67, MTHFR, KNDC1, KCNJ12, EGR1, ITGA2	CD5, CDCP1, CEL, CHRM4, CISH, CREM, CTGF, CXCL11, CYP1A1, CYP2S1, DEGS2, DUSP6, E4F1, EFNA1, EGR1, ENTPD5, EPHA5, ETS1, ETV5, FBN1, FBN2, FES, FGF11, FGF13, FOS, FOXQ1, FZD9, G0S2, GABRA2, GALR1, GBP7, GDF15, GEM, GJB6, GLCE, GNE, GPR182, GPR3, GRIN2A, H3F3A/H3F3B, HAS3, HBEGF, HCAR1, HES1, HHEX, HLX, HPX, HTR3A, HYAL2, ID4, IKZF3, IL16, ITGA2B, ITGA5, KCND3, KCNH1, KCNJ2, KCNQ1, KEAP1, KLF11, KLF2, Kng1/Kng1l1, LGALS1, LIFR, LIN9, LMNB2, LRP5, LRRC4C, LRRK2, LTB, MAFA, MAFB, MAP2K6, Mt1, MX1, Myo16, MZF1, NDNF, NEUROD4, NFIB, NFKB2, NFKBID, NKX6-1, NMNAT1, NOTCH1,	EPHB1, EPHB3, FBN1, FES, G0S2, GPC5, GPR3, GRHL2, GSTP1, HBEGF, HCK, HLX, HPX, ID4, IFNLR1, Irx5, ITGA2B, JAG1, JDP2, KCNQ1, Kng1/Kng1l1, LCAT, LIFR, LIN9, MAFA, MAP2K6, MICALL2, MPZ, NPTX1, NR4A1, NRIP1, ORAI1, PDIA5, PFKFB3, PLK3, PNOC, POU2F2, PROK2, RGS16, S1PR2, SCD, SH2B2, SLAMF1, SLC6A4, SLC7A11, SPRY4, SRGAP1, SRGAP3, ST6GAL1, TIMM8A, TRIB3	NGFR, NRG1, NTRK3, PDGFB, PDLIM2, PHLDA1, PIM1, PLAGL1, PLK3, RASSF1, RRM2, RUNX1T1, SOCS2, SPRY4, TLR2

	Cellular growth and proliferation	**Subset of Genes (Upregulated/ downregulated)**		NPY1R, NR4A1, NTN1, NTN4, ORAI1, OXTR, PACSIN2, PAPSS2, PDGFB, PDIA5, PDPN, PER1, PFKFB3, PIWIL1, PLCD1, PLK3, PLK5, PNOC, PRICKLE2, PRLR, PTGS1, PYCARD, RASGRP2, RASSF1, RGS19, RRM2, RUNX1T1, RYR2, S1PR2, SERPINE2, SESN1, SH2B2, SIPA1, SLAMF1, SLC22A1, SLC26A2, SLC30A1, SLC39A10, SLC6A4, SLIT2, SLX4, SMAD7, SOCS2, SOCS3, SPDYA, SPRY4, SRGAP3, ST6GAL1, STK38L, TAGLN3, TGFB2, THG1L, TIFA, Timd2, TNFRSF25, TP53INP1, TRA2A, TRPC4, TRPM4, UNC5B, VAV3		
	DISEASES					
	Metabolic Disease	**p-value range**	$1.83 \times 10^{-04} – 1.66 \times 10^{-02}$	$1.07 \times 10^{-05} – 1.23 \times 10^{-04}$	$8.30 \times 10^{-04} – 8.61 \times 10^{-03}$	$7.41 \times 10^{-09} – 3.85 \times 10^{-04}$
		Subset of Genes (Upregulated/	MT-ND3, MT-ND6, APOE, ALB, CD59, MTHFR,	ADA, HLX, PAPSS2, PLVAP, ALB, ALDH1A1, ARX,	EBF1, EHHADH, GATM, GSTP1, HBEGF, MFSD2A,	AANAT, ACACB, ACAT2, ALB, AR, ARX, ATF3,

		downregulated)	D2HGDH	ATP1A2, BMP2, CA9, CAMTA1, CARTPT, CASP4, CD200, CD5, CEL, CHRM4, CREM, ENTPD5, FOS, FRMD3, GABRA2, GABRG2, GDF15, GLIS3, GRIN2A, HES1, HHEX, HSD17B1, HTR3A, HYAL2, IKZF3, IRF7, Irs3, ITGA2B, KCNJ2, KCNQ1, KLF11, LIN9, LRP5, MAFA, Mt1, MTNR1A, NKX2-2, NKX6-1, NPY1R, NR0B2, NR4A1, PDE4B, PDE7B, PHACTR3, PREX2, PRLR, PSMB8,	NR4A1, NRIP1, PDE4B, SCD , ALB, SLC7A11, ADCY1, ATP1A2, CD7, GSTP1, HCN1, HERC6, ITGA2B, KCNE2, KCNQ1, LIN9, MAFA, NR4A1, PDE4B, PSMB8, SCD, SLC6A4, SLC7A11, TAP2, TH, TMEM116, MAGT1, LCAT, DUOX2	ATP10A, BACH2, BCL2, BHLHE40, CAMTA1, CAPSL, CARTPT, CASP4, CAV1, CD200, CD5, CHRM4, COL5A3, COX6A2, CPT1A, CREM, DGAT2, EDN1, EPM2A, FGF1, GABRA2, GDF15, GIPR, GSTP1, HDC, HLA-A, HMBOX1, HMGCR, HSD17B1, ID1, Ifi47, IFIH1, IGF1, IGFBP2, IL15, IL1R2, INS, IRS2, Irs3, KCNK3, KLF11, LDLR, LIN9, MAFA, MAGI2, MERTK, MSH5, Mt1, MTNR1A, MYC, NKX2-2, NKX6-1, NLRP3, NOS3, NPY1R, NR0B2, OAS1, OGT, ONECUT1, PCDH15, PDE4B, PDE4C, PLAGL1, PPAP2B, PPARGC1A, PRKCQ, PTGER4, PTPRO, RNF39, RTP4, S100A4, SAMD4A,
	Metabolic Disease	**Subset of Genes (Upregulated/ downregulated)**				

						SLC17A4, SLC22A1, SPRED1, TIMP1, TLR2, TNFRSF9, TRIB1, TRIB3, TXNIP, XAF1, ZBTB1
	Cancer	p-value range	$2.18 \times 10^{-03} – 1.73 \times 10^{-02}$	$7.68 \times 10^{-08} – 4.07 \times 10^{-03}$	$7.15 \times 10^{-04} – 1.19 \times 10^{-02}$	$2.55 \times 10^{-12} – 5.75 \times 10^{-04}$
		Subset of Genes (Upregulated/ downregulated)	CCDC155, FAM107A, FJX1, GABARAPL2, HIST1H2BI, HNRNPA0, KCNJ12, LRRC34, MSS51, MT-ND3, RAP2B, TMEM176B, ANTXR1, EGR1, CD59, ALB, ANTXR1, APOE, CDH3, TGM1, EGR4, ERBB3, FOS, NPTX1, ALB, CD59, FBXL2, KITLG, NR4A1	ARHGAP4, CACNA1H, CASP4, CEL, CHRNA2, CNKSR3, CTGF, DHODH, DOCK10, DPYD, E4F1, EHHADH, EPHA5, ETS1, ETV5, F13A1, FBN2, FLRT2, FLRT3, FOS, FUBP1, GDF15, GRIN2A, HAPLN3, HBEGF, HCAR1, KLF11, KLHL24, LGALS1, LRRC18, LRRK2, MYH13, NFKBID, NID2, NPY1R, NTN4, PITPNC1, RRM2, RUNX1T1, RYR1, SCN1A, SCN7A, SEMA3E, SERPINE2, SLCO1A2, SLIT2, ST6GAL1, SYNE2, TGFB2, THSD1, TLE3, TP53INP1, TTLL12, WDR24, WDR49,	ABCG4, ADCY1, ALB, ANTXR1, APLNR, ATL1, ATP1A2, BCL6, BEGAIN, BEX4, CAMK2A, CCDC141, CCNG2, CD6, CD7, CHAC1, CITED2, CSF1R, CYP1A1, Cyp2c44, CYTIP, DNAH6, EBF1, EFNA4, EGR4, EHHADH, EPHB1, FBN1, FLNC, FNIP1, GPC5, GPR27, GRHL2, GSTP1, GUCA1B, HBEGF, HCK, HCN1, HERC6, HLX, HPX, ID4, IGDCC4, IRF5, ITGA10, ITGA2B, JAG1, JDP2, KIAA1107, KPNA5, LCAT, LIFR, MAFA, MARCH10, MDFIC, MFSD2A, MGARP,	BCL2, CASR, CAV1, EDN1, EGR1, EPHA2, ERBB2, F2RL1, FGF1, FHL2, GDF15, GLS, HMGCR, ID1, ID2, IGF1, IL15, JAG1, MYC, NOV, NRG1, PDGFB, PIM1, PLAGL1, TFF3, TXNIP, VEGFC, ALB, AR, CD59, DEPTOR, DHCR7, ETS1, FBXL2, HBEGF, MAP2K6, NGFR, PHLDA1, SERPINB9, TAF1B, TIMP1, TRIB1, VASH1 ALB, SLC7A11, ADCY1, ATP1A2, CD7, GSTP1, HCN1, HERC6, ITGA2B, KCNE2, KCNQ1, LIN9, MAFA, NR4A1, PDE4B,

	Cancer	**Subset of Genes (Upregulated/ downregulated)**		ZFPM2, ZNF407	MICALL2, MIDN, MMP13, MSC, NPTX1, NR4A1, NRIP1, NUAK2, NYAP2, ORAI1, P2RX2, PCNXL2, PDE10A, PDE4B, PDHA2, PDIA5, PEAR1, PFKFB3, PLEKHG4, PLK3, POU2F2, PPP1R3C, PRR35, PSMB8, RAB27B, RASL12, RASSF2, RDH16, RHBG, RPL13A, RPL37, RPL7A, RPL9, S1PR2, SAMD14, SCD, SLAMF1, SLC5A11, SLC6A4, SLC7A11, SNX33, SPATA2L, SPRY4, SRGAP1, SRGAP3, ST6GAL1, TAP2, THSD1, TRIB3, TTBK1, TTC28, WDR49, ZNF407	PSMB8, SCD, SLC6A4, SLC7A11, TAP2, TH, TMEM116, MAGT1, LCAT, DUOX2

Table 5.6 A: Top canonical pathways predicted to be activated based on the genes regulated response to GLP-1.

(A) Two highly enriched pathways that were predicted to be activated across multiple time-dependent treatments of GLP-1 (30 min, 2 h, 6 h and 24 h) relative in INS-1 832/3 cells. The analysis was performed using Ingenuity Pathway Analysis software and P<0.05 was considered statistically significant. ND = not detected at this time point. Genes highlighted in red represents up-regulated genes, while genes highlighted in green indicate down-regulated genes. (B) Canonical pathways that were predicted to be activated or inhibited based on the gene expression profiles of GLP-1 treatments at 30 min, 2 h, 6 h or 24 h.

		GLP-1 for 30 min (G_30)	**GLP-1 for 2 h (G_2)**	**GLP-1 for 6 h (G_6)**	**GLP-1 for 24 h (G_24)**
Canonical Pathways	**Number of significantly enriched canonical pathways**	7	35	15	45
	Endocytosis signalling				
		Caveolar –mediated	Caveolar –mediated	Caveolar –mediated	Clathrin-mediated
	p-value	6.61×10^{-04}	2.42×10^{-02}	3.3×10^{-03}	1.77×10^{-02}
	Genes present in the pathway				
	Upregulated	ITGA2B, ITGA2, FLNC	ITGA2B, ZBTB12	ITGA2B, FLNC	LDLR, FGF1, AAK1, FGF11, PDGFB, INS, TFRC
	Downregulated	ALB	ITGA10, ITGA5, ALB	ITGA10, ALB	IGF1, VEGFC, ITGA5, ALB
	Protein kinase A (PKA) signalling				
	p-value	ND	1.8×10^{-02}	6.29×10^{-03}	2.9×10^{-02}
	Genes present in the pathway				
	Upregulated	ND	RYR1, PLCD1, NTN1, TH, PDE4B, CAMK2A, NFKB2,	ADCY1, HHAT, PPP1R3C, DUSP15, TH, FLNC, PDE4B,	ADCY8, CREM, DUSP6, DUSP4, PDE4B, PDE4C

			CREM, PDE7B, DUSP6	CAMK2A	
	Downregulated	ND	AKAP2, GNB1L, H1f0, H3F3A/H3F3B, TGFB2, RYR2	PDE10A	PRKCQ, H3F3A/H3F3B, PTPRO, CDC25C, ADCY10, GNB1L, , NGFR, , NOS3, H1f0, EPM2A, PTPN7, H1FX

(B) Canonical pathways that were predicted to be activated or inhibited based on the gene expression profiles of GLP-1 treatments at 30 min, 2 h, 6 h or 24 h.

Canonical pathways predicted to be activated by GLP-1	Canonical pathways predicted to be inhibited by GLP-1
Caveolin-mediated endocytotic signalling	Tgfβ signalling
PKA signalling	ILK signalling
GPCR-mediated signalling	EGT signalling
cAMP-mediated signalling	Purinergic signalling
Gαs signalling	ERK5 signalling
Gβγ signalling	CD40 signalling
CREB signalling	NGF signalling
nNOS signalling	HGF signalling
Notch signalling	P70S6K signalling
PPAR and PPARα signalling	
STAT 3 pathway	
EIF2 signalling	
ERB signalling	
JAK/STAT signalling	
Corticotropin-mediated signalling	
GNRH signalling	
PI3-kinase signalling	
Wnt/Ca^{2+} signalling	
IGF1 signalling	
Paxillin signalling	
Signalling by Rho family GTPases	
VEGF signalling	
P38 MAPkinase signalling	
P53 signalling	
Integrin signalling	

5.3.5.2 Investigation of signal bias and differential regulation induced transcriptome alteration in INS-1 832/3 cells through IPA analysis

A global analysis of differentially regulated genes was performed to compare 100 nM GLP-1 and 100 nM exendin-4 and the results are represented as a venn diagram (Figure 5.6). Comparison of gene expression changes at 30 min treatment of INS-1 832/3 cells in presence of 100 nM GLP-1 (G_30) compared with 100 nM exendin-4 (Ex_30) treatment showed differential regulation of 43 genes while there were 196 commonly regulated genes (Figure 5.6A; Appendix 4,Table S5.6 contains a full list of these GLP-1R regulated genes). Similarly, comparison involving the prolonged treatment (24 h) of the two peptides revealed a differential regulation of 44 genes with 95 commonly regulated genes (Figure 5.6 B; Appendix 4, Table S5.7 contains a full list of GLP-1R regulated genes).

Similar to the GLP-1 time course, a vast array of functional clusters, with significantly enriched genes/molecules, were observed post analysis (heat maps not displayed). Likewise, a number of established signalling pathways were commonly and differentially regulated between GLP-1 and exendin-4, at 30 min and 24 h (Table 5.7). In functional analysis, both ligands were able to regulate a large number of genes (both at 30 min and 24 h) that have been associated with diabetes or metabolic disease. Caveolar-mediated endocytosis signalling was identified as one of the commonly regulated pathways by both peptides after 30 min treatment. Corticotropin releasing hormone signalling and molecular mechanisms of cancer were two of the differentially regulated signalling pathways in response to acute treatment with GLP-1, where the former is related to cellular growth, proliferation and repair and the latter linked to cell death, survival and cell cycle (Table 5.7). At 24 h, both the peptides showed significantly regulated genes enriching the eIF2 signalling pathway that regulates protein synthesis, gene expression, cell death and survival. Regulation of cellular mechanics by calpain protease that has been linked to cellular growth, proliferation and development was also regulated by both ligands (Table 5.7). Enrichment of NRF2-mediated oxidative stress response was significantly modulated by GLP-1 at 24 h but not exendin-4 and this is related to signalling pathways linked to cell death and survival. ILK signalling that is linked to both cell survival and inflammatory responses was predicted to be regulated by exendin-4 but not GLP-1 (Table 5.7).

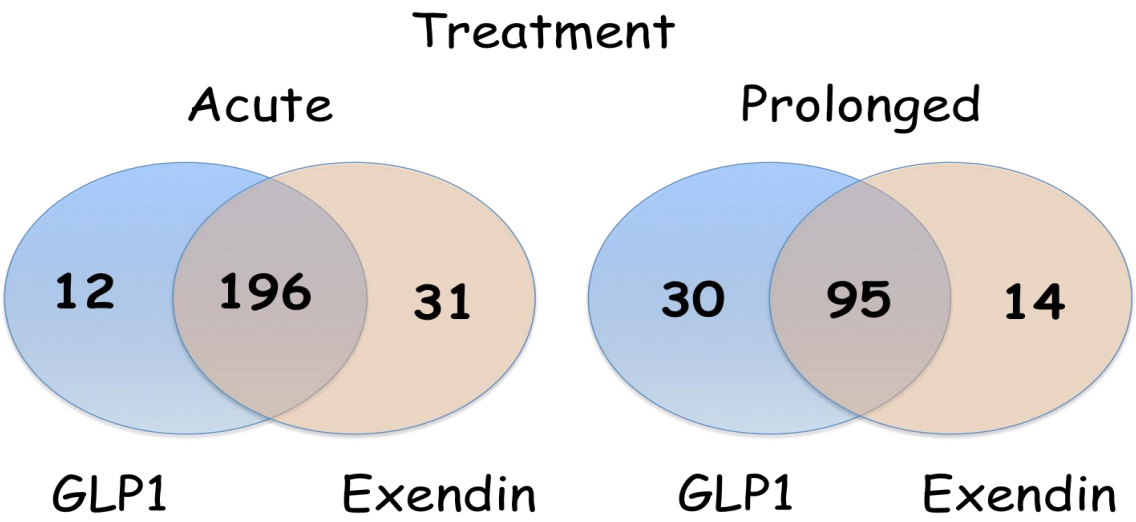

Figure 5.6 Global Analysis. Venn diagrams showing overlap of differentially ($p < 0.05$) expressed genes at different time points (30 min (acute) and 24 h (prolonged)) in the presence of 100 nM GLP-1 (G_30 and G_24) and 100 nM exendin-4 (Ex_30 and Ex_24) compared to 11 mM glucose at the same time points (U_30 and U_24). (A) Comparison of genes coregulated and differentially regulated between GLP-1 and exendin-4 treatments at 30 min and (B) comparison of genes coregulated and differentially regulated between GLP-1 and exendin-4 treatments at 24 h.

Table 5.7: Canonical pathways affected by differential regulation of genes in response to acute and chronic treatment with glucose alone, GLP-1 and exendin-4 relative to the appropriate vehicle control in INS-1 832/3 cells. The analysis was performed using Ingenuity Pathway Analysis software. Genes highlighted in red represents up-regulated genes, while genes highlighted in green indicate down-regulated genes.

Treatment groups	**Canonical pathways**		
	Name	**p-value**	**Genes/molecules**
GLP-1 at 30 min (U_30 vs G_30)	Caveolar-mediated Endocytosis Signaling	6.61×10^{-04}	ALB, FLNC, HLA-A ITGA2, ITGA2B
	Molecular Mechanisms of Cancer	1.64×10^{-02}	ADCY1, FOS, HHAT, WNT9B, RAP2B, ITGA2
	Corticotropin releasing hormone signalling	2.41×10^{-02}	ADCY1, FOS, NR4A1
Exendin-4 at 30 min (U_30 vs Ex_30)	Caveolar-mediated Endocytosis Signaling	3.26×10^{-04}	ALB, FLNC, HLA-A, ITGA10, ITGA2B
	nNos signalling	9.96×10^{-03}	CAPN3, RYR3, SNTB1
	Communication between innate and adaptive immune cells	6.71×10^{-03}	CCR7, HLA-A, IL15, TLR5
GLP-1at 24 h (U_24 vs G_24)	Regulation of Cellular Mechanics by Calpain Protease	2.64×10^{-04}	ACTN2, CAPN6, CNGB3

	NRF2-mediated Oxidative Stress Response	2.63×10^{-03}	ACTC1, AOX1, FOS, FTL
	EIF2 Signaling	$2.24\ 10^{-03}$	RPL9, RPL37, RPL41, RPS20
Exendin-4 at 24 h (U_24 vs Ex_24)	EIF2 Signaling	9.61×10^{-03}	RPL9, RPL41, RPS20, RPS29
	ILK signalling	9.46×10^{-03}	ACTC1, ACTN2, CREB1, CREB3 FOS, VIM,
	Regulation of Cellular Mechanics by Calpain Protease	7.71×10^{-03}	ACTN2, CNGB3

Table 5.8. Examples of genes linked to functions of interest when considering GLP-1R activation for therapeutic development. Assorted sub-list of co-regulated genes at either 30 min or 24 h in response to GLP-1 and exendin-4 compared to glucose control (vehicle). Listed are genes lined to cell to cell signalling, signal transduction, cell death and survival and genes linked to type 2 diabetes. Green coloured genes indicate down regulated genes and red colour represents up-regulated genes in the data set. Highlighted in pink are some of the genes already reported to be linked to GLP-1R function and diabetes; yellow are various GPCRs regulated, blue are some transcription factors and white are genes previously not linked to GLP-1R mediated activation.

Cell to cell signalling	Signal transduction	Proliferation	Cell death and survival	Linked to type 2 diabetes
ADM	GPR27	Abcb1b	ACTC1	RAMP1
CCKAR	CHRNA2	ADC41	ALB	CALCR
Tp53	Taar4	CD59	ERBB3	MAFA
SLC12A1	Tas1R	NOTCH2	CASP4	Mt1
ApoE	GIP	NR4A1	FBXL2	NR4A3
EGFR	IGF1R	IGF2	GCK	KCNQ1
FOS	SOCS2	IGF1R	BCL2	GBP6
S100A4	GNRH1	CAG3	EGR1	NEBL
WNT9B	SRC	Mt1	IGF1R	CPNE4
Sik1	ANTXR1	JUN	PAX6	CCND1
SOCS3	TIRAP	VIM	TGM1	MZB1
SLAMF1	NPFFR2	TGM1	SOCS3	PHACTR3
TLR	KITLG	MTHFR	MTHFR	CACNA1F

A large number of genes were also identified that were regulated by both GLP-1 and exendin-4 at either 30 min or the 24 h timepoint. While Table 5.8 highlights come of these coregulated genes, it is important to note that in some cases, the time for which the particular gene was regulated was not always the same for both ligands, and in a few cases the direction of change was not always the same. Within this list includes a large range of genes linked to functions such as cell to cell signalling and signal transduction, proliferation, cell death and survival and genes that have been linked to type 2 diabetes, all functions that are important when considering GLP-1R activation for therapeutic targeting. In addition, a number of these genes are also GPCRs suggesting a significant level of coregulation of GPCR signalling between different receptors in this superfamily (Table 5.8).

5.3.5.3 Designing an RT-qPCR array

The ingenuity knowledge database, NetAge, and Type 2 diabetes network (IBAB) were the tools employed to choose significantly and differentially regulated genes for designing an RT-qPCR array. Various criteria were taken into consideration during the selection process including (i) control genes (process or PCR control); 2 genes, (ii) housekeeping genes; 5 genes, (iii) genes known to be involved in GLP-1R signalling; 15 genes, (iv) genes differentially regulated by both GLP-1 and exendin-4 at 30 min and 24 h; 84 genes, (v) genes commonly regulated by both GLP-1 and exendin-4 at 30 min and 24 h but in opposite directions; 9 genes (vi) genes commonly regulated by both GLP-1 and exendin-4 at 30 min and 24 h that are connected to diabetes and associated networks; 33 genes and (vi) genes commonly regulated by both GLP-1 and exendin-4 at 30 min and 24 h involved with proliferation, apoptosis and cell signalling; 44 genes (Appendix 4, Table S5.6). The primers designed for this array are included in Appendix 4, Table S5.8. Subsequently this array will be used for validation of transcriptomic data and identification of differentially regulated genes in response to other GLP-1R peptides and allosteric ligands. However, due to time constraints this still has to be completed.

5.4. DISCUSSION

RNA-seq is a highly parallelized sequencing technology that allows for comprehensive transcriptome characterization and quantification (Wang *et al.*, 2009). RNA-seq offers distinct advantages over the other methods that were developed earlier (probe-based sequencing and hybridization-based microarray) including significantly improved detection accuracy, the ability to identify transcripts without probe dependency and *de novo* analysis of novel transcripts (Lee *et al.*, 2011; Song *et al.*, 2012).

The study in this chapter was performed to obtain unbiased data on the cellular responses mediated upon activation of the GLP-1R by various agonists. The aim was to identify gene products involved in GLP-1R dependent signalling, to identify pathways that potentially could be involved in potentiation of GSIS, proliferation and anti-apoptotic effects in pancreatic β-islets, or pathways that may lead to disease. Furthermore, this study attempts to identify the molecular networks/molecules differentially activated by GLP-1R peptide ligands to attempt to understand GLP-1R biased signalling at the global level. In this work, deep sequencing was performed on pooled samples (different replicates of same time point and treatment) with the rationale to capture the snapshot of the transcriptome at distinct stages, ranging from an early time point (30 min) through to intermediate (2 h and 6 h) and late time point of 24 h for GLP-1. However, only 30 min and 24 h exposure was performed for exendin-4, oxyntomodulin as well as a vehicle control (11 mM glucose alone). RNA-seq enabled identification of various genes/metabolic pathways and networks inclusive of an extensive catalog of expression values over the range of distinct analytical (30 min, 2 h, 6 h and 24 h) stages (Figure 5.2). On average 53.5 million sequenced reads were obtained per sample, amongst which on average 39.8 million reads uniquely mapped to the reference genome without mismatch, and 27.3 million reads on average mapped perfectly to the annotated genes of the rat sequence. Ingenuity Pathway Analysis (IPA) connects the molecules based on the Ingenuity Knowledge Base, its database of information on biomolecules and their relationships and this software allowed comprehensive analysis of all data sets obtained within the experiments described in this chapter.

5.4.1 Transcriptomic regulation in response to GLP-1

Type 2 diabetes is a metabolic disorder defined by chronic hyperglycemia and relative insulin insensitivity and is accompanied by disregulation in carbohydrate, lipids and protein metabolism. Although there are some predisposing genotypes, type 2 diabetes is primarily caused by an excess of energy consumption over expenditure coupled with a sedentary lifestyle. Obesity, in particular central adiposity, is a key risk factor for type 2 diabetes. It has been demonstrated that activation of the GLP-1R has the potential to improve glucose-homeostasis and energy metabolism by both peripheral (increasing the level of glucose dependent insulin secretion in the pancreas) and central (appetite regulation, reduced gastric emptying and reduction in hepatic glucose production) mechanisms (Drucker, 2006; Baggio and Drucker, 2007). GLP-1R peptide agonists are used in the clinic for management of type 2 diabetes and obesity, however the downstream pancreatic effects are not fully known. Thus, here we have applied a network biology approach to investigate and identify the molecular targets that may contribute to the underlying physiological and therapeutic effects of GLP-1.

Biological/canonical pathway information is useful for the better understanding the mechanisms affected by patho/physiological state. Biofunctional and pathway analysis of the genes regulated across the timecourse of treatments assessed for GLP-1 demonstrated enrichment of pathways and clusters based on the significantly regulated genes that were associated with metabolic disorders, as well as metabolism of lipids and carbohydrates. This outcome was not unexpected, given that GLP-1 promotes glucoregulatory and insulinotropic effects. GLP-1 has been demonstrated to augment GSIS by both PKA-dependent and -independent (Epac activation) mechanisms where it regulates the activity of K^{+}_{ATP} ion channel, Ca^{2+}concentration and insulin granule exocytosis (Ozaki *et al.*, 2000; Kang *et al.*, 2001; Eliasson *et al.*, 2003). Activation of Akt/PKB subsequently inhibiting AMPK has been implicated in various metabolic effects including lipolysis and glucose transport (Wullschleger *et al.*, 2006; Hardie, 2007). GLP-1R activation has been shown to regulate adipogenesis by co-ordinating early events of adipocyte differentiation inclusive of PPARδ, C/ebpβ and C/ebpδ (Challa *et al.*, 2011). Activation of c-jun, Akt, ERK1/2, PKCβII are other putative downstream regulators of this process (Challa *et al.*, 2011). In addition, various adipokines secreted from the adipose including leptin, adiponectin and resistin have been reported to regulate energy homeostasis (Ahima and Lazar, 2008; Rajala and Scherer, 2003). Of these proteins, some of their genes showed altered expression levels with GLP-1 treatment (for example c-jun, insulin and various different K^{+} channels), however not all were identified. This does not mean the data is inconsistent with activation of these other pathways that have been reported in the literature. One limitation of assessing changes in mRNA expression levels is that gene regulation changes do not always directly correlate with protein expression levels. In addition, although only a small number of the genes for these reported proteins were altered, changes in the expression levels of genes upstream or downstream of some of these pathways were significantly up or downregulated, indicating that these pathways are important. For example, a large number of genes involved in PKA-mediated signalling were significantly upregulated across the entire GLP-1 timecourse with IPA predicting PKA mediated signalling is activated by GLP-1 (Table 5.2 A). In addition, genes associated with Gαs and cAMP (upstream mediators of PKA and Epac) were predicted to be activated based on the genes regulated (Table 5.2 B). This is not surprising due to the known roles of cAMP, PKA and Epac in GLP-1R-mediated insulin secretion and insulin secretion/biosynthesis (Drucker *et al.*, 1987; Taylor *et al.*, 1990; Dyachok *et al.*, 2006). In addition, genes associated with PPAR signalling were also regulated with the up/downregulation profile of these genes consistent with activation of this signalling pathway (Table 5.3).

While our transcriptome data did not identify up/downregulation of all genes of signalling proteins known to be activated by GLP-1, there are a number of genes identified that were consistent with

those already been reported in the literature to be were regulated by GLP-1. This includes, but is not limited to IRS1, CREB, CREM Ins1, Adcy1, BCL2 Nfkb1, Foxo1, EGR1, NeuroD4, SMAD7, SOCS2 and Mafa. These genes play roles in cellular signalling (Adcy1, CREM, CREB, Ins1, Irs1) and cell survival pathways (Nfkb1, CREM, EGR1, Foxo1, Bcl2, NeuroD4, SMAD7, SOCS2). Their appearance in our lists of regulated genes provides some confidence in the datasets that were obtained from the transcriptomics data presented in this chapter.

In addition to known genes linked to GLP-1R activation, our transcriptome sequencing has also revealed a large array of genes that have not previously been reported or linked to GLP-1R activation (Table 5.1). Some of these cluster in a list of biofunctions corresponding to cellular growth and proliferation, cell death and survival and therefore may play roles in GLP-1R mediated proliferative and anti-apoptotic mechanisms that can be linked to β-cell function and growth. Of particular interest are NOTCH1, KIT ligand (KITLG), 5-hydroxytryptamine (serotonin) receptor 1D, G protein-coupled (5HTR1D), glycine N-methyltransferase (GNMT), serum/glucocorticoid regulated kinase 2 (SGK2), nuclear RNA export factor 3 (NXF3). Further work will be required to identify if these genes and the pathways by which they regulate function, are important for GLP-1R mediated β-cell survival and function. Following up this work will be important to identify novel pathways that may be useful to exploit therapeutically. To validate and further analyse the regulation of some of these interesting genes/transcription factors (in addition to others), a RT-qPCR array has been designed (listed in Appendix 4, Table S5.8). However, due to time constraints, additional work for the array could not be completed for this thesis.

As mentioned, pathway analysis predicted many signalling pathways to be activated by GLP-1 that were not unexpected due to the reported signalling profiles for this receptor (for example PKA signalling, cAMP-mediated signalling, CREB signalling, Gαs signalling, ERK signalling, PI3 kinase signalling, STAT3 pathway IGF1 signalling). However, a large number of pathways were also predicted to be either activated or inhibited by GLP-1 treatment that have not been extensively explored before in the literature for the GLP-1R (Table 5.2 B). One of these pathways, endocytosis signalling, was predicted to be activated based on the transcriptome profile at all four timepoints that were assessed.

There are different mechanisms for endocytic internalization including clathrin-mediated endocytosis, caveolar-mediated endocytosis, macropinocytosis and non-clathrin, non-caveolae endocytosis. These processes are associated with fusion of early endosomes, cell trafficking and vesicle transport (Gruenberg and Maxfield, 1995; Seachrist and Ferguson, 2003; Grant and

Donaldson, 2009). Endocytotic internalization is one method by which GPCRs can be desensitized where receptors are uncoupled from the regulatory proteins including G proteins and directed to either caveolae or clathrin coated pits. However, it is now well established that internalization does not always desensitize GPCRs, but that they can continue signalling from intracellular compartments. In our study genes involved in caveolar-mediated (30 min, 2 h and 6 h) as well as clathrin-mediated endocytotic signalling (24 h) were regulated by GLP-1 treatment. This occurred at different time points and both endocytic pathways have been previously reported to be responsible for agonist-dependent GLP-1R internalisation (Vázquez *et al.,* 2005; Syme *et al.,* 2006).

Caveolin-1 is the major component of caveolae anchored by filamin (FLNC), which binds to the actin cytoskeleton with internalization of caveolae induced by numerous stimuli. Caveolar mediated endocytosis plays a role in various cellular processes such as cellular signalling, cell trafficking, lipid recycling, fusion with early endosomes and transport of vesicles, whereas clathrin-mediated endocytosis is the major pathway for the internalization of nutrients, hormones, receptors and other signalling molecules from the plasma membrane into intracellular compartments. Both caveolin and clathrin-mediated endocytosis have been reported to regulate cell surface levels of the GLP-1R (Marchese *et al.,* 2003; Syme *et al.,* 2006). Following endocytosis, the receptor can be either trafficked back to the plasma membrane or degraded in the lysosomes. However, while internalized, there is also evidence that the GLP-1R can promote cellular signalling. Activation and endosomal trafficking of the GLP-1R has been explored where compartmentalized cAMP generation from intracellular sites has been demonstrated to, in part, regulate insulin granule exocytosis in cultured pancreatic β-cells before being sorted to lysosome for degradation (Kuna *et al.,* 2013). There may, therefore, be some regulatory feedback between GLP-1R activation and upregulation of genes involved in receptor cycling and/or internalized signaling. Additionally, there are some literature reports that support a model in which clathrin-mediated endocytosis is linked to stimulated exocytosis of insulin (MacDonald and Rorsman, 2007; Deisl *et al.,* 2014). It is therefore tempting to speculate that upregulation of these clathrin pathway genes may contribute to the observed increases in medium term GSIS in response to GLP-1 mimetics.

IPA analysis of diseases revealed metabolic disease as the most significant disease area associated with the significantly regulated genes. Given the known roles of GLP-1R in metabolic processes, this was not surprising. There were are large number of genes that have been specifically linked in the literature to type 2 diabetes, many of which have not been reported previously to be involved in physiological processes downstream of GLP-1R activation (some are listed in Table 5.8). This is particularly interesting given the therapeutic potential of GLP-1R agonists in treatment and

management of this disease. Potentially all of these would be interesting to pursue further to confirm the extent of their involvement in GLP-1R functions. All of these genes have been included (Appendix 4, Table S5.8) in the designed RT-qPCR array mentioned previously to confirm the importance before additional follow up work will be pursued. The IPA analysis of disease also revealed cancer as one of the highly linked diseases in response to GLP-1 treatment. The GLP-1R has been associated with cell proliferation and survival effects both in the literature and with bio-function anlaysis within IPA. Many of the cancer-associated genes overlap with genes associated with cellular growth, development, function and survival and therefore, it may not be unexpected that cancer was predicted. Moreover, the β-cell model employed for the study was derived from a rat tumor, which may also be one of the reasons for cancer emerging as one of the most enriched diseases during the analysis. However, it may be interesting to explore some of these genes further, in relation to their regulation by different GLP-1R agonists, as currently GLP-1R peptide mimetics that are used clinically have been associated with an increased risk for the development of various cancers, including pancreatic cancers and thyroid tumors (Elashoff *et al.,* 2011; Singh *et al.,* 2013; Drucker *et al.,* 2013). Understanding pathways that may lead to this increased risk, may aid in future development of drugs with less side effect profiles.

5.4.2. Differential regulation of transcriptome in presence of GLP-1 and exendin-4

Using different signalling (pERK1/2 and cAMP) and functional endpoints (insulin secretion, apoptosis and proliferation), chapter 4 highlighted that GLP-1R peptide ligands exhibit bias at the therapeutically relevant endpoints of proliferation and apoptosis that control β-cell mass. There was also some bias observed in acute signalling pathways such as pERK1/2. However, these studies cannot define which intermediaries contribute/promote this signalling bias. In addition, using only a limited number of preselected endpoints as assessed in chapter 4 does not have the capacity to reveal the full extend of ligand-directed signalling bias that may be exerted by these peptide ligands. Identification of the full extent of bias induced by GLP-1R ligands may provide insights into different clinical efficacies of various ligand acting at the same receptor, in addition to observed differences in the extent and magnitude of side effect profiles induced by different ligands. By analysis of the transcriptomic data described in this chapter, genes differentially regulated were identified in response to individual GLP-1R peptides.

Given the sequence conservation between GLP-1 and exendin-4, and the fact that exendin-4 is used clinically to mimic GLP-1, it was not surprising to find that a large number of genes were significantly regulated in the same direction by both of these peptides. To summarize the findings from different sub-analysis performed using IPA, a subset of genes that were regulated by both

peptides were categorized into five categories based on identifying signalling molecules/genes/networks contributing to physiological and therapeutic effects mediated by GLP-1R activation including cellular signalling and improved β-cell function and mass. These include cell to cell signalling, signal transduction, proliferation, cell death and survival and genes previously linked to type 2 diabetes. A number of the genes listed in Table 5.4 (highlighted in pink; not all are listed), including EGFR, FOS, IGF-1R, IGF2, GCK, BCL2, EGR1 and KCNQ1, have been reported in the literature to be either regulated at the gene level or known to be involved in GLP-1R function and were expected to be expressed (Cornu *et al.*, 2009; Park *et al.*, 2012; Quoyer *et al.*, 2010; Yamagata *et al.*, 2011).

There were also a number of identified coregulated genes that have been linked to either cell survival mechanisms or differentiation specifically in β-islets cells but that had not been previously linked to GLP-1R signalling. These include PAX6 (Paired Box 6), TGM1 (transglutaminase 1) and SOCS3. PAX6 is a transcription factor that regulates differentiation, proliferation, and cell cycle progression and has been identified to be crucial for β-cell function, insulin biosynthesis, and glucose-induced insulin secretion (Gosmain *et al.*, 2012). TGM1 is a membrane protein that has been associated with cell death and survival in different cells (Antonyak *et al.*, 2006; Baso *et al.*, 2012). SOCS3 is STAT-induced STAT inhibitor (SSI), also known as suppressor of cytokine signaling (SOCS). The expression of this gene is induced by various cytokines, including interleukin 6 (IL6) and 10 (IL10) and interferon (IFN)-gamma. Regulation of SOCS3 is associated with wide range of functions including cell viability, growth, cell death and proliferation (Karlsen *et al.*, 2001; Rezende *et al.*, 2012), glucose uptake (Ueki *et al.*, 2004) and insulin secretion and thus, it is not surprising that these genes may also be involved in GLP-1 mediated responses (Rønn *et al.*, 2002).

Moreover, in this list of genes co regulated by both GLP-1 and exendin-4, there were also a number of GPCR genes, GPCR modulators, ligand gated ion channels and GPCR ligands that were up or down-regulated. This includes of ADM (adrenomedullin), CCKAR (cholecystokinin A receptor), GPR27 (G protein-coupled receptor 27), CHRNA2 (Cholinergic receptor, nicotinic, alpha polypeptide 2), Taar4 (trace amine-associated receptor 4), Tas1R (taste receptor, type 1, member 1), GIP (gastric inhibitory polypeptide), RAMP1 (receptor activity modifying protein 1), and CALCR (calcitonin receptor). GIP is an incretin hormone belonging to the glucagon superfamily and aids maintaining glucose homeostasis as it is a potent stimulator of insulin secretion from pancreatic β-cells following food ingestion and nutrient absorption (Ishihara *et al.*, 2011). RAMP1 is single pass transmembrane proteins that can heterodimerise with both CALCR and the calcitonin-receptor-like

receptor (CLR). In the presence of this (RAMP1) protein, CLR functions as a CGRP receptor. CALCR is a GPCR that binds to calcitonin and is involved in calcium homeostasis and regulates cell fate (Evdokiou *et al.,* 1999). The heterodimer of RAMP1 and CALCR is a high affinity receptor for amylin, a peptide hormone co-secreted from β-cells with insulin. Amylin slows gastric emptying and promotes satiety, assisting in limiting post-prandial glucose excursion. In this context it is interesting that the receptor for amylin appears to be differentially regulated by GLP-1R ligands. ADM is a peptide hormone with several functions, including vasodilation, regulation of hormone secretion, promotion of angiogenesis, and antimicrobial activity. Additionally, ADM promotes cell growth, proliferation and survival by binding to adrenomeullin receptors (Ramachandaran *et al.,* 2007; Maybin *et al.,* 2011; Ishikawa *et al.,* 2003). CCKAR is also a GPCR that has been reported to regulate satiety and the release of β-endorphin and dopamine (Kopin *et al.,* 1999). However, Taar4 and Tas1R and GPR27 are GPCRs whose role still needs to be established in terms of regulation of pancreatic β-cell structure and functions.

The ability of GLP-1 treatment to alter expression levels of genes encoding proteins for other GPCRs, suggests that there may be tightly coordinated function/crosstalk between different GPCRs that may be involved in tightly regulating pancreatic β cell functions. To date, there are only a few studies that have specifically assessed the role of other GPCR functions on that of the GLP-1R. Co expression of the GIP receptor with the GLP-1R identified interplay of signalling between these two receptors. These receptors have the ability to heterodimerise, which alters the signalling profile of the GLP-1R for β arrestins and calcium mobilisation (compared to the GLP-1R expressed alone) (Schelshorn *et al.,* 2012). In addition, cross talk between the GLP-1R and GIP receptor signalling and trafficking was identified, where the GIP receptor reduced the rate and extent of internalisation of the GLP-1R. This was coupled with impaired GLP-1R mediated signalling (Roed *et al.,* 2015). This interplay of signalling by GLP-1R and GIP receptor is not only interesting, but could have therapeutic implications, as expression of the GIP receptor is reduced in type 2 diabetes, however the GLP-1R is not (Meier *et al.,* 2001; Vilsboll *et al.,* 2002). Therefore, the crosstalk between the two receptors will be lost in these conditions altering the signalling properties and kinetics of trafficking of the GLP-1R. Based on this transcripomic data, it would be interesting to assess GLP-1R crosstalk with these other GPCRs and to understand how their relative expression levels alter in disease states.

While a large number of genes were coregulated by both GLP-1 and exendin-4, there were a substantial number (87 in total) that were identified as differentially regulated between the two ligands (Figure 5.6; Appendix 4, Table S5.6 and S5.7) at 30 min and/or 24 h. This reveals that

ligand-induced signalling bias can be detected at the global level, and further highlights that exendin-4, although used clinically to mimic GLP-1, does not activate the GLP-1R in the same manner. IPA analysis on the various pathways activated by the two ligands revealed large arrays of pathways were similarly enriched by the sets of regulated genes for both ligands. Within the top pathways, both caveolar-mediated endocytosis signalling was identified for both peptides after 30 min treatment. Corticotropin releasing hormone signalling and molecular mechanisms of cancer were within the top pathways for GLP-1 and these pathways are related to cellular growth, proliferation and repair, cell death, survival and cell cycle (Table 5.7). The ability of GLP-1 to activate these pathways with a higher prediction score (compared to exendin-4, where this pathway was not evident) may be related to the ability of GLP-1 to promote greater relative levels of cell proliferation and protection against apoptosis compared to exendin-4 (as identified in chapter 4). At 24 h, both the peptides showed significantly regulated genes enriching the eIF2 signalling and regulation of cellular mechanics by calpain protease. These pathways regulate protein synthesis, gene expression, cell death and survival, cellular growth, proliferation and development. While the studies in chapter 4 showed GLP-1 produced more proliferation and anti-apoptosis relative to cAMP compared to exendin-4, exendin-4 was still capable of promoting these effects. From these transcriptomics studies, it can be speculated that observed differences in the bias profile of these ligands may be linked to the kinetics of promoting changes linked to cell survival pathways, with GLP-1 promoting both acute and prolonged effects, but exendin-4 only activating signalling linked to these pathways in prolonged conditions. Genes modulated by GLP-1 treatment also downregulated genes linked NRF2-mediated oxidative stress response pathways that are linked to cell death and survival at 24 h. In contrast, ILK signalling that is linked to proliferation, apoptotic pathways as well as inflammatory responses, was predicted to be upregulated by exendin-4 but not GLP-1 (Table 5.7). The different mechanisms in terms of pathways predicted to be activated by GLP-1 compared to exendin-4 that are linked functions of cell survival and cell death may also account for some of the observed differences in the bias of GLP-1 and exendin-4 when considering proliferative and apoptotic pathways. In addition, interestingly, the clinical use of exendin-4 has be associated with an increased risk of pancreatitis, therefore activation of pathways (such as ILK signalling) that promote inflammatory responses may account for some of these observations. This should be pursued further as identification of signalling that may account for these increased risks associated with use of the current GLP-1R drugs, may aid in designing better therapeutics in the future.

All of the genes that differentially regulated by GLP-1 and exendin-4 in this study, were selected for validation through the RT-qPCR array. Subsequently, genes that are validated and confirmed as

being regulated differentially by these ligands in this array will be followed up by using various pharmacological and siRNA approaches. The effect of knock down of these proteins or their function, will be assessed by measuring changes to downstream signalling, including cAMP, pERK1/2, insulin secretion, apoptosis and proliferation, as optimised and characterised in previous chapters (Chapter 3 and 4). This will identify if the proteins encoded by these genes are involved in the observed bias profiles observed by the two ligands when assessing these pathways.

Chapter 4 identified distinct ligand bias signalling profiles of GLP-1R agonists in different glucose concentrations. Future studies will also include investigation of GLP-1R peptide mediated alterations in the transcriptome at low glucose (2.8 mM glucose), mimicking the fasting state, normal glucose levels (5 mM glucose), as well as sustained elevated glucose levels that would mimic the pathophysiological state. These investigations at low, normal and sustained elevated glucose concentrations will help in defining the effects of long-acting GLP-1 peptide therapeutics including exenatide, liraglutide and dulaglutide. When administered, these long acting GLP-1 mimetics remain in circulation even in the fasting state altering the cellular RNA pool when administered chronically and therefore understanding how these drugs behave on these conditions is critical.

5.4.3. Differential regulation of transcriptome in presence of GLP-1 and oxytnomodulin

The endogenous ligand oxyntomodulin is a biased ligand compared to GLP-1 and exendin-4, and this has been identified in both recombinant systems (Koole *et al.*, 2010; Willard *et al.*, 2012) and in insulinoma cells (chapter 4). Analysis of the effect of oxntomodulin treatment on the trranscriptome identified some genes that were coregulated by ocyntomodulin, GLP-1 and exendin-4. This was expected as oxyntomodulin can also promote insulin secretion. However there were genes differentially modulated by oxyntomodulin compared to GLP-1 (63 at 30 min, 45 at 24 h) and exendin-4 (55 at 30 min, 39 at 24 h) (Figure 5.2). This data confirms previous reports, that oxyntomodulin is a biased agonist with the ability to present a different pattern of gene regulation, highlighting potential bias at the global level. At this point in time, analysis of the distinct functions and effects of these genes has not been preformed. This is due to the fact that oxyntomodulin can actually activate both the GLP-1R and the glucagon receptor at the concentrations used for this study and our transcriptome data revealed that these two receptors were expressed at equivalent levels in the insulinoma cells assessed. This is problematic as at this stage it is impossible to distinguish effects mediated by the GLP-1R and those mediated by the glucagon receptor. Future work, assessing the transcriptome (or at a minimum the designed RT qPCR array) will include knocking down either GLP-1R or glucagon receptor expression in the INS-1 832/3 cells using gene

editing technology (ie clustered regularly interspaced short palindromic repeats, CRISPR) and assessing the effects of oxytomodulin in each of these modified cell lines. This will provide the ability to assess global gene changes from activating the GLP-1R, the glucagon receptor or both receptors simultaneously by oxyntomodulin. Oxyntomodulin reduces body weight in obese subjects through increased energy expenditure and decreased energy intake (Pocai *et al.,* 2009). In addition, development of novel ligands that activate both the GLP-1R and glucagon receptor exhibit superior weight loss, lipid-lowering activity, and antihyperglycemic efficacy compared to agonists that activate the GLP-1R alone. These drugs also showed improvements in metabolic markers, including insulin, leptin, adionectin that were more pronounced than compared with activation of the GLP-1R alone. Additionally, studies in both GLP-1R KO mice and glucagon receptor KO mice showed that both receptors were required for this improved anti-obesity effect of these dual ligands (Pocai *et al.,* 2009). Therefore pursuing studies to understand global changes in gene expression profiles following activation of either GLP-1R, glucagon receptor or both simultaneously using oxyntomoduin may aid in identification of potential differences in the signalling pathways underlying the improved therapeutic effect of dual receptor agonism compared to activation of the GLP-1R alone.

5.5 CONCLUSION

In conclusion, the current transcriptome analysis provided a list of potential genes expressed in INS-1 832/3 cells that were regulated in response to various GLP-1R peptide agonists at different time points. This valuable dataset can be utilized for future functional studies in insulinoma cells to gain mechanistic insights into the physiological effects mediated by activation of the GLP-1R, along with acting as the basis for molecular target identification, new drug design and treatment for diabetes management. It also assisted in identifying the gaps in the existing knowledge both at the level of experimental designing and planning in terms of future studies required.

CHAPTER 6:
FUTURE DIRECTIONS AND PERSPECTIVES

Summary and Future directions

G protein-coupled receptors (GPCRs) belong to a superfamily of cell surface signalling proteins that have a pivotal role in many physiological functions and in multiple diseases. Classically, a number of drugs based on GPCRs have been developed for different indications including cardiovascular, metabolic, neurodegenerative, psychiatric, and oncologic diseases. Two striking paradigms associated with GPCRs that are been looked upon as potential approaches for development of new therapeutics include allosteric modulation and ligand-directed stimulus bias (Kenakin, 2005; Koole *et al.*, 2010; Wootten *et al.*, 2011).

Potential advantages of allosteric modulators include the scope of structural/conformational modifications that can independently control both affinity and efficacy separately, resulting in the fine-tuning of GPCR activity in a manner that depends on the presence of the endogenous ligand (Kenakin, 2009). Also, these molecules possess the capability of preserving temporal and spatial endogenous tone while fine-tuning the desired biological signalling outcome. Furthermore, the demonstration of a ceiling to the effect that is limited by the extent of cooperativity and the potential for enhanced subtype selectivity can aid in minimizing side effects (Melancol *et al.*, 2012).

The leveraging of biased signalling (promotion of one signalling pathway at the expense of another at the same receptor) and probe dependence (differing signalling outcomes based on the identity of the chosen orthosteric ligand at a given receptor) may be exploited as novel modalities toward the treatment of disease. In the context of GPCRs that were described as “undruggable”, including Class B GPCRs, there is scope for these to be modulated allosterically by synthetically accessible small molecules, opening a new avenue for drug development of targets that were previously unassailable (Wootten *et al.*, 2013).

Though the advantages that have propelled the exploitation of these intrinsic characteristics of GPCRs includes, filling in the gaps in knowledge of how these receptors function, as well as providing new opportunities in drug design, they also present a unique set of challenges, for instance, differences in the allosteric site of the same receptor between species that can affect the translational research. The potential of probe dependence of allosteric modulators necessitates careful selection of orthosteric ligands for assays. Allosteric modulator design may suffer from flat structure-activity relationships if only binding affinity and efficacy are considered without full appreciation of other key parameters such as the impact of co-operativity between allosteric and orthosteric ligand’s binding affinity and efficacy (Wild *et al.*, 2014). Further, the rate of target innovation is debilitated by poor and incomplete understanding of the pharmacology and signalling

mechanisms associated with these surface proteins, particularly in the context of physiological and/or pathophysiological signalling.

Most GPCR therapies are based on chronic exposure of the receptor to orthosteric ligands, which raises the important issue of understanding and investigating the long term regulatory processes of the receptors and the implications for decreased clinical efficacy due to desensitization and up/down regulation of the target receptor. Thus, it also emphasizes the increased complexity in how these receptors function, and the need for further investigations to assist in rational drug design and development.

The GLP-1R promotes glucoregulatory and insulinotropic effects in conjunction with modulating gastric emptying and appetite resulting in effective weight loss. These attributes of the GLP-1R make it an influential target to pursue for the development of effective therapeutics for metabolic disorders including diabetes and obesity. This thesis addresses key questions associated with GLP-1R activation and physiology in a cell system that mimics the functional attributes of pancreatic β-islets. Knowing that the GLP-1R activates a plethora of signalling pathways, various endogenous (GLP-1 and oxyntomodulin) and exogenous (exendin-4) orthosteric ligands, along with two identified allosteric modulators (compound 2 and BETP) were profiled and subsequently used to investigate the consequences of signalling bias, allosteric modulation and probe-dependence in physiologically relevant end points in both low and high glucose conditions. The downstream targeted signalling/events included both acute signalling pathways that have been assessed in recombinant cell systems (cAMP, pERK1/2 and calcium) for direct comparison to the CHO FlpIn cells, in addition to physiologically relevant endpoints downstream of GLP-1R activation, including insulin secretion and cell survival assays (proliferation and anti-apoptosis). Furthermore, to gain deeper insight, and to enable identification of the signalling networks/molecules that regulate the physiological functions mediated by GLP-1R activation and associated biased agonism, a global analysis of cellular response via transcriptomics was undertaken. Thus, this thesis employs the reductionist and non-reductionist/ emergentistic approaches to understand the glucoregulatory, proliferation and survival effects mediated by GLP-1R activation on model pancreatic islet cells.

The major drivers of our research were that the drugs used clinically (exenatide, liraglutide and dulaglutide) are suboptimal, as they are only available as injectable therapeutics, and they have been associated with side effect profiles including nausea, increased risk of pancreatitis, pancreatic and thyroid cancers. Thus, there is interest in development of orally available drugs that would overcome the side effect profiles. A number of small molecule ligands have been developed, two of

which, compound 2 and BETP, are allosteric and used in the current study. While these compounds are not drug-like molecules, they provide important research tools for understanding the pharmacology of this receptor. Furthermore, the GLP-1R system is quite complex and has multiple ligands including four endogenous forms of GLP-1, oxyntomodulin, and three clinically used mimetic peptide ligands, thus the prospect of ligand-directed stimulus bias needs to be considered, along with the potential for this to impact on physiological or pathological responses (May *et al.*, 2007; Koole *et al.*, 2010; Wootten *et al.*, 2013). To date, the majority of studies investigating biased agonism have been performed in recombinant cell systems that overexpress the GLP-1R. While these studies identify fingerprints for distinct ligands, and identify those that have biased signalling behaviour, it is unclear what the physiological impact of this is, and how this information may be used to exploit biased signalling therapeutically.

Despite a huge investment from the pharmaceutical industry, there has been a very slow rate in the development of an orally available, drug-like, molecule to activate or modulate the GLP-1R. While this speaks to the relative intractability of the target, such development is also limited by our relatively poor understanding of the physiology and signalling that occurs following GLP-1R activation. We believe that understanding the very basic pharmacology and physiology of this receptor and its signalling properties could aid in the identification and design of better therapeutics, both for peptidic and non-peptidic ligands.

This thesis expands the current knowledge around GLP-1R ligand-directed signalling bias and allostery. My work contributes to the elucidation of the various pathways that might be essential for GLP-1R-mediated physiological functions, and highlights the importance of understanding signalling bias profiles of ligands in different cell backgrounds. In addition, the assessment of signalling bias in two physiologically relevant glucose conditions highlights the need to not only understand the impact of signalling bias on physiologically relevant events, but also the context in which these phenomena are studied, as the bias observed changes under these different conditions.
During the course of optimization and ligand profiling (Chapter 3 and 4) we identified that cAMP accumulation, proliferation and anti-apoptosis that were facilitated by GLP-1, exendin-4 and oxyntomodulin, occurred independent of glucose concentration, whereas, augmentation of GSIS, $[Ca^{2+}]_i$ mobilization and aspects of the ERK1/2 phosphorylation kinetics were observed to be glucose-dependent. These distinct patterns of response cannot be determined using a transfected cell system that lacks the capacity to respond to glucose regulation. Nonetheless, there were parallels between elements of the response profile in CHO FlpIn cells with those in the INS-1 cells. For instance, transient activation of ERK1/2 in low glucose was observed to be consistent with the

profile of ERK1/2 observed in CHO FlpIn cells (Koole *et al.*, 2010; Wootten *et al.*, 2013). However, the full effects of GLP-1R function in β-islets, can only be observed in a system that displays glucose-dependence. We observed a characteristic profile of pERK1/2 in high glucose conditions represented by a transient peak, trough and sustained response that is distinct from the transient response seen in low glucose. Though transient and sustained activation of ERK1/2 have been physiologically associated with distinct physiological functions, such as insulin secretion and cell survival, respectively (Sonoda *et al.*, 2008; Quoyer *et al.*, 2010), the attenuation of glucose-mediated activation of ERK1/2 by GLP-1R peptide observed at 5 min appears to be a novel observation. Future studies need to be planned so as to explore the physiological relevance of this phase of ERK1/2, including studies in primary islets from mice and humans.

In order to quantify bias in the INS-1 832/3 cells, the Black/Leff operational model was applied to derive transduction ratios (Log tau/K_A), which are measures of the intrinsic efficacy that is unique for each ligand in individual pathways. Normalising the data to a reference ligand (GLP-1), and reference pathway (cAMP), can be utilized to generate a web of bias that gives us a visual representation of the amount of biased agonism engendered by the GLP-1R ligands. The first conclusion that we can draw from these webs (Figure 4.13) is that GLP-1R peptide ligands behave differently in the presence of different physiologically relevant glucose concentrations. In addition, there is also quite a distinct bias profile between the different ligands in the two glucose conditions. Specifically, in low glucose, oxyntomodulin is biased compared to the other ligands in that, for the same amount of cAMP, it produces significantly more transient ERK. This cAMP to transient ERK profile is also observed in high glucose, and is consistent with previous observations in a recombinant system (Koole *et al.*, 2010; Wootten *et al.*, 2013, Wootten *et al.*, 2013b).

However, the web of bias generated for high glucose conditions provides a higher level of information than previously obtained in recombinant cell systems. As expected, no peptide-mediated ligand-directed signalling bias was observed between cAMP and insulin responses, consistent with the known correlation between cAMP production and insulin secretion. However, a large degree of bias was observed between the ligands at the therapeutically relevant endpoints of proliferation and apoptosis that control beta cell mass. For equivalent amounts of cAMP generated, GLP-1 was a more efficient ligand, when compared to exendin-4 and oxyntomodulin, in promoting proliferation, and cell survival under conditions of staurosporine-induced apoptosis. This data suggests that in high glucose conditions, distinct mechanisms downstream of GLP-1R activation may be driving ligand-induced cell survival pathways to those in low glucose conditions where these ligands were equivalent at promoting cAMP, proliferation and anti-apoptosis. Moreover, no

bias with respect to cAMP was observed with any of the ligand for sustained ERK1/2 activation determined in presence of high glucose. This suggests that while sustained activation of pERK1/2 and production of cAMP may contribute to cell survival mechanisms that promote enhanced beta cell mass (Quoyer *et al.*, 2010; Yusta *et al.*, 2006), they may not be the most significant drivers of proliferative and anti-apoptotic effects mediated downstream of GLP-1R activation in high glucose conditions.

With small molecule ligands we see bias between cAMP production and insulin secretion that was not observed with the peptide ligands. Presumably there is also a large degree of bias in terms of apoptosis and proliferation as the small molecule ligands could not promote these responses at the concentrations tested. Thus, some elements of GLP-1R ligand bias for these compounds translates from recombinant cells (CHO FlpIn) to insulinoma cells (i.e. transient ERK and cAMP), however, in high glucose, while the transient pERK profile of both the small molecules was similar, BETP was unable to generate sustained ERK phosphorylation. In addition, BETP only allosterically modulated oxyntomodulin-mediated cAMP production and insulin secretion with no significant effect on the other two peptides. This action is consistent with previous in vivo and ex vivo studies with BETP (Willard *et al.*, 2012; Wootten *et al.*, 2013a).

Thus, deciphering pathways that may explain this bias associated with GLP-1R in different glucose conditions could provide avenues to improve profiles of potential drug candidates. It is therefore important to extend the types of studies described in this thesis (chapter 4) to explore additional downstream pathways of GLP-1R activation that may be linked to proliferative or inhibition of apoptotic pathways. Potentially, proteins such as PKC and Akt (protein kinase B), PI-3 kinase inhibition of caspases, NFkB and Foxo1 could play a role in these cell survival mechanisms mediated by the GLP-1R as activation of these proteins have been linked to proliferation and differentiation of β-cells (Urosova *et al.*, 2004; Brubaker *et al.*, 2004). The GLP-1R is known to activate PI-3 kinase, potentially through Gβγ and/or transactivation of EGRF that can result in activation of numerous downstream effectors including PKC, IRS2 and phosphorylation of Akt (protein kinase B) (Buteau *et al.*, 2003; Egan *et al.*, 2003), although to date, these have not been specifically linked to proliferation and apoptosis when activated downstream of the GLP-1R.

It has been reported that both intracellular calcium mobilisation and β-arrestin-1 are also important for GLP-1 mediated insulin secretion (Chapter 1 subsection 1.6.3.2). Interestingly, in CHO FlpIn cells BETP is biased towards both of these pathways, producing significantly more calcium and β-arrestin-1 recruitment for equivalent amounts of cAMP (compared to GLP-1) (Wootten *et al.*,

2012). In addition, in these recombinant cells, compound 2 is also biased towards β-arrestin1 recruitment (Wootten *et al.*, 2012), however, these compounds exhibit bias towards cAMP production over insulin secretion (Chapter 4, Figure 4.13). This may suggest that β-arrestin and intracellular calcium related pathways are not responsible for the observed differences the bias profile of these small molecule agonists compared to GLP-1. Nonetheless, given that the ligand bias profiles of the peptide ligands differ between the two glucose concentrations, it would be important to measure both calcium mobilisation and β-arrestin 1 recruitment in high and low glucose conditions in the insulinoma cells to establish if the bias profile observed in CHO FlpIn cells translates across the cell backgrounds before further conclusions around this can be drawn. Identification of relative contribution of individual signalling pathways that could account for the observed differences in the amount of cAMP vs insulin secretion produced by the small molecule ligands vs GLP-1 may aid in identification of additional signalling pathways could engender an improved therapeutic profile in terms of insulin secretion in drug development.

There is an interplay between allosteric interactions and biased signalling, in that the co-binding of an allosteric ligand, with an orthosteric ligand, has the potential to alter the orthosteric ligand signalling profile and this may occur in a pathway dependent manner, (one pathway can be enhanced while another pathway is reduced) or in a probe-dependent manner (May *et al.*, 2007). Understanding of both the probe- and pathway- dependent nature of allosteric modulation has the potential to affect the success/failure of allosteric drugs during clinical development. However, for these concepts to be exploited, a detailed understanding of what these allosteric ligands do to the signalling profile of orthosteric ligands, and particularly those that are endogenously expressed, are required.

In this thesis, I have demonstrated that BETP and Compound 2 induce altered signalling bias in a peptide-dependent manner in the INS-1832/3 cells. The results from these studies are summarized in Figures 6.1 and 6.2 that highlight the extent of modulation of various different signalling pathways. Furthermore, from these figures, it is clear to see that these allosteric effects are influenced by the glucose concentration in the cells, which has clinical relevance for the development of allosteric drugs. In low glucose, the allosteric effect of compound 2 was similar for all peptides with positive modulation of cAMP, and pERK1/2. However, the magnitude of the modulation varied between the ligands with exendin-4 not reaching statistical significance for any pathway. Comparison of the low glucose effects to the high glucose effects, reveals that there is quite a different profile and clear evidence of biased modulation between the three peptide ligands. Firstly, while both cAMP and transient ERK are positively modulated for both GLP-1 and

oxyntomodulin, only the oxyntomodulin-mediated insulin response was enhanced. In addition, there was some weak modulation of insulin with exendin-4, however, in this case, while transient pERK was modulated cAMP production was not. While cAMP is essential for insulin secretion, it is not the only effector modulating the magnitude of effect (Chapter 1, section 1.6.3.1). The data support a role for factors other than cAMP being required for insulin secretion, because there is a disconnect between the level of compound 2-mediated modulation of cAMP production versus modulation of insulin secretion across the three peptides; only in the case of oxyntomodulin was the magnitude of effect equivalent for these two pathways (Figure 6.1).

With BETP as the allosteric ligand, a distinct pattern of modulation of the peptides was seen, in both low and high glucose (Figure 6.2). In low glucose, this was most evident in the modulation of cAMP accumulation, where oxyntomodulin was the only peptide with enhanced signalling. In high glucose, further differences in the extent of modulation of insulin secretion were observed (compare Figure 6.1 and 6.2), though, like compound 2, transient pERK was positively modulated by BETP for most peptides. Interestingly, BETP also modulated the unexpected reduction in glucose-stimulated pERK1/2, seen at the 5 min time point, where BETP enhanced the pEC_{50} of the inverse agonism of all three peptide ligands. In contrast, Compound 2 was unable to modulate this inhibitory response of the orthosteric ligands.

Collectively, the data illustrate the likelihood that allosteric ligands will change the profile of endogenous ligand responses, with parallel effects on transient pERK seen with GLP-1 and oxyntomodulin, but preferential enhancement of oxyntomodulin-mediated cAMP production and insulin secretion. Although not studied in the INS-1 832/3 cells, BETP also alters the signalling profile of the GLP-1 metabolite, GLP-1(9-36)NH_2, with selective and potent enhancement of cAMP accumulation that is linked to enhanced insulin secretion (Wootten *et al.*, 2012), thus how this peptide functions in physiological target cells in the presence of modulators is an important area for future study, in the context of future allosteric drug development.

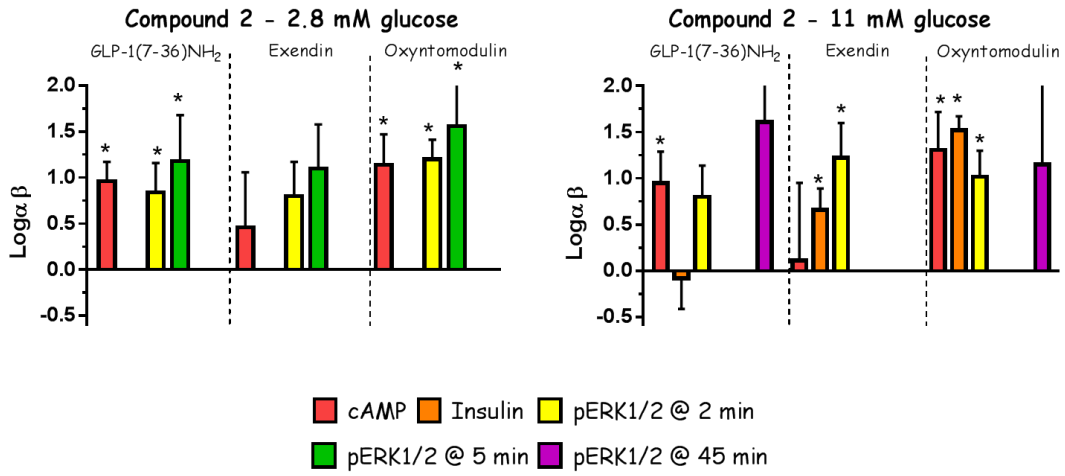

Figure 6.1 Probe dependence, signal bias and physiological relevance in presence of compound 2 and GLP-1R peptides. Cooperativity values (logαβ) derived from application of the operational model of allostery to concentration response data for various different peptide agonists in the presence of compound 2 using multiple functional outputs. These were derived from the data presented in chapter 4.

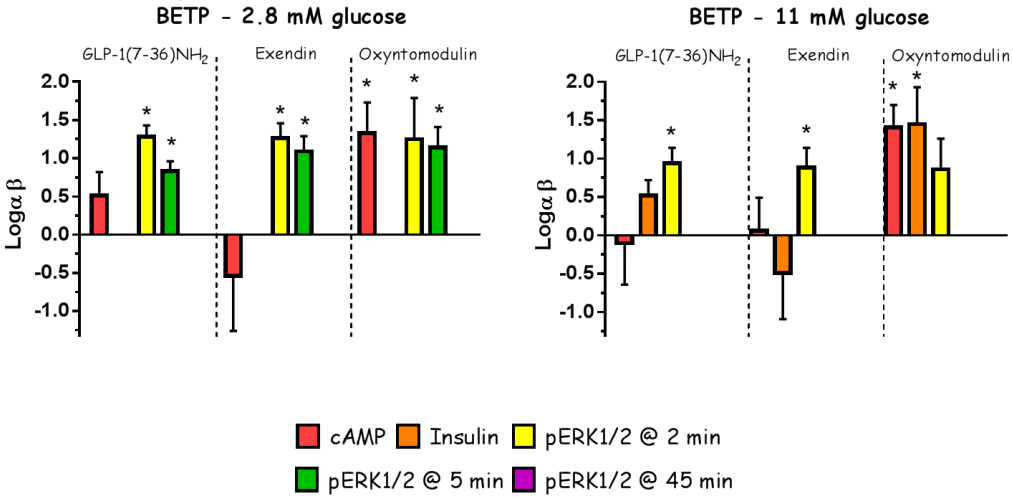

Figure 6.2 Probe dependence, signal bias and physiological relevance in presence of BETP and GLP-1R peptides. Cooperativity values (logαβ) derived from application of the operational model of allostery to concentration response data for various different peptide agonists in the presence of BETP using multiple functional outputs. These were derived from the data presented in chapter 4.

Currently, based on the data in this thesis, it is still not clear what are the most important pathways for therapeutic modulation. As mentioned earlier, calcium signalling, β-arrestin-1 and sustained pERK1/2 have been reported to have a role in insulin secretion, while the convergent network of pathways linked to other functional endpoints (proliferation, apoptosis, insulin synthesis) are yet to be fully elucidated. Analysis of β-arrestin recruitment and analysis of the pathways downstream of this scaffolding protein will be important for understanding of these processes, but additional knowledge of how β-islet-like cells more broadly respond to peptide and non-peptidic ligands is also required, and this formed the basis for work in chapter 5.

Thus, in this thesis I have identified additional information to that previously known around biased ligands and allosteric modulation. In addition, while the work presented here explores biased signalling and allostery to try to understand elements of GLP-1R signalling in β-islets, for many therapeutically important effects of GLP-1R activation, including decreased appetite, delayed gastric emptying, cardio-protective and neuroprotective effects, the underlying GLP-1R mediated signalling pathways are very poorly studied, and this requires further exploration. From the results presented in chapter 4, it could be predicted that the GLP-1R will display distinct signalling profiles depending on its location in the body, and the nature of the activating ligand. Therefore therapeutic targeting of the GLP-1R for specific diseases such as diabetes, neurodegeneration or cardiovascular disease will require an understanding of the importance of different signalling cascades and how these are affected by biased agonists in the different tissue beds, such as the pancreas, brain and heart.

All the studies performed in Chapters 3 and 4, and the significant findings discussed above, were the result of reductionist approach in that we have selected pathways to assess, based on those we know have physiological relevance. However, we can only get limited information from this and it also has been difficult to link effects of ligands (particularly allosteric effects) on acute signalling pathways to physiological endpoints. This is because GLP-1R signalling is very complex. In an attempt to overcome this I employed a non-reductionist approach in Chapter 5, where signalling was assessed at a global level using transcriptomics.

The analysis of global sequencing of RNA identified a large set of genes whose expression was regulated by the binding of both GLP-1 and exendin-4 to the GLP-1R on INS-1 832/3 cells. The elucidation of this complex gene-regulatory network is essential for a better understanding of the physiological and pharmacological effects of GLP-1, as well as for deciphering the mechanisms

underlying the diverse repertoire of GLP-1 action in pancreatic β-islets. Furthermore, the work provides an initial window into the extent of genes differentially regulated by the two peptide ligands, and networks that might explain some of the biased agonism displayed by these peptides.

Various studies performed in-vitro using recombinant and primary cell lines and ex-vivo on isolated pancreatic β-islets, as well as limited data from whole animal models and clinical trials, suggests that activation of GLP-1R, promotes β-cell mass, and that this occurs by increasing β-cell proliferation, inhibiting β-cell apoptosis and inducing the differentiation of β-cells from progenitor cells (Quoyer *et al.*, 2010; Yusta *et al.*, 2006, Puddu *et al.*, 2013). While data from these varied studies implicate multitude of factors and signalling intermediates in these events (Chapter 1, section 1.6.3.3), it is clear that preservation/growth of β-cell mass requires a complex interplay of pathways at the cellular and molecular levels. In Chapter 5, transcriptomic data identified global changes in gene expression downstream of GLP-1R activation in insulinoma cells and many of these gene expression changes can be linked to functional consequences, such as cell survival and endocrine functions.

To understand the biased agonism exhibited at the GLP-1R by different ligands (Table 6.1 and 6.2), at a global level, oxyntomodulin and exendin-4 were included along with GLP-1 in the study. However, the transcriptome analysis revealed that both the GLP-1R and the glucagon receptor are expressed in INS-1 832/3 cells at the same levels, complicating the interpretation of data from the oxyntomodulin experiments, as this ligand binds to both of these receptors. As a consequence, the gene regulation observed for oxyntomodulin likely represents a cumulative response to activation of both receptors, and thus, discriminating bias at the GLP-1R from the co-activation of the glucagon receptor requires additional experiments. Future experiments, to explore the GLP-1R dependent pattern of transcriptional changes mediated by oxyntomodulin, could include (i) knocking down the glucagon receptors in INS-1 832/3 cells using siRNA, or by gene deletion using CRISP/Cas9 technology, or (ii) blocking/inhibiting the activation of glucagon receptor by oxyntomodulin using selective antagonists. A potential flaw accompanying the second approach is the limited knowledge of the potential of the antagonist/inhibitors to independently elicit a response (i.e. they may have intrinsic efficacy for unexplored pathways). Additional experiments could be performed on islets derived from both GLP-1R KO and glucagon receptor KO animals, in addition to wild type animals to distinguish effects of oxyntomodulin mediated by each of these receptors.

A substantial number of genes were differentially regulated by exendin-4 and GLP-1 at both 30 min and 24 h. These genes may contribute to the signalling bias displayed by these peptide agonists at

GLP-1R. Thus, future follow up studies could include use of various pharmacological (pathway inhibitors), siRNA and proteomic approaches to provide more definitive links between the transcriptomic changes and the signalling events related to biased agonism.

Furthermore, as presented and identified in chapter 4, the glucose levels regulate the nature of the biased agonism seen at GLP-1R, and as such, there arises a need to investigate GLP-1R peptide mediated alterations in the transcriptome at low glucose (2.8 mM glucose), indicating the physiological fasting state as well as at normal physiological glucose levels (5 mM glucose) and both acute and sustained high glucose conditions to mimic the normal physiological responses rises in glucose levels, and the pathophysiological state observed in individuals with poorly controlled diabetes. These investigations at low and normal glucose concentrations will help in understanding the effects of long-acting GLP-1 peptide therapeutics, including FDA approved drugs such as exenatide, liraglutide and dulaglutide that, when administered to diabetic/obese subjects, would remain in the biological system even after achieving gluco-homeostasis. Thus, they could have distinct effects on the cellular RNA pool related to their different pharmacokinetics, when administered chronically.

A number of the genes as listed in Table 5.4 (highlighted in pink) including EGFR, FOS, IGF-1R, IGF2, GCK, BCL2, EGR1 and KCNQ1, have been previously reported to be either regulated at the gene level or are known to be involved in GLP-1R function and were expected to be expressed in the INS-1 832/3 cells, and regulated in response to GLP-1 (Cornu *et al.*, 2009; Park *et al.*, 2012; Quoyer *et al.*, 2010; Yamagata *et al.*, 2011). In addition to these genes, we also identified multiple genes that have been linked to either cell survival mechanisms or differentiation specifically in beta islets cells but that not been previously linked to GLP-1R signalling, and these include PAX6, TGM1 and SOCS3. Moreover, there were also a number of genes for GPCRs and GPCR ligands that were up or down-regulated and comprise ADM, CCKAR, GPR27, CHRNA2, Taar4, Tas1R, GIP, RAMP1, and CALCR. This implies that perhaps there is some crosstalk between the GLP-1R and other GPCR or GPCR-mediated signalling, that could be of interest for drug development, and may be worth investigating further to understand the extent of such interaction.

Future studies can also be designed to target identification of differentially regulated transcription factors. Regulation by TFs or drugs does not only have effects on one pathway but also has effects on downstream processes. This integration leads to improved insight and also a much clearer illustration of the overall process, and the most important elements.

While the current transcriptomic analysis provides initial insight into peptide-dependent gene regulation, the work requires validation and further exploration of the time and concentration dependent components of ligand action. Consequently, data from the studies in Chapter 5 was used to design gene arrays to confirm the transcriptomic data and to assess biased agonism at the global level. The genes for the arrays were selected based on their association with functions of cell to cell signalling, signal transduction, proliferation, cell death and survival and also included some that have been previously linked to type 2 diabetes. This may be used to identify ligand response fingerprints including that of endogenous peptides, clinically used peptide mimetics, and small molecule agonists, which can be linked to physiological profiling of ligands in *in vivo* and in *ex vivo* experiments.

In conclusion, this thesis expanded the knowledge of GLP-1 signalling using both reductionist and non-reductionist approaches with regard to signal bias, allosteric modulation and probe dependence associated with GLP-1R in a system that possesses glucose-dependence, and has the hallmarks of native β-islet cells.

REFERENCES

Abdulla, F. A.; Smith, P. A., Nociceptin inhibits T-type Ca2+ channel current in rat sensory neurons by a G-protein-independent mechanism. *Journal of Neuroscience***1997,** 17, (22), 8721-8728.

Abdul-Ridha, A.; Lane, J. R.; Sexton, P. M.; Canals, M.; Christopoulos, A., Allosteric modulation of a chemogenetically modified G protein-coupled receptor. *Molecular Pharmacology***2013,** 83, (2), 521-530.

Abe, H.; Urao, T.; Ito, T.; Seki, M.; Shinozaki, K.; Yamaguchi-Shinozaki, K., Arabidopsis AtMYC2 (bHLH) and AtMYB2 (MYB) function as transcriptional activators in abscisic acid signaling. *The Plant Cell* **2003,** 15, (1), 63-78.

AC't Hoen, P.; Ariyurek, Y.; Thygesen, H. H.; Vreugdenhil, E.; Vossen, R. H.; de Menezes, R. X.; Boer, J. M.; van Ommen, G.-J. B.; den Dunnen, J. T., Deep sequencing-based expression analysis shows major advances in robustness, resolution and inter-lab portability over five microarray platforms. *Nucleic Acids Research***2008,** 36, (21), e141-e141.

Adachi, T.; Kar, S.; Wang, M.; Carr, B. I., Transient and sustained ERK phosphorylation and nuclear translocation in growth control. *Journal of Cellular Physiology* **2002,** 192, (2), 151-159.

Adler, E.; Hoon, M. A.; Mueller, K. L.; Chandrashekar, J.; Ryba, N. J. P.; Zuker, C. S., A novel family of mammalian taste receptors. *Cell* **2000,** 100, (6), 693-702.

Ahima, R. S.; Lazar, M. A., Adipokines and the peripheral and neural control of energy balance. *Molecular Endocrinology***2008,** 22, (5), 1023-1031.

Ahn, S.; Kim, J.; Hara, M. R.; Ren, X. R.; Lefkowitz, R. J., beta-Arrestin-2 Mediates Anti-apoptotic Signaling through Regulation of BAD Phosphorylation. *Journal Biological Chemistry***2009,** 284, (13), 8846-8856.

Ahrén, B., Glucagon-like peptide-1 (GLP-1): A gut hormone of potential interest in the treatment of diabetes. *BioEssays* **1998,** 20, (8), 642-651.

Ahren, B.; Hughes, T. E., Inhibition of dipeptidyl peptidase-4 augments insulin secretion in response to exogenously administered glucagon-like peptide-1, glucose-dependent insulinotropic polypeptide, pituitary adenylate cyclase-activating polypeptide, and gastrin-releasing peptide in mice. *Endocrinology* **2005,** 146, (4), 2055-9.

Ahren, B.; Schmitz, O., GLP-1 receptor agonists and DPP-4 inhibitors in the treatment of type 2 diabetes. *Hormone and Metabolic Research***2004,** 36, (11-12), 867-76.

Akeno, N.; Smith, E. P.; Stefan, M.; Huber, A. K.; Zhang, W.; Keddache, M.; Tomer, Y., IFN-α mediates the development of autoimmunity both by direct tissue toxicity and through immune cell recruitment mechanisms. *The Journal of Immunology* **2011,** 186, (8), 4693-4706.

Alarcon, C.; Wicksteed, B. & Rhodes, C. Exendin 4 controls insulin production in rat islet beta cells predominantly by potentiation of glucose-stimulated proinsulin biosynthesis at the translational level. *Diabetologia* **2006,** 49(12), 2920-2929.

Alcantara, A. I.; Morales, M.; Delgado, E.; Lopez-Delgado, M. I.; Clemente, F.; Luque, M. A.; Malaisse, W. J.; Valverde, I.; Villanueva-Penacarrillo, M. L., Exendin-4 agonist and exendin(9-39)amide antagonist of the GLP-1(7-36)amide effects in liver and muscle. *Archivesof Biochemistryand Biophysics***1997,** 341, (1), 1-7.

Alejandro, E. U.; Kalynyak, T. B.; Taghizadeh, F.; Gwiazda, K. S.; Rawstron, E. K.; Jacob, K. J.; Johnson, J. D., Acute insulin signaling in pancreatic beta-cells is mediated by multiple Raf-1 dependent pathways. *Endocrinology* **2010,** 151, (2), 502-12.

Ali, M. S.; Sayeski, P. P.; Bernstein, K. E., Jak2 acts as both a STAT1 kinase and as a molecular bridge linking STAT1 to the angiotensin II AT(1) receptor. *Journal of Biological Chemistry***2000,** 275, (20), 15586-15593.

Ali, M. S.; Sayeski, P. P.; Dirksen, L. B.; Hayzer, D. J.; Marrero, M. B.; Bernstein, K. E., Dependence on the motif YIPP for the physical association of Jak2 kinase with the intracellular carboxyl tail of the angiotensin II AT(1) receptor. *Journal of Biological Chemistry***1997,** 272, (37), 23382-23388.

Allen, J. A.; Roth, B. L., Strategies to Discover Unexpected Targets for Drugs Active at G Protein-Coupled Receptors. In *Annual Review of Pharmacology and Toxicology, Vol 51, 2011*, Cho, A. K., Ed. Annual Reviews: Palo Alto, 2011; Vol. 51, pp 117-144.

Alonso, L. C.; Yokoe, T.; Zhang, P.; Scott, D. K.; Kim, S. K.; O'Donnell, C. P.; Garcia-Ocaña, A., Glucose infusion in mice a new model to induce β-cell replication. *Diabetes* **2007,** 56, (7), 1792-1801.

Amori, R. E.; Lau, J.; Pittas, A. G., Efficacy and safety of incretin therapy in type 2 diabetes: systematic review and meta-analysis. *JAMA* **2007,** 298, (2), 194-206.

Andersen, D. K.; Elahi, D.; Brown, J. C.; Tobin, J. D.; Andres, R., Oral glucose augmentation of insulin secretion. Interactions of gastric inhibitory polypeptide with ambient glucose and insulin levels. *The Journal of Clinical Investigation***1978,** 62, (1), 152-61.

Arakawa, M.; Mita, T.; Azuma, K.; Ebato, C.; Goto, H.; Nomiyama, T.; Fujitani, Y.; Hirose, T.; Kawamori, R.; Watada, H., Inhibition of monocyte adhesion to endothelial cells and attenuation of atherosclerotic lesion by a glucagon-like peptide-1 receptor agonist, exendin-4. *Diabetes* **2010,** 59, (4), 1030-7.

Arkan, M. C.; Hevener, A. L.; Greten, F. R.; Maeda, S.; Li, Z.-W.; Long, J. M.; Wynshaw-Boris, A.; Poli, G.; Olefsky, J.; Karin, M., IKK-beta links inflammation to obesity-induced insulin resistance. *Nature Medicine***2005,** 11, 191-198.

Arnette, D.; Gibson, T. B.; Lawrence, M. C.; January, B.; Khoo, S.; McGlynn, K.; Vanderbilt, C. A.; Cobb, M. H., Regulation of ERK1 and ERK2 by glucose and peptide hormones in pancreatic beta cells. *Journal of Biological Chemistry***2003,** 278, (35), 32517-25.

Arnés, L.; Moreno, P.; Nuche-Berenguer, B.; Valverde, I.; & Villanueva-Peñacarrillo, M. L.. Effect of exendin-4 treatment upon glucose uptake parameters in rat liver and muscle, in normal and type 2 diabetic state. *Regulatory peptides,***2009**, 153(1), 88-92.

Arnette, D.; Gibson, T. B.; Lawrence, M. C.; January, B.; Khoo, S.; McGlynn, K.; Vanderbilt, C. A.; Cobb, M. H., Regulation of ERK1 and ERK2 by glucose and peptide hormones in pancreatic β cells. *Journal of Biological Chemistry***2003,** 278, (35), 32517-32525.

Arnolds, S.; Dellweg, S.; Clair, J.; Dain, M. P.; Nauck, M. A.; Rave, K.; Kapitza, C., Further improvement in postprandial glucose control with addition of exenatide or sitagliptin to combination therapy with insulin glargine and metformin: a proof-of-concept study. *Diabetes Care* **2010,** 33, 1509-1515.

Arnolds, S.; Heckermann, S.; Heise, T.; Sawicki, P. T., Spectrum of Diabetes Research does not Reflect Patients' Scientific Preferences: A Longitudinal Evaluation of Diabetes Research Areas 2010-2013 vs. a Cross-sectional Survey in Patients with Diabetes. *Experimental and Clinical Endocrinology and Diabetes* **2015,** 123, (5), 299-302.

Arnolds, S.; Kuglin, B.; Kapitza, C.; Heise, T., How pharmacokinetic and pharmacodynamic principles pave the way for optimal basal insulin therapy in type 2 diabetes. *International Journal of Clinical Practice***2010,** 64, (10), 1415-24.

Aronoff, S. L.; Berkowitz, K.; Shreiner, B.; Want, L., Glucose metabolism and regulation: beyond insulin and glucagon. *Diabetes Spectrum* **2004,** 17, (3), 183-190.

Asfari, M.; Janjic, D.; Meda, P.; Li, G.; Halban, P. A.; Wollheim, C. B., Establishment of 2-mercaptoethanol-dependent differentiated insulin-secreting cell lines. *Endocrinology* **1992,** 130, (1), 167-178.

Assefa, Z.; Lavens, A.; Steyaert, C.; Stangé, G.; Martens, G. A.; Ling, Z.; Hellemans, K.; Pipeleers, D., Glucose Regulates Rat Beta Cell Number through Age-Dependent Effects on Beta Cell Survival and Proliferation. *PLoS One* **2014,** 9, (1).

Assmann, A.; Ueki, K.; Winnay, J. N.; Kadowaki, T.; Kulkarni, R. N., Glucose effects on beta-cell growth and survival require activation of insulin receptors and insulin receptor substrate 2. *Molecular and Cellular Biology* **2009,** 29, (11), 3219-3228.

Atz, M.; Walsh, D.; Cartagena, P.; Li, J.; Evans, S.; Choudary, P.; Overman, K.; Stein, R.; Tomita, H.; Potkin, S., Methodological considerations for gene expression profiling of human brain. *Journal of Neuroscience Methods* **2007,** 163, (2), 295-309.

Auer, P. L.; Doerge, R., Statistical design and analysis of RNA sequencing data. *Genetics* **2010,** 185, (2), 405-416.

Auer, P. L.; Srivastava, S.; Doerge, R., Differential expression—the next generation and beyond. *Briefings in Functional Genomics* **2011**, elr041.

Aulinger, B. A.; Bedorf, A.; Kutscherauer, G., de Heer; J., Holst, J. J.; Göke, B. & Schirra, J.. Defining the role of GLP-1 in the enteroinsulinar axis in type 2 diabetes using DPP-4 inhibition and GLP-1 receptor blockade. *Diabetes* **2014**, 63(3), 1079-1092.

Aviv, V.; Meivar-Levy, I.; Rachmut, I. H.; Rubinek, T.; Mor, E.; Ferber, S., Exendin-4 promotes liver cell proliferation and enhances the PDX-1-induced liver to pancreas transdifferentiation process. *Journal of Biological Chemistry***2009,** 284, (48), 33509-33520.

Avruch, J., MAP kinase pathways: the first twenty years. *Biochimica et Biophysica Acta (BBA)-Molecular Cell Research* **2007,** 1773, (8), 1150-1160.

Ayala, J. E.; Bracy, D. P.; James, F. D.; Burmeister, M. A.; Wasserman, D. H.; Drucker, D. J., Glucagon-like peptide-1 receptor knockout mice are protected from high-fat diet-induced insulin resistance. *Endocrinology* **2010,** 151, (10), 4678-87.

Baggio, L. L.; Drucker, D. J., Biology of incretins: GLP-1 and GIP. *Gastroenterology* **2007,** 132, (6), 2131-57.

Baggio, L. L.; Huang, Q.; Brown, T. J.; Drucker, D. J., Oxyntomodulin and glucagon-like peptide-1 differentially regulate murine food intake and energy expenditure. *Gastroenterology* **2004,** 127, 546-558.

Baggio, L. L.; Kim, J. G.; Drucker, D. J., Chronic exposure to GLP-1R agonists promotes homologous GLP-1 receptor desensitization in vitro but does not attenuate GLP-1R-dependent glucose homeostasis in vivo. *Diabetes* **2004,** 53 Suppl 3, S205-14.

Baggio, L. L.; Kim, J.-G.; Drucker, D. J., Chronic exposure to GLP-1r agonists promotes homologous GLP-1 receptor desensitization in vitro but does not attenuate GLP-1r–dependent glucose homeostasis in vivo. *Diabetes* **2004,** 53, (suppl 3), S205-S214.

Baldissera, F. G.; Holst, J. J.; Knuhtsen, S.; Hilsted, L, & Nielsen, O. V.. Oxyntomodulin (glicentin-(33–69)): pharmacokinetics, binding to liver cell membranes, effects on isolated perfused pig pancreas, and secretion from isolated perfused lower small intestine of pigs. *Regulatory peptides* **1988**, 21(1), 151-166.

Ballesteros, J. A.; Shi, L.; Javitch, J. A., Structural mimicry in G protein-coupled receptors: Implications of the high-resolution structure of rhodopsin for structure-function analysis of rhodopsin-like receptors. *Molecular Pharmacology* **2001,** 60, (1), 1-19.

Ban, K.; Kim, K. H.; Cho, C. K.; Sauvé, M.; Diamandis, E. P.; Backx, P. H.; Drucker, D. J.; Husain, M., Glucagon-like peptide (GLP)-1(9-36)amide-mediated cytoprotection is blocked by exendin(9-39) yet does not require the known GLP-1 receptor. *Endocrinology* **2010,** 151, (4), 1520-1531.

Ban, K.; Noyan-Ashraf, M. H.; Hoefer, J.; Bolz, S. S.; Drucker, D. J.; Husain, M., Cardioprotective and vasodilatory actions of glucagon-like peptide1receptor are mediated through both glucagon-like peptide 1 receptor-dependent and -independent pathways. *Circulation* **2008,** 117, 2340-2350.

Barabási, A.-L.; Gulbahce, N.; Loscalzo, J., Network medicine: a network-based approach to human disease. *Nature Reviews Genetics* **2011,** 12, (1), 56-68.

Barnes, W. G.; Reiter, E.; Violin, J. D.; Ren, X. R.; Milligan, G.; Lefkowitz, R. J., beta-arrestin 1 and G(alpha q/11) coordinately activate RhoA and stress fiber formation following receptor stimulation. *Journal of Biological Chemistry***2005,** 280, (9), 8041-8050.

Barragan, J. M.; Eng, J.; Rodriguez, R.; Blazquez, E., Neural contribution to the effect of glucagon-like peptide-1-(7-36) amide on arterial blood pressure in rats. *The American Journal of Physiology* **1999,** 277, (5 Pt 1), E784-91.

Barragan, J. M.; Rodriguez, R. E.; Blazquez, E., Changes in arterial blood pressure and heart rate induced by glucagon-like peptide-1-(7-36) amide in rats. *The American Journal of Physiology***1994,** 266, (3 Pt 1), E459-66.

Bastien-Dionne, P. O.; Valenti, L.; Kon, N.; Gu, W.; Buteau, J., Glucagon-like peptide 1 inhibits the sirtuin deacetylase SirT1 to stimulate pancreatic beta-cell mass expansion. *Diabetes* **2011,** 60, (12), 3217-22.

Baud, V.; Chissoe, S. L.; Viegaspequignot, E.; Diriong, S.; Nguyen, V. C.; Roe, B. A.; Lipinski, M., EMR1, An unusual member in the family of hormone receptors with 7 transmembrane segments.*Genomics* **1995,** 26, (2), 334-344.

Bavec, A.; Hällbrink, M.; Langel, Ü.; Zorko, M., Different role of intracellular loops of glucagon-like peptide-1 receptor in G-protein coupling. *Regulatory Peptides* **2003,** 111, (1), 137-144.

Beane, J.; Vick, J.; Schembri, F.; Anderlind, C.; Gower, A.; Campbell, J.; Luo, L.; Zhang, X. H.; Xiao, J.; Alekseyev, Y. O., Characterizing the impact of smoking and lung cancer on the airway transcriptome using RNA-Seq. *Cancer Prevention Research* **2011,** 4, (6), 803-817.

Beaulieu, J. M.; Sotnikova, T. D.; Marion, S.; Lefkowitz, R. J.; Gainetdinov, R. R.; Caron, M. G., An Akt/beta-arrestin 2/PP2A signaling complex mediates dopaminergic neurotransmission and behavior. *Cell* **2005,** 122, (2), 261-273.

Becamel, C.; Figge, A.; Poliak, S.; Dumuis, A.; Peles, E.; Bockaert, J.; Lubbert, H.; Ullmer, C., Interaction of serotonin 5-hydroxytryptamine type 2C receptors with PDZ10 of the multi-PDZ domain protein MUPP1. *Journal of Biological Chemisttry***2001,** 276, (16), 12974-12982.

Bell, G. I.; Sanchez-Pescador, R.; Laybourn, P. J.; Najarian, R. C., Exon duplication and divergence in the human preproglucagon gene. *Nature* **1983,** 304, 368-371.

Benes, C.; Poitout, V.; Marie, J.; Martin-Perez, J.; Roisin, M.; Fagard, R., Mode of regulation of the extracellular signal-regulated kinases in the pancreatic β-cell line MIN6 and their implication in the regulation of insulin gene transcription. *Biochemical Journal***1999,** 340, 219-225.

Benes, C.; Roisin, M. P.; Van Tan, H.; Creuzet, C.; Miyazaki, J.-i.; Fagard, R., Rapid activation and nuclear translocation of mitogen-activated protein kinases in response to physiological concentration of glucose in the MIN6 pancreatic β cell line. *Journal of Biological Chemisttry***1998,** 273, (25), 15507-15513.

Benito, E.; Blazquez, E.; Bosch, M. A., Glucagon-like peptide-1-(7-36)amide increases pulmonary surfactant secretion through a cyclic adenosine 3',5'-monophosphate-dependent protein kinase mechanism in rat type II pneumocytes. *Endocrinology* **1998,** 139, (5), 2363-8.

Berg, J. K.; Shenouda, S. K.; Heilmann, C. R.; Gray, A. L.; Holcombe, J. H., Effects of exenatide twice daily versus sitagliptin on 24-h glucose, glucoregulatory and hormonal measures: a randomized, double-blind, crossover study. *Diabetes, Obesity &Metabolism* **2011,** 13, (11), 982-9.

Berger, B.; Peng, J.; Singh, M., Computational solutions for omics data. *Nature Reviews Genetics* **2013,** 14, (5), 333-346.

Bernal-Mizrachi, E.; Wen, W.; Srinivasan, S.; Klenk, A.; Cohen, D.; Permutt, M. A., Activation of Elk-1, an Ets transcription factor, by glucose and EGF treatment of insulinoma cells. *American Journal of Physiology-Endocrinology and Metabolism* **2001,** 281, (6), E1286-E1299.

Bernal-Mizrachi, E.; Wice, B.; Inoue, H.; Permutt, M. A., Activation of serum response factor in the depolarization induction of Egr-1 transcription in pancreatic islet β-cells. *Journal of Biological Chemisttry***2000,** 275, (33), 25681-25689.

Bertin, R.; Roscigno, M.; Colombo, R.; Spagnolo, D.; Ferrari, A.; Rigatti, P., Herniation of the amniotic sac into the bladder through a vesico-uterine fistula in the 32nd week of pregnancy. *BJOG - An International Journal of Obstetrics and Gynaecology***2001,** 108, (12), 1300-1.

Bhanot, P.; Brink, M.; Samos, C. H.; Hsieh, J. C.; Wang, Y. S.; Macke, J. P.; Andrew, D.; Nathans, J.; Nusse, R., A new member of the frizzled family from Drosophila functions as a Wingless receptor. *Nature* **1996,** 382, (6588), 225-230.

Bhavsar, S.; Mudaliar, S.; Cherrington, A., Evolution of exenatide as a diabetes therapeutic. *Current Diabetes Reviews* **2013,** 9, (2), 161-93.

Bird, P. A.; Shnier, R.; Edmonds, J. P., Questioning the sensitivity of magnetic resonance imaging in early septic spondylodiscitis. *Journal of Clinical Rheumatology***2001,** 7, (3), 184-7.

Bjarnadottir, T. K.; Fredriksson, R.; Hoglund, P. J.; Gloriam, D. E.; Lagerstrom, M. C.; Schioth, H. B., The human and mouse repertoire of the adhesion family of G-protein-coupled receptors. *Genomics* **2004,** 84, (1), 23-33.

Black, J.; Leff, P., Operational models of pharmacological agonism. *Proceedings of the Royal Society of London B: Biological Sciences* **1983,** 220, (1219), 141-162.

Black, J. W.; Leff, P., Operational models of pharmacological agonism. *Proceedings of the Royal Society of London. Series B, Biological sciences* **1983,** 220, (1219), 141-62.

Block, G. A.; Martin, K. J.; de Francisco, A. L.; Turner, S. A.; Avram, M. M.; Suranyi, M. G.; Hercz, G.; Cunningham, J.; Abu-Alfa, A. K.; Messa, P., Cinacalcet for secondary hyperparathyroidism in patients receiving hemodialysis. *New England Journal of Medicine* **2004,** 350, (15), 1516-1525.

Bataille, D.; Tatemoto, K.; Gespach, C.; Jörnvall, H.; Rosselin, G. & Mutt, V. Isolation of glucagon-37 (bioactive enteroglucagon/oxyntomodulin) from porcine jejuno-ileum. *FEBS letters* **1982**, 146(1), 79-86.

Bode, H.-P.; Moormann, B.; Dabew, R.; Göke, B., Glucagon-Like Peptide 1 Elevates Cytosolic Calcium in Pancreaticβ-Cells Independently of Protein Kinase A 1. *Endocrinology* **1999,** 140, (9), 3919-3927.

Bonner-Weir, S.; Smith, F. E., Islet cell growth and the growth factors involved. *Trends in Endocrinology & Metabolism* **1994,** 5, (2), 60-64.

Bootman, M. D.; Berridge, M. J., The elemental principles of calcium signaling. *Cell* **1995,** 83, (5), 675-8.

Bose, A. K.; Mocanu, M. M.; Carr, R. D.; Yellon, D. M., Glucagon like peptide-1 is protective against myocardial ischemia/reperfusion injury when given either as a preconditioning mimetic or at reperfusion in an isolated rat heart model. *Cardiovascular drugs and therapy / sponsored by the International Society of Cardiovascular Pharmacotherapy* **2005,** 19, (1), 9-11.

Boudin, H.; Craig, A. M., Molecular determinants for PICK1 synaptic aggregation and mGluR7a receptor coclustering. *Journal of Biological Chemisttry***2001,** 276, (32), 30270-30276.

Bourne, H. R.; Sanders, D. A.; McCormick, F., The GTPase superfamily - conserved structure and molecular mechanism.*Nature* **1991,** 349, (6305), 117-127.

Boushey, R. P.; Yusta, B.; & Drucker, D. J. Glucagon-like peptide 2 decreases mortality and reduces the severity of indomethacin-induced murine enteritis. *American Journal of Physiology-Endocrinology and Metabolism* **1999,** 277(5), E937-E947.

Boushey, R. P.; Yusta, B. & Drucker, D. J. Glucagon-like peptide (GLP)-2 reduces chemotherapy-associated mortality and enhances cell survival in cells expressing a transfected GLP-2 receptor. *Cancer research* **2001**, 61(2), 687-693.

Boutant, M.; Ramos, O.; Tourrel-Cuzin, C.; Movassat, J.; Ilias, A.; Vallois, D.; Planchais, J.; Pégorier, J.-P.; Schuit, F.; Petit, P. X., COUP-TFII controls mouse pancreatic β-cell mass through GLP-1-β-catenin signaling pathways. *PLoS One* **2012,** 7, (1), e30847.

Bouwens, L.; Rooman, I., Regulation of pancreatic beta-cell mass. *Physiologial Reviews***2005,** 85, (4), 1255-1270.

Brady, R. A.; Bruno, V. M.; Burns, D. L., RNA-Seq Analysis of the Host Response to Staphylococcus aureus Skin and Soft Tissue Infection in a Mouse Model. PLOS One, **2015,** 10, (4), e0124877.

Brandt, I.; Joossens, J.; Chen, X.; Maes, M. B.; Scharpe, S.; De Meester, I.; Lambeir, A. M., Inhibition of dipeptidyl-peptidase IV catalyzed peptide truncation by Vildagliptin ((2S)-{[(3-hydroxyadamantan-1-yl)amino]acetyl}-pyrrolidine-2-carbonitrile). *Biochemical Pharmacology* **2005,** 70, (1), 134-43.

Brauner-Osborne, H.; Jensen, A. A.; Sheppard, P. O.; O'Hara, P.; Krogsgaard-Larsen, P., The agonist-binding domain of the calcium-sensing receptor is located at the amino-terminal domain. *Journal of Biological Chemisttry***1999,** 274, (26), 18382-18386.

Brennan, E. P.; Morine, M. J.; Walsh, D. W.; Roxburgh, S. A.; Lindenmeyer, M. T.; Brazil, D. P.; Gaora, P. Ó.; Roche, H. M.; Sadlier, D. M.; Cohen, C. D., Next-generation sequencing identifies TGF-β1-associated gene expression profiles in renal epithelial cells reiterated in human diabetic nephropathy. *Biochimica et Biophysica Acta (BBA)-Molecular Basis of Disease* **2012,** 1822, (4), 589-599.

Brenneman, D. E., Neuroprotection: A comparative view of vasoactive intestinal peptide and pituitary adenylate cyclase-activating polypeptide. *Peptides* **2007,** 28, (9), 1720-1726.

Briaud, I.; Lingohr, M. K.; Dickson, L. M.; Wrede, C. E.; Rhodes, C. J., Differential activation mechanisms of Erk-1/2 and p70(S6K) by glucose in pancreatic beta-cells. *Diabetes* **2003,** 52, (4), 974-83.

Broadbent, H. M.; Peden, J. F.; Lorkowski, S.; Goel, A.; Ongen, H.; Green, F.; Clarke, R.; Collins, R.; Franzosi, M. G.; Tognoni, G., Susceptibility to coronary artery disease and diabetes is encoded by distinct, tightly linked SNPs in the ANRIL locus on chromosome 9p. *Human molecular genetics* **2008,** 17, (6), 806-814.

Broca, C.; Quoyer, J.; Costes, S.; Linck, N.; Varrault, A.; Deffayet, P. M.; Bockaert, J.; Dalle, S.; Bertrand, G., beta-Arrestin 1 is required for PAC1 receptor-mediated potentiation of long-lasting ERK1/2 activation by glucose in pancreatic beta-cells. *Journal of Biological Chemisttry***2009,** 284, (7), 4332-42.

Brown, E. M., Clinical lessons from the calcium-sensing receptor. *Nature Clinical Practce Endocrinology and Metabolism.* **2007,** 3, (2), 122-133.

Brubaker, P. L.; Drucker, D. J., Minireview: Glucagon-like peptides regulate cell proliferation and apoptosis in the pancreas, gut, and central nervous system. *Endocrinology* **2004,** 145, (6), 2653-9.

Brun, T.; Duhamel, D. L.; Hu He, K. H.; Wollheim, C. B.; Gauthier, B. R., The transcription factor PAX4 acts as a survival gene in INS-1E insulinoma cells. *Oncogene* **2007,** 26, (29), 4261-71.

Bufe, B.; Hofmann, T.; Krautwurst, D.; Raguse, J. D.; Meyerhof, W., The human TAS2R16 receptor mediates bitter taste in response to beta-glucopyranosides. *Nature Genetics* **2002,** 32, (3), 397-401.

Burrin, D. G.; Petersen, Y.; Stoll, B. & Sangild, P. Glucagon-like peptide 2: a nutrient-responsive gut growth factor. *The Journal of nutrition* **2001**, 131(3), 709-712.

Bullock, B. P.; Heller, R. S.; Habener, J. F., Tissue distribution of messenger ribonucleic acid encoding the rat glucagon-like peptide-1 receptor. *Endocrinology* **1996,** 137, (7), 2968-78.

Buse, J. B.; Nauck, M.; Forst, T.; Sheu, W. H.; Shenouda, S. K.; Heilmann, C. R.; Hoogwerf, B. J.; Gao, A.; Boardman, M. K.; Fineman, M.; Porter, L.; Schernthaner, G., Exenatide once weekly versus liraglutide once daily in patients with type 2 diabetes (DURATION-6): a randomised, open-label study. *Lancet* **2013,** 381, (9861), 117-24.

Buse, J. B.; Rosenstock, J.; Sesti, G.; Schmidt, W. E.; Montanya, E.; Brett, J. H.; Zychma, M.; Blonde, L., Liraglutide once a day versus exenatide twice a day for type 2 diabetes: a 26-week randomised, parallel-group, multinational, open-label trial (LEAD-6). *Lancet* **2009,** 374, (9683), 39-47.

Busso, N.; Wagtmann, N.; Herling, C.; Chobaz-Peclat, V.; Bischof-Delaloye, A.; So, A.; Grouzmann, E., Circulating CD26 is negatively associated with inflammation in human and experimental arthritis. *The American Journal of Pathology***2005,** 166, (2), 433-42.

Buteau, J.; Foisy, S.; Joly, E.; Prentki, M., Glucagon-like peptide 1 induces pancreatic beta-cell proliferation via transactivation of the epidermal growth factor receptor. *Diabetes* **2003,** 52, (1), 124-32.

Buteau, J.; Foisy, S.; Rhodes, C. J.; Carpenter, L.; Biden, T. J.; Prentki, M., Protein kinase Czeta activation mediates glucagon-like peptide-1-induced pancreatic beta-cell proliferation. *Diabetes* **2001,** 50, (10), 2237-43.

Buteau, J.; Roduit, R.; Susini, S.; Prentki, M., Glucagon-like peptide-1 promotes DNA synthesis, activates phosphatidylinositol 3-kinase and increases transcription factor pancreatic and duodenal homeobox gene 1 (PDX-1) DNA binding activity in beta (INS-1)-cells. *Diabetologia* **1999,** 42, (7), 856-64.

Buteau, J.; Spatz, M. L.; Accili, D., Transcription factor FoxO1 mediates glucagon-like peptide-1 effects on pancreatic beta-cell mass. *Diabetes* **2006,** 55, (5), 1190-6.

Butler, A. E.; Campbell-Thompson, M.; Gurlo, T.; Dawson, D. W.; Atkinson, M.; Butler, P. C., Marked expansion of exocrine and endocrine pancreas with incretin therapy in humans with increased exocrine pancreas dysplasia and the potential for glucagon-producing neuroendocrine tumors. *Diabetes* **2013,** 62, (7), 2595-2604.

Butler, A. E.; Janson, J.; Soeller, W. C.; Butler, P. C., Increased beta-cell apoptosis prevents adaptive increase in beta-cell mass in mouse model of type 2 diabetes: evidence for role of islet amyloid formation rather than direct action of amyloid. *Diabetes* **2003,** 52, (9), 2304-14.

Butler, N. S.; Dandekar, A. A.; Perlman, S., Antiviral antibodies are necessary to prevent cytotoxic T-lymphocyte escape in mice infected with a coronavirus. *Journal of Virology***2007,** 81, (24), 13291-8.

Buysschaert, M.; Tennstedt, D.; Preumont, V., Improvement of psoriasis during exenatide treatment in a patient with diabetes. *Diabetes and Metabolism***2012,** 38, (1), 86-8.

Cabou, C.; Campistron, G.; Marsollier, N.; Leloup, C.; Cruciani-Guglielmacci, C.; Penicaud, L.; Drucker, D. J.; Magnan, C.; Burcelin, R., Brain glucagon-like peptide-1 regulates arterial blood flow, heart rate, and insulin sensitivity. *Diabetes* **2008,** 57, (10), 2577-87.

Campbell, R. M.; Bongers, J.; Felix, A. M., Rational design, synthesis, and biological evaluation of novel growth-hormone releasing-factor analogs.*Biopolymers* **1995,** 37, (2), 67-88.

Campos, R. V.; Lee, Y. C.; Drucker, D. J., Divergent tissue-specific and developmental expression of receptors for glucagon and glucagon-like peptide-1 in the mouse. *Endocrinology* **1994,** 134, (5), 2156-64.

Canals, M.; Sexton, P. M.; Christopoulos, A., Allostery in GPCRs:‘MWC’revisited. *Trends in Biochemical Sciences***2011,** 36, (12), 663-672.

Carraro-Lacroix, L. R.; Malnic, G.; Girardi, A. C., Regulation of Na+/H+ exchanger NHE3 by glucagon-like peptide 1 receptor agonist exendin-4 in renal proximal tubule cells. *The American Journal of Physiology - Renal Physiology***2009,** 297, (6), F1647-55.

Challa, T. D.; Beaton, N.; Arnold, M.; Rudofsky, G.; Langhans, W.; Wolfrum, C., Regulation of adipocyte formation by GLP-1/GLP-1R signaling. *Journal of Biological Chemistry***2012,** 287, (9), 6421-30.

Chambard, J.-C.; Lefloch, R.; Pouysségur, J.; Lenormand, P., ERK implication in cell cycle regulation. *Biochimica et Biophysica Acta (BBA)-Molecular Cell Research* **2007,** 1773, (8), 1299-1310.

Cha-Molstad, H.; Saxena, G.; Chen, J.; Shalev, A., Glucose-stimulated expression of Txnip is mediated by carbohydrate response element-binding protein, p300, and histone H4 acetylation in pancreatic beta cells. *Journal of Biological Chemistry***2009,** 284, (25), 16898-905.

Chandramohan, R.; Wu, P.-Y.; Phan, J. H.; Wang, M. D. In *Benchmarking RNA-Seq quantification tools*, Engineering in Medicine and Biology Society (EMBC), 2013 35th Annual International Conference of the IEEE, 2013; IEEE: 2013; pp 647-650.

Chang, S.-Y.; Kim, D.-B.; Ryu, G. R.; Ko, S.-H.; Jeong, I.-K.; Ahn, Y.-B.; Jo, Y.-H.; Kim, M.-J., Exendin-4 Inhibits iNOS Expression at the Protein Level in LPS-Stimulated Raw264.7 Macrophage by the Activation of cAMP/PKA Pathway. *Journal of Cellular Biochemistry* **2013,** 114, 844-853.

Chang, T. I.; Horal, M.; Jain, S. K.; Wang, F.; Patel, R.; Loeken, M. R., Oxidant regulation of gene expression and neural tube development: Insights gained from diabetic pregnancy on molecular causes of neural tube defects. *Diabetologia* **2003,** 46, (4), 538-45.

Charest, P. G.; Oligny-Longpre, G.; Bonin, H.; Azzi, M.; Bouvier, M., The V2 vasopressin receptor stimulates ERK1/2 activity independently of heterotrimeric G protein signalling. *Cellular Signalling***2007,** 19, (1), 32-41.

Charo, I. F.; Ransohoff, R. M., The many roles of chemokines and chemokine receptors in inflammation. *New England Journal of Medicine* **2006,** 354, (6), 610-621.

Chen, C. A.; Manning, D. R., Regulation of G proteins by covalent modification. *Oncogene* **2001,** 20, (13), 1643-1652.

Chen, D.; Liao, J.; Li, N.; Zhou, C.; Liu, Q.; Wang, G.; Zhang, R.; Zhang, S.; Lin, L.; Chen, K., A nonpeptidic agonist of glucagon-like peptide 1 receptors with efficacy in diabetic db/db mice. *Proceedings of the National Academy of Sciences* **2007,** 104, (3), 943-948.

Chen, H.; Gu, X.; Liu, Y.; Wang, J.; Wirt, S. E.; Bottino, R.; Schorle, H.; Sage, J.; Kim, S. K., PDGF signalling controls age-dependent proliferation in pancreatic [bgr]-cells. *Nature* **2011,** 478, (7369), 349-355.

Chen, I. M.; Wu, K. C.; Chien, Y. L.; Chen, Y. H.; Lee, S. T., Missing link in community psychiatry: When a patient with schizophrenia was expelled from her home. *Journal of Formosan Medical Association***2015,** 114, (6), 553-7.

Chen, K.; Deng, S.; Lu, H.; Zheng, Y.; Yang, G.; Kim, D.; Cao, Q.; Wu, J. Q., RNA-seq characterization of spinal cord injury transcriptome in acute/subacute phases: a resource for understanding the pathology at the systems level. *PLoS One* **2013,** 8, (8).

Chen, Y.; Zhu, J.; Lum, P. Y.; Yang, X.; Pinto, S.; MacNeil, D. J.; Zhang, C.; Lamb, J.; Edwards, S.; Sieberts, S. K., Variations in DNA elucidate molecular networks that cause disease. *Nature* **2008,** 452, (7186), 429-435.

Chen, Z. W.; Wan, Y.; Yao, K. W., [Tuberculosis complicated with acquired hemophilia A--a case report]. *Zhongguo Zhong Xi Yi Jie He Za Zhi* **2007,** 27, (11), 1044-5.

Cheng, J.; Kapranov, P.; Drenkow, J.; Dike, S.; Brubaker, S.; Patel, S.; Long, J.; Stern, D.; Tammana, H.; Helt, G., Transcriptional maps of 10 human chromosomes at 5-nucleotide resolution. *Science* **2005,** 308, (5725), 1149-1154.

Chen, J.; Yu, L., Wang, L.; Fang, X.; Li, L. & Li, W. Stability of synthetic exendin-4 in human plasma in vitro. *Protein and peptide letters* **2007**, 14(1), 19-25.

Chen, T.; Kwok, H.; Ivanyi, C.; & Shaw, C. Isolation and cloning of exendin precursor cDNAs from single samples of venom from the Mexican beaded lizard (Heloderma horridum) and the Gila monster (Heloderma suspectum). *Toxicon* **2006**, **47**(3), 288-295.

Cheong, Y.-H.; Kim, M.-K.; Son, M.-H.; Kaang, B.-K., Two small molecule agonists of glucagon-like peptide-1 receptor modulate the receptor activation response differently. *Biochemical and Biophysical Research Communications***2012,** 417, (1), 558-563.

Cheeseman, C. I. & Tsang, R. The effect of GIP and glucagon-like peptides on intestinal basolateral membrane hexose transport. *American Journal of Physiology-Gastrointestinal and Liver Physiology* **1996**, 271(3), G477-G482.

Christopoulos, A., Advances in G protein-coupled receptor allostery: From function to structure. *Molecular Pharmacology***2014,** 86, (5), 463-478.

Christopoulos, A.; Grant, M. K.; El-Fakahany, E. E., Transducer abstraction: a novel approach to the detection of partial agonist efficacy in radioligand binding studies. *Journal of Pharmacological and Toxicological Methods* **2000,** 43, (1), 55-67.

Christopoulos, A.; Kenakin, T., G protein-coupled receptor allosterism and complexing. *Pharmacological Reviews***2002,** 54, (2), 323-74.

Colledge, M.; Scott, J. D., AKAPs: from structure to function. *Trends in Cell Biology***1999,** 9, (6), 216-221.

Concannon, P.; Rich, S. S.; Nepom, G. T., Genetics of type 1A diabetes. *New England Journal of Medicine* **2009,** 360, (16), 1646-1654.

Conigrave, A. D.; Quinn, S. J.; Brown, E. M., L-amino acid sensing by the extracellular Ca2+-sensing receptor. *Proceedings of the National Academy of Sciences* **2000,** 97, (9), 4814-4819.

Conte, C.; Ebeling, M.; Marcuz, A.; Nef, P.; Andres-Barquin, P. J., Identification and characterization of human taste receptor genes belonging to the TAS2R family. *Cytogeneticand Genome Research***2002,** 98, (1), 45-53.

Coopman, K.; Huang, Y.; Johnston, N.; Bradley, S. J.; Wilkinson, G. F.; Willars, G. B., Comparative effects of the endogenous agonist glucagon-like peptide-1 (GLP-1)-(7-36) amide and the small-molecule ago-allosteric agent “compound 2” at the GLP-1 receptor. *Journal of Pharmacology and Experimental Therapeutics* **2010,** 334, (3), 795-808.

Cornu, M.; Modi, H.; Kawamori, D.; Kulkarni, R. N.; Joffraud, M.; Thorens, B., Glucagon-like peptide-1 increases β-cell glucose competence and proliferation by translational induction of insulin-like growth factor-1 receptor expression. *Journal of Biological Chemistry***2010,** 285, (14), 10538-10545.

Cornu, M.; Thorens, B., GLP-1 protects beta-cells against apoptosis by enhancing the activity of an IGF-2/IGF1-receptor autocrine loop. *Islets* **2009,** 1, (3), 280-2.

Cornu, M.; Yang, J.-Y.; Jaccard, E.; Poussin, C.; Widmann, C.; Thorens, B., Glucagon-like peptide-1 protects β-cells against apoptosis by increasing the activity of an IGF-2/IGF-1 receptor autocrine loop. *Diabetes* **2009,** 58, (8), 1816-1825.

Collie, N. L.; Zhu, Z.; Jordan, S. & Reeve, J. Oxyntomodulin stimulates intestinal glucose uptake in rats. *Gastroenterology* **1997**, 112(6), 1961-1970.

Costa, V.; Angelini, C.; D'Apice, L.; Mutarelli, M.; Casamassimi, A.; Sommese, L.; Gallo, M. A.; Aprile, M.; Esposito, R.; Leone, L., Massive-scale RNA-Seq analysis of non ribosomal transcriptome in human trisomy 21. *PLoS One* **2011,** 6, (4), e18493.

Costa, V.; Angelini, C.; De Feis, I.; Ciccodicola, A., Uncovering the complexity of transcriptomes with RNA-Seq. *BioMed Research International* **2010,** 2010.

Costa, V.; Aprile, M.; Esposito, R.; Ciccodicola, A., RNA-Seq and human complex diseases: recent accomplishments and future perspectives. *European Journal of Human Genetics* **2013,** 21, (2), 134-142.

Costes, S.; Broca, C.; Bertrand, G.; Lajoix, A. D.; Bataille, D.; Bockaert, J.; Dalle, S., ERK1/2 control phosphorylation and protein level of cAMP-responsive element-binding protein: a key role in glucose-mediated pancreatic beta-cell survival. *Diabetes* **2006,** 55, (8), 2220-30.

Courtois, G.; Gilmore, T., Mutations in the NF-κB signaling pathway: implications for human disease. *Oncogene* **2006,** 25, (51), 6831-6843.

Crajoinas, R. O.; Lessa, L. M.; Carraro-Lacroix, L. R.; Davel, A. P.; Pacheco, B. P.; Rossoni, L. V.; Malnic, G.; Girardi, A. C., Posttranslational mechanisms associated with reduced NHE3 activity in adult vs. young prehypertensive SHR. *The American Journal of Physiology - Renal Physiology***2010,** 299, (4), F872-81.

Creutzfeldt, W., The incretin concept today. *Diabetologia* **1979,** 16, 75-85.

Creutzfeldt, W.; Nauck, M., Gut hormones and diabetes mellitus. *Diabetes/Metabolism Research and Reviews***1992,** 8, 149-177.

Creutzfeldt, W. O.; Kleine, N.; Willms, B.; Orskov, C.; Holst, J. J.; Nauck, M. A., Glucagonostatic actions and reduction of fasting hyperglycemia by exogenous glucagon-like peptide I(7-36) amide in type I diabetic patients. *Diabetes Care* **1996,** 19, (6), 580-6.

Croze, E., Differential gene expression and translational approaches to identify biomarkers of interferon beta activity in multiple sclerosis. *Journal of Interferon &Cytokine Research* **2010,** 30, (10), 743-749.

Cypryk, K.; Vilsbøll, T.; Nadel, I.; Smyczynska, J.; Holst, J. J.; Lewinski, A., Normal secretion of the incretin hormones glucose-dependent insulinotropic polypeptide and glucagon-like peptide-1 during gestational diabetes mellitus. *Gynecological Endocrinology* **2007,** 23, (1), 58-62.

Dadon, D.; Tornovsky-Babaey, S.; Furth-Lavi, J.; Ben-Zvi, D.; Ziv, O.; Schyr-Ben-Haroush, R.; Stolovich-Rain, M.; Hija, A.; Porat, S.; Granot, Z., Glucose metabolism: key endogenous regulator of β-cell replication and survival. *Diabetes, Obesity and Metabolism* **2012,** 14, (s3), 101-108.

Dai, H.; Gustavson, S. M.; Preston, G.M.; Eskra, J.D.; Calle, R.; Hirshberg, B., Non-linear increase in GLP-1 levels in response to DPP-IV inhibition in healthy adult subjects. *Diabetes, Obesity and Metabolism*, **2008**, 10(6), 506-513.

Dakin, C. L.; Gunn, I.; Small, C. J.; Edwards, C. M.; Hay, D. L.; Smith, D. M.; Ghatei, M. A.; Bloom, S. R., Oxyntomodulin inhibits food intake in the rat. *Endocrinology* **2001,** 142, 4244-4250.

Deacon, C. F.; Nauck, M. A.; Toft-Nielsen, M.; Pridal, L.; Willms, B. & Holst, J. J. Both subcutaneously and intravenously administered glucagon-like peptide I are rapidly degraded from the NH2-terminus in type II diabetic patients and in healthy subjects. *Diabetes* **1995**, 44(9), 1126-1131.

D'Alessio, D. A.; Kahn, S. E.; Leusner, C. R.; Ensinck, J. W., Glucagon-like peptide 1 enhances glucose tolerance both by stimulation of insulin release and by increasing insulin-independent glucose disposal. *Journal of Clinical Investigation* **1994,** 93, (5), 2263.

Dann, C. E.; Hsieh, J. C.; Rattner, A.; Sharma, D.; Nathans, J.; Leahy, D. J., Insights into Wnt binding and signalling from the structures of two Frizzled cysteine-rich domains. *Nature* **2001,** 412, (6842), 86-90.

Dardevet, D.; Moore, M. C.; Neal, D.; DiCostanzo, C. A.; Snead, W.; Cherrington, A. D., Insulin-independent effects of GLP-1 on canine liver glucose metabolism: duration of infusion and involvement of hepatoportal region. *The American Journal of Physiology - Endocrinology and Metabolism***2004,** 287, (1), E75-81.

Davey, A. E.; Leach, K.; Valant, C.; Conigrave, A. D.; Sexton, P. M.; Christopoulos, A., Positive and negative allosteric modulators promote biased signaling at the calcium-sensing receptor. *Endocrinology* **2011,** 153, (3), 1232-1241.

Davidson, R., Psychiatry and homosexuality in mid-twentieth-century Edinburgh: the view from Jordanburn Nerve Hospital. *History of Psychiatry* **2009,** 20, (80 Pt 4), 403-24.

Deacon, C. F., Therapeutic strategies based on glucagon-like peptide 1. *Diabetes* **2004,** 53, (9), 2181-2189.

Deacon, C. F.; Holst, J. J., Dipeptidyl peptidase IV inhibitors: a promising new therapeutic approach for the management of type 2 diabetes. *International JOurnal of Biochemistry and Cell Biology***2006,** 38, 831-844.

Deacon, C. F.; Johnsen, A. H.; Holst, J. J., Degradation of glucagon-like peptide-1 by human plasma in vitro yields an N-terminally truncated peptide that is a major endogenous metabolite in vivo. *Journal of Clinical Endocrinology and Metabolism***1995,** 80, 952-957.

Deacon, C. F.; Nauck, M. A.; Toft-Nielsen, M.; Pridal, L.; Willms, B.; Holst, J. J., Both subcutaneously and intravenously administered glucagon-like peptide I are rapidly degraded from the NH2-terminus in type II diabetic patients and in healthy subjects. *Diabetes* **1995,** 44, (9), 1126-1131.

DeFronzo, R. A.; Fleck, P. R.; Wilson, C. A.; Mekki, Q., Efficacy and safety of the dipeptidyl peptidase-4 inhibitor alogliptin in patients with type 2 diabetes and inadequate glycemic control: a randomized, double-blind, placebo-controlled study. *Diabetes care* **2008,** 31, (12), 2315-7.

DeFronzo, R. A.; Hissa, M. N.; Garber, A. J.; Luiz Gross, J.; Yuyan Duan, R.; Ravichandran, S.; Chen, R. S., The efficacy and safety of saxagliptin when added to metformin therapy in patients with inadequately controlled type 2 diabetes with metformin alone. *Diabetes Care* **2009,** 32, (9), 1649-55.

Delgado-Aros, S.; Kim, D. Y.; Burton, D. D.; Thomforde, G. M.; Stephens, D.; Brinkmann, B. H.; Vella, A.; Camilleri, M., Effect of GLP-1 on gastric volume, emptying, maximum volume ingested, and postprandial symptoms in humans. *American journal of physiology. Gastrointestinal and Liver Physiology* **2002,** 282, (3), G424-31.

DeLuca, D. S.; Levin, J. Z.; Sivachenko, A.; Fennell, T.; Nazaire, M.-D.; Williams, C.; Reich, M.; Winckler, W.; Getz, G., RNA-SeQC: RNA-seq metrics for quality control and process optimization. *Bioinformatics* **2012,** 28, (11), 1530-1532.

Depigny, C.; Lupo, B.; Kervran, A.; Bataille, D., Demonstration of a specific receptor site for glucagon-37 (oxyntomodulin/bioactive enteroglucagon) in rat oxyntic glands. *Comptes Rendus de l'Académie des Sciences - Series III* **1984,** 299, (16), 677-680.

Dewire, S. M.; Kim, J.; Whalen, E. J.; Ahn, S.; Chen, M.; Lefkowitz, R. J., beta-arrestin-mediated signaling regulates protein synthesis. *Journal of Biological Chemistry***2008,** 283, (16), 10611-10620.

Dive, C.; Gregory, C. D.; Phipps, D. J.; Evans, D. L.; Milner, A. E.; Wyllie, A. H., Analysis and discrimination of necrosis and apoptosis (programmed cell death) by multiparameter flow cytometry. *Biochimica et Biophysica Acta (BBA)-Molecular Cell Research* **1992,** 1133, (3), 275-285.

Dong, M. Q.; Li, Z. J.; Pinon, D. I.; Lybrand, T. P.; Miller, L. J., Spatial approximation between the amino terminus of a peptide agonist and the top of the sixth transmembrane segment of the secretin receptor. *Journal of Biological Chemistry***2004,** 279, (4), 2894-2903.

Dong, M. Q.; Pinon, D. I.; Cox, R. F.; Miller, L. J., Importance of the amino terminus in secretin family G protein-coupled receptors - Intrinsic photoaffinity labeling establishes initial docking constraints for the calcitonin receptor. *Journal of Biological Chemistry***2004,** 279, (2), 1167-1175.

Dong, Z.; Chen, Y., Transcriptomics: advances and approaches. *Science China Life Sciences* **2013,** 56, (10), 960-967.

Downes, G. B.; Gautam, N., The G protein subunit gene families. *Genomics* **1999,** 62, (3), 544-552.

Doyle, M. E.; Egan, J. M., Mechanisms of action of glucagon-like peptide 1 in the pancreas. *Pharmacology and Therapeutics***2007,** 113, (3), 546-593.

Drucker, D. J., Glucagon-like peptides: regulators of cell proliferation, differentiation, and apoptosis. *Molecular Endocrinology***2003,** 17, (2), 161-171.

Drucker, D. J., Enhancing incretin action for the treatment of type 2 diabetes. *Diabetes Care* **2003,** 26, (10), 2929-2940.

Drucker, D. J., The biology of incretin hormones. *Cell Metabolism.* **2006,** 3, (3), 153-165.

Drucker, D. J.; DeForest, L.; Brubaker, P. L., Intestinal response to growth factors administered alone or in combination with human [Gly2]glucagon-like peptide 2. *The American Journal of Physiology* **1997,** 273, (6 Pt 1), G1252-62.

Drucker, D. J.; Nauck, M. A., The incretin system: glucagon-like peptide-1 receptor agonists and dipeptidyl peptidase-4 inhibitors in type 2 diabetes. *Lancet* **2006,** 368, (9548), 1696-1705.

Drucker, D. J.; Philippe, J.; Jepeal, L.; Habener, J. F., Glucagon gene 5'-flanking sequences promote islet cell-specific gene transcription. *Journal of Biological Chemistry***1987,** 262, (32), 15659-65.

Drucker, D. J.; Philippe, J.; Mojsov, S.; Chick, W. L.; Habener, J. F., Glucagon-like peptide I stimulates insulin gene expression and increases cyclic AMP levels in a rat islet cell line. *Proceedings of the National Academy of Sciences* **1987,** 84, (10), 3434-3438.

Drucker, D. J.; Sherman, S. I.; Bergenstal, R. M.; Buse, J. B., The safety of incretin-based therapies—review of the scientific evidence. *The Journal of Clinical Endocrinology & Metabolism* **2011,** 96, (7), 2027-2031.

Drucker, D. Gut adaptation and the glucagon-like peptides. *Gut* **2002**, 50(3), 428-435.

Dukes, I. D.; Philipson, L. H., K+ channels: generating excitement in pancreatic beta-cells. *Diabetes* **1996,** 45, (7), 845-53.

Dunphy, J. L.; Taylor, R. G.; Fuller, P. J., Tissue distribution of rat glucagon receptor and GLP-1 receptor gene expression. *Molecular and Cellular Endocrinology* **1998,** 141, (1), 179-186.

Dupre, J.; Ross, S. A.; Watson, D.; Brown, J. C., Stimulation of insulin secretion by gastric inhibitory polypeptide in man. *The Journal of Clinical Endocrinology & Metabolism***1973,** 37, (5), 826-8.

Dyachok, O.; Gylfe, E., Ca2+-induced Ca2+ release via inositol 1, 4, 5-trisphosphate receptors is amplified by protein kinase A and triggers exocytosis in pancreatic β-cells. *Journal of Biological Chemistry***2004,** 279, (44), 45455-45461.

Dyachok, O.; Isakov, Y.; Sagetorp, J.; Tengholm A., Oscillations of cyclic AMP in hormone-stimulated insulin-secreting b-cells. *Nature* **2006,** 439, 349-352.

Dzhura, I.; Chepurny, O. G.; Kelley, G. G.; Leech, C. A.; Roe, M. W.; Dzhura, E.; Afshari, P.; Malik, S.; Rindler, M. J.; Xu, X., Epac2-dependent mobilization of intracellular Ca2+ by glucagon-like peptide-1 receptor agonist exendin-4 is disrupted in β-cells of phospholipase C-ε knockout mice. *The Journal of Physiology* **2010,** 588, (24), 4871-4889.

Dzhura, I.; Chepurny, O. G.; Leech, C. A.; Roe, M. W.; Dzhura, E.; Xu, X.; Lu, Y.; Schwede, F.; Genieser, H. G.; Smrcka, A. V.; Holz, G. G., Phospholipase C-epsilon links Epac2 activation to the potentiation of glucose-stimulated insulin secretion from mouse islets of Langerhans. *Islets* **2011,** 3, (3), 121-8.

Ebisuya, M.; Kondoh, K.; Nishida, E., The duration, magnitude and compartmentalization of ERK MAP kinase activity: mechanisms for providing signaling specificity. *Journal of Cell Science* **2005,** 118, (14), 2997-3002.

Edvell, A.; Lindström, P., Initiation of Increased Pancreatic Islet Growth in Young Normoglycemic Mice (Umeå+/?) 1. *Endocrinology* **1999,** 140, (2), 778-783.

Efrat, S.; Linde, S.; Kofod, H.; Spector, D.; Delannoy, M.; Grant, S.; Hanahan, D.; Baekkeskov, S., Beta-cell lines derived from transgenic mice expressing a hybrid insulin gene-oncogene. *Proceedings of the National Academy of Sciences* **1988,** 85, (23), 9037-9041.

Egan, J. M.; Bulotta, A.; Hui, H.; Perfetti, R., GLP-1 receptor agonists are growth and differentiation factors for pancreatic islet beta cells. *Diabetes/Metabolism Research and Reviews* **2003,** 19, (2), 115-123.

Egan, J. M.; Bulotta, A.; Hui, H.; Perfetti, R., GLP-1 receptor agonists are growth and differentiation factors for pancreatic islet beta cells. *Diabetes/Metabolism Research and Reviews***2003,** 19, (2), 115-23.

Egan, J. M.; Montrose-Rafizadeh, C.; Wang, Y.; Bernier, M.; Roth, J., Glucagon-like peptide-1(7-36) amide (GLP-1) enhances insulin-stimulated glucose metabolism in 3T3-L1 adipocytes: one of several potential extrapancreatic sites of GLP-1 action. *Endocrinology* **1994,** 135, (5), 2070-5.

Egefjord, L.; Jensen, J. L.; Bang-Berthelsen, C. H.; Petersen, A. B.; Smidt, K.; Schmitz, O.; Karlsen, A. E.; Pociot, F.; Chimienti, F.; Rungby, J.; Magnusson, N. E., Zinc transporter gene expression is regulated by pro-inflammatory cytokines: a potential role for zinc transporters in beta-cell apoptosis? *BMC Endocrine Disorders***2009,** 9, 7.

Ehlert, F., Estimation of the affinities of allosteric ligands using radioligand binding and pharmacological null methods. *Molecular Pharmacology***1988,** 33, (2), 187-194.

Ehlert, F. J., Means of clarifying mechanisms of desensitization. Energetics of conformational changes in receptors. *Trends in Pharmacological Sciences***1988,** 9, (11), 393-4.

Ehlert, F. J., Analysis of allosterism in functional assays. *Journal of Pharmacology and Experimental Therapeutics***2005,** 315, (2), 740-54.

Ehses, J. A.; Casilla, V. R.; Doty, T.; Pospisilik, J. A.; Winter, K. D.; Demuth, H.-U. & McIntosh, C. H. Glucose-dependent insulinotropic polypeptide promotes β-(INS-1) cell survival via cyclic adenosine monophosphate-mediated caspase-3 inhibition and regulation of p38 mitogen-activated protein kinase. *Endocrinology* **2003**, 144(10), 4433-4445.

Eizirik, D. L.; Moore, F.; Flamez, D.; Ortis, F., Use of a systems biology approach to understand pancreatic beta-cell death in Type 1 diabetes. *Biochemical Society Transactions* **2008,** 36, (3), 321.

Eizirik, D. L.; Sammeth, M.; Bouckenooghe, T.; Bottu, G.; Sisino, G.; Igoillo-Esteve, M.; Ortis, F.; Santin, I.; Colli, M. L.; Barthson, J., The human pancreatic islet transcriptome: expression of candidate genes for type 1 diabetes and the impact of pro-inflammatory cytokines. *PLoS Genetics* **2012,** 8, (3), e1002552.

Elahi, D.; Egan, J. M.; Shannon, R. P.; Meneilly, G. S.; Khatri, A.; Habener, J. F.; Andersen, D. K., GLP-1 (9-36) amide, cleavage product of GLP-1 (7-36) amide, is a glucoregulatory peptide. *Obesity* **2008,** 16, 1501-1509.

Elashoff, M.; Matveyenko, A. V.; Gier, B.; Elashoff, R.; Butler, P. C., Pancreatitis, pancreatic, and thyroid cancer with glucagon-like peptide-1–based therapies. *Gastroenterology* **2011,** 141, (1), 150-156.

Eliasson, L.; Abdulkader, F.; Braun, M.; Galvanovskis, J.; Hoppa, M. B.; Rorsman, P., Novel aspects of the molecular mechanisms controlling insulin secretion. *The Journal of Physiology* **2008,** 586, (14), 3313-3324.

Elrick, H.; Stimmler, L.; Hlad, C.; Arai, Y., Plasma insulin response to oral and intravenous glucose administration. *Journal of* Clinical Endocrinology Metabolism **1964,** 24, 1076-1082.

Eng, J.; Kleinman, W.; Singh, L.; Singh, G. & Raufman, J.-P. (1992). Isolation and characterization of exendin-4, an exendin-3 analogue, from Heloderma suspectum venom. Further evidence for an exendin receptor on dispersed acini from guinea pig pancreas. *Journal of Biological Chemistry* **1992**, 267(11), 7402-7405.

Epstein, S., Is cortical bone hip? What determines cortical bone properties? *Bone* **2007,** 41, (1), S3-S8.

Estall, J. L.; Drucker, D. J., Glucagon-like peptide-2. *Annual Review of Nutrition* **2006,** 26, 391-411.

Farilla, L.; Bulotta, A.; Hirshberg, B.; Li Calzi, S.; Khoury, N.; Noushmehr, H.; Bertolotto, C.; Di Mario, U.; Harlan, D. M.; Perfetti, R., Glucagon-like peptide 1 inhibits cell apoptosis and improves glucose responsiveness of freshly isolated human islets. *Endocrinology* **2003,** 144, (12), 5149-5158.

Farilla, L.; Hui, H.; Bertolotto, C.; Kang, E.; Bulotta, A.; Di Mario, U.; Perfetti, R., Glucagon-like peptide-1 promotes islet cell growth and inhibits apoptosis in Zucker diabetic rats. *Endocrinology* **2002,** 143, (11), 4397-4408.

Fätkenheuer, G.; Pozniak, A. L.; Johnson, M. A.; Plettenberg, A.; Staszewski, S.; Hoepelman, A. I.; Saag, M. S.; Goebel, F. D.; Rockstroh, J. K.; Dezube, B. J., Efficacy of short-term monotherapy with maraviroc, a new CCR5 antagonist, in patients infected with HIV-1. *Nature medicine* **2005,** 11, (11), 1170-1172.

Faurschou, A.; Pedersen, J.; Gyldenlove, M.; Poulsen, S. S.; Holst, J. J.; Thyssen, J. P.; Zachariae, C.; Vilsboll, T.; Skov, L.; Knop, F. K., Increased expression of glucagon-like peptide-1 receptors in psoriasis plaques. Experimental Dermatology **2013,** 22, (2), 150-2.

Faurschou, A.; Zachariae, C.; Skov, L.; Vilsboll, T.; Knop, F. K., Gastric bypass surgery: improving psoriasis through a GLP-1-dependent mechanism? *Medical Hypotheses* **2011,** 77, (6), 1098-101.

Favaro, E.; Granata, R.; Miceli, I.; Baragli, A.; Settanni, F.; Perin, P. C.; Ghigo, E.; Camussi, G.; Zanone, M., The ghrelin gene products and exendin-4 promote survival of human pancreatic islet endothelial cells in hyperglycaemic conditions, through phosphoinositide 3-kinase/Akt, extracellular signal-related kinase (ERK) 1/2 and cAMP/protein kinase A (PKA) signalling pathways. *Diabetologia* **2012,** 55, (4), 1058-1070.

Feero, W. G.; Guttmacher, A. E.; McCarthy, M. I., Genomics, type 2 diabetes, and obesity. *New England Journal of Medicine* **2010,** 363, (24), 2339-2350.

Fehmann, H. C.; Goke, R.; Goke, B., Cell and molecular biology of the incretin hormones glucagon-like peptide-I and glucose-dependent insulin releasing polypeptide. *Endocrine Reviews* **1995,** 16, (3), 390-410.

Feng, J.; Zhang, Z.; Wallace, M. B.; Stafford, J. A.; Kaldor, S. W.; Kassel, D. B.; Navre, M.; Shi, L.; Skene, R. J.; Asakawa, T.; Takeuchi, K.; Xu, R.; Webb, D. R.; Gwaltney, S. L., 2nd, Discovery of alogliptin: a potent, selective, bioavailable, and efficacious inhibitor of dipeptidyl peptidase IV. *Journal of Medicinal Chemistry* **2007,** 50, (10), 2297-300.

Feng, J.; Zhang, Z.; Wallace, M. B.; Stafford, J. A.; Kaldor, S. W.; Kassel, D. B.; Navre, M.; Shi, L.; Skene, R. J.; Asakawa, T.; Takeuchi, K.; Xu, R.; Webb, D. R.; Gwaltney, S. L. n., Discovery of alogliptin: a potent, selective, bioavailable, and efficacious inhibitor of dipeptidyl peptidase IV. *Journal of Medicinal Chemistry* **2007,** 50, (10), 2297-300.

Feng, Z. C.; Donnelly, L.; Li, J.; Krishnamurthy, M.; Riopel, M.; Wang, R., Inhibition of Gsk3beta activity improves beta-cell function in c-KitWv/+ male mice. *Lab Invest* **2012,** 92, (4), 543-55.

Ferrer, J., Glucose as a mitogenic hormone. *Cell Metabolism* **2011,** 13, (4), 357-358.

Fisyunov, A. I., Molecular Mechanisms of G Protein-Independent Signaling Mediated by 7-Transmembrane Receptors. *Neurophysiology* **2012,** 44, (3), 255-264.

Flamez, D.; Gilon, P.; Moens, K.; Van Breusegem, A.; Delmeire, D.; Scrocchi, L. A.; Henquin, J. C.; Drucker, D. J.; Schuit, F., Altered cAMP and Ca2+ signaling in mouse pancreatic islets with glucagon-like peptide-1 receptor null phenotype. *Diabetes* **1999,** 48, (10), 1979-86.

Flint, A.; Raben, A.; Astrup, A., & Holst, J. J. Glucagon-like peptide 1 promotes satiety and suppresses energy intake in humans. *Journal of Clinical Investigation* **1998**, 101(3), 515.

Florez, J., Newly identified loci highlight beta cell dysfunction as a key cause of type 2 diabetes: where are the insulin resistance genes? *Diabetologia* **2008,** 51, (7), 1100-1110.

Flower, D. R., Modelling G-protein-coupled receptors for drug design. *Biochimica et Biophysica Acta (BBA) - Reviews on Biomembranes* **1999,** 1422, (3), 207-234.

Foord, S. M.; Bonner, T. I.; Neubig, R. R.; Rosser, E. M.; Pin, J. P.; Davenport, A. P.; Spedding, M.; Harmar, A. J., International Union of Pharmacology. XLVI. G protein-coupled receptor list. *Pharmacological Reviews* **2005,** 57, (2), 279-288.

Fredriksson, R.; Lagerstrom, M. C.; Lundin, L. G.; Schioth, H. B., The G-protein-coupled receptors in the human genome form five main families. Phylogenetic analysis, paralogon groups, and fingerprints. *Molecular Pharmacology* **2003,** 63, (6), 1256-1272.

Fu, Z.; Kuang, H. Y.; Hao, M.; Gao, X. Y.; Liu, Y.; Shao, N., Protection of exenatide for retinal ganglion cells with different glucose concentrations. *Peptides* **2012,** 37, (1), 25-31.

Furuta, M.; Zhou, A.; Webb, G.; Carroll, R.; Ravazzola, M.; Orci, L.; Steiner, D. F., Severe defect in proglucagon processing in islet A-cells of prohormone convertase 2 null mice. *Journal of Biological Chemistry* **2001,** 276, (29), 27197-27202.

Furman, B. L. The development of Byetta (exenatide) from the venom of the Gila monster as an anti-diabetic agent. *Toxicon* **2012**, 59(4), 464-471.

Gaddy, D. F.; Riedel, M. J.; Pejawar-Gaddy, S.; Kieffer, T. J.; Robbins, P. D., In vivo expression of HGF/NK1 and GLP-1 from dsAAV vectors enhances pancreatic β-cell proliferation and improves pathology in the db/db mouse model of diabetes. *Diabetes* **2010,** 59, (12), 3108-3116.

Gallwitz, B. Exenatide in type 2 diabetes: treatment effects in clinical studies and animal study data. *International journal of clinical practice* **2006**, 60(12), 1654-1661.

Garber, A. J., Restaging insulin therapy for patients with type 2 diabetes. *Diabetes, Obesity & Metabolism* **2009,** 11 Suppl 5, 1-5.

Garber, M.; Grabherr, M. G.; Guttman, M.; Trapnell, C., Computational methods for transcriptome annotation and quantification using RNA-seq. *Nature Methods* **2011,** 8, (6), 469-477.

Gardella, T. J.; Ju, H., Interaction of PTH and PTHrP with their receptors. *Reviews in Endocrine and Metabolic Disorders* **2000,** 1, (4), 317-329.

Gaulton, K. J.; Nammo, T.; Pasquali, L.; Simon, J. M.; Giresi, P. G.; Fogarty, M. P.; Panhuis, T. M.; Mieczkowski, P.; Secchi, A.; Bosco, D., A map of open chromatin in human pancreatic islets. *Nature Genetics* **2010,** 42, (3), 255-259.

Gesty-Palmer, D.; Luttrell, L. M., Heptahelical terpsichory. Who calls the tune? Journal of Receptors and Signal Transduction **2008,** 28, (1-2), 39-58.

Gevaert, O.; De Moor, B., Prediction of cancer outcome using DNA microarray technology: past, present and future. *Expert Opinion on Medical Diagnostics,* **2009,** 3 (2) , 157 - 165 .

Gilligan, P. J.; Li, Y. W., Corticotropin-releasing factor antogonists: Recent advances and exciting prospects for the treatment of human diseases. Current Opinion in Drug Discovery & Development **2004,** 7, (4), 487-497.

Glauser, D. A.; Brun, T.; Gauthier, B. R.; Schlegel, W., Transcriptional response of pancreatic beta cells to metabolic stimulation: large scale identification of immediate-early and secondary response genes. *BMC Molecular Biology* **2007,** 8, (1), 54.

Glauser, D. A.; Schlegel, W., Sequential actions of ERK1/2 on the AP-1 transcription factor allow temporal integration of metabolic signals in pancreatic β cells. *The FASEB Journal* **2007,** 21, (12), 3240-3249.

Gloriam, D. E.; Fredriksson, R.; Schioth, H. B., The G protein-coupled receptor subset of the rat genome. *BMC Genomics* **2007,** 8.

Go, Y.; Satta, Y.; Takenaka, O.; Takahata, N., Lineage-specific loss of function of bitter taste receptor genes in humans and nonhuman primates. *Genetics* **2005,** 170, (1), 313-326.

Göke, R., Fehmann; H.-C., Linn, T.; Schmidt, H.; Krause, M.; Eng, J. & Göke, B. Exendin-4 is a high potency agonist and truncated exendin-(9-39)-amide an antagonist at the glucagon-like peptide 1-(7-36)-amide receptor of insulin-secreting beta-cells. *Journal of Biological Chemistry* **1993**, 268(26), 19650-19655.

Golpon, H. A.; Puechner, A.; Welte, T.; Wichert, P. V.; Feddersen, C. O., Vasorelaxant effect of glucagon-like peptide-(7-36)amide and amylin on the pulmonary circulation of the rat. Regulatory Peptides **2001,** 102, (2-3), 81-6.

Gomariz, R. P.; Martinez, C.; Abad, C.; Leceta, J.; Delgado, M., Immunology of VIP: A review and therapeutical perspectives. Current Pharmaceutical Design **2001,** 7, (2), 89-111.

Gomez, E.; Pritchard, C.; Herbert, T. P., cAMP-dependent protein kinase and Ca2+ influx through L-type voltage-gated calcium channels mediate Raf-independent activation of extracellular regulated kinase in response to glucagon-like peptide-1 in pancreatic beta-cells. *Journal Biological Chemistry* **2002,** 277, (50), 48146-51.

Gomez, E.; Pritchard, C.; Herbert, T. P., cAMP-dependent protein kinase and Ca2+ influx through L-type voltage-gated calcium channels mediate Raf-independent activation of extracellular regulated kinase in response to glucagon-like peptide-1 in pancreatic β-cells. *Journal Biological Chemistry* **2002,** 277, (50), 48146-48151.

Grace, C. R. R.; Perrin, M. H.; DiGruccio, M. R.; Miller, C. L.; Rivier, J. E.; Vale, W. W.; Riek, R., NMR structure and peptide hormone binding site of the first extracellular domain of a type B1 G protein-coupled receptor. *Proceedings of the National Academy of Sciences of the United States of America* **2004,** 101, (35), 12836-12841.

Grant, B. D.; Donaldson, J. G., Pathways and mechanisms of endocytic recycling. *Nature Reviews Molecular Cell Biology* **2009,** 10, (9), 597-608.

Gregory, K. J.; Hall, N. E.; Tobin, A. B.; Sexton, P. M.; Christopoulos, A., Identification of orthosteric and allosteric site mutations in M2 muscarinic acetylcholine receptors that contribute to ligand-selective signaling bias. *Journal of Biological Chemistry* **2010,** 285, (10), 7459-74.

Gregory, K. J.; Sexton, P. M.; Tobin, A. B.; Christopoulos, A., Stimulus bias provides evidence for conformational constraints in the structure of a G protein-coupled receptor. *Journal of Biological Chemistry* **2012,** 287, (44), 37066-37077.

Gromada, J.; Ding, W.-G.; Barg, S.; Renström, E. & Rorsman, P. Multisite regulation of insulin secretion by cAMP-increasing agonists: evidence that glucagon-like peptide 1 and glucagon act via distinct receptors. *Pflügers Archiv* **1997**, 434(5), 515-524.

Gros, L.; Thorens, B.; Bataille, D. & Kervran, A. Glucagon-like peptide-1-(7-36) amide, oxyntomodulin, and glucagon interact with a common receptor in a somatostatin-secreting cell line. *Endocrinology* **1993**, 133(2), 631-638.

Gromada, J.; Bark, C.; Smidt, K.; Efanov, A. M.; Janson, J.; Mandic, S. A.; Webb, D. L.; Zhang, W.; Meister, B.; Jeromin, A.; Berggren, P. O., Neuronal calcium sensor-1 potentiates glucose-dependent exocytosis in pancreatic beta cells through activation of phosphatidylinositol 4-kinase beta. *Proceedings of the National Academy of Sciences of the United States of America* **2005,** 102, (29), 10303-8.

Gromada, J.; Dissing, S.; Bokvist, K.; Renström, E.; Frøkjær-Jensen, J.; Wulff, B. S.; Rorsman, P., Glucagon-like peptide I increases cytoplasmic calcium in insulin-secreting βTC3-cells by enhancement of intracellular calcium mobilization. *Diabetes* **1995,** 44, (7), 767-774.

Gromada, J.; Holst, J. J.; Rorsman, P., Cellular regulation of islet hormone secretion by the incretin hormone glucagon-like peptide 1. *Pflügers Archiv: European Journal of Physiology* **1998,** 435, (5), 583-594.

Gromada, J.; Rorsman, P., Molecular mechanism underlying glucagon-like peptide 1 induced calcium mobilization from internal stores in insulin-secreting bTC3 cells. *Acta Physiologica Scandinavica* **1996,** 157, (3), 349-351.

Gros, R.; You, X.; Baggio, L. L.; Kabir, M. G.; Sadi, A. M.; Mungrue, I. N.; Parker, T. G.; Huang, Q.; Drucker, D. J.; Husain, M., Cardiac function in mice lacking the glucagon-like peptide-1 receptor. *Endocrinology* **2003,** 144, (6), 2242-52.

Gruenberg, J.; Maxfield, F. R., Membrane transport in the endocytic pathway. *Curr. Opin. Cell Biol.* **1995,** 7, (4), 552-563.

Gui, T.; Sun, Y.; Shimokado, A.; Muragaki, Y., The roles of mitogen-activated protein kinase pathways in TGF-β-induced epithelial-mesenchymal transition. *Journal of signal transduction* **2012,** 2012.

Guo, S., Insulin signaling, resistance, and metabolic syndrome: insights from mouse models into disease mechanisms. *Journal of Endocrinology* **2014,** 220, (2), T1-T23.

Gupta, N. A.; Mells, J.; Dunham, R. M.; Grakoui, A.; Handy, J.; Saxena, N. K.; Anania, F. A., Glucagon-like peptide-1 receptor is present on human hepatocytes and has a direct role in decreasing hepatic steatosis in vitro by modulating elements of the insulin signaling pathway. *Hepatology* **2010,** 51, (5), 1584-92.

Gurzov, E. N.; Barthson, J.; Marhfour, I.; Ortis, F.; Naamane, N.; Igoillo-Esteve, M.; Gysemans, C.; Mathieu, C.; Kitajima, S.; Marchetti, P., Pancreatic β-cells activate a JunB/ATF3-dependent survival pathway during inflammation. *Oncogene* **2012,** 31, (13), 1723-1732.

Guttmann-Raviv, N.; Shraga-Heled, N.; Varshavsky, A.; Guimaraes-Sternberg, C.; Kessler, O.; Neufeld, G., Semaphorin-3A and semaphorin-3F work together to repel endothelial cells

and to inhibit their survival by induction of apoptosis. *J. Biol. Chem.* **2007,** 282, (36), 26294-26305.

Gutzwiller, J.; Göke, B.; Drewe, J.; Hildebrand, P.; Ketterer, S.; Handschin, D.; Beglinger, C. Glucagon-like peptide-1: a potent regulator of food intake in humans. *Gut* **1999**, 44(1), 81-86.

Gutzwiller, J.-P.;Drewe, J.; Göke, B.; Schmidt, H.; Rohrer, B.; Lareida, J., & Beglinger, C. Glucagon-like peptide-1 promotes satiety and reduces food intake in patients with diabetes mellitus type 2. *American Journal of Physiology-Regulatory, Integrative and Comparative Physiology* **1999**, 276(5), R1541-R1544.

Habib, A. M.; Richards, P.; Cairns, L. S.; Rogers, G. J.; Bannon, C. A.; Parker, H. E.; Morley, T. C.; Yeo, G. S.; Reimann, F.; Gribble, F. M., Overlap of endocrine hormone expression in the mouse intestine revealed by transcriptional profiling and flow cytometry. *Endocrinology* **2012,** 153, 3054-3065.

Hall, D. A., Modeling the functional effects of allosteric modulators at pharmacological receptors: an extension of the two-state model of receptor activation. *Molecular Pharmacology* **2000,** 58, (6), 1412-23.

Hall, R. A.; Lefkowitz, R. J., Regulation of G protein-coupled receptor signaling by scaffold proteins. *Circulation Research* **2002,** 91, (8), 672-680.

Hall, R. A.; Premont, R. T.; Chow, C. W.; Blitzer, J. T.; Pitcher, J. A.; Claing, A.; Stoffel, R. H.; Barak, L. S.; Shenolikar, S.; Weinman, E. J.; Grinstein, S.; Lefkowitz, R. J., The beta(2)-adrenergic receptor interacts with the Na+/H+-exchanger regulatory factor to control Na+/H+ exchange. *Nature* **1998,** 392, (6676), 626-630.

Hällbrink, M.; Holmqvist, T.; Olsson, M.; Östenson, C.-G.; Efendic, S.; Langel, Ü., Different domains in the third intracellular loop of the GLP-1 receptor are responsible for Gα s and Gα i/Gα o activation. *Biochimica et Biophysica Acta (BBA)-Protein Structure and Molecular Enzymology* **2001,** 1546, (1), 79-86.

Halls, M.; Westhuizen, E. d.; Bathgate, R.; Summers, R., Relaxin family peptide receptors–former orphans reunite with their parent ligands to activate multiple signalling pathways. *British Journal of Pharmacology* **2007,** 150, (6), 677-691.

Han, H.; Bearss, D. J.; Browne, L. W.; Calaluce, R.; Nagle, R. B.; Von Hoff, D. D., Identification of differentially expressed genes in pancreatic cancer cells using cDNA microarray. *Cancer Research* **2002,** 62, (10), 2890-2896.

Hansen, L.; Deacon, C. F.; Orskov, C.; Holst, J. J., Glucagon-like peptide-1-(7-36) amide is transformed to glucagon-like-peptide-1-(9-36) amide by dipeptidyi peptidase IVin the cappillaries supplying the L-cells of porcine intestine. *Endocrinology* **1999,** 140, 5356-5363.

Hardie, D. G., AMP-activated/SNF1 protein kinases: conserved guardians of cellular energy. *Nature Reviews Molecular Cell Biology* **2007,** 8, (10), 774-785.

Hardy, O. T.; Hohmeier, H. E.; Becker, T. C.; Manduchi, E.; Doliba, N. M.; Gupta, R. K.; White, P.; Stoeckert, C. J., Jr.; Matschinsky, F. M.; Newgard, C. B.; Kaestner, K. H., Functional genomics of the beta-cell: short-chain 3-hydroxyacyl-coenzyme A dehydrogenase regulates

insulin secretion independent of K+ currents. *Molecular Endocrinology* **2007,** 21, (3), 765-73.

Harmar, A. J., Family-B G-protein-coupled receptors. *Genome Biology* **2001,** 2, (12).

Hartmann, B.; Harr, M. B.; Jeppesen, P. B.; Wojdemann, M.; Deacon, C. F.; Mortensen, P. B.; Holst, J. J., In vivo and in vitro degradation of glucagon-like peptide-2 in humans. *Journal of Clinical Endocrinology and Metabolism* **2000,** 85, (8), 2884-8.

Hartmann, B.; Thulesen, J.; Kissow, H.; Thulesen, S.; Orskov, C.; Ropke, C.; Poulsen, S. S.; Holst, J. J., Dipeptidyl peptidase IV inhibition enhances the intestinotrophic effect of glucagon-like peptide-2 in rats and mice. *Endocrinology* **2000,** 141, (11), 4013-20.

Hatzis, C.; Sun, H.; Yao, H.; Hubbard, R. E.; Meric-Bernstam, F.; Babiera, G. V.; Wu, Y.; Pusztai, L.; Symmans, W. F., Effects of tissue handling on RNA integrity and microarray measurements from resected breast cancers. *Journal of the National Cancer Institute* **2011,** 103, (24), 1871-1883.

Head, S. R.; Komori, H. K.; LaMere, S. A.; Whisenant, T.; Van Nieuwerburgh, F.; Salomon, D. R., & Ordoukhanian, P. Library construction for next-generation sequencing: overviews and challenges. *Biotechniques* **2014**, 56(2), 61.

Hectors, T.; Vanparys, C.; Pereira-Fernandes, A.; Martens, G. A.; Blust, R., Evaluation of the INS-1 832/13 cell line as a beta-cell based screening system to assess pollutant effects on beta-cell function. *PLoS One* **2013,** 8, (3), 21.

Heit, J. J.; Karnik, S. K.; Kim, S. K., Intrinsic regulators of pancreatic β-cell proliferation. Annual Review of Cell and Developmental Biology **2006,** 22, 311-338.

Hennige, A. M.; Ozcan, U.; Okada, T.; Jhala, U. S.; Schubert, M.; White, M. F.; Kulkarni, R. N., Alterations in growth and apoptosis of insulin receptor substrate-1-deficient β-cells. *American Journal of Physiology-Endocrinology and Metabolism* **2005,** 289, (2), E337-E346.

Henry, M., Reliability of the 8 Week Time Point for Single Assessment of Midcarpal Fusion by CT Scan. Journal of Hand and Microsurgery **2011,** 3, (1), 1-5.

Herman, G. A.; Stevens, C.; Van Dyck, K.; Bergman, A.; Yi, B.; De Smet, M.; Snyder, K.; Hilliard, D.; Tanen, M.; Tanaka, W.; Wang, A. Q.; Zeng, W.; Musson, D.; Winchell, G.; Davies, M. J.; Ramael, S.; Gottesdiener, K. M.; Wagner, J. A., Pharmacokinetics and pharmacodynamics of sitagliptin, an inhibitor of dipeptidyl peptidase IV, in healthy subjects: results from two randomized, double-blind, placebo-controlled studies with single oral doses. Clinical Pharmacology & Therapeutics **2005,** 78, (6), 675-88.

Herrmann, C.; Goke, R.; Richter, G.; Fehmann, H. C.; Arnold, R.; Goke, B., Glucagon-like peptide-1 and glucose-dependent insulin-releasing polypeptide plasma levels in response to nutrients. *Digestion* **1995,** 56, (2), 117-26.

Heruth, D. P.; Gibson, M.; Grigoryev, D. N.; Zhang, L. Q.; Ye, S. Q., RNA-seq analysis of synovial fibroblasts brings new insights into rheumatoid arthritis. Cell & Bioscience **2012,** 2, (1), 43.

Heuss, C.; Scanziani, M.; Gahwiler, B. H.; Gerber, U., G-protein-independent signaling mediated by metabotropic glutamate receptors. Nature Neuroscience **1999,** 2, (12), 1070-1077.

Heymann, E.; Mentlein, R., Liver dipeptidyl aminopeptidase IV hydrolyzes substance P. *FEBS Letters* **1978,** 91, (2), 360-4.

Hinke, S. A.; Hellemans, K.; Schuit, F. C., Plasticity of the β cell insulin secretory competence: preparing the pancreatic β cell for the next meal. *The Journal of Physiology* **2004,** 558, (2), 369-380.

Hirata, K.; Kume, S.; Araki, S.; Sakaguchi, M.; Chin-Kanasaki, M.; Isshiki, K.; Sugimoto, T.; Nishiyama, A.; Koya, D.; Haneda, M.; Kashiwagi, A.; Uzu, T., Exendin-4 has an anti-hypertensive effect in salt-sensitive mice model. *Biochemical and Biophysical Research Communications* **2009,** 380, (1), 44-9.

Ho, T. W.; Edvinsson, L.; Goadsby, P. J., CGRP and its receptors provide new insights into migraine pathophysiology. Nature Reviews Neurology **2010,** 6, (10), 573-582.

Hoare, S. R. J., Mechanisms of peptide and nonpeptide ligand binding to class B G-protein coupled receptors. *Drug Discovery Today* **2005,** 10, (6), 417-427.

Hofmann, B. A.; Sydow, S.; Jahn, O.; Van Werven, L.; Liepold, T.; Eckart, K.; Spiess, J., Functional and protein chemical characterization of the N-terminal domain of the rat corticotropin-releasing factor receptor 1. *Protein Science* **2001,** 10, (10), 2050-2062.

Hohmeier, H. E.; Mulder, H.; Chen, G.; Henkel-Rieger, R.; Prentki, M.; Newgard, C. B., Isolation of INS-1-derived cell lines with robust ATP-sensitive K+ channel-dependent and-independent glucose-stimulated insulin secretion. *Diabetes* **2000,** 49, (3), 424-430.

Hollenstein, K.; Kean, J.; Bortolato, A.; Cheng, R. K. Y.; Dore, A. S.; Jazayeri, A.; Cooke, R. M.; Weir, M.; Marshall, F. H., Structure of class B GPCR corticotropin-releasing factor receptor 1. *Nature* **2013,** 499, (7459), 438-+.

Holst, J. J.; Bersani, M.; Johnsen, A. H.; Kofod, H.; Hartmann, B., & Orskov, C. Proglucagon processing in porcine and human pancreas. *Journal of Biological Chemistry* **1994**, 269(29), 18827-18833.

Holst, J. J., The physiology of glucagon-like peptide 1. *Physiological Reviews* **2007,** 87, (4), 1409-1439.

Holst, J. J.; Orskov, C., Incretin hormones-an update. Scandinavian Journal of Clinical and Laboratory Investigation **2001,** 234(suppl), 75-85.

Holst, J. J.; Orskov, C.; Van Nielsen, O.; Schwartz, T. W., Truncated glucagon-like peptide I, an insulin-releasing hormone from the distal gut. *FEBS Letters* **1987,** 211, 169-173.

Holz, G. G., Epac: a new cAMP-binding protein in support of glucagon-like peptide-1 receptor-mediated signal transduction in the pancreatic β-cell. *Diabetes* **2004,** 53, (1), 5-13.

Holz, G. G.; Leech, C. A.; Heller, R. S.; Castonguay, M.; Habener, J. F., cAMP-dependent mobilization of intracellular Ca2+ stores by activation of ryanodine receptors in pancreatic

beta-cells. A Ca2+ signaling system stimulated by the insulinotropic hormone glucagon-like peptide-1-(7-37). Journal of Biological Chemistry **1999,** 274, (20), 14147-56.

Holz, G. G.; Leech, C. A.; Heller, R. S.; Castonguay, M.; Habener, J. F., cAMP-dependent Mobilization of Intracellular Ca2+ Stores by Activation of Ryanodine Receptors in Pancreatic β-Cells A Ca2+ signaling system stimulated by the insulinotropic hormone glucagon-like peptide-1-(7–37). Journal of Biological Chemistry **1999,** 274, (20), 14147-14156.

Holz, G. G. t.; Leech, C. A.; Habener, J. F., Activation of a cAMP-regulated Ca(2+)-signaling pathway in pancreatic beta-cells by the insulinotropic hormone glucagon-like peptide-1. Journal of Biological Chemistry **1995,** 270, (30), 17749-57.

Holz IV, G. G.; Kühtreiber, W. M.; Habener, J. F., Pancreatic beta-cells are rendered glucose-competent by the insulinotropic hormone glucagon-like peptide-1 (7-37). *Nature* **1993,** 361, (6410), 362.

Hoorens, A.; Van de Casteele, M.; Klöppel, G.; Pipeleers, D., Glucose promotes survival of rat pancreatic beta cells by activating synthesis of proteins which suppress a constitutive apoptotic program. *Journal of Clinical Investigation* **1996,** 98, (7), 1568.

Hornby, P. J., & Moore, B. A. The therapeutic potential of targeting the glucagon-like peptide-2 receptor in gastrointestinal disease. *Expert opinion on therapeutic targets* **2011**, 15(5), 637-646.

Hosokawa, Y. A.; Hosokawa, H.; Chen, C.; Leahy, J. L., Mechanism of impaired glucose-potentiated insulin secretion in diabetic 90% pancreatectomy rats. Study using glucagonlike peptide-1 (7-37). *Journal of Clinical Investigation* **1996,** 97, (1), 180-6.

Hou, R.; Yang, Z.; Li, M.; Xiao, H., Impact of the next-generation sequencing data depth on various biological result inferences. *Science China Life Sciences* **2013,** 56, (2), 104-109.

Hu, L. Y. A.; Tang, Y. T.; Miller, W. E.; Cong, M.; Lau, A. G.; Lefkowitz, R. J.; Hall, R. A., beta 1-adrenergic receptor association with PSD-95 - Inhibition of receptor internalization and facilitation of beta(1)-adrenergic receptor interaction with N-methyl-D-aspartate receptors. Journal of Biological Chemistry **2000,** 275, (49), 38659-38666.

Hügl, S. R.; White, M. F.; Rhodes, C. J., Insulin-like growth factor I (IGF-I)-stimulated pancreatic β-cell growth is glucose-dependent synergistic activation of insulin receptor substrate-mediated signal transduction pathways by glucose and IGF-I in INS-1 cells. Journal of Biological Chemistry **1998,** 273, (28), 17771-17779.

Hui, H.; Nourparvar, A.; Zhao, X.; Perfetti, R., Glucagon-like peptide-1 inhibits apoptosis of insulin-secreting cells via a cyclic 5′-adenosine monophosphate-dependent protein kinase A- and a phosphatidylinositol 3-kinase-dependent pathway. *Endocrinology* **2003,** 144, (4), 1444-1455.

Hui, H.; Perfetti, R., Pancreas duodenum homeobox-1 regulates pancreas development during embryogenesis and islet cell function in adulthood. *European Journal of Endocrinology* **2002,** 146, (2), 129-141.

Hui, H.; Tang, Y. G.; Zhu, L.; Khoury, N.; Hui, Z.; Wang, K. Y.; Perfetti, R.; Go, V. L. W., Glucagon like peptide-1-directed human embryonic stem cells differentiation into insulin-producing cells via hedgehog, cAMP, and PI3K pathways. *Pancreas* **2010,** 39, (3), 315-322.

Hui, H.; Wright, C.; Perfetti, R., Glucagon-like peptide 1 induces differentiation of islet duodenal homeobox-1–positive pancreatic ductal cells into insulin-secreting cells. *Diabetes* **2001,** 50, (4), 785-796.

Huising, M. O.; van der Meulen, T.; Vaughan, J. M.; Matsumoto, M.; Donaldson, C. J.; Park, H.; Billestrup, N.; Vale, W. W., CRFR1 is expressed on pancreatic β cells, promotes β cell proliferation, and potentiates insulin secretion in a glucose-dependent manner. *Proceedings of the National Academy of Sciences* **2010,** 107, (2), 912-917.

Hupe-Sodmann, K.; McGregor, G. P.; Bridenbaugh, R.; Goke, R.; Goke, B.; Thole, H.; Zimmermann, B.; Voigt, K., Characterisation of the processing by human neutral endopeptidase 24.11 of GLP-1(7-36) amide and comparison of the substrate specificity of the enzyme for other glucagon-like peptides. *Regulatory Peptides* **1995** 58, 149-156.

Hurd, P. J.; Nelson, C. J., Advantages of next-generation sequencing versus the microarray in epigenetic research. *Briefings in Functional Genomics* **2009**, elp013.

Inouye, M.; Silander, K.; Hamalainen, E.; Salomaa, V.; Harald, K.; Jousilahti, P.; Mannisto, S.; Eriksson, J. G.; Saarela, J.; Ripatti, S., An immune response network associated with blood lipid levels. *PLoS Genetics* **2010,** 6, (9), e1001113.

Inzucchi, S. E.; McGuire, D. K., New drugs for the treatment of diabetes - Part II: Incretin-based therapy and beyond. *Circulation* **2008,** 117, (4), 574-584.

Irwin, D. M., Evolution of genes for incretin hormones and their receptors. *Vitamins and Hormones* **2010,** 84, 1-20.

Irwin, N.; Flatt, P. R.; Patterson, S.; Green, B. D., Insulin-releasing and metabolic effects of small molecule GLP-1 receptor agonist 6, 7-dichloro-2-methylsulfonyl-3-N-tert-butylaminoquinoxaline. *European Journal of Pharmacology* **2010,** 628, (1), 268-273.

Ishibashi, Y.; Nishino, Y.; Matsui, T.; Takeuchi, M.; Yamagishi, S., Glucagon-like peptide-1 suppresses advanced glycation end product-induced monocyte chemoattractant protein-1 expression in mesangial cells by reducing advanced glycation end product receptor level. *Metabolism Clinical and Experimental* **2011,** 60 1271-1277.

Ishihara, H.; Asano, T.; Tsukuda, K.; Katagiri, H.; Inukai, K.; Anai, M.; Kikuchi, M.; Yazaki, Y.; Miyazaki, J.-I.; Oka, Y., Pancreatic beta cell line MIN6 exhibits characteristics of glucose metabolism and glucose-stimulated insulin secretion similar to those of normal islets. *Diabetologia* **1993,** 36, (11), 1139-1145.

Islam, M. S., Calcium signaling in the islets. In *The Islets of Langerhans*, Springer: 2010; pp 235-259.

Islam, M. S.; Rorsman, P.; Berggren, P.-O., Ca 2+-induced Ca 2+ release in insulin-secreting cells. *FEBS Letters* **1992,** 296, (3), 287-291.

Jacoby, E.; Bouhelal, R.; Gerspacher, M.; Seuwen, K., The 7TM G-protein-coupled receptor target family. *ChemMedChem* **2006,** 1, (8), 760-782.

Jarrousse, C.; Bataille, D., & Jeanrenaud, B. A Pure Enteroglucagon, Oxyntomodulin (Glucagon 37), Stimulates Insulin Release in Perfused Rat Pancreas*. *Endocrinology* **1984**, 115(1), 102-105.

Jaques, F.; Jousset, H.; Tomas, A.; Prost, A.-L.; Wollheim, C. B.; Irminger, J.-C.; Demaurex, N.; Halban, P. A., Dual effect of cell-cell contact disruption on cytosolic calcium and insulin secretion. *Endocrinology* **2008,** 149, (5), 2494-2505.

Jeppesen, P. Clinical significance of GLP-2 in short-bowel syndrome. *The Journal of nutrition* **2003**, 133(11), 3721-3724.

Jeppesen, P. B;, Hartmann, B.; Thulesen, J.; Graff, J.; Lohmann, J.; Hansen, B. S. & Holst, J. J. Glucagon-like peptide 2 improves nutrient absorption and nutritional status in short-bowel patients with no colon. *Gastroenterology* **2001**, 120(4), 806-815.

Jeppesen, P.; Sanguinetti, E.; Buckman, A.; Howard, L.; Scolapio, J.; Ziegler, T. & Mortensen, P. Teduglutide (ALX-0600), a dipeptidyl-peptidase-IV resistant glucagon-like-2 analog improves intestinal function in short bowel syndrome patients. *Gut 2005*, 54(9):1224-31.

Jeppesen, P. B., Glucagon-like peptide-2: Update of the recent clinical trials. *Gastroenterology* **2006,** 130, (2), S127-S131.

Jhala, U. S.; Canettieri, G.; Screaton, R. A.; Kulkarni, R. N.; Krajewski, S.; Reed, J.; Walker, J.; Lin, X.; White, M.; Montminy, M., cAMP promotes pancreatic beta-cell survival via CREB-mediated induction of IRS2. *Genes Development* **2003,** 17, (13), 1575-80.

Jin, S. L.; Han, V. K.; Simmons, J. G.; Towle, A. C.; Lauder, J. M.; Lund, P. K., Distribution of glucagonlike peptide I (GLP-I), glucagon, and glicentin in the rat brain: an immunocytochemical study. *The Journal of Comparative Neurology* **1988,** 271, (4), 519-32.

Jolivalt, C. G.; Fineman, M.; Deacon, C. F.; Carr, R. D.; Calcutt, N. A., GLP-1 signals via ERK in peripheral nerve and prevents nerve dysfunction in diabetic mice. *Diabetes, Obesity & Metabolism* **2011,** 13, (11), 990-1000.

Jonas, J.-C.; Sharma, A.; Hasenkamp, W.; Ilkova, H.; Patanè, G.; Laybutt, R.; Bonner-Weir, S.; Weir, G. C., Chronic hyperglycemia triggers loss of pancreatic β cell differentiation in an animal model of diabetes. *Journal Biological Chemistry* **1999,** 274, (20), 14112-14121.

Jones, P. M.; Persaud, S. J., Protein Kinases, Protein Phosphorylation, and the Regulation of Insulin Secretion from Pancreatic β-Cells. Endocrine Reviews **1998,** 19, (4), 429-461.

Jorgensen, R.; Kubale, V.; Vrecl, M.; Schwartz, T. W.; Elling, C. E., Oxyntomodulin differentially affects glucagon-like peptide-1 receptor beta-arrestin recruitment and signaling through Galpha(s). Journal of Pharmacology and Experimental Therapeutics **2007,** 322, (1), 148-154.

Josefsen, K.; Sørensen, L.; Buschard, K.; Birkenbach, M., Glucose induces early growth response gene (Egr-1) expression in pancreatic beta cells. *Diabetologia* **1999,** 42, (2), 195-203.

Kahn, C. R., Knockout mice challenge our concepts of glucose homeostasis and the pathogenesis of diabetes. Experimental Diabesity Research **2003,** 4, (3), 169-82.

Kahvejian, A.; Quackenbush, J.; Thompson, J. F., What would you do if you could sequence everything? *Nature biotechnology* **2008,** 26, (10), 1125-1133.

Kaiser, S.; Nisenbaum, L. K., Evaluation of common gene expression patterns in the rat nervous system. *Physiological Genomics* **2003,** 16, (1), 1-7.

Kalwat, M. A.; Thurmond, D. C., Signaling mechanisms of glucose-induced F-actin remodeling in pancreatic islet β cells. *Experimental & Molecular Medicine* **2013,** 45, (8), e37.

Kandpal, R. P.; Rajasimha, H. K.; Brooks, M. J.; Nellissery, J.; Wan, J.; Qian, J.; Kern, T. S.; Swaroop, A., Transcriptome analysis using next generation sequencing reveals molecular signatures of diabetic retinopathy and efficacy of candidate drugs. *Molecular Vision* **2012,** 18, 1123.

Kanehisa, M.; Goto, S., KEGG: kyoto encyclopedia of genes and genomes. *Nucleic Acids Research* **2000,** 28, (1), 27-30.

Kaneto, H.; Matsuoka, T. A.; Nakatani, Y.; Kawamori, D.; Matsuhisa, M.; Yamasaki, Y., Oxidative stress and the JNK pathway in diabetes. Current Diabetes Reviews 2005, 1, (1), 65-72.

Kang, G.; Chepurny, O. G.; Holz, G. G., cAMP-regulated guanine nucleotide exchange factor II (Epac2) mediates Ca2+-induced Ca2+ release in INS-1 pancreatic beta-cells. *The Journal of Physiology* **2001,** 536, (Pt 2), 375-85.

Kang, G.; Chepurny, O. G.; Malester, B.; Rindler, M. J.; Rehmann, H.; Bos, J. L.; Schwede, F.; Coetzee, W. A.; Holz, G. G., cAMP sensor Epac as a determinant of ATP-sensitive potassium channel activity in human pancreatic β cells and rat INS-1 cells. *The Journal of physiology* **2006,** 573, (3), 595-609.

Kang, G.; Holz, G. G., Amplification of exocytosis by Ca2+-induced Ca2+ release in INS-1 pancreatic β cells. *The Journal of physiology* **2003,** 546, (1), 175-189.

Kang, G.; Joseph, J. W.; Chepurny, O. G.; Monaco, M.; Wheeler, M. B.; Bos, J. L.; Schwede, F.; Genieser, H. G.; Holz, G. G., Epac-selective cAMP analog 8-pCPT-2'-O-Me-cAMP as a stimulus for Ca2+-induced Ca2+ release and exocytosis in pancreatic beta-cells. *Journal of Biological Chemistry* **2003,** 278, (10), 8279-85.

Kang, U. G.; Jeon, W. J.; Kim, Y.; Chung, C. K.; Park, J. B.; Juhnn, Y. S.; Kim, Y. S., Transient activation of protein phosphatase 2A induced by electroconvulsive shock in the rat frontal cortex. *Neuroscience Letters* **2005,** 390, (3), 171-5.

Kanse, S. M.; Kreymann, B.; Ghatei, M. A.; Bloom, S. R., Identification and characterization of glucagon-like peptide-1 7-36 amide-binding sites in the rat brain and lung. *FEBS Letters* **1988,** 241, (1-2), 209-12.

Kappo, M. A.; Eiso, A.; Hassem, F.; Atkinson, R. A.; Faro, A.; Muleya, V.; Mulaudzi, T.; Poole, J. O.; McKenzie, J. M.; Chibi, M., Solution structure of RING finger-like domain of retinoblastoma-binding protein-6 (RBBP6) suggests it functions as a U-box. *Journal of Biological Chemistry* **2012,** 287, (10), 7146-7158.

Kapranov, P.; Cawley, S. E.; Drenkow, J.; Bekiranov, S.; Strausberg, R. L.; Fodor, S. P.; Gingeras, T. R., Large-scale transcriptional activity in chromosomes 21 and 22. *Science* **2002,** 296, (5569), 916-919.

Kapranov, P.; Drenkow, J.; Cheng, J.; Long, J.; Helt, G.; Dike, S.; Gingeras, T. R., Examples of the complex architecture of the human transcriptome revealed by RACE and high-density tiling arrays. *Genome Research* **2005,** 15, (7), 987-997.

Kara, E.; Crepieux, P.; Gauthier, C.; Martinat, N.; Piketty, V.; Guillou, F.; Reiter, E., A phosphorylation cluster of five serine and threonine residues in the C-terminus of the follicle-stimulating hormone receptor is important for desensitization but not for beta-arrestin-mediated ERK activation. *Molecular Endocrinology* **2006,** 20, (11), 3014-3026.

Kashima, Y.; Miki, T.; Shibasaki, T.; Ozaki, N.; Miyazaki, M.; Yano, H.; Seino, S., Critical role of cAMP-GEFII· Rim2 complex in incretin-potentiated insulin secretion. *Journal of Biological Chemistry* **2001,** 276, (49), 46046-46053.

Kato, T.; Nagatsu, T.; Fukasawa, K.; Harada, M.; Nagatsu, I.; Sakakibara, S., Successive cleavage of N-terminal Arg1--Pro2 and Lys3-Pro4 from substance P but no release of Arg1-Pro2 from bradykinin, by X-Pro dipeptidyl-aminopeptidase. Biochimica et Biophysica Acta **1978,** 525, (2), 417-22.

Kawasaki, H.; Springett, G. M.; Mochizuki, N.; Toki, S.; Nakaya, M.; Matsuda, M.; Housman, D. E.; Graybiel, A. M., A family of cAMP-binding proteins that directly activate Rap1. *Science* **1998,** 282, 2275-2279.

Keire, D. A.; Bowers, C. W.; Solomon, T. E.; Reeve, J. R., Jr., Structure and receptor binding of PYY analogs. *Peptides* **2002,** 23, (2), 305-21.

Kenakin, T., Principles: Receptor theory in pharmacology. Trends in Pharmacological Sciences **2004,** 25, (4), 186-192.

Kenakin, T., New concepts in drug discovery: collateral efficacy and permissive antagonism. *Nature Reviews. Drug discovery* **2005,** 4, (11), 919-27.

Kenakin, T., Allosteric theory: taking therapeutic advantage of the malleable nature of GPCRs. *Current Neuropharmacology* **2007,** 5, (3), 149-56.

Kenakin, T., Collateral efficacy in drug discovery: taking advantage of the good (allosteric) nature of 7TM receptors. Trends in Pharmacological Sciences **2007,** 28, (8), 407-415.

Kenakin, T., Functional selectivity in GPCR modulator screening. *Combinatorial Chemistry & High Throughput Screening* **2008,** 11, (5), 337-43.

Kenakin, T., Functional selectivity and biased receptor signaling. Journal of Pharmacology and Experimental Therapeutics **2011,** 336, (2), 296-302.

Kenakin, T.; Christopoulos, A., Signalling bias in new drug discovery: detection, quantification and therapeutic impact. Nature Reviews Drug Discovery **2013,** 12, (3), 205-216.

Kenakin, T.; Miller, L. J., Seven transmembrane receptors as shapeshifting proteins: the impact of allosteric modulation and functional selectivity on new drug discovery. *Pharmacological Reviews* **2010,** 62, (2), 265-304.

Kenakin, T. P., '7TM receptor allostery: putting numbers to shapeshifting proteins. Trends in Pharmacological Sciences **2009,** 30, (9), 460-9.

Kenny, A. D.; Ahearn, D. J.; Maher, J. F., Improved method for determining parathyroid hormone in biological material. Biochemical Medicine **1976,** 16, (3), 201-10.

Kervran, A.; Blache, P & Bataille, D. Distribution of Oxyntomodulin and Glucagon in the Gastrointestinal Tract and the Plasma of the Rat*. *Endocrinology* **1987**, 121(2), 704-713.

Keov, P.; Sexton, P. M.; Christopoulos, A., Allosteric modulation of G protein-coupled receptors: a pharmacological perspective. *Neuropharmacology* **2011,** 60, (1), 24-35.

Khin, E. E.; Kikkawa, F.; Ino, K.; Suzuki, T.; Shibata, K.; Kajiyama, H.; Tamakoshi, K.; Mizutani, S., Neutral endopeptidase/CD10 expression in the stroma of epithelial ovarian carcinoma. International Journal of Gynecological Pathology **2003,** 22, (2), 175-80.

Khoo, S.; Cobb, M. H., Activation of mitogen-activating protein kinase by glucose is not required for insulin secretion. *Proceedings of the National Academy of Sciences* **1997,** 94, (11), 5599-5604.

Khoo, S.; Griffen, S. C.; Xia, Y.; Baer, R. J.; German, M. S.; Cobb, M. H., Regulation of insulin gene transcription by ERK1 and ERK2 in pancreatic β cells. *Journal Biological Chemistry* **2003,** 278, (35), 32969-32977.

Khoury, E.; Clément, S.; Laporte, S. A., Allosteric and biased g protein-coupled receptor signaling regulation: potentials for new therapeutics. *Frontiers in Endocrinology* **2014,** 5.

Kieffer, T. J.; McIntosh, C. H.; Pederson, R. A., Degradation of glucose-dependent insulinotropic polypeptide and truncated glucagon-like peptide 1 in vitro and in vivo by dipeptidyl peptidase IV. *Endocrinology* **1995,** 136, (8), 3585-96.

Kieffer, T. J.; McIntosh, C., & Pederson, R. A. Degradation of glucose-dependent insulinotropic polypeptide and truncated glucagon-like peptide 1 in vitro and in vivo by dipeptidyl peptidase IV. *Endocrinology* **1995**, 136(8), 3585-3596.

Kiekens, R.; In't Veld, P.; Mahler, T.; Schuit, F.; Van De Winkel, M.; Pipeleers, D., Differences in glucose recognition by individual rat pancreatic B cells are associated with intercellular differences in glucose-induced biosynthetic activity. *Journal of Clinical Investigation* **1992,** 89, (1), 117.

Kim, D.; MacConell, L.; Zhuang, D.; Kothare, P. A.; Trautmann, M.; Fineman, M., & Taylor, K. Effects of once-weekly dosing of a long-acting release formulation of exenatide on glucose control and body weight in subjects with type 2 diabetes. *Diabetes Care* **2007**, 30(6), 1487-1493.

Kim Chung le, T.; Hosaka, T.; Yoshida, M.; Harada, N.; Sakaue, H.; Sakai, T.; Nakaya, Y., Exendin-4, a GLP-1 receptor agonist, directly induces adiponectin expression through

protein kinase A pathway and prevents inflammatory adipokine expression. Biochemical and Biophysical Research Communications **2009,** 390, (3), 613-8.

Kim, D.; Wang, L.; Beconi, M.; Eiermann, G. J.; Fisher, M. H.; He, H.; Hickey, G. J.; Kowalchick, J. E.; Leiting, B.; Lyons, K.; Marsilio, F.; McCann, M. E.; Patel, R. A.; Petrov, A.; Scapin, G.; Patel, S. B.; Roy, R. S.; Wu, J. K.; Wyvratt, M. J.; Zhang, B. B.; Zhu, L.; Thornberry, N. A.; Weber, A. E., (2R)-4-oxo-4-[3-(trifluoromethyl)-5,6-dihydro[1,2,4]triazolo[4,3-a]pyrazin-7(8H)-yl]-1-(2,4,5-trifluorophenyl)butan-2-amine: a potent, orally active dipeptidyl peptidase IV inhibitor for the treatment of type 2 diabetes. Journal of Medicinal Chemistry **2005,** 13, (48(1)), 141-51.

Kim, J.; Ahn, S.; Ren, X. R.; Whalen, E. J.; Reiter, E.; Wei, H. J.; Lefkowitz, R. J., Functional antagonism of different G protein-coupled receptor kinases for beta-arrestin-mediated angiotensin II receptor signaling. *Proceedings of the National Academy of Sciences of the United States of America* **2005,** 102, (5), 1442-1447.

Kim, J.-Y.; Lee, S.-K.; Jo, K.-J.; Song, D.-Y.; Lim, D.-M.; Park, K.-Y.; Bonewald, L. F.; Kim, B.-J., Exendin-4 increases bone mineral density in type 2 diabetic OLETF rats potentially through the down-regulation of SOST/sclerostin in osteocytes. *Life sciences* **2013,** 92, (10), 533-40.

Kim, K. R.; Rhee, S. D.; Kim, H. Y.; Jung, W. H.; Yang, S. D.; Kim, S. S.; Ahn, J. H.; Cheon, H. G., KR-62436, 6-{2-[2-(5-cyano-4,5-dihydropyrazol-1-yl)-2-oxoethylamino]ethylamino}nicotinonitr ile, is a novel dipeptidyl peptidase-IV (DPP-IV) inhibitor with anti-hyperglycemic activity. European Journal of Pharmacology **2005,** 518, (1), 63-70.

Kim, M.; Platt, M. J.; Shibasaki, T.; Quaggin, S. E.; Backx, P. H.; Seino, S.; Simpson, J. A.; Drucker, D. J., GLP-1 receptor activation and Epac2 link atrial natriuretic peptide secretion to control of blood pressure. *Nature Medicine* **2013,** 19, (5), 567-75.

Kim, W.; Egan, J. M., The role of incretins in glucose homeostasis and diabetes treatment. *Pharmacological Reviews* **2008,** 60, (4), 470-512.

Kim, Y. N.; Kim, S.; Kim, I.-Y.; Shin, J. H.; Cho, S.; Yi, S. S.; Kim, W. K.; Kim, K.-S.; Lee, S.; Seong, J. K., Transcriptomic analysis of insulin-sensitive tissues from anti-diabetic drug treated Zdf rats, a T2Dm animal model. *PLoS One* **2013,** 8, (7), e69624.

Klinger, S.; Poussin, C.; Debril, M. B.; Dolci, W.; Halban, P. A.; Thorens, B., Increasing GLP-1-induced beta-cell proliferation by silencing the negative regulators of signaling cAMP response element modulator-alpha and DUSP14. *Diabetes* **2008,** 57, (3), 584-93.

Knaack, D.; Fiore, D. M.; Surana, M.; Leiser, M.; Laurance, M.; Fusco-DeMane, D.; Hegre, O. D.; Fleischer, N.; Efrat, S., Clonal insulinoma cell line that stably maintains correct glucose responsiveness. *Diabetes* **1994,** 43, (12), 1413-1417.

Knudsen, K., [Doctored drinks and drugs more myth than reality in rape cases]. *Lakartidningen* **2007,** 104, (37), 2603-5.

Knudsen, L. B.; Kiel, D.; Teng, M.; Behrens, C.; Bhumralkar, D.; Kodra, J. T.; Holst, J. J.; Jeppesen, C. B.; Johnson, M. D.; de Jong, J. C.; Jorgensen, A. S.; Kercher, T.; Kostrowicki, J.; Madsen, P.; Olesen, P. H.; Petersen, J. S.; Poulsen, F.; Sidelmann, U. G.; Sturis, J.;

Truesdale, L.; May, J.; Lau, J., Small-molecule agonists for the glucagon-like peptide 1 receptor. *Proceedings of the National Academy of Sciences of the United States of America* **2007,** 104, (3), 937-42.

Knudsen, L. B.; Pridal, L., Glucagon-like peptide-1- (9 -36) amide is a major metabolite of glucagon-like peptide-1- (7-36) amide after in vivo administration to dogs, it acts as an antagonist on the pancreatic receptor. *European Journal of Pharmacology* **1996,** 318, 429-435.

Kodera, R.; Shikata, K.; Kataoka, H. U.; Takatsuka, T.; Miyamoto, S.; Sasaki, M.; Kajitani, N.; Nishishita, S.; Sarai, K.; Hirota, D.; Sato, C.; Ogawa, D.; Makino, H., Glucagon-like peptide-1 receptor agonist ameliorates renal injury through its anti-inflammatory action without lowering blood glucose level in a rat model of type 1 diabetes. *Diabetologia* **2011,** 54, (4), 965-78.

Kolakowski, L. F., GCRDB - A G-protein-coupled receptor database. *Receptors and Channels* **1994,** 2, (1), 1-7.

Koole, C.; Wootten, D.; Simms, J.; Miller, L. J.; Christopoulos, A., & Sexton, P. M. Differential impact of amino acid substitutions on critical residues of the human glucagon-like peptide-1 receptor involved in peptide activity and small-molecule allostery. *Journal of Pharmacology and Experimental Therapeutics* **2015**, 353(1), 52-63.

Koole, C.; Wootten, D.; Simms, J.; Savage, E. E.; Miller, L. J.; Christopoulos, A., & Sexton, P. M. Second extracellular loop of human glucagon-like peptide-1 receptor (GLP-1R) differentially regulates orthosteric but not allosteric agonist binding and function. *Journal of Biological Chemistry* **2012**, 287(6), 3659-3673.

Koole, C.; Pabreja, K.; Savage, E. E.; Wootten, D.; Furness, S.; Miller, L. J.; Christopoulos, A.; Sexton, P. M., Recent advances in understanding GLP-1R (glucagon-like peptide-1 receptor) function. Biochemical Society Transactions **2013,** 41, (1), 172-179.

Koole, C.; Savage, E. E.; Christopoulos, A.; Miller, L. J.; Sexton, P. M.; Wootten, D., Minireview: signal bias, allosterism, and polymorphic variation at the GLP-1R: implications for drug discovery. *Molecular Endocrinology* **2013,** 27, (8), 1234-1244.

Koole, C.; Wootten, D.; Simms, J.; Miller, L. J.; Christopoulos, A.; Sexton, P. M., Second extracellular loop of human glucagon-like peptide-1 receptor (GLP-1R) has a critical role in GLP-1 peptide binding and receptor activation. *Journal Biological Chemistry* **2012,** 287, (6), 3642-3658.

Koole, C.; Wootten, D.; Simms, J.; Valant, C.; Miller, L. J.; Christopoulos, A.; Sexton, P. M., Polymorphism and ligand dependent changes in human glucagon-like peptide-1 receptor (GLP-1R) function: allosteric rescue of loss of function mutation. *Molecular Pharmacology* **2011,** 80, (3), 486-497.

Koole, C.; Wootten, D.; Simms, J.; Valant, C.; Sridhar, R.; Woodman, O. L.; Miller, L. J.; Summers, R. J.; Christopoulos, A.; Sexton, P. M., Allosteric ligands of the glucagon-like peptide 1 receptor (GLP-1R) differentially modulate endogenous and exogenous peptide responses in a pathway-selective manner: implications for drug screening. *Molecular Pharmacology* **2010,** 78, (3), 456-65.

Koole, O.; Colebunders, R., ART in low-resource settings: how to do more with less. *Lancet* **2010,** 376, (9739), 396-8.

Krämer, A.; Green, J.; Pollard, J.; Tugendreich, S., Causal Analysis Approaches in Ingenuity Pathway Analysis (IPA). *Bioinformatics* **2013**, btt703.

Krasnoperov, V. G.; Bittner, M. A.; Beavis, R.; Kuang, Y. N.; Salnikow, K. V.; Chepurny, O. G.; Little, A. R.; Plotnikov, A. N.; Wu, D. Q.; Holz, R. W.; Petrenko, A. G., alpha-latrotoxin stimulates exocytosis by the interaction with a neuronal G-protein-coupled receptor. *Neuron* **1997,** 18, (6), 925-937.

Krause, R. M.; Buisson, B.; Bertrand, S.; Corringer, P.-J.; Galzi, J.-L.; Changeux, J.-P.; Bertrand, D., Ivermectin: a positive allosteric effector of the α7 neuronal nicotinic acetylcholine receptor. *Molecular Pharmacology* **1998,** 53, (2), 283-294.

Kreymann, B.; Ghatei, M. A.; Williams, G.; Bloom, S. R., Glucagonlike peptide-1 (7-36): a physiological incretin in man. *Lancet* **1987,** 2, 1300-1304.

Kristiansen, K., Molecular mechanisms of ligand binding, signaling, and regulation within the superfamily of G-protein-coupled receptors: molecular modeling and mutagenesis approaches to receptor structure and function. *Pharmacology and Therapeutics* **2004,** 103, (1), 21-80.

Kumar, S.; Pioszak, A.; Zhang, C. H.; Swaminathan, K.; Xu, H. E., Crystal Structure of the PAC1R Extracellular Domain Unifies a Consensus Fold for Hormone Recognition by Class B G-Protein Coupled Receptors. *PLoS One* **2011,** 6, (5).

Kunishima, N.; Shimada, Y.; Tsuji, Y.; Sato, T.; Yamamoto, M.; Kumasaka, T.; Nakanishi, S.; Jingami, H.; Morikawa, K., Structural basis of glutamate recognition by a dimeric metabotropic glutamate receptor. *Nature* **2000,** 407, (6807), 971-977.

Kushner, J. A.; Simpson, L.; Wartschow, L. M.; Guo, S.; Rankin, M. M.; Parsons, R.; White, M. F., Phosphatase and tensin homolog regulation of islet growth and glucose homeostasis. *Journal Biological Chemistry* **2005,** 280, (47), 39388-39393.

Kwon, G.; Marshall, C. A.; Liu, H.; Pappan, K. L.; Remedi, M. S.; McDaniel, M. L., Glucose-stimulated DNA Synthesis through Mammalian Target of Rapamycin (mTOR) Is Regulated by KATP Channels. Effects on cell cycle progression in rodent islets. *Journal Biological Chemistry* **2006,** 281, (6), 3261-3267.

Kwon, G.; Marshall, C. A.; Pappan, K. L.; Remedi, M. S.; McDaniel, M. L., Signaling elements involved in the metabolic regulation of mTOR by nutrients, incretins, and growth factors in islets. *Diabetes* **2004,** 53, (suppl 3), S225-S232.

Lagerstrom, M. C.; Schioth, H. B., Structural diversity of G protein-coupled receptors and significance for drug discovery. Nature Reviews Drug Discovery **2008,** 7, (4), 339-357.

Lambeir, A. M.; Durinx, C.; Proost, P.; Van Damme, J.; Scharpe, S.; De Meester, I., Kinetic study of the processing by dipeptidyl-peptidase IV/CD26 of neuropeptides involved in pancreatic insulin secretion. *FEBS Letters* **2001,** 507, (3), 327-30.

Lambright, D. G.; Noel, J. P.; Hamm, H. E.; Sigler, P. B., Structural determinants for activation of the alpha-subunit of a heterotrimeric g-protein. *Nature* **1994,** 369, (6482), 621-628.

Lamont, B. J.; Li, Y.; Kwan, E.; Brown, T. J.; Gaisano, H.; Drucker, D. J., Pancreatic GLP-1 receptor activation is sufficient for incretin control of glucose metabolism in mice. *The Journal of Clinical Investigation* **2012,** 122, (1), 388.

Langmead, C. J.; Christopoulos, A., Allosteric agonists of 7TM receptors: expanding the pharmacological toolbox. *Trends in Pharmacological Sciences* **2006,** 27, (9), 475-81.

Langmead, C. J.; Christopoulos, A., Functional and structural perspectives on allosteric modulation of GPCRs. *Current Opinion in Cell Biology* **2014,** 27, 94-101.

Larsen, J.; Hylleberg, B.; Ng, K.; Damsbo, P., Glucagon-like peptide-1 infusion must be maintained for 24 h/day to obtain acceptable glycemia in type 2 diabetic patients who are poorly controlled on sulphonylurea treatment. *Diabetes Care* **2001,** 24, (8), 1416-1421.

Larsen, P. J.; Tang-Christensen, M.; Jessop, D. S., Central administration of glucagon-like peptide-1 activates hypothalamic neuroendocrine neurons in the rat. *Endocrinology* **1997,** 138, (10), 4445-55.

Lawrence, M. C.; McGlynn, K.; Naziruddin, B.; Levy, M. F.; Cobb, M. H., Differential regulation of CHOP-10/GADD153 gene expression by MAPK signaling in pancreatic beta-cells. *Proceedings of the National Academy of Sciences of the United States of America* **2007,** 104, (28), 11518-25.

Lawrence, M. C.; McGlynn, K.; Park, B. H.; Cobb, M. H., ERK1/2-dependent activation of transcription factors required for acute and chronic effects of glucose on the insulin gene promoter. *Journal of Biological Chemistry* **2005,** 280, (29), 26751-9.

Lazareno, S.; Birdsall, N. J., Detection, quantitation, and verification of allosteric interactions of agents with labeled and unlabeled ligands at G protein-coupled receptors: interactions of strychnine and acetylcholine at muscarinic receptors. *Molecular Pharmacology* **1995,** 48, (2), 362-78.

Leach, K.; Sexton, P. M.; Christopoulos, A., Allosteric GPCR modulators: taking advantage of permissive receptor pharmacology. *Trends in Pharmacological Sciences* **2007,** 28, (8), 382-9.

Ledford, H., The death of microarrays? *Nature News* **2008,** 455, (7215), 847-847.

Lee, J.-H.; Gao, C.; Peng, G.; Greer, C.; Ren, S.; Wang, Y.; Xiao, X., Analysis of transcriptome complexity through RNA sequencing in normal and failing murine hearts. *Circulation Research* **2011,** 109, (12), 1332-1341.

Lee, Y. S.; Park, M. S.; Choung, J. S.; Kim, S. S.; Oh, H. H.; Choi, C. S.; Ha, S. Y.; Kang, Y.; Kim, Y.; Jun, H. S., Glucagon-like peptide-1 inhibits adipose tissue macrophage infiltration and inflammation in an obese mouse model of diabetes. *Diabetologia* **2012,** 55, (9), 2456-68.

Leech, C. A.; Dzhura, I.; Chepurny, O. G.; Kang, G.; Schwede, F.; Genieser, H.-G.; Holz, G. G., Molecular physiology of glucagon-like peptide-1 insulin secretagogue action in pancreatic β cells. *Progress in Biophysics and Molecular Biology* **2011,** 107, (2), 236-247.

Lefkowitz, R. J., G protein-coupled receptors III. New roles for receptor kinases and beta-arrestins in receptor signaling and desensitization. *Journal of Biological Chemistry* **1998,** 273, (30), 18677-18680.

Leftowitz, R. J.; Shenoy, S. K., Transduction of receptor signals by beta-arrestins. *Science* **2005,** 308, (5721), 512-517.

Levin, J. Z.; Yassour, M.; Adiconis, X.; Nusbaum, C.; Thompson, D. A.; Friedman, N.; Gnirke, A.; Regev, A., Comprehensive comparative analysis of strand-specific RNA sequencing methods. *Nature Methods* **2010,** 7, (9), 709-715.

Li, N.; Lu, J.; Willars, G. B., Allosteric modulation of the activity of the glucagon-like peptide-1 (GLP-1) metabolite GLP-1 9–36 amide at the GLP-1 receptor. *PLOS One,* **2012,** 7, (10), e47936.

Li, S.; Tighe, S. W.; Nicolet, C. M.; Grove, D.; Levy, S.; Farmerie, W.; Viale, A.; Wright, C.; Schweitzer, P. A.; Gao, Y., Multi-platform assessment of transcriptome profiling using RNA-seq in the ABRF next-generation sequencing study. *Nature Biotechnology* **2014,** 32, (9), 915-925.

Li, Y.; Cao, X.; Li, L.-X.; Brubaker, P. L.; Edlund, H.; Drucker, D. J., β-Cell Pdx1 expression is essential for the glucoregulatory, proliferative, and cytoprotective actions of glucagon-like peptide-1. *Diabetes* **2005,** 54, (2), 482-491.

Li, Y.; Hansotia, T.; Yusta, B.; Ris, F.; Halban, P. A.; Drucker, D. J., Glucagon-like peptide-1 receptor signaling modulates β cell apoptosis. *Journal of Biological Chemistry* **2003,** 278, (1), 471-478.

Li, Y.; Hansotia, T.; Yusta, B.; Ris, F.; Halban, P. A.; Drucker, D. J., Glucagon-like peptide-1 receptor signaling modulates beta cell apoptosis. *Journal of Biological Chemistry* **2003,** 278, (1), 471-8.

Liang, C. P.; Han, S.; Li, G.; Tabas, I.; Tall, A. R., Impaired MEK signaling and SERCA expression promote ER stress and apoptosis in insulin-resistant macrophages and are reversed by exenatide treatment. *Diabetes* **2012,** 61, (10), 2609-2620.

Liang, W. S.; Craig, D. W.; Carpten, J.; Borad, M. J.; Demeure, M. J.; Weiss, G. J.; Izatt, T.; Sinari, S.; Christoforides, A.; Aldrich, J., Genome-wide characterization of pancreatic adenocarcinoma patients using next generation sequencing. *Plos One,* **2012,** 7, (10), e43192.

Ling, Z.; Hannaert, J.; Pipeleers, D., Effect of nutrients, hormones and serum on survival of rat islet beta cells in culture. *Diabetologia* **1994,** 37, (1), 15-21.

Ling, Z.; Kiekens, R.; Mahler, T.; Schuit, F. C.; Pipeleers-Marichal, M.; Sener, A.; Klöppel, G.; Malaisse, W. J.; Pipeleers, D. G., Effects of chronically elevated glucose levels on the functional properties of rat pancreatic β-cells. *Diabetes* **1996,** 45, (12), 1774-1782.

Ling, Z.; Pipeleers, D. G., Preservation of glucose-responsive islet beta-cells during serum-free culture. *Endocrinology* **1994,** 134, (6), 2614-2621.

Ling, Z.; Wu, D.; Zambre, Y.; Flamez, D.; Drucker, D.; Pipeleers, D. G.; Schuit, F. C., Glucagon-like peptide 1 receptor signaling influences topography of islet cells in mice. *Virchows Archiv: The European Journal of Pathology* **2001,** 438, (4), 382-387.

Lingohr, M. K.; Dickson, L. M.; McCuaig, J. F.; Hugl, S. R.; Twardzik, D. R.; Rhodes, C. J., Activation of IRS-2—Mediated Signal Transduction by IGF-1, but not TGF-α or EGF, Augments Pancreatic β-Cell Proliferation. *Diabetes* **2002,** 51, (4), 966-976.

Liao, S.; Liang, Y.; Zhang, Z.; Li, J.; Wang, J.; Wang, X.;Liu, K. In Vitro Metabolic Stability of Exendin-4: Pharmacokinetics and Identification of Cleavage Products. *PloS one* **2015**, 10(2), e0116805.

Linnebjerg, H.; Park, S.; Kothare, P. A.; Trautmann, M. E.; Mace, K.; Fineman, M.; Horowitz, M. Effect of exenatide on gastric emptying and relationship to postprandial glycemia in type 2 diabetes. *Regulatory peptides* **2008**, 151(1), 123-129.

List, J. F.; He, H.; Habener, J. F., Glucagon-like peptide-1 receptor and proglucagon expression in mouse skin. Regulatory Peptides **2006,** 134, (2-3), 149-57.

Liu, F.; Wan, Q.; Pristupa, Z. B.; Yu, X. M.; Wang, Y. T.; Niznik, H. B., Direct protein-protein coupling enables cross-talk between dopamine D5 and gamma-aminobutyric acid A receptors. *Nature* **2000,** 403, (6767), 274-280.

Liu, Y. L.; Ford, H. E.; Druce, M. R.; Minnion, J. S.; Field, B. C.; Shillito, J. C.; Baxter, J.; Murphy, K. G.; Ghatei, M. A.; Bloom, S. R., Subcutaneous oxyntomodulin analogue administration reduces body weight in lean and obese rodents. *International Journal of Obesity* **2010,** 34, (12), 1715-25.

Liu, Z.; Habener, J. F., Glucagon-like peptide-1 activation of TCF7L2-dependent Wnt signaling enhances pancreatic beta cell proliferation. *Journal of Biological Chemistry* **2008,** 283, (13), 8723-35.

Liu, Z.; Pan, X.; Zhang, X., Total knee arthroplasty using navigation system for severe osteoarthritis with extra-articular deformity. *European Journal of Orthopaedic Surgery & Traumatology* **2013,** 23, (1), 93-6.

Lopez-Delgado, M. I.; Morales, M.; Villanueva-Penacarrillo, M. L.; Malaisse, W. J.; Valverde, I., Effects of glucagon-like peptide 1 on the kinetics of glycogen synthase a in hepatocytes from normal and diabetic rats. *Endocrinology* **1998,** 139, (6), 2811-7.

Lue, H.; Kapurniotu, A.; Fingerle-Rowson, G.; Roger, T.; Leng, L.; Thiele, M.; Calandra, T.; Bucala, R.; Bernhagen, J., Rapid and transient activation of the ERK MAPK signalling pathway by macrophage migration inhibitory factor (MIF) and dependence on JAB1/CSN5 and Src kinase activity. *Cell Signalling* **2006,** 18, (5), 688-703.

Luttrell, L. M., Reviews in molecular biology and biotechnology: Transmembrane signaling by G protein-coupled receptors. *Molecular Biotechnology* **2008,** 39, (3), 239-264.

Luttrell, L. M.; Daaka, Y.; Lefkowitz, R. J., Regulation of tyrosine kinase cascades by G-protein-coupled receptors. *Current Opinion in Cell Biology* **1999,** 11, (2), 177-183.

Luttrell, L. M.; Roudabush, F. L.; Choy, E. W.; Miller, W. E.; Field, M. E.; Pierce, K. L.; Lefkowitz, R. J., Activation and targeting of extracellular signal-regulated kinases by beta-arrestin scaffolds. *Proceedings of the National Academy of Sciences of the United States of America* **2001,** 98, (5), 2449-2454.

Ma, X.; Meng, J.; Jia, M.; Bi, L.; Zhou, Y.; Wang, Y.; Hu, J.; He, G.; Luo, X., Exendin-4, a glucagon-like peptide-1 receptor agonist, prevents osteopenia by promoting bone formation and suppressing bone resorption in aged ovariectomized rats. *Journal of Bone and Mineral Research* **2013,** 28, (7), 1641-52.

MacDonald, P. E.; El-kholy, W.; Riedel, M. J.; Salapatek, A. M. F.; Light, P. E.; Wheeler, M. B., The multiple actions of GLP-1 on the process of glucose-stimulated insulin secretion. *Diabetes* **2002,** 51, (suppl 3), S434-S442.

MacDonald, P. E.; Salapatek, A. M. F.; Wheeler, M. B., Glucagon-Like Peptide-1 Receptor Activation Antagonizes Voltage-Dependent Repolarizing K+ Currents in β-Cells A Possible Glucose-Dependent Insulinotropic Mechanism. *Diabetes* **2002,** 51, (suppl 3), S443-S447.

MacDonald, P. E.; Wang, X.; Xia, F.; El-kholy, W.; Targonsky, E. D.; Tsushima, R. G.; Wheeler, M. B., Antagonism of rat beta-cell voltage-dependent K+ currents by exendin 4 requires dual activation of the cAMP/protein kinase A and phosphatidylinositol 3-kinase signaling pathways. *Journal of Biological Chemistry* **2003,** 278, (52), 52446-53.

MacDonald, P. E.; Wang, X.; Xia, F.; El-Kholy, W.; Targonsky, E. D.; Tsushima, R. G.; Wheeler, M. B., Antagonism of rat β-cell voltage-dependent K+ currents by exendin 4 requires dual activation of the cAMP/protein kinase A and phosphatidylinositol 3-kinase signaling pathways. *Journal of Biological Chemistry* **2003,** 278, (52), 52446-52453.

Mack, C.; Moore, C.; Jodka, C.; Bhavsar, S.; Wilson, J.; Hoyt, J. & Parkes, D. Antiobesity action of peripheral exenatide (exendin-4) in rodents: effects on food intake, body weight, metabolic status and side-effect measures. *International journal of obesity* **2006**, 30(9), 1332-1340.

Maida, A.; Lovshin, J. A.; Baggio, L. L.; Drucker, D. J., The glucagon-like peptide-1 receptor agonist oxyntomodulin enhances β-cell function but does not inhibit gastric emptying in mice. *Endocrinology* **2008,** 149, (11), 5670-5678.

Maida, A.; Hansotia, T.; Longuet, C.; Seino, Y., & Drucker, D. J. Differential importance of glucose-dependent insulinotropic polypeptide vs glucagon-like peptide 1 receptor signaling for beta cell survival in mice. *Gastroenterology* **2009**, 137(6), 2146-2157.

Makita, N.; Sato, J.; Manaka, K.; Shoji, Y.; Oishi, A.; Hashimoto, M.; Fujita, T.; Iiri, T., An acquired hypocalciuric hypercalcemia autoantibody induces allosteric transition among active human Ca-sensing receptor conformations. *Proceedings of the National Academy of Sciences* **2007,** 104, (13), 5443-5448.

Malbon, C. C., Frizzleds: New members of the superfamily of G-protein-coupled receptors. *Frontiers in Bioscience* **2004,** 9, 1048-1058.

Malitschek, B.; Schweizer, C.; Keir, M.; Heid, J.; Froestl, W.; Mosbacher, J.; Kuhn, R.; Henley, J.; Joly, C.; Pin, J. P.; Kaupmann, K.; Bettler, B., The N-terminal domain of gamma-aminobutyric acid(B) receptors is sufficient to specify agonist and antagonist binding. *Molecular Pharmacology* **1999,** 56, (2), 448-454.

Mancuso, F.; Basta, G.; Calvitti, M.; Luca, G.; Guido, L.; Racanicchi, L.; Montanucci, P.; Becchetti, E.; Calafiore, R., Long-term cultured neonatal porcine islet cell monolayers: a potential tissue source for transplant in diabetes. *Xenotransplantation* **2006,** 13, (4), 289-298.

Marathe, C. S.; Rayner, C. K.; Jones, K. L., & Horowitz, M. Glucagon-like peptides 1 and 2 in health and disease: a review. *Peptides* **2013**, 44, 75-86.

Marguerat, S.; Wilhelm, B. T.; Bähler, J., British Yeast Group Meeting 2008: Next-generation sequencing: applications beyond genomes. *Biochemical Society Transactions* **2008,** 36, (Pt 5), 1091.

Marguet, D.; Baggio, L.; Kobayashi, T.; Bernard, A. M.; Pierres, M.; Nielsen, P. F.; Ribel, U.; Watanabe, T.; Drucker, D. J.; Wagtmann, N., Enhanced insulin secretion and improved glucose tolerance in mice lacking CD26. *Proceedings of the National Academy of Sciences of the United States of America* **2000,** 97, (12), 6874-9.

Marie, S.; Diaz-Guerra, M.-J.; Miquerol, L.; Kahn, A.; Iynedjian, P., The pyruvate kinase gene as a model for studies of glucose-dependent regulation of gene expression in the endocrine pancreatic beta-cell type. *Journal of Biological Chemistry* **1993,** 268, (32), 23881-23890.

Marinissen, M. J.; Gutkind, J. S., G-protein-coupled receptors and signaling networks: emerging paradigms. *Trends in Pharmacological Sciences* **2001,** 22, (7), 368-376.

Marquardt, J. U.; Seo, D.; Andersen, J. B.; Gillen, M. C.; Kim, M. S.; Conner, E. A.; Galle, P. R.; Factor, V. M.; Park, Y. N.; Thorgeirsson, S. S., Sequential transcriptome analysis of human liver cancer indicates late stage acquisition of malignant traits. *Journal of Hepatology* **2014,** 60, (2), 346-353.

Marquez, L.; Trapote, M.; Luque, M. A.; Valverde, I.; Villanueva-Penacarrillo, M. L., Inositolphosphoglycans Possibly Mediate the E€ ects of Glucagon-Like Peptide-1(7-36)amide on Rat Liver and Adipose Tissue. *Cell Biochemistry and Function* **1998,** 16, 51-56

Marselli, L.; Thorne, J.; Dahiya, S.; Sgroi, D. C.; Sharma, A.; Bonner-Weir, S.; Marchetti, P.; Weir, G. C., Gene expression profiles of Beta-cell enriched tissue obtained by laser capture microdissection from subjects with type 2 diabetes. *PLoS One* **2010,** 5, (7), e11499.

Marshall, C., Specificity of receptor tyrosine kinase signaling: transient versus sustained extracellular signal-regulated kinase activation. *Cell* **1995,** 80, (2), 179-185.

Martens, G. A.; Cai, Y.; Hinke, S.; Stangé, G.; Van de Casteele, M.; Pipeleers, D., Glucose suppresses superoxide generation in metabolically responsive pancreatic β cells. *Journal of Biological Chemistry* **2005,** 280, (21), 20389-20396.

Marti-Solano, M.; Guixa-Gonzalez, R.; Sanz, F.; Pastor, M.; Selent, J., Novel insights into biased agonism at G protein-coupled receptors and their potential for drug design. *Current Pharmaceutical Design* **2013,** 19, (28), 5156-5166.

Matsunami, H.; Montmayeur, J. P.; Buck, L. B., A family of candidate taste receptors in human and mouse. *Nature* **2000,** 404, (6778), 601-+.

May, L. T.; Leach, K.; Sexton, P. M.; Christopoulos, A., Allosteric modulation of G protein-coupled receptors. *The Annual Review of Pharmacology and Toxicology.* **2007,** 47, 1-51.

Mayo, C. S.; Urie, M. M., A systematic benchmark method for analysis and comparison of IMRT treatment planning algorithms. *Medical Dosimetry* **2003,** 28, (4), 235-42.

Mayo, K. E.; Miller, L. J.; Bataille, D.; Dalle, S.; Goke, B.; Thorens, B.; Drucker, D. J., International Union of Pharmacology: XXXV. The glucagon receptor family. *Pharmacological Reviews* **2003,** 55, 167-194.

McClenaghan, N. H.; Barnett, C. R.; Ah-Sing, E.; Abdel-Wahab, Y. H.; O'Harte, F. P.; Yoon, T.-W.; Swanston-Flatt, S. K.; Flatt, P. R., Characterization of a novel glucose-responsive insulin-secreting cell line, BRIN-BD11, produced by electrofusion. *Diabetes* **1996,** 45, (8), 1132-1140.

McDaniel, M. L.; Marshall, C. A.; Pappan, K. L.; Kwon, G., Metabolic and autocrine regulation of the mammalian target of rapamycin by pancreatic β-cells. *Diabetes* **2002,** 51, (10), 2877-2885.

Meeran, K.; O'Shea, D.; Edwards, C. M.; Turton, M. D.; Heath, M. M.; Gunn, I.; Abusnana, S.; Rossi, M.; Small, C. J.; Goldstone, A. P.; Taylor, G. M.; Sunter, D.; Steere, J.; Choi, S. J.; Ghatei, M. A.; Bloom, S. R., Repeated intracerebroventricular administration of glucagon-like peptide-1-(7-36) amide or exendin-(9-39) alters body weight in the rat. *Endocrinology* **1999,** 140, (1), 244-50.

Meier, J. J.; Nauck, M. A.; Pott, A.; Heinze, K.; Goetze, O.; Bulut, K. & Holst, J. J. Glucagon-like peptide 2 stimulates glucagon secretion, enhances lipid absorption, and inhibits gastric acid secretion in humans. *Gastroenterology* **2006**, 130(1), 44-54.

Meier, J., Beta cell mass in diabetes: a realistic therapeutic target? *Diabetologia* **2008,** 51, (5), 703-713.

Meier, J.; Breuer, T.; Bonadonna, R.; Tannapfel, A.; Uhl, W.; Schmidt, W.; Schrader, H.; Menge, B., Pancreatic diabetes manifests when beta cell area declines by approximately 65% in humans. *Diabetologia* **2012,** 55, (5), 1346-1354.

Meier, J. J.; Gallwitz, B.; Salmen, S.; Goetze, O.; Holst, J. J.; Schmidt, W. E.; Nauck, M. A., Normalization of glucose concentrations and deceleration of gastric emptying after solid meals during intravenous glucagon-like peptide 1 in patients with type 2 diabetes. *The Journal of Clinical Endocrinology & Metabolism* **2003,** 88, (6), 2719-2725.

Meier, J. J.; Hücking, K.; Holst, J. J.; Deacon, C. F.; Schmiegel, W. H.; Nauck, M. A., Reduced insulinotropic effect of gastric inhibitory polypeptide in first-degree relatives of patients with type 2 diabetes. *Diabetes* **2001,** 50, (11), 2497-2504.

Melancon, B. J.; Hopkins, C. R.; Wood, M. R.; Emmitte, K. A.; Niswender, C. M.; Christopoulos, A.; Conn, P. J.; Lindsley, C. W., Allosteric modulation of seven transmembrane spanning

receptors: theory, practice, and opportunities for central nervous system drug discovery. *The Journal of Medicinal Chemistry* **2012,** 55, (4), 1445-64.

Mentlein, R., Dipeptidyl-peptidase IV (CD26)--role in the inactivation of regulatory peptides. *Regulatory Peptides* **1999,** 85, (1), 9-24.

Mentlein, R.; Dahms, P.; Grandt, D.; Kruger, R., Proteolytic processing of neuropeptide Y and peptide YY by dipeptidyl peptidase IV. *Regulatory Peptides* **1993,** 49, (2), 133-44.

Mentlein, R.; Gallwitz, B.; Schmidt, W. E., Dipeptidyl-peptidase IV hydrolyses gastric inhibitory polypeptide, glucagon-like peptide-1(7-36)amide, peptide histidine methionine and is responsible for their degradation in human serum. *European Journal of Biochemistry* **1993,** 214, (3), 829-35.

Merglen, A.; Theander, S.; Rubi, B.; Chaffard, G.; Wollheim, CB. & Maechler P. Glucose sensitivity and metabolism-secretion coupling studied during two-year continuous culture in INS-1E insulinoma cells. **2004,** 145(2): 667-678.

Merida, E.; Delgado, E.; Molina, L. M.; Villanueva-Penacarrillo, M. L.; Valverde, I., Presence of glucagon and glucagon-like peptide-1-(7-36)amide receptors in solubilized membranes of human adipose tissue. *The Journal of Clinical Endocrinology & Metabolism* **1993,** 77, (6), 1654-7.

Metukuri, M. R.; Zhang, P.; Basantani, M. K.; Chin, C.; Stamateris, R. E.; Alonso, L. C.; Takane, K. K.; Gramignoli, R.; Strom, S. C.; O'Doherty, R. M., ChREBP mediates glucose-stimulated pancreatic β-cell proliferation. *Diabetes* **2012,** 61, (8), 2004-2015.

Michel, M. C.; Beck-Sickinger, A.; Cox, H.; Doods, H. N.; Herzog, H.; Larhammar, D.; Quirion, R.; Schwartz, T.; Westfall, T., XVI. International Union of Pharmacology recommendations for the nomenclature of neuropeptide Y, peptide YY, and pancreatic polypeptide receptors. *Pharmacological Reviews* **1998,** 50, (1), 143-50.

Miller, W. E.; Maudsley, S.; Ahn, S.; Khan, K. D.; Luttrell, L. M.; Lefkowitz, R. J., beta-arrestin1 interacts with the catalytic domain of the tyrosine kinase c-SRC - Role of beta-arrestin1-dependent targeting of c-SRC in receptor endocytosis. *Journal of Biological Chemistry* **2000,** 275, (15), 11312-11319.

Mima, A.; Hiraoka-Yamomoto, J.; Li, Q.; Kitada, M.; Li, C.; Geraldes, P.; Matsumoto., M.; Mizutani., K.; Park, K.; Cahill, C.; Nishikawa, S.-I.; Rask-Madsen, C.; King, G. L., Protective effects of GLP-1 on glomerular endothelium and its inhibition by PKCb activation in diabetes. *Diabetes* **2012,** 61, 2967-2979.

Minakami, R.; Kato, A.; Sugiyama, H., Interaction of Vesl-1L/Homer 1c with syntaxin 13. *Biochemical and Biophysical Research Communications* **2000,** 272, (2), 466-471.

Minn, A. H.; Hafele, C.; Shalev, A., Thioredoxin-interacting protein is stimulated by glucose through a carbohydrate response element and induces beta-cell apoptosis. *Endocrinology* **2005,** 146, (5), 2397-405.

Miyazaki, J.-I.; Araki, K.; Yamato, E.; Ikegami, H.; Asano, T.; Shibasaki, Y.; Oka, Y.; Yamamura, K.-I., Establishment of a Pancreatic β Cell Line That Retains Glucose-Inducible Insulin

Secretion: Special Reference to Expression of Glucose Transporter Isoforms*. *Endocrinology* **1990,** 127, (1), 126-132.

Mohr, K.; Trankle, C.; Kostenis, E.; Barocelli, E.; De Amici, M.; Holzgrabe, U., Rational design of dualsteric GPCR ligands: quests and promise. *British Journal of Pharmacology* **2010,** 159, (5), 997-1008.

Mojsov, S.; Heinrich, G.; Wilson, I. B.; Ravazzola, M.; Orci, L., & Habener, J. F. Preproglucagon gene expression in pancreas and intestine diversifies at the level of post-translational processing. *Journal of Biological Chemistry* **1986**, 261(25), 11880-11889.

Mojsov, S.; Weir, G. C.; Habener, J. F., Insulinotropin: glucagon-like peptide-I(7-37) co-encoded in the glucagon gene is a potent stimulator of insulin release in the perfused rat pancreas. *Journal of Clinical Investigation* **1987,** 79, 616-619.

Monod, J.; Changeux, J. P.; Jacob, F., Allosteric proteins and cellular control systems. *Journal of Molecular Biology* **1963,** 6, 306-29.

Monoranu, C. M.; Apfelbacher, M.; Grünblatt, E.; Puppe, B.; Alafuzoff, I.; Ferrer, I.; Al-Saraj, S.; Keyvani, K.; Schmitt, A.; Falkai, P., pH measurement as quality control on human post mortem brain tissue: a study of the BrainNet Europe consortium. *Neuropathology and Applied Neurobiology* **2009,** 35, (3), 329-337.

Moore, C. E.; Omikorede, O.; Gomez, E.; Willars, G. B.; Herbert, T. P., PERK activation at low glucose concentration is mediated by SERCA pump inhibition and confers preemptive cytoprotection to pancreatic β-cells. *Molecular Endocrinology* **2010,** 25, (2), 315-326.

Morales, M.; Lopez-Delgado, M. I.; Alcantara, A.; Luque, M. A.; Clemente, F.; Marquez, L.; Puente, J.; Vinambres, C.; Malaisse, W. J.; Villanueva-Penacarrillo, M. L.; Valverde, I., Preserved GLP-1 effects on glycogen synthase a activity and glucose metabolism in hepatocytes and skeletal muscle from diabetic rats. *Diabetes* **1997,** 46, (8), 1264 -1269.

Moreno, P.; Nuche-Berenguer, B.; Gutierrez-Rojas, I.; Acitores, A.; Sancho, V.; Valverde, I.; Gonzalez, N.; Villanueva-Penacarrillo, M. L., Normalizing action of exendin-4 and GLP-1 in the glucose metabolism of extrapancreatic tissues in insulin-resistant and type 2 diabetic states. *Journal of Molecular Endocrinology* **2012,** 48, (1), 37-47.

Mortazavi, A.; Williams, B. A.; McCue, K.; Schaeffer, L.; Wold, B., Mapping and quantifying mammalian transcriptomes by RNA-Seq. *Nature Methods* **2008,** 5, (7), 621-628.

Mosedale, M.; Egodage, S.; Calma, R. C.; Chi, N. W.; Chessler, S. D., Neurexin-1alpha contributes to insulin-containing secretory granule docking. *Journal of Biological Chemistry* **2012,** 287, (9), 6350-61.

Mulder, J. E.; Kolatkar, N. S.; LeBoff, M. S., Drug insight: Existing and emerging therapies for osteoporosis. *Nature Clinical Practice- Endocrinology & metabolism* **2006,** 2, (12), 670-680.

Murone, M.; Rosenthal, A.; de Sauvage, F. J., Sonic hedgehog signaling by the patched-smoothened receptor complex. *Current Biology* **1999,** 9, (2), 76-84.

Murphy, L. O.; Smith, S.; Chen, R.-H.; Fingar, D. C.; Blenis, J., Molecular interpretation of ERK signal duration by immediate early gene products. *Nature Cell Biology* **2002,** 4, (8), 556-564.

Mutz, K.-O.; Heilkenbrinker, A.; Lönne, M.; Walter, J.-G.; Stahl, F., Transcriptome analysis using next-generation sequencing. *Current Opinion in Biotechnology* **2013,** 24, (1), 22-30.

Myojo, S.; Tsujikawa, T.; Sasaki, M.; Fujiyama, Y. & Bamba, T. Trophic effects of glicentin on rat small-intestinal mucosa in vivo and in vitro. *Journal of gastroenterology* **1997**, 32(3), 300-305.

Nauck, M. A., Is glucagon-like peptide 1 an incretin hormone? *Diabetologia* **1999,** 42, (3), 373-379.

Nauck, M. A.; Bartels, E.; Orskov, C.; Ebert, R.; Creutzfeldt, W., Additive insulinotropic effects of exogenous synthetic human gastric inhibitory polypeptide and glucagon-like peptide-1-(7-36) amide infused at near-physiological insulinotropic hormone and glucose concentrations. *The Journal of Clinical Endocrinology & Metabolism* **1993,** 76, (4), 912-7.

Nauck, M. A.; Heimesaat, M. M.; Behle, K.; Holst, J. J.; Nauck, M. S.; Ritzel, R.; Hüfner, M.; Schmiegel, W. H., Effects of glucagon-like peptide 1 on counterregulatory hormone responses, cognitive functions, and insulin secretion during hyperinsulinemic, stepped hypoglycemic clamp experiments in healthy volunteers. *The Journal of Clinical Endocrinology & Metabolism* **2002,** 87, (3), 1239-1246.

Nauck, M. A.; Homberger, E.; Siegel, E. G.; Allen, R. C.; Eaton, R. P.; Ebert, R.; Creutzfeldt, W., Incretin effects of increasing glucose loads in man calculated from venous insulin and Cpeptide responses. *The Journal of Clinical Endocrinology & Metabolism* **1986,** 63, 492-498.

Nauck, M. A.; Kemmeries, G.; Holst, J. J.; Meier, J. J., Rapid tachyphylaxis of the glucagon-like peptide 1–induced deceleration of gastric emptying in humans. *Diabetes* **2011,** 60, (5), 1561-1565.

Nauck, M. A.; Kleine, N.; Orskov, C.; Holst, J. J.; Willms, B.; Creutzfeldt, W., Normalization of fasting hyperglycaemia by exogenous glucagon-like peptide 1 (7-36 amide) in type 2 (non-insulin-dependent) diabetic patients. *Diabetologia* **1993,** 36, (8), 741-4.

Nauck, M. A.; Meier, J. J., Glucagon-like peptide 1 (GLP-1) and its derivatives in the treatment of diabetes. *Regulatory Peptides* **2005,** 124(suppl), 135-148.

Nawaratne, V.; Leach, K.; Felder, C. C.; Sexton, P. M.; Christopoulos, A., Structural Determinants of Allosteric Agonism and Modulation at the M4 Muscarinic Acetylcholine Receptor identification of ligand-specific and global activation mechanisms. *Journal of Biological Chemistry* **2010,** 285, (25), 19012-19021.

Neubig, R. R.; Spedding, M.; Kenakin, T.; Christopoulos, A., International Union of Pharmacology Committee on Receptor Nomenclature and Drug Classification. XXXVIII. Update on terms and symbols in quantitative pharmacology. *Pharmacoogical Reiews* **2003,** 55, (4), 597-606.

Neubig, R. R.; Spedding, M.; Kenakin, T.; Christopoulos, A.; International Union of Pharmacology Committee on Receptor, N.; Drug, C., International Union of Pharmacology Committee on

Receptor Nomenclature and Drug Classification. XXXVIII. Update on terms and symbols in quantitative pharmacology. *Pharmacological Reviews* **2003,** 55, (4), 597-606.

Newgard, C. B.; An, J.; Bain, J. R.; Muehlbauer, M. J.; Stevens, R. D.; Lien, L. F.; Haqq, A. M.; Shah, S. H.; Arlotto, M.; Slentz, C. A., A branched-chain amino acid-related metabolic signature that differentiates obese and lean humans and contributes to insulin resistance. *Cell Metabolism.* **2009,** 9, (4), 311-326.

Nielsen, L. L.; Young, A. A.; & Parkes, D. G. Pharmacology of exenatide (synthetic exendin-4): a potential therapeutic for improved glycemic control of type 2 diabetes. *Regulatory peptides* **2004**, 117(2), 77-88.

Nielsen, J. H.; Galsgaard, E. D.; Møldrup, A.; Friedrichsen, B. N.; Billestrup, N.; Hansen, J. A.; Lee, Y. C.; Carlsson, C., Regulation of beta-cell mass by hormones and growth factors. *Diabetes* **2001,** 50, (suppl 1), S25.

Nikolaidis, L. A.; Doverspike, A.; Hentosz, T.; Zourelias, L.; Shen, Y. T.; Elahi, D.; Shannon, R. P., Glucagon-like peptide-1 limits myocardial stunning following brief coronary occlusion and reperfusion in conscious canines. *The Journal of Pharmacology and Experimental Therapeutics* **2005,** 312, (1), 303-8.

Nikolaidis, L. A.; Elahi, D.; Hentosz, T.; Doverspike, A.; Huerbin, R.; Zourelias, L.; Stolarski, C.; Shen, Y. T.; Shannon, R. P., Recombinant glucagon-like peptide-1 increases myocardial glucose uptake and improves left ventricular performance in conscious dogs with pacing-induced dilated cardiomyopathy. *Circulation* **2004,** 110, (8), 955-61.

Nikolaidis, L. A.; Elahi, D.; Shen, Y. T.; Shannon, R. P., Active metabolite of GLP-1 mediates myocardial glucose uptake and improves left ventricular performance in conscious dogs with dilated cardiomyopathy. *American Journal of Physiology - Heart and Circulatory Physiology* **2005b,** 289, H2401-H2408.

Nikolaidis, L. A.; Mankad, S.; Sokos, G. G.; Miske, G.; Shah, A.; Elahi, D.; Shannon, R. P., Effects of glucagon-like peptide-1 in patients with acute myocardial infarction and left ventricular dysfunction after successful reperfusion. *Circulation* **2004,** 109, (8), 962-5.

Noel, J. P.; Hamm, H. E.; Sigler, P. B., The 2.2-angstrom crystal-structure of transducin-alpha complexed with gtp-gamma-s. *Nature* **1993,** 366, (6456), 654-663.

Nuche-Berenguer, B.; Moreno, P.; Esbrit, P.; Dapia, S.; Caeiro, J. R.; Cancelas, J.; Haro-Mora, J. J.; Villanueva-Penacarrillo, M. L., Effect of GLP-1 treatment on bone turnover in normal, type 2 diabetic, and insulin-resistant states. *Calcified Tissue International* **2009,** 84, (6), 453-61.

Nolte, W.M.; Fortin, J-P.; Stevens, B.D.; Aspnes, G.E.; Griffith, D.A.; Hoth, L.R.; Ruggeri, R.B.; Mathiowetz, A.M.; Limberakis, C.; Hepworth, D., A potentiator of orthosteric ligand activity at GLP-1R acts via covalent modification. *Nature Chemical Biology* 2014, 10, (8), 629-631.

Nuche-Berenguer, B.; Portal-Nunez, S.; Moreno, P.; Gonzalez, N.; Acitores, A.; Lopez-Herradon, A.; Esbrit, P.; Valverde, I.; Villanueva-Penacarrillo, M. L., Presence of a functional receptor for GLP-1 in osteoblastic cells, independent of the cAMP-linked GLP-1 receptor. *Journal of Cellular Physiology* **2010,** 225, (2), 585-92.

Nystrom, T.; Gutniak, M. K.; Zhang, Q.; Zhang, F.; Holst, J. J.; Ahren, B.; Sjoholm, A., Effects of glucagon-like peptide-1 on endothelial function in type 2 diabetes patients with stable coronary artery disease. *The American Journal of Physiology - Endocrinology and Metabolism* **2004,** 287, (6), E1209-15.

Oben, J.; Morgan, L.; Fletcher, J.; Marks, V., Effect of the entero-pancreatic hormones, gastric inhibitory polypeptide and glucagon-like polypeptide-1(7-36) amide, on fatty acid synthesis in explants of rat adipose tissue. *Journal of Endocrinology* **1991,** 130, (2), 267-72.

Ohara, P. J.; Sheppard, P. O.; Thogersen, H.; Venezia, D.; Haldeman, B. A.; McGrane, V.; Houamed, K. M.; Thomsen, C.; Gilbert, T. L.; Mulvihill, E. R., The ligand-binding domain in metabotropic glutamate receptors is related to bacterial periplasmic binding-proteins. *Neuron* **1993,** 11, (1), 41-52.

Ohara-Imaizumi, M.; Fujiwara, T.; Nakamichi, Y.; Okamura, T.; Akimoto, Y.; Kawai, J.; Matsushima, S.; Kawakami, H.; Watanabe, T.; Akagawa, K.; Nagamatsu, S., Imaging analysis reveals mechanistic differences between first- and second-phase insulin exocytosis. *Journal of Cell Biology* **2007,** 177, (4), 695-705.

Ohsugi, M.; Cras-Méneur, C.; Zhou, Y.; Warren, W.; Bernal-Mizrachi, E.; Permutt, M. A., Glucose and insulin treatment of insulinoma cells results in transcriptional regulation of a common set of genes. *Diabetes* **2004,** 53, (6), 1496-1508.

Ohtsuki, T.; Hosono, O.; Kobayashi, H.; Munakata, Y.; Souta, A.; Shioda, T.; Morimoto, C., Negative regulation of the anti-human immunodeficiency virus and chemotactic activity of human stromal cell-derived factor 1alpha by CD26/dipeptidyl peptidase IV. *FEBS Letters* **1998,** 431, (2), 236-40.

Ojima, A.; Ishibashi, Y.; Matsui, T.; Maeda, S.; Nishino, Y.; Takeuchi, M.; Fukami, K.; Yamagishi, S., Glucagon-like peptide-1 receptor agonist inhibits asymmetric dimethylarginine generation in the kidney of streptozotocin-induced diabetic rats by blocking advanced glycation end product-induced protein arginine methyltranferase-1 expression. *The American Journal of Pathology* **2013,** 182, (1), 132-41.

Okamoto, T.; Sekiyama, N.; Otsu, M.; Shimada, Y.; Sato, A.; Nakanishi, S.; Jingami, H., Expression and purification of the extracellular ligand binding region of metabotropic glutamate receptor subtype 1. *Journal of Biological Chemistry* **1998,** 273, (21), 13089-13096.

Olansky, L., Q: Do incretin drugs for type 2 diabetes increase the risk of acute pancreatitis? *Cleveland Clinic Journal of Medicine* **2010,** 77, (8), 503-505.

Oldham, W. M.; Hamm, H. E., Heterotrimeric G protein activation by G-protein-coupled receptors. *Nature Reviews Molecular Cell Biology.* **2008,** 9, (1), 60-71.

Oravecz, T.; Pall, M.; Roderiquez, G.; Gorrell, M. D.; Ditto, M.; Nguyen, N. Y.; Boykins, R.; Unsworth, E.; Norcross, M. A., Regulation of the receptor specificity and function of the chemokine RANTES (regulated on activation, normal T cell expressed and secreted) by dipeptidyl peptidase IV (CD26)-mediated cleavage. *Journal Experimental Medicine* **1997,** 186, (11), 1865-72.

Orskov, C.; Bersani, M.; Johnsen, A.; Højrup, P., & Holst, J. Complete sequences of glucagon-like peptide-1 from human and pig small intestine. *Journal of Biological Chemistry* **1989**, 264(22), 12826-12829.

Ørskov, C;, Holst, J. J.; Knuhtsen, S.; Baldissera, F. G.; Poulsen, S. S., & Nielsen, O. V. Glucagon-Like Peptides GLP-1 and GLP-2, Predicted Products of the Glucagon Gene, Are Secreted Separately from Pig Small Intestine but Not Pancreas*. *Endocrinology* **1986**, 119(4), 1467-1475.

Ørskov, C.; Holst, J.; Nielsen, O., Effect of truncated glucagon-like peptide-1 [proglucagon-(78–107) amide] on endocrine secretion from pig pancreas, antrum, and nonantral stomach. *Endocrinology* **1988,** 123, (4), 2009-2013.

Orskov, C.; Rabenhoj, L.; Wettergren, A.; Kofod, H.; Holst, J. J., Tissue and plasma concentrations of amidated and glycine-extended glucagon-like peptide I in humans. *Diabetes* **1994,** 43, (4), 535-539.

Orskov, C.; Wettergren, A.; Holst, J. J., Secretion of the incretin hormones glucagon-like peptide-1 and gastric inhibitory polypeptide correlates with insulin secretion in normal man throughout the day. *Scandinavian Journal of Gastroenterology* **1996,** 31, (7), 665-70.

Orskov, L.; Worm, M.; Schmitz, O.; Mengel, A.; Sidenius, P., Nerve conduction velocity in man: influence of glucose, somatostatin and electrolytes. *Diabetologia* **1994,** 37, (12), 1216-20.

Ortis, F.; Naamane, N.; Flamez, D.; Ladrière, L.; Moore, F.; Cunha, D. A.; Colli, M. L.; Thykjaer, T.; Thorsen, K.; Ørntoft, T. F., Cytokines interleukin-1β and tumor necrosis factor-α regulate different transcriptional and alternative splicing networks in primary β-cells. *Diabetes* **2010,** 59, (2), 358-374.

Ozsolak, F.; Milos, P. M., RNA sequencing: advances, challenges and opportunities. *Nature Reviews Genetics* **2011,** 12, (2), 87-98.

Pabreja, K.; Mohd, M.; Koole, C.; Wootten, D.; Furness, S., Molecular mechanisms underlying physiological and receptor pleiotropic effects mediated by GLP-1R activation. *British Journal of Pharmacology* **2014,** 171, (5), 1114-1128.

Pal, K.; Melcher, K.; Xu, H. E., Structure and mechanism for recognition of peptide hormones by Class B G-protein-coupled receptors. *Acta Pharmacologica Sinica* **2012,** 33, (3), 300-311.

Panjwani, N.; Mulvihill, E. E.; Longuet, C.; Yusta, B.; Campbell, J. E.; Brown, T. J.; Streutker, C.; Holland, D.; Cao, X.; Baggio, L. L.; Drucker, D. J., GLP-1 receptor activation indirectly reduces hepatic lipid accumulation but does not attenuate development of atherosclerosis in diabetic male ApoE(-/-) mice. *Endocrinology* **2013,** 154, (1), 127-39.

Papapetropoulos, S.; Shehadeh, L.; McCorquodale, D., Optimizing human post-mortem brain tissue gene expression profiling in Parkinson's disease and other neurodegenerative disorders: From target “fishing” to translational breakthroughs. *Journal of Neuroscience Research* **2007,** 85, (14), 3013-3024.

Parkes, D. G.; Mace, K. F., & Trautmann, M. E. Discovery and development of exenatide: the first antidiabetic agent to leverage the multiple benefits of the incretin hormone, GLP-1. *Expert opinion on drug discovery* **2013**, 8(2), 219-244.

Park, C. W.; Kim, H. W.; Ko, S. H.; Lim, J. H.; Ryu, G. R.; Chung, H. W.; Han, S. W.; Shin, S. J.; Bang, B. K.; Breyer, M. D.; Chang, Y. S., Long-term treatment of glucagon-like peptide-1 analog exendin-4 ameliorates diabetic nephropathy through improving metabolic anomalies in db/db mice. *Journal of the American Society of Nephrology* **2007,** 18, (4), 1227-38.

Park, J. H.; Kim, S. J.; Park, S. H.; Son, D. G.; Bae, J. H.; Kim, H. K.; Han, J.; Song, D. K., Glucagon-like peptide-1 enhances glucokinase activity in pancreatic beta-cells through the association of Epac2 with Rim2 and Rab3A. *Endocrinology* **2012,** 153, (2), 574-82.

Park, S.; Dong, X.; Fisher, T. L.; Dunn, S.; Omer, A. K.; Weir, G.; White, M. F., Exendin-4 uses Irs2 signaling to mediate pancreatic beta cell growth and function. *Journal of Biological Chemistry* **2006,** 281, (2), 1159-68.

Park, Y.; Ao, Z.; Kieffer, T.; Chen, H.; Safikhan, N.; Thompson, D.; Meloche, M.; Warnock, G.; Marzban, L., The glucagon-like peptide-1 receptor agonist exenatide restores impaired pro-islet amyloid polypeptide processing in cultured human islets: implications in type 2 diabetes and islet transplantation. *Diabetologia* **2013,** 56, (3), 508-519.

Parker, H. E.; Reimann, F.; Gribble, F. M., Molecular mechanisms underlying nutrient-stimulated incretin secretion. *Expert Reviews in Molecular Medicine* **2010,** 12, e1.

Parker, S.; Stitzel, M.; Taylor, D.; Orozco, J.; Erdos, M.; Akiyama, J.; van Bueren, K.; Chines, P.; Narisu, N.; Black, B., National Institutes of Health Intramural Sequencing Center Comparative Sequencing Program Authors; NISC Comparative Sequencing Program Authors (2013). Chromatin stretch enhancer states drive cell-specific gene regulation and harbor human disease risk variants. *Proceedings of the National Academy of Sciences of the U.S.A.* 110, 17921-17926.

Parlevliet, E. T.; Heijboer, A. C.; Schroder-van der Elst, J. P.; Havekes, L. M.; Romijn, J. A.; Pijl, H.; Corssmit, E. P., Oxyntomodulin ameliorates glucose intolerance in mice fed a high-fat diet. *American Journal of Physiology - Endocrinology and Metabolism* **2008,** 294, E142-E147.

Parlevliet, J. M.; Paccamonti, D. L.; Barker, S. A., Cefquinome concentrations in endometrium after intrauterine treatment of cobactan 4.5% in mares and inflammatory response of the endometrium to this treatment. *Reproduction in Domestic Animals* **2009,** 44, (2), 189-93.

Parthier, C.; Reedtz-Runge, S.; Rudolph, R.; Stubbs, M. T., Passing the baton in class B GPCRs: peptide hormone activation via helix induction? *Trends in Biochemical Sciences.* **2009,** 34, (6), 303-310.

Paszkiewicz, K. H.; Farbos, A.; O'Neill, P.; Moore, K., Quality control on the frontier. *Frontiers in Genetics* **2014,** 5.

Patzelt, C., & Schiltz, E. Conversion of proglucagon in pancreatic alpha cells: the major endproducts are glucagon and a single peptide, the major proglucagon fragment, that contains two glucagon-like sequences. *Proceedings of the National Academy of Sciences* **1984**, 81(16), 5007-5011.

Patzelt, C., Tager, H., Carroll, R., & Steiner, D. Identification and processing of proglucagon in pancreatic islets. *Nature* **1979**, 282(5736), 260-266.

Pederson, R. A.; Satkunarajah, M.; McIntosh, C.; Scrocchi, L. A.; Flamez, D.; Schuit, F.; Drucker, D. J.; Wheeler, M. B., Enhanced glucose-dependent insulinotropic polypeptide secretion and insulinotropic action in glucagon-like peptide 1 receptor-/-mice. *Diabetes* **1998,** 47, (7), 1046-1052.

Perfetti, R.; Zhou, J.; Doyle, M. E.; Egan, J. M., Glucagon-like peptide-1 induces cell proliferation and pancreatic-duodenum homeobox-1 expression and increases endocrine cell mass in the pancreas of old, glucose-intolerant rats. *Endocrinology* **2000,** 141, (12), 4600-5.

Perry, S. J.; Lefkowitz, R. J., Arresting developments in heptahelical receptor signaling and regulation. *Trends in Cell Biology* **2002,** 12, (3), 130-8.

Perry, T.; Greig, N. H., Enhancing central nervous system endogenous GLP-1 receptor pathways for intervention in Alzheimer's disease. *Current Alzheimer Research* **2005,** 2, (3), 377-85.

Perry, T.; Holloway, H. W.; Weerasuriya, A.; Mouton, P. R.; Duffy, K.; Mattison, J. A.; Greig, N. H., Evidence of GLP-1-mediated neuroprotection in an animal model of pyridoxine-induced peripheral sensory neuropathy. *Experimental Neurology* **2007,** 203, (2), 293-301.

Pérez-Arana, G.; Blandino-Rosano, M.; Prada-Oliveira, A.; Aguilar-Diosdado, M.. & Segundo, C. Decrease in β-cell proliferation precedes apoptosis during diabetes development in bio-breeding/worcester rat: beneficial role of exendin-4. *Endocrinology* **2010**, 151(6), 2538-2546.

Pin, J. P.; Kniazeff, J.; Binet, V.; Liu, J. F.; Maurel, D.; Galvez, T.; Duthey, W.; Havlickova, M.; Blahos, J.; Prezeau, L.; Rondard, P., Activation mechanism of the heterodimeric GABA(B) receptor. *Biochemical Pharmacology* **2004,** 68, (8), 1565-1572.

Pioszak, A. A.; Parker, N. R.; Suino-Powell, K.; Xu, H. E., Molecular Recognition of Corticotropin-releasing Factor by Its G-protein-coupled Receptor CRFR1. *Journal of Biological Chemistry* **2008,** 283, (47), 32900-32912.

Pioszak, A. A.; Xu, H. E., Molecular recognition of parathyroid hormone by its G protein-coupled receptor. *Proceedings of the National Academy of Sciences of the U. S. A.* **2008,** 105, (13), 5034-5039.

Pipeleers, D.; Schuit, F.; In't Veld, P.; Maes, E.; Hooghe-Peters, E.; WINKEL, M. V. D.; Gepts, W., Interplay of Nutrients and Hormones in the Regulation of Insulin Release*. *Endocrinology* **1985,** 117, (3), 824-833.

Pocai, A. Unraveling oxyntomodulin, GLP1's enigmatic brother. *Journal of Endocrinology* **2012**, 215(3), 335-346.

Pocai, A. Action and therapeutic potential of oxyntomodulin. *Molecular metabolism* **2014**, 3(3), 241-251.

Pop, M.; Salzberg, S. L., Bioinformatics challenges of new sequencing technology. *Trends in Genetics* **2008,** 24, (3), 142-149.

Porat, S.; Weinberg-Corem, N.; Tornovsky-Babaey, S.; Schyr-Ben-Haroush, R.; Hija, A.; Stolovich-Rain, M.; Dadon, D.; Granot, Z.; Ben-Hur, V.; White, P., Control of pancreatic β cell regeneration by glucose metabolism. *Cell Metabolism* **2011,** 13, (4), 440-449.

Porcheray, F.; Viaud, S.; Rimaniol, A. C.; Leone, C.; Samah, B.; Dereuddre-Bosquet, N.; Dormont, D.; Gras, G., Macrophage activation switching: an asset for the resolution of inflammation. *Clinical and Experimental Immunology* **2005,** 142, 481-489.

Poy, M. N.; Eliasson, L.; Krutzfeldt, J.; Kuwajima, S.; Ma, X.; MacDonald, P. E.; Pfeffer, S.; Tuschl, T.; Rajewsky, N.; Rorsman, P., A pancreatic islet-specific microRNA regulates insulin secretion. *Nature* **2004,** 432, (7014), 226-230.

Poyner, D. R.; Sexton, P. M.; Marshall, I.; Smith, D. M.; Quirion, R.; Born, W.; Muff, R.; Fischer, J. A.; Foord, S. M., International Union of Pharmacology. XXXII. The mammalian calcitonin gene-related peptides, adrenomedullin, amylin, and calcitonin receptors. *Pharmacological Reviews* **2002,** 54, (2), 233-246.

Pratley, R.; Nauck, M.; Bailey, T.; Montanya, E.; Cuddihy, R.; Filetti, S.; Garber, A.; Thomsen, A. B.; Hartvig, H.; Davies, M., One year of liraglutide treatment offers sustained and more effective glycaemic control and weight reduction compared with sitagliptin, both in combination with metformin, in patients with type 2 diabetes: a randomised, parallel-group, open-label trial. *International Journal of Clinical Practice* **2011,** 65, (4), 397-407.

Pratley, R. E.; Gilbert, M., Targeting Incretins in Type 2 Diabetes: Role of GLP-1 Receptor Agonists and DPP-4 Inhibitors. *The Review of Diabetic Studies* **2008,** 5, (2), 73-94.

Pratley, R. E.; Nauck, M.; Bailey, T.; Montanya, E.; Cuddihy, R.; Filetti, S.; Thomsen, A. B.; Sondergaard, R. E.; Davies, M., Liraglutide versus sitagliptin for patients with type 2 diabetes who did not have adequate glycaemic control with metformin: a 26-week, randomised, parallel-group, open-label trial. *Lancet* **2010,** 375, 1447-1456.

Price, M. R.; Baillie, G. L.; Thomas, A.; Stevenson, L. A.; Easson, M.; Goodwin, R.; McLean, A.; McIntosh, L.; Goodwin, G.; Walker, G.; Westwood, P.; Marrs, J.; Thomson, F.; Cowley, P.; Christopoulos, A.; Pertwee, R. G.; Ross, R. A., Allosteric modulation of the cannabinoid CB1 receptor. *Molecular Pharmacology* **2005,** 68, (5), 1484-95.

Prigeon, R. L.; Quddusi, S.; Paty, B.; D'Alessio, D. A., Suppression of glucose production by GLP-1 independent of islet hormones: a novel extrapancreatic effect. *American journal of physiology-Endocrinology and metabolism* **2003,** 285, (4), E701-7.

Primeaux, S. D.; Barnes, M. J.; Braymer, H. D.; & Bray, G. A. Sensitivity to the satiating effects of exendin 4 is decreased in obesity-prone Osborne–Mendel rats compared to obesity-resistant S5B/Pl rats. *International journal of obesity* **2010**, 34(9), 1427-1433.

Proost, P.; Menten, P.; Struyf, S.; Schutyser, E.; De Meester, I.; Van Damme, J., Cleavage by CD26/dipeptidyl peptidase IV converts the chemokine LD78beta into a most efficient monocyte attractant and CCR1 agonist. *Blood* **2000,** 96, (5), 1674-80.

Proost, P.; Struyf, S.; Schols, D.; Durinx, C.; Wuyts, A.; Lenaerts, J. P.; De Clercq, E.; De Meester, I.; Van Damme, J., Processing by CD26/dipeptidyl-peptidase IV reduces the chemotactic and anti-HIV-1 activity of stromal-cell-derived factor-1alpha. *FEBS Letters* **1998,** 432, (1-2), 73-6.

Proost, P.; Struyf, S.; Schols, D.; Opdenakker, G.; Sozzani, S.; Allavena, P.; Mantovani, A.; Augustyns, K.; Bal, G.; Haemers, A.; Lambeir, A. M.; Scharpe, S.; Van Damme, J.; De Meester, I., Truncation of macrophage-derived chemokine by CD26/ dipeptidyl-peptidase IV beyond its predicted cleavage site affects chemotactic activity and CC chemokine receptor 4 interaction. *Journal of Biological Chemistry* **1999,** 274, (7), 3988-93.

Proost, P.; Struyf, S.; Wuyts, A.; Menten, P.; De Meester, I.; Lambeir, A. M.; Scharpe, S.; Schols, D.; De Clercq, E.; Van Damme, J., Isolation and identification of naturally modified C-C chemokines MCP-1, MCP-2 and RANTES: effects of posttranslational modifications on receptor usage, chemotactic and anti-HIV-1 activity. *European Cytokine Network* **1998,** 9, (3 Suppl), 73-5.

Puddu, A.; Sanguineti, R.; Montecucco, F.; Viviani, G. L., Retinal pigment epithelial cells express a functional receptor for glucagon-like peptide-1 (GLP-1). *Mediators of Inflammation* **2013,** 2013, 975032.

Puddu, A.; Storace, D.; Durante, A.; Odetti, P.; Viviani, G. L., Glucagon-like peptide-1 counteracts the detrimental effects of Advanced Glycation End-Products in the pancreatic beta cell line HIT-T 15. *Biochemical and Biophysical Research Communications* **2010,** 398, (3), 462-6.

Quoyer, J.; Longuet, C.; Broca, C.; Linck, N.; Costes, S.; Varin, E.; Bockaert, J.; Bertrand, G.; Dalle, S., GLP-1 Mediates Antiapoptotic Effect by Phosphorylating Bad through a beta-Arrestin 1-mediated ERK1/2 Activation in Pancreatic beta-Cells. *Journal of Biological Chemistry* **2010,** 285, (3), 1989-2002

Rahmani, M.; Wong, B. W.; Ang, L.; Cheung, C. C.; Carthy, J. M.; Walinski, H.; McManus, B. M., Versican: signaling to transcriptional control pathways This paper is one of a selection of papers published in this Special Issue, entitled Young Investigator's Forum. *Canadian Journal of Physiology and Pharmacology* **2006,** 84, (1), 77-92.

Rajagopal, S.; Ahn, S.; Rominger, D. H.; Gowen-MacDonald, W.; Lam, C. M.; DeWire, S. M.; Violin, J. D.; Lefkowitz, R. J., Quantifying ligand bias at seven-transmembrane receptors. *Molecular Pharmacology.* **2011,** 80, (3), 367-377.

Rajagopal, S.; Rajagopal, K.; Lefkowitz, R. J., Teaching old receptors new tricks: biasing seven-transmembrane receptors. *Nature Reviews Drug Discovery* **2010,** 9, (5), 373-386.

Rajala, M. W.; Scherer, P. E., Minireview: the adipocyte—at the crossroads of energy homeostasis, inflammation, and atherosclerosis. *Endocrinology* **2003,** 144, (9), 3765-3773.

Rajan, S.; Torres, J.; Thompson, M. S.; Philipson, L. H., SUMO downregulates GLP-1-stimulated cAMP generation and insulin secretion. *The American Journal of Physiology - Endocrinology and Metabolism* **2012,** 302, (6), E714-23.

Raman, I. M.; Tong, G.; Jahr, C. E., beta-adrenergic regulation of synaptic NMDA receptors by cAMP-dependent protein kinase. *Neuron* **1996,** 16, (2), 415-421.

Raman, M.; Chen, W.; Cobb, M. H., Differential regulation and properties of MAPKs. *Oncogene* **2007,** 26, (22), 3100-12.

Rask-Andersen, M.; Almen, M. S.; Schioth, H. B., Trends in the exploitation of novel drug targets. *Nature Reiews. Drug Discovery*. **2011,** 10, (8), 579-590.

Rau, A.; Gallopin, M.; Celeux, G.; Jaffrézic, F., Data-based filtering for replicated high-throughput transcriptome sequencing experiments. *Bioinformatics* **2013,** 29, (17), 2146-2152.

Redondo, A.; Trigo, M. V.; Acitores, A.; Valverde, I.; Villanueva-Penacarrillo, M. L., Cell signalling of the GLP-1 action in rat liver. *Molecular and Cellular Endocrinology* **2003,** 204 43-50.

Reiter, E.; Lefkowitz, R. J., GRKs and beta-arrestins: roles in receptor silencing, trafficking and signaling. *Trends in Endocrinology & Metabolism* **2006,** 17, (4), 159-165.

Ren, X. R.; Reiter, E.; Ahn, S.; Kim, J.; Chen, W.; Lefkowitz, R. J., Different G protein-coupled receptor kinases govern G protein and beta-arrestin-mediated signaling of V2 vasopressin receptor. *Proceedings of the National Academy of Sciences of the. U. S. A.* **2005,** 102, (5), 1448-1453.

Renstrom, E.; Eliasson, L.; Rorsman, P., Protein kinase A-dependent and -independent stimulation of exocytosis by cAMP in mouse pancreatic B-cells. *The Journal of Physiology* **1997,** 502 (Pt 1), 105-18.

Rhodes, M. E.; Talluri, J.; Harney, J. P.; Frye, C. A., Ketogenic diet decreases circulating concentrations of neuroactive steroids of female rats. *Epilepsy & Behavior* **2005,** 7, (2), 231-9.

Richard, H.; Schulz, M. H.; Sultan, M.; Nürnberger, A.; Schrinner, S.; Balzereit, D.; Dagand, E.; Rasche, A.; Lehrach, H.; Vingron, M., Prediction of alternative isoforms from exon expression levels in RNA-Seq experiments. *Nucleic Acids Research* **2010,** 38, (10), e112-e112.

Richter, G.; Feddersen, O.; Wagner, U.; Barth, P.; Goke, R.; Goke, B., GLP-1 stimulates secretion of macromolecules from airways and relaxes pulmonary artery. *The American Journal of Physiology* **1993,** 265, (4 Pt 1), L374-81.

Richter, G.; Goke, R.; Goke, B.; Arnold, R., Characterization of receptors for glucagon-like peptide-1(7-36)amide on rat lung membranes. *FEBS Letters* **1990,** 267, (1), 78-80.

Rieg, T.; Gerasimova, M.; Murray, F.; Masuda, T.; Tang, T.; Rose, M.; Drucker, D. J.; Vallon, V., Natriuretic effect by exendin-4, but not the DPP-4 inhibitor alogliptin, is mediated via the GLP-1 receptor and preserved in obese type 2 diabetic mice. *American journal of physiology-Renal physiology* **2012,** 303, (7), F963-F971.

Ronnebaum, S. M.; Jensen, M. V.; Hohmeier, H. E.; Burgess, S. C.; Zhou, Y.-P.; Qian, S.; MacNeil, D.; Howard, A.; Thornberry, N.; Ilkayeva, O., Silencing of cytosolic or mitochondrial isoforms of malic enzyme has no effect on glucose-stimulated insulin secretion from rodent islets. *Journal of Biological Chemistry* **2008,** 283, (43), 28909-28917.

Roques, B. P.; Noble, F.; Daug, V.; Fournie-Zaluski, M. C.; Beaumont, A., Neutral endopeptidase 24.11: Structure, inhibition and experimental and clinical pharmacology. *Pharmacological Reviews* **1993,** 45, 87-146.

Rosen, O. M., After insulin binds. *Science* **1987,** 237, (4821), 1452-1458.

Rouille, Y.; Westermark, G.; Martin, S. K.; Steiner, D. F., Proglucagon is processed to glucagon by prohormone convertase PC2 in a TC1-6 cells. *Proceedings of the National Academy of Sciences of the U.S.A.* **1994,** 91 (8), 3242-3246.

Rouillé, Y.; Martin, S.; & Steiner, D. F. Differential processing of proglucagon by the subtilisin-like prohormone convertases PC2 and PC3 to generate either glucagon or glucagon-like peptide. *Journal of Biological Chemistry* **1995**, 270(44), 26488-26496.

Ruiz-Grande, C.; Alarcon, C.; Merida, E.; Valverde, I., Lipolytic action of glucagon-like peptides in isolated rat adipocytes. *Peptides* **1992,** 13, (1), 13-6.

Runge, S.; Thogersen, H.; Madsen, K.; Lau, J.; Rudolph, R., Crystal structure of the ligand-bound glucagon-like peptide-1 receptor extracellular domain. *Journal of Biological Chemistry* **2008,** 283, (17), 11340-11347.

Rutter, G. A., Nutrient–secretion coupling in the pancreatic islet β-cell: recent advances. *Molecular Aspects of Medicine* **2001,** 22, (6), 247-284.

Sakurada, K.; Toida, I.; Sakai, I.; Sekiguchi, K.; Shiraishi, T.; Takatori, T., The BCG scar after percutaneous multiple puncture vaccination may help establish the nationalities of unidentified cadavers. *Journal of Clinical Forensic Medicine* **2003,** 10, (4), 235-41.

Sakurada, S.; Hang, N. T.; Ishizuka, N.; Toyota, E.; Hung le, D.; Chuc, P. T.; Lien, L. T.; Thuong, P. H.; Bich, P. T.; Keicho, N.; Kobayashi, N., Inter-rater agreement in the assessment of abnormal chest X-ray findings for tuberculosis between two Asian countries. *BMC Infectious Diseases* **2012,** 12, 31.

Salpeter, S. J.; Klein, A. M.; Huangfu, D.; Grimsby, J.; Dor, Y., Glucose and aging control the quiescence period that follows pancreatic beta cell replication. *Development* **2010,** 137, (19), 3205-13.

Saltiel, A. R.; Kahn, C. R., Insulin signalling and the regulation of glucose and lipid metabolism. *Nature* **2001,** 414, (6865), 799-806.

Sánchez-Pla, A.; Reverter, F.; de Villa, M. C. R.; Comabella, M., Transcriptomics: mRNA and alternative splicing. *Journal of Neuroimmunology* **2012,** 248, (1), 23-31.

Sancho, V.; Nuche, B.; Arnes, L.; Cancelas, J.; Gonzalez, N.; Diaz-Miguel, M.; Martin-Duce, A.; Valverde, I.; Villanueva-Penacarrillo, M. L., The action of GLP-1 and exendins upon glucose transport in normal human adipocytes, and on kinase activity as compared to morbidly obese patients. *International Journal of Molecular Medicine* **2007,** 19, (6), 961-6.

Sancho, V.; Trigo, M. V.; Gonzalez, N.; Valverde, I.; Malaisse, W. J.; Villanueva-Penacarrillo, M. L., Effects of glucagon-like peptide-1 and exendins on kinase acyivity, glucose transport and lipid metabolism in adipocytes from normal and type-2 diabetic rats. *Journal of Molecular Endocrinology* **2005,** 35, 27-38.

Sanz, C.; Vazquez, P.; Blazquez, C.; Barrio, P. A.; Alvarez Mdel, M.; Blazquez, E., Signaling and biological effects of glucagon-like peptide 1 on the differentiation of mesenchymal stem

cells from human bone marrow. *American journal of physiology. Endocrinology and metabolism* **2010,** 298, (3), E634-43.

Sayeski, P. P.; Ali, M. S.; Frank, S. J.; Bernstein, K. E., The angotensin II-dependent nuclear translocation of Stat1 is mediated by the Jak2 protein motif (YRFRR)-Y-231. *Journal of Biological Chemistry* **2001,** 276, (13), 10556-10563.

Schadt, E. E.; Monks, S. A.; Drake, T. A.; Lusis, A. J.; Che, N.; Colinayo, V.; Ruff, T. G.; Milligan, S. B.; Lamb, J. R.; Cavet, G., Genetics of gene expression surveyed in maize, mouse and man. *Nature* **2003,** 422, (6929), 297-302.

Schepp, W.; Dehne, K.; Riedel, T.; Schmidtler, J.; Schaffer, K.; Classen, M., Oxyntomodulin: a cAMP-dependent stimulus of rat parietal cell function via the receptor for glucagon-like peptide-1 (7-36)NH2. *Digestion* **1996,** 57, (6), 398-405.

Schirra, J.; Nicolaus, M.; Roggel, R.; Katschinski, M.; Storr, M.; Woerle, H. J.; Goke, B., Endogenous glucagon-like peptide 1 controls endocrine pancreatic secretion and antro-pyloro-duodenal motility in humans. *Gut* **2006,** 55, (2), 243-51.

Schisler, J. C.; Jensen, P. B.; Taylor, D. G.; Becker, T. C.; Knop, F. K.; Takekawa, S.; German, M.; Weir, G. C.; Lu, D.; Mirmira, R. G.; Newgard, C. B., The Nkx6.1 homeodomain transcription factor suppresses glucagon expression and regulates glucose-stimulated insulin secretion in islet beta cells. *Proceedings of the National Academy of Sciencesof the U.S.A.* **2005,** 102, (20), 7297-302.

Schlatter, P.; Beglinger, C.; Drewe, J.; Gutmann, H., Glucagon-like peptide 1 receptor expression in primary porcine proximal tubular cells. *Regulatory Peptides* **2007,** 141, 120-128.

Schnabel, C. A.; Wintle, M.; Kolterman, O., Metabolic effects of the incretin mimetic exenatide in the treatment of type 2 diabetes. *Vascular Health and Risk Management* **2006,** 2, (1), 69-77.

Schneider, M.; Kostin, S.; Strøm, C. C.; Aplin, M.; Lyngbæk, S.; Theilade, J.; Grigorian, M.; Andersen, C. B.; Lukanidin, E.; Hansen, J. L., S100A4 is upregulated in injured myocardium and promotes growth and survival of cardiac myocytes. *Cardiovascular Research* **2007,** 75, (1), 40-50.

Schuit, F.; Flamez, D.; De Vos, A.; Pipeleers, D., Glucose-regulated gene expression maintaining the glucose-responsive state of β-cells. *Diabetes* **2002,** 51, (suppl 3), S326-S332.

Schuit, F.; In't Veld, P.; Pipeleers, D., Glucose stimulates proinsulin biosynthesis by a dose-dependent recruitment of pancreatic beta cells. *Proceedings of the National Academy of Sciencesof the U.S.A.* **1988,** 85, (11), 3865-3869.

Schuit, F. C.; Huypens, P.; Heimberg, H.; Pipeleers, D. G., Glucose sensing in pancreatic β-cells a model for the study of other glucose-regulated cells in gut, pancreas, and hypothalamus. *Diabetes* **2001,** 50, (1), 1-11.

Seachrist, J. L.; Ferguson, S. S., Regulation of G protein-coupled receptor endocytosis and trafficking by Rab GTPases. *Life Sciences* **2003,** 74, (2), 225-235.

Shao, W.; Yu, Z.; Fantus, I. G.; Jin, T., Cyclic AMP signaling stimulates proteasome degradation of thioredoxin interacting protein (TxNIP) in pancreatic beta-cells. *Cellular Signalling* **2010,** 22, (8), 1240-6.

Shaw, A. J.; Cox, C. J.; Buck, W. R.; Devos, N.; Buchanan, A. M.; Cave, L.; Seppelt, R.; Shaw, B.; Larrain, J.; Andrus, R.; Greilhuber, J.; Temsch, E. M., Newly resolved relationships in an early land plant lineage: Bryophyta class Sphagnopsida (peat mosses). *American Journal of Botany* **2010,** 97, (9), 1511-31.

Shen, H.; Cheng, X.; Cai, K.; Hu, M.-B., Detect overlapping and hierarchical community structure in networks. *Physica A: Statistical Mechanics and its Applications* **2009,** 388, (8), 1706-1712.

Shendure, J., The beginning of the end for microarrays? *Nature Methods* **2008,** 5, (7), 585-587.

Shenoy, S. K.; Drake, M. T.; Nelson, C. D.; Houtz, D. A.; Xiao, K. H.; Madabushi, S.; Reiter, E.; Premont, R. T.; Lichtarge, O.; Lefkowitz, R. J., beta-arrestin-dependent, G protein-independent ERK1/2 activation by the beta 2 adrenergic receptor. *Journal of Bioogical Chemistry* **2006,** 281, (2), 1261-1273.

Sherwood, N. M.; Krueckl, S. L.; McRory, J. E., The origin and function of the pituitary adenylate cyclase-activating polypeptide (PACAP)/glucagon superfamily. *Endocrine Reviews* **2000,** 21, (6), 619-670.

Shi, P.; Zhang, J. Z.; Yang, H.; Zhang, Y. P., Adaptive diversification of bitter taste receptor genes in mammalian evolution. *Molecular Biology and Evolution* **2003,** 20, (5), 805-814.

Shibasaki, T.; Takahashi, H.; Miki, T.; Sunaga, Y.; Matsumura, K.; Yamanaka, M.; Zhang, C.; Tamamoto, A.; Satoh, T.; Miyazaki, J.; Seino, S., Essential role of Epac2/Rap1 signaling in regulation of insulin granule dynamics by cAMP. *Proceedings of the National Academy of Sciences of the U.S.A* **2007,** 104, (49), 19333-8.

Shih, M. L.; Lin, F. B.; Scott, J. D.; Wang, H. Y.; Malbon, C. C., Dynamic complexes of beta(2)-adrenergic receptors with protein kinases and phosphatases and the role of gravin. *Journal of Biological Chemistry* **1999,** 274, (3), 1588-1595.

Shin, S.; Le Lay, J.; Everett, L. J.; Gupta, R.; Rafiq, K.; Kaestner, K. H., CREB mediates the insulinotropic and anti-apoptotic effects of GLP-1 signaling in adult mouse β-cells. *Molecular Metabolism* **2014,** 3, (8), 803-812.

Shiraishi, D.; Fujiwara, Y.; Komohara, Y.; Mizuta, H.; Takeya, M., Glucagon-like peptide-1 (GLP-1) induces M2 polarization of human macrophages via STAT3 activation. *Biochemical and Biophysical Research Communications* **2012,** 425, 304-308.

Shoelson, S. E.; Lee, J.; Goldfine, A. B., Inflammation and insulin resistance. *Journal of Clinical Investigation* **2006,** 116, (7), 1793.

Shonberg, J.; Lopez, L.; Scammells, P. J.; Christopoulos, A.; Capuano, B.; Lane, J. R., Biased Agonism at G Protein-Coupled Receptors: The Promise and the Challenges—A Medicinal Chemistry Perspective. *Medicinal Research Reviews* **2014,** 34, (6), 1286-1330.

Simon, M. I.; Strathmann, M. P.; Gautam, N., Diversity of G-Proteins in Signal Transduction. *Science* **1991,** 252, (5007), 802-808.

Singh, S.; Chang, H.-Y.; Richards, T. M.; Weiner, J. P.; Clark, J. M.; Segal, J. B., Glucagonlike peptide 1–based therapies and risk of hospitalization for acute pancreatitis in type 2 diabetes mellitus: a population-based matched case-control study. *JAMA Internal Medicine* **2013,** 173, (7), 534-539.

Silvestre, R. A.; Rodríguez-Gallardo, J.; Egido, E. M., & Marco, J. Interrelationship among insulin, glucagon and somatostatin secretory responses to exendin-4 in the perfused rat pancreas. *European journal of pharmacology* **2003**, 469(1), 195-200.

Siu, F. Y.; He, M.; de Graaf, C.; Han, G. W.; Yang, D. H.; Zhang, Z. Y.; Zhou, C. H.; Xu, Q. P.; Wacker, D.; Joseph, J. S.; Liu, W.; Lau, J.; Cherezov, V.; Katritch, V.; Wang, M. W.; Stevens, R. C., Structure of the human glucagon class B G-protein-coupled receptor. *Nature* **2013,** 499, (7459), 444-+.

Skelin, M.; Rupnik, M.; Cencic, A., Pancreatic beta cell lines and their applications in diabetes mellitus research. *Altex* **2010,** 27, (2), 105-113.

Sloop, K. W.; Willard, F. S.; Brenner, M. B.; Ficorilli, J.; Valasek, K.; Showalter, A. D.; Farb, T. B.; Cao, J. X.; Cox, A. L.; Michael, M. D., Novel small molecule glucagon-like peptide-1 receptor agonist stimulates insulin secretion in rodents and from human islets. *Diabetes* **2010,** 59, (12), 3099-3107.

Smotrys, J. E.; Linder, M. E., Palmitoylation of intracellular signaling proteins: Regulation and function. *Annual Review of Biochemistry* **2004,** 73, 559-587.

Sokos, G. G.; Bolukoglu, H.; German, J.; Hentosz, T.; Magovern, G. J., Jr.; Maher, T. D.; Dean, D. A.; Bailey, S. H.; Marrone, G.; Benckart, D. H.; Elahi, D.; Shannon, R. P., Effect of glucagon-like peptide-1 (GLP-1) on glycemic control and left ventricular function in patients undergoing coronary artery bypass grafting. *The American Journal of Cardiology* **2007,** 100, (5), 824-9.

Sokos, G. G.; Nikolaidis, L. A.; Mankad, S.; Elahi, D.; Shannon, R. P., Glucagon-like peptide-1 infusion improves left ventricular ejection fraction and functional status in patients with chronic heart failure. *Journal of Cardiac Failure* **2006,** 12, (9), 694-9.

Song, W.-J.; Schreiber, W. E.; Zhong, E.; Liu, F.-F.; Kornfeld, B. D.; Wondisford, F. E., & Hussain, M. A. Exendin-4 stimulation of cyclin A2 in β-cell proliferation. *Diabetes* **2008**, 57(9), 2371-2381.

Song, H. K.; Hong, S.-E.; Kim, T.; Kim, D. H., Deep RNA sequencing reveals novel cardiac transcriptomic signatures for physiological and pathological hypertrophy. *PLoS One* **2012,** 7, (4), e35552.

Sonoda, N.; Imamura, T.; Yoshizaki, T.; Babendure, J. L.; Lu, J.; Olefsky, J. M., β-Arrestin-1 mediates glucagon-like peptide-1 signaling to insulin secretion in cultured pancreatic β-cells. *Proceedings of the National Academy of Sciences of the U.S.A* **2008,** 105, (18), 6614-6619.

Sonoda, N.; Imamura, T.; Yoshizaki, T.; Babendure, J. L.; Lu, J. C.; Olefsky, J. M., beta-Arrestin-1 mediates glucagon-like peptide-1 signaling to insulin secretion in cultured pancreatic beta cells. *Proceedings of the National Academy of Sciences of the U.S.A* **2008,** 105, (18), 6614-6619

Sonoda, Y.; Hada, N.; Kaneda, T.; Suzuki, T.; Ohshio, T.; Takeda, T.; Kasahara, T., A synthetic glycosphingolipid-induced antiproliferative effect in melanoma cells is associated with suppression of FAK, Akt, and Erk activation. *Biological & Pharmaceutical Bulletin* **2008,** 31, (6), 1279-83.

Stacey, M.; Lin, H. H.; Gordon, S.; McKnight, A. J., LNB-TM7, a group of seven-transmembrane proteins related to family-B G-protein-coupled receptors. *Trends in Biochemical Sciences.* **2000,** 25, (6), 284-289.

Stanley, S.; Wynne, K.; Bloom, S., Gastrointestinal satiety signals III. Glucagon-like peptide 1, oxyntomodulin, peptide YY, and pancreatic polypeptide. *American Journal of Physiology-Gastrointestinal and Liver Physiology* **2004,** 286, (5), G693-G697.

Stockton, J. M.; Birdsall, N. J.; Burgen, A. S.; Hulme, E. C., Modification of the binding properties of muscarinic receptors by gallamine. *Molecular Pharmacology* **1983,** 23, (3), 551-7.

Stoffers, D. A.; Kieffer, T. J.; Hussain, M. A.; Drucker, D. J.; Bonner-Weir, S.; Habener, J. F.; Egan, J. M., Insulinotropic glucagon-like peptide 1 agonists stimulate expression of homeodomain protein IDX-1 and increase islet size in mouse pancreas. *Diabetes* **2000,** 49, (5), 741-748.

Stolovich-Rain, M.; Hija, A.; Grimsby, J.; Glaser, B.; Dor, Y., Pancreatic beta cells in very old mice retain capacity for compensatory proliferation. *Journal of Bioogical. Chemistry* **2012,** 287, (33), 27407-27414.

St-Pierre, C.; Brochu, S.; Vanegas, J. R.; Dumont-Lagacé, M.; Lemieux, S.; Perreault, C., Transcriptome sequencing of neonatal thymic epithelial cells. *Scientific Reports* **2013,** 3.

Struyf, S.; Proost, P.; Schols, D.; De Clercq, E.; Opdenakker, G.; Lenaerts, J. P.; Detheux, M.; Parmentier, M.; De Meester, I.; Scharpe, S.; Van Damme, J., CD26/dipeptidyl-peptidase IV down-regulates the eosinophil chemotactic potency, but not the anti-HIV activity of human eotaxin by affecting its interaction with CC chemokine receptor 3. *Journal of Immunology* **1999,** 162, (8), 4903-9.

Su, S.; Lu, S. X.; Xu, W. G., Photocatalytic Degradation of Reactive Brilliant Blue X-BR in Aqueous Solution Using Quantum-sized ZnO. *Materials Research Bulletin* **2008,** 43, (8-9), 2172-2178.

Suckow, A. T.; Comoletti, D.; Waldrop, M. A.; Mosedale, M.; Egodage, S.; Taylor, P.; Chessler, S. D., Expression of neurexin, neuroligin, and their cytoplasmic binding partners in the pancreatic beta-cells and the involvement of neuroligin in insulin secretion. *Endocrinology* **2008,** 149, (12), 6006-17.

Suckow, A. T.; Zhang, C.; Egodage, S.; Comoletti, D.; Taylor, P.; Miller, M. T.; Sweet, I. R.; Chessler, S. D., Transcellular neuroligin-2 interactions enhance insulin secretion and are

integral to pancreatic beta cell function. *Journal of Biological Chemistry* **2012,** 287, (24), 19816-26.

Sultan, M.; Schulz, M. H.; Richard, H.; Magen, A.; Klingenhoff, A.; Scherf, M.; Seifert, M.; Borodina, T.; Soldatov, A.; Parkhomchuk, D., A global view of gene activity and alternative splicing by deep sequencing of the human transcriptome. *Science* **2008,** 321, (5891), 956-960.

Sun, X. J.; Wang, L.-M.; Zhang, Y., Role of IR5-2 in insulin and. *Nature* **1995,** 377, 173.

Suratman, S.; Leach, K.; Sexton, P.; Felder, C.; Loiacono, R.; Christopoulos, A., Impact of species variability and 'probe-dependence'on the detection and in vivo validation of allosteric modulation at the M4 muscarinic acetylcholine receptor. *British Journal of Pharmacology* **2011,** 162, (7), 1659-1670.

Susini, S.; Roche, E.; Prentki, M.; Schlegel, W., Glucose and glucoincretin peptides synergize to induce c-fos, c-jun, junB, zif-268, and nur-77 gene expression in pancreatic β (INS-1) cells. *The FASEB Journal* **1998,** 12, (12), 1173-1182.

Susini, S.; Van Haasteren, G.; Li, S.; Prentki, M.; Schlegel, W., Essentiality of intron control in the induction of c-fos by glucose and glucoincretin peptides in INS-1 β-cells. *The FASEB Journal* **2000,** 14, (1), 128-136.

Sutherland, G. T.; Janitz, M.; Kril, J. J., Understanding the pathogenesis of Alzheimer's disease: will RNA-Seq realize the promise of transcriptomics? *Journal of Neurochemistry* **2011,** 116, (6), 937-946.

Svegliati-Baroni, G.; Saccomanno, S.; Rychlicki, C.; Agostinelli, L.; De Minicis, S.; Candelaresi, C.; Faraci, G.; Pacetti, D.; Vivarelli, M.; Nicolini, D.; Garelli, P.; Casini, A.; Manco, M.; Mingrone, G.; Risaliti, A.; Frega, G. N.; Benedetti, A.; Gastaldelli, A., Glucagon-like peptide-1 receptor activation stimulates hepatic lipid oxidation and restores hepatic signalling alteration induced by a high-fat diet in nonalcoholic steatohepatitis. *Liver International* **2011,** 31, (9), 1285-97.

Swenne, I., The role of glucose in the in vitro regulation of cell cycle kinetics and proliferation of fetal pancreatic B-cells. *Diabetes* **1982,** 31, (9), 754-760.

Szayna, M.; Doyle, M. E.; Betkey, J. A.; Holloway, H. W.; Spencer, R. G.; Greig, N. H.; Egan, J. M., Exendin-4 decelerates food intake, weight gain, and fat deposition in Zucker rats. *Endocrinology* **2000,** 141, (6), 1936-41.

Talbot, J.; Joly, E.; Prentki, M.; Buteau, J., beta-Arrestin1-mediated recruitment of c-Src underlies the proliferative action of glucagon-like peptide-1 in pancreatic beta INS832/13 cells. *Molecular and Cellular Endocrinology* **2012,** 364, (1-2), 65-70.

Taneera, J.; Lang, S.; Sharma, A.; Fadista, J.; Zhou, Y.; Ahlqvist, E.; Jonsson, A.; Lyssenko, V.; Vikman, P.; Hansson, O., A systems genetics approach identifies genes and pathways for type 2 diabetes in human islets. *Cell Metabolism* **2012,** 16, (1), 122-134.

Tang, F.; Barbacioru, C.; Nordman, E.; Li, B.; Xu, N.; Bashkirov, V. I.; Lao, K.; Surani, M. A., RNA-Seq analysis to capture the transcriptome landscape of a single cell. *Nature Protocols* **2010,** 5, (3), 516-535.

Tang, F.; Barbacioru, C.; Wang, Y.; Nordman, E.; Lee, C.; Xu, N.; Wang, X.; Bodeau, J.; Tuch, B. B.; Siddiqui, A., mRNA-Seq whole-transcriptome analysis of a single cell. *Nature Methods* **2009,** 6, (5), 377-382.

Tang-Christensen, M.; Larsen, P. J.; Goke, R.; Fink-Jensen, A.; Jessop, D. S.; Moller, M.; Sheikh, S. P., Central administration of GLP-1-(7-36) amide inhibits food and water intake in rats. *The American Journal of Physiology* **1996,** 271, (4 Pt 2), R848-56.

Tao, Y.-X., The melanocortin-4 receptor: physiology, pharmacology, and pathophysiology. *Endocrine Reviews* **2010,** 31, (4), 506-543.

Tateyama, M.; Kubo, Y., Dual signaling is differentially activated by different active states of the metabotropic glutamate receptor 1alpha. *Proceedings of the National Academy of Sciences of the U S A* **2006,** 103, (4), 1124-8.

Tavares, W.; Drucker, D. J.; Brubaker, P. L., Enzymatic- and renal-dependent catabolism of the intestinotropic hormone glucagon-like peptide-2 in rats. *The American Journal of Physiology - Endocrinology and Metabolism* **2000,** 278, (1), E134-9.

Terauchi, Y.; Takamoto, I.; Kubota, N.; Matsui, J.; Suzuki, R.; Komeda, K.; Hara, A.; Toyoda, Y.; Miwa, I.; Aizawa, S., Glucokinase and IRS-2 are required for compensatory β cell hyperplasia in response to high-fat diet–induced insulin resistance. *Journal of Clinical Investigation* **2007,** 117, (1), 246.

Tfelt-Hansen, J.; Brown, E. M., The calcium-sensing receptor in normal physiology and pathophysiology: A review. *Critical Reviews in Clinical Laboratory Sciences.* **2005,** 42, (1), 35-70.

Thim, L., & Moody, A. J. Purification and chemical characterization of a glicentin-related pancreatic peptide (proglucagon fragment) from porcine pancreas. *Biochimica et Biophysica Acta (BBA)-Protein Structure and Molecular Enzymology* **1982**, 703(2), 134-141.

Thomas, M. K.; Tsang, S. W.; Yeung, M. L.; Leung, P. S.; Yao, K. M., The roles of the PDZ-containing proteins bridge-1 and PDZD2 in the regulation of insulin production and pancreatic beta-cell mass. *Current Protein & Peptide Science* **2009,** 10, (1), 30-6.

Thorens, B., Expression cloning of the pancreatic beta cell receptor for the gluco-incretin hormone glucagon-like peptide 1. *Proceedings of the National Academy of Sciencesof the U.S.A* **1992,** 89, (18), 8641-8645.

Thorens, B., Expression cloning of the pancreatic beta cell receptor for the gluco-incretin hormone glucagonlike peptide 1. *Proceedings of the National Academy of Sciences of the U S A* **1992,** 89, 8641-8645.

Thorens, B.; Porret, A.; Bühler, L.; Deng, S.-P.; Morel, P., & Widmann, C. Cloning and functional expression of the human islet GLP-1 receptor: demonstration that exendin-4 is an agonist and exendin-(9–39) an antagonist of the receptor. *Diabetes* **1993**, 42(11), 1678-1682.

Tian, L.; Gao, J.; Weng, G.; Yi, H.; Tian, B.; O'Brien, T. D.; Guo, Z., Comparison of exendin-4 on beta-cell replication in mouse and human islet grafts. *Transplant International* **2011,** 24, (8), 856-864.

Tibaduiza, E. C.; Chen, C.; Beinborn, M., A small molecule ligand of the glucagon-like peptide 1 receptor targets its amino-terminal hormone binding domain. *Journal of Biological Chemistry* **2001,** 276, (41), 37787-93.

Trapote, M. A.; Clemente, F.; Galera, C.; Morales, M.; Alcantara, A. I.; Lopez-Delgado, M. I.; Villanueva-Penacarrillo, M. L.; Valverde, I., Inositolphosphoglycans are possible mediators of the glucagon-like peptide 1 (7-36)amide action in the liver. *Journal Of Endocrinological Investigation* **1996,** 19, (2), 114-8.

Trumper, A.; Trumper, K.; Trusheim, H.; Arnold, R.; Goke, B.; Horsch, D., Glucose-dependent insulinotropic polypeptide is a growth factor for beta (INS-1) cells by pleiotropic signaling. *Molecular Endocrinology* **2001,** 15, (9), 1559-70.

Tsuboi, T.; da SILVA, X. G.; Holz, G.; Jouaville, L.; Thomas, A.; Rutter, G., Glucagon-like peptide-1 mobilizes intracellular Ca2+ and stimulates mitochondrial ATP synthesis in pancreatic MIN6 beta-cells. *Biochemical Journal* **2003,** 369, 287-299.

Tsuchiya, D.; Kunishima, N.; Kamiya, N.; Jingami, H.; Morikawa, K., Structural views of the ligand-binding cores of a metabotropic glutamate receptor complexed with an antagonist and both glutamate and Gd3+. *Proceedings of the National Academy of Sciences* **2002,** 99, (5), 2660-2665.

Tu, J. C.; Xiao, B.; Naisbitt, S.; Yuan, J. P.; Petralia, R. S.; Brakeman, P.; Doan, A.; Aakalu, V. K.; Lanahan, A. A.; Sheng, M.; Worley, P. F., Coupling of mGluR/Homer and PSD-95 complexes by the shank family of postsynaptic density proteins. *Neuron* **1999,** 23, (3), 583-592.

Tu, J. C.; Xiao, B.; Yuan, J. P.; Lanahan, A. A.; Leoffert, K.; Li, M.; Linden, D. J.; Worley, P. F., Homer binds a novel proline-rich motif and links group 1 metabotropic glutamate receptors with IP3 receptors. *Neuron* **1998,** 21, (4), 717-726.

Tucker, J. D.; Dhanvantari, S., & Brubaker, P. L. Proglucagon processing in islet and intestinal cell lines. *Regulatory peptides* **1996**, 62(1), 29-35.

Turton, M. D.; O'Shea, D.; Gunn, I.; Beak, S. A.; Edwards, C. M.; Meeran, K.; Choi, S. J.; Taylor, G. M.; Heath, M. M.; Lambert, P. D.; Wilding, J. P.; Smith, D. M.; Ghatei, M. A.; Herbert, J.; Bloom, S. R., A role for glucagon-like peptide-1 in the central regulation of feeding. *Nature* **1996,** 379, (6560), 69-72.

Tyndall, J. D. A.; Sandilya, R., GPCR Agonists and Antagonists in the Clinic. Journal of *Medicinal Chemistry* **2005,** 1, (4), 405-421.

Ullmer, C.; Schmuck, K.; Figge, A.; Lubbert, H., Cloning and characterization of MUPP1, a novel PDZ domain protein. *FEBS Letters* **1998,** 424, (1-2), 63-68.

Underwood, C. R.; Garibay, P.; Knudsen, L. B.; Hastrup, S.; Peters, G. H.; Rudolph, R.; Reedtz-Runge, S., Crystal Structure of Glucagon-like Peptide-1 in Complex with the Extracellular Domain of the Glucagon-like Peptide-1 Receptor. *Journal of Biological Chemistry* **2010,** 285, (1), 723-730.

Unson, C. G.; Wu, C. R.; Jiang, Y. W.; Yoo, B.; Cheung, C.; Sakmar, T. P.; Merrifield, R. B., Roles of specific extracellular domains of the glucagon receptor in ligand binding and signaling. *Biochemistry* **2002,** 41, (39), 11795-11803.

Urusova, I. A.; Farilla, L.; Hui, H.; D'Amico, E.; Perfetti, R., GLP-1 inhibition of pancreatic islet cell apoptosis. *Trends in Endocrinology & Metabolism* **2004,** 15, (1), 27-33.

Usui, I.; Imamura, T.; Huang, J.; Satoh, H.; Shenoy, S. K.; Lefkowitz, R. J.; Hupfeld, C. J.; Olefsky, J. M., beta-arrestin-1 competitively inhibits insulin-induced ubiquitination and degradation of insulin receptor substrate 1. *Molecular and Cellular Biology* **2004,** 24, (20), 8929-37.

Valant, C.; Felder, C. C.; Sexton, P. M.; Christopoulos, A., Probe dependence in the allosteric modulation of a G protein-coupled receptor: implications for detection and validation of allosteric ligand effects. *Molecular Pharmacology* **2012,** 81, (1), 41-52.

Valant, C.; Sexton, P. M.; Christopoulos, A., Orthosteric/allosteric bitopic ligands: going hybrid at GPCRs. *Molecular Interventions* **2009,** 9, (3), 125-35.

Valverde, I.; Merida, E.; Delgado, E.; Trapote, M. A.; Villanueva-Penacarrillo, M. L., Presence and characterization of glucagon-like peptide-1(7-36) amide receptors in solubilized membranes of rat adipose tissue. *Endocrinology* **1993,** 132, (1), 75-9.

Valverde, I.; Morales, M.; Clemente, F.; Lopez-Delgado, M. I.; Delgado, E.; Perea, A.; Villanueva-Penacarrillo, M. L., Glucagon-like peptide 1: a potent glycogenic hormone. *FEBS Letters* **1994,** 349, (2), 313-6.

Van Bakel, H.; Nislow, C.; Blencowe, B. J.; Hughes, T. R., Most “dark matter” transcripts are associated with known genes. *PLOS Biology* **2010,** 8, (5), e1000371.

Van der Westhuizen, E. T.; Breton, B.; Christopoulos, A.; Bouvier, M., Quantification of ligand bias for clinically relevant β2-adrenergic receptor ligands: implications for drug taxonomy. *Molecular Pharmacology* **2014,** 85, (3), 492-509.

Van Dijk, G.; Thiele, T. E.; Donahey, J. C.; Campfield, L. A.; Smith, F. J.; Burn, P.; Bernstein, I. L.; Woods, S. C.; Seeley, R. J., Central infusions of leptin and GLP-1-(7-36) amide differentially stimulate c-FLI in the rat brain. *The American Journal of Physiology* **1996,** 271, (4 Pt 2), R1096-100.

Vara, E.; Arias-Diaz, J.; Garcia, C.; Balibrea, J. L.; Blazquez, E., Glucagon-like peptide-1(7-36) amide stimulates surfactant secretion in human type II pneumocytes. *American Journal of Respiratory and Critical Care Medicine* **2001,** 163, (4), 840-6.

Vara, E.; Arias-Diaz, J.; Garcia, C.; Balibrea, J. L.; Blazquez, E., Glucagon-like Peptide-1(7–36) Amide Stimulates Surfactant Secretion in Human Type II Pneumocytes. *American Journal of Respiratory and Critical Care Medicine* **2001,** 163, 840-846.

Vella, A.; Shah, P.; Reed, A.; Adkins, A.; Basu, R.; Rizza, R., Lack of effect of exendin-4 and glucagon-like peptide-1-(7, 36)-amide on insulin action in non-diabetic humans. *Diabetologia* **2002,** 45, (10), 1410-1415.

Vendrell, J.; El Bekay, R.; Peral, B.; Garcia-Fuentes, E.; Megia, A.; Macias-Gonzalez, M.; Fernandez Real, J.; Jimenez-Gomez, Y.; Escote, X.; Pachon, G.; Simo, R.; Selva, D. M.; Malagon, M. M.; Tinahones, F. J., Study of the potential association of adipose tissue GLP-1 receptor with obesity and insulin resistance. *Endocrinology* **2011,** 152, (11), 4072-9.

Vidal, M.; Cusick, M. E.; Barabasi, A.-L., Interactome networks and human disease. *Cell* **2011,** 144, (6), 986-998.

Villanueva-Penacarrillo, M. L.; Alcantara, A. I.; Clemente, F.; Delgado, E.; Valverde, I., Potent glycogenic effect of GLP-1(7-36)amide in rat skeletal muscle. *Diabetologia* **1994,** 37, (11), 1163-6.

Vilsbøll, T.; Agersø, H.; Krarup, T.; Holst, J. J., Similar elimination rates of glucagon-like peptide-1 in obese type 2 diabetic patients and healthy subjects. *The Journal of Clinical Endocrinology & Metabolism* **2003,** 88, (1), 220-224.

Vilsboll, T.; Knop, F. K., Long-acting GLP-1 analogs for the treatment of type 2 diabetes mellitus. *BioDrugs* **2008,** 22, (4), 251-7.

Vilsboll, T.; Krarup, T.; Deacon, C. F.; Madsbad, S.; Holst, J. J., Reduced postprandial concentrations of intact biologically active glucagon-like peptide 1 in type 2 diabetic patients. *Diabetes* **2001,** 50, (3), 609-13.

Vilsbøll, T.; Krarup, T.; Madsbad, S.; Holst, J., Defective amplification of the late phase insulin response to glucose by GIP in obese Type II diabetic patients. *Diabetologia* **2002,** 45, (8), 1111-1119.

Vilsboll, T.; Krarup, T.; Madsbad, S.; Holst, J. J., No reactive hypoglycaemia in Type 2 diabetic patients after subcutaneous administration of GLP-1 and intravenous glucose. *Diabetic Medicine* **2001,** 18, (2), 144-9.

Vitale, M.; Zamai, L.; Mazzotti, G.; Cataldi, A.; Falcieri, E., Differential kinetics of propidium iodide uptake in apoptotic and necrotic thymocytes. *Histochemistry* **1993,** 100, (3), 223-229.

Voight, B. F.; Scott, L. J.; Steinthorsdottir, V.; Morris, A. P.; Dina, C.; Welch, R. P.; Zeggini, E.; Huth, C.; Aulchenko, Y. S.; Thorleifsson, G., Twelve type 2 diabetes susceptibility loci identified through large-scale association analysis. *Nature Genetics.* **2010,** 42, (7), 579-589.

Volmat, V.; Camps, M.; Arkinstall, S.; Pouysségur, J.; Lenormand, P., The nucleus, a site for signal termination by sequestration and inactivation of p42/p44 MAP kinases. *Journal of Cell Science* **2001,** 114, (19), 3433-3443.

Wang, L.-X.; Wang, Y.-P.; Chen, Z.; Liu, X.-Y.; Liu, X.-H.; Liu, L.; Liu, L.-B. Exendin-4 protects murine pancreatic β-cells from dexamethasone-induced apoptosis through PKA and PI-3K signaling. *Diabetes research and clinical practice* **2010**, 90(3), 297-304.

Wang, A.; Dorso, C.; Kopcho, L.; Locke, G.; Langish, R.; Harstad, E.; Shipkova, P.; Marcinkeviciene, J.; Hamann, L.; Kirby, M. S., Potency, selectivity and prolonged binding of saxagliptin to DPP4: maintenance of DPP4 inhibition by saxagliptin in vitro and ex vivo when compared to a rapidly-dissociating DPP4 inhibitor. *BMC Pharmacology* **2012,** 12, (2).

Wang, D.; Pascual, J. M.; De Vivo, D., Glucose Transporter Type 1 Deficiency Syndrome. In *Gene Reviews(R)*, Pagon, R. A.; Adam, M. P.; Ardinger, H. H.; Wallace, S. E.; Amemiya, A.; Bean, L. J. H.; Bird, T. D.; Dolan, C. R.; Fong, C. T.; Smith, R. J. H.; Stephens, K., Eds. University of Washington, Seattle: Seattle WA, **1993.**

Wang, H. J.; Chiang, B. H., Anti-diabetic effect of a traditional Chinese medicine formula. *Food and Function* **2012,** 3, (11), 1161-9.

Wang, L.; Feng, Z.; Wang, X.; Wang, X.; Zhang, X., DEGseq: an R package for identifying differentially expressed genes from RNA-seq data. *Bioinformatics* **2010,** 26, (1), 136-138.

Wang, Q.; Li, L.; Xu, E.; Wong, V.; Rhodes, C.; Brubaker, P., Glucagon-like peptide-1 regulates proliferation and apoptosis via activation of protein kinase B in pancreatic INS-1 beta cells. *Diabetologia* **2004,** 47, (3), 478-487.

Wang, T. J.; Larson, M. G.; Vasan, R. S.; Cheng, S.; Rhee, E. P.; McCabe, E.; Lewis, G. D.; Fox, C. S.; Jacques, P. F.; Fernandez, C., Metabolite profiles and the risk of developing diabetes. *Nature Medicine* **2011,** 17, (4), 448-453.

Wang, X.; Cahill, C. M.; Pineyro, M. A.; Zhou, J.; Doyle, M. E.; Egan, J. M., Glucagon-like peptide-1 regulates the beta cell transcription factor, PDX-1, in insulinoma cells. *Endocrinology* **1999,** 140, (10), 4904-7.

Wang, X.; Zhou, J.; Doyle, M. E.; Egan, J. M., Glucagon-like peptide-1 causes pancreatic duodenal homeobox-1 protein translocation from the cytoplasm to the nucleus of pancreatic beta-cells by a cyclic adenosine monophosphate/protein kinase A-dependent mechanism. *Endocrinology* **2001,** 142, (5), 1820-7.

Wang, Y. S.; Macke, J. P.; Abella, B. S.; Andreasson, K.; Worley, P.; Gilbert, D. J.; Copeland, N. G.; Jenkins, N. A.; Nathans, J., A large family of putative transmembrane receptors homologous to the product of the Drosophila tissue polarity gene frizzled. *Journal of Biological Chemistry* **1996,** 271, (8), 4468-4476.

Wang, Z.; Gerstein, M.; Snyder, M., RNA-Seq: a revolutionary tool for transcriptomics. *Nature Reviews Genetics* **2009,** 10, (1), 57-63.

Washington, M. C.; Raboin, S. J.; Thompson, W.; Larsen, C. J., & Sayegh, A. I. Exenatide reduces food intake and activates the enteric nervous system of the gastrointestinal tract and the dorsal vagal complex of the hindbrain in the rat by a GLP-1 receptor. *Brain research* **2010**, 1344, 124-133.

Watson, M., Quality assessment and control of high-throughput sequencing data. *Frontiers in Genetics* **2014,** 5.

Webb, G. C.; Akbar, M. S.; Zhao, C.; Steiner, D. F., Expression profiling of pancreatic β cells: glucose regulation of secretory and metabolic pathway genes. *Proceedings of the National Academy of Sciences* **2000,** 97, (11), 5773-5778.

Weber, P. J.; Weber, G.; Eckerskorn, C., Isolation of organelles and prefractionation of protein extracts using free-flow electrophoresis. *Current Protocols in Protein Science* **2004,** Chapter 22, Unit 22 5.

Wei, P.; Shi, M.; Barnum, S.; Cho, H.; Carlson, T.; Fraser, J., Effects of glucokinase activators GKA50 and LY2121260 on proliferation and apoptosis in pancreatic INS-1 beta cells. *Diabetologia* **2009,** 52, (10), 2142-2150.

Weinman, E. J.; Minkoff, C.; Shenolikar, S., Signal complex regulation of renal transport proteins: NHERF and regulation of NHE3 by PKA. *American journal of physiology-Renal physiology.* **2000,** 279, (3), F393-F399.

Weir, G. C.; Bonner-Weir, S., Five stages of evolving beta-cell dysfunction during progression to diabetes. *Diabetes* **2004,** 53, (suppl 3), S16-S21.

Weir, G. C.; Bonner-Weir, S., A dominant role for glucose in β cell compensation of insulin resistance. *Journal of Clinical Investigation* **2007,** 117, (1), 81.

Wente, W.; Efanov, A. M.; Brenner, M.; Kharitonenkov, A.; Köster, A.; Sandusky, G. E.; Sewing, S.; Treinies, I.; Zitzer, H.; Gromada, J., Fibroblast growth factor-21 improves pancreatic β-cell function and survival by activation of extracellular signal–regulated kinase 1/2 and Akt signaling pathways. *Diabetes* **2006,** 55, (9), 2470-2478.

Werner, T., Next generation sequencing in functional genomics. *Briefings in Bioinformatics* **2010,** 11, (5), 499-511.

Werry, T. D.; Sexton, P. M.; Christopoulos, A., "Ins and outs" of seven-transmembrane receptor signalling to ERK. *Trends in Endocrinology & Metabolism* **2005,** 16, (1), 26-33.

Weston, C.; Poyner, D.; Patel, V.; Dowell, S.; Ladds, G., Investigating G protein signalling bias at the glucagon-like peptide-1 receptor in yeast. *British Journal of Pharmacology* **2014,** 171, (15), 3651-3665.

Wettschureck, N.; Offermanns, S., Mammalian G proteins and their cell type specific functions. *Physiological Reviews* **2005,** 85, (4), 1159-1204.

Weytjens, C.; Keymeulen, B.; Van Haleweyn, C.; Somers, G.; Bossuyt, A., Rapid gastric emptying of a liquid meal in long-term Type 2 diabetes mellitus. *Diabetic Medicine* **1998,** 15, (12), 1022-7.

Wild, D.; Fani, M.; Fischer, R.; Del Pozzo, L.; Kaul, F.; Krebs, S.; Fischer, R.; Rivier, J. E.; Reubi, J. C.; Maecke, H. R.; Weber, W. A., Comparison of somatostatin receptor agonist and antagonist for peptide receptor radionuclide therapy: a pilot study. *Journal Of Nuclear Medicine* **2014,** 55, (8), 1248-52.

Willard, F. S.; Bueno, A. B.; Sloop, K. W., Small molecule drug discovery at the glucagon-like peptide-1 receptor. *Experimental Diabetes Research* **2012,** 2012.

Willard, F. S.; Wootten, D.; Showalter, A. D.; Savage, E. E.; Ficorilli, J.; Farb, T. B.; Bokvist, K.; Alsina-Fernandez, J.; Furness, S. G.; Christopoulos, A., Small molecule allosteric modulation of the glucagon-like peptide-1 receptor enhances the insulinotropic effect of oxyntomodulin. *Molecular Pharmacology.* **2012,** 82, (6), 1066-1073.

Willard, F. S.; Wootten, D.; Showalter, A. D.; Savage, E. E.; Ficorilli, J.; Farb, T. B.; Bokvist, K.; Alsina-Fernandez, J.; Furness, S. G.; Christopoulos, A.; Sexton, P. M.; Sloop, K. W., Small

molecule allosteric modulation of the glucagon-like Peptide-1 receptor enhances the insulinotropic effect of oxyntomodulin. *Molecular Pharmacology* **2012,** 82, (6), 1066-73.

Willard, S. S.; Koochekpour, S., Regulators of gene expression as biomarkers for prostate cancer. *American Journal of Cancer Research* **2012,** 2, (6), 620-57.

Willie, A., Cell death: the significance of apoptosis. *International Review of Cytology.* **1980,** 68, 251-306.

Witherow, D. S.; Garrison, T. R.; Miller, W. E.; Lefkowitz, R. J., beta-Arrestin inhibits NF-kappa B activity by means of its interaction with the NF-kappa B inhibitor I kappa B alpha. *Proceedings of the National Academy of Sciences of the U. S. A.* **2004,** 101, (23), 8603-8607.

Wollheim, C., Beta-cell mitochondria in the regulation of insulin secretion: a new culprit in type II diabetes. *Diabetologia* **2000,** 43, (3), 265-277.

Wood, A.; Armour, D., The discovery of the CCR5 receptor antagonist, UK-427,857, a new agent for the treatment of HIV infection and AIDS. *Progress in Medicinal Chemistry* **2005,** 43, 239-271.

Wood, S. L.; Westbrook, J. A.; Brown, J. E., Omic-profiling in breast cancer metastasis to bone: implications for mechanisms, biomarkers and treatment. *Cancer Treatment Reviews* **2014,** 40, (1), 139-152.

Wootten, D.; Christopoulos, A.; Sexton, P. M., Emerging paradigms in GPCR allostery: implications for drug discovery. *Nature Reviews. Drug Discovery* **2013,** 12, (8), 630-44.

Wootten, D.; Lindmark, H.; Kadmiel, M.; Willcockson, H.; Caron, K. M.; Barwell, J.; Drmota, T.; Poyner, D. R., Receptor activity modifying proteins (RAMPs) interact with the VPAC2 receptor and CRF1 receptors and modulate their function. *British Journal of Pharmacology* **2013,** 168, (4), 822-34.

Wootten, D.; Savage, E. E.; Valant, C.; May, L. T.; Sloop, K. W.; Ficorilli, J.; Showalter, A. D.; Willard, F. S.; Christopoulos, A.; Sexton, P. M., Allosteric modulation of endogenous metabolites as an avenue for drug discovery. *Molecular Pharmacology* **2012,** 82, (2), 281-90.

Wootten, D.; Savage, E. E.; Willard, F. S.; Bueno, A. B.; Sloop, K. W.; Christopoulos, A.; Sexton, P. M., Differential activation and modulation of the glucagon-like peptide-1 receptor by small molecule ligands. *Molecular Pharmacology* **2013,** 83, (4), 822-34.

Wootten, D.; Simms, J.; Koole, C.; Woodman, O. L.; Summers, R. J.; Christopoulos, A.; Sexton, P. M., Modulation of the glucagon-like peptide-1 receptor signaling by naturally occurring and synthetic flavonoids. *Journal of Pharmacology and Experimental Therapeutics* **2011,** 336, (2), 540-50.

Wootten, D. L.; Simms, J.; Massoura, A. J.; Trim, J. E.; Wheatley, M., Agonist-specific requirement for a glutamate in transmembrane helix 1 of the oxytocin receptor. *Molecular and Cellular Endocrinology* **2011,** 333, (1), 20-7.

Wright, J. R.; Clements, J. A., Metabolism and turnover of lung surfactant. *The American Review of Respiratory Disease* **1987,** 136, (2), 426-44.

Wullschleger, S.; Loewith, R.; Hall, M. N., TOR signaling in growth and metabolism. *Cell* **2006,** 124, (3), 471-484.

Wynne, K.; Park, A. J.; Small, C. J.; Patterson, M.; Ellis, S. M.; Murphy, K. G. & hatei, M. A. Subcutaneous oxyntomodulin reduces body weight in overweight and obese subjects a double-blind, randomized, controlled trial. *Diabetes* **2005**, 54(8), 2390-2395.

Wynne, K.; Park, A.; Small, C.; Meeran, K.; Ghatei, M.; Frost, G., & Bloom, S. Oxyntomodulin increases energy expenditure in addition to decreasing energy intake in overweight and obese humans: a randomised controlled trial. *International journal of obesity* **2006**, 30(12), 1729-1736.

Xiao, K.; McClatchy, D. B.; Shukla, A. K.; Zhao, Y.; Chen, M.; Shenoy, S. K.; Yates, J. R.; Lefkowitz, R. J., Functional specialization of beta-arrestin interactions revealed by proteornic analysis. *Proceedings of the National Academy of Sciences of the U. S. A.* **2007,** 104, (29), 12011-12016.

Xiao, K. H.; Sun, J. P.; Kim, J.; Rajagopal, S.; Zhai, B.; Villen, J.; Haas, W.; Kovacs, J. J.; Shukla, A. K.; Hara, M. R.; Hernandez, M.; Lachmann, A.; Zhao, S.; Lin, Y. A.; Cheng, Y. S.; Mizuno, K.; Ma'ayan, A.; Gygi, S. P.; Lefkowitz, R. J., Global phosphorylation analysis of beta-arrestin-mediated signaling downstream of a seven transmembrane receptor (7TMR). *Proceedings of the National Academy of Sciences of the U. S. A.* **2010,** 107, (34), 15299-15304.

Xu, G.; Stoffers, D. A.; Habener, J. F.; Bonner-Weir, S., Exendin-4 stimulates both beta-cell replication and neogenesis, resulting in increased beta-cell mass and improved glucose tolerance in diabetic rats. *Diabetes* **1999,** 48, (12), 2270-2276.

Xue, S.; Wasserfall, C.; Parker, M.; McGrail, S.; McGrail, K.; Campbell-Thompson M.;Haller, M. J. Exendin-4 treatment of nonobese diabetic mice increases beta-cell proliferation and fractional insulin reactive area. *Journal of diabetes and its complications* **2010**, 24(3), 163-167.

Yamada, C.; Yamada, Y.; Tsukiyama, K.; Yamada, K.; Udagawa, N.; Takahashi, N.; Tanaka, K.; Drucker, D. J.; Seino, Y.; Inagaki, N., The murine glucagon-like peptide-1 receptor is essential for control of bone resorption. *Endocrinology* **2008,** 149, (2), 574-9.

Yamagata, K.; Senokuchi, T.; Lu, M.; Takemoto, M.; Fazlul Karim, M.; Go, C.; Sato, Y.; Hatta, M.; Yoshizawa, T.; Araki, E.; Miyazaki, J.; Song, W. J., Voltage-gated K+ channel KCNQ1 regulates insulin secretion in MIN6 beta-cell line. *Biochemical and Biophysical Research Communications* **2011,** 407, (3), 620-5.

Yamagata, K.; Senokuchi, T.; Lu, M.; Takemoto, M.; Karim, M. F.; Go, C.; Sato, Y.; Hatta, M.; Yoshizawa, T.; Araki, E., Voltage-gated K+ channel KCNQ1 regulates insulin secretion in MIN6 β-cell line. *Biochemical and Biophysical Research Communications* **2011,** 407, (3), 620-625.

Yamamoto, H.; Lee, C. E.; Marcus, J. N.; Williams, T. D.; Overton, J. M.; Lopez, M. E.; Hollenberg, A. N.; Baggio, L.; Saper, C. B.; Drucker, D. J.; Elmquist, J. K., Glucagon-like

peptide-1 receptor stimulation increases blood pressure and heart rate and activates autonomic regulatory neurons. *The Journal of Clinical Investigation* **2002,** 110, (1), 43-52.

Yaney, G. C.; Civelek, V. N.; Richard, A. M.; Dillon, J. S.; Deeney, J. T.; Hamilton, J. A.; Korchak, H. M.; Tornheim, K.; Corkey, B. E.; Boyd, A. E., 3rd, Glucagon-like peptide 1 stimulates lipolysis in clonal pancreatic beta-cells (HIT). *Diabetes* **2001,** 50, (1), 56-62.

Yang, H. J.; Kim, N.; Seong, K. M.; Youn, H.; Youn, B., Investigation of radiation-induced transcriptome profile of radioresistant non-small cell lung cancer A549 cells using RNA-seq. *PLoS One* **2013,** 8, (3), e59319.

Yang, S.; Fransson, U.; Fagerhus, L.; Stenson Holst, L.; Hohmeier, H. E.; Renström, E.; Mulder, H., Enhanced cAMP protein kinase A signaling determines improved insulin secretion in a clonal insulin-producing β-cell line (INS-1 832/13). Molecular Endocrinology **2004,** 18, (9), 2312-2320.

Yip, R. G.; Wolfe, M. M., GIP biology and fat metabolism. *Life Sciences* **2000,** 66, (2), 91-103.

Young, A. A.; Gedulin, B. R.; Bhavsar, S.; Bodkin, N.; Jodka, C.; Hansen, B.; Denaro, M., Glucose-lowering and insulin-sensitizing actions of exendin-4: studies in obese diabetic (ob/ob, db/db) mice, diabetic fatty Zucker rats, and diabetic rhesus monkeys (Macaca mulatta). *Diabetes* **1999,** 48, (5), 1026-34.

Yusta, B.; Baggio, L. L.; Estall, J. L.; Koehler, J. A.; Holland, D. P.; Li, H.; Pipeleers, D.; Ling, Z.; Drucker, D. J., GLP-1 receptor activation improves β cell function and survival following induction of endoplasmic reticulum stress. *Cell Metabolism.* **2006,** 4, (5), 391-406.

Zander, M.; Madsbad, S.; Madsen, J. L.; Holst, J. J., Effect of 6-week course of glucagon-like peptide 1 on glycaemic control, insulin sensitivity, and beta-cell function in type 2 diabetes: a parallel-group study. *Lancet* **2002,** 359, (9309), 824-30.

Zawalich, W.; Tesz, G.; Zawalich, K., Inhibitors of phosphatidylinositol 3-kinase amplify insulin release from islets of lean but not obese mice. *Journal of Endocrinology* **2002,** 174, (2), 247-258.

Zhang, L. Q.; Cheranova, D.; Gibson, M.; Ding, S.; Heruth, D. P.; Fang, D.; Ye, S. Q., RNA-seq reveals novel transcriptome of genes and their isoforms in human pulmonary microvascular endothelial cells treated with thrombin. *PLoS One* **2012,** 7, (2), e31229.

Zhang, Y.; Wang, Q.; Zhang, J.; Lei, X.; Xu, G. T.; Ye, W., Protection of exendin-4 analogue in early experimental diabetic retinopathy. *Graefe's Archive for Clinical and Experimental Ophthalmology* **2009,** 247, (5), 699-706.

Zhang, Y.; Zhang, J.; Wang, Q.; Lei, X.; Chu, Q.; Xu, G.-T.; Ye, W., Intravitreal injection of exendin-4 analogue protects retinal cells in early diabetic rats. *Investigative Ophthalmology and Visual Science* **2011,** 52, (1), 278-285.

Zhao, P.; Metcalf, M.; Bunnett, N. W., Biased signaling of protease-activated receptors. *Frontiers in Endocrinology* **2014,** 5.

Zhao, X.; Tang, Y. G.; Wu, S. V.; Wang, C.; Perfetti, R.; Khoury, N.; Cai, D.; He, F.; Su, X.; Go, V. L. W., The Global Transcriptional Response of Isolated Human Islets of Langerhans to Glucagon-Like Peptide-1 Receptor Agonist Liraglutide. *ISRN Endocrinology* **2012,** 2012.

Zheng, Q.; Wang, X.-J., GOEAST: a web-based software toolkit for Gene Ontology enrichment analysis. *Nucleic Acids Research* **2008,** 36, (suppl 2), W358-W363.

Zhu, D.; Zhang, Y.; Lam, P. P.; Dolai, S.; Liu, Y.; Cai, E. P.; Choi, D.; Schroer, S. A.; Kang, Y.; Allister, E. M.; Qin, T.; Wheeler, M. B.; Wang, C. C.; Hong, W. J.; Woo, M.; Gaisano, H. Y., Dual role of VAMP8 in regulating insulin exocytosis and islet beta cell growth. *Cell Metabolism* **2012,** 16, (2), 238-49.

Zhu, L.; Tamvakopoulos, C.; Xie, D.; Dragovic, J.; Shen, X.; Fenyk-Melody, J. E.; Schmidt, K.; Bagchi, A.; Griffin, P. R.; Thornberry, N. A.; Sinha Roy, R., The role of dipeptidyl peptidase IV in the cleavage of glucagon family peptides: in vivo metabolism of pituitary adenylate cyclase activating polypeptide-(1-38). *Journal of Biological Chemistry* **2003,** 278, (25), 22418-23.

Zwemer, L. M.; Hui, L.; Wick, H. C.; Bianchi, D. W., RNA-Seq and expression microarray highlight different aspects of the fetal amniotic fluid transcriptome. *Prenatal Diagnosis* **2014,** 34, (10), 1006-1014.